Title

Studies Pertaining to Amide C—N Bond Activation and Strained Heterocyclic Allenes

Author

Mehta, Milauni

Publication Date

2023

Peer reviewed|Thesis/dissertation

UNIVERSITY OF CALIFORNIA

Los Angeles

Studies Pertaining to Amide C–N Bond Activation and Strained Heterocyclic Allenes

A dissertation submitted in partial satisfaction of the

requirements for the degree Doctor of Philosophy

in Chemistry

by

Milauni Mehta

2023

ABSTRACT OF THE DISSERTATION

Studies Pertaining to Amide C–N Bond Activation and Strained Heterocyclic Allenes

by

Milauni Mehta

Doctor of Philosophy in Chemistry

University of California, Los Angeles, 2023

Professor Neil K. Garg, Chair

This dissertation describes the development of reaction methodologies that utilize unconventional building blocks. One major effort involves the development of a strategy to improve the practicality of the nickel-catalyzed Suzuki–Miyaura cross-coupling of amide electrophiles and a strategy for a base-mediated reduction of ketones to secondary alcohols. Furthermore, a one-pot reductive arylation of amides wherein two different nucleophiles are added to the amide carbonyl carbon is reported. This reaction, which proceeds by way of a sequential nickel-catalyzed Suzuki–Miyaura coupling and base-catalyzed reduction cascade process, directly converts amide starting materials to chiral secondary alkyl–aryl alcohol products. Finally, investigations into strained heterocyclic allenes are described. These studies detail the cyclic allene

approach to the core of the manzamine alkaloid keramaphidin B, where the key step hinges on a cycloaddition of an azacyclic allene intermediate. Furthermore, the parameters controlling the regioselectivity of the Diels–Alder cycloaddition of heterocyclic allenes with α-pyrones is reported. Each of the methodologies presented is expected to expand the synthetic toolbox by leveraging unique reactivity.

Chapter one outlines a strategy for performing nickel-catalyzed Suzuki–Miyaura couplings of aliphatic amides on the benchtop. In this approach, air- and moisture-sensitive reagents are stored in paraffin capsules, allowing for air-sensitive transition-metal-catalyzed cross-couplings to be carried out without the need for glovebox manipulations. This study is anticipated to advance the utility of amides as acyl synthons for C–C bond-forming cross-coupling reactions.

Chapters two and three concern the development of a base-catalyzed reduction of aryl ketones and its application toward a one-pot reductive arylation of aliphatic amides. In chapter two, the use of an electron-rich benzylic alcohol reductant to achieve a Meerwein–Ponndorf–Verley (MPV)-type reduction of ketones is reported. This approach avoids the use of the hydride source as the solvent, proceeds under mildly basic conditions, reduces aromatic and *O*- and *S*-containing heteroaromatic ketones, and delivers enantioenriched alcohol products through a stereospecific reduction when using an enantioenriched reductant. These studies expand the field of base-catalyzed MPV-type reductions of carbonyls and address several limitations associated with prior methodologies. Chapter three describes the application of this mild ketone reduction protocol toward a one-pot reductive arylation of amides. Specifically, this methodology, which proceeds by way of a nickel-catalyzed Suzuki–Miyaura coupling of aliphatic amides and subsequent base-catalyzed transfer hydrogenation of ketone intermediates, provides direct access to chiral secondary alkyl–aryl alcohols from amide starting materials. This study represents the

first catalytic method for the direct intermolecular addition of two different nucleophiles to the amide carbonyl carbon. Moreover, these efforts are expected to promote the development of additional catalytic approaches to directly convert carboxylic acids and their derivatives to functional groups bearing stereogenic centers.

Chapter four describes the cyclic allene approach to the core of the manzamine alkaloid keramaphidin B. This approach to access the azadecalin core of the natural product relies on the strain-promoted Diels–Alder cycloaddition of an azacyclic allene with a pyrone trapping partner. It is demonstrated that the cycloaddition is tolerant of nitrile and primary amide functional groups and can be dovetailed with a subsequent retro-Diels–Alder step to access advanced intermediates. These studies highlight that strained cyclic allenes can be used to build significant structural complexity and should encourage further exploration of these fleeting intermediates in complex molecule synthesis.

Finally, chapter five describes the study of parameters affecting the regioselectivity of the strain-promoted Diels–Alder cycloaddition cyclic allenes and α-pyrones. This report investigates the scope of methyl-substituted heterocyclic allenes as dienophiles, substituent effects on both cycloaddition partners for the regioselectivity of the reaction, and relative reactivity of furans vs pyrones as trapping partners with both methyl- and ester-substituted cyclic allenes in competition experiments. Additionally, the first example of ester-substituted oxacyclic allenes in a Diels–Alder reaction with α-pyrone is reported. These studies provide insight into the fundamental reactivity of cyclic allenes and offer a starting point for determining the predictive capacity of Diels–Alder cycloadditions of heterocyclic allenes and pyrones.

The dissertation of Milauni Mehta is approved.

Kendall N. Houk

Abigail G. Doyle

Yi Tang

Neil K. Garg, Committee Chair

University of California, Los Angeles

2023

“Even the darkest night will end and the sun will rise.”

– Victor Hugo

For my family

TABLE OF CONTENTS

ABSTRACT OF THE DISSERTATION ii

COMMITTEE PAGE v

DEDICATION PAGE vi

TABLE OF CONTENTS vii

LIST OF FIGURES xiii

LIST OF TABLES xxiv

LIST OF ABBREVIATIONS xxiv

ACKNOWLEDGEMENTS xxxi

BIOGRAPHICAL SKETCH xli

CHAPTER ONE: Ni-Catalyzed Suzuki–Miyaura Cross-Coupling of Aliphatic Amides on the Benchtop 1

1.1 Abstract 1

1.2 Introduction 1

1.3 Reaction Discovery and Optimization 3

1.4 Scope of the Boronic Ester Coupling Partner 4

1.5 Scope of the Amide Substrate 5

1.6 Demonstration of Coupling on Gram-Scale 6

1.7 Conclusion 7

1.8 Experimental Section 8

1.8.1 Materials and Methods 8

1.8.2 Experimental Procedures 9

1.8.2.1 Preparation of Paraffin Wax Capsules 9

1.8.2.2 Preparation of Paraffin Wax Capsules for Gram-Scale Coupling 13

1.8.2.3 Optimization of Methodology 16

1.8.2.4 Scope of Methodology 18

1.8.2.5 Gram-Scale Benchtop Suzuki–Miyaura Cross-Coupling 25

1.9 Spectra Relevant to Chapter One 27

1.10 Notes and References 35

CHAPTER TWO: Based-Mediated Meerwein–Ponndorf–Verley Reduction of Aromatic and Heterocyclic Ketones 45

2.1 Abstract 45

2.2 Introduction 45

2.3 Reaction Discovery and Optimization 47

2.4 Scope of Methodology 48

2.5 Gram-Scale and Stereospecific Reductions 50

2.6 Conclusion 51

2.7 Experimental Section 53

2.7.1 Materials and Methods 53

2.7.2 Experimental Procedures 55

2.7.2.1 Syntheses of Ketone Substrates 55

2.7.2.2 Syntheses of Alcohol Reductant **2.5** 56

2.7.2.3 Syntheses of Enantioenriched Alcohol Reductant (*R*)-**2.5** 57

2.7.2.4 Initial Survey of Reaction Conditions and Relevant Control Experiments 58

2.7.2.5 Trace Metal Analysis of Reagents 60

2.7.2.6 Scope of Methodology 64

2.7.2.7 Gram-Scale Reduction 72

2.7.2.8 Stereospecific Reduction 73

2.7.2.9 Verification of Enantiopurity 74

2.7.2.9.1 Chiral SFC & HPLC Assays of Alcohol Reductant 74

2.7.2.9.2 Stereospecific Reduction of Ketone **2.6** 76

2.8 Spectra Relevant to Chapter Two 78

2.9 Notes and References 91

CHAPTER THREE: Reductive Arylation of Amides via a Nickel-Catalyzed Suzuki–Miyaura Coupling and Transfer Hydrogenation Cascade 101

3.1 Abstract 101

3.2 Introduction 101

3.3 Reaction Discovery and Optimization 104

3.4 Scope of the Aliphatic Amide Substrate and Robustness Screen 106

3.5 Scope of Aryl Boronic Ester Coupling Partner 109

3.6 Synthetic Applications of the Methodology 110

3.7 Conclusion 112

3.8 Experimental Section 113

3.8.1 Materials and Methods 113

3.8.2 Experimental Procedures 114

3.8.2.1 Syntheses of Amide Substrates 114

3.8.2.2 Relevant Control Experiments 119

3.8.2.3 General Procedures for Methodology 121

3.8.2.3.1 General Procedures A 121

3.8.2.3.2 General Procedures B 121

3.8.2.3.3 General Procedures C 122

3.8.2.4 Scope of Amide Substrates 123

3.8.2.5 Scope of Boronate Ester Nucleophiles 132

3.8.2.6 Syntheses of Alcohols **3.40** and **3.43** 139

3.8.2.7 Syntheses of Authentic Samples of Alcohols **3.13** and **3.37** 140

3.8.2.8 Robustness Screen 143

3.8.2.9 Benchtop Variants of Methodology 144

3.8.2.9.1 Procedure A: Employing a paraffin wax encapsulation approach. 144

3.8.2.9.1 Procedure B: Employing an air-stable Ni(II) precatalyst. 145

3.8.2.10 Enantioselectivity Experiments 146

3.8.2.11 Verification of Enantioenrichment 147

3.8.2.12 Deuterium Incorporation Experiments 149

3.8.2.12.1 Preparation of deuterated reducing agent *d*-DMPE (***d*-3.7**) 149

3.8.2.12.2 Deuterium incorporation experiments using *d*-DMPE (***d*-3.7**) 150

3.9 Spectra Relevant to Chapter Three 151

3.10 Notes and References 178

CHAPTER FOUR: Cyclic Allene Approach to the Manzamine Alkaloid Keramaphidin B 193

4.1 Abstract 193

4.2 Introduction 193

4.3 Retrosynthetic Analysis 195

4.4 Model System Studies 196

4.5 Revised Strategy and Experimental Results 198

4.6 Conclusion 201

4.7 Experimental Section 203

4.7.1 Materials and Methods 203

4.7.2 Experimental Procedures 205

4.7.2.1 Synthesis of Compound **4.16** 205

4.7.2.2 Syntheses of Silyl Triflates **4.22a** and **4.22b** 211

4.7.2.3 Syntheses of Trienes **4.23a** and **4.23b** 215

4.8 Spectra Relevant to Chapter Four 218

4.9 Notes and References 232

CHAPTER FIVE: Strain-Promoted Diels–Alder Cycloadditions of Heterocyclic Allenes and α-Pyrones 240

5.1 Abstract 240

5.2 Introduction 240

5.3 Scope of Cycloadditions with Methyl-Substituted Heterocyclic Allenes 243

5.4 Cycloadditions with Ester-Substituted Oxacyclic Allenes 246

5.5 Competition Experiments 248

5.6 1 mmol Scale Reaction 249

5.7 Conclusion 250

5.8 Experimental Section 251

5.8.1 Materials and Methods 251

5.8.2 Experimental Procedures 253

5.8.2.1 Synthesis of Silyl Triflates 253

5.8.2.2 Scope of Cycloadditions with Methyl-Substituted Heterocyclic Allenes 258

5.8.2.3 Cycloadditions with Ester-Substituted Oxacyclic Allenes 266

5.8.2.4 Competition Experiments 270

5.8.2.5 1 mmol Scale Reaction 271

5.9 Spectra Relevant to Chapter Five 273

5.10 Notes and References 321

LIST OF FIGURES

CHAPTER ONE

Figure 1.1 Methods for the conversion of amides to ketones, prior studies of Ni-catalyzed Suzuki–Miyaura couplings that utilize a glovebox, and paraffin encapsulation strategy for benchtop delivery (present study) 3

Figure 1.2 Preparation of $Ni(cod)_2$/Benz-ICy•HCl–paraffin capsules and their use in the benchtop Suzuki–Miyaura coupling of piperidinyl amide **1.4** and pyrrole boronic ester **1.5** under optimized conditions 4

Figure 1.3 Scope of the boronic ester coupling partner 5

Figure 1.4 Scope of the amide substrate 6

Figure 1.5 Gram-scale Suzuki–Miyaura coupling of amide **1.1** with boronate ester **1.18** to generate ketone **1.19** 7

Figure 1.6 ^1H NMR (500 MHz, $CDCl_3$) of compound **1.6** 28

Figure 1.7 ^{1}H NMR (500 MHz, $CDCl_3$) of compound **1.7** 28

Figure 1.8 ^{1}H NMR (500 MHz, $CDCl_3$) of compound **1.8** 29

Figure 1.9 ^{1}H NMR (500 MHz, $CDCl_3$) of compound **1.9** 29

Figure 1.10 ^{1}H NMR (600 MHz, $CDCl_3$) of compound **1.10** 30

Figure 1.11 ^{1}H NMR (500 MHz, $CDCl_3$) of compound **1.11** 30

Figure 1.12 ^{1}H NMR (400 MHz, $CDCl_3$) of compound **1.12** 31

Figure 1.13 ^{1}H NMR (500 MHz, $CDCl_3$) of compound **1.13** 31

Figure 1.14 ^{1}H NMR (500 MHz, $CDCl_3$) of compound **1.14** 32

Figure 1.15 ^{1}H NMR (500 MHz, $CDCl_3$) of compound **1.15** 32

Figure 1.16 ^{1}H NMR (500 MHz, $CDCl_3$) of compound **1.16** 33

Figure 1.17 ^{1}H NMR (500 MHz, $CDCl_3$) of compound **1.17** 33

Figure 1.18 ^{1}H NMR (500 MHz, $CDCl_3$) of compound **1.19** 34

Figure 1.19 ^{13}C NMR (125 MHz, $CDCl_3$) of compound **1.19** 34

CHAPTER TWO

Figure 2.1 Traditional MPV reduction of ketones and base-mediated variant (prior studies) 46

Figure 2.2 Scope of the base-mediated MPV reduction of aromatic ketones 49

Figure 2.3 Scope of the base-mediated MPV reduction of heteroaromatic ketones 50

Figure 2.4 Gram-scale reduction and stereochemical transfer studies demonstrating the synthetic utility of the base-mediated MPV reduction 51

Figure 2.5 SFC trace of *rac*-**2.5** (Table 2.6, Entry 1) 75

Figure 2.6 SFC trace of (*R*)-**2.5** (Table 2.6, Entry 2) 75

Figure 2.7 HPLC trace of *rac*-**2.6** (Table 2.7, Entry 1) 76

Figure 2.8 HPLC trace of (*R*)-**2.6** (Table 2.7, Entry 2) 77

Figure 2.9 ^{1}H NMR (600 MHz, $CDCl_3$) of compound **2.24** 79

Figure 2.10 ^{13}C NMR (125 MHz, $CDCl_3$) of compound **2.24** 79

Figure 2.11 ^{1}H NMR (500 MHz, $CDCl_3$) of compound **2.20** 80

Figure 2.12 ^{1}H NMR (500 MHz, $CDCl_3$) of compound **2.5** 80

Figure 2.13 ^{1}H NMR (500 MHz, $CDCl_3$) of compound **2.2** 81

Figure 2.14 ^{1}H NMR (500 MHz, $CDCl_3$) of compound **2.6** 81

Figure 2.15 ^{1}H NMR (500 MHz, $CDCl_3$) of compound **2.7** 82

Figure 2.16 ^{1}H NMR (500 MHz, $CDCl_3$) of compound **2.8** 82

Figure 2.17 ^{1}H NMR (500 MHz, $CDCl_3$) of compound **2.9** 83

Figure 2.18 ^{1}H NMR (500 MHz, $CDCl_3$) of compound **2.10** 83

Figure 2.19 ^{1}H NMR (500 MHz, $CDCl_3$) of compound **2.11** 84

Figure 2.20 ^{1}H NMR (500 MHz, $CDCl_3$) of compound **2.12** 84

Figure 2.21 ^{1}H NMR (500 MHz, $CDCl_3$) of compound **2.13** 85

Figure 2.22 ^{1}H NMR (400 MHz, $CDCl_3$) of compound **2.14** 85

Figure 2.23 ^{13}C NMR (125 MHz, $CDCl_3$) of compound **2.14** 86

Figure 2.24 ^{1}H NMR (400 MHz, $CDCl_3$) of compound **2.15** 86

Figure 2.25 ^{1}H NMR (500 MHz, $CDCl_3$) of compound **2.16** 87

Figure 2.26 ^{13}C NMR (125 MHz, $CDCl_3$) of compound **2.16** 87

Figure 2.27 ^{1}H NMR (500 MHz, $CDCl_3$) of compound **2.17** 88

Figure 2.28 ^{1}H NMR (500 MHz, $CDCl_3$) of compound **2.18** 88

Figure 2.29 ^{13}C NMR (125 MHz, $CDCl_3$) of compound **2.18** 89

Figure 2.30 ^{1}H NMR (500 MHz, $CDCl_3$) of compound **2.19** 89

Figure 2.31 ^{13}C NMR (125 MHz, $CDCl_3$) of compound **2.19** 90

CHAPTER THREE

Figure 3.1 (a) Common reaction pathways for nucleophilic additions to carboxylic acid derivatives. (b) Direct catalytic approaches to chiral amines or alcohols from carboxylic acid derivatives..... 103

Figure 3.2 Overview of current study involving the conversion of aliphatic amides to alkyl–aryl alcohols via a Suzuki–Miyaura coupling / transfer hydrogenation cascade .. 104

Figure 3.3 Evaluation of reaction conditions for the nickel-catalyzed Suzuki–Miyaura coupling / transfer hydrogenation cascade of amide **3.1** with phenyl boronates and reductants. 106

Figure 3.4 Scope of the reductive arylation of aliphatic amides and boronate **3.6** 108

Figure 3.5 Scope of the reductive arylation of aliphatic amides and aryl boronates 110

Figure 3.6 (a) Synthesis of alcohol **3.40**, an intermediate in the synthesis of γ-secretase modulator **3.41**. (b) Synthesis of alcohol **3.43**, intercepting a known synthetic route toward Prozac® (**3.44**, fluoxetine) 111

Figure 3.7 SFC trace of *rac*-**3.4** (Table 3.3, Entry 1). 148

Figure 3.8 SFC trace of *enantionenriched*-**3.4** (Table 3.3, Entry 2) 148

Figure 3.9 ^{1}H NMR (600 MHz, $CDCl_3$) of compound **3.55** 152

Figure 3.10 ^{13}C NMR (125 MHz, $CDCl_3$) of compound **3.55** 152

Figure 3.11 ^{1}H NMR (500 MHz, $CDCl_3$) of compound **3.57** 153

Figure 3.12 ^{13}C NMR (125 MHz, $CDCl_3$) of compound **3.57** 153

Figure 3.13 ^{1}H NMR (500 MHz, $CDCl_3$) of compound **3.42** 154

Figure 3.14 ^{13}C NMR (125 MHz, $CDCl_3$) of compound **3.42** 154

Figure 3.15 ^{1}H NMR (600 MHz, $CDCl_3$) of compound **3.4** 155

Figure 3.16 ^{1}H NMR (500 MHz, $CDCl_3$) of compound **3.8** 155

Figure 3.17 ^{1}H NMR (500 MHz, $CDCl_3$) of compound **3.9** 156

Figure 3.18 ^{1}H NMR (500 MHz, $CDCl_3$) of compound **3.10** 156

Figure 3.19 ^{1}H NMR (600 MHz, $CDCl_3$) of compound **3.11** 157

Figure 3.20 ^{1}H NMR (600 MHz, $CDCl_3$) of compound **3.12** 157

Figure 3.21 ^{1}H NMR (400 MHz, $CDCl_3$) of compound **3.13** 158

Figure 3.22 ^{1}H NMR (600 MHz, $CDCl_3$) of compound **3.13** 158

Figure 3.23 ^{13}C NMR (125 MHz, $CDCl_3$) of compound **3.13** 159

Figure 3.24 ^{1}H NMR (600 MHz, $CDCl_3$) of compound **3.14** 159

Figure 3.25 ^{13}C NMR (125 MHz, $CDCl_3$) of compound **3.14** 160

Figure 3.26 ^{1}H NMR (500 MHz, $CDCl_3$) of compound **3.15** 160

Figure 3.27 ^{13}C NMR (125 MHz, $CDCl_3$) of compound **3.15** 161

Figure 3.28 ^{1}H NMR (500 MHz, $CDCl_3$) of compound **3.16** 161

Figure 3.29 ^{1}H NMR (500 MHz, $CDCl_3$) of compound **3.17** 162

Figure 3.30 ^{13}C NMR (125 MHz, $CDCl_3$) of compound **3.17** 162

Figure 3.31 ^{1}H NMR (500 MHz, $CDCl_3$) of compound **3.18** 163

Figure 3.32 ^{1}H NMR (500 MHz, $CDCl_3$) of compound **3.19** 163

Figure 3.33 ^{13}C NMR (125 MHz, $CDCl_3$) of compound **3.19** 164

Figure 3.34 ^{1}H NMR (500 MHz, $CDCl_3$) of compound **3.20** 164

Figure 3.35 ^{1}H NMR (500 MHz, $CDCl_3$) of compound **3.28** 165

Figure 3.36 ^{13}C NMR (125 MHz, $CDCl_3$) of compound **3.28** 165

Figure 3.37 ^{1}H NMR (600 MHz, $CDCl_3$) of compound **3.29** 166

Figure 3.38 ^{13}C NMR (125 MHz, $CDCl_3$) of compound **3.29** 166

Figure 3.39 ^{1}H NMR (500 MHz, $CDCl_3$) of compound **3.30** 167

Figure 3.40 ^{13}C NMR (125 MHz, $CDCl_3$) of compound **3.30** 167

Figure 3.41 ^{1}H NMR (600 MHz, $CDCl_3$) of compound **3.31** 168

Figure 3.42 ^{13}C NMR (125 MHz, $CDCl_3$) of compound **3.31** 168

Figure 3.43 ^{1}H NMR (500 MHz, $CDCl_3$) of compound **3.32** 169

Figure 3.44 ^{13}C NMR (125 MHz, $CDCl_3$) of compound **3.32** 169

Figure 3.45 ^{1}H NMR (500 MHz, $CDCl_3$) of compound **3.33** 170

Figure 3.46 ^{13}C NMR (125 MHz, $CDCl_3$) of compound **3.33** 170

Figure 3.47 ^{1}H NMR (500 MHz, $CDCl_3$) of compound **3.34** 171

Figure 3.48 ^{13}C NMR (125 MHz, $CDCl_3$) of compound **3.34** 171

Figure 3.49 ^{1}H NMR (500 MHz, $CDCl_3$) of compound **3.35** 172

Figure 3.50 ^{13}C NMR (125 MHz, $CDCl_3$) of compound **3.35** 172

Figure 3.51 ^{1}H NMR (500 MHz, $CDCl_3$) of compound **3.36** 173

Figure 3.52 ^{13}C NMR (125 MHz, $CDCl_3$) of compound **3.36** 173

Figure 3.53 ^{1}H NMR (500 MHz, $CDCl_3$) of compound **3.37** 174

Figure 3.54 ^{1}H NMR (500 MHz, $CDCl_3$) of compound **3.37** 174

Figure 3.55 ^{13}C NMR (125 MHz, $CDCl_3$) of compound **3.37** 175

Figure 3.56 ^{1}H NMR (500 MHz, $CDCl_3$) of compound **3.40** 175

Figure 3.57 ^{13}C NMR (125 MHz, $CDCl_3$) of compound **3.40** 176

Figure 3.58 ^{1}H NMR (500 MHz, $CDCl_3$) of compound **3.43** 176

Figure 3.59 ^{1}H NMR (500 MHz, $CDCl_3$) of compound **3.70** 177

Figure 3.60 ^{1}H NMR (400 MHz, $CDCl_3$) of compound ***d*-3.7** 177

CHAPTER FOUR

Figure 4.1 (–)-Keramaphidin B (**4.1**), a complex manzamine alkaloid and azacyclic allenes **4.2**, an underutilized synthetic building block 194

Figure 4.2 Retrosynthetic analysis of (–)-keramaphidin B (**4.1**)..... 196

Figure 4.3 Model system for assembly of azadecalin scaffold (**4.4**)..... 197

Figure 4.4 Synthesis of ImDA precursor **4.16** and evaluation of intramolecular ImDA reaction..... 198

Figure 4.5 Revised strategy to construct the [2.2.2]-azabicycle 199

Figure 4.6 Synthesis of allene precursors **4.22a** and **4.22b**..... 200

Figure 4.7 One-pot cycloaddition and CO_2 extrusion to generate trienes **4.23a** and **4.23b** 201

Figure 4.8 ^{1}H NMR (500 MHz, $CDCl_3$) of compound **4.10** 219

Figure 4.9 ^{13}C NMR (125 MHz, $CDCl_3$) of compound **4.10** 219

Figure 4.10 ^{1}H NMR (500 MHz, $CDCl_3$) of compound **4.11** 220

Figure 4.11 ^{13}C NMR (125 MHz, $CDCl_3$) of compound **4.11** 220

Figure 4.12 ^{19}F NMR (376 MHz, $CDCl_3$) of compound **4.11**..... 221

Figure 4.13 ^{1}H NMR (500 MHz, $CDCl_3$) of compound **4.14** 221

Figure 4.14 ^{13}C NMR (125 MHz, $CDCl_3$) of compound **4.14** 222

Figure 4.15 ^{1}H NMR (500 MHz, $CDCl_3$) of compound **4.15** 222

Figure 4.16 NOESY (600 MHz, $CDCl_3$) of compound **4.15** 223

Figure 4.17 ^{13}C NMR (125 MHz, $CDCl_3$) of compound **4.15** 224

Figure 4.18 ^{1}H NMR (500 MHz, MeOD) of compound **4.16**..... 224

Figure 4.19 ^{13}C NMR (125 MHz, MeOD) of compound **4.16**..... 225

Figure 4.20 ^{1}H NMR (500 MHz, $CDCl_3$) of compound **4.21** 225

Figure 4.21 ^{13}C NMR (125 MHz, $CDCl_3$) of compound **4.21** 226

Figure 4.22 ^{19}F NMR (376 MHz, $CDCl_3$) of compound **4.21** 226

Figure 4.23 ^{1}H NMR (500 MHz, $CDCl_3$) of compound **4.22a** 227

Figure 4.24 ^{13}C NMR (125 MHz, $CDCl_3$) of compound **4.22a** 227

Figure 4.25 ^{19}F NMR (376 MHz, $CDCl_3$) of compound **4.22a** 228

Figure 4.26 ^{1}H NMR (500 MHz, MeOD) of compound **4.22b** 228

Figure 4.27 ^{13}C NMR (125 MHz, MeOD) of compound **4.22b** 229

Figure 4.28 ^{19}F NMR (376 MHz, MeOD) of compound **4.22b** 229

Figure 4.29 ^{1}H NMR (500 MHz, $CDCl_3$) of compound **4.23a** 230

Figure 4.30 ^{13}C NMR (150 MHz, $CDCl_3$) of compound **4.23a** 230

Figure 4.31 ^{1}H NMR (500 MHz, $CDCl_3$) of compound **4.23b** 231

Figure 4.32 ^{13}C NMR (150 MHz, $CDCl_3$) of compound **4.23b** 231

CHAPTER FIVE

Figure 5.1 Overview of scaffolds accessible from strain-promoted Diels–Alder cycloadditions of strained cyclic intermediates (**5.3** or **5.6**) with furans (**5.2**) or pyrones (**5.4**) 242

Figure 5.2 Scope of the DA cycloaddition with methyl-substituted oxa and azacyclic allenes (**5.12**) and pyrones **5.15**, **5.18**, **5.21**, and **5.24** 245

Figure 5.3 Cycloaddition reactions with α-pyrones (**5.28**) and 2,5-dimethylfuran (**5.30**) with ester-substituted oxacyclic allene (**5.27**) and di-substituted oxacyclic allene (**5.32**) 247

Figure 5.4 Competition experiments with allene precursors **5.35** and **5.38** with 2,5-dimethylfuran (**5.28**) and α-pyrone (**5.30**) 249

Figure 5.5 Strain-promoted DA cycloaddition with allene precursor **5.40** and pyrone **5.24** on one mmol scale. 250

Figure 5.6 ^{1}H NMR (500 MHz, $CDCl_3$) of compound **5.39** 274

Figure 5.7 ^{13}C NMR (150 MHz, $CDCl_3$) of compound **5.39** 274

Figure 5.8 ^{1}H NMR (600 MHz, $CDCl_3$) of compound **5.34** 275

Figure 5.9 ^{13}C NMR (125 MHz, $CDCl_3$) of compound **5.34** 275

Figure 5.10 ^{19}F NMR (376 MHz, $CDCl_3$) of compound **5.34** 276

Figure 5.11 ^{1}H NMR (500 MHz, $CDCl_3$) of compound **5.35** 277

Figure 5.12 ^{13}C NMR (125 MHz, $CDCl_3$) of compound **5.35** 277

Figure 5.13 ^{19}F NMR (376 MHz, $CDCl_3$) of compound **5.35** 278

Figure 5.14 ^{1}H NMR (500 MHz, $CDCl_3$) of compound **5.41** 279

Figure 5.15 ^{13}C NMR (125 MHz, $CDCl_3$) of compound **5.41** 279

Figure 5.16 ^{1}H NMR (500 MHz, $CDCl_3$) of compound **5.42** 280

Figure 5.17 ^{13}C NMR (125 MHz, $CDCl_3$) of compound **5.42** 280

Figure 5.18 ^{19}F NMR (376 MHz, $CDCl_3$) of compound **5.42** 281

Figure 5.19 ^{1}H NMR (500 MHz, $CDCl_3$) of compound **5.19a** 282

Figure 5.20 ^{13}C NMR (125 MHz, $CDCl_3$) of compound **5.19a** 282

Figure 5.21 ^{1}H NMR (500 MHz, $CDCl_3$) of compound **5.21a** 283

Figure 5.22 ^{13}C NMR (125 MHz, $CDCl_3$) of compound **5.21a** 283

Figure 5.23 ^{1}H NMR (500 MHz, $CDCl_3$) of compound **5.25** 284

Figure 5.24 ^{13}C NMR (125 MHz, $CDCl_3$) of compound **5.25** 284

Figure 5.25 ^{1}H NMR (400 MHz, $CDCl_3$) of compound **5.23** 285

Figure 5.26 ^{13}C NMR (100 MHz, $CDCl_3$) of compound **5.23** 285

Figure 5.27 ^{1}H NMR (500 MHz, $CDCl_3$) of compound **5.20a** and **5.20b** 286

Figure 5.28 ^{13}C NMR (125 MHz, $CDCl_3$) of compound **5.20a** and **5.20b** 286

Figure 5.29 ^{1}H NMR (500 MHz, $CDCl_3$) of compound **5.22a** 287

Figure 5.30 ^{13}C NMR (125 MHz, $CDCl_3$) of compound **5.22a** 287

Figure 5.31 ^{1}H NMR (500 MHz, $CDCl_3$) of compound **5.26** 288

Figure 5.32 ^{13}C NMR (125 MHz, $CDCl_3$) of compound **5.26** 288

Figure 5.33 ^{1}H NMR (500 MHz, $CDCl_3$) of compound **5.24** 289

Figure 5.34 ^{13}C NMR (125 MHz, $CDCl_3$) of compound **5.24** 289

Figure 5.35 ^{1}H NMR (500 MHz, $CDCl_3$) of compound **5.30** 290

Figure 5.36 ^{13}C NMR (125 MHz, $CDCl_3$) of compound **5.30** 290

Figure 5.37 ^{1}H NMR (500 MHz, $CDCl_3$) of compound **5.28** 291

Figure 5.38 ^{13}C NMR (125 MHz, $CDCl_3$) of compound **5.28** 291

Figure 5.39 ^{1}H NMR (500 MHz, $CDCl_3$) of compound **5.33** 292

Figure 5.40 ^{13}C NMR (125 MHz, $CDCl_3$) of compound **5.33** 292

Figure 5.41 ^{1}H NMR (600 MHz, $CDCl_3$) of compound **5.32** 293

Figure 5.42 ^{13}C NMR (125 MHz, $CDCl_3$) of compound **5.32** 293

Figure 5.43 ^{1}H NMR (600 MHz, $CDCl_3$) of compound **5.44** 294

Figure 5.44 ^{13}C NMR (125 MHz, $CDCl_3$) of compound **5.44** 294

Figure 5.45 ^{1}H NMR (500 MHz, DMSO-d_6) of compound **5.37** 295

Figure 5.46 ^{13}C NMR (125 MHz, DMSO-d_6) of compound **5.37** 295

Figure 5.47 NOESY (500 MHz, DMSO-d_6) of compound **5.37** 296

Figure 5.48 HSQC (600 MHz, DMSO-d_6) of compound **5.37** 297

Figure 5.49 NOESY (600 MHz, $CDCl_3$) of compound **5.19a** 298

Figure 5.50 HSQC (600 MHz, $CDCl_3$) of compound **5.19a** 299

Figure 5.51 NOESY (600 MHz, $CDCl_3$) of compound **5.21a** 300

Figure 5.52 HSQC (400 MHz, $CDCl_3$) of compound **5.21a** 301

Figure 5.53 NOESY (600 MHz, $CDCl_3$) of compound **5.25** 302

Figure 5.54 HSQC (600 MHz, $CDCl_3$) of compound **5.25** 303

Figure 5.55 HMBC (600 MHz, $CDCl_3$) of compound **5.25** 304

Figure 5.56 NOESY (600 MHz, $CDCl_3$) of compound **5.20a** and **5.20b** 305

Figure 5.57 HSQC (600 MHz, $CDCl_3$) of compound **5.20a** and **5.20b** 306

Figure 5.58 HMBC (600 MHz, $CDCl_3$) of compound **5.20a** and **5.20b** 307

Figure 5.59 NOESY (600 MHz, $CDCl_3$) of compound **5.28** 308

Figure 5.60 HSQC (600 MHz, $CDCl_3$) of compound **5.28** 309

Figure 5.61 HMBC (600 MHz, $CDCl_3$) of compound **5.28** 310

Figure 5.62 NOESY (600 MHz, $CDCl_3$) of compound **5.30** 311

Figure 5.63 NOESY (600 MHz, $CDCl_3$) of compound **5.33** 312

Figure 5.64 HSQC (600 MHz, $CDCl_3$) of compound **5.33** 313

Figure 5.65 HMBC (600 MHz, $CDCl_3$) of compound **5.33** 314

Figure 5.66 NOESY (600 MHz, $CDCl_3$) of compound **5.32** 315

Figure 5.67 HMBC (600 MHz, $CDCl_3$) of compound **5.32** 316

Figure 5.68 NOESY (600 MHz, $CDCl_3$) of compound **5.44** 317

Figure 5.69 HMBC (600 MHz, $CDCl_3$) of compound **5.44** 318

Figure 5.70 NOESY (600 MHz, $CDCl_3$) of compound **5.22a** 319

Figure 5.71 NOESY (600 MHz, $CDCl_3$) of compound **5.26** 320

LIST OF TABLES

CHAPTER ONE

Table 1.1 Optimization studies 18

CHAPTER TWO

Table 2.1 Optimization of reaction conditions 48

Table 2.2 Survey of reaction conditions and relevant control experiments 60

Table 2.3 Trace metal analysis of K_3PO_4 61

Table 2.4 Trace metal analysis of 1,4-dioxane 62

Table 2.5 Trace metal analysis of alcohol reductant **2.5** 63

Table 2.6 Conditions and results of chiral SFC analysis of alcohol reductant **2.5** 74

Table 2.7 Conditions and results of chiral HPLC analysis of alcohol products 76

CHAPTER THREE

Table 3.1 Relevant control experiments 120

Table 3.2 Evaluation of functional group compatibility in the Suzuki–Miyaura coupling and transfer hydrogenation cascade 143

Table 3.3 Conditions and results of chiral SFC analysis of alcohol products 147

LIST OF ABBREVIATIONS

α	alpha
β	beta
γ	gamma

λ	wavelength
μ	micro
π	pi
δ	chemical shift
Δ	heat
(Het)	hetero
[H]	reduction
[O]	oxidation
$[\alpha]_D$	specific rotation at wavelength of sodium D line
°C	degrees Celsius
Å	angstrom
AcOH	acetic acid
$AlCl_3$	aluminum trichloride
Alk	alkyl
APCI	atmospheric-pressure chemical ionization
app.	apparent
aq.	aqueous
Ar	aryl
Au	gold
B(pin)	pinacol borane
Benz-ICy•HCl	1,3-dicyclohexylbenzimidazolium chloride
BF_3•Et_2O	boron trifluoride diethyl etherate
Bn	benzyl
$BnNH_2$	benzylamine
Boc	*tert*-butoxycarbonyl
Boc_2O	di-*tert*-butyl dicarbonate
Bu	butyl
Bz	benzoyl
c	centi
c	concentration for specific rotation measurements
C	carbon
C_6D_6	deuterated benzene
C_6H_6	benzene
CaH_2	calcium hydride
cal	calorie

calcd	calculated
cat.	catalytic or catalyst
CD_3CN	deuterated acetonitrile
$CDCl_3$	deuterated chloroform
CF_3	trifluoromethyl
CH_2Cl_2	dichloromethane
CH_3	methyl
CH_3CN	acetonitrile
$CHCl_3$	chloroform
CO_2	carbon dioxide
cod	1,5-cyclooctadiene
d	doublet
DART	direct analysis in real time
DMAP	4-dimethylaminopyridine
DMF	*N*,*N*-dimethylformamide
DMSO-d_6	deuterated dimethyl sulfoxide
DMSO	dimethyl sulfoxide
EDC	1-ethyl-3-(3-dimethylaminopropyl)carbodiimide
EDC•HCl	1-ethyl-3-(3-dimethylaminopropyl)carbodiimide hydrochloride
eds.	editors
EDTA	ethylenediaminetetraacetic acid
ee	enantiomeric excess
equiv	equivalent
ESI	electrospray ionization
Et	ethyl
Et_2O	diethyl ether
Et_3N	triethylamine
EtOAc	ethyl acetate
FAQ	frequently asked questions
FT	Fourier transform
g	gram(s)
GC-MS	gas chromatography mass spectrometry(er)
h	hour(s)
H	proton

$h\nu$	light
HCl	hydrochloric acid
HMB	hexamethylbenzene
HOBt	hydroxybenzatriazole
HPLC	high-performance liquid chromatography
HRMS	high resolution mass spectroscopy
Hz	hertz
i-Bu	isobutyl
i-Pr	*iso*-propyl
i-$PrNH_2$	*iso*-propyl amine
i-PrOAc	*iso*-propyl acetate
i-PrOH	*iso*-propyl alcohol
I_2	iodine
ICy•HCl	1,3-dicyclohexylimidazolium chloride
IPr	1,3-Bis(2,6-diisopropylphenyl)-imidazol-2-ylidene
IR	infrared (spectroscopy)
J	coupling constant
KHMDS	potassium bis(trimethylsilyl)amide
K_3PO_4	potassium phosphate tribasic
KO*t*-Bu	potassium *tert*-butoxide
KRED	ketoreductase
L	liter
LDA	lithium diisopropylamide
$LiAlH_4$	lithium aluminum hydride
LiCl	lithium chloride
LiHMDS	lithium bis(trimethylsilyl)amide
m	multiplet or milli or meter
M	molecular mass, molar, or metal
m-	meta
m/z	mass to charge ratio
Me	methyl
$MgSO_4$	magnesium sulfate
MHz	megahertz
min	minute(s)
Mo	molybdenum

mol	mole(s)
mp	melting point
MS	molecular sieves
N	normal
n-Bu	butyl (linear)
n-BuLi	butyl (linear) lithium
N_2	nitrogen gas
Na^0	sodium metal
NaHMDS	sodium bis(trimethylsilyl)amide
$Na_2S_2O_3$	sodium thiosulfate
Na_2SO_4	sodium sulfate
NADP	nicotinamide adenine dinucleotide phosphate
NaH	sodium hydride
$NaHCO_3$	sodium bicarbonate
NaOH	sodium hydroxide
NaO*t*-Bu	sodium *tert*-butoxide
NH_4Cl	ammonium chloride
NHC	*N*-heterocyclic carbene
Ni	nickel
nM	nanomolar
NMR	nuclear magnetic resonance
NOESY	nuclear overhauser effect spectroscopy
o-	ortho
OMe	methoxy
p-	para
Pd	palladium
PDB	protein data bank
Ph	phenyl
$PhCOCF_3$	2,2,2-trifluoroacetophenone
PhH	benzene
PhMe	toluene
Piv	pivaloyl
PPh_3	triphenylphosphine
ppm	parts per million
Pr	Propyl

Pt	platinum
PTFE	polytetrafluoroethylene
q	quartet
quint.	quintet
rac	racemic
R_f	retention factor
rpm/RPM	revolutions per minute
Ru	ruthenium
s	singlet or second
sat.	saturated
sext.	sextet
SFC	supercritical fluid chromatography
SiPr	1,3-Bis(2,6-diisopropylphenyl)-1,3-dihydro-2*H*-imidazol-2-ylidene
SiPr•HCl	1,3-Bis(2,6-diisopropylphenyl)-1,3-dihydro-2*H*-imidazol-2-ylidene hydrochloride
SmI_2	samarium diiodide
t	triplet
t-Bu	*tert*-butyl
t-$BuNH_2$	*tert*-butyl amine
t-BuOH	*tert*-butyl alcohol
TA	teaching assistant
TBDPS	*tert*-butyldiphenylsilyl
TBDPSCl	*tert*-butyldiphenylchlorosilane
TCI	Tokyo Chemical Industry Co.
temp	temperature
THF	tetrahydrofuran
Ti	titanium
TLC	thin layer chromatography
TMB	1,3,5-trimethoxybenzene
TESCl	chlorotriethylsilane
TMSCl	chlorotrimethylsilane
t_R	retention time
Trit	trityl
Ts	tosyl

UHP	ultra-high purity
UV	ultraviolet
WT	wild-type
$ZnEt_2$	diethyl zinc
Zr	zirconium

ACKNOWLEDGEMENTS

When I was a first year graduate student, I had asked the fifth year I worked next to, right before he graduated, what he would remember the most about his experience. Without hesitation, he mentioned that the people he overlapped with were the most memorable part. That response stuck with me for the five years I've been at UCLA and here, in these few pages, I will try to do justice to all of the people who have supported me through my PhD.

First and foremost, I'd like to thank my advisor, Prof. Neil Garg. Neil and I have developed a remarkably honest rapport during my graduate school experience and I would not have it any other way. Neil consistently created space for me to be able to share how I felt and constantly encouraged me to push my boundaries to become the best chemist and professional I could be. I feel incredibly honored to have learned from him and feel incredibly lucky to have an advisor who was always looking out for my best interests academically, professionally, and personally. Thank you, Neil, for the endless support and encouragement you have provided through the hard times and sticking firmly to the 'work hard, play hard' mentality by ensuring the celebration of personal and group successes.

I would like to thank the members of my committee, Professors Ken Houk, Yi Tang, Hosea Nelson, and Abigail Doyle. I have appreciated all of your advice and guidance you have provided me during my time at UCLA.

The major driving force for my decision to pursue graduate school was inspired by Dr. Chris Callam's sophomore organic chemistry class that I took in 2014 at The Ohio State University. Thank you Dr. Callam for teaching the fundamental concepts of this subject so wonderfully and introducing me to Dr. T. V. RajanBabu, who was my undergraduate research advisor for two years. Through my time in the Babu group, I was able to develop my technical

skills in the lab and capitalized on the opportunities provided to travel for research. Thank you, Dr. Babu, for encouraging me to stay committed to research as an undergraduate student and supporting me through all my travel adventures presenting the group's research. I will always be grateful for the time I spent in your group.

The graduate students and postdocs that I overlapped with over my five years at UCLA have been some of the most impactful humans in my life. There are countless memories shared with everyone both in and out of the lab/office space that have made graduate school an enjoyable experience.

When I first joined the lab, the fifth years at the time, Drs. Lucas Morrill, Bryan Simmons, and Joyann Donaldson, were incredibly helpful. Lucas was in 5235 with me and always answered my curiosity questions with the utmost enthusiasm. I will always cherish 'Apple Fritter Fridays' instilled by Lucas that the rest of 5235 enjoyed for his last few months in lab. Bryan and I had an interesting friendship filled with lots of joking and poking fun at each other. But when I really needed him to support me, Bryan was always there to provide words of encouragement and his fifth year wisdom always helped me keep appropriate perspective on any challenges I was facing. Hey Bryan, you up?? Joyann was undoubtedly one of the most positive students in the lab. I sincerely appreciated her optimism and her willingness to help me any time I had any questions.

The next class of graduate students, self-proclaimed as 'The Fellas', consisted of Drs. Jacob Dander, Michael Yamano, Jordan Dotson, and Rob Susick. Jacob quickly became a close mentor and friend to me as we are cut from the same cloth. I had the privilege of not only being his mentee, but also his apartment-mate for a few months in 2020. Those three months were filled with movies, laughter, and of course, the start of the infamous Cake-Thirty. I would be remiss to not mention an honorary member of this class, Ryan Kauffmann, who is Jacob's husband but, more

importantly, my twin flame. I am ever so grateful that grad school introduced me to Jacob and Ryan and that I can call them close friends to this day. Michael has the sharpest wit I have ever encountered in a person. His good-natured pranks, hilarious magician videos, and quick retorts always kept the lab festive. I am very much looking forward to working with Michael at Amgen this year and watching our friendship flourish over all the future skiing trips I am *sure* we will go on. Jordan Dotson is undoubtedly one of the most brilliant chemists I have ever met. He was so incredibly helpful during my candidacy exam and ever-so-patiently explained concepts to me over Zoom. Although, my favorite memory with Jordan will always be the midterm exam he wrote up for our Synth 2 class.

Drs. Tim Boit, Sarah Anthony, and Melissa Ramirez were third years when I joined the lab. Over the years that we overlapped, Melissa possessed an unfailingly positive attitude and a tireless work ethic, all while being available to support the younger students as often as she could. Melissa is a continued inspiration for women of color in STEM and I am excited to see her career grow as a research advisor. Sarah and Tim were both in 5235 with me for my first two years of grad school, so I got to know the both of them incredibly well. Sarah was my go-to person for scream-singing songs in lab, beach days, wine nights, and long chats about being women in STEM. I could always count on her to bring the energy of the room up every time she arrived in the morning with a cheerful 'good morning!' or wrapping up a long day at work with some good ol' Taylor Swift or Jordin Sparks or any other female pop ballad songs. Tim started off as my mentor when I joined the group and my project partner for three(!!!) projects and eventually became a dear friend. Tim's chemical prowess was initially quite intimidating but I quickly realized how fortunate I was to have such a diligent and helpful mentor support me through my first few years of grad school. I could wax poetic about how deeply I admire Tim and how grateful I am to have

been his mentee, but I'll keep it succinct and say that I feel extremely fortunate to know Tim Boit and I am excited to stay absolute best friends with him forever.

The class above me consisted of Drs. Rachel Knapp, Francesca Ippoliti, and Jason Chari. Affectionally nicknamed our Woke King, Jason infused 29 with a unique positive energy. His love for Rihanna and most female pop vocalists (except for Adele… still unclear why), willingness to have a dance party at any point in the day, and unbelievable athletic ability make Jason one of the most pleasant people to be around. At work, Francesca was my total synthesis queen and I felt very comfortable asking her questions about anything and everything chemistry, Garg Lab, or life-related. Outside of work, Francesca was truly the life of the party (the Francesca to Jessica to Rebecca arc is one of my favorite transformations). Fran is one of those rare people who possesses a truly beautiful spirit - I am excited to see her inspire the next generation of chemists as a professor! Rachel quickly became one of my dearest friends in the program. From our daily unpacking sessions, to the unwavering support she provided during especially difficult professional, and personal moments to just being an all-around incredible person, Rachel helped me discover my confidence by being an excellent role model and a friend who accepted all of my emotions and anxiety-ridden ramblings without any judgment. I am forever grateful for your friendship Rachel!

The postdocs in the lab have been wonderful chemists to learn from. Drs. Evan Darzi and Maude Giroud were the postdocs in the group when I first joined the lab. Both Evan and Maude were incredibly friendly and never hesitated to answer any questions I had. The next class of postdocs included Drs. Logan Bachman and Veronica Tona. Logan and I shared the battlefield of getting a total synthesis project off the ground together. Not only was Logan a gifted chemist, he was also one of the kindest people I've worked with. Thank you for helping me rediscover my

love of organic chemistry, for so patiently teaching me the ways of the 'total synthesis mindset' and for introducing me to yee-haw chemistry and terrifyingly aggressive music. Let me know if you ever need a ride to the airport Logie, I got you. Veronica's bold personality matched mine very well and we became fast friends during the lab's shift schedule. Some of my favorite memories with Vero include several pasta nights, my 24th birthday prom night, and the assuredness with which she lived her life.

Drs. Daniel Nasrallah and Nathan Adamson joined the group during my fourth year. Nathan was one of my favorite people to ask chemistry advice from, especially since he had performed every reaction underneath the sun. Dan is one of the most thoughtful people – he not only cares about cool experiments I was running but also made sure to inquire about my life generally to check in and make sure things were going all right. While I am constantly disapproving of Dan's sneaky exits from lab events, I'll greatly miss his optimistic attitude and Festive Friday shirts. Drs. Jacob Sorrentino and Lukas Wein are the newest postdocs in the group. I've really enjoyed learning from Jacob about the med chem ways through working on a collaboration project together this past year. Lukas' deadpan delivery of one-line zingers will always be one of the most entertaining dynamics of 29 – I'm happy I got to work in the same room as him for this past year!

Katie Ann Spence and Andrew Vincent Kelleghan have been my day ones, my ride or dies. As Milandie, the three of us could not have more different personalities that somehow figured out how to become close friends. I would not have wanted to go through first year classes, second year milestones, candidacy, job interviews, conferences, and many more shared experiences with anyone other than these two people. Without a doubt, Andrew is a tremendously gifted chemist and one of the kindest, humblest, and sweetest people. I'll miss stopping by your hood to chat your

ear off about random nonsense, but don't worry Drewseph, I'll call all the time even if you never call me. Katie's chaotic energy is unmatched. She is one of the absolute most fun people to be around and I am forever admiring Katie's ability to brush things off and maintain a positive, 'let's move forward' attitude. From going to Vegas as first years, red-eye flights and sleeping in airports at 5am, late-night dance parties in lab, to road trips to San Diego, and so many other memories over these past five years to graduating together in a couple weeks, I am so glad to have had Katie by my side as the ultimate hype woman. Thank you, Katie and Andrew, for being there for me whenever I needed to laugh, cry, or vent. I am so proud to call these two goofballs my friends, and I am confident that both of you will absolutely thrive at Gilead next year.

The class a year younger than me consisted of Ana Bulger, Matthew McVeigh, and Laura Wonilowicz. Laura has been a wonderful project partner for the pyrone project and I was so happy to be able to share my love of reading and Taylor Swift with her! I really enjoyed our singing sessions in 5235 during my second year. Laura is such an empathetic person and will continue to be a phenomenal resource to the younger students during her fifth year. Matt is naturally one of the funniest people I have met, which makes him not only a wonderful coworker but also a great roommate from when we lived together for two years. Matt truly was one of my favorite roommates, especially in comparison to some of the more interesting characters we used to live with. I'll always cherish our memories at Los Leones with sweet Sisi and I'm so excited to see you crush the job interview process! Being placed in a room next to Ana was one of the absolute best things to happen to me in graduate school. Words in this section will never do justice to the depth of love, respect, and admiration I have for her. I am going to sorely miss hanging out with my best friend every day in MolSci 5229 and sharing every single thought that crosses my mind with her in real time. I am so thankful to be only a 40 minute drive away so we can continue our movie

nights, long emotional walks, chocolate time, dinners at trendy restaurants, and whatever else we want to get up to. I love you, Egg, and I am so thankful to have you in my life (and to be on the wall in your home!).

The current third years, Dominick Witkowski, Luca McDermott Catena, and Arismel Tena Meza, are quite a formidable class. It's been an absolute pleasure being in the same room as Luca and bonding over his family wines, psychedelic trance/jazz music, and being in the same subgroup for almost two years straight. Luca's unwavering passion for chemistry is truly admirable, and I am so excited to see the finished story of Dodeca hopefully soon! I've really enjoyed being on the OCDS board with Ari and having someone to relate to about being women of color in STEM over free wine. While Ari may be 'not concerned' about some things, her diligent work ethic and positive attitude is commendable. Dominick is my coffee run/mid-morning walk buddy, social event coordinator protégée, and fellow glovebox caretaker. I'm so happy we were put on so many group jobs together as it brought us closer as friends which led to some really fun memories by the Los Leones pool and the beach!

Jordan Gonzalez and Georgia Scherer are the current second year class. Georgia is an amazing person, and I am glad I had the opportunity to get to know her better when we worked on a medicinal chemistry project together. Outside of chemistry, we've bonded over books, running (mainly me being in awe of her ability to run for a full twenty-six miles), and our love for cats! I am excited to see Georgia grow as a chemist over these next few years, and I promise that if I'm invited, I'll come back for your graduation. I had the distinct privilege of mentoring Jordan for his first year of grad school and being his project partner for Kermit. Jordan has grown into an incredibly competent chemist who is currently tackling a very difficult problem with a relentlessly positive attitude. Some of my favorite memories with Jordan include him leaving notes everywhere

in 5229, bringing in lab pickles, playing lofi beats at all hours of the day, reluctantly accepting me shouting 'Jordan!!!!' every time he walks into a room, and being a consistent pillar of support for me. I am so happy he dovetailed both mine and Nathan's wisdom as his mentors and am so proud of his growth over these two years.

Finally, the newest members of the group are Zach Walter, Dani Turner, and Allison Hands. I can always rely on Dani to brighten up our room with his wonderfully colorful outfits and matching earrings. Zach's ceaseless positive attitude is a phenomenal addition to Team Dodeca and I have really enjoyed working in the hood right next to his for my last year! Allison is incredibly sweet, and I am happy we got to share fun memories at St. Felix and with Taylor Tomlinson.

Quite honestly, I would be nowhere without the support of my family and friends. To my best friends, Dr. Nishma Jain and Sukanya Maulik, thank you for always reminding me of my roots and cheering me on. Both of you have been so crucial for all my life milestones and I am so happy to be able to share this one with you two in person! To my cousin sister, Diksha Mehta, thank you for the hours and hours of phone calls over these years where you've so patiently listened to everything I've had to say and provided emotional support (for the last 26 years). To my younger brother, Maunil, thanks for always being level-headed and reminding me that most things aren't as big of a deal as I think they are.

To Saketh Undurty – I am so happy we found each other. The unwavering faith you provided during the job interview process kept me sane and helped manage a lot of my anxiety of the unknown. Thank you for the immense amount of joy you have brought into my life this past year and some change. I am so excited for our future together!

Finally, to my parents, Manisha and Mehul Mehta – thank you for everything. I am so appreciative of my mom for always being my emotional sounding board and of my dad for always being willing to take care of any real-life things so I wouldn't have to worry about it. Thank you for letting me go to school so far away from home and believing that I will be able to handle it, thank you for being willing to hop on a flight to come stay with me in LA whenever I hinted at being homesick, thank you for putting up with the emotional roller coaster these last five years have been, thank you for loving me so much and giving me all the freedom in the world to pursue whatever I wanted to.

Chapter 1 is a version of Mehta, M. M.;† Boit, T. B.;† Dander, J. E.;† Garg, N. K. *Org. Lett.* **2020**, *22*, 1–5. Mehta, Boit, and Dander were responsible for experimental work.

Chapter 2 is a version of Boit, T. B.; Mehta, M. M.; Garg, N. K. *Org, Lett.* **2019**, *1*, 6447–6451. Boit and Mehta were responsible for experimental work.

Chapter 3 is a version of Mehta, M. M.;† Boit, T. B.;† Kim, J.; Baker, E. L.; Garg, N. K. *Angew. Chem., Int. Ed.* **2021**, *60*, 2472–2477. Mehta, Boit, Kim, and Baker were responsible for experimental work.

Chapter 4 is a version of Mehta, M. M.; Gonzalez, J. A. M.; Bachman, J. L.; Garg, N. K. *Manuscript submitted*. Mehta, Gonzalez, and Bachman were responsible for experimental work.

Chapter 5 is a version of Mehta, M. M.;† Wonilowicz, L. G.;† Garg, N. K. *Manuscript in preparation*. Mehta and Wonilowicz were responsible for experimental work.

BIOGRAPHICAL SKETCH

Education:

University of California, Los Angeles, CA

- Ph.D., Organic Chemistry, anticipated Spring 2023.
- 2020–2023 NSF GRFP Fellow.
- Current GPA: 3.8/4.0.

The Ohio State University, Columbus, OH

- B.A. in Chemistry, minor in Molecular Genetics (May 2018).
- Cumulative GPA: 3.5/4.0.
- Humanities Scholar (2014 – 2016).

Professional and Academic Experience:

Graduate Research Assistant: University of California, Los Angeles, CA.

- August 2018 – present; Advisor: Prof. Neil K. Garg.
  - Investigated strain-promoted Diels–Alder cycloadditions of heterocyclic allenes and pyrones to determine the parameters that influence regioselectivity of the reaction.
  - Designed and tested Diels–Alder substrates to construct the azadecalin core of (–)-Keramaphidin B using strained cyclic allene chemistry.
  - Currently evaluating an intramolecular iminium Diels–Alder cycloaddition approach to build the isoquinuclidine core of (–)-keramaphidin B, en route to completion of the total synthesis.
  - Developed a one-pot reductive arylation of amides to form chiral secondary alcohols via a Suzuki–Miyaura coupling and transfer-hydrogenation cascade.
  - Expanded the scope of boronic ester coupling partners for benchtop delivery of nickel-catalyzed Suzuki-Miyaura cross-coupling of aliphatic amides using paraffin wax capsules.
  - Developed a base-mediated MPV-type reduction of heterocycles bearing ketones to give secondary alcohols.

Graduate Teaching Assistant: University of California, Los Angeles, CA.

- Undergraduate organic chemistry laboratory for physical science majors (Fall 2018, Winter 2019, Spring 2019, Fall 2020).
  - Instructed undergraduate students, both in person and virtually, in developing basic laboratory skills through various experiments including epoxidations, biocatalytic reductions, and polymerizations.

Summer Course Instructor: University of California, Los Angeles, CA

- Chem 101: Catalysis in Modern Drug Discovery (Summer 2021, Summer 2022)
  - Taught an upper-level elective course at UCLA focused on transition-metal catalysis in the drug development process. Additionally, the course featured a guest lecture series where guests included Dr. Margaret Chu-Moyer (Amgen), Dr. Rebecca Ruck (Merck & Co.), and Professor Michael E. Jung (UCLA).

Undergraduate Research Assistant: The Ohio State University, Columbus, OH.

- May 2016 – May 2018; Advisor: Prof. Thaliyil V. RajanBabu.
  - Optimized reaction conditions for cobalt-catalyzed asymmetric hydroboration of 1,3-(*E*)-dienes and 1,4-heterodimerization of 1,3-(*E*)-dienes with methyl acrylates.
- Merck & Co., Rahway, NJ; May 2018 – August 2018; Supervisors: Dr. Niki Patel and Dr. Heather Johnson.
  - Optimized reaction conditions for zinc/BINOL-catalyzed asymmetric alkylation of ketones using alkyl Grignard reagents.
- Karlsruhe Institute of Technology, Karlsruhe, Germany; May 2017 – August 2017; Supervisor: Prof. Stefan Bräse.

- Synthesized 1,5-cyclooctadienyl (COD) alcohol and ketone derivatives to generate a new class of COD-platinum complexes.

Honors & Awards

- 2022 Ralph & Charlene Bauer Award – University of California, Los Angeles
- 2022 Royal Society of Chemistry Horizon Prize in Education.
- 2021 Trueblood Tutor Fellowship – University of California, Los Angeles.
- 2020–2023 NSF Graduate Research Fellowship.
- 2020 Michael E. Jung Excellence in Teaching Award – University of California, Los Angeles, CA.
- 2019 Irving & Jean Stone Fellowship Award – University of California, Los Angeles, CA.
- 2018 Bertram Thomas Memorial Fund – The Ohio State University, Columbus, OH.
- 2017 DAAD RISE Scholarship – Karlsruhe Institute of Technology, Karlsruhe, Germany.
- 2016–2018 Dean's List – The Ohio State University, Columbus, OH.

Publications

Graduate

1. Mehta, M. M.;[†]* Wonilowicz, L. G.;[†] Garg, N. K. "Strain-promoted Diels–Alder Cycloadditions of Heterocyclic Allenes and α-Pyrones." *Manuscript in Preparation.*

2. Mehta, M. M.;* Gonzalez, J. A. M.; Bachman, J. L.; Garg, N. K. "Cyclic Allene Approach to the Manzamine Alkaloid Keramaphidin B." *Manuscript Submitted.*

3. Spence, K. A.; Mehta, M. M.;* Garg, N. K. "Synthesis of Triphenylene via the Palladium-Catalyzed Annulation of Benzyne." *Org. Synth.* **2022**, *99*, 174–189.

4. Mehta, M. M.;* Kelleghan, A. V.; Garg, N. K. "Palladium-Catalyzed Acetylation of Arylbromides." *Org. Synth.* **2021**, *98*, 68–83.

5. Mehta, M. M.;[†]* Boit, T. B.;[†] Kim, J.; Baker, E. L.; Garg, N. K. "Reductive Arylation of Amides via a Nickel-Catalyzed Suzuki–Miyaura Coupling and Transfer Hydrogenation Cascade." *Angew. Chem., Int. Ed.* **2021**, *60*, 2472–2477.

6. Mehta, M. M.;[†]* Boit, T. B.;[†] Dander, J. E.;[†] Garg, N. K. "Ni-Catalyzed Suzuki–Miyaura Cross-Coupling of Aliphatic Amides on the Benchtop." *Org. Lett.* **2020**, *22*, 1–5.

7. Anthony, S. M.; Kelleghan, A. V.; Mehta, M. M.;* Garg, N. K. "From Heavy Water to Heavy Aldehydes." *Nature Catal.* **2019**, *2*, 1058–1059.

8. Boit, T. B.; Mehta, M. M.;* Garg, N. K. "Base-Mediated Meerwein–Ponndorf–Verley Reduction of Aromatic and Heteroaromatic Ketones." *Org. Lett.* **2019**, *21*, 6447–6451.

Undergraduate

1. Duvvuri, K.;[†] Dewese, K. R.;[†] Parsutkar, M. M.;[†] Jing, S. J.; Mehta, M. M.;* Gallucci, J. C.; RajanBabu, T.V. "Cationic Co(I)-Intermediates for Hydrofunctionalization Reactions: Regio- and Enantioselective Cobalt-Catalyzed 1,2- Hydroboration of 1,3-Dienes." *J. Am. Chem. Soc.* **2019**, *141*, 7365–7375.

[†]Authors Contributed Equally.

CHAPTER ONE

Ni-Catalyzed Suzuki–Miyaura Cross-Coupling of Aliphatic Amides on the Benchtop

Milauni M. Mehta,[†] Timothy B. Boit,[†] Jacob E. Dander,[†] and Neil K. Garg.

Org. Lett. **2020**, *22*, 1–5.

1.1 Abstract

Suzuki–Miyaura cross-couplings of amides offer an approach to the synthesis of ketones that avoids the use of basic or pyrophoric nucleophiles. However, these reactions require glovebox manipulations, thus limiting their practicality. We report a benchtop protocol for Suzuki–Miyaura cross-couplings of aliphatic amides that utilizes a paraffin capsule containing a Ni(0) pre-catalyst and NHC ligand. This methodology is broad in scope, scalable, and provides a user-friendly approach to convert aliphatic amides to alkyl–aryl ketones.

1.2 Introduction

The conversion of carboxylic acid derivatives to ketones is a fundamental transformation in synthetic chemistry (Figure 1.1).[1] A common strategy to achieve this conversion is the Weinreb ketone synthesis, in which a *N*-methoxy-*N*-methyl amide undergoes net substitution with an organometallic nucleophile.[2] An alternative strategy lies in the development of transition metal-catalyzed cross-couplings of acyl electrophiles,[1c,3] which avoid the use of strongly basic and pyrophoric organometallic reagents. Our laboratory and others have shown that amides, which are well suited for multi-step synthesis due to their pronounced stability, are particularly useful in this

context.[4] Specifically, Ni-[5,6] and Pd-catalysis[7] have enabled the mild activation of the amide C–N bond for cross-coupling with boronic acids and esters,[8] as well as organozinc reagents.[9]

We recently reported a Ni-catalyzed Suzuki–Miyaura coupling of aliphatic amides to generate alkyl–aryl ketones (Figure 1.1, e.g. **1.1** + **1.2** → **1.3**).[10,11] This methodology is broad in scope, but requires the use of a glovebox, thus limiting its practical utility.[12] We questioned if a paraffin encapsulation strategy, analogous to that pioneered by Buchwald, could prove useful.[13] In this approach, air-sensitive reagents are stored in paraffin capsules, ultimately providing a user-friendly means to perform air-sensitive transition metal-catalyzed reactions. Previously, we showed the promise of this strategy for the Suzuki–Miyaura cross-coupling of a single benzamide-derived substrate utilizing paraffin–Ni(cod)$_2$/SIPr capsules.[14] However, this pre-catalyst and ligand combination is ineffective in the coupling of amides derived from aliphatic carboxylic acids.[10] Moreover, only a single example of a glovebox-free arylation of an aliphatic amide derivative has been reported, which uses a bench-stable Pd(II) pre-catalyst.[15] We report the realization of a paraffin encapsulation strategy to achieve the nickel-catalyzed Suzuki–Miyaura coupling of aliphatic amides on the benchtop.

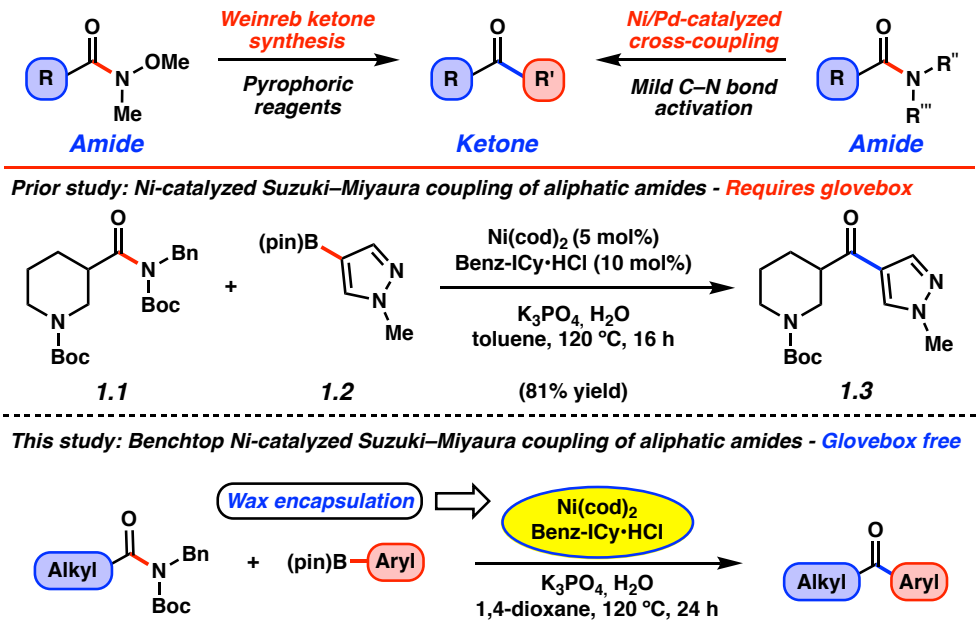

Figure 1.1. Methods for the conversion of amides to ketones, prior studies of Ni-catalyzed Suzuki–Miyaura couplings that utilize a glovebox, and paraffin encapsulation strategy for benchtop delivery (present study).

1.3 Reaction Discovery and Optimization

Our studies were initiated by preparing the desired paraffin capsules, using a molding process analogous to one we had previously reported (Figure 1.2).[14] These capsules were charged with Ni(cod)$_2$ and Benz-ICy•HCl, as this pre-catalyst/ligand combination had proven effective in our original studies on the Suzuki–Miyaura coupling of aliphatic amides using a glovebox.[10] Next, we assessed the utility of these capsules in the benchtop Suzuki–Miyaura coupling of amide **1.4** with *N*-methylpyrrole-2-boronic acid pinacol ester (**1.5**), using 5 mol% Ni. Unfortunately, the use of our literature conditions resulted in poor yield of ketone **1.6**.[16] Specifically, the coupling of **1.4** and **1.5** employing paraffin-encapsulated Ni(cod)$_2$/Benz-ICy•HCl, 2.5 equiv of **1.5**, toluene as the reaction solvent, and a stir rate of 400 RPM for 16 h at 120 °C provided ketone **1.6** in 28% ^{1}H NMR yield.[17] After extensive experimentation, it was found that employing higher equivalents of **1.5** (2.5 to 5.0), utilizing 1,4-dioxane as the reaction solvent, and extending the reaction time to 24

hours proved beneficial. This provided ketone **1.6** in 91% yield on the benchtop. Additionally, these capsules displayed long-term air and moisture stability when stored outside of a glovebox. After two months of storage, a benchtop coupling of **1.4** and **1.5** generated **1.6** in comparable yield.[16] These capsules are currently undergoing commercialization to enable their widespread use.[18]

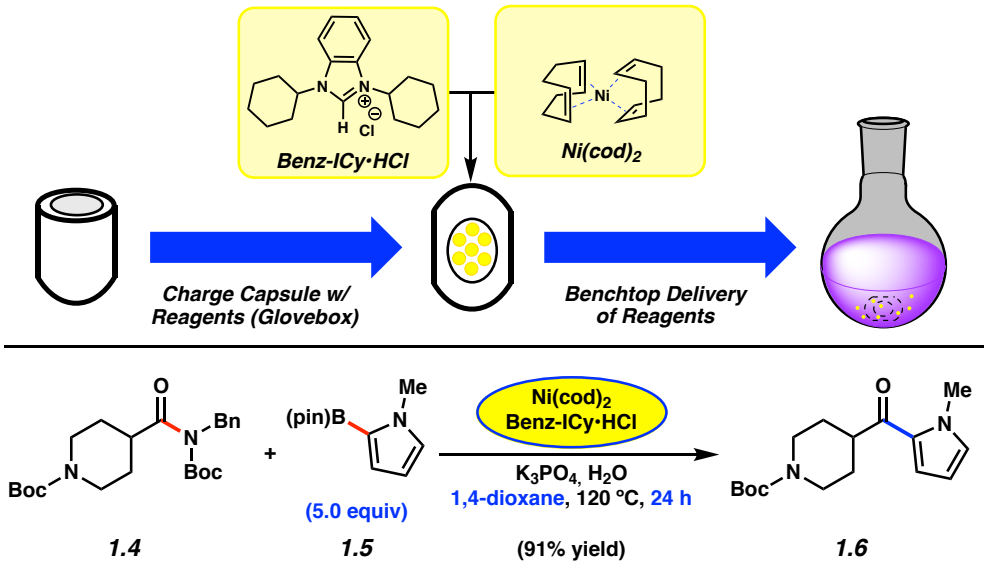

Figure 1.2. Preparation of Ni(cod)$_2$/Benz-ICy•HCl–paraffin capsules and their use in the benchtop Suzuki–Miyaura coupling of piperidinyl amide **1.4** and pyrrole boronic ester **1.5** under optimized conditions. Yield was determined by ^{1}H NMR analysis using 1,3,5-trimethoxybenzene as an external standard.

1.4 Scope of the Boronic Ester Coupling Partner

Having validated our encapsulation approach and arrived at optimized reaction conditions, we evaluated the scope of this transformation with respect to the boronate ester coupling partner. A variety of aryl boronate esters were assessed in couplings with piperidinylamide **1.4** (Figure 1.3). The methodology was found to be tolerant of medicinally privileged *N*-heterocyclic aryl boronates[19] as evidenced by the formation of ketones **1.6**–**1.8**, in good to excellent yields. Additionally, electron-poor *p*-CF_3 and sterically encumbered *o*-CH_3 substituted phenyl boronate

esters could be employed in the coupling, providing ketones **1.9** and **1.10** in 53% and 74% yields, respectively. Boronate esters featuring extended aromatic ring systems were also competent nucleophiles in the methodology, as demonstrated by the formation of naphthyl ketone **1.11** in 71% yield. Of note, in all cases, benchtop yields of the desired ketone products were comparable to those obtained when using literature conditions requiring a glovebox (yields using the glovebox protocol are shown in parentheses in Figures 1.3 and 1.4).[10]

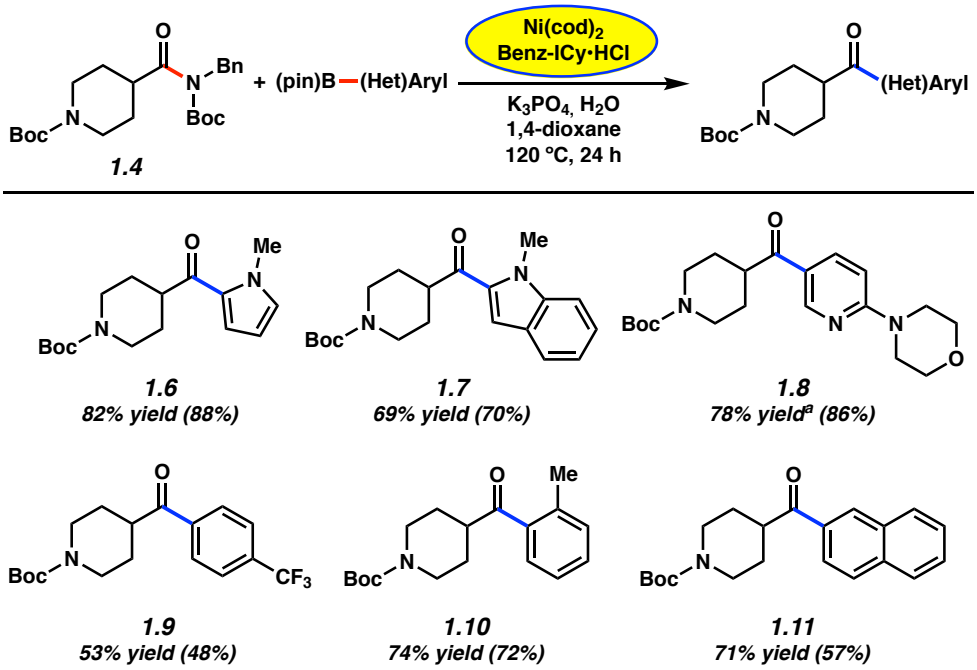

Figure 1.3. Scope of the boronic ester coupling partner. Unless otherwise noted, yields reflect the average of two isolation experiments. Yields in parentheses were obtained by carrying out the reaction in a glovebox utilizing literature conditions without encapsulating $Ni(cod)_2$ and Benz-ICy•HCl in paraffin. [a]Yield was determined by ^1H NMR analysis using 1,3,5-trimethoxybenzene as an external standard.

1.5 Scope of the Amide Substrate

We next surveyed a range of amide substrates in the Suzuki–Miyaura coupling with pyrroloboronate **1.5** (Figure 1.4).[20] An additional piperidine-derived amide substrate could be used in the coupling to furnish **1.12** in excellent yield. Furthermore, amides derived from isomeric 3-

and 4-tetrahydropyrancarboxylic acids were competent substrates, giving rise to ketones **1.13** and **1.14** in 79% and 84% yield, respectively. We also evaluated the coupling of non-heterocyclic amides. Linear and carbocyclic amides underwent the reaction smoothly, as demonstrated by the formation of **1.15** and **1.16** in 83% yield and 89% yield, respectively. Notably, steric bulk adjacent to the amide carbonyl did not hinder the Suzuki–Miyaura coupling as the use of a pivalamide substrate gave ketone **1.17** in 90% yield.

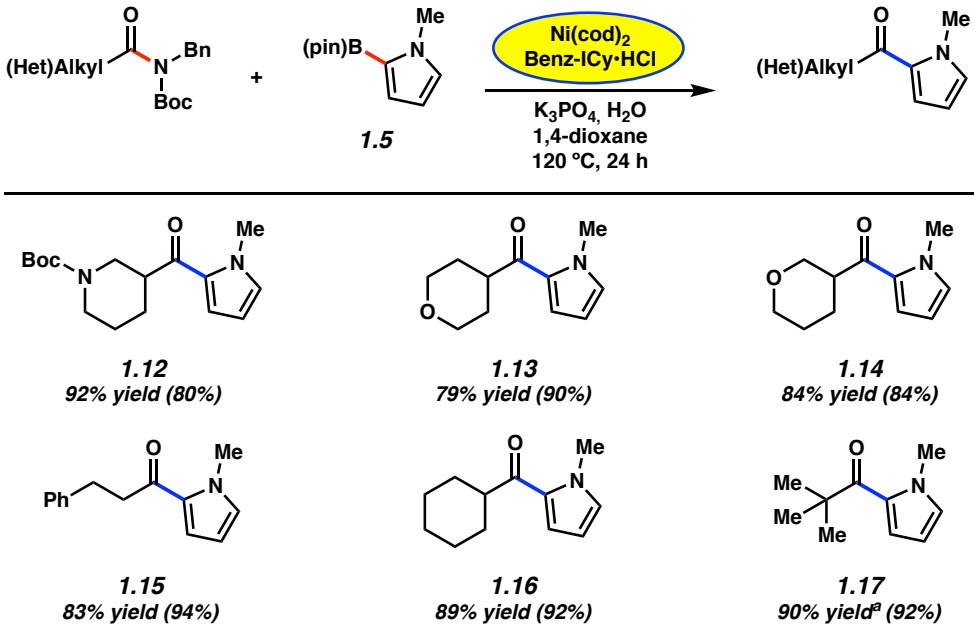

Figure 1.4. Scope of the amide substrate. Unless otherwise noted, yields reflect the average of two isolation experiments. Yields in parentheses were obtained by carrying out the reaction in a glovebox utilizing literature conditions without encapsulating $Ni(cod)_2$ and Benz-ICy•HCl in paraffin. [a]Yield was determined by ^1H NMR analysis using 1,3,5-trimethoxybenzene as an external standard.

1.6 Demonstration of Coupling on Gram-Scale

Finally, we assessed the Suzuki–Miyaura coupling of piperidine amide **1.1** with *N*-methylindole-2-boronic ester **1.18** on gram-scale as shown in Figure 1.5. Using 5 mol% Ni, the coupling proceeded smoothly to deliver ketone **1.19** in 73% yield. We view this result as promising

in the context of the scalable construction of biologically-relevant bis-heterocyclic ketones[19] where the enolizable alkyl–aryl ketone provides a valuable synthetic handle for further manipulation.

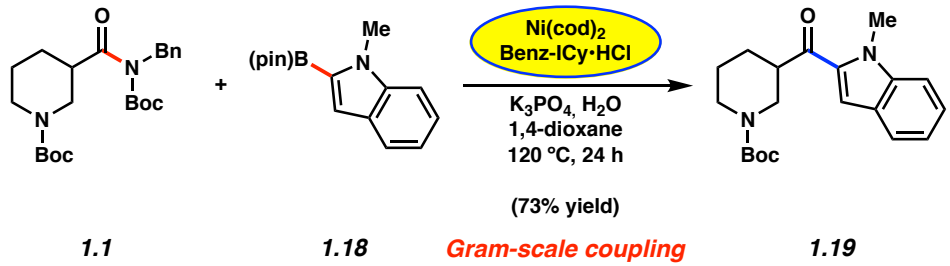

Figure 1.5. Gram-scale Suzuki–Miyaura coupling of amide **1.1** with boronate ester **1.18** to generate ketone **1.19**.

1.7 Conclusion

We have developed a benchtop protocol for the Suzuki–Miyaura cross-coupling of aliphatic amides to access alkyl–aryl ketones. Our strategy leverages mild Ni-catalyzed C–N bond activation to avoid the use of strongly basic and pyrophoric reagents typically employed in amide to ketone conversions. Additionally, the $Ni(cod)_2$/Benz-ICy•HCl–paraffin capsules, which are currently undergoing commercialization,[18] obviate the need to setup the reactions in a glovebox. Notably, this methodology enables the coupling of heterocyclic and aliphatic amides with a variety of aryl boronic esters for the formation of C–C bonds. Moreover, this transformation is scalable and, further, provides a valuable approach to the synthesis of alkyl–aryl ketones from amides, which benefits further from the use of base-metal catalysis and commercially available boronic ester nucleophiles. Thus, we hope these studies promote the use of Ni-mediated Suzuki–Miyaura couplings of aliphatic amides as a complement to traditional synthetic strategies.

1.8 Experimental Section

1.8.1 Materials and Methods

Unless stated otherwise, reactions were conducted in flame-dried glassware under an atmosphere of nitrogen or argon and commercially obtained reagents were used as received. Boronate esters **1.5**, **1.18**, **1.27**–**1.30** were obtained from Combi-Blocks. $Ni(cod)_2$ and Benz-ICy•HCl were obtained from Strem Chemicals. Potassium phosphate (K_3PO_4) was obtained from Acros. 1,4-Dioxane was obtained from Fisher Scientific and purified by distillation (over Na^0 and benzophenone) and degassed by sparging with N_2 for 1 h prior to use. Deionized water was degassed by sparging with N_2 for ≥10 min prior to use. Paraffin wax (mp 53–57 °C ASTM D 87) was obtained from Sigma-Aldrich and used as received. 1,3,5-trimethoxybenzene was obtained from Alfa Aesar and used as received. Reaction temperatures were controlled using an IKAmag temperature modulator, and unless stated otherwise, reactions were performed at room temperature (approximately 23 °C). Thin-layer chromatography (TLC) was conducted with EMD gel 60 F254 pre-coated plates (0.25 mm for analytical chromatography and 0.50 mm for preparative chromatography) and visualized using a combination of UV, anisaldehyde, iodine, and potassium permanganate staining techniques. Silicycle Siliaflash P60 (particle size 0.040–0.063 mm) was used for flash column chromatography. ^{1}H NMR spectra were recorded on Bruker spectrometers (400, 500, and 600 MHz) and are reported relative to residual solvent signals. Data for ^{1}H NMR spectra are reported as follows: chemical shift (δ ppm), multiplicity, coupling constant (Hz), integration. Data for ^{13}C NMR are reported in terms of chemical shift (at 125 MHz). IR spectra were recorded on a Perkin-Elmer UATR Two FT-IR spectrometer and are reported in terms of absorption frequency (cm^{-1}). DART-MS spectra were collected on a Thermo Exactive Plus MSD (Thermo Scientific) equipped with an ID-CUBE ion source and a Vapur Interface (IonSense Inc.).

Both the source and MSD were controlled by Excalibur software v. 3.0. The analyte was spotted onto OpenSpot sampling cards (IonSense Inc.) using $CHCl_3$, $CDCl_3$, or CH_2Cl_2 as the solvent. Ionization was accomplished using UHP He plasma with no additional ionization agents. The mass calibration was carried out using Pierce LTQ Velos ESI (+) and (–) Ion calibration solutions (Thermo Fisher Scientific).

Note: Supporting information for the syntheses of amides **1.1**, **1.4**, **1.20**, **1.21**,[5g] and **1.22**–**1.24**[10] have been published and spectral data match those previously reported.

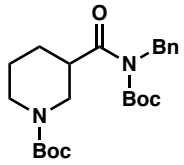

1.1

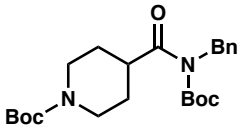

1.4

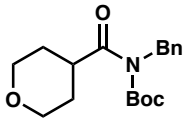

1.20

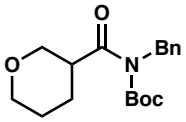

1.21

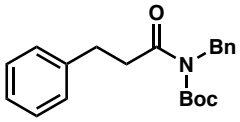

1.22

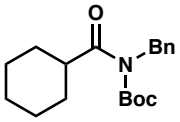

1.23

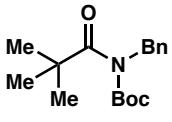

1.24

1.8.2 Experimental Procedures

1.8.2.1 Preparation of Paraffin Wax Capsules

Representative Procedure for the preparation of paraffin wax capsules for use in Sections 1.8.2.3 and 1.8.2.4. Paraffin wax (mp 53–57 °C ASTM D 87) was melted in a 250 mL beaker suspended in an oil bath maintained at 80 °C.

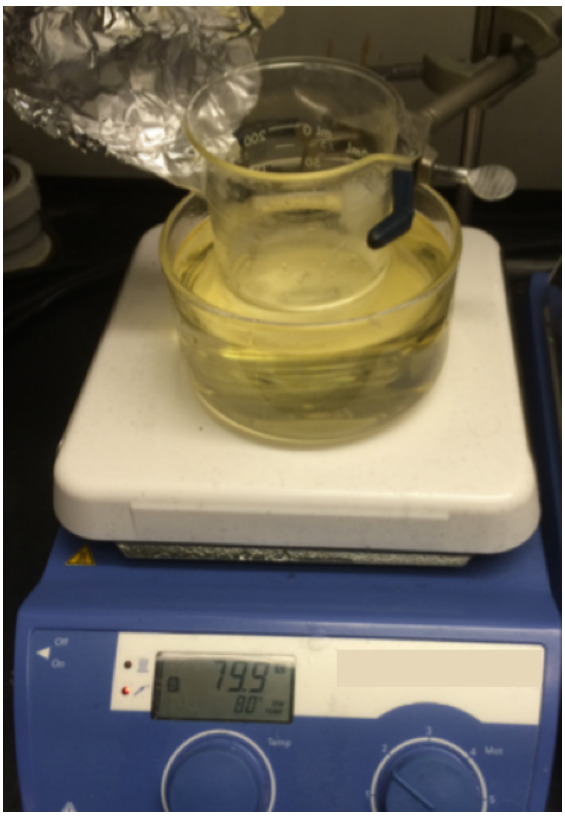

The molten paraffin was then pipetted into a standard brass mold (Brass Nipple, 1/8 in x close) using a 5 3/4 in glass pipette and pipette bulb.

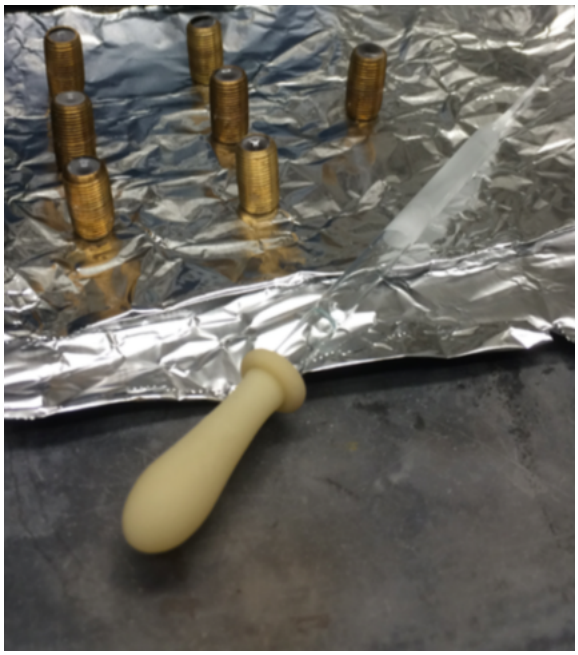

After cooling, the resulting wax cylinder was removed from the brass mold and trimmed to approximately 1 cm in length using a razor blade.

Next, a cavity was bored in the wax cylinder using a standard drill bit (5/32 in, black oxide), taking care not to bore through the entire cylinder.

The resulting hollow and open capsule was brought into a glovebox, inserted into a 14/20 septum for ease of handling, and charged with $Ni(cod)_2$ (5.5 mg, 0.020 mmol, 5 mol%) and Benz-ICy•HCl (12.8 mg, 0.040 mmol, 10 mol%).

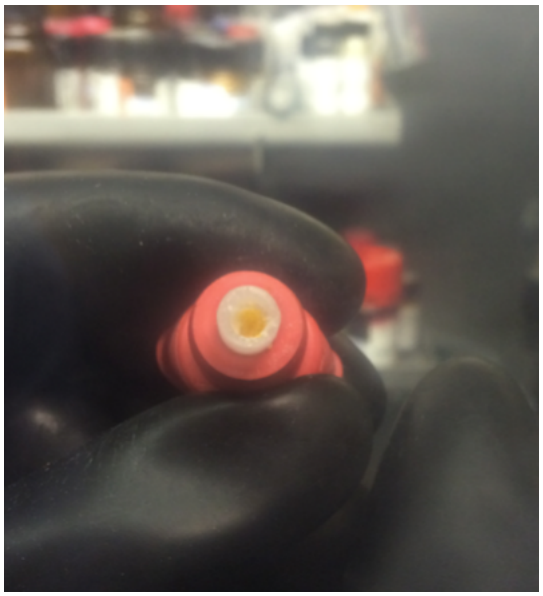

After charging the capsule, a warm metal spatula (maintained at approximately 80 °C using a hot plate in the glovebox) was used to melt the top of the capsule closed. Removal from the glovebox and re-dipping in molten wax twice (to ensure a proper seal) gave the desired capsules that were ready for use on the benchtop. The capsules were stored in a freezer maintained at –20 °C under an atmosphere of air until use.

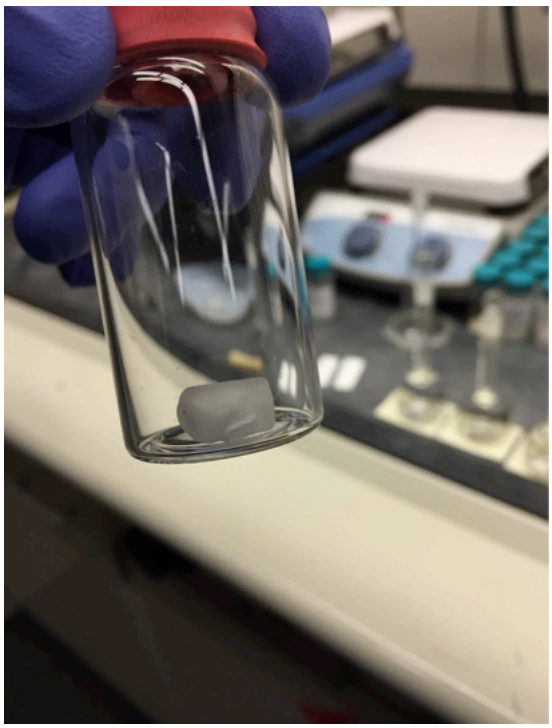

Note: Supporting information for the preparation of similar paraffin capsules has been previously disclosed.[14] Typically, paraffin wax capsules generated in this way were used within 1–2 weeks of being prepared. The stability of paraffin capsules to air and moisture was examined over a period of two months (See Section 1.8.2.3).

1.8.2.2 Preparation of Paraffin Wax Capsules for Gram-Scale Coupling

Representative Procedure for preparation of paraffin wax capsules for use in Section 1.8.2.5. Paraffin wax (mp 53–57 °C ASTM D 87) was melted in a 250 mL beaker suspended in an oil bath maintained at 80 °C. The molten paraffin (approximately 4 mL) was then pipetted into a standard glass VWR culture tube (12 x 75 mm) using a 5 3/4 in glass pipette and pipette bulb. After cooling, the resulting wax cylinder was removed from the culture tube (by scoring and carefully breaking

the glass away from the paraffin) and trimmed to approximately 2.0 cm in length using a razor blade.

Next, a cavity was bored in the wax cylinder using a standard drill bit (15/64 in, black oxide), taking care not to bore through the entire cylinder.

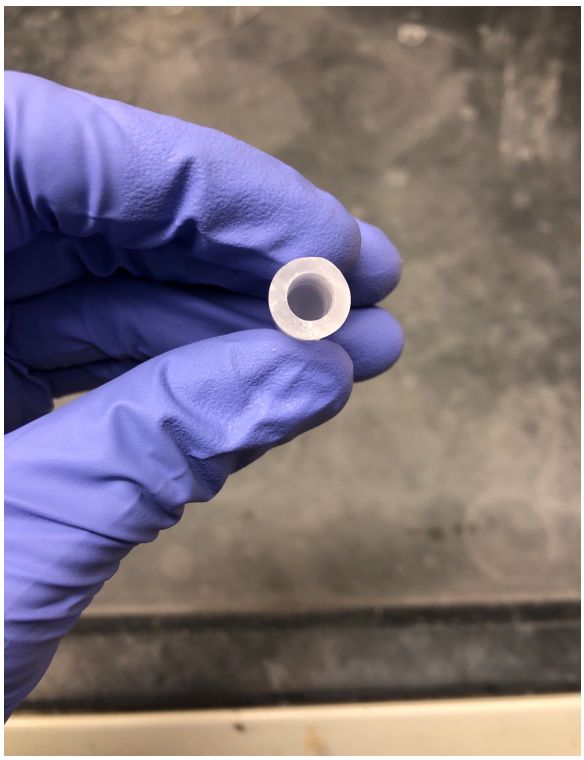

The resulting hollow and open capsule was brought into a glovebox and charged with $Ni(cod)_2$ (32.9 mg, 0.119 mmol, 5 mol%) and Benz-ICy•HCl (76.2 mg, 0.239 mmol, 10 mol%). After charging the capsule, a warm metal spatula (maintained at approximately 80 °C using a hot plate in the glovebox) was used to melt the top of the capsule closed. Removal from the glovebox and re-dipping in molten wax twice (to ensure a proper seal) gave the desired capsules that were ready for use on the benchtop (See Section 1.8.2.5)

Note: Supporting information for the preparation of similar gram-scale paraffin capsules has been previously disclosed.[14]

1.8.2.3 Optimization of Methodology

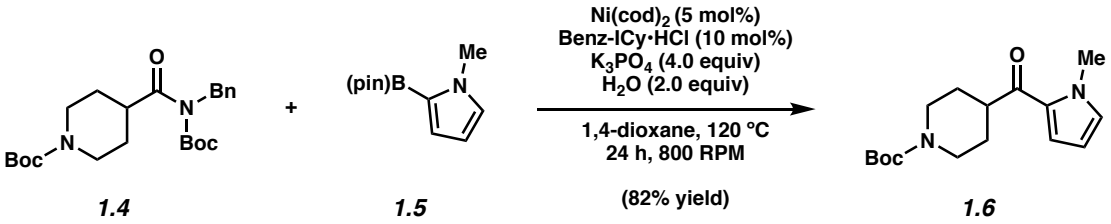

Representative Procedure for Table 1.1 (coupling of amide 1.4 and *N*-methylpyrrole-2-boronic acid pinacol ester (1.5) is used as an example). Ketone 1.6. A 2-dram vial was charged with anhydrous powder K_3PO_4 (340 mg, 1.60 mmol, 4.00 equiv) and a magnetic stir bar (egg-shaped 3/8 x 3/16 in). The vial and its contents were flame-dried under reduced pressure and

allowed to cool under N_2. The vial was then charged with amide substrate **1.4** (167 mg, 0.40 mmol, 1.00 equiv), *N*-methylpyrrole-2-boronic acid pinacol ester (**1.5**, 414 mg, 2.00 mmol, 5.00 equiv), and a paraffin wax capsule containing $Ni(cod)_2$ (5.50 mg, 0.02 mmol, 0.05 equiv) and Benz-ICy•HCl (12.8 mg, 0.04 mmol, 0.10 equiv) prepared as described in Section 1.8.2.1. The vial was purged with N_2 and subsequently deionized water (14.0 μL, 0.80 mmol, 2.00 equiv) and 1,4-dioxane (0.40 mL, 1.00 M) were added. The vial was capped with a Teflon-lined screw cap under a flow of N_2 and the reaction mixture was stirred vigorously (800 RPM) at 120 ºC for 24 h. After removing the vial from heat, the reaction mixture was transferred to a 100 mL pear-shaped flask containing 2.0 g of silica gel with hexanes (6 mL) and CH_2Cl_2 (6 mL). The mixture was adsorbed onto the silica gel under reduced pressure and filtered over a plug of silica gel (4.0 cm OD x 3.0 cm, 300 mL of hexanes eluent to remove paraffin, then 250 mL of EtOAc eluent). The volatiles were removed under reduced pressure and the yield of ketone **1.6** was determined by ^1H NMR analysis with 1,3,5-trimethoxybenzene as an external standard.[10]

Any modifications of the conditions shown in the representative procedure above are specified below in Table 1.1.

Table 1.1. Optimization studies.

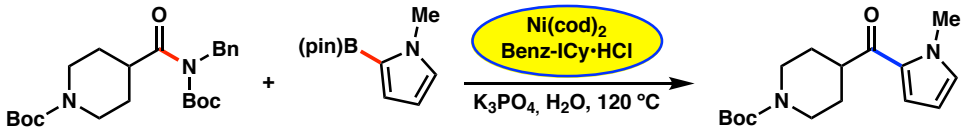

1.4 *1.5* *1.6*

Entry	*Solvent (1.0 M)*	*equiv. 1.5*	*Time*	*Stir Rate*	*Yield of 1.6*[a]
1	toluene	2.5	16	400 RPM	28%
2	1,4-dioxane	2.5	16	400 RPM	71%
3	1,4-dioxane	5.0	24	800 RPM	91%
4[b]	1,4-dioxane	2 month stability test			97%

[a]Yields were determined by ^{1}H NMR analysis using 1,3,5-trimethoxybenzene as an external standard and reflect the average of two experiments. [b]Reaction performed using conditions outlined in Entry 3.

1.8.2.4 Scope of Methodology

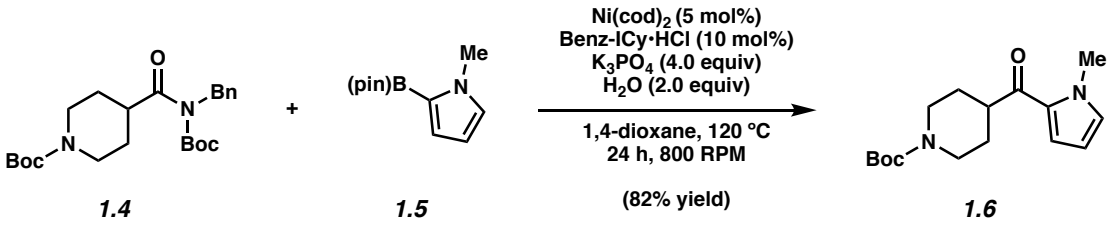

1.4 *1.5* *1.6*

Representative Procedure for Figures 1.3 and 1.4 (coupling of amide 1.4 and *N*-methylpyrrole-2-boronic acid pinacol ester (1.5) is used as an example). Ketone 1.6. A 2-dram vial was charged with anhydrous powder K_3PO_4 (340 mg, 1.60 mmol, 4.00 equiv) and a magnetic stir bar (egg-shaped 3/8 x 3/16 in). The vial and its contents were flame-dried under reduced pressure and allowed to cool under N_2. The vial was then charged with amide substrate **1.4** (167 mg, 0.40 mmol, 1.00 equiv), *N*-methylpyrrole-2-boronic acid pinacol ester **1.5** (414 mg, 2.00 mmol, 5.0 equiv), and a paraffin wax capsule containing $Ni(cod)_2$ (5.50 mg, 0.02 mmol, 0.05 equiv) and Benz-ICy•HCl (12.8 mg, 0.04 mmol, 0.10 equiv) prepared as described in Section 1.8.2.1. The vial was purged with N_2 and subsequently deionized water (14.0 µL, 0.8 mmol, 2.00

equiv) and 1,4-dioxane (0.40 mL, 1.00 M) were added. The vial was capped with a Teflon-lined screw cap under a flow of N_2 and the reaction mixture was stirred vigorously (800 RPM) at 120 ºC for 24 h. After removing the vial from heat, the reaction mixture was transferred to a 100 mL pear-shaped flask containing 2.0 g of silica gel with hexanes (6 mL) and CH_2Cl_2 (6 mL). The mixture was adsorbed onto the silica gel under reduced pressure and filtered over a plug of silica gel (4.0 cm OD x 3.0 cm, 300 mL of hexanes eluent to remove paraffin, then 250 mL of EtOAc eluent). The volatiles were removed under reduced pressure and the crude residue was purified by flash column chromatography (19:1 Hexanes:EtOAc → 9:1 Hexanes:EtOAc) to yield ketone **1.6** (82% yield, average of two experiments) as a yellow oil. Ketone **1.6**: R_f 0.25 (5:1 Hexanes:EtOAc). ^{1}H NMR (500 MHz, $CDCl_3$): δ 6.98 (dd, J = 4.1, 1.7, 1H), 6.83 (t, J = 2.0, 1H), 6.14 (dd, J = 2.6, 1.7, 1H), 4.18 (br s, 2H), 3.93 (s, 3H), 3.21–3.10 (m, 1H), 2.82 (br s, 2H), 1.85–1.64 (m, 4H), 1.47 (s, 9H). Spectral data match those previously reported.[10]

Any modifications of the conditions shown in the representative procedure above are specified in the following schemes, which depict all of the results shown in Figures 1.3 and 1.4.

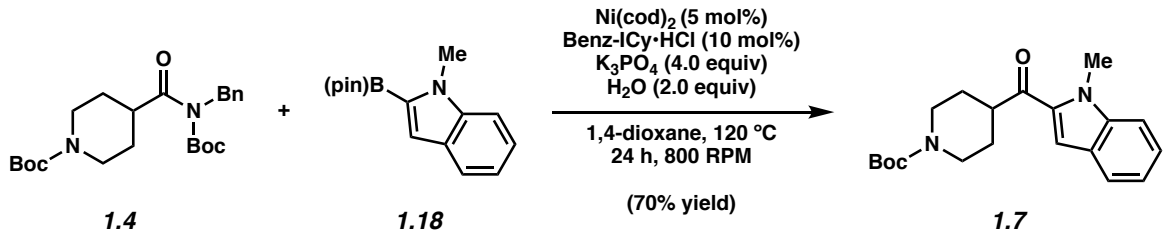

1.4 *1.18* *1.7*

Ketone 1.7. Purification by flash chromatography (19:1 Hexanes:EtOAc → 9:1 Hexanes:EtOAc) generated ketone **1.7** (70% yield, average of two experiments) as a white solid. Ketone **1.7**: R_f 0.33 (5:1 Hexanes:EtOAc). ^{1}H NMR (500 MHz, $CDCl_3$): δ 7.70 (d, J = 7.9, 1H), 7.39 (d, J = 3.9, 2H),

7.33 (s, 1H), 7.20–7.14 (m, 1H) 4.21 (br s, 2H), 4.07 (s, 3H), 3.47–3.32 (m, 1H), 2.88 (br s, 2H), 1.86 (br s, 2H), 1.82–1.70 (m, 2H), 1.48 (s, 9H). Spectral data match those previously reported.[10]

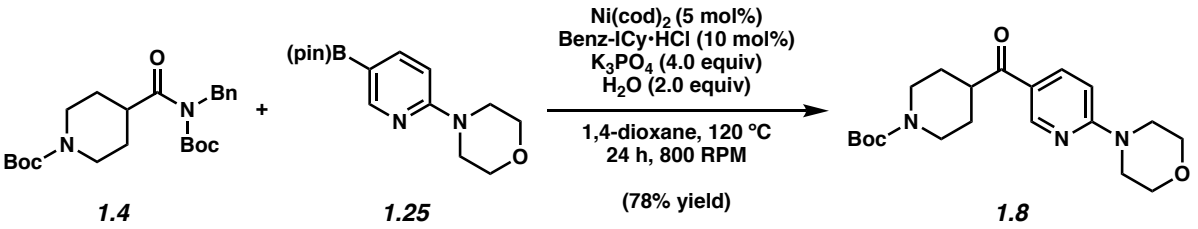

Ketone 1.8. ^{1}H NMR analysis of the crude reaction mixture indicated a 78% yield of ketone **1.8** relative to a 1,3,5-trimethoxybenzene external standard (average of two experiments). Purification by preparative thin-layer chromatography (1:1 Hexanes:EtOAc) provided an analytical sample of ketone **1.8** as a white solid. Ketone **1.8**: R_f 0.30 (1:1 Hexanes:EtOAc). ^{1}H NMR (500 MHz, $CDCl_3$): δ 8.78 (d, J = 2.6, 1H), 8.05 (dd, J = 9.1, 2.5, 1H), 6.63 (d, J = 9.1, 1H), 4.16 (br s, 2H), 3.81 (t, J = 5.2, 4H), 3.68 (t, J = 4.7, 4H), 3.32–3.21 (m, 1H), 2.87 (br s, 2H), 1.79 (br s, 2H), 1.76–1.65 (m, 2H), 1.46 (s, 9H). Spectral data match those previously reported.[10]

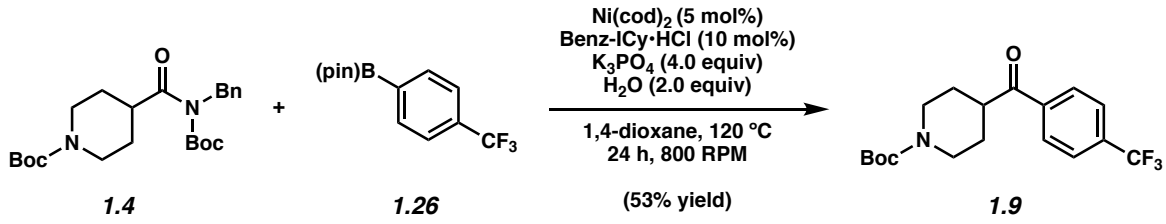

Ketone 1.9. Purification by flash chromatography (19:1 Hexanes:EtOAc → 9:1 Hexanes:EtOAc) generated ketone **1.9** (53% yield, average of two experiments) as a white solid. Ketone **1.9**: R_f 0.33 (5:1 Hexanes:EtOAc). ^{1}H NMR (500 MHz, $CDCl_3$): δ 8.03 (d, J = 8.4, 2H), 7.74 (d, J = 8.4, 2H), 4.16 (br s, 2H), 3.46–3.31 (m, 1H), 2.91 (br s, 2H), 1.85 (d, J = 13.3, 2H), 1.76–1.64 (m, 2H), 1.46 (d, J = 4.0, 9H). Spectral data match those previously reported.[10]

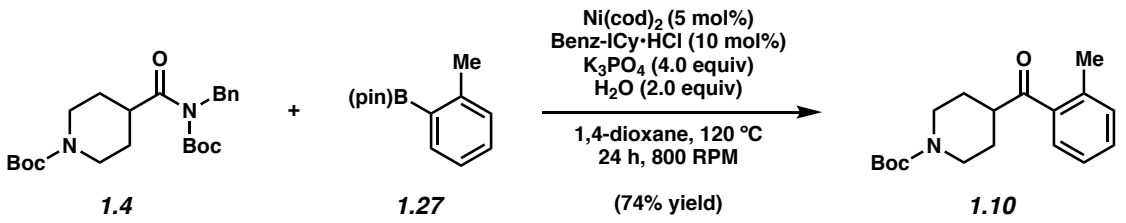

Ketone 1.10. Purification by flash chromatography (24:1 Hexanes:EtOAc → 5:1 Hexanes:EtOAc) generated ketone **1.10** (74% yield, average of two experiments) as a yellow oil. Ketone **1.10**: R_f 0.16 (9:1 Hexanes:EtOAc). ^{1}H NMR (600 MHz, $CDCl_3$): δ 7.50 (dd, J = 7.8, 1.4 Hz, 1H), 7.36 (td, J = 7.4, 1.3, 1H), 7.26–7.22 (m, 2H), 4.12 (br s, 2H), 3.18 (tt, J = 11.2, 3.6, 1H), 2.84 (br s, 2H), 2.41 (s, 3H), 1.81 (d, J = 13.1, 2H), 1.60–1.58 (m, 2H), 1.46 (s, 9H). Spectral data match those previously reported.[10]

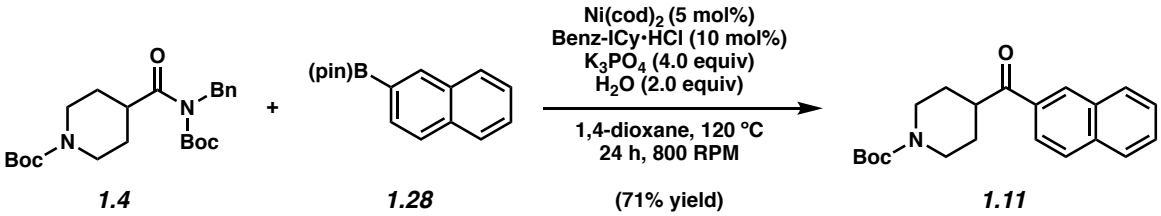

Ketone 1.11. Purification by flash chromatography (19:1 Hexanes:EtOAc → 14:1 Hexanes:EtOAc) generated ketone **1.11** (71% yield, average of two experiments) as a white solid. Ketone **1.11**: R_f 0.16 (9:1 Hexanes:EtOAc). ^{1}H NMR (500 MHz, $CDCl_3$): δ 8.45 (s, 1H), 8.04–7.85 (m, 4H), 7.65–7.53 (m, 2H), 4.20 (br s, 2H), 3.58 (tt, J = 11.2, 4.0, 1H), 2.96 (t, J = 2.8, 2H), 1.90 (br s, 2H), 1.83–1.69 (m, 2H), 1.48 (s, 9H). Spectral data match those previously reported.[10]

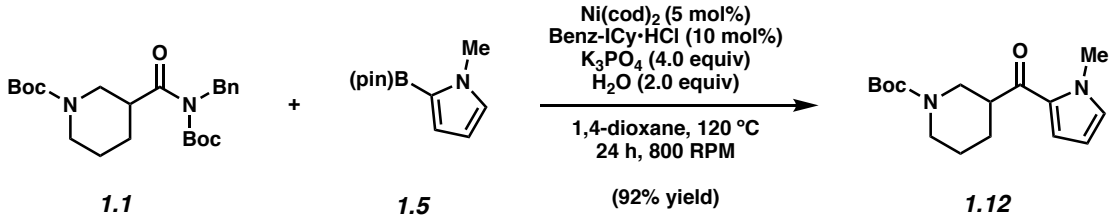

1.1 *1.5* *1.12*

Ketone 1.12. Purification by flash chromatography (19:1 Hexanes:EtOAc → 9:1 Hexanes:EtOAc) generated ketone **1.12** (92% yield, average of two experiments) as a light brown oil. Ketone **1.12**: R_f 0.26 (5:1 Hexanes:EtOAc). ^{1}H NMR (400 MHz, $CDCl_3$): δ 7.05 (dd, *J* = 4.2, 1.6, 1H), 6.82 (t, *J* = 1.9, 1H), 6.14 (dd, *J* = 4.1, 2.5, 1H), 4.25 (br d, *J* = 13.5, 1H), 4.12 (br d, *J* = 11.7, 1H), 3.93 (br s, 3H), 3.16 (tt, *J* = 11.4, 3.6, 1H), 2.94–2.83 (m, 1H), 2.70 (td, *J* = 12.7, 2.4, 1H), 2.02–1.92 (m, 1H), 1.79–1.68 (m, 2H), 1.61–1.50 (m, 1H), 1.47 (s, 9H). Spectral data match those previously reported.[10]

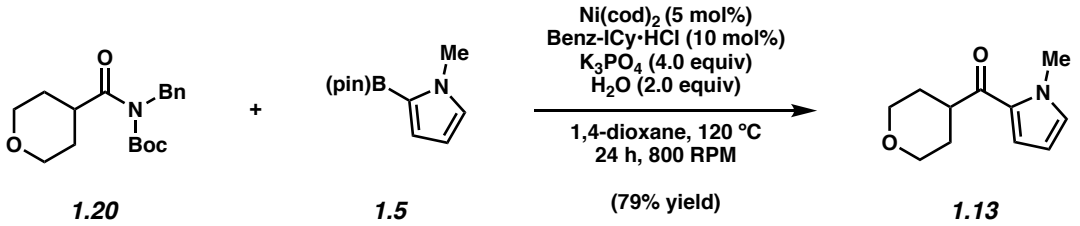

1.20 *1.5* *1.13*

Ketone 1.13. Purification by sequential preparative thin-layer chromatography (9:1 Hexanes:EtOAc and 5:1 Hexanes:EtOAc) generated ketone **1.13** (79% yield, average of two experiments) as a white solid. Ketone **1.13**: R_f 0.17 (5:1 Hexanes:EtOAc). ^{1}H NMR (500 MHz, $CDCl_3$): δ 6.99 (dd, *J* = 4.1, 1.6, 1H), 6.83 (t, *J* = 1.9, 1H), 6.14 (dd, *J* = 4.1, 2.5, 1H), 4.09–4.00 (m, 2H), 3.94 (s, 3H), 3.52 (td, *J* = 11.8, 2.1, 2H), 3.26 (tt, *J* = 11.5, 3.8, 1H), 1.97–1.86 (m, 2H), 1.74–1.67 (m, 2H). Spectral data match those previously reported.[10]

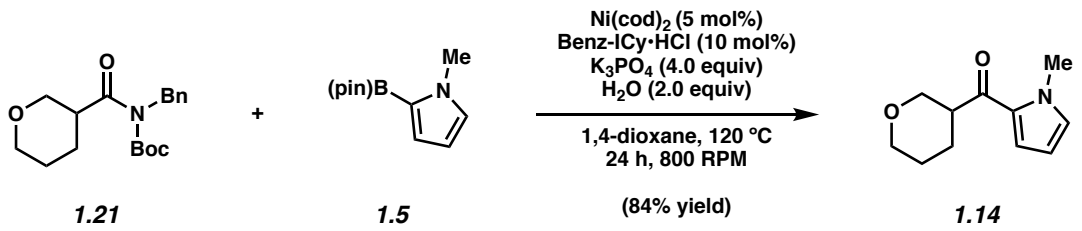

Ketone 1.14. Purification by flash chromatography (9:1 Hexanes:EtOAc) generated ketone **1.14** (84% yield, average of two experiments) as a colorless oil. Ketone **1.14**: R_f 0.22 (5:1 Hexanes:EtOAc). ^{1}H NMR (500 MHz, $CDCl_3$): δ 7.03 (dd, *J* = 4.2, 1.7, 1H), 6.82 (t, *J* = 1.9, 1H), 6.14 (dd, *J* = 4.2, 2.5, 1H), 4.10–4.04 (m, 1H), 3.99–3.93 (m, 1H), 3.92 (s, 3H), 3.53 (t, *J* = 10.8, 1H), 3.46–3.34 (m, 2H), 2.02–1.94 (m, 1H), 1.91–1.80 (m, 1H), 1.80–1.65 (m, 2H). Spectral data match those previously reported.[10]

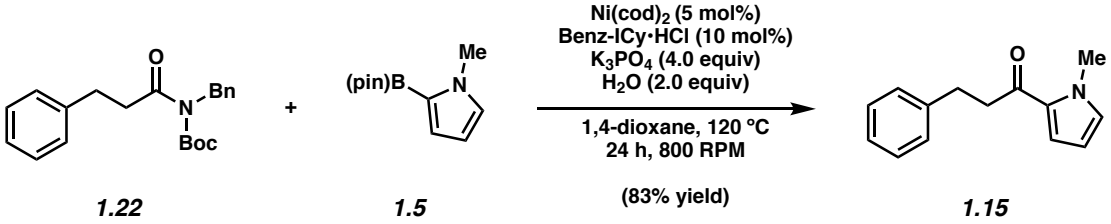

Ketone 1.15. Purification by flash chromatography (19:1 Hexanes:EtOAc) generated ketone **1.15** (83% yield, average of two experiments) as a colorless oil. Ketone **1.15**: R_f 0.40 (5:1 Hexanes:EtOAc). ^{1}H NMR (500 MHz, $CDCl_3$): δ 7.32–7.17 (m, 2H), 7.26–7.23 (m, 2H), 7.22–7.17 (m, 1H), 6.94 (dd, *J* = 4.1, 1.7, 1H), 6.80 (t, *J* = 1.9, 1H), 6.11 (dd, *J* = 4.1, 2.4, 1H), 3.95 (s, 3H), 3.14–3.08 (m, 2H), 3.05–2.99 (m, 2H). Spectral data match those previously reported.[10]

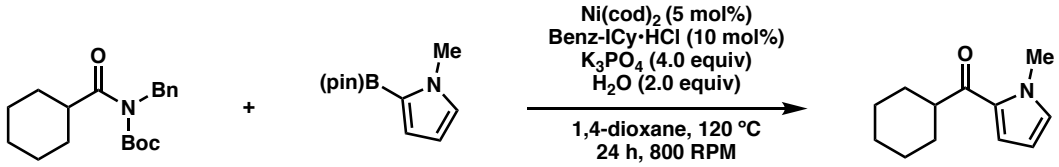

Ketone 1.16. Purification by flash chromatography (25:4:1 Hexanes:PhH:Et_2O) generated ketone **1.16** (89% yield, average of two experiments) as a colorless oil. Ketone **1.16**: R_f 0.55 (5:1 Hexanes:EtOAc). ^{1}H NMR (500 MHz, $CDCl_3$): δ 6.97 (dd, *J* = 4.1, 1.7, 1H), 6.80 (t, *J* = 1.9, 1H), 6.12 (dd, *J* = 4.1, 2.5, 1H), 3.93 (s, 3H), 3.02 (tt, *J* = 11.7, 3.2, 1H), 1.88–1.79 (m, 4H), 1.76–1.67 (m, 1H), 1.56–1.45 (m, 2H), 1.41–1.30 (m, 2H), 1.29–1.19 (m, 1H). Spectral data match those previously reported.[10]

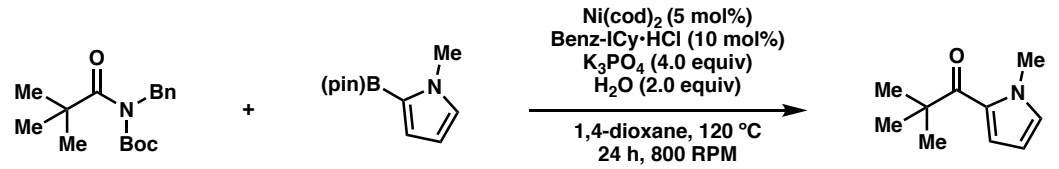

Ketone 1.17. ^{1}H NMR analysis of the crude reaction mixture indicated a 90% yield of ketone **1.17** relative to a 1,3,5-trimethoxybenzene external standard. Purification by preparative thin-layer chromatography (49:1 Cyclohexane:EtOAc), eluted twice, provided an analytical sample of ketone **1.17** as a colorless oil. Ketone **1.17**: R_f 0.65 (4:1 Hexanes:EtOAc). ^{1}H NMR (500 MHz, $CDCl_3$): δ 7.03 (dd, *J* = 4.1, 1.6, 1H), 6.75 (t, *J* = 1.9, 1H), 6.11 (dd, *J* = 4.1, 2.5, 1H), 3.90 (s, 3H), 1.36 (m, 9H). Spectral data match those previously reported.[10]

1.8.2.5 Gram-Scale Benchtop Suzuki–Miyaura Cross-Coupling

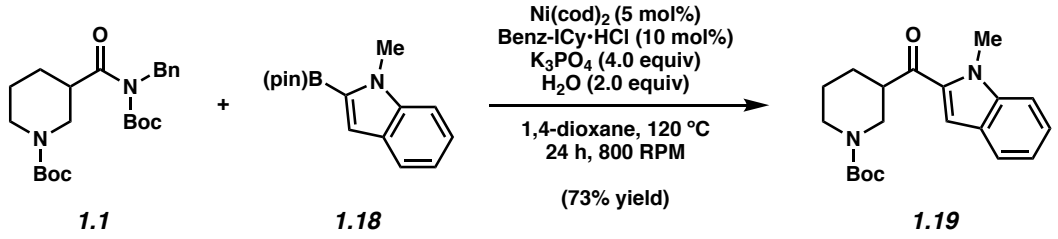

Ketone 1.19. A 20-mL scintillation vial was charged with anhydrous powder K_3PO_4 (2.03 g, 9.56 mmol, 4.00 equiv) and a magnetic stir bar (football shaped, 0.5 x 1.5 cm). The vial and its contents were flame-dried under reduced pressure and allowed to cool under N_2. The vial was charged with amide substrate **1.1** (1.00 g, 2.39 mmol, 1.00 equiv), boronic ester **1.18** (3.07 g, 11.9 mmol, 5.00 equiv), and a paraffin wax capsule containing $Ni(cod)_2$ (32.9 mg, 0.119 mmol, 0.050 equiv) and Benz-ICy•HCl (76.2 mg, 0.239 mmol, 0.100 equiv) prepared as described in Section 1.8.2.3. The vial was purged with N_2 and subsequently deionized water (86.1 μL, 4.78 mmol, 2.00 equiv) and 1,4-dioxane (2.39 mL, 1.00 M) were added. The vial was capped with a Teflon-lined screw cap under a flow of N_2 and the reaction mixture was stirred vigorously (800 RPM) at 120 ºC for 24 h. After removing the vial from heat, the reaction mixture was transferred to a 100 mL pear-shaped flask containing 12.0 g of silica gel with hexanes (10 mL) and CH_2Cl_2 (10 mL). The mixture was adsorbed onto the silica gel under reduced pressure and filtered over a plug of silica gel (4.0 cm OD x 3.0 cm, 300 mL of hexanes eluent to remove paraffin, then 250 mL of EtOAc eluent). The volatiles were removed under reduced pressure and the crude residue was purified by flash column chromatography (14:1 Hexanes:Et_2O → 4:1 Hexanes:Et_2O) to yield ketone **1.19** (73% yield, average of two experiments) as a white amorphous solid. Ketone **1.19**: R_f 0.25 (5:1 Hexanes:EtOAc); ^{1}H NMR (500 MHz, $CDCl_3$): δ 7.70 (d, J = 8.1, 1H), 7.44–7.34 (m, 3H), 7.20–7.11 (m, 1H), 4.32 (br s, 1H), 4.24–3.96 (m, 4H), 3.47–3.27 (m, 1H), 2.98 (br s, 1H), 2.74 (br s, 1H), 2.12–2.00 (m, 1H), 1.84–1.68 (m, 2H), 1.67–1.54 (m, 2H), 1.49 (s, 9H); ^{13}C NMR (125 MHz,

$CDCl_3$): δ 195.3, 154.9, 140.5, 133.9, 126.3, 125.9, 123.2, 121.0, 111.9, 110.5, 79.9, 47.9, 46.2, 44.9, 44.0, 32.4, 28.64, 28.61, 24.8; IR (film): 2973, 2938, 2861, 1691, 1656, 1614, 1423, 1168, 1146, 970 cm^{-1}; HRMS-APCI (m/z) $[M + H]^+$ calcd for $C_{20}H_{27}N_2O_3$, 343.2016; found 343.2010.

*Note: Ketone **1.19** was obtained as a mixture of conformers. These data represent empirically observed chemical shifts from the ^{13}C NMR spectrum.*

1.9 Spectra Relevant to Chapter One:

Ni-Catalyzed Suzuki–Miyaura Cross-Coupling of Aliphatic Amides on the Benchtop

Milauni M. Mehta,† Timothy B. Boit,† Jacob E. Dander,† and Neil K. Garg.

Org. Lett. **2020**, *22*, 1–5.

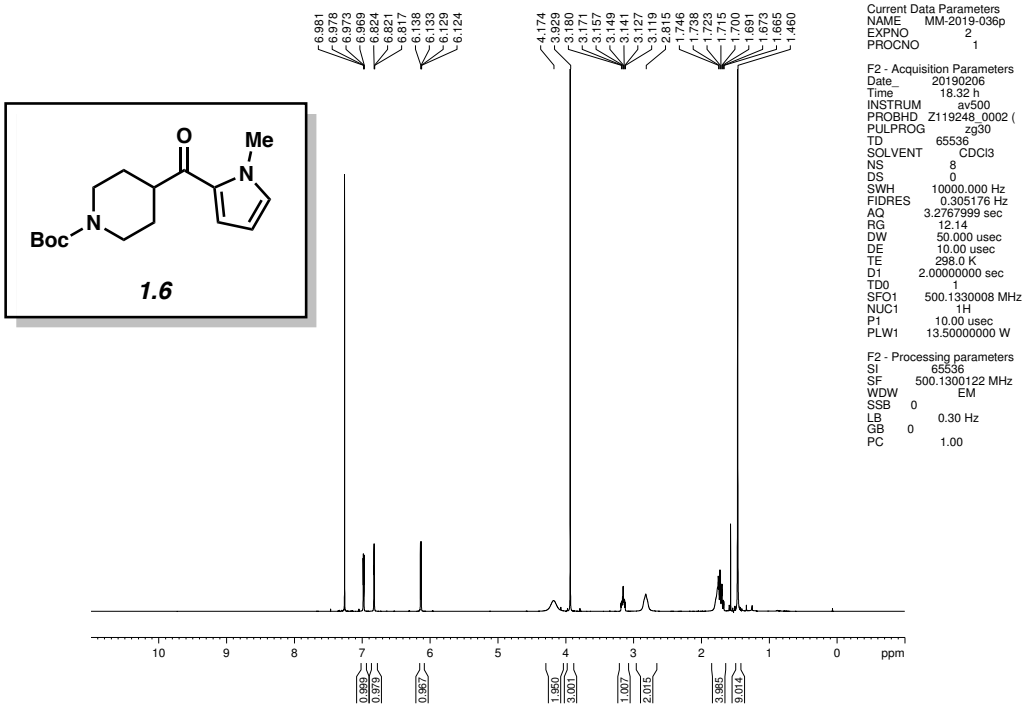

Figure 1.6 ^{1}H NMR (500 MHz, $CDCl_3$) of compound **1.6**.

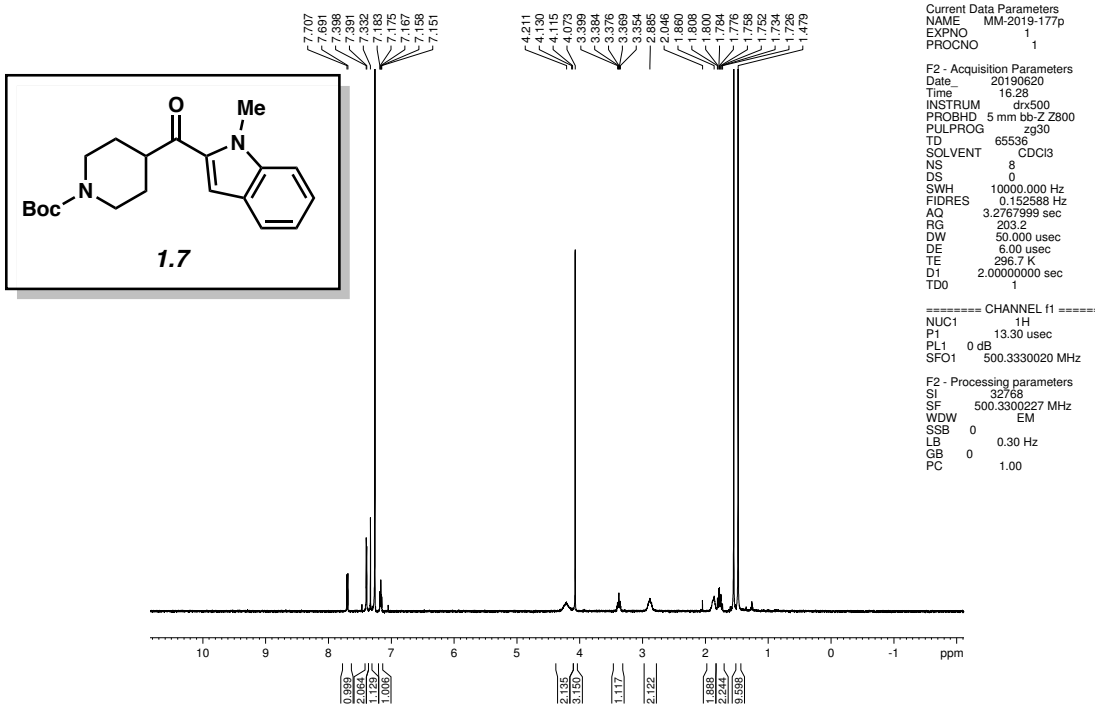

Figure 1.7 ^{1}H NMR (500 MHz, $CDCl_3$) of compound **1.7**.

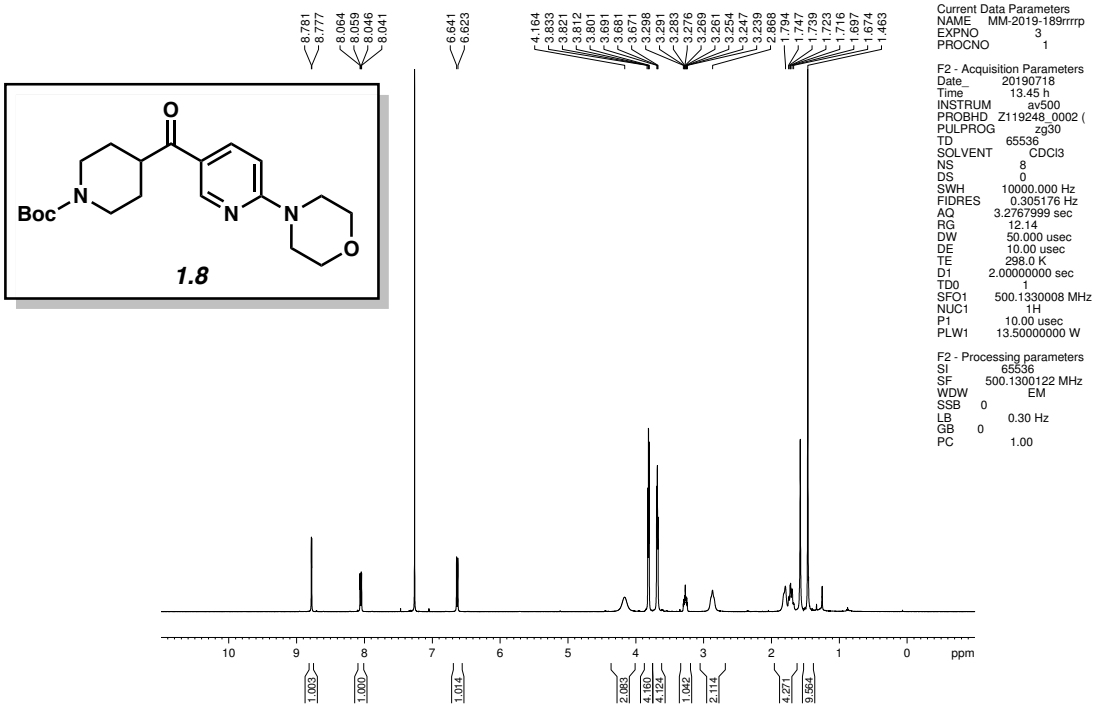

Figure 1.8 ^{1}H NMR (500 MHz, $CDCl_3$) of compound **1.8**.

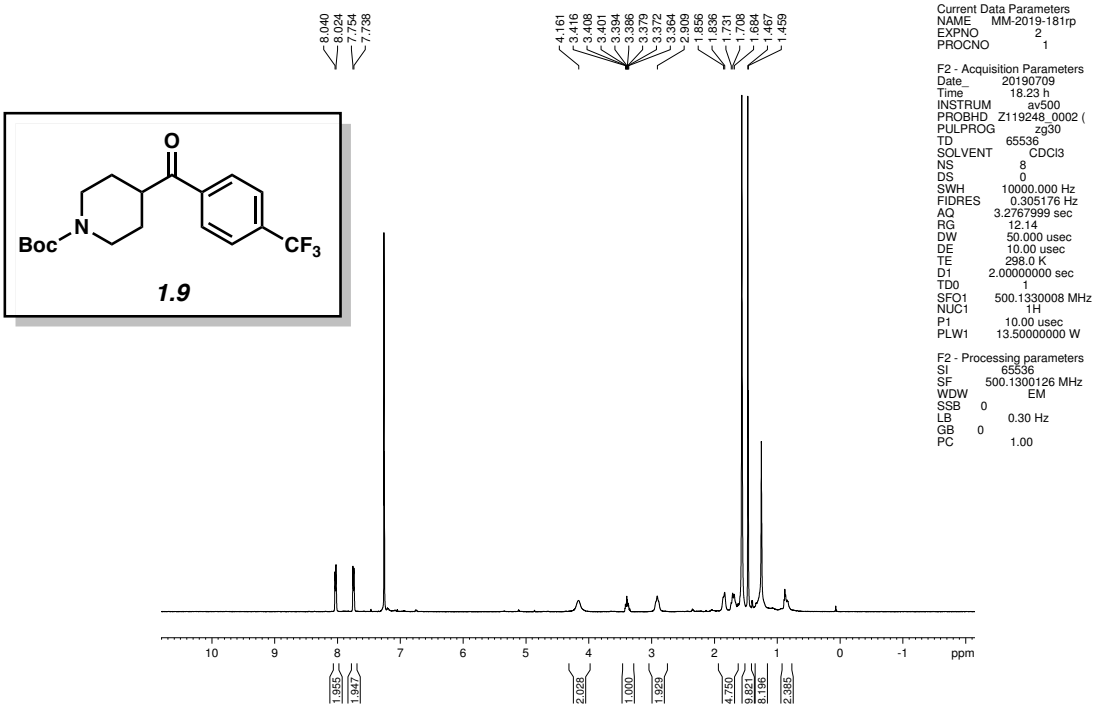

Figure 1.9 ^{1}H NMR (500 MHz, $CDCl_3$) of compound **1.9**.

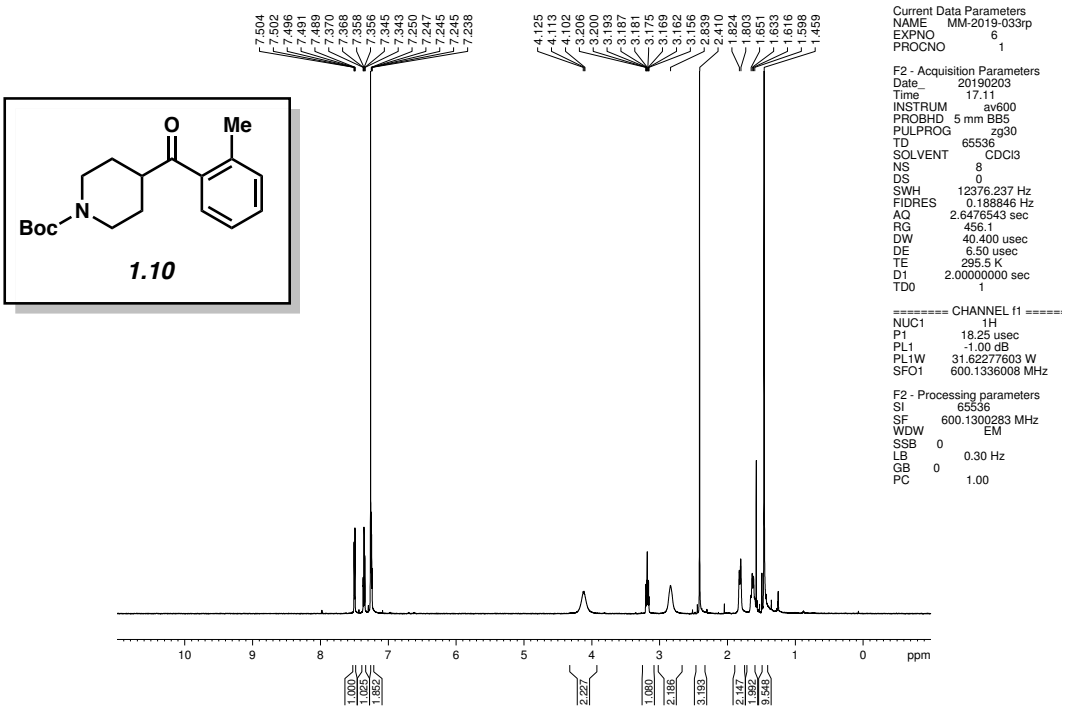

Figure 1.10 ^{1}H NMR (600 MHz, $CDCl_3$) of compound **1.10**.

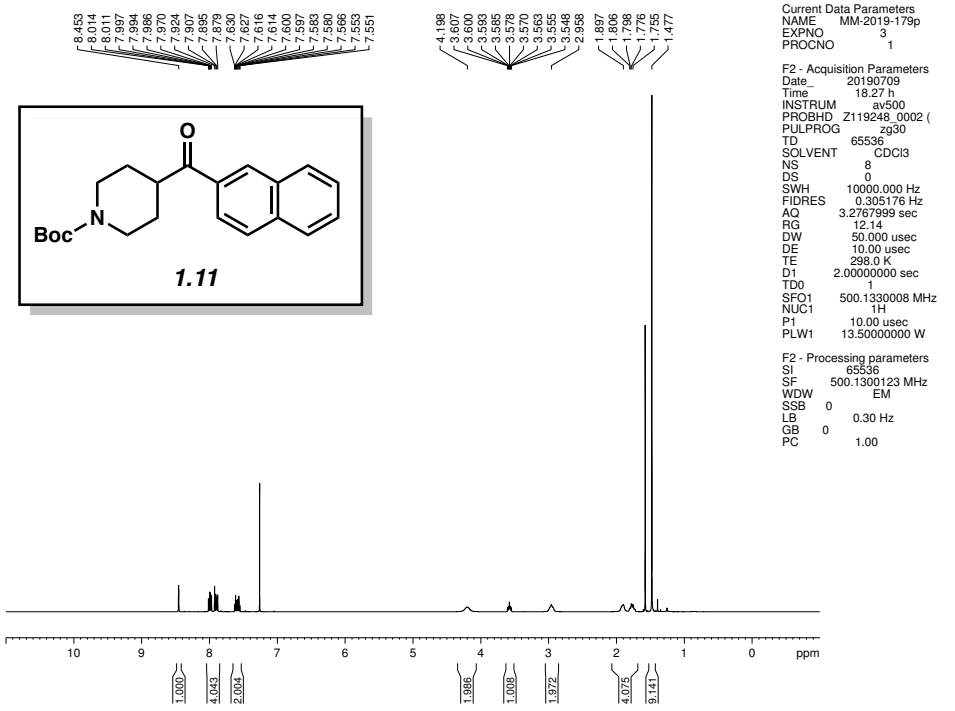

Figure 1.11 ^{1}H NMR (500 MHz, $CDCl_3$) of compound **1.11**.

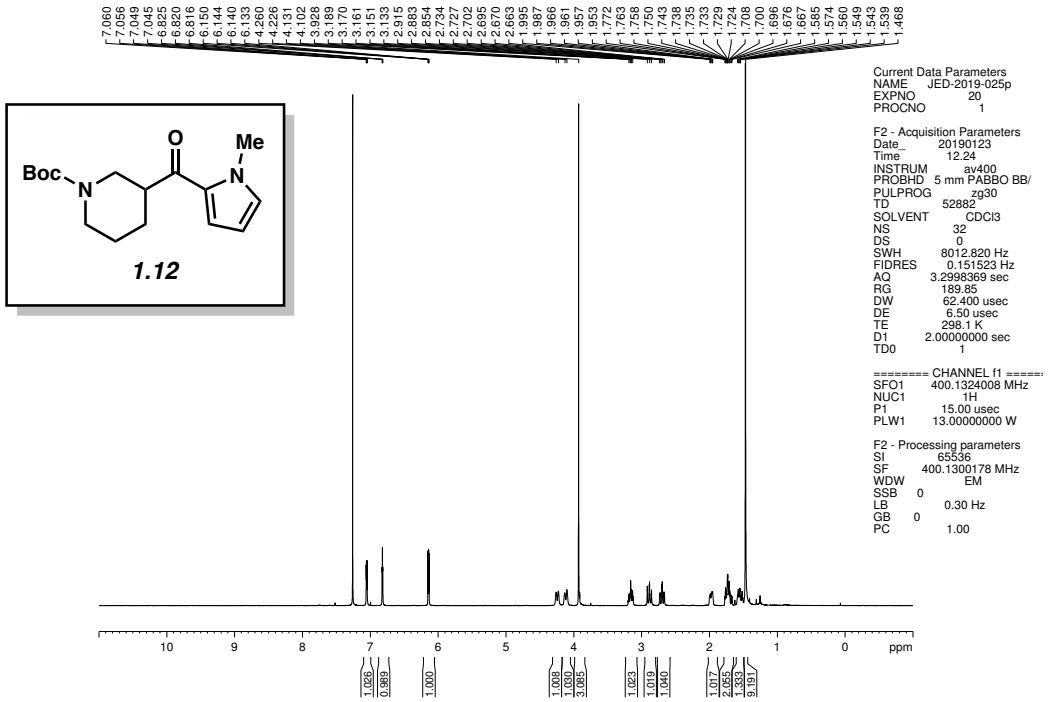

Figure 1.12 ^{1}H NMR (400 MHz, $CDCl_3$) of compound **1.12**.

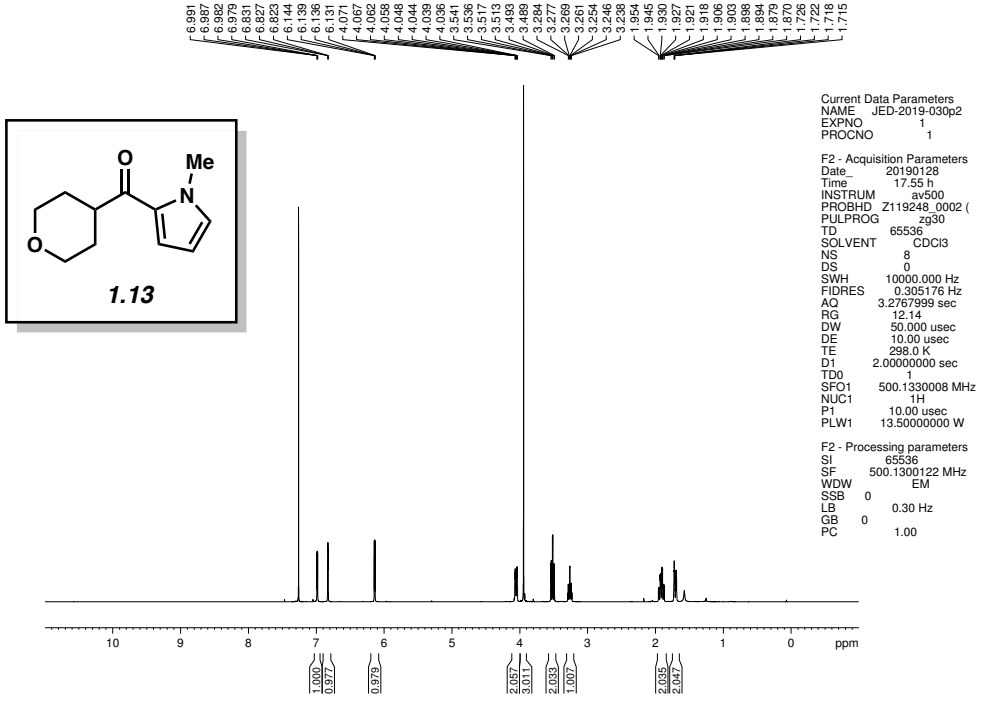

Figure 1.13 ^{1}H NMR (500 MHz, $CDCl_3$) of compound **1.13**.

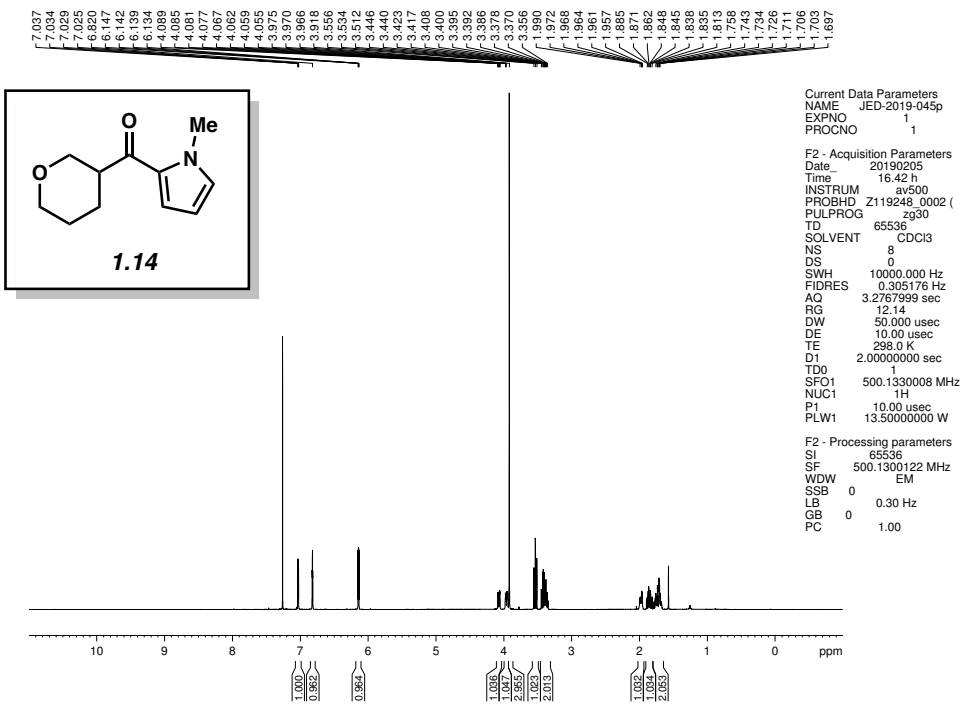

Figure 1.14 ^{1}H NMR (500 MHz, $CDCl_3$) of compound **1.14**.

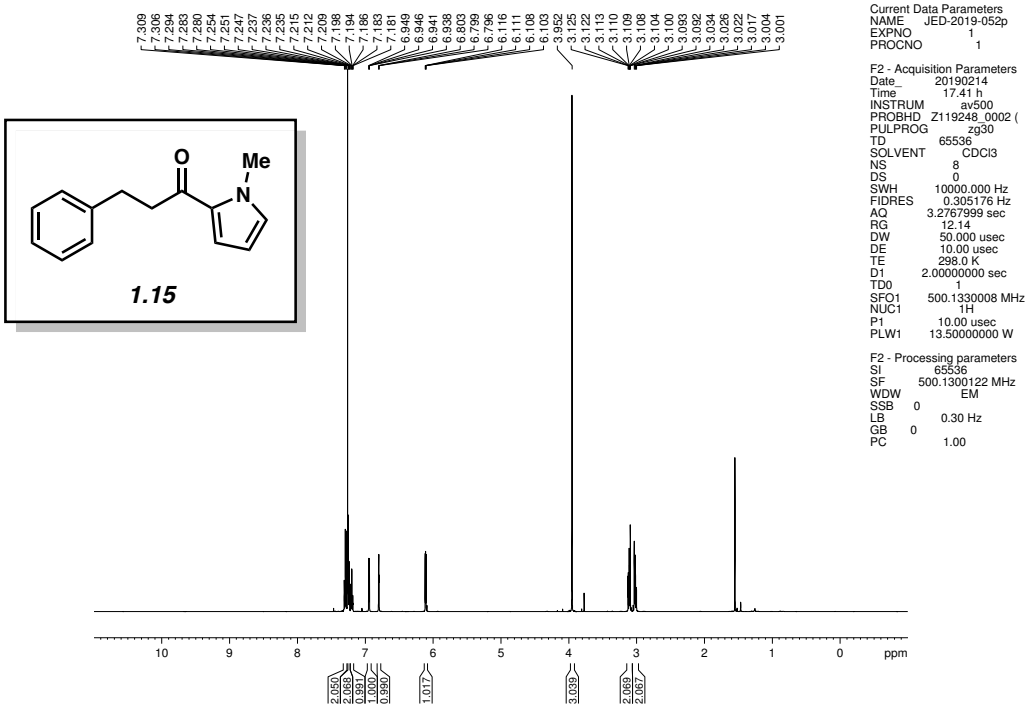

Figure 1.15 ^{1}H NMR (500 MHz, $CDCl_3$) of compound **1.15**.

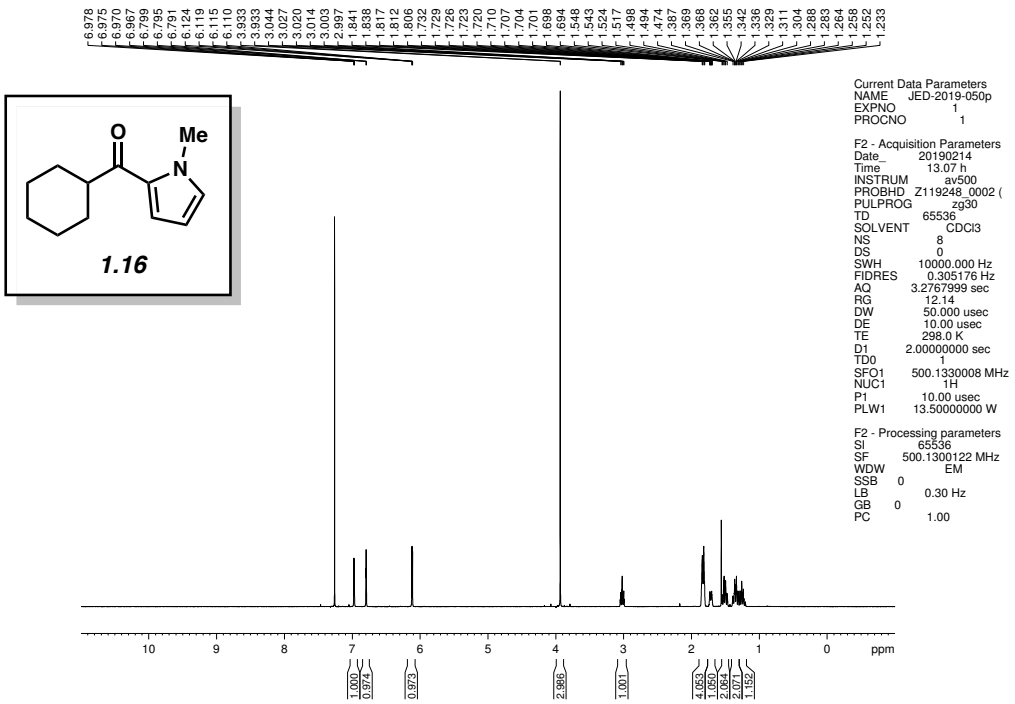

Figure 1.16 ^{1}H NMR (500 MHz, $CDCl_3$) of compound **1.16**.

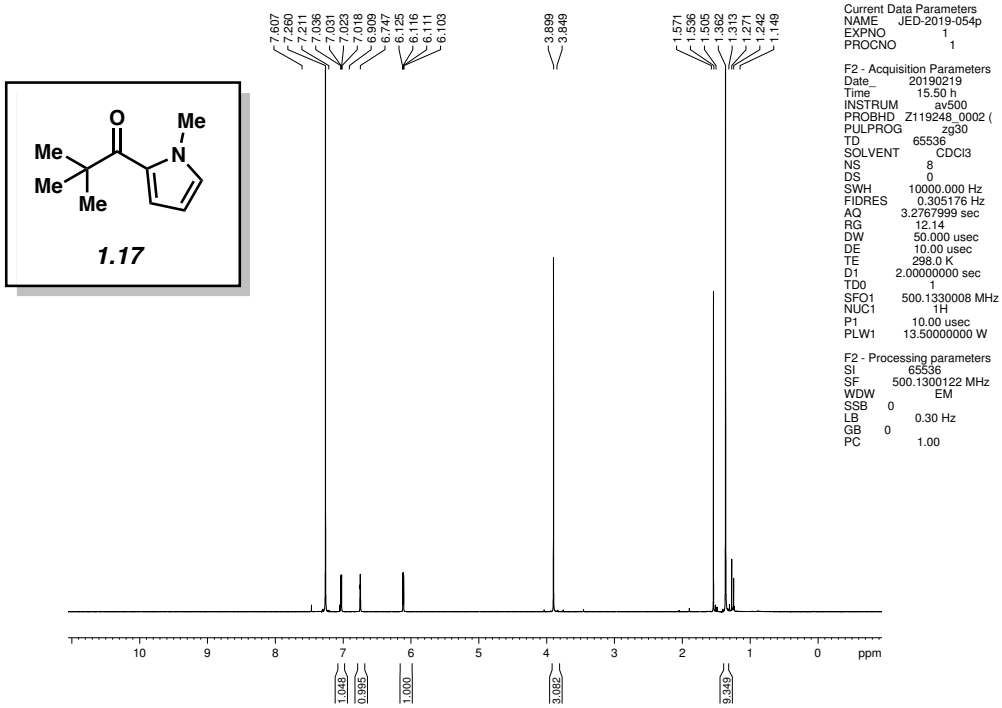

Figure 1.17 ^{1}H NMR (500 MHz, $CDCl_3$) of compound **1.17**.

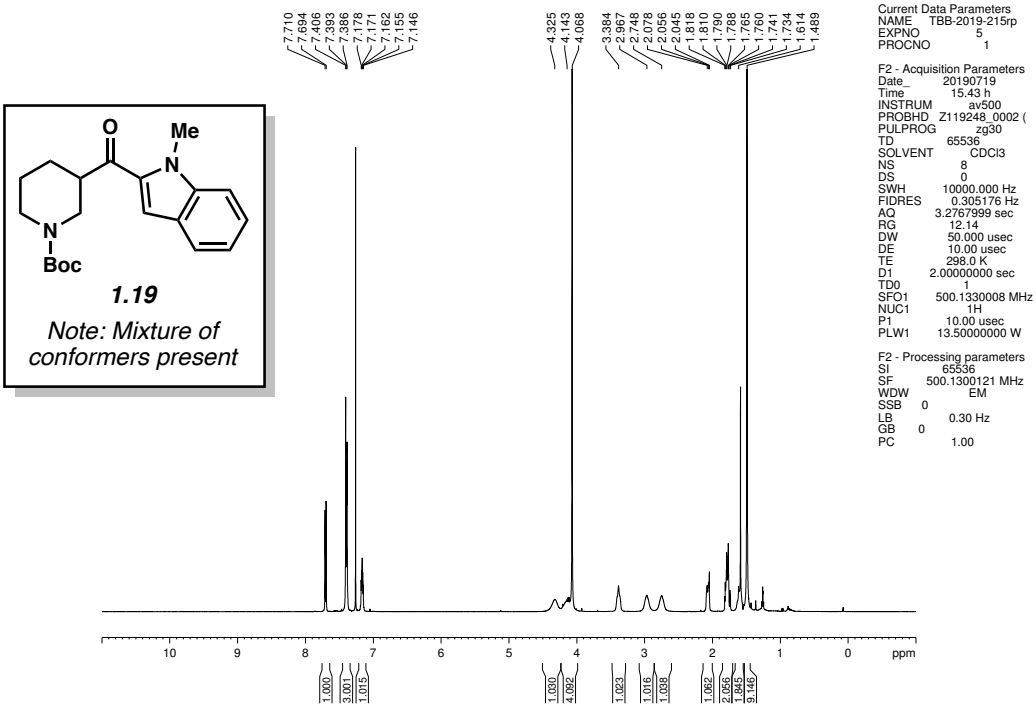

Figure 1.18 ^{1}H NMR (500 MHz, $CDCl_3$) of compound **1.19**.

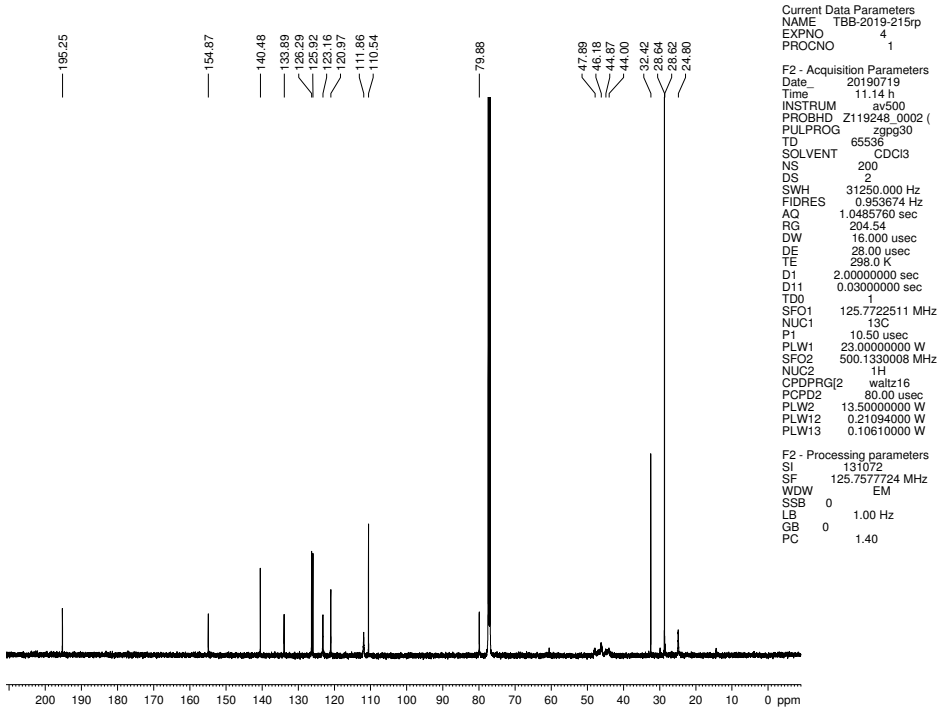

Figure 1.19 ^{13}C NMR (125 MHz, $CDCl_3$) of compound **1.19**.

1.10 Notes and References

(1) (a) Larock, R. C. Comprehensive Organic Transformations: A Guide to Functional Group Preparations; VCH: New York, 1989; pp 685−702. (b) Nicholson, J. W.; Wilson, A. D. Carboxylic. *J. Chem. Educ.* **2004**, *81*, 1362–1366. (c) Amani, J.; Molander, G. A. Direct Conversion of Carboxylic Acids to Alkyl Ketones. *Org. Lett.* **2017**, *19*, 3612–3615.

(2) (a) Nahm, S.; Weinreb, S. M. *N*-Methoxy-*N*-Methylamides as Effective Acylating Agents. *Tetrahedron Lett.* **1981**, *22*, 3815–3818. (b) Balasubramaniam, S.; Aidhen, I. S. The Growing Synthetic Utility of the Weinreb Amide. *Synthesis* **2002**, *23*, 3707–3738.

(3) For couplings of acyl halides, anhydrides, esters, and thioesters, see: (a) Labadie, J. W.; Tueting, D.; Stille, J. K. Synthetic Utility of the Palladium-Catalyzed Coupling Reaction of Acid Chlorides with Organotins. *J. Org. Chem.* **1983**, *48*, 4634−4642. (b) Stille, J. K. The Palladium-Catalyzed Cross-Coupling Reactions of Organotin Reagents with Organic Electrophiles. *Angew. Chem., Int. Ed.* **1986**, *25*, 508−524. (c) Stephan, M. S.; Teunissen, A. J. J. M.; de Vries, J. G. Heck Reactions without Salt Formation: Aromatic Carboxylic Anhydrides as Arylating Agents. *Angew. Chem., Int. Ed.* **1998**, *37*, 662−664. (d) Gooßen, L. J.; Ghosh, K. Palladium-Catalyzed Synthesis of Aryl Ketones from Boronic Acids and Carboxylic Acids Activated in situ by Pivalic Anhydride. *Angew. Chem., Int. Ed.* **2001**, *40*, 3458−3460. (e) Kakino, R.; Narahashi, H.; Shimizu, I.; Yamamoto, A. Palladium-Catalyzed Direct Conversion of Carboxylic Acids into Ketones with Organoboronic Acids Promoted by Anhydride Activators. *Bull. Chem. Soc. Jpn.* **2002**, *75*, 1333−1345. (f) Bykov, V. V.; Korolev, D. N.; Bumagin, N. A. Palladium-Catalyzed Reactions of Organoboron Compounds with Acyl Chlorides. *Russ. Chem. Bull.* **1997**, *46*, 1631−1632. (g) Zhang, L.; Wu, J.; Shi, L.; Xia,

C.; Li, F. *Tetrahedron Lett.* **2011**, *52*, 3897−3901. (h) Kakino, R.; Shimizu, I.; Yamamoto, A. Synthesis of Trifluoromethyl Ketones by Palladium-Catalyzed Cross-Coupling Reaction of Phenyl Trifluoroacetate with Organoboron Compounds. *Bull. Chem. Soc. Jpn.* **2001**, *74*, 371−376. (i) Cherney, A. H.; Reisman, S. E. Pd-Catalyzed Fukuyama Cross-Coupling of Secondary Organozinc Reagents for the Direct Synthesis of Unsymmetrical Ketones. *Tetrahedron* **2014**, *70*, 3259−3265. (j) Harada, T.; Kotani, Y.; Katsuhira, T.; Oku, A. Novel Method for Generation of Secondary Organozinc Reagent: Application to Tandem Carbon-Carbon Bond Formation Reaction of 1,1-Dibromoalkane. *Tetrahedron Lett.* **1991**, *32*, 1573−1576. (k) Negishi, E.-I.; Bagheri, V.; Chatterjee, S.; Luo, F.-T.; Miller, J. A.; Stoll, A. T. Palladium-Catalyzed Acylation of Organozincs and Other Organometallics as a Convenient Route to Ketones. *Tetrahedron Lett.* **1983**, *24*, 5181−5184. (l) Iwai, T.; Nakai, T.; Mihara, M.; Ito, T.; Mizuno, T.; Ohno, T. Pd-Catalyzed Cross-Coupling Reactions of Pyridine Carboxylic Acid Chlorides with Alkylzinc Reagents. *Synlett* **2009**, *20*, 1091−1094. (m) Grey, R. A. A Palladium-Catalyzed Synthesis of Ketones from Acid Chlorides and Organozinc Compounds. *J. Org. Chem.* **1984**, *49*, 2288−2289. (n) Bercot, E. A.; Rovis, T. A Mild and Efficient Catalytic Alkylative Monofunctionalization of Cyclic Anhydrides. *J. Am. Chem. Soc.* **2002**, *124*, 174−175. (o) Bercot, E. A.; Rovis, T. A Palladium-Catalyzed Enantioselective Alkylative Desymmetrization of *meso*-Succinic Anhydrides. *J. Am. Chem. Soc.* **2004**, *126*, 10248−10249. (p) Johnson, J. B.; Yu, R. T.; Fink, P.; Bercot, E. A.; Rovis, T. Selective Substituent Transfer from Mixed Zinc Reagents in Ni-Catalyzed Anhydride Alkylation. *Org. Lett.* **2006**, *8*, 4307−4310. (q) Tokuyama, H.; Yokoshima, S.; Yamashita, T.; Fukuyama, T. A Novel Ketone Synthesis by a Palladium-Catalyzed Reaction of Thiol Esters and Organozinc

Reagents. *Tetrahedron Lett.* **1998**, *39*, 3189−3192. (r) Mori, Y.; Seki, M. A Novel Procedure for the Synthesis of Multifunctional Ketones Through the Fukuyama Coupling Reaction Employing Dialkylzincs. *Tetrahedron Lett.* **2004**, *45*, 7343−7345. (s) Miyazaki, T.; Han-ya, Y.; Tokuyama, H.; Fukuyama, T. New Odorless Protocols for the Synthesis of Aldehydes and Ketones from Thiol Esters. *Synlett* **2004**, *3*, 477−480. (t) Dieter, R. K. Reaction of Acyl Chlorides with Organometallic Reagents: A Banquet Table of Metals for Ketone Synthesis. *Tetrahedron* **1999**, *55*, 4177–4236. (u) Shi, S.; Nolan, S. P.; Szostak, M. Well-Defined Palladium(II)–NHC Precatalysts for Cross-Coupling Reactions of Amides and Esters by Selective N–C/O–C Cleavage. *Acc. Chem. Res.* **2018**, *51*, 2589–2599. (v) Halima, T. B.; Zhang, W.; Yalaoui, T.; Hong, X.; Yang, Y.-F.; Houk, K. N.; Newman, S. G. Palladium-Catalyzed Suzuki–Miyaura Coupling of Aryl Esters. *J. Am. Chem. Soc.* **2017**, *139*, 1311–1318.

(4) For recent reviews, see: (a) Dander, J. E.; Garg, N. K. Breaking Amides using Nickel Catalysis. *ACS Catal.* **2017**, *7*, 1413−1423. (b) Meng, G.; Shi, S.; Szostak, M. Cross-Coupling of Amides by N–C Bond Activation. *Synlett* **2016**, *27*, 2530–2540. (c) Takise, R.; Muto, K.; Yamaguchi, J. Cross-Coupling of Aromatic Esters and Amides. *Chem. Soc. Rev.* **2017**, *46*, 5864–5888. (d) Kaiser, D.; Bauer, A.; Lemmerer, M.; Maulide, N. Amide Activation: An Emerging Tool for Chemoselective Synthesis. *Chem. Soc. Rev.* **2018**, *47*, 7899–7925.

(5) For nickel-catalyzed reactions proceeding with cleavage of the amide C−N bond, see: (a) Hie, L.; Fine Nathel, N. F.; Shah, T. K.; Baker, E. L.; Hong, X.; Yang, Y.-F.; Liu, P.; Houk, K. N.; Garg, N. K. Conversion of Amides to Esters by the Nickel-Catalysed Activation of Amide C–N Bonds. *Nature* **2015**, *524*, 79−83. (b) Weires, N. A.; Baker, E. L.; Garg, N. K. Nickel-

Catalysed Suzuki–Miyaura Coupling of Amides. *Nat. Chem.* **2016**, *8*, 75−79. (c) Baker, E. L.; Yamano, M. M.; Zhou, Y.; Anthony, S. M.; Garg, N. K. A Two-Step Approach to Achieve Secondary Amide Transamidation Enabled by Nickel Catalysis. *Nat. Commun.* **2016**, *7*, 11554. (d) Simmons, B. J.; Weires, N. A.; Dander, J. E.; Garg, N. K. Nickel-Catalyzed Alkylation of Amide Derivatives. *ACS Catal.* **2016**, *6*, 3176−3179. (e) Shi, S.; Szostak, M. Nickel-Catalyzed Diaryl Ketone Synthesis by N–C Cleavage: Direct Negishi Cross-Coupling of Primary Amides by Site-Selective *N*,*N*-Di-Boc Activation. *Org. Lett.* **2016**, *18*, 5872−5875. (f) Shi, S.; Szostak, M. Efficient Synthesis of Diaryl Ketones by Nickel-Catalyzed Negishi Cross-Coupling of Amides by Carbon–Nitrogen Bond Cleavage at Room Temperature Accelerated by a Solvent Effect. *Chem. Eur. J.* **2016**, *22*, 10420−10424. (g) Hie, L.; Baker, E. L.; Anthony, S. M.; Desrosiers, J.-N.; Senanayake, C.; Garg, N. K. Nickel-Catalyzed Esterification of Aliphatic Amides. *Angew. Chem., Int. Ed.* **2016**, *55*, 15129−15132. (h) Dey, A.; Sasmal, S.; Seth, K.; Lahiri, G. K.; Maiti, D. Nickel-Catalyzed Deamidative Step-Down Reduction of Amides to Aromatic Hydrocarbons. *ACS Catal.* **2017**, *7*, 433−437. (i) Ni, S.; Zhang, W.; Mei, H.; Han, J.; Pan, Y. Ni-Catalyzed Reductive Cross-Coupling of Amides with Aryl Iodide Electrophiles via C–N Bond Activation. *Org. Lett.* **2017**, *19*, 2536−2539. (j) Medina, J. M.; Moreno, J.; Racine, S.; Du, S.; Garg, N. K. Mizoroki–Heck Cyclizations of Amide Derivatives for the Introduction of Quaternary Centers. *Angew. Chem., Int. Ed.* **2017**, *56*, 6567−6571. (k) Hu, J.; Wang, M.; Pu, X.; Shi, Z. Nickel-Catalysed Retro-Hydroamidocarbonylation of Aliphatic Amides to Olefins. *Nat. Commun.* **2017**, *8*, 14993. (l) Weires, N. A.; Caspi, D. D.; Garg, N. K. (m) Shi, S.; Szostak, M. Nickel-Catalyzed Negishi Cross-Coupling of *N*-Acylsuccinimides: Stable, Amide-Based, Twist-Controlled Acyl-

Transfer Reagents via N–C Activation. *Synthesis* **2017**, *49*, 3602−3608. (n) Dander, J. E.; Baker, E. L.; Garg, N. K. Nickel-Catalyzed Transamidation of Aliphatic Amide Derivatives. *Chem. Sci.* **2017**, *8*, 6433−6438. (o) Huang, P.-Q.; Chen, H. Ni-Catalyzed Cross-Coupling Reactions of *N*-Acylpyrrole-Type Amides with Organoboron Reagents. *Chem. Commun.* **2017**, *53*, 12584−12587. (p) Deguchi, T.; Xin, H.-L.; Morimoto, H.; Ohshima, T. Direct Catalytic Alcoholysis of Unactivated 8-Aminoquinoline Amides. *ACS Catal.* **2017**, *7*, 3157−3161.

(6) For nickel-catalyzed decarbonylative coupling reactions of amides, see: (a) Shi, S.; Meng, G.; Szostak, M. Synthesis of Biaryls through Nickel-Catalyzed Suzuki–Miyaura Coupling of Amides by Carbon–Nitrogen Bond Cleavage. *Angew. Chem., Int. Ed.* **2016**, *55*, 6959−6963. (b) Hu, J.; Zhao, Y.; Liu, J.; Zhang, Y.; Shi, Z. Nickel-Catalyzed Decarbonylative Borylation of Amides: Evidence for Acyl C−N Bond Activation. *Angew. Chem., Int. Ed.* **2016**, *55*, 8718−8722. (c) Srimontree, W.; Chatupheeraphat, A.; Liao, H.-H.; Rueping, M. Amide to Alkyne Interconversion via a Nickel/Copper-Catalyzed Deamidative Cross-Coupling of Aryl and Alkenyl Amides. *Org. Lett.* **2017**, *19*, 3091−3094. (d) Liu, C.; Szostak, M. Decarbonylative Phosphorylation of Amides by Palladium and Nickel Catalysis: The Hirao Cross-Coupling of Amide Derivatives. *Angew. Chem., Int. Ed.* **2017**, *56*, 12718−12722. (e) Yue, H.; Guo, L.; Liao, H.-H.; Cai, Y.; Zhu, C.; Rueping, M. Catalytic Ester and Amide to Amine Interconversion: Nickel-Catalyzed Decarbonylative Amination of Esters and Amides by C−O and C−C Bond Activation. *Angew. Chem., Int. Ed.* **2017**, *56*, 4282−4285. (f) Chatupheeraphat, A.; Liao, H.-H.; Lee, S.-C.; Rueping, M. Nickel-Catalyzed C–CN Bond Formation via Decarbonylative Cyanation of Esters, Amides, and Intramolecular

Recombination Fragment Coupling of Acyl Cyanides. *Org. Lett.* **2017**, *19*, 4255−4258. (g) Yue, H.; Guo, L.; Lee, S.-C.; Liu, X.; Rueping, M. Selective Reductive Removal of Ester and Amide Groups from Arenes and Heteroarenes through Nickel-Catalyzed C−O and C−N Bond Activation. *Angew. Chem., Int. Ed.* **2017**, *56*, 3972−3976. (h) Lee, S.-C.; Guo, L.; Yue, H.; Liao, H.-H.; Rueping, M. Nickel-Catalyzed Decarbonylative Silylation, Borylation, and Amination of Arylamides via a Deamidative Reaction Pathway. *Synlett* **2017**, *28*, 2594−2598.

(7) For Pd-catalyzed amide C–N bond activation, see: (a) Li, X.; Zou, G. Acylative Suzuki Coupling of Amides: Acyl-Nitrogen Activation via Synergy of Independently Modifiable Activating Groups. *Chem. Commun.* **2015**, *51*, 5089−5092. (b) Yada, A.; Okajima, S.; Murakami, M. Palladium-Catalyzed Intramolecular Insertion of Alkenes into the Carbon–Nitrogen Bond of *β*-Lactams. *J. Am. Chem. Soc.* **2015**, *137*, 8708−8711. (c) Meng, G.; Szostak, M. Palladium-Catalyzed Suzuki–Miyaura Coupling of Amides by Carbon–Nitrogen Cleavage: General Strategy for Amide N–C Bond Activation. *Org. Biomol. Chem.* **2016**, *14*, 5690−5705. (d) Meng, G.; Szostak, M. General Olefin Synthesis by the Palladium-Catalyzed Heck Reaction of Amides: Sterically Controlled Chemoselective N–C Activation. *Angew. Chem., Int. Ed.* **2015**, *54*, 14518−14522. (e) Meng, G.; Szostak, M. Sterically Controlled Pd-Catalyzed Chemoselective Ketone Synthesis via N–C Cleavage in Twisted Amides. *Org. Lett.* **2015**, *17*, 4364−4367. (f) Liu, C.; Meng, G.; Liu, Y.; Liu, R.; Lalancette, R.; Szostak, R.; Szostak, M. *N*-Acylsaccharins: Stable Electrophilic Amide-Based Acyl Transfer Reagents in Pd-Catalyzed Suzuki–Miyaura Coupling via N–C Cleavage. *Org. Lett.* **2016**, *18*, 4194−4197. (g) Lei, P.; Meng, G.; Szostak, M. General Method for the Suzuki–Miyaura Cross-Coupling of Amides Using Commercially Available, Air- and Moisture-Stable Palladium/NHC (NHC

= *N*-Heterocyclic Carbene) Complexes. *ACS Catal.* **2017**, *7*, 1960−1965. (h) Liu, C.; Liu, Y.; Liu, R.; Lalancette, R.; Szostak, R.; Szostak, M. Palladium-Catalyzed Suzuki–Miyaura Cross-Coupling of *N*-Mesylamides by N–C Cleavage: Electronic Effect of the Mesyl Group. *Org. Lett.* **2017**, *19*, 1434−1437. (i) Liu, C.; Meng, G.; Szostak, M. *N*-Acylsaccharins as Amide-Based Arylating Reagents via Chemoselective N–C Cleavage: Pd-Catalyzed Decarbonylative Heck Reaction. *J. Org. Chem.* **2016**, *81*, 12023−12030. (j) Meng, G.; Shi, S.; Szostak, M. Palladium-Catalyzed Suzuki–Miyaura Cross-Coupling of Amides via Site-Selective N–C Bond Cleavage by Cooperative Catalysis. *ACS Catal.* **2016**, *6*, 7335−7339. (k) Cui, M.; Wu, H.; Jian, J.; Wang, H.; Liu, C.; Stelck, D.; Zeng, Z. Palladium-Catalyzed Sonogashira Coupling of Amides: Access to Ynones via C–N Bond Cleavage. *Chem. Commun.* **2016**, *52*, 12076−12079. (l) Wu, H.; Li, Y.; Cui, M.; Jian, J.; Zeng, Z. Suzuki Coupling of Amides via Palladium-Catalyzed C–N Cleavage of *N*-Acylsaccharins. *Adv. Synth. Catal.* **2016**, *358*, 3876−3880. (m) Shi, S.; Szostak, M. Decarbonylative Cyanation of Amides by Palladium Catalysis. *Org. Lett.* **2017**, *19*, 3095−3098. (n) Lei, P.; Meng, G.; Ling, Y.; An, J.; Szostak, M. Pd-PEPPSI: Pd-NHC Precatalyst for Suzuki–Miyaura Cross-Coupling Reactions of Amides. *J. Org. Chem.* **2017**, *82*, 6638−6646. (o) Meng, G.; Szostak, R.; Szostak, M. Suzuki–Miyaura Cross-Coupling of *N*-Acylpyrroles and Pyrazoles: Planar, Electronically Activated Amides in Catalytic N–C Cleavage. *Org. Lett.* **2017**, *19*, 3596−3599. (p) Meng, G.; Lalancette, R.; Szostak, R.; Szostak, M. *N*-Methylamino Pyrimidyl Amides (MAPA): Highly Reactive, Electronically-Activated Amides in Catalytic N–C(O) Cleavage. *Org. Lett.* **2017**, *19*, 4656−4659. (q) Osumi, Y.; Szostak, M. *N*-Acylsuccinimides: Twist-Controlled, Acyl-Transfer Reagents in Suzuki–Miyaura Cross-Coupling by N–C Amide Bond Activation. *Org.*

Biomol. Chem. **2017**, *15*, 8867−8871. (r) Lei, P.; Meng, G.; Ling, Y.; An, J.; Nolan, S. P.; Szostak, M. General Method for the Suzuki–Miyaura Cross-Coupling of Primary Amide-Derived Electrophiles Enabled by [Pd(NHC)(cin)Cl] at Room Temperature. *Org. Lett.* **2017**, *19*, 6510−6513. (s) Li, X.; Zou, G. Palladium-Catalyzed Acylative Cross-Coupling of Amides with Diarylborinic Acids and Sodium Tetraarylborates. *J. Organomet. Chem.* **2015**, *794*, 136–145. (t) Liu, C.; Li, G.; Shi, S.; Meng, G.; Lalancette, R.; Szostak, R.; Szostak, M. Acyl and Decarbonylative Suzuki Coupling of *N*-Acetyl Amides: Electronic Tuning of Twisted, Acyclic Amides in Catalytic Carbon–Nitrogen Bond Cleavage. *ACS Catal.* **2018**, *8*, 9131–9139. (u) Meng, G.; Szostak, M. Palladium/NHC (NHC = *N*-Heterocyclic Carbene)-Catalyzed B-Alkyl Suzuki Cross-Coupling of Amides by Selective N–C Bond Cleavage. *Org. Lett.* **2018**, *20*, 6789–6793. (v) Shi, S.; Szostak, M. Decarbonylative Borylation of Amides by Palladium Catalysis. *ACS Omega* **2019**, *4*, 4901–4907. (w) Zhou, T.; Li, G.; Nolan, S. P.; Szostak, M. [Pd(NHC)(acac)Cl]: Well-Defined, Air-Stable, and Readily Available Precatalysts for Suzuki and Buchwald–Hartwig Cross-coupling (Transamidation) of Amides and Esters by N–C/O–C Activation. *Org. Lett.* **2019**, *21*, 3304–3309.

(8) For Ni- and Pd-catalyzed cross-couplings of amides with aryl boronic esters or acids, See Section 1.10, references: 5b,o; 6a,b; 7a,c,f–h,j,n,o,q–s,t,u,w.

(9) For Ni- and Pd-catalyzed cross-couplings of amides with alkyl zinc reagents, See Section 1.10, references: 5d–f,m.

(10) Boit, T. B.; Weires, N. A.; Kim, J.; Garg, N. K. Nickel-Catalyzed Suzuki–Miyaura Coupling of Aliphatic Amides. *ACS Catal.* **2018**, *8*, 1003–1008.

(11) The Molander group has reported a dual-metal photoredox approach to the synthesis of alkyl–alkyl ketones using alkyltrifluoroborate salts and aliphatic acyl succinimides, see: Amani, J.; Alam, R.; Badir, S.; Molander, G. A. Synergistic Visible-Light Photoredox/Nickel-Catalyzed Synthesis of Aliphatic Ketones via N–C Cleavage of Imides. *Org. Lett.* **2017**, *19*, 2426–2429.

(12) The use of air-stable Ni(II) precatalysts represents a complementary strategy for avoiding glovebox manipulations, see: (a) Shields, J. D.; Gray, E. E.; Doyle, A. G. A Modular, Air-Stable Nickel Precatalyst. *Org. Lett.* **2015**, *17*, 2166–2169. (b) Magano, J.; Monfette, S. Development of an Air-Stable, Broadly Applicable Nickel Source for Nickel-Catalyzed Cross-Coupling. *ACS Catal*. **2015**, *5*, 3120–3123. (c) Standley, E. A.; Jamison, T. F. Simplifying Nickel(0) Catalysis: An Air-Stable Nickel Precatalyst for the Internally Selective Benzylation of Terminal Alkenes. *J. Am. Chem. Soc.* **2013**, *135*, 1585–1592. (d) Park. N. H.; Teverovskiy, G.; Buchwald, S. L. Development of an Air-Stable Nickel Precatalyst for the Amination of Aryl Chlorides, Sulfamates, Mesylates, and Triflates. *Org. Lett.* **2014**, *16*, 220–223. (e) Ge, S.; Hartwig, J. F. Highly Reactive, Single-Component Nickel Catalyst Precursor for Suzuki–Miyuara Cross-Coupling of Heteroaryl Boronic Acids with Heteroaryl Halides. *Angew. Chem., Int. Ed.* **2012**, *51*, 12837–12841.

(13) (a) Sather, A. C.; Lee, H. G.; Colombe, J. R.; Zhang, A.; Buchwald, S. L. Dosage Delivery of Sensitive Reagents Enables Glove-Box-Free Synthesis. *Nature* **2015**, *524*, 208–211. (b) Fang, Y.; Liu, Y.; Ke, Y.; Guo, C.; Zhu, N.; Mi, X.; Ma, Z.; Hu, Y. A New Chromium-Based Catalyst Coated with Paraffin for Ethylene Oligomerization and the Effect of Chromium State on Oligomerization Selectivity. *Appl. Cat. A* **2002**, *235*, 33–38. (c) Taber, D. F.; Frankowski,

K. J. Grubbs' Catalyst in Paraffin: An Air-Stable Preparation for Alkene Metathesis. *J. Org. Chem.* **2003**, *68*, 6047–6048.

(14) (a) Dander, J. E.; Weires, N. A.; Garg, N. K. Benchtop Delivery of $Ni(cod)_2$ using Paraffin Capsules. *Org. Lett.* **2016**, *18*, 3934–3936. (b) Dander, J. E.; Morrill, L. A.; Nguyen, M. M.; Chen, S.; Garg, N. K. Breaking Amide C–N Bonds in an Undergraduate Organic Chemistry Laboratory. *J. Chem. Ed.* **2019**, *96*, 776–780.

(15) Lei, P.; Meng, G.; Shi, S.; Ling, Y.; An, J.; Szostak, R.; Szostak, M. Suzuki–Miyaura Cross-Coupling of Amides and Esters at Room Temperature: Correlation with Barriers to Rotation Around C–N and C–O Bonds. *Chem. Sci.* **2017**, *8*, 6525–6530.

(16) See Section 1.8.2.3 for details.

(17) See Section 1.8.2.3 for full optimization details.

(18) TCI Chemicals is commercializing the capsules containing $Ni(cod)_2$ and Benz-ICy•HCl.

(19) (a) Vitaku, E.; Smith, D. T.; Njardarson, J. T. Analysis of the Structural Diversity, Substitution Patterns, and Frequency of Nitrogen Heterocycles among U.S. FDA Approved Pharmaceuticals. *J. Med. Chem.* **2014**, *57*, 10257–10257. (b) Hirata, T.; Funatsu, T.; Keto, Y.; Nakata, M.; Sasamata, M. Pharmacological Profile of Ramosetron, a Novel Therapeutic Agent for IBS. *Inflammopharmacology* **2007**, *15*, 5–9.

(20) Amide derivatives featuring various *N*-substituents have been employed successfully in cross-coupling reactions. *N*-Bn-*N*-Boc derivatives were selected for the present study due to their utility in the glovebox methodology and ease of preparation.

CHAPTER TWO

Base-Mediated Meerwein–Ponndorf–Verley Reduction of Aromatic Ketones and Heterocyclic Ketones

Timothy B. Boit, Milauni M. Mehta, and Neil K. Garg.

Org. Lett. **2019**, *21*, 6447–6451.

2.1 Abstract

An experimental protocol to achieve the Meerwein–Ponndorf–Verley (MPV) reduction of ketones under mildly basic conditions is reported. The transformation is tolerant of a range of ketone substrates, including *O*- and *S*-containing heterocycles, is scalable, and shows potential to be used as platform to access enantioenriched products. These studies provide a general method for achieving the reduction of ketones under mildly basic conditions and offer an alternative protocol to more well-known Al-based MPV reduction conditions.

2.2 Introduction

The Meerwein–Ponndorf–Verley (MPV) reaction is an important and powerful tool for the reduction of ketones and aldehydes because of its chemoselectivity, mild reaction conditions, scalability, and low operational cost.[1] Discovered nearly a century ago,[2] the traditional MPV reduction employs an aluminum alkoxide catalyst generated from a secondary alcohol (most commonly isopropanol) to achieve the reversible transfer hydrogenation of carbonyl substrates (Figure 2.1).[3] This venerable reaction has been featured in the syntheses of several natural products[4] and spurred numerous experimental[5] and computational studies.[6] Despite the synthetic

utility of the traditional MPV reduction, several drawbacks exist. These include long reaction times, the need for a large excess of reducing agent, competing side reactions such as aldol condensation and the Tishchenko reduction of aldehydes, and low enantioselectivities in the case of intermolecular asymmetric variants.[1,3] Methodological advances to address these limitations include the use of additives,[7] microwave irradiation,[8] and the development of novel aluminum,[9] organoboron[10] and metal alkoxide catalysts (i.e. transition[11] and lanthanide[12]). A particularly efficient aluminum siloxide catalyst has been reported by the Krempner group.[9c]

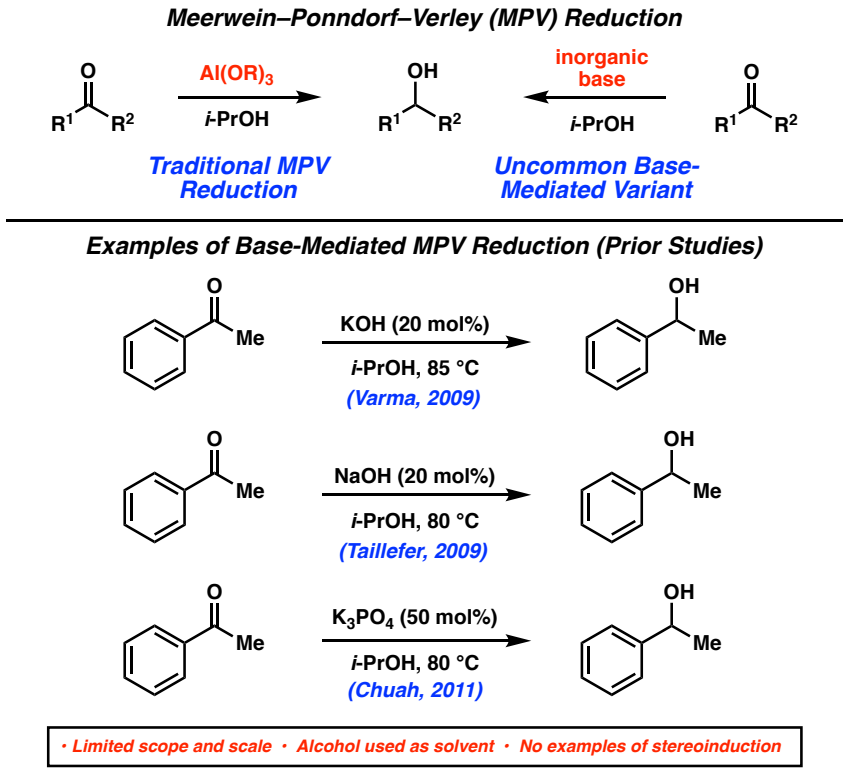

Figure 2.1. Traditional MPV reduction of ketones and base-mediated variant (prior studies).

A largely unexplored approach to the MPV-type reduction of carbonyls uses simple alkali metal alkoxides. (Figure 2.1).[13,14] This variant of the MPV reaction has several benefits including its avoidance of metal catalysts, operational simplicity, and compatibility with heteroatoms known

to inhibit metal catalysis.[3,13] Specifically, isopropoxide catalysts generated from strong alkali bases, such as NaOH[13a] and KOH[13b] and milder bases such as K_3PO_4,[13c] have been employed in the reduction of aldehydes and ketones. Nevertheless, a number of limitations of the base-mediated MPV reduction remain unaddressed including a limited scope and the reliance on *i*-PrOH as the solvent and hydride source.[15] Additionally, no examples of stereoselective base-mediated MPV reactions exist. We report the use of a simple potassium alkoxide reductant, generated in situ from the corresponding alcohol and K_3PO_4, for the reduction of a wide range of aromatic ketones. This methodology is tolerant of heterocycles, scalable, and shows potential for the asymmetric reduction of alkyl–aryl ketones.

2.3 Reaction Discovery and Optimization

To initiate our studies, we examined the reduction of dihydrochalcone (**2.1**) using alkyl–alkyl secondary alcohols and K_3PO_4, a readily available and mild base (Table 2.1).[16] Subjecting **2.1** to catalytic K_3PO_4 using isopropanol or 3-pentanol (**2.3**) (2.5 equivalents) in 1,4-dioxane at 80 °C provided none of the desired alcohol product **2.2** (entries 1 and 2).[16,17,18] Owing to the potential reversibility of the reaction,[1a–c,16] we turned to the use of aryl–alkyl reductants to bias the reaction equilibrium. Importantly, this class of alcohol enabled a greater control of the redox properties of the reductant. We evaluated alcohol **2.4** and the more electron-rich derivative **2.5** as reductants,[19] anticipating that the stability of the respective aryl ketone and doubly vinylogous amide byproducts would drive the forward reaction to yield **2.2**. Gratifyingly, the use of 2.5 equivalents of **2.4** or **2.5** provided **2.2** in 40% and 61% yield, respectively (entries 3 and 4). Employing reductant **2.5** at 120 °C furnished desired product **2.2** in 92% yield (entry 5). Finally, alcohol **2.2** was obtained in near quantitative yield by utilizing excess base (entry 6).

Table 2.1. Optimization of reaction conditions

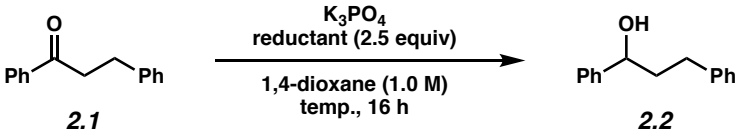

2.1 *2.2*

Entry	Reductant	Equiv K_3PO_4	Temp (°C)	Yield[a]
1	*i*-PrOH	0.50	80	0%
2	3	0.50	80	0%
3	4	0.50	80	40%
4	5	0.50	80	61%
5	5	0.50	120	92%
6	5	4.0	120	99%

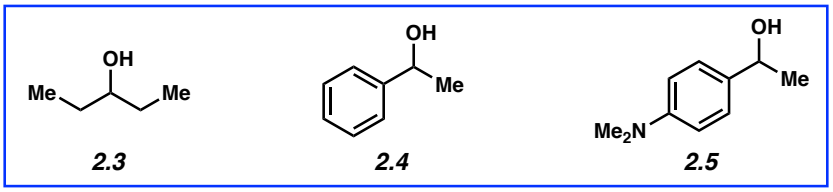

2.3 *2.4* *2.5*

[a]General conditions unless otherwise stated: substrate **2.1** (1.0 equiv, 0.10 mmol), K_3PO_4 (0.50–4.0 equiv), reductant (2.5 equiv), and 1,4-dioxane (1.0 M) heated at 80–120 °C for 16 h in a sealed vial under an atmosphere of N_2. Yields determined by ^1H NMR analysis using 1,3,5-trimethoxybenzene as an external standard.

2.4 Scope of Methodology

With optimized conditions in hand, we examined a range of aryl ketone substrates in the reduction (Figure 2.2). Linear and α-branched substrates smoothly underwent reduction, giving rise to alcohols **2.2** and **2.6**–**2.8** in good yields. Of note, steric bulk on the alkyl substituent of the ketone was tolerated, as shown by the successful reduction of *tert*-butyl phenyl ketone to furnish alcohol **2.8** in 83% yield. The reduction of α-tetralone to give α-tetralol (**2.9**) in 86% yield demonstrates competence of a cyclic ketone substrate in this transformation. Notably, we found that electron-rich aromatic ketones and those highly decorated with heteroatom substituents underwent facile reduction, as demonstrated by the formation of alcohols **2.10** and **2.11** in 81%

and 87% yield, respectively. Finally, both electron-rich and electron-deficient benzophenone derivatives were suitable substrates, as shown by the production of alcohol products **2.12** and **2.13** in good yields.

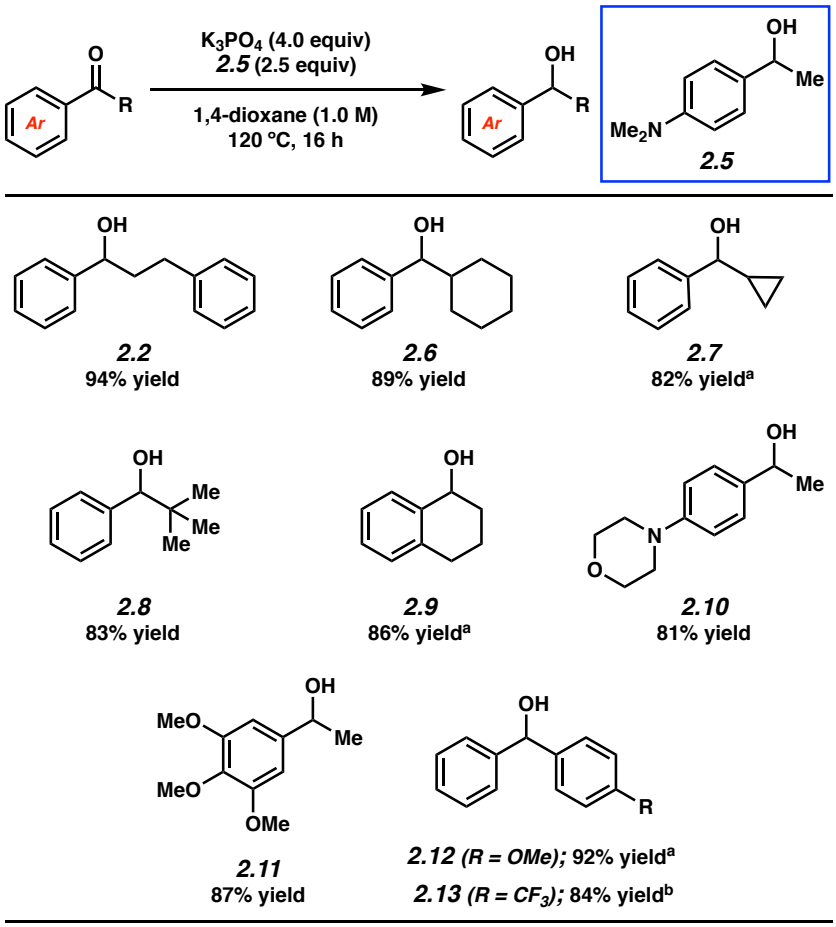

Figure 2.2. Scope of the base-mediated MPV reduction of aromatic ketones. Conditions: substrate (1.0 equiv, 0.10 mmol), K_3PO_4 (4.0 equiv), reductant (2.5 equiv), and 1,4-dioxane (1.0 M) heated at 120 °C for 16 h in a sealed vial under an atmosphere of N_2. Unless otherwise noted, yields reflect the average of two isolation experiments. [a]Yield determined by ^{1}H NMR analysis using hexamethylbenzene as an external standard. [b]Reaction heated at 80 °C for 16 h.

We next set out to evaluate the reactivity of a number of heterocyclic ketone substrates, as only a handful of examples of base-mediated MPV reductions of heterocyclic ketones have been previously reported (Figure 2.3).[20] Benzofuran- and dibenzofuran-containing ketones underwent

reduction to provide alcohols **2.14** and **2.15** in 73% and 76% yield, respectively. Benzodioxole and benzodioxane moieties were also well tolerated, as seen by the formation of alcohols **2.16** and **2.17** in good yields. Lastly, ketones bearing thiophenes were successfully employed, as judged by the formation of benzothiophene **2.18** and tetrahydrobenzothiophene **2.19** in 70% and 73% yield, respectively.[21]

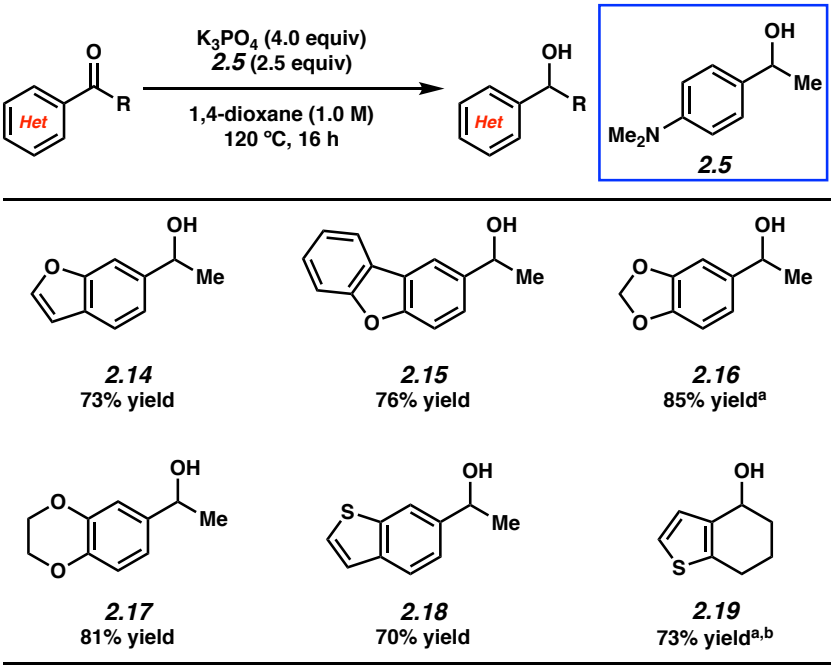

Figure 2.3. Scope of the base-mediated MPV reduction of heteroaromatic ketones. Conditions: substrate (1.0 equiv, 0.10 mmol), K_3PO_4 (4.0 equiv), reductant (2.5 equiv), and 1,4-dioxane (1.0 M) heated at 120 °C for 16 h in a sealed vial under an atmosphere of N_2. Unless otherwise noted, yields reflect the average of two isolation experiments. [a]Yield determined by ^1H NMR analysis using hexamethylbenzene as an external standard. [b]Reaction heated at 130 °C for 16 h.

2.5 Gram-Scale and Stereospecific Reductions

As a demonstration of the utility of the base-mediated MPV reduction of ketones, we performed the additional studies shown in Figure 2.4. In the first, we performed a gram-scale reduction of acetyldibenzofuran **2.20**.[22] Carrying out the reaction at 130 °C for 24 h delivered alcohol **2.15** in 66% yield, thus demonstrating the scalability of this methodology. Next, we

questioned whether this reaction could be used for the synthesis of enantioenriched alcohols. Toward this end, we performed the reduction of phenylcyclohexyl ketone **2.21** using enantioenriched (*R*)-**2.5**. This proceeded to give alcohol (*S*)-**2.6** with 50% stereochemical transfer (96% *ee* of (*R*)-**2.5** → 48% *ee* (*S*)-**2.6**. This result underscores the potential of the base-mediated MPV reduction to generate enantioenriched products.[1e,12d,23]

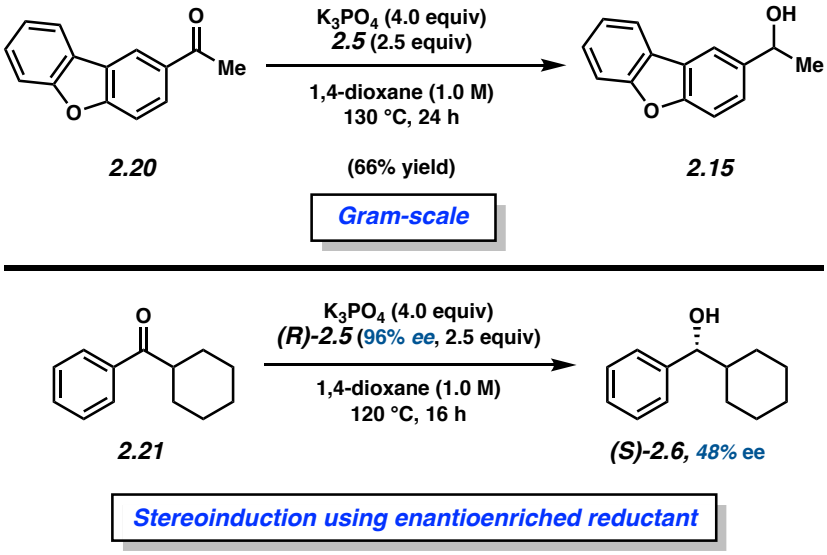

Figure 2.4. Gram-scale reduction and stereochemical transfer studies demonstrating the synthetic utility of the base-mediated MPV reduction. Conditions: substrate (1.0 equiv), K_3PO_4 (4.0 equiv), reductant (2.5 equiv), and 1,4-dioxane (1.0 M) heated at the indicated temperature and time in a sealed vial under an atmosphere of N_2.

2.6 Conclusion

In summary, we have developed the base-mediated MPV reduction of aromatic and heteroaromatic ketones. This methodology employs the simple combination of K_3PO_4 as a mild base and secondary alcohol **2.5** as the reductant. The transformation is tolerant of a range of ketone substrates, including *O*- and *S*-containing heterocycles, and avoids the hydride source being used as the solvent. The reduction has been demonstrated on gram scale and shows potential to be used

as platform to provide enantioenriched products. These studies provide a general platform for achieving the reduction of ketones under mildly basic MPV conditions and offer an alternative protocol to the more classic Al-based MPV reduction. We hope this study will enable the greater utilization of the uncommon base-mediated variant of the MPV reduction in chemical synthesis.

2.7 Experimental Section

2.7.1 Materials and Methods

Unless stated otherwise, reactions were conducted in flame-dried glassware under an atmosphere of nitrogen or argon and commercially obtained reagents were used as received. Not-commercially available ketone substrates were synthesized following protocols specified in Section A in the Experimental Procedures. Alcohols **2.5** and (*R*)-**2.5** were synthesized following protocols specified in Section B and C in the Experimental Procedures, respectively. 1,2-Dicholoroethane, 1,4-dioxane, and isopropanol were obtained from Fischer Scientific and purified by distillation. 3-Pentanol (**2.3**) and 1-phenylethanol (**2.4**) were obtained from Sigma-Aldrich and purified by distillation. Prior to use, 1,4-dioxane, isopropanol, 3-pentanol (**2.3**) and 1-phenylethanol (**2.4**) were degassed by sparging with N_2 for 1 h. Ketone **2.1**[24] and **2.36**[25] were prepared according to literature procedures. **2.22**, **2.28**, **2.29**, **2.30**, **2.31**, and **2.34** were obtained from Sigma-Aldrich. **2.26**, **2.21**, **2.27**, **2.32**, **2.35**, and **2.37** was obtained from Combi-Blocks. Ketone **2.26** was obtained from Oxchem. Ketone **2.33** was obtained from Alfa Aesar. $Pd(PPh_3)_4$ (99%) was obtained from Strem Chemicals. Acetyltrimethylsilane (**2.23**) (97%) was obtained from Sigma-Aldrich. Cesium fluoride (99%+) was obtained from Strem Chemicals. Potassium phosphate (K_3PO_4) was obtained from Acros. Reaction temperatures were controlled using an IKAmag temperature modulator, and unless stated otherwise, reactions were performed at room temperature (approximately 23 °C). Thin-layer chromatography (TLC) was conducted with EMD gel 60 F254 pre-coated plates (0.25 mm for analytical chromatography and 0.50 mm for preparative chromatography) and visualized using a combination of UV, anisaldehyde, iodine, and potassium permanganate staining techniques. Silicycle Siliaflash P60 (particle size 0.040–0.063 mm) was used for flash column chromatography. ^{1}H NMR spectra were recorded on Bruker

spectrometers (at 300, 400, 500, and 600 MHz) and are reported relative to residual solvent signals. Data for ^{1}H NMR spectra are reported as follows: chemical shift (δ ppm), multiplicity, coupling constant (Hz), integration. Data for ^{13}C NMR are reported in terms of chemical shift (at 75 and 125 MHz). IR spectra were recorded on a Perkin-Elmer UATR Two FT-IR spectrometer and are reported in terms of frequency absorption (cm^{-1}). DART-MS spectra were collected on a Thermo Exactive Plus MSD (Thermo Scientific) equipped with an ID-CUBE ion source and a Vapur Interface (IonSense Inc.). Both the source and MSD were controlled by Excalibur software v. 3.0. The analyte was spotted onto OpenSpot sampling cards (IonSense Inc.) using $CHCl_3$ or CH_2Cl_2 as the solvent. Ionization was accomplished using UHP He plasma with no additional ionization agents. The mass calibration was carried out using Pierce LTQ Velos ESI (+) and (–) Ion calibration solutions (Thermo Fisher Scientific). Optical rotations were measured with a Rudolf Autopol III Automatic Polarimeter. Trace metal analysis was determined by inductively coupled plasma mass spectrometry on an Agilent 8800 Triple Quadrupole ICP-MS instrument. The level of all analytes of interest was determined in MS/MS mode, measured using He in the collision/reaction cell using an environmental calibration standard (elements not included in this standard: B, Ti, Rb, Ru, Rh, Pd, Ir, and Pt). The quantification was done using the ICP-MS MassHunter WorkStation v4.3, through the QuickScan acquisition. Nitric acid was obtained from Fisher Scientific (A467500). Determination of enantiopurity was carried out on a Mettler Toledo SFC (supercritical fluid chromatography) or Agilent HPLC (high performance liquid chromatography) using Daicel ChiralPak IC–3 and Daicel ChiralPak OD–H columns. Data for SFC and HPLC spectra are reported in enantiomeric excess (ee). For SFC and HPLC chromatograms see Section 2.7.2.9 of Experimental Procedures.

2.7.2 Experimental Procedures

2.7.2.1 Syntheses of Ketone Substrates

Representative Procedure for the Synthesis of Ketone Substrates (synthesis of ketone 2.24 is used as an example).

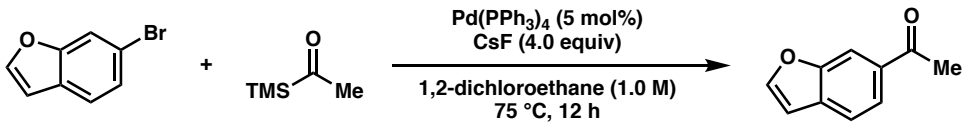

2.22 *2.23* *2.24*

Ketone 2.24. A flame-dried 1-dram vial was charged 6-bromobenzofuran (**2.22**) (130 mg, 0.660 mmol, 1.00 equiv) and a magnetic stir bar. In the glove box, CsF (401 mg, 2.64 mmol, 4.00 equiv) and $Pd(PPh_3)_4$ (38.1 mg, 0.0330 mmol, 0.0500 equiv) were added to the vial. The vessel was removed from the glove box and placed under an atmosphere of N_2 on the bench. Distilled 1,2-dichloroethane (0.700 mL, 1.00 M) and silane **2.23** (189 µL, 1.32 mmol, 2.0 equiv) were added and the vial was sealed with a Teflon-lined screw cap. The heterogeneous mixture was heated to 75 ºC for 12 h. After cooling to 23 ºC, the mixture was diluted with hexanes (0.5 mL), filtered over a plug of silica gel (1.00 cm OD x 5.00 cm, 10 mL EtOAc eluent), and the volatiles were removed under reduced pressure. The crude residue was purified by flash chromatography (19:1 Hexanes:EtOAc → 14:1 Hexanes:EtOAc) to yield ketone **2.24** (57.0 mg, 54% yield) as a yellow oil. Ketone **2.24**: R_f 0.42 (5:1 Hexanes:EtOAc); ^{1}H NMR (600 MHz, $CDCl_3$): δ 8.13 (s, 1H), 7.89 (dd, *J* = 8.30, 1.38 Hz, 1H), 7.79 (d, *J* = 2.17 Hz, 1H), 7.66 (d, *J* = 8.30 Hz, 1H), 6.87–6.89 (m, 1H), 2.67 (s, 3H); ^{13}C NMR (125 MHz, $CDCl_3$): δ 197.8, 154.8, 148.4, 134.0, 132.0, 123.3, 121.2, 112.0, 107.0, 27.0; IR (film): 3118, 3003, 1673, 1425, 1271 cm^{-1}; HRMS-APCI (*m/z*) $[M+NH_4]^+$ calcd for $C_{10}H_{12}O_2N^+$, 178.08626; found 178.08536.

Note: Supporting information for the synthesis of ketone **2.36** has previously been reported.[25] The synthesis of the remaining substrate, **2.20**, is as follows:

Any modifications of the conditions shown in the representative procedure above are specified in the following scheme.

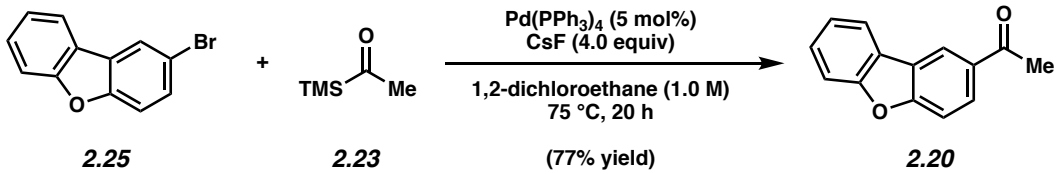

2.25 ***2.23*** **(77% yield)** ***2.20***

Ketone 2.20. Purification by flash chromatography (49:1 Hexanes:EtOAc) generated ketone **2.20** (263 mg, 77% yield) as a white solid. Ketone **2.20**: R_f 0.33 (9:1 Hexanes:EtOAc). Spectral data match those previously reported.[26]

2.7.2.2 Syntheses of Alcohol Reductant 2.5

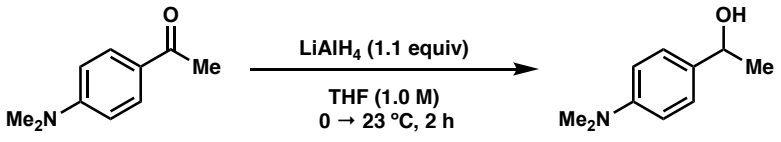

2.26 **(93% yield)** ***2.5***

To a flame-dried flask equipped with a magnetic stir bar was added $LiAlH_4$ (2.56 g, 67.4 mmol, 1.10 equiv) in a glovebox. The flask was removed from the glovebox, THF (61.0 mL) was added, and the solution was cooled to 0 °C. To the solution was then added ketone **2.26** (2.00 g, 61.5 mmol each, 0.200 equiv) in 5 aliquots over 25 min. The reaction was then warmed to 23 °C. After stirring for 2 h, the reaction was cooled to 0 °C and quenched by the sequential addition of deionized water (5 mL), 10% aq. NaOH (7 ml), MeOH (20 mL), and deionized water (10 mL).

The mixture was then warmed to 23 °C and stirred for 30 min. The mixture was then filtered over a pad of celite (100 mL EtOAc eluent). The resulting organic layer was dried over Na_2SO_4, filtered, and the volatiles were removed under reduced pressure. The crude residue was purified by flash chromatography (5:1 Hexanes:EtOAc → 3:1 Hexanes:EtOAc) to yield alcohol **2.5** (9.42 g, 93% yield) as a white solid. Alcohol **2.5**: R_f 0.33 (3:1 Hexanes:EtOAc). Spectral data match those previously reported.[27]

2.7.2.3 Syntheses of Enantioenriched Alcohol Reductant (*R*)-2.5

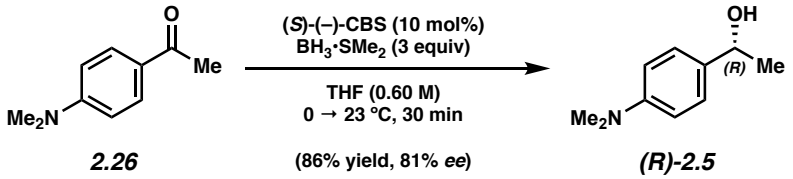

2.26 (86% yield, 81% *ee*) *(R)-2.5*

To a flame-dried flask equipped with a magnetic stir bar was added (S)-(–)-CBS catalyst (170 mg, 0.613 mmol, 0.100 equiv). The flask was removed from the glovebox and THF (6.13 mL) was added. Next, **2.26** (1.00 g, 6.13 mmol, 1.00 equiv) in a solution of THF (2.50 mL) was added to the reaction flask, which was then stirred to give a clear homogeneous solution and cooled to 0 °C. Subsequently, BH_3•SMe_2 (1.70 mL, 18.4 mmol, 3.00 equiv) was added (1 drop/2 sec) over 7.50 min. The reaction was stirred at 0 °C for 2 min, then warmed to 23 °C. After stirring for 30 min, the reaction was cooled to 0 °C and quenched by the dropwise addition of methanol (20 mL) and water (20 mL) and diluted with Et_2O (50 mL). The layers were separated and the aqueous layer was extracted with Et_2O (3 x 50 mL). The combined organic layers were washed with sat. aq. NH_4Cl (80 mL), sat. aq. $NaHCO_3$ (80 mL), and brine (80 mL). The organic layer was then dried over Na_2SO_4, filtered, and the volatiles were removed under reduced pressure. The crude residue was purified by flash chromatography (10:1 Hexanes:EtOAc → 3:1 Hexanes:EtOAc) to yield

alcohol (*R*)-**2.5** (871 mg, 86% yield, 81% ee) as a white solid. Alcohol (*R*)-**2.5**: R_f 0.33 (3:1 Hexanes:EtOAc). The spectral data match those previously reported in the literature for *rac*-**2.5**.[27] The SFC data match those reported in the Experimental Procedures Section 2.7.2.7.

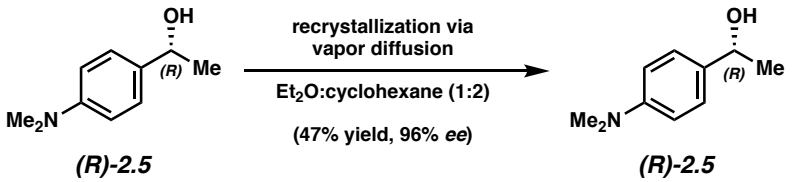

A solution of (*R*)-**2.5** (25.0 mg, 0.151 mmol, 1.00 equiv) in Et_2O (1.00 mL) was filtered through a 0.45 μm Millipore Millex PTFE filter into a 1-dram vial. The vial was then placed within a 20 mL scintillation vial containing cyclohexane (2.00 mL). The scintillation vial was sealed and allowed to stand at 23 °C for 24 h, which led to the formation of white crystals. This vapor diffusion crystallization process was repeated three times to lead to the recovery of alcohol (*R*)-**2.5** (11.8 mg, 47% yield, 96% ee) as a white crystalline solid. $[\alpha]_D^{23.1} = +51.6$ ($c = 1.00$, $CHCl_3$). The spectral data match those previously reported in the literature for *rac*-**2.5**.[27] The major enantiomer product was assigned by comparison to published $[\alpha]_D$ values for (*R*)-**2.5**.[28]

2.7.2.4 Initial Survey of Reaction Conditions and Relevant Control Experiments

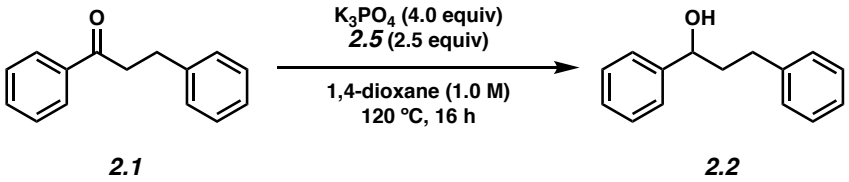

Representative Procedure for Base-Mediated MPV Reduction from Table 2.2 (reduction of ketone 2.1 with alcohol 2.5 is used as an example). A 1-dram vial was charged with anhydrous powdered K_3PO_4 (85.0 mg, 0.400 mmol, 4.00 equiv) and a magnetic stir bar. The vial and its

contents were flame-dried under reduced pressure, then allowed to cool under N_2. Ketone substrate **2.1** (21.0 mg, 0.100 mmol, 1.00 equiv) and alcohol reductant **2.5** (41.3 mg, 0.250 mmol, 2.50 equiv) were added. The vial was flushed with N_2, and then 1,4-dioxane (0.100 mL, 1.00 M) was added. Under a stream of N_2, the vial septum cap was quickly switched for a Teflon-lined screw cap, sealed, then further sealed with electrical tape. The reaction was stirred vigorously (800 rpm) at 120 °C for 16 h. After cooling to 23 °C, the mixture was diluted with hexanes (0.5 mL) and filtered over a plug of silica gel (1 cm OD x 5 cm, 10 mL EtOAc eluent). The volatiles were removed under reduced pressure and the yield of alcohol **2.2** was determined by ^{1}H NMR analysis with 1,3,5-trimethoxybenzene as an external standard.

Any modifications of the conditions shown in the representative procedure above are specified below in Table 2.2.

Table 2.2. Survey of reaction conditions and relevant control experiments

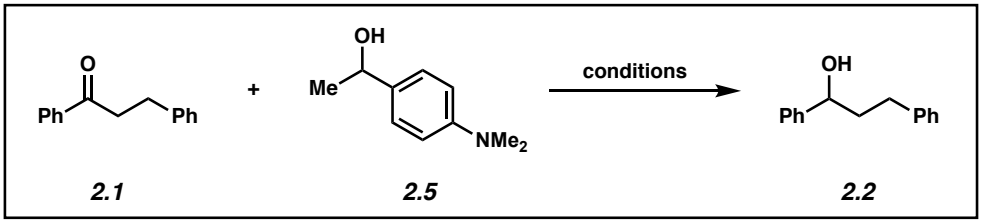

Reaction Conditions	Experimental Results[a] 2.1	2.2
2.5 (2.5 equiv), K_3PO_4 (4.0 equiv), dioxane (1.0 M), 120 °C, 16 h	0%	99%
2.5 (2.5 equiv), K_3PO_4 (4.0 equiv), dioxane (1.0 M), 80 °C, 16 h	0%	99%
2.5 (2.5 equiv), K_3PO_4 (4.0 equiv), dioxane (1.0 M), 120 °C, 3 h	<5%	98%
2.5 (2.5 equiv), K_3PO_4 (4.0 equiv), 2-Me THF (1.0 M), 80 °C, 16 h	0%	99%
2.5 (2.5 equiv), K_3PO_4 (4.0 equiv), *t*-amyl alcohol (1.0 M), 80 °C, 16 h	<5%	98%
2.5 (2.5 equiv), K_3PO_4 (4.0 equiv), *n*-heptane (1.0 M), 80 °C, 16 h	11%	89%
Control Experiments:		
2.5 (2.5 equiv), K_3PO_4 (4.0 equiv), dioxane (1.0 M), 120 °C, 16 h *Ran in the dark*	0%	99%
2.5 (2.5 equiv), K_3PO_4 (4.0 equiv), H_2O (2.0 equiv), dioxane (1.0 M), 120 °C, 16 h	<5%	95%
2.5 (2.5 equiv), K_3PO_4 (4.0 equiv), dioxane (1.0 M), 120 °C, 16 h *Ran under an atmosphere of air*	12%	88%

[a]Yields were determined by ^{1}H NMR analysis using 1,3,5-trimethoxybenzene as an external standard.

2.7.2.5 Trace Metal Analysis of Reagents

Representative Procedure for Trace Metal Analysis (preparation of K_3PO_4 is used as an example). A 15-mL conical tube was charged with K_3PO_4 (95.2 mg, 1.00 equiv) and the sample was diluted with milli-Q water (6.8 mL) to a final concentration of 1.4% (w/w). Subsequently, ICP-MS-grade 70% nitric acid (200 µl) was added to each sample (2% final nitric acid concentration).

Table 2.3. Trace metal analysis of K_3PO_4

Sample: K_3PO_4	
Metal	**Concentration (ppm) (average of two samples)**
Fe	0.00809
Al	0.000
Co	0.000
B	0.0240
Ti	0.0420
Mg	0.00189
Mn	7.84×10^{-5}
Sc	0.000
Rb	0.203
Ni	0.0303
Cu	0.000
Zn	0.000
Ru	9.46×10^{-6}
Rh	0.000
Pd	1.53×10^{-5}
Ag	0.000
Ir	1.17×10^{-6}
Pt	0.000

Table 2.4. Trace metal analysis of 1,4-dioxane

Sample: 1,4-dioxane	
Metal	**Concentration (ppm) (average of two samples)**
Fe	0.00369
Al	0.00384
Co	0.000130
B	0.00570
Ti	0.00250
Mg	0.01780
Mn	0.000151
Sc	0.00190
Rb	3.41×10^{-5}
Ni	0.354
Cu	0.000
Zn	0.000
Ru	0.000
Rh	0.000
Pd	1.06×10^{-5}
Ag	2.85×10^{-5}
Ir	0.000
Pt	0.000

Table 2.5. Trace metal analysis of alcohol reductant **2.5**

Sample: Alcohol Reductant 2.5	
Metal	**Concentration (ppm) (average of two samples)**
Fe	0.00352
Al	0.00121
Co	3.20×10^{-5}
B	0.0211
Ti	0.000642
Mg	0.0125
Mn	1.81×10^{-5}
Sc	0.000962
Rb	5.15×10^{-6}
Ni	0.113
Cu	0.000
Zn	0.000
Ru	0.000
Rh	9.31×10^{-7}
Pd	3.00×10^{-6}
Ag	7.91×10^{-6}
Ir	0.000
Pt	1.76×10^{-6}

2.7.2.6 Scope of Methodology

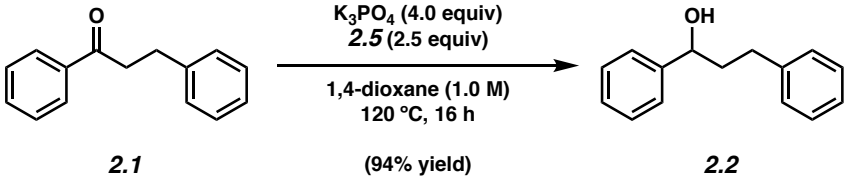

Representative Procedure for Base-Mediated MPV Reduction from Figure 2.2 (reduction of ketone 2.1 with alcohol 2.5 is used as an example). Alcohol 2.2. A 1-dram vial was charged with anhydrous powdered K_3PO_4 (85.0 mg, 0.400 mmol, 4.00 equiv) and a magnetic stir bar. The vial and its contents were flame-dried under reduced pressure, then allowed to cool under N_2. Ketone substrate **2.1** (21.0 mg, 0.100 mmol, 1.00 equiv) and alcohol reductant **2.5** (41.3 mg, 0.250 mmol, 2.50 equiv) were added. The vial was purged with N_2, and then 1,4-dioxane (0.100 mL, 1.00 M) was added. Under a stream of N_2, the vial septum cap was quickly switched for a Teflon-lined screw cap, sealed, then further sealed with electrical tape. The reaction was stirred vigorously (800 rpm) at 120 °C for 16 h. After cooling to 23 °C, the reaction was quenched by the addition of sat. aq. NH_4Cl (1.00 mL) and diluted with EtOAc (2.00 mL) and the layers were separated. The aqueous layer was extracted with EtOAc (3 x 2.00 mL) and the combined organic layers were passed through a plug (1.00 cm OD) of silica gel (3.00 cm tall) and Na_2SO_4 (3.00 cm tall) using EtOAc (10.0 mL) as eluent. The volatiles were removed under reduced pressure. The crude residue was purified by flash chromatography (99:1 Hexanes:EtOAc → 19:1 Hexanes:EtOAc) to yield alcohol **2.2** (20 mg, 94% yield, average of two experiments) as a clear oil. Alcohol **2.2**: R_f 0.32 (5:1 Hexanes:EtOAc). ^{1}H NMR (500 MHz, $CDCl_3$): δ 7.41–7.33 (m, 4H), 7.32–7.26 (m, 3H), 7.23–7.16 (m, 3H), 4.78–4.61 (m, 1H), 2.85–2.61 (m, 2H), 2.23–1.97 (m, 2H), 1.87 (d, J = 3.5 Hz, 1H). Spectral data match those previously reported.[29]

Any modifications of the conditions shown in the representative procedure above are specified in the following schemes, which depict all of the results shown in Figures 2.2 and 2.3.

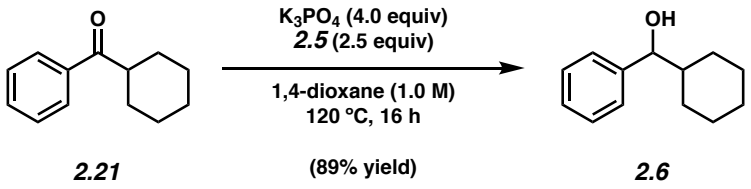

Alcohol 2.6. Purification by flash chromatography (99:1 Hexanes:EtOAc → 19:1 Hexanes:EtOAc) generated alcohol **2.6** (17 mg, 89% yield, average of two experiments) as a crystalline white solid. Alcohol **2.6**: R_f 0.39 (5:1 Hexanes:EtOAc).). ^{1}H NMR (500 MHz, $CDCl_3$): δ 7.38–7.25 (m, 5H), 4.37 (dd, *J* = 7.2 Hz, 3.3 Hz, 1H), 2.03–1.92 (m, 1H), 1.84–1.72 (m, 2H), 1.71–1.57 (m, 3H), 1.41–1.33 (m, 1H), 1.29–1.00 (m, 4H), 0.99–0.87 (m, 1H). Spectral data match those previously reported.[30]

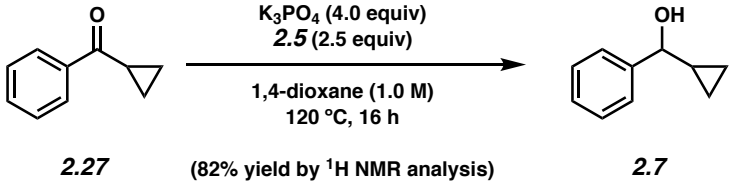

Alcohol 2.7. ^{1}H NMR analysis of the crude reaction mixture indicated an 82% yield of alcohol **2.7** relative to hexamethylbenzene external standard (average of two experiments). Purification by preparative thin-layer chromatography (3:1 Hexanes:EtOAc) provided an analytical sample of alcohol **2.7** as a clear oil. Alcohol **2.7**: R_f 0.30 (5:1 Hexanes:EtOAc). ^{1}H NMR (500 MHz, $CDCl_3$): δ 7.46–7.40 (m, 2H), 7.39–7.33 (m, 2H), 7.32–7.27 (m, 1H), 4.02 (dd, *J* = 8.3, 3.0, 1H), 1.90 (d, *J*

= 3.0, 1H), 1.28–1.18 (m, 1H), 0.69–0.61 (m, 1H), 0.60–0.52 (m, 1H), 0.52–0.44 (m, 1H), 0.42–0.34 (m, 1H). Spectral data match those previously reported.[31]

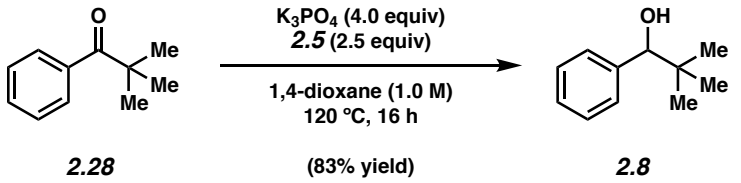

Alcohol 2.8. Purification by flash chromatography (24:1 Hexanes:EtOAc) generated alcohol **2.8** (14 mg, 83% yield, average of two experiments) as a white crystalline solid. Alcohol **2.8**: R_f 0.52 (5:1 Hexanes:EtOAc). ^{1}H NMR (500 MHz, $CDCl_3$): δ 7.35–7.30 (m, 4H), 7.29–7.26 (m, 1H), 4.40 (d, J = 2.8, 1H), 1.84 (d, J = 2.8, 1H), 0.93 (s, 9H). Spectral data match those previously reported.[32]

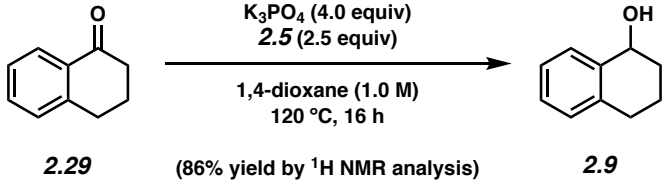

Alcohol 2.9. ^{1}H NMR analysis of the crude reaction mixture indicated an 86% yield of alcohol **2.9** relative to hexamethylbenzene external standard (average of two experiments). Purification by preparative thin-layer chromatography (9:1 PhH:Acetone) provided an analytical sample of alcohol **2.9** as a clear oil. Alcohol **2.9**: R_f 0.50 (9:1 PhH:Acetone). ^{1}H NMR (500 MHz, $CDCl_3$): δ 7.48–7.39 (m, 1H), 7.24–7.17 (m, 2H), 7.14–7.05 (m, 1H), 4.84–4.71 (m, 1H), 2.88–2.78 (m, 1H), 2.87–2.67 (m, 1H), 2.05–1.95 (m, 2H), 1.95–1.87 (m, 1H), 1.85–1.73 (m, 1H), 1.71–1.60 (m, 1H). Spectral data match those previously reported.[33]

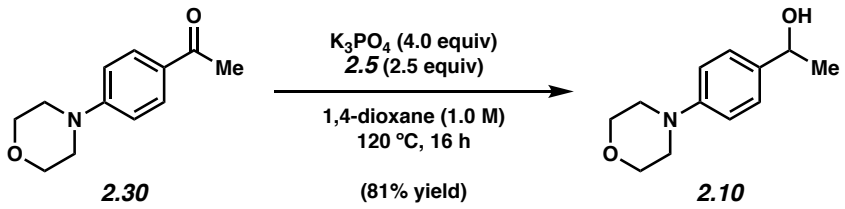

Alcohol 2.10. Purification by flash chromatography (2:2:1 CH_2Cl_2:Et_2O:Hexanes) generated alcohol **2.10** (17 mg, 81% yield, average of two experiments) as a pale yellow solid. Alcohol **2.10**: R_f 0.24 (1:1:1 CH_2Cl_2:Et_2O:Hexanes). ^{1}H NMR (500 MHz, $CDCl_3$): δ 7.33–7.28 (m, 2H), 6.93–6.87 (m, 2H), 4.85 (dq, J = 6.4, 3.5, 1H), 3.90–3.83 (m, 4H), 3.19–3.12 (m, 4H), 1.67 (d, J = 3.5, 1H), 1.48 (d, J = 6.4, 3H). Spectral data match those previously reported.[34]

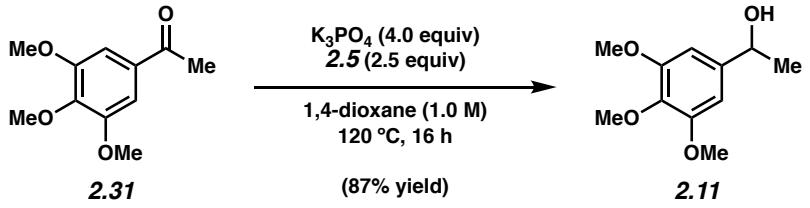

Alcohol 2.11. Purification by flash chromatography (9:1 Hexanes:EtOAc → 2:1 Hexanes:EtOAc) generated alcohol **2.11** (18 mg, 87% yield, average of two experiments) as a clear oil. Alcohol **2.11**: R_f 0.33 (1:1 Hexanes:EtOAc). ^{1}H NMR (500 MHz, $CDCl_3$): δ 6.60 (s, 2H), 4.89–4.77 (m, 1H), 3.86 (s, 6H), 3.83 (s, 3H), 1.99–1.80 (m, 1H), 1.48 (d, J = 6.4, 3H). Spectral data match those previously reported.[34]

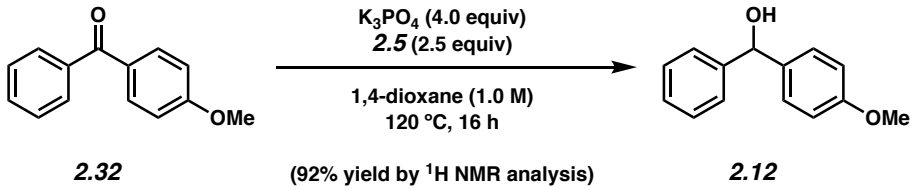

Alcohol 2.12. ^{1}H NMR analysis of the crude reaction mixture indicated a 92% yield of alcohol **2.12** relative to hexamethylbenzene external standard (average of two experiments). Purification by preparative thin-layer chromatography (3:3:2 CH_2Cl_2:Et_2O:Hexanes) provided an analytical sample of alcohol **2.12** as a pale yellow solid. Alcohol **2.12**: R_f 0.70 (1:1:1 CH_2Cl_2:Et_2O:Hexanes). ^{1}H NMR (500 MHz, $CDCl_3$): δ 7.40–7.31 (m, 4H), 7.31–7.23 (m, 3H), 6.93–6.81 (m, 2H), 5.82 (d, J = 3.0, 1H), 3.79 (s, 3H), 2.15 (d, J = 3.4, 1H). Spectral data match those previously reported.[30]

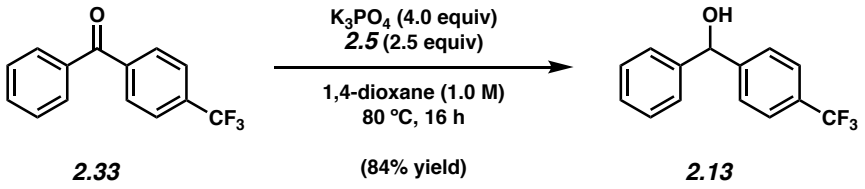

Alcohol 2.13. Purification by flash chromatography (9:1 Hexanes:Et_2O → 3:1 Hexanes:Et_2O) generated alcohol **2.13** (21 mg, 84% yield, average of two experiments) as a clear oil. Alcohol **2.13**: R_f 0.30 (5:1 Hexanes:Et_2O). ^{1}H NMR (500 MHz, $CDCl_3$): δ 7.60 (d, J = 8.3, 2H), 7.51 (d, J = 8.3, 2H), 7.42–7.34 (m, 4H), 7.34–7.28 (m, 1H), 5.88 (s, 1H), 2.46–2.32 (m, 1H). Spectral data match those previously reported.[30]

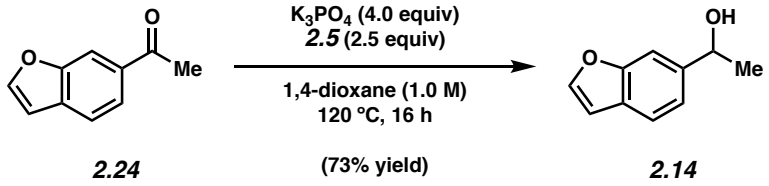

Alcohol 2.14. Purification by flash chromatography (90:9:1 → 15:9:1 Hexanes:PhH:Acetone) generated alcohol **2.14** (12 mg, 73% yield, average of two experiments) as a yellow oil. Alcohol **2.14**: R_f 0.39 (9:1 PhH:Acetone); ^{1}H NMR (500 MHz, C_6D_6): δ 7.50–7.46 (m, 1H), 7.35 (d, J = 8.1 Hz, 1H), 7.12 (ddd, J = 8.1, 1.4, 0.5 Hz, 1H), 6.35 (dd, J = 2.2, 1.1 Hz, 1H), 4.59 (q, J = 6.5 Hz, 1H), 1.29 (d, J = 6.5 Hz, 3H), 1.14, (br s, 1H); ^{13}C NMR (125 MHz, $CDCl_3$): δ 155.3, 145.4, 142.8, 126.9, 121.2, 120.6, 108.4, 106.5, 70.7, 25.6; IR (film): 3350, 2972, 2926, 1430, 1265 cm^{-1}; HRMS-APCI (*m/z*) $[M + H]^+$ calcd for $C_{10}H_{11}O_2^+$, 163.0754; found 163.0746.

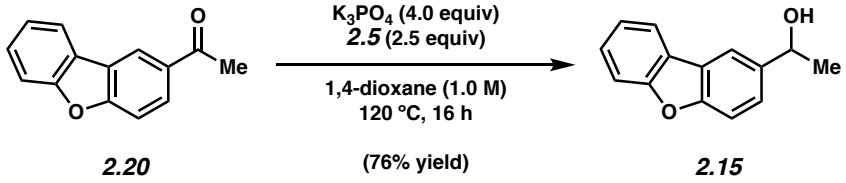

Alcohol 2.15. Purification by flash chromatography (90:9:1 → 25:9:1 Hexanes:PhH:Acetone) generated alcohol **2.15** (16 mg, 76% yield, average of two experiments) as a yellow solid. Alcohol **2.15**: R_f 0.35 (9:1 PhH:Acetone). ^{1}H NMR (400 MHz, $CDCl_3$): δ 8.03–7.91 (m, 2H), 7.60–7.51 (m, 2H), 7.50–7.43 (m, 2H), 7.35 (td, J = 7.5, 1.0, 1H), 5.09 (dq, J = 6.4, 3.3, 1H), 1.90 (d, J = 3.3, 1H), 1.60 (d, J = 6.4, 3H). Spectral data match those previously reported.[35]

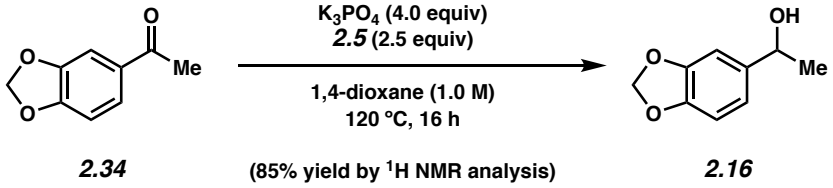

Alcohol 2.16. ^{1}H NMR analysis of the crude reaction mixture indicated an 85% yield of alcohol **2.16** relative to hexamethylbenzene external standard. Purification by preparative thin-layer chromatography (13:1:1 PhH:Et_2O:CH_3CN) provided an analytical sample of alcohol **2.16** as a yellow oil. Alcohol **2.16**: R_f 0.30 (13:1:1 PhH:Et_2O:CH_3CN); ^{1}H NMR (500 MHz, $CDCl_3$): δ 6.90 (s, 1H), 6.82 (dd, *J* = 8.1, 1.7 Hz, 1H), 6.77 (d, *J* = 8.1 Hz, 1H), 5.95 (s, 2H), 4.86–4.79 (m, 1H), 1.70 (d, *J* = 3.4 Hz, 1H), 1.46 (d, *J* = 6.4 Hz, 3H); ^{13}C NMR (125 MHz, $CDCl_3$): δ 147.9, 147.0, 140.1, 118.8, 108.2, 106.2, 101.1, 70.4, 25.3; IR (film): 3361, 2972, 2890, 1487, 1240 cm^{-1}; HRMS-APCI (*m/z*) $[M + H]^+$ calcd for $C_9H_{11}O_3^+$, 167.0703; found 167.0699.

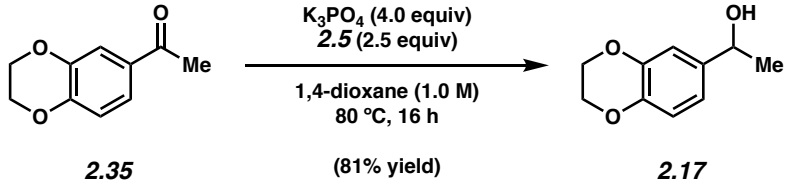

Alcohol 2.17. Purification by flash chromatography (98:1:1 → 28:1:1 PhH:Et_2O:CH_3CN) generated alcohol **2.17** (15 mg, 81% yield, average of two experiments) as a yellow oil. Alcohol **2.17**: R_f 0.32 (13:1:1 PhH:Et_2O:CH_3CN). ^{1}H NMR (500 MHz, $CDCl_3$): δ 6.92–6.88 (m, 1H), 6.86–6.81 (m, 2H), 4.80 (dq, *J* = 6.4, 3.6, 1H), 4.25 (s, 4H), 1.69 (d, *J* = 3.6, 1H), 1.46 (d, *J* = 6.4, 3H). Spectral data match those previously reported.[36]

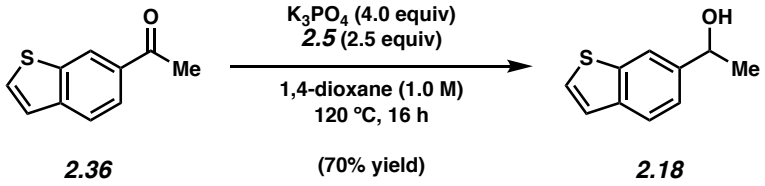

Alcohol 2.18. Purification by flash chromatography (90:9:1 → 40:9:1 Hexanes:PhH:Acetone) generated alcohol **2.18** (12 mg, 70% yield, average of two experiments) as a yellow oil. Alcohol **2.18**: R_f 0.38 (9:1 PhH:Acetone); ^{1}H NMR (500 MHz, $CDCl_3$): δ 7.91 (s, 1H), 7.80 (d, J = 8.2 Hz, 1H), 7.43 (d, J = 5.5 Hz, 1H), 7.38 (dd, J = 8.3, 1.3 Hz, 1H), 7.32 (d, J = 5.5 Hz, 1H), 5.10–5.0 (m, 1H), 1.85 (d, J = 3.4 Hz, 1H), 1.56 (d, J = 6.5 Hz, 3H); ^{13}C NMR (125 MHz, $CDCl_3$): δ 142.3, 140.1, 139.2, 126.6, 123.8, 123.7, 122.3, 119.2, 70.7, 25.5; IR (film): 3351, 2971, 1398, 1197, 1074 cm^{-1}; HRMS-APCI (*m/z*) $[M]^+$ calcd for $C_{10}H_{10}OS^+$, 178.0447; found 178.0437.

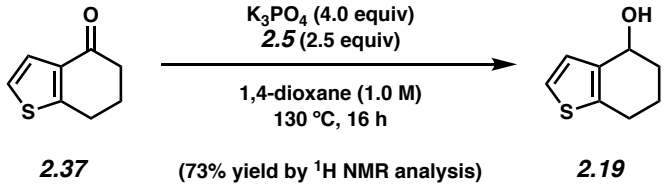

Alcohol 2.19. ^{1}H NMR analysis of the crude reaction mixture indicated a 73% yield of alcohol **2.19** relative to hexamethylbenzene external standard. Purification by preparative thin-layer chromatography (1:1:1 Hexanes:Et_2O:CH_2Cl_2) provided an analytical sample of alcohol **2.19** as a white crystalline solid. Alcohol **2.19**: R_f 0.48 (1:1:1 Hexanes:Et_2O:CH_2Cl_2); ^{1}H NMR (500 MHz, $CDCl_3$): δ 7.10 (dt, J = 5.2, 0.7 Hz, 1H), 7.03 (d, J = 5.2 Hz, 1H), 4.82–4.75 (m, 1H), 2.89–2.79 (m, 1H), 2.77–2.67 (m, 1H), 2.06–1.94 (m, 2H), 1.93–1.79 (m, 2H), 1.64 (d, J = 7.0 Hz 1H); ^{13}C NMR (125 MHz, $CDCl_3$): δ 139.0, 138.1, 126.7, 122.9, 65.6, 32.5, 25.2, 20.1; IR (film): 3235,

2936, 2921, 1431, 982 cm^{-1}; HRMS-APCI (*m/z*) $[M + H]^+$ calcd for $C_8H_{11}OS^+$, 155.0525; found 155.0521.

2.7.2.7 Gram-Scale Reduction

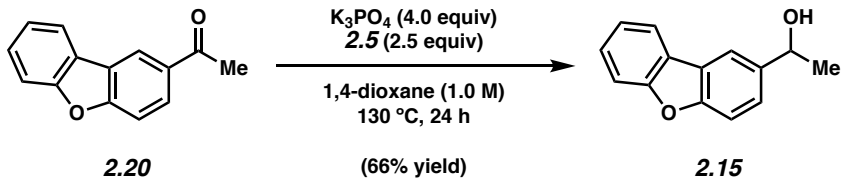

Alcohol 2.15. An 8-dram vial was charged with anhydrous powdered K_3PO_4 (4.04 g, 19.0 mmol, 4.00 equiv) and a magnetic stir bar. The vial and its contents were flame-dried under reduced pressure, then allowed to cool under N_2. Ketone substrate **2.20** (1.00 g, 4.76 mmol, 1.00 equiv) and alcohol reductant **2.5** (1.96 g, 11.9 mmol, 2.50 equiv) were then added. The vial was flushed with N_2 and subsequently 1,4-dioxane (4.76 mL, 1.00 M) was added. Under a stream of N_2, the vial septum cap was quickly switched for a Teflon-lined screw cap, sealed, then further sealed with electrical tape. The reaction was then stirred vigorously (800 rpm) at 130 °C for 24 h. After cooling to 23 °C, the reaction was quenched by the addition of sat. aq. NH_4Cl (8.00 mL) and diluted with EtOAc (6.00 mL) and the layers were separated. The aqueous layer was extracted with EtOAc (3 x 6.00 mL) and the combined organic layers were passed through a plug (1.00 cm OD) of silica gel (3.00 cm tall) and Na_2SO_4 (3.00 cm tall) using EtOAc (10.0 mL) as eluent. The volatiles were removed under reduced pressure. The crude residue was purified by flash chromatography (60:9:1 Hexanes:PhH:Acetone → 5:9:1 Hexanes:PhH:Acetone) to yield alcohol **2.15** (664 mg, 66% yield) as a yellow solid. Alcohol **2.15**: R_f 0.32 (5:1 Hexanes:EtOAc). Spectral data match those previously reported.[35]

2.7.2.8 Stereospecific Reduction

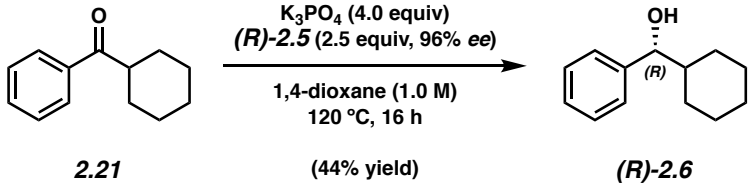

Alcohol (*R*)-2.6. A 1-dram vial was charged with anhydrous powdered K_3PO_4 (85.0 mg, 0.400 mmol, 4.00 equiv) and a magnetic stir bar. The vial and its contents were flame-dried under reduced pressure, then allowed to cool under N_2. Ketone substrate **2.21** (18.8 mg, 0.100 mmol, 1.00 equiv) and alcohol reductant (*R*)-**2.5** (41.3 mg, 0.250 mmol, 2.50 equiv) were added. The vial was purged with N_2 and subsequently, 1,4-dioxane (0.100 mL, 1.00 M) was added. Under a stream of N_2, the vial septum cap was quickly switched for a Teflon-lined screw cap, sealed, then further sealed with electrical tape. The reaction was stirred vigorously (800 rpm) at 120 °C for 16 h. After cooling to 23 °C, the reaction was quenched by the addition of sat. aq. NH_4Cl (1.00 mL) and diluted with EtOAc (2.00 mL) and the layers were separated. The aqueous layer was extracted with EtOAc (3 x 2.00 mL) and the combined organic layers were passed through a plug (1.00 cm OD) of silica gel (3.00 cm tall) and Na_2SO_4 (3.00 cm tall) using EtOAc (10.0 mL) as eluent. The volatiles were removed under reduced pressure. The crude residue was purified by flash chromatography (99:1 Hexanes:EtOAc → 19:1 Hexanes:EtOAc) to yield alcohol (*R*)-**2.6** (8.4 mg, 44% yield, 48% ee) as a white crystalline solid. Alcohol (*R*)-**2.6**: R_f 0.39 (5:1 Hexanes:EtOAc). $[\alpha]_D^{21.1}$ = +20.8 (c = 0.50, $CHCl_3$). The spectral data match those previously reported in the literature for *rac*-**2.6**.[30] The major enantiomer product was assigned by comparison to published $[\alpha]_D$ values for (*R*)-**2.6**.[37]

2.7.2.9 Verification of Enantiopurity

2.7.2.9.1 Chiral SFC & HPLC Assays of Alcohol Reductant

Table 2.6. Conditions and results of chiral SFC analysis of alcohol reductant **2.5**.

Compound	SFC Method Column/Temp. Abs. Wavelength	Solvent	Method Flow Rate	Retention Times (min)	Enantiomeric Ratio (er)
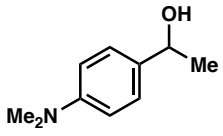 ***rac-2.5***	Daicel ChiralPak IC-3/35 °C λ_{abs} = 210 nm	5% isopropanol in CO_2	3.5 mL/min	7.88/8.61	50:50
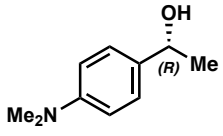 ***(R)-2.5***	Daicel ChiralPak IC-3/35 °C λ_{abs} = 210 nm	5% isopropanol in CO_2	3.5 mL/min	7.58/8.22	98:2

Figure 2.5. SFC trace of *rac*-**2.5** (Table 2.6, Entry 1).

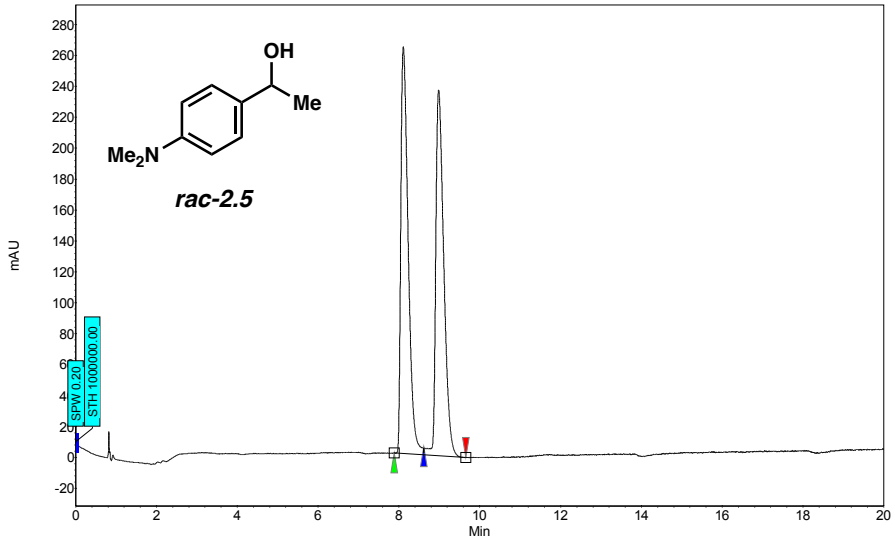

Index	Name	Start	Time	End	RT Offset	Quantity	Height	Area	Area
		[Min]	[Min]	[Min]	[Min]	[% Area]	[µV]	[µV.Min]	[%]
1	UNKNOWN	7.88	8.11	8.61	0.00	50.43	263.1	55.4	50.434
2	UNKNOWN	8.61	8.99	9.66	0.00	49.57	236.6	54.5	49.566
Total						100.00	499.7	109.9	100.000

Figure 2.6. SFC trace of (*R*)-**2.5** (Table 2.6, Entry 2).

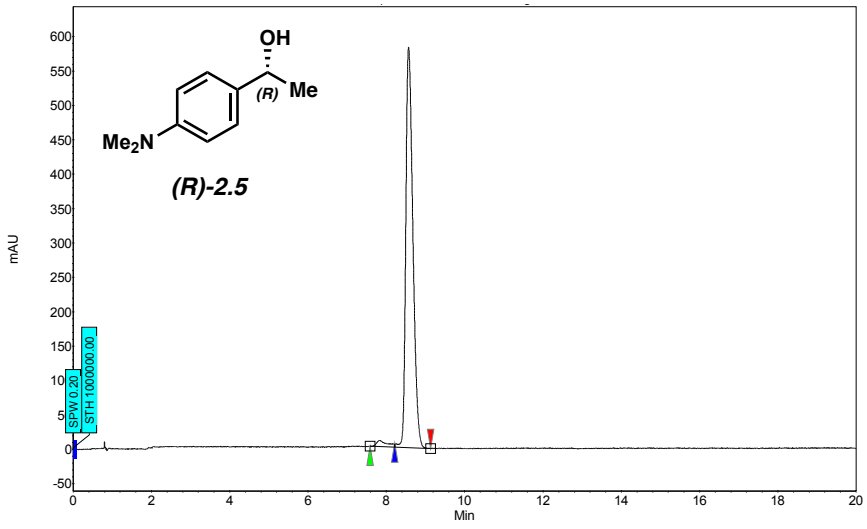

Index	Name	Start	Time	End	RT Offset	Quantity	Height	Area	Area
		[Min]	[Min]	[Min]	[Min]	[% Area]	[µV]	[µV.Min]	[%]
1	UNKNOWN	7.58	7.82	8.22	0.00	2.18	8.7	2.7	2.176
2	UNKNOWN	8.22	8.57	9.13	0.00	97.82	582.5	122.1	97.824
Total						100.00	591.1	124.8	100.000

2.7.2.9.2 Stereospecific Reduction of Ketone 2.6

Table 2.7. Conditions and results of chiral HPLC analysis of alcohol products.

Compound	HPLC Method Column/Temp. Abs. Wavelength	Solvent	Method Flow Rate	Retention Times (min)	Enantiomeric Ratio (er)
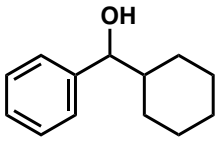 ***rac-2.6***	Daicel ChiralPak OD-H/23 °C λ_{abs} = 210 nm	10% isopropanol in Hexanes	1 mL/min	5.14/5.77	50:50
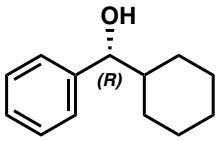 ***(R)-2.6***	Daicel ChiralPak OD-H/23 °C λ_{abs} = 210 nm	10% isopropanol in Hexanes	1 mL/min	5.16/5.70	74:26

Figure 2.7. HPLC trace of *rac*-**2.6** (Table 2.7, Entry 1).

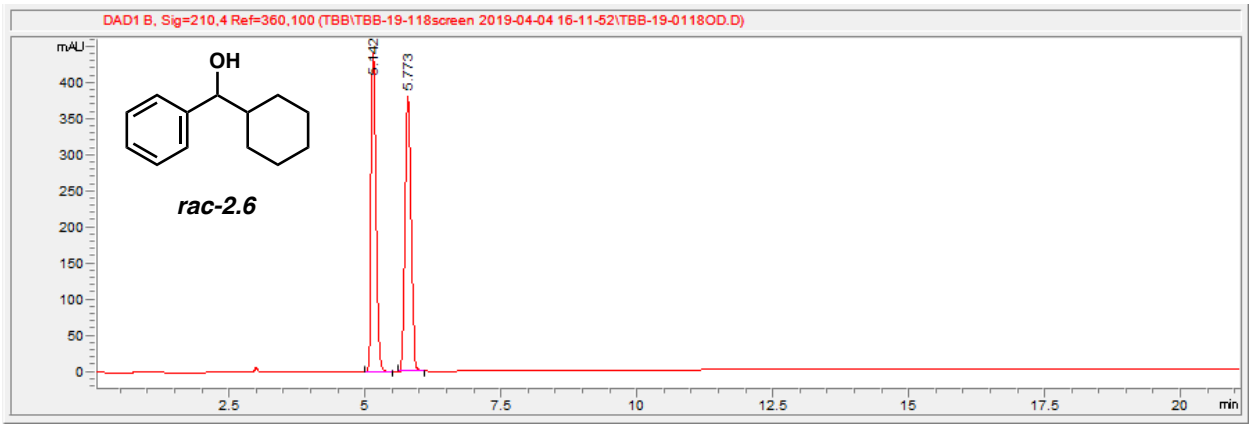

#	Time	Area	Height	Width	Area%	Symmetry
1	5.142	2774.2	442.1	0.0972	50.021	0.833
2	5.773	2771.9	380.2	0.113	49.979	0.836

Figure 2.8. HPLC trace of (*R*)-**2.6** (Table 2.7, Entry 2).

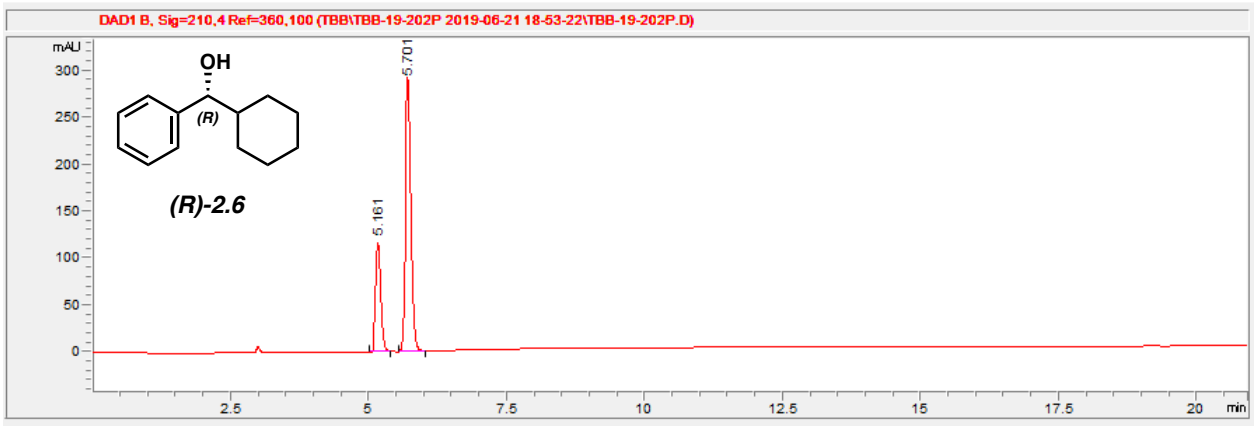

#	Time	Area	Height	Width	Area%	Symmetry
1	5.161	732.7	116.3	0.0975	25.919	0.834
2	5.701	2094.1	291.8	0.1107	74.081	0.837

2.8 Spectra Relevant to Chapter Two:

Base-Mediated Meerwein–Ponndorf–Verley Reduction of Aromatic Ketones and Heterocyclic Ketones

Timothy B. Boit,† Milauni M. Mehta, and Neil K. Garg.

Org. Lett. **2019**, *21*, 6447–6451.

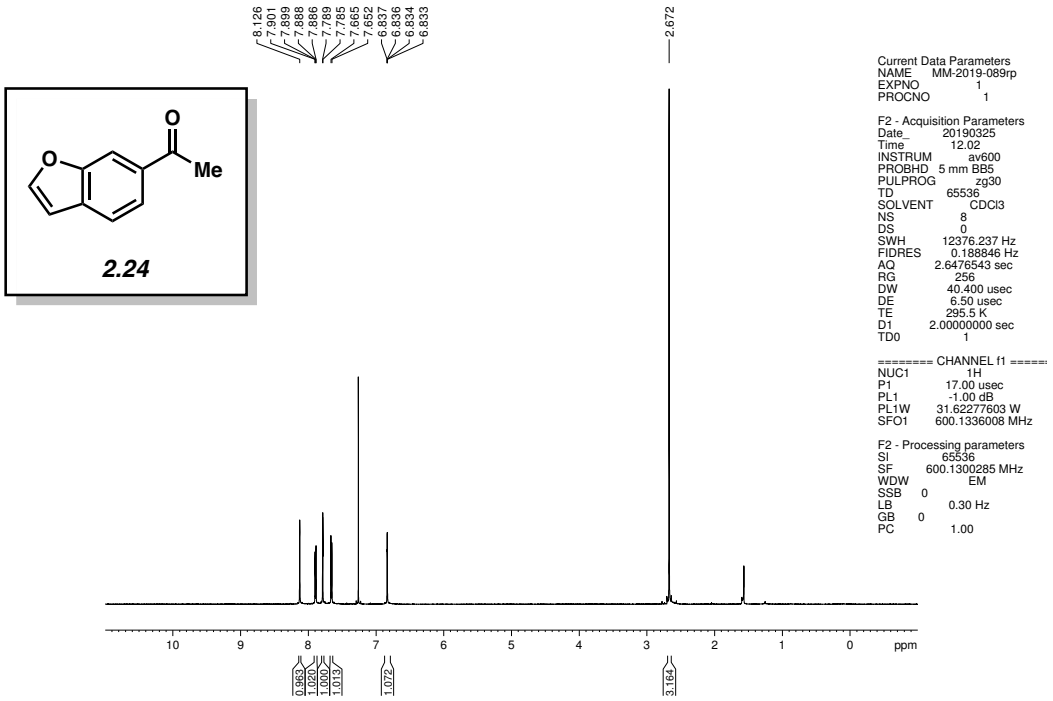

Figure 2.9 ^{1}H NMR (600 MHz, $CDCl_3$) of compound **2.24**.

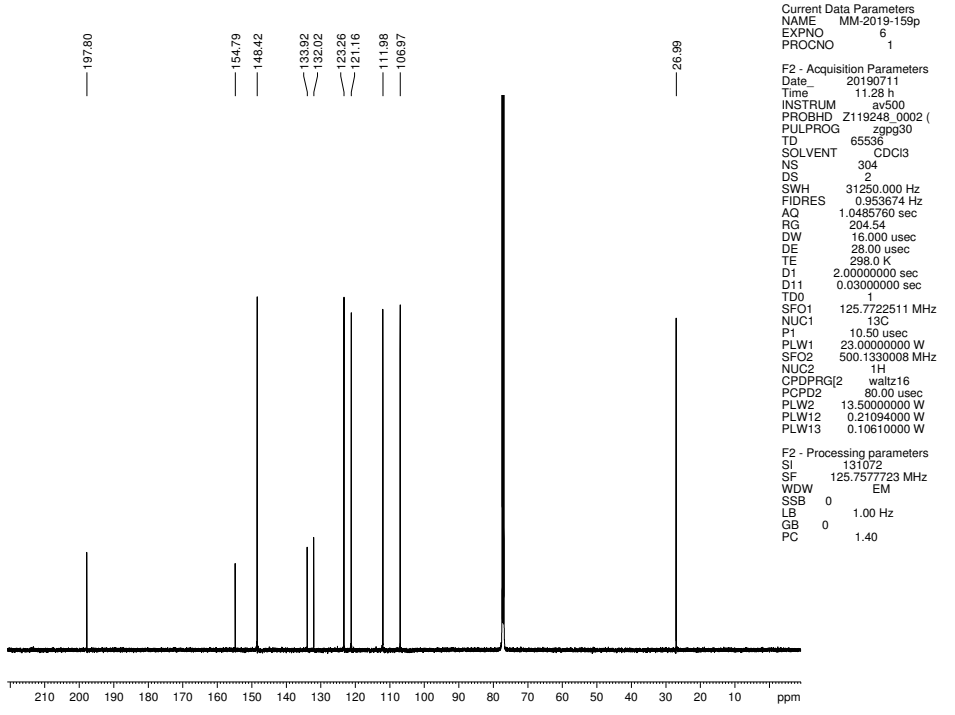

Figure 2.10 ^{13}C NMR (125 MHz, $CDCl_3$) of compound **2.24**.

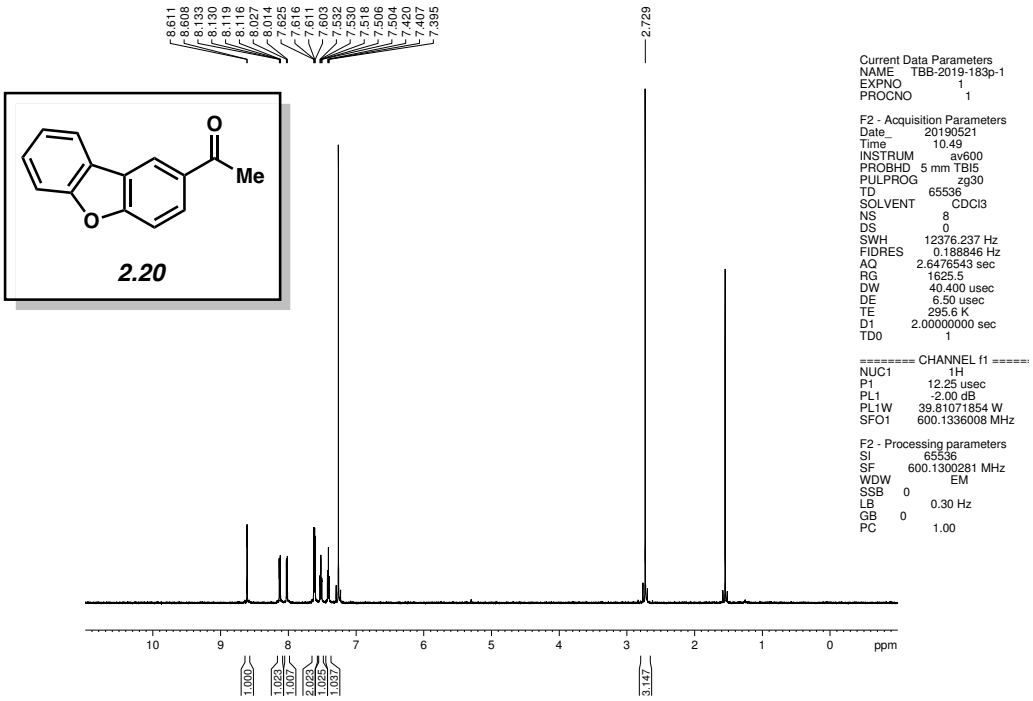

Figure 2.11 ^{1}H NMR (500 MHz, $CDCl_3$) of compound **2.20**.

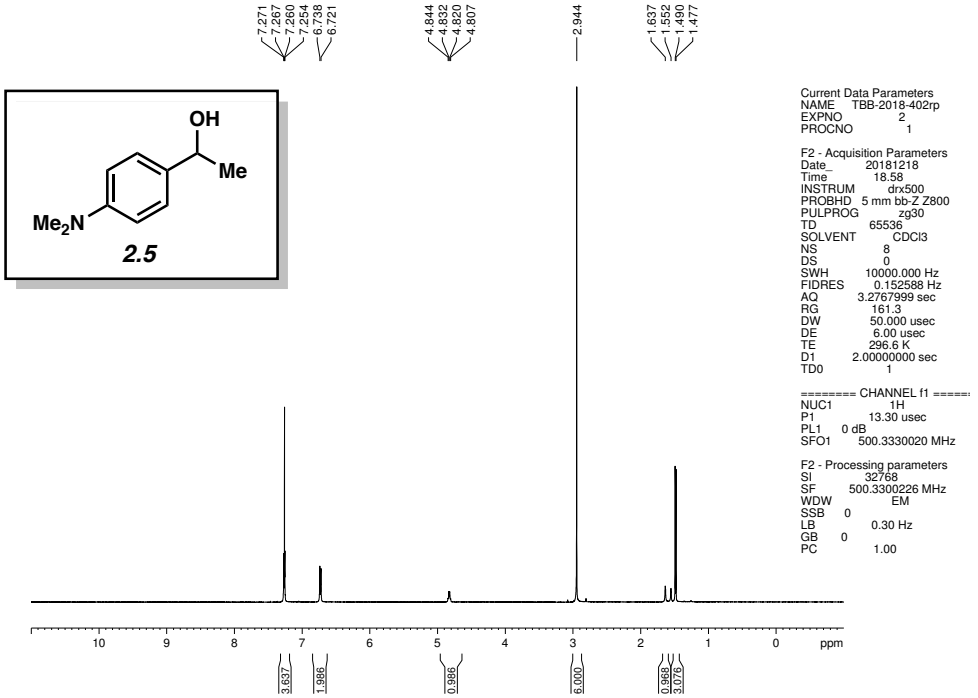

Figure 2.12 ^{1}H NMR (500 MHz, $CDCl_3$) of compound **2.5**.

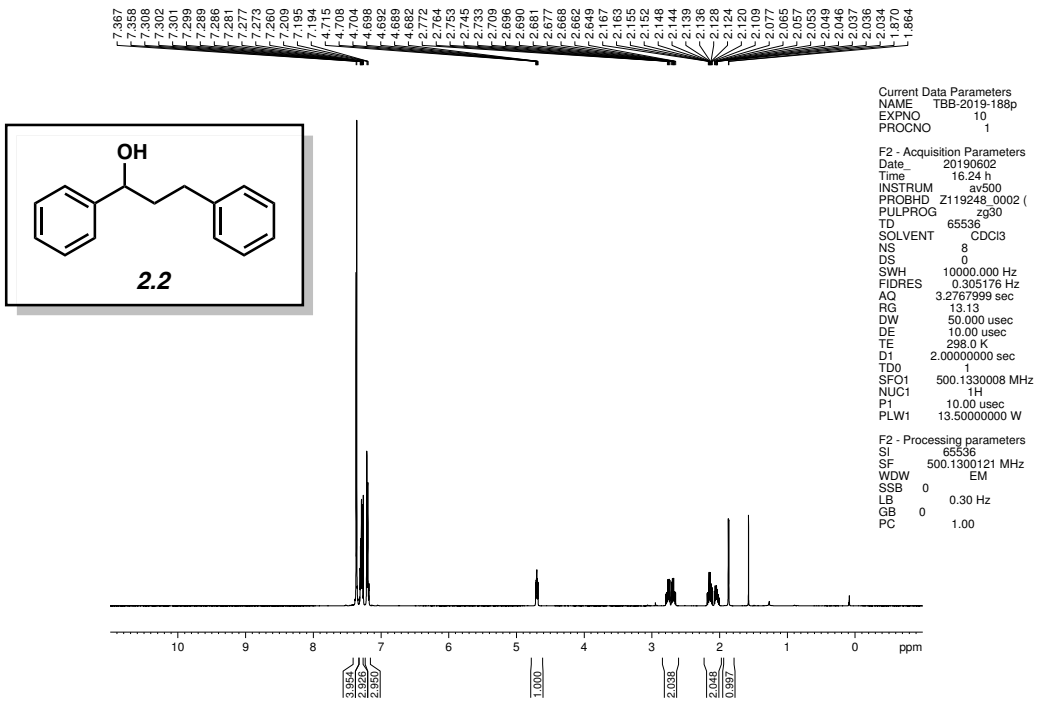

Figure 2.13 ^{1}H NMR (500 MHz, $CDCl_3$) of compound **2.2**.

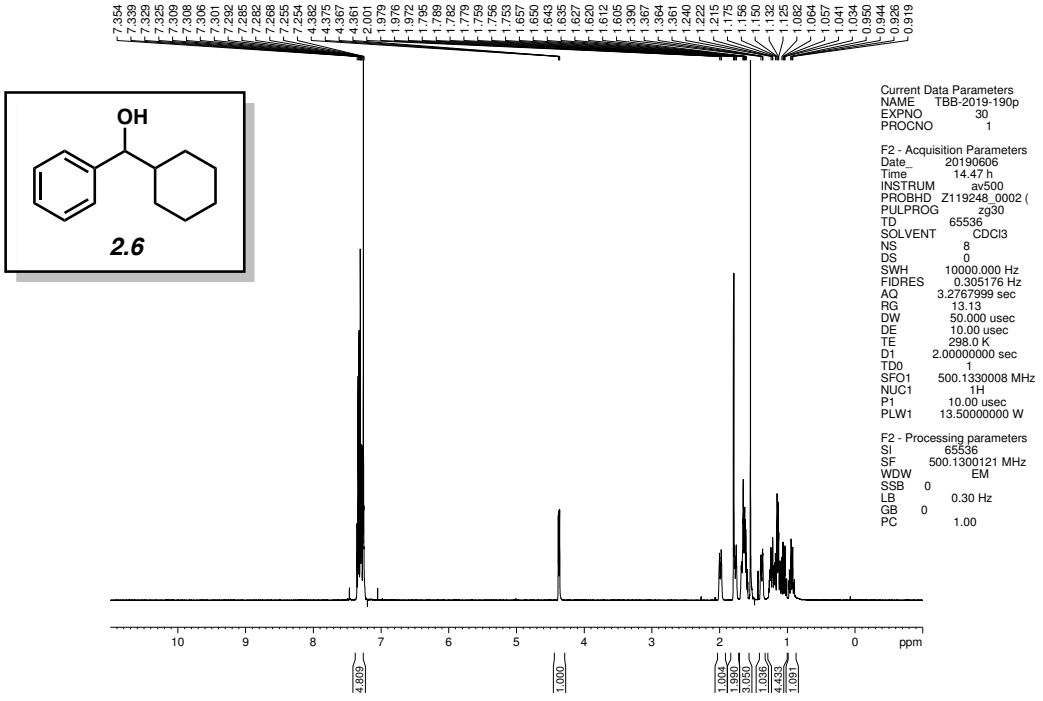

Figure 2.14 ^{1}H NMR (500 MHz, $CDCl_3$) of compound **2.6**.

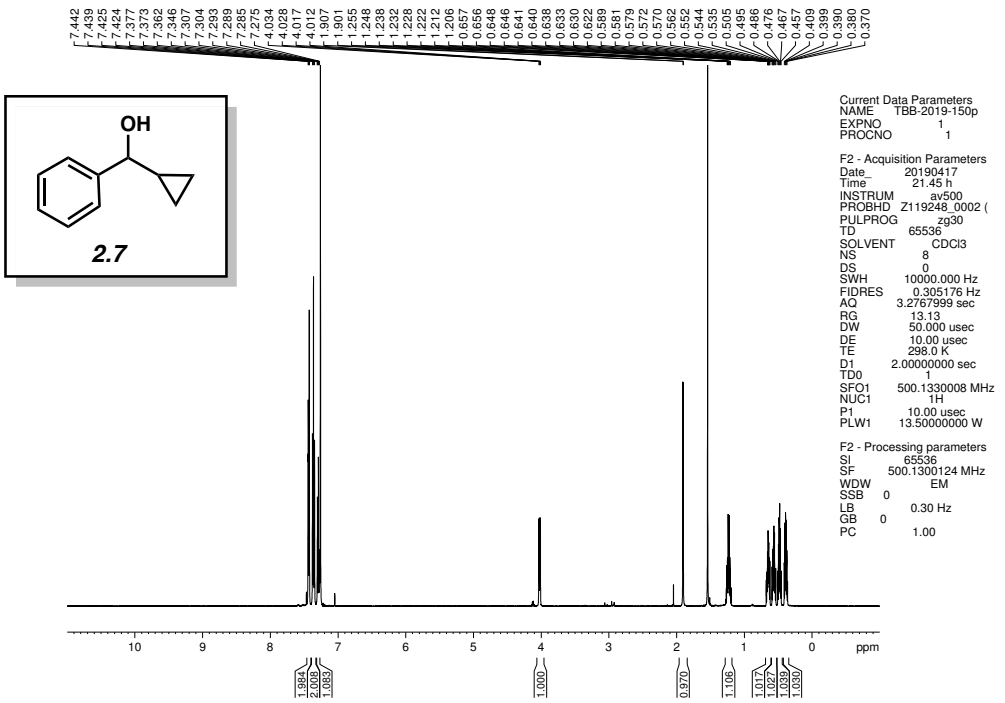

Figure 2.15 ^{1}H NMR (500 MHz, $CDCl_3$) of compound **2.7**.

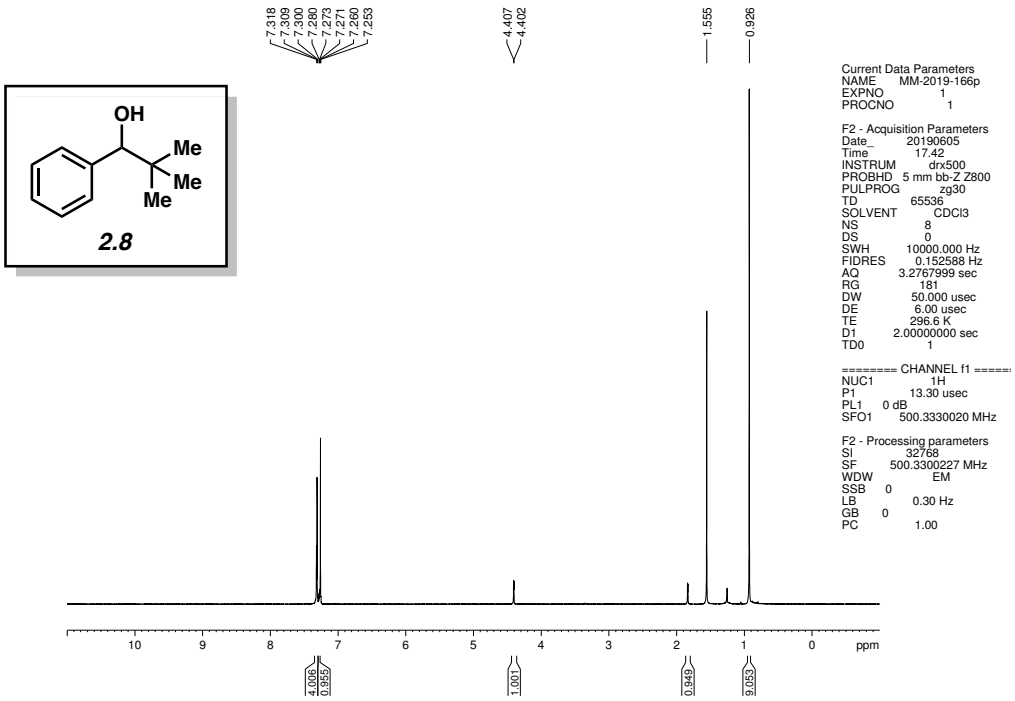

Figure 2.16 ^{1}H NMR (500 MHz, $CDCl_3$) of compound **2.8**.

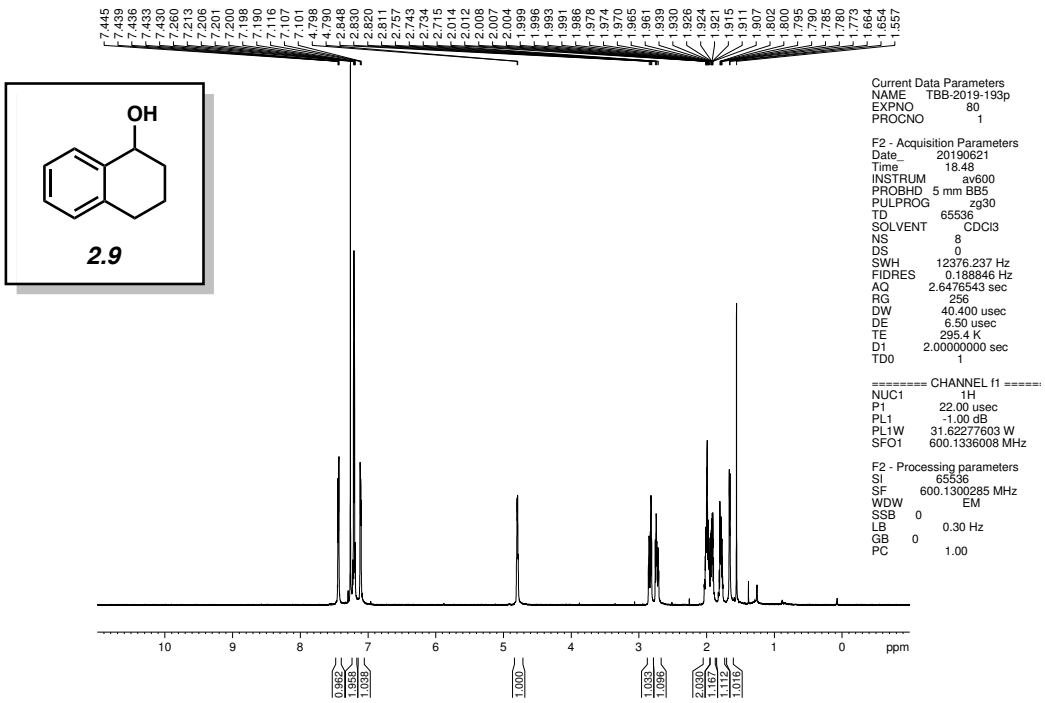

Figure 2.17 ^{1}H NMR (500 MHz, $CDCl_3$) of compound **2.9**.

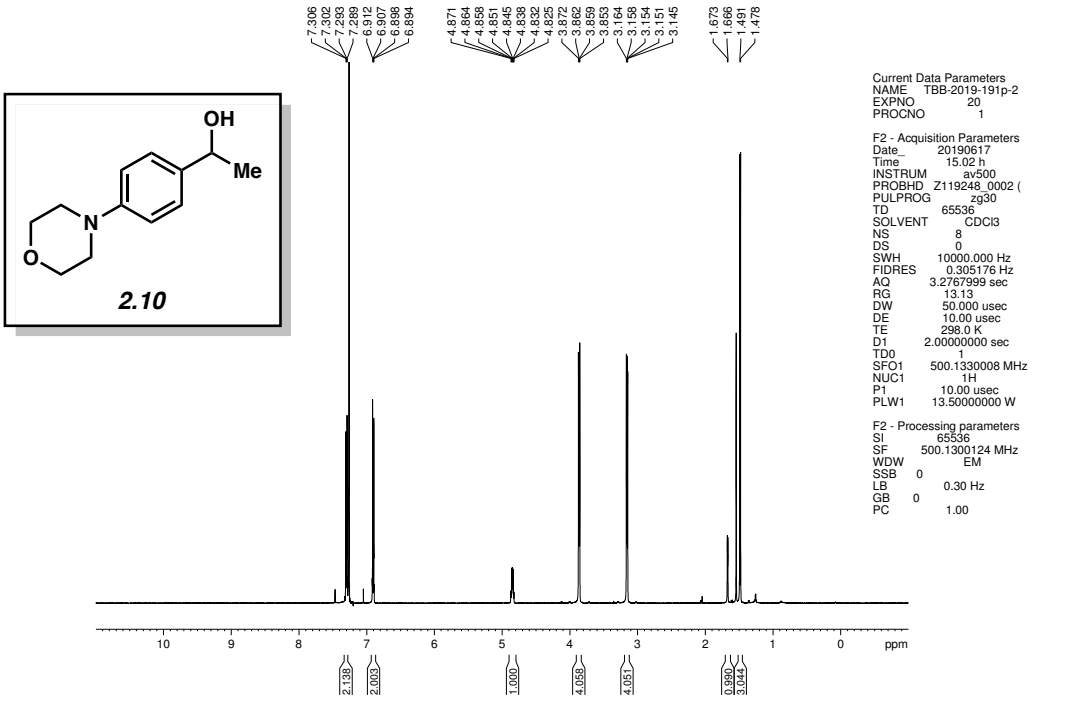

Figure 2.18 ^{1}H NMR (500 MHz, $CDCl_3$) of compound **2.10**.

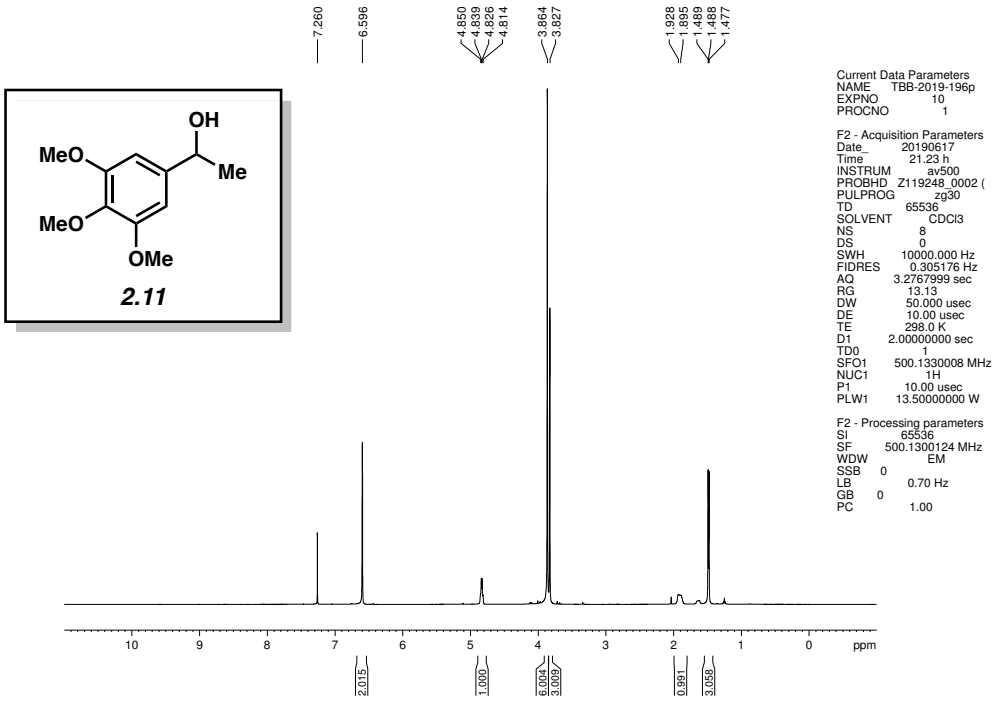

Figure 2.19 ^{1}H NMR (500 MHz, $CDCl_3$) of compound **2.11**.

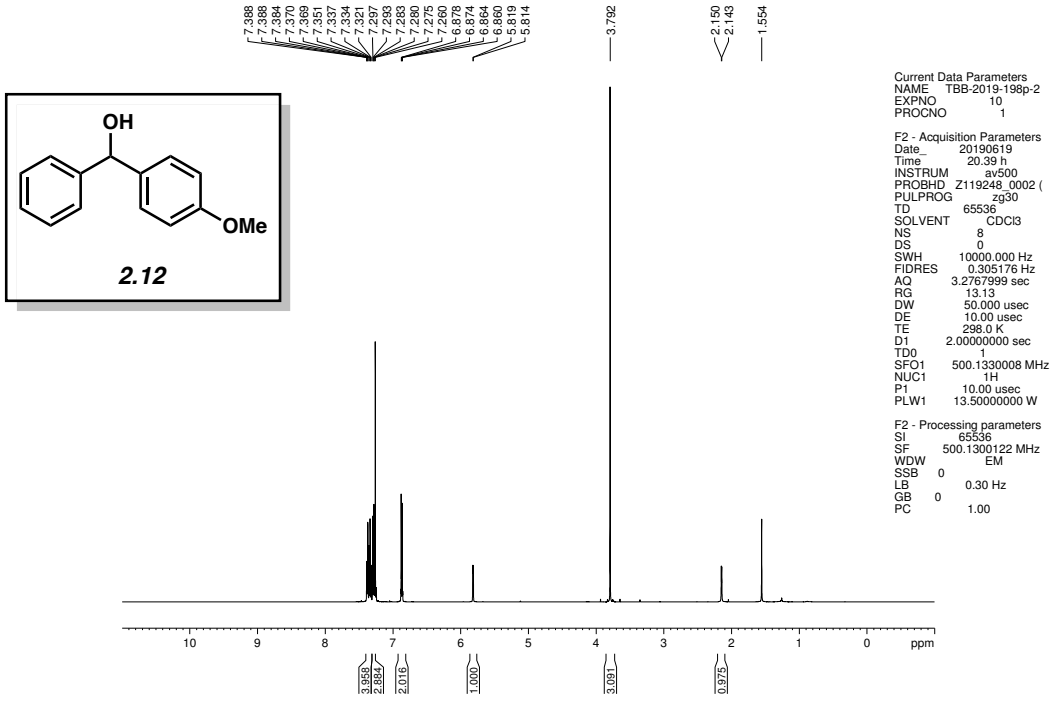

Figure 2.20 ^{1}H NMR (500 MHz, $CDCl_3$) of compound **2.12**.

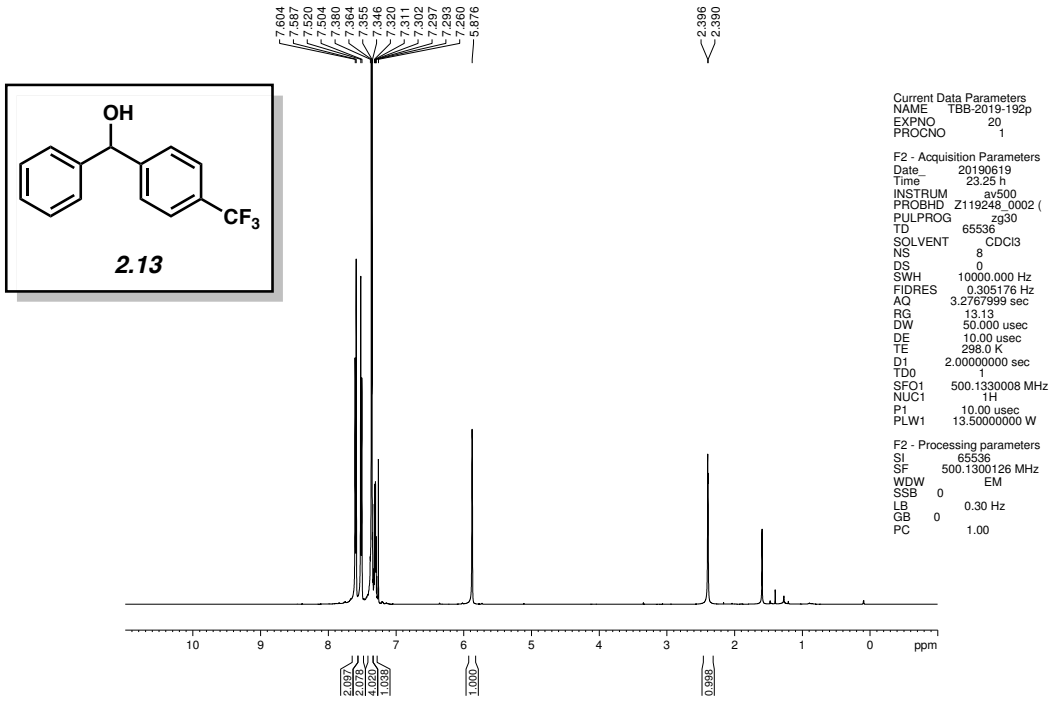

Figure 2.21 ^{1}H NMR (500 MHz, $CDCl_3$) of compound **2.13**.

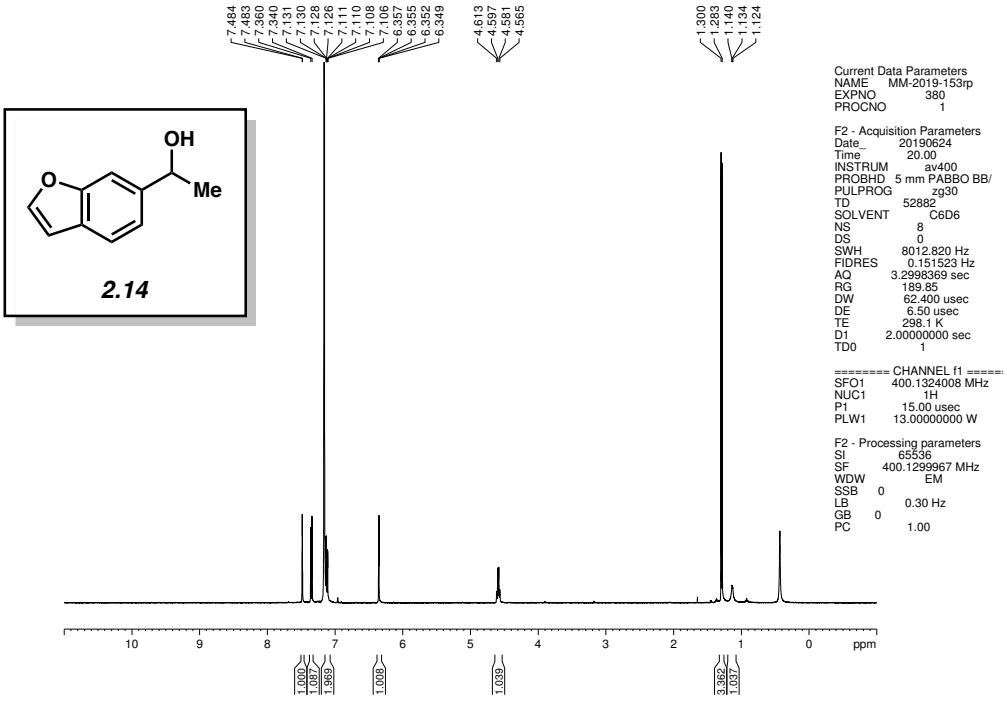

Figure 2.22 ^{1}H NMR (400 MHz, $CDCl_3$) of compound **2.14**.

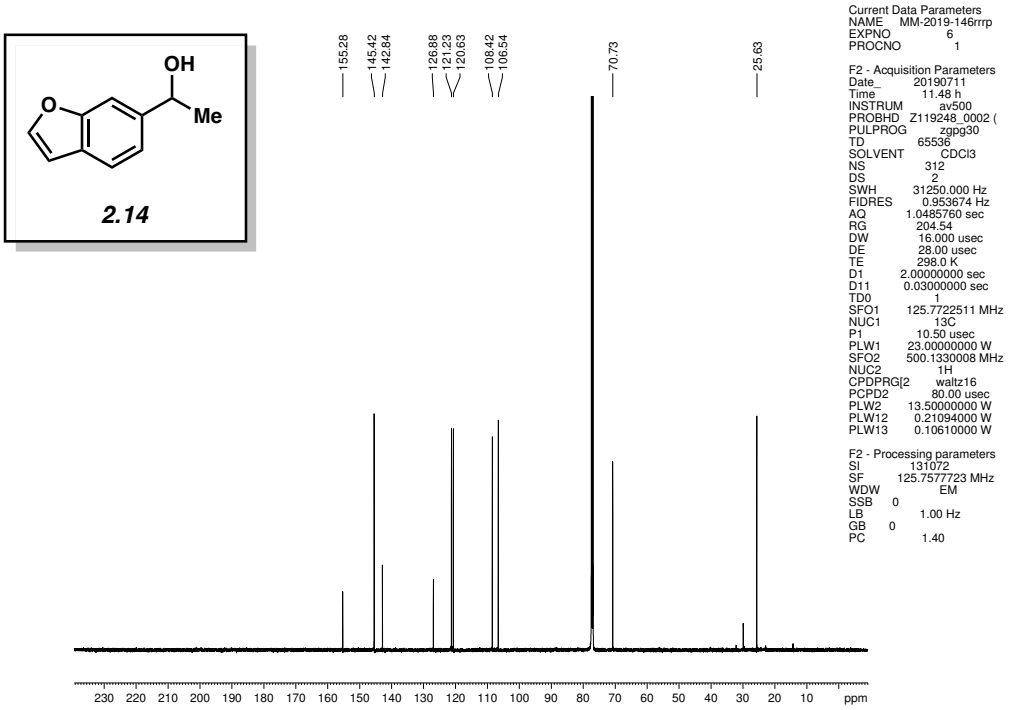

Figure 2.23 ^{13}C NMR (125 MHz, $CDCl_3$) of compound **2.14**.

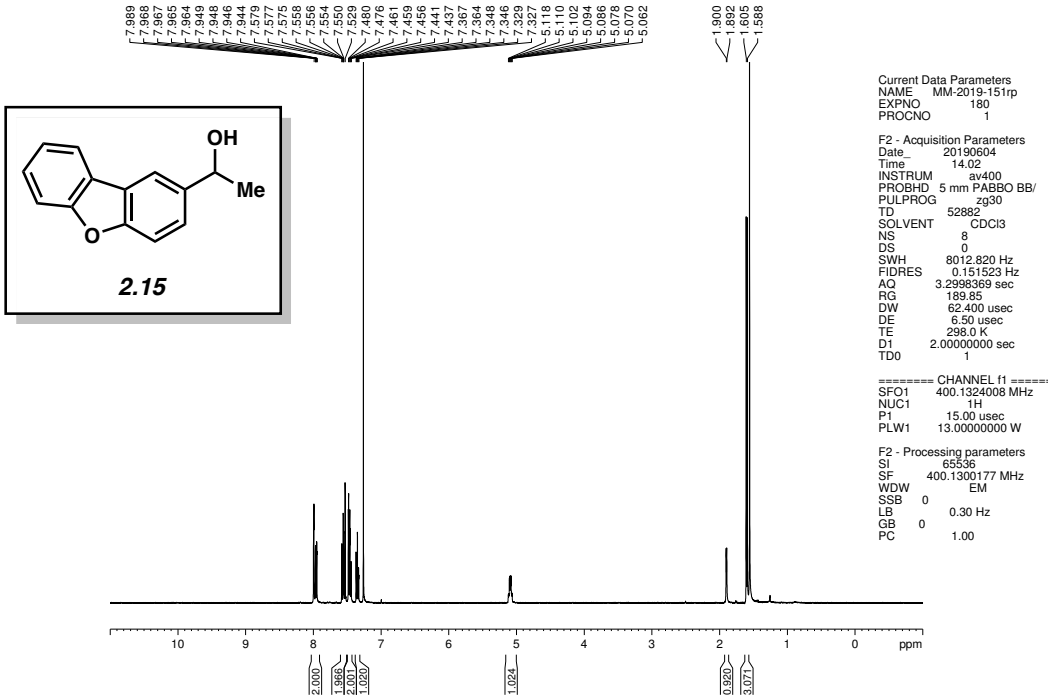

Figure 2.24 ^{1}H NMR (400 MHz, $CDCl_3$) of compound **2.15**.

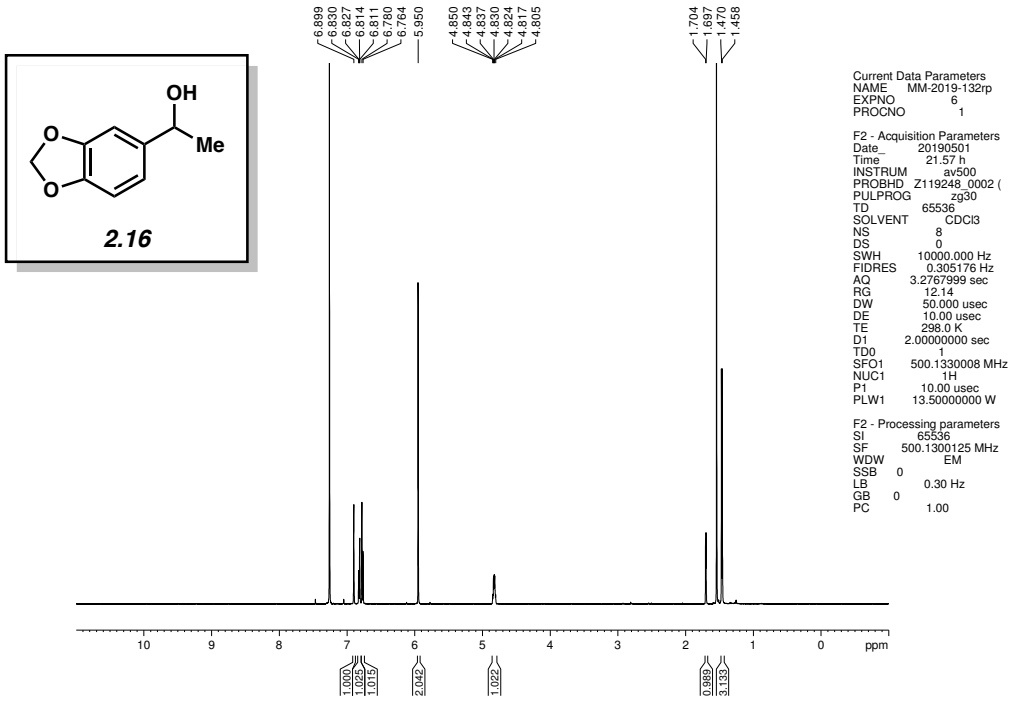

Figure 2.25 ^{1}H NMR (500 MHz, $CDCl_3$) of compound **2.16**.

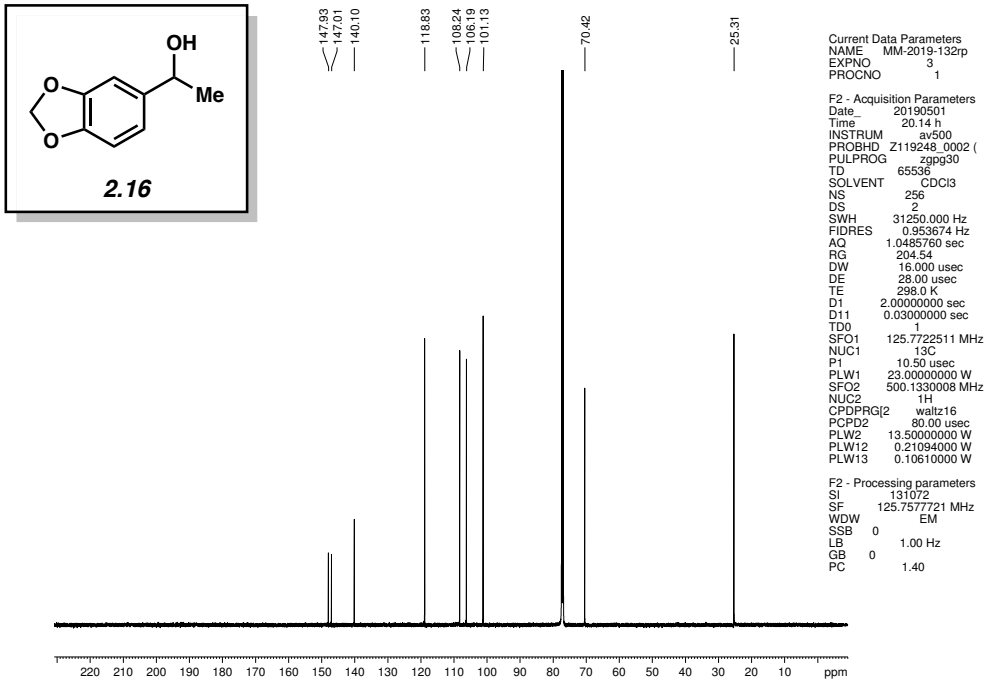

Figure 2.26 ^{13}C NMR (125 MHz, $CDCl_3$) of compound **2.16**.

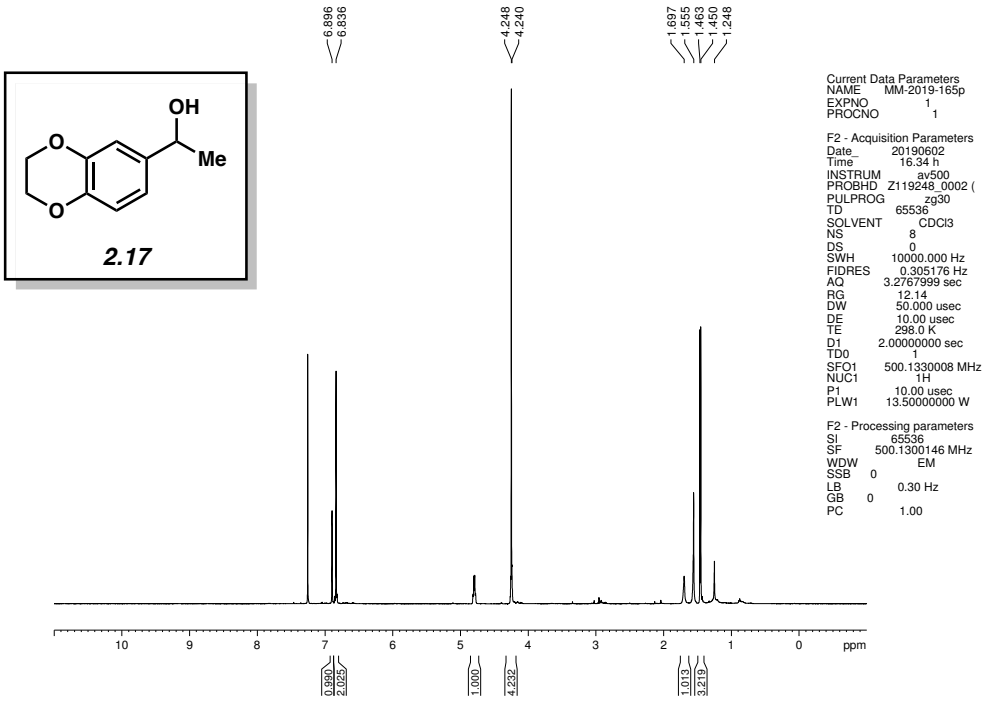

Figure 2.27 ^{1}H NMR (500 MHz, $CDCl_3$) of compound **2.17**.

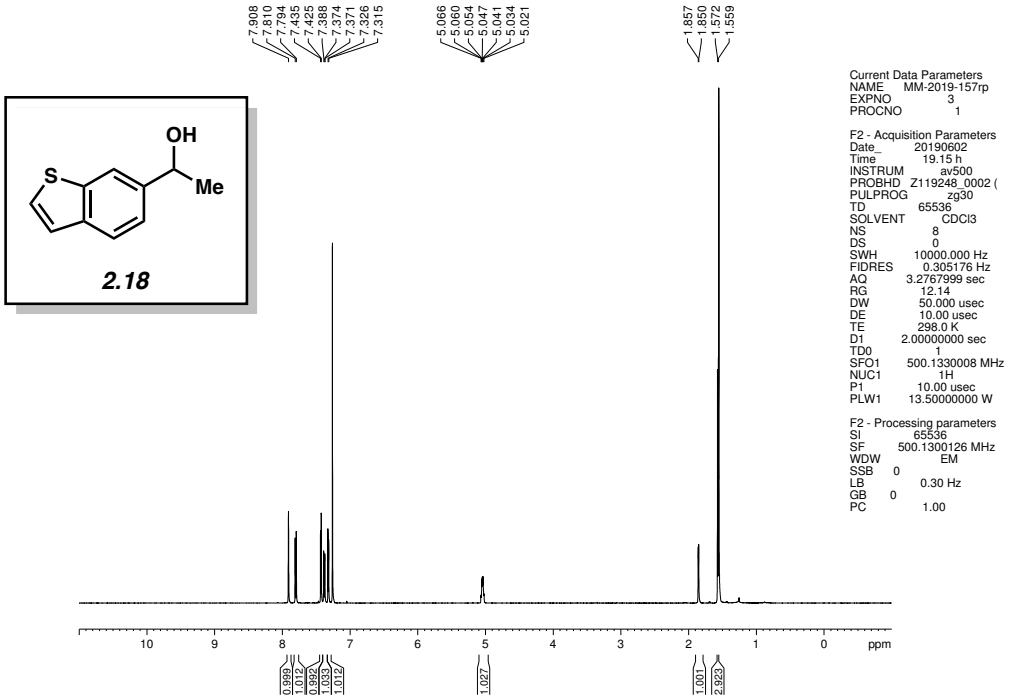

Figure 2.28 ^{1}H NMR (500 MHz, $CDCl_3$) of compound **2.18**.

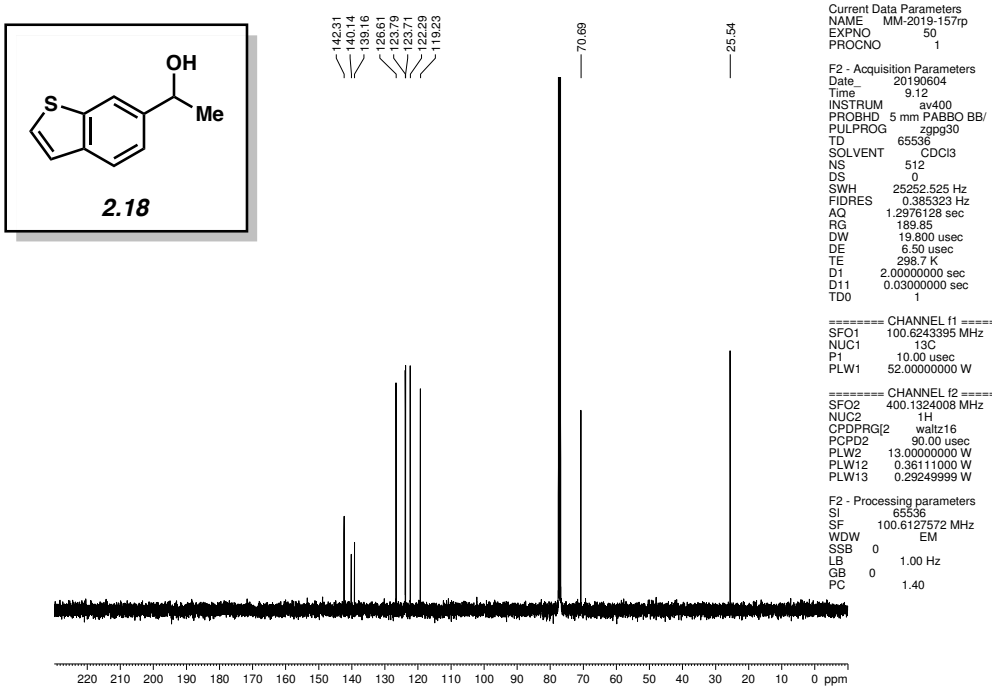

Figure 2.29 ^{13}C NMR (125 MHz, $CDCl_3$) of compound **2.18**.

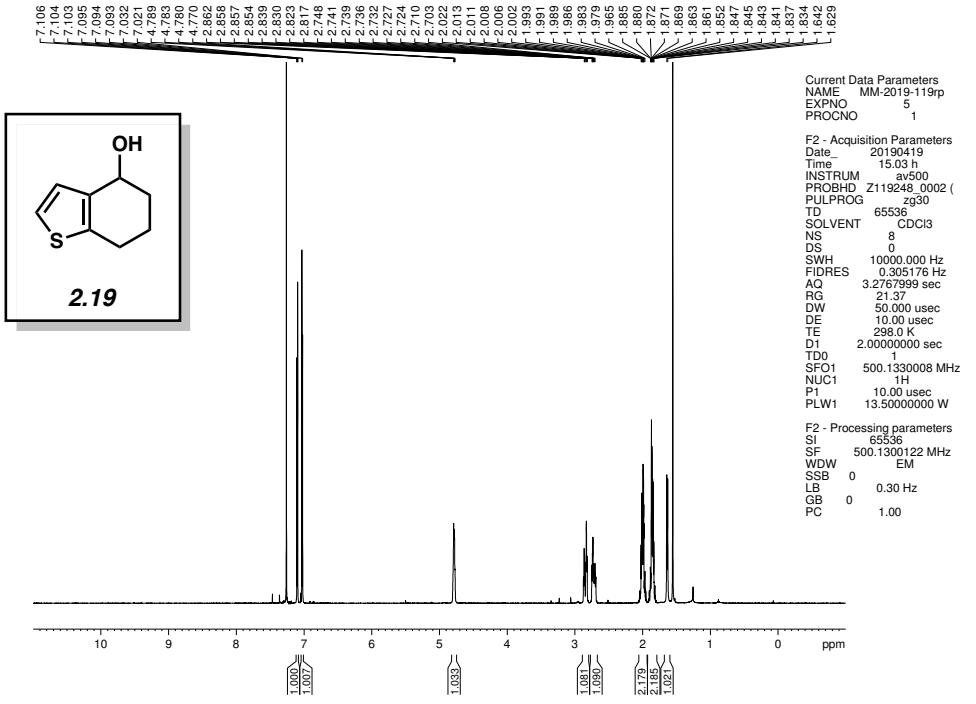

Figure 2.30 ^{1}H NMR (500 MHz, $CDCl_3$) of compound **2.19**.

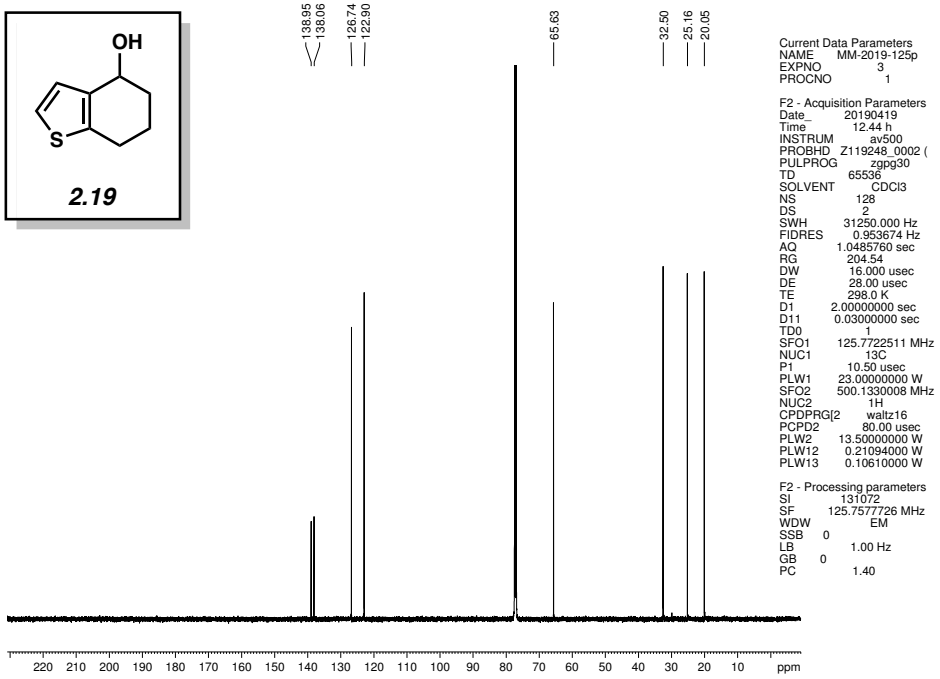

Figure 2.31 ^{13}C NMR (125 MHz, $CDCl_3$) of compound **2.19**.

2.9 Notes and References

(1) For reviews, see: (a) Johnstone, R. A. W.; Wilby, A. H.; Entwistle, I. D. Heterogeneous Catalytic Transfer Hydrogenation and its Relation to Other Methods for Reduction of Organic Compounds. *Chem. Rev.* **1985**, *85*, 129–170. (b) Cha, J. S. Recent Developments in the Meerwein–Ponndorf–Verley and Related Reactions for the Reduction of Organic Functional Groups using Aluminum, Boron, and Other Metal Reagents: A Review. *Org. Proc. Res. Dev.* **2006**, *10*, 1032–1053. (c) de Graauw, C. F.; Peters, J. A.; van Bekkum, H.; Husken, J. Meerwein–Ponndorf–Verley Reductions and Oppenauer Oxidations: An Integrated Approach. *Synthesis* **1994**, 1007–1017. (d) Inch, T. D. Asymmetric Synthesis. *Synthesis* **1970**, *2*, 466–473. (e) Nishide, K.; Node, M. Recent Development of Asymmetric Syntheses Based on the Meerwein–Ponndorf–Verley Reduction. *Chirality* **2002**, *14*, 759–767. (f) Ooi, T.; Miura, T.; Itagaki, Y.; Ichikawa, H.; Maruoka, K. Catalytic Meerwein–Ponndorf–Verley (MPV) and Oppenauer (OPP) Reactions: Remarkable Acceleration of Hydride Transfer by Powerful Bidentate Aluminum Alkoxides. *Synthesis* **2002**, 279–291. (g) Zassinovich, G.; Mestroni, G. Asymmetric Hydrogen Transfer Reactions Promoted by Homogeneous Transition Metal Catalysts. *Chem. Rev.* **1992**, *92*, 1051–1069. (h) Wilds, A. L. Reduction with Aluminum Alkoxides. *Org. React.* **1944**, *2*, 178–223. (i) Djerassi, C. The Oppenauer oxidation. *Org. React* **1951**, *6*, 207–272.

(2) For seminal publications, see: (a) Meerwein, H.; Schmidt, R. Ein neues Verfahren zur Reduktion von Aldehyden und Ketonen. *Liebigs Ann*. **1925**, *444*, 221–238. (b) Verley, A. The Exchange of Functional Groups Between Two Molecules: The Passage of Ketones to

Alcohols and the Reverse. *Bull. Soc. Chim. Fr.* **1925**, *37*, 871–874. (c) Ponndorf, W. Z. The Reversible Exchange of Oxygen Between Aldehydes or Ketones on the One Hand and Primary or Secondary Alcohols on the Other Hand. *Angew. Chem.,* **1926**, *39*, 138–143.

(3) Woodward, R. B.; Wendler, N. L.; Brutschy, F. J. Quininone. *J. Am. Chem. Soc.* **1945**, *67*, 1425–1429.

(4) (a) Gammill, R. B. The Synthesis and Chemistry of Functionalized Furochromones. 2. The Synthesis, Sommelet-Hauser Rearrangement, and Conversion of 4,9-dimethoxy-7-[(methylthio)methyl]-5H-furo(3,2-g)benzopyran-5-one to Ammiol. *J. Org. Chem.* **1984**, *49*, 5035–5041. (b) Sano, T.; Toda, J.; Maehara, N.; Tsuda, Y. Synthesis of Erythrina and Related Alkaloids. 17. Total Synthesis of *dl*-Coccuvinine and *dl*-Coccolinine. *Can. J. Chem.* **1987**, *65*, 94–98. (c) Evans, D. A.; Reiger, D. L.; Jones, T. K.; Kaldor, S. W. Assignment of Stereochemistry in the Oligomycin/Rutamycin/Cytovaricin Family of Antibiotics. Asymmetric Synthesis of the Rutamycin Spiroketal Synthon. *J. Org. Chem.* **1990***, 55*, 6260–6268. (d) Toyota, M.; Odashima, T.; Wada, T.; Ihara, M. Application of Palladium-Catalyzed Cycloalkenylation Reaction to C_{20} Gibberellin Synthesis: Formal Syntheses of GA_{12}, GA_{111}, and GA_{112}. *J. Am. Chem. Soc.* **2000**, *122*, 9036–9037.

(5) (a) Doering, W. v. E.; Aschner, T. C. Mechanism of the Alkoxide-Catalyzed Carbinol–Carbonyl Equilibrium. *J. Am. Chem. Soc.* **1953***, 75*, 393–397. (b) Moulton, W. N.; Van Atta, R. E.; Ruch, R. R. Mechanism of the Meerwein–Ponndorf–Verley Reduction. *J. Org. Chem.* **1961**, *26*, 290–292. (c) Yager, B. J.; Hancock, C. K. Equilibrium and Kinetic Studies of the Meerwein–Ponndorf–Verley–Oppenauer (MPVO) Reaction. *J. Org. Chem.* **1965**, *30*, 1174–

1179. (d) Screttas, C. G.; Cazianis, C. T. Mechanism of Meerwein–Ponndorf–Verley type reductions. *Tetrahedron* **1978**, *34*, 933–940. (e) Ashby, E. C.; Argyropoulos, J. N. Single Electron Transfer in the Meerwein–Ponndorf–Verley Reduction of Benzophenone by Lithium Alkoxides. *J. Org. Chem.* **1986**, *51*, 3593–3597. (f) Shiner Jr., V. J.; Whittaker, D. Kinetics of the Meerwein–Ponndorf–Verley Reaction. *J. Am. Chem. Soc.* **1969**, *91*, 394–398.

(6) (a) Cohen, R.; Graves, C. R.; Nguyen, S. T.; Martin, J. M. L.; Ratner, M. A. The Mechanism of Aluminum-Catalyzed Meerwein−Schmidt−Ponndorf−Verley Reduction of Carbonyls to Alcohols. *J. Am. Chem. Soc.* **2004**, *126*, 14796–14803. (b) Boronat, M.; Corma, A.; Renz, M. Mechanism of the Meerwein−Ponndorf−Verley−Oppenauer (MPVO) Redox Equilibrium on Sn− and Zr−Beta Zeolite Catalysts. *J. Phys. Chem. B* **2006**, *110*, 21168–21174. (c) Sominsky, L.; Rozental, E.; Gottlieb, H.; Gedanken, A.; Hoz, S. Uncatalyzed Meerwein−Ponndorf−Oppenauer−Verley Reduction of Aldehydes and Ketones Under Supercritical Conditions. *J. Org. Chem.* **2004**, *69*, 1492–1496.

(7) (a) Kow, R.; Nugren, R.; Rathke, M. W. Rate Enhancement of the Meerwein–Ponndorf–Verley–Oppenauer Reaction in the Presence of Proton Acids. *J. Org. Chem.* **1977**, *42*, 826–827. (b) Akamanchi, K. G.; Varalakshmy, N. R. Aluminium Isopropoxide - TFA, a Modified Catalyst for Highly Accelerated Meerwein–Ponndorf–Verley (MPV) Reduction. *Tetrahedron Lett.* **1995**, *36*, 3571–3572. (c) Akamanchi, K. G.; Varalakshmy, N. R. Truly Catalytic Meerwein–Ponndorf–Verley (MPV) Reduction. *Tetrahedron Lett.* **1995**, *36*, 5085–5088.

(8) Barbry, D.; Torchy, S. Accelerated Reduction of Carbonyl Compounds under Microwave Irradiation. *Tetrahedron Lett.* **1997**, *38*, 2959–2960.

(9) (a) Graves, C. R.; Scheidt, K. A.; Nguyen, S. T. Enantioselective MSPV Reduction of Ketimines Using 2-Propanol and (BINOL)Al^{III}. *Org. Lett.* **2006***, 8,* 1229–1232. (b) Campbell, E. J.; Zhou, H.; Nguyen, S. T. The Asymmetric Meerwein–Schmidt–Ponndorf–Verley Reduction of Prochiral Ketones with *i*PrOH Catalyzed by Al Catalysts. *Angew. Chem., Int. Ed.,* **2002***, 41,* 1020–1022. (c) McNerney, B.; Whittlesey, B.; Cordes, D. B.; Krempner, C. A Well-Defined Monomeric Aluminum Complex as an Efficient and General Catalyst in the Meerwein-PonndorfVerley Reduction. *Chem. - Eur. J.* **2014**, *20*, 14959−14964.

(10) (a) Midland, M. M.; Tramontano, A. B-Alkyl-9-borabicyclo[3.3.1]nonanes as Mild, Chemoselective Reducing Agents for Aldehydes. *J. Org. Chem*. **1978**, *43*, 1470–1471. (b) Chandrasekharan, J.; Ramachandran, P. V.; Brown, H. C. Diisopinocampheylchloroborane, a Remarkably Efficient Chiral Reducing Agent for Aromatic Prochiral Ketones. *J. Org. Chem.* **1985**, *50*, 5446–5448.

(11) Krohn, K.; Knauer, B. The Diastereoselectivity of Zirconium Alkoxide Catalysed Meerwein–Ponndorf–Verley Reductions. *Liebigs Ann.* **1995**, 1347–1351.

(12) (a) Kagan, H. B.; Namy, J. L. Lanthanides in Organic Synthesis. *Tetrahedron* **1986**, *42*, 6573–6614. (b) Namy, J. L.; Souppe, J.; Collin, J.; Kagan H. B. New Preparations of Lanthanide Alkoxides and their Catalytical Activity in Meerwein–Ponndorf–Verley–Oppenauer Reactions. *J. Org. Chem.* **1984**, *49*, 2045–2049. (c) Okano, T.; Matsuoka, M.; Konishi, H.;

Kiji, J. Meerwein–Ponndorf–Verley Reduction of Ketones and Aldehydes Catalyzed by Lanthanide Tri-2-propoxides. *Chem. Lett.* **1987**, 181–184. (d) Evans, D. A.; Nelson, S. G.; Gagné, M. R.; Muci, A. R. A Chiral Samarium-Based Catalyst for the Asymmetric Meerwein–Ponndorf–Verley Reduction. *J. Am. Chem. Soc.* **1993**, *115*, 9800–9801. (e) Molander G. A.; McKie, J. A. Samarium(II) Iodide Induced Sequential Intramolecular Nucleophilic Acyl Substitution and Stereospecific Intramolecular Meerwein–Ponndorf–Verley Reduction/Oppenauer Oxidation. *J. Am. Chem. Soc.* **1993**, *115*, 5821–5822. (f) Hu, X.; Kellogg, R. M. Asymmetric Reduction and Meerwein–Ponndorf–Verley Reaction of Prochiral Aromatic Ketones in the Presence of Optically Pure 1-aryl-2, 2-dimethylpropane-1, 3-diols. *Recl. Trav. Chim. Pays-Bas.* **1996**, *115*, 410–417.

(13) (a) Ouali, A.; Majoral, J.-P.; Caminade, A.-M.; Taillefer, M. NaOH-promoted Hydrogen Transfer: Does NaOH or Traces of Transition Metals Catalyze the Reaction? *ChemCatChem* **2009**, *1*, 504–509. (b) Polshettiwar, V.; Varma, R. S. Revisiting the Meerwein–Ponndorf–Verley Reduction: A Sustainable Protocol for Transfer Hydrogenation of Aldehydes and Ketones. *Green Chem.* **2009**, *11*, 1313–1316. (c) Radhakrishan, R.; Do, D. M.; Jaenicke, S.; Sasson, Y.; Chuah, G.-K. Potassium Phosphate as a Solid Base Catalyst for the Catalytic Transfer Hydrogenation of Aldehydes and Ketones. *ACS Catal.* **2011**, *1*, 1631–1636.

(14) Mojtahedi, M. M.; Zkbarzadeh, E.; Sharifi, R.; Abaee, M. S. Lithium Bromide as a Flexible, Mild, and Recyclable Reagent for Solvent-Free Cannizzaro, Tishchenko, and Meerwein−Ponndorf−Verley Reactions. *Org. Lett.* **2007**, *9*, 2791–2793.

(15) Under the conditions reported by Chuah and coworkers (ref. 12c), only cyclohexanone, 4-*tert*-butyl cyclohexanone, and acetophenone were evaluated for reactivity using K_3PO_4/*i*-PrOH affording the respective alcohol products in 55%, 30%, and 38% yield.

(16) Subjecting dihydrochalcone (**2.1**) to previously reported conditions for the reduction of ketones using catalytic K_3PO_4 using *i*-PrOH as a solvent gave the desired product **2.2** in only 47% yield.

(17) Although 1,4-dioxane was chosen for these studies, we found other solvents could be employed (see section 2.7.2 for details).

(18) K_3PO_4 is roughly 10^3 less basic than NaOH and KOH. For the pKa of KH_2PO_4 and H_2O respectively, see: (a) Bruice, P. Y. *Organic Chemistry*. 6th ed. Boston: Prentice Hall, 2011. (b) Bordwell, F. G. Equilibrium Acidities in Dimethylsulfoxide Solution. *Acc. Chem. Res.* **1988**, *21*, 456–463.

(19) Using DFT calculations (M06-2X/6-31G(d)), we estimate that the conversion of **2.1** and **2.5** to **2.2** and reduced **2.5** is thermodynamically favorable by ~2 kcal/mol.

(20) Previous reports on the base-mediated MPV reductions of ketones using NaOH and KOH have shown only a handful of heterocyclic substrates undergoing reduction (see refs. 12a and 12b). The base-mediated MPV reduction of heterocyclic ketones using K_3PO_4 has not been previously reported.

(21) Subjecting *N*-containing heterocyclic ketones such as *N*-MOM 4-acetyl indole and 4-acetyl pyridine to base-mediated MPV reduction conditions led to lower yields of the products (20% and 11% yield, respectively).

(22) Dibenzofurans have found application in OLED's, bioactive molecules, and chemical probes: (a) Kim, S.-Y.; Hwang, S.-H.; Kim, Y.-K.; Jung, H.-J.; Lim, J.-O.; Han, S.-H.; Jeong, E.-J.; Park, J.-H.; Lee, E.-Y.; Lee, B.-R.; Lee, J.-H. Condensed-Cyclic Compound and Organic Light-Emitting Device. U.S. Patent 20180248127, Jul. 25, 2012. (b) Patpi, S. R.; Pulipati, L.; Yogeeswari, P.; Sriram, D.; Jain, N.; Sridhar, B.; Murthy, R.; Devi, T. A.; Kalivendi, S., V.; Kantevari, S. Design, Synthesis, and Structure–Activity Correlations of Novel Dibenzo[b,d]furan, dibenzo[b,d]thiophene, and *N*-Methylcarbazole Clubbed 1,2,3-triazoles as Potent Inhibitors of *Mycobacterium tuberculosis. J. Med. Chem.* **2012**, *55*, 3911–3922. (c) Liu, L.-X., Wang, X.-Q.; Yan, J.-M.; Li, Y.; Sun, C.-J.; Chen, W.; Zhou, H.-B.; Yang, X.-D. Synthesis and Antitumor Activities of Novel Dibenzo[b,d]furan–imidazole Hybrid Compounds. *Eur. J. Med. Chem.* **2013**, *66*, 423–437. (d) Lusic, H.; Uprety, R.; Deiter, A. Improved Synthesis of the Two-photon Caging Group 3-nitro-2-ethyldibenzofuran and its Application to a Caged Thymidine Phosphoramidite. *Org. Lett.* **2010**, *12*, 916–919.

(23) For select examples of intermolecular asymmetric MPV reductions of ketones, see: (a) Doering, W. E.; Young, R. W. Partially asymmetric Meerwein–Ponndorf–Verley reductions. *J. Am. Chem. Soc.* **1950**, *72*, 631. (b) Nandi, P.; Solovyov, A.; Okrut, A.; Katz, A. Al^{III}–calix[4]arene Catalysts for Asymmetric Meerwein–Ponndorf–Verley Reduction. *ACS Catal.* **2014**, *4*, 2492–2495. (c) Wu, W.; Zou, S.; Lin, L.; Ji, J.; Zhang, Y.; Ma, B.; Liu, X.; Feng, X. Catalytic Asymmetric Meerwein–Ponndorf–Verley Reduction of Glyoxylates Induced by a Chiral N,N′-dioxide/$Y(OTf)_3$ Complex. *Chem. Commun.* **2017**, *53*, 3232–3235. (d) Ooi, T.; Miura, T.; Maruoka, K. Highly Efficient, Catalytic Meerwein–Ponndorf–Verley

Reduction with a Novel Bidentate Aluminum Catalyst. *Angew. Chem., Int. Ed.* **1998**, *37*, 2347–2349.

(24) Mori, A.; Miyakawa, Y.; Ohashi, E.; Haga, T.; Maegawa, T.; Sajiki, H. Pd/C-Catalyzed Chemoselective Hydrogenation in the Presence of Diphenylsulfide. *Org. Lett.* **2006**, *8*, 3279–3281.

(25) Ramgren, S. D.; Garg, N. K. Pd-Catalyzed Acetylation of Arenes. *Org. Lett.* **2014**, *16*, 824–827.

(26) Xiao, B.; Gong, T.-J.; Liu, Z.-J.; Liu, J.-H.; Luo, D.-F.; Xu, J.; Liu, L. Synthesis of Dibenzofurans via Palladium-Catalyzed Phenol-Directed C–H Activation/C–O Cyclization. *J. Am. Chem. Soc.* **2011**, *133*, 9250–9253.

(27) Guyon, C.; Baron, M.; Lemaire, M.; Popowycz, F.; Métay, E. Commutative Reduction of Aromatic Ketones to Arylmethylenes/Alcohols by Hypophosphites Catalyzed by Pd/C Under Biphasic Conditions. *Tetrahedron* **2014**, *70*, 2088–2095.

(28) Xu, J.; Wei, T.; Zhang, Q. Influences of Electronic Effects and Anions on the Enantioselectivity in the Oxazaborolidine-Catalyzed Asymmetric Borane Reduction of Ketones. *J. Org. Chem.* **2004**, *69*, 6860–6886.

(29) Genç, S.; Arslan, B.; Gülcemal, S.; Günnaz, S.; Çetinkaya, B.; Gülcemal, D. Iridium(I)-Catalyzed C–C and C–N Bond Formation Reactions via the Borrowing Hydrogen Strategy. *J. Org. Chem.* **2019**, *84*, 6286–6297.

(30) Gaykar, R, N.; Bhunia, A.; Biju, A. T. Employing Arynes for the Generation of Aryl Anion Equivalents and Subsequent Reaction with Aldehydes. *J. Org. Chem.* **2018**, *83*, 11333–11340.

(31) Zeng, H.; Wu, J.; Li, S.; Hui, C.; Ta, A.; Cheng, S.-Y.; Zheng, S.; Shang, G. Copper(II)-catalyzed Selective Hydroboration of Ketones and Aldehydes. *Org. Lett.* **2019**, *21*, 401–406.

(32) Rahaim Jr., R. J.; Maleczka Jr., R. E. C–O Hydrogenolysis Catalyzed by Pd-PMHS Nanoparticles in the company of Chloroarenes. *Org. Lett.* **2011**, *13*, 584–587.

(33) Puls, F.; Knölker, H.-J. Conversion of Olefins into Ketones by an Iron-catalyzed Wacker-type Oxidation using Oxygen as the Sole Oxidant. *Angew. Chem., Int. Ed.* **2018**, *57*, 1222–1226.

(34) Wang, S.; Huang, H.; Tsareva, S.; Bruneau, C.; Fischmeister, C. Silver-catalyzed Hydrogenation of Ketones under Mild Conditions. *Adv. Synth. Catal.* **2019**, *361*, 786–790.

(35) Patpi, S. R.; Pulipati, L.; Yogeeswari, P.; Sriram, D.; Jain, N.; Sridhari, B.; Murthy, R.; Devi T., A.; Kalivendi, S. V.; Kantevar, S. Design, Synthesis, and Structure–Activity correlations of Novel Dibenzo[b,d]furan, Dibenzo[b,d]thiophene, and N-Methylcarbazole Clubbed 1,2,3-Triazoles as Potent Inhibitors of Mycobacterium Tuberculosis. *J. Med. Chem.* **2012**, *55*, 3911–3922.

(36) Moine, E.; Dimier-Poisson, I.; Enguihard-Gueiffier, C.; Logé, C.; Pénichon, M.; Moiré, N.; Delebouzé, C.; Foll-Josselin, B.; Ruchaud, S.; Bach, S.; Gueiffier, A.; Debierre-Grockiego, F.; Denevault-Sabourin, C. Development of New Highly Potent Imidazo[1,2-b]pyridazines Targeting Toxoplasma Gondii Calcium-Dependent Protein Kinase 1. *Eur. J. Med. Chem.* **2015**, *105*, 80–105.

(37) Stepanenko, V.; De Jesús, M.; Correa, W.; Guzmán, I.; Vázquez, C.; de la Cruz, W.; Ortiz-Marciales, M.; Barnes, C. L. Enantioselective Reduction of Prochiral Ketones Using Spiroborate Esters as Catalysts. *Tetrahedron Lett.* **2007**, *48*, 5799–5802.

CHAPTER THREE

Reductive Arylation of Amides via a Nickel-Catalyzed Suzuki–Miyaura Coupling and Transfer Hydrogenation Cascade

Milauni M. Mehta,[†] Timothy B. Boit,[†] Junyong Kim, Emma L. Baker and Neil K. Garg.

Angew. Chem., Int. Ed. **2021**, *60*, 2472–2477.

3.1 Abstract

We report a means to achieve the addition of two disparate nucleophiles to the amide carbonyl carbon in a single operational step. Our method takes advantage of non-precious-metal catalysis and allows for the facile conversion of amides to chiral alcohols via a one-pot Suzuki–Miyaura cross-coupling / transfer hydrogenation process. This study is anticipated to promote the development of new transformations that allow for the conversion of carboxylic acid derivatives to functional groups bearing stereogenic centers via cascade processes.

3.2 Introduction

The synthetic manipulation of carboxylic acid derivatives has become central to organic chemistry after more than a century of methodological development.[1] Though the field has a rich history, strategies for nucleophilic addition to carboxylic acid derivatives may be largely characterized by two primary mechanisms (Figure 3.1a). The first involves an addition-elimination sequence to produce carbonyl derivatives via a tetrahedral intermediate.[2] Notably, this traditional strategy has limitations in the context of organometallic nucleophiles, as the ketone products resulting from initial acyl substitution are susceptible to further nucleophilic attack to give achiral

alcohol products. Specialized acyl derivatives such as *N*-methyl-*N*-methoxy amides, or "Weinreb amides," are often required to avoid such undesired reactivity and necessitate two-step protocols.[2,3] A complementary approach employs transition metal catalysis,[4] where mild substrate activation affords an acyl-metal intermediate and allows for cross-coupling with a variety of nucleophiles.[4a,5] This alternative pathway differentiates the reactivity of the substrate from the product carbonyl to overcome the selectivity challenges mentioned above. An exciting opportunity offered by the latter strategy is the addition of a second, *different* nucleophile to the intermediate resulting from the initial cross-coupling reaction to generate chiral products. Cascade reactions of this type would provide efficient access to important chiral products in racemic or enantioenriched form from achiral starting materials.[6]

Despite the widely recognized importance of cross-couplings, methods to leverage this platform for the addition of disparate nucleophiles to carboxylic acid derivatives remain underexplored.[7] We envisioned that amides could provide a viable entry to address this challenge, given their recent popularization as cross-coupling handles.[4j–o,8,9] Amides have been shown to undergo a variety of couplings through the intermediacy of acyl-metal species using either non-precious or precious metal catalysis (e.g., Ni or Pd). Additionally, we viewed them as ideal substrates for one-pot cascade reactions, as their stability under non-metal catalyzed conditions could allow for the orchestration of orthogonal bond-forming events.[10] Dixon has reported an elegant intramolecular reductive cyclization of a tertiary lactam substrate mediated by Vaska's Ir complex,[11] however, no examples exist for the intermolecular addition of two distinct nucleophiles to amides using catalysis in a single operation.[12,13] Indeed, a reductive alkylation of aryl pyridyl esters reported by Chen and coworkers in 2019 represents the only known example of a carboxylic acid derivative undergoing direct catalytic addition of two nucleophiles through a cross-coupling

approach (Figure 3.1b).[14] Though mechanistically distinct and not involving acyl metal species, two additional relevant methodologies should be highlighted. Buchwald and coworkers have reported a copper-catalyzed reductive alkylation of symmetric anhydrides to afford enantioenriched secondary alcohols,[15] and more recently the Hoveyda group reported a copper-catalyzed asymmetric reductive allylation of nitriles to access enantioenriched homoallylic amines (Figure 3.1b).[16] Together, these examples illustrate some of the potential advantages of cascade reactions that add disparate nucleophiles to a single reactive center of an achiral substrate and uncover synergistic reactivity beyond the capabilities of one reaction manifold.[17]

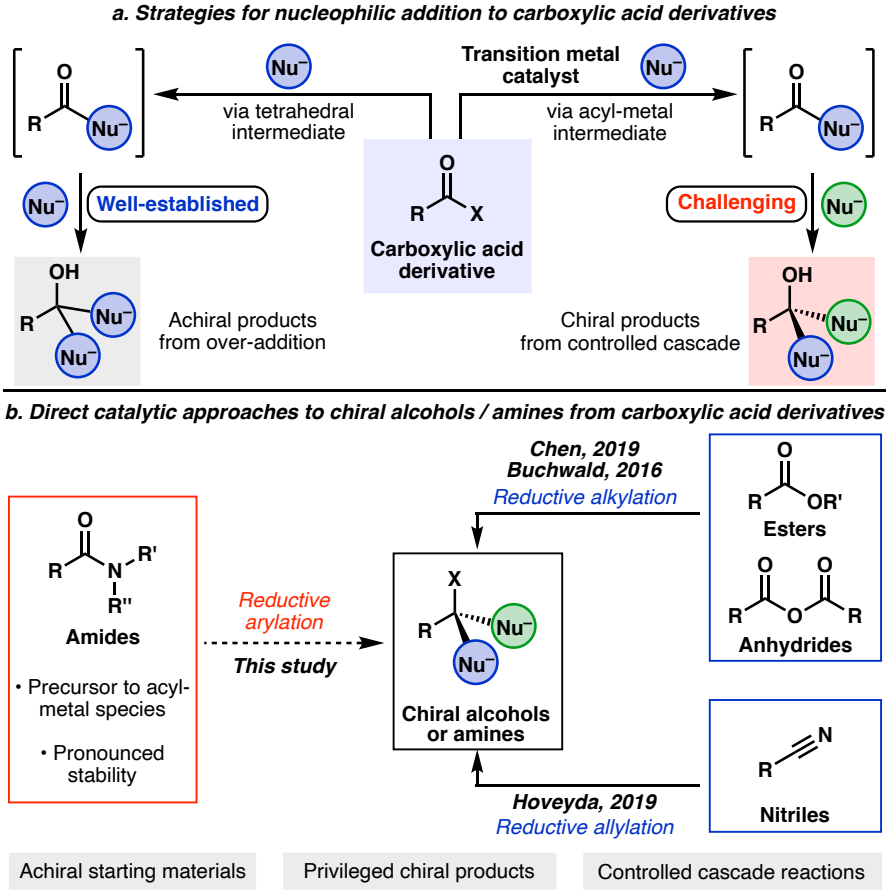

Figure 3.1. (a) Common reaction pathways for nucleophilic additions to carboxylic acid derivatives. (b) Direct catalytic approaches to chiral amines or alcohols from carboxylic acid derivatives.

In this manuscript, we describe a synthetic method for achieving the addition of two different nucleophiles to a carboxylic acid derivative using nickel catalysis.[18] The overall transformation relies on a Suzuki–Miyaura cross-coupling / transfer hydrogenation cascade reaction of amide starting materials to form a C–C and C–H bond,[19,20] consecutively, and ultimately furnish alcohol products (Figure 3.2).[21] The results presented herein not only reinforce the notion that amides are versatile building blocks for transition-metal catalyzed reactions, but also validate their utility as synthons for directly generating sp^3 carbon centers from the amide carbonyl.

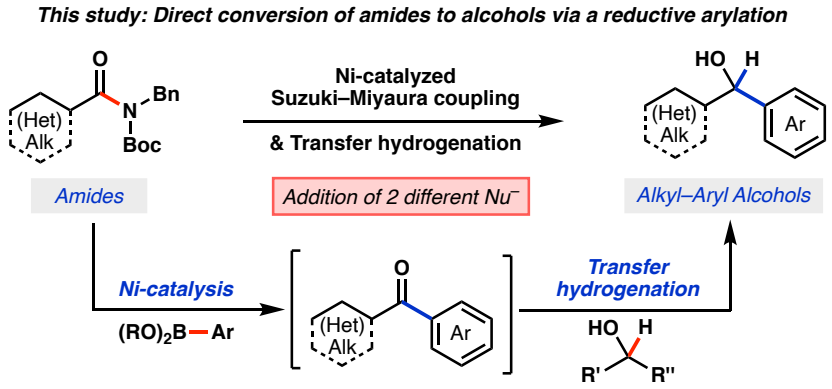

Figure 3.2. Overview of current study involving the conversion of aliphatic amides to alkyl–aryl alcohols via a Suzuki–Miyaura coupling / transfer hydrogenation cascade.

3.3 Reaction Discovery and Optimization

We initiated our study by examining the Ni-catalyzed Suzuki–Miyaura coupling and in situ reduction of dihydrocinnamic acid-derived amide **3.1** as shown in Figure 3.3.[19b] In the absence of a reducing agent, the Suzuki–Miyaura coupling with boronate **3.5** delivered ketone **3.3** in nearly quantitative yield (entry 1).[22,23,24] With the aim of developing the reductive variant, we questioned whether the use of a secondary alcohol reductant could effect the in situ transfer hydrogenation of ketone **3.3** to deliver alcohol **3.4**. In this regard, we attempted the use of *i*-PrOH as solvent, reminiscent of common Meerwein–Ponndorf–Verley (MPV) reduction conditions.[25,26]

Unfortunately, this change resulted in low yields of **3.4** (entries 2 and 3).[27] By shifting to the use of *i*-PrOH as an additive while using toluene as solvent, we obtained the desired product **3.4** in a slightly improved yield of 32%, with 18% of ketone **3.3** remaining (entry 4). Given our lab's recent success in using 1-4-(dimethylamino)phenyl)-1-ethanol (DMPE, **3.7**) in base-catalyzed MPV reductions,[28] we also tested this benzylic alcohol in our system.[29] By simply replacing *i*-PrOH with **3.7**, alcohol **3.4** was obtained in 51% yield (entry 5). Finally, switching the solvent to 1,4-dioxane (entry 6) and using boronate **3.6** in place of boronate **3.5** (entry 7) led to further improvements, delivering alcohol **3.4** in 82% yield.[30,31,32]

It is worth noting that these optimized conditions satisfy a challenging balance of reactivity required for the success of the amide to alcohol conversion. Specifically, reducing agent **3.7** does not significantly impede the nickel-catalyzed cross-coupling step, yet is reactive enough to efficiently reduce ketone **3.3**. Furthermore, as will be shown, other carbonyl functional groups are tolerated by the methodology's mild reducing conditions.

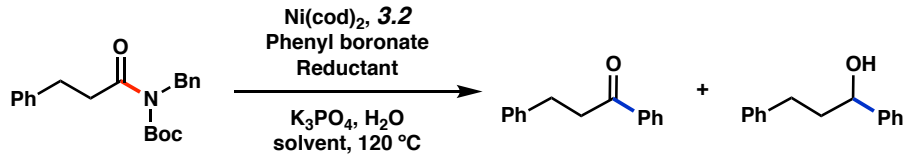

3.1 *3.3* *3.4*

Entry	$Ni(cod)_2$ (mol%)	*3.2* (mol%)	Boronate (equiv)	Solvent	Reductant (equiv)	Yield[a] *3.3*	Yield[a] *3.4*
1	5	10	*3.5* (2.5)	PhMe	–	98%	0%
2	5	10	*3.5* (2.5)	*i*-PrOH	solvent	0%	14%
3	10	20	*3.5* (4.0)	*i*-PrOH	solvent	0%	21%
4	10	20	*3.5* (4.0)	PhMe	*i*-PrOH (2.5)	18%	32%
5	10	20	*3.5* (4.0)	PhMe	*3.7* (2.5)	3%	51%
6	10	20	*3.5* (4.0)	1,4-dioxane	*3.7* (2.5)	0%	78%
7	10	20	*3.6* (4.0)	1,4-dioxane	*3.7* (2.5)	0%	82%

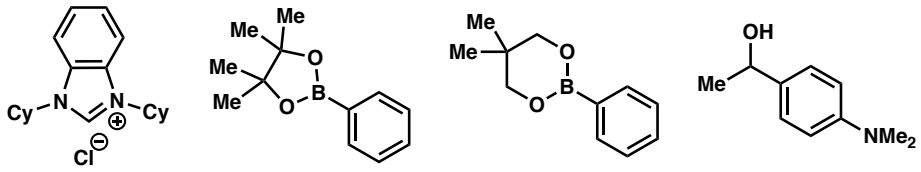

Benz-ICy·HCl (3.2)
Cy = cyclohexyl

Ph–B(pin) (3.5)

Ph–B(nep) (3.6)

DMPE (3.7)

Figure 3.3. Evaluation of reaction conditions for the nickel-catalyzed Suzuki–Miyaura coupling / transfer hydrogenation cascade of amide **3.1** with phenyl boronates and reductants. Standard conditions unless otherwise noted: amide substrate (0.20 mmol, 1.0 equiv); phenyl boronate (0.50–0.80 mmol, 2.5–4.0 equiv); reductant (0.50 equiv, 2.5 equiv); K_3PO_4 (0.80 mmol, 4.0 equiv); H_2O (0.40 mmol, 2.0 equiv); $Ni(cod)_2$ (0.010–0.020 mmol, 5–10 mol%); **3.2** (0.020–0.040 mmol, 10–20 mol%); solvent (1.0 M); 120 °C; 16 h in a sealed vial. [a]Yield determined by ^1H NMR analysis using 1,3,5-trimethoxybenzene as an external standard.

3.4 Scope of the Aliphatic Amide Substrate and Robustness Screen

With optimized conditions in hand, we evaluated the scope of the reaction with respect to the aliphatic amide[33] coupling partner using phenyl boronate **3.6**, which afforded a range of alkyl–aryl alcohol products (Figure 3.4). Beginning with the parent dihydrocinnamic acid-derived amide substrate used in optimization studies (i.e., **3.1**), the reductive arylation furnished alcohol **3.4** in 76% isolated yield. Additionally, the use of an unbranched amide derived from decanoic acid provided alcohol **3.8** in 82% yield. Carrying out the reaction at 130 °C allowed for the reductive

arylation of sterically encumbered substrates, as demonstrated by the formation of alcohol **3.9** in 61% yield. The compatibility of carbocyclic amides with boronate **3.6** was explored as well and gave alcohols **3.10**–**3.14** in good yields. We also evaluated an amide substrate bearing an epimerizable stereocenter α to the amide carbonyl. As shown by the formation of alcohol **3.15** from the corresponding *trans* amide substrate, minimal erosion of stereochemistry was observed.[34] Of note, the ester moiety was not disturbed, demonstrating both the preferential cleavage of the amide C–N bond over the ester C–O bond and the mildness of the reducing conditions.[35] The tolerance of the methodology toward heterocycles was also determined. Notably, tetrahydropyrans, pyrrolidines, and piperidines, all of which are valuable in medicinal chemistry,[36] could be employed as evidenced by the synthesis of alcohols **3.16**–**3.20**, respectively.

With the aim of further improving the synthetic utility of the reductive arylation, we performed a robustness screen to assess the compatibility of the reaction with various functional groups and heterocycles (Figure 3.4).[37] Results indicated the tolerance of functional groups including tertiary alcohols, secondary anilines, and secondary amides, as demonstrated by moderate to good yields of alcohol **3.20** and appreciable recoveries of additives **3.22**–**3.24**, respectively. Additionally, heterocycles such as quinoline (**3.25**), dibenzofuran (**3.26**), and *N*-methyl indole (**3.27**) were found to be stable under our standard reductive arylation conditions with minimal to no inhibition of reactivity.[38] These results complement those presented in the scope of the reaction and further demonstrate the methodology's robustness toward several heteroatom-containing functional groups.

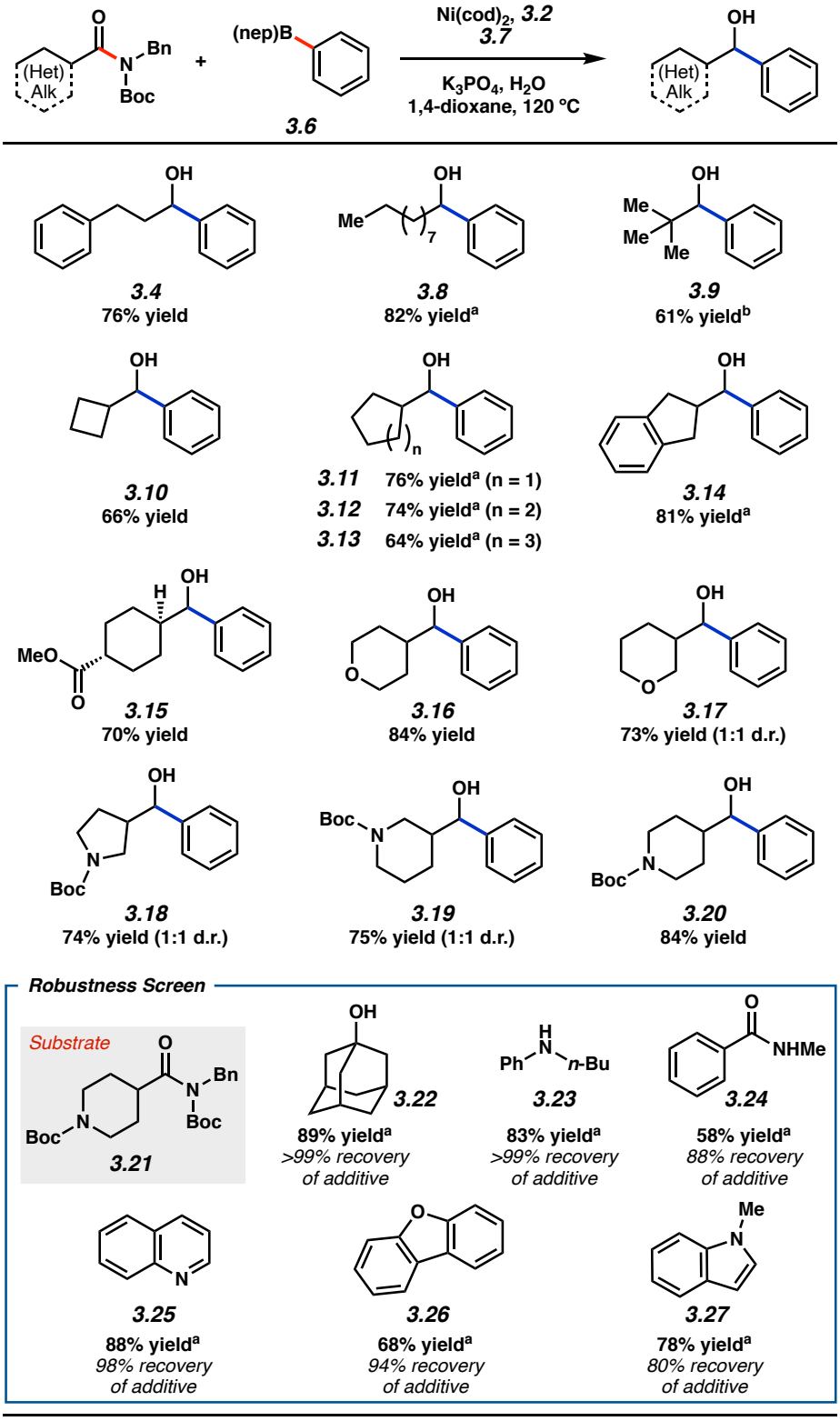

Figure 3.4. Scope of the reductive arylation of aliphatic amides and boronate **3.6**. Standard conditions unless otherwise noted: amide substrate (0.20 mmol, 1.0 equiv); phenyl boronate **3.6** (0.80 mmol, 4.0 equiv); 7 (0.50 mmol, 2.5 equiv); K_3PO_4 (0.80 mmol, 4.0 equiv); H_2O (0.40 mmol,

2.0 equiv); $Ni(cod)_2$ (0.020 mmol, 10 mol%); **3.2** (0.040 mmol, 20 mol%); solvent (1.0 M); 120 °C; 16 h. Unless otherwise noted, yields reflect the average of two isolation experiments. [a]Yield determined by ^1H NMR analysis using 1,3,5-trimethoxybenzene as an external standard. [b]Reaction ran at 130 °C.

3.5 Scope of Aryl Boronic Ester Coupling Partner

The scope of the aryl boronate component was also examined by coupling pinacol boronates with various amides (Figure 3.5).[31,39] Methyl substitution at the ortho, meta, or para positions of the aryl boronate was tolerated, as demonstrated by the formation of alcohols **3.28**–**3.30** in synthetically useful yields. We also evaluated aryl boronic ester nucleophiles bearing either a trimethylsilyl or trifluoromethyl group, which furnished alcohols **3.31** and **3.32**, respectively, in good yields. Additionally, a naphthyl boronate ester underwent the reductive arylation to afford alcohol **3.33** in 58% yield. We also tested several boronates that possess functional groups that have been demonstrated to be reactive to nickel catalysis. To our delight, an aryl ester,[35] an ether,[40] and a dimethyl amine were tolerated,[41] thus giving rise to alcohols **3.34**–**3.36**, respectively. Furthermore, a boronic ester containing a morpholinopyridine motif was employed to furnish alcohol **3.37**, showing the reaction's tolerance of this heteroatom-rich unit.[42]

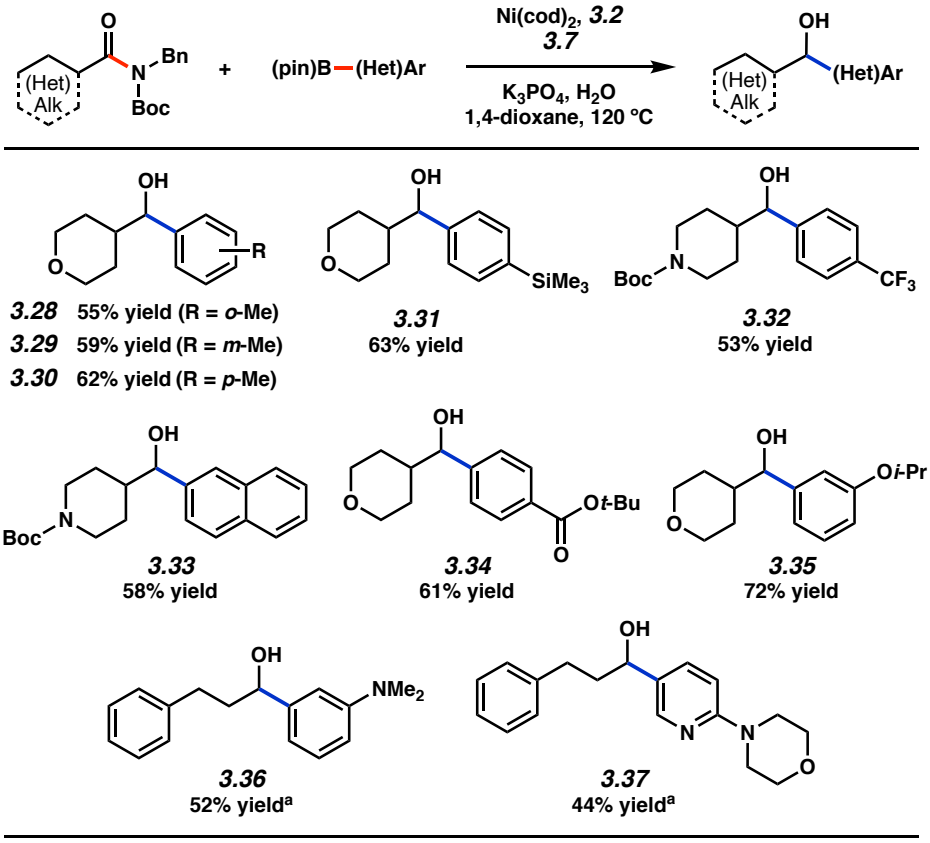

Figure 3.5. Scope of the reductive arylation of aliphatic amides and aryl boronates. Standard conditions unless otherwise noted: amide substrate (0.20 mmol, 1.0 equiv); aryl boronate (0.80–1.2 mmol, 4.0–6.0 equiv); **3.7** (0.50 mmol, 2.5 equiv); K_3PO_4 (0.80 mmol, 4.0 equiv); H_2O (0.40 mmol, 2.0 equiv); $Ni(cod)_2$ (0.020–0.040 mmol, 10–20 mol%); **3.2** (0.040–0.080 mmol, 20–40 mol%); solvent (1.0 M); 120 °C; 16–24 h**.** Unless otherwise noted, yields reflect the average of two isolation experiments. [a]Yield determined by ^1H NMR analysis using 1,3,5-trimethoxybenzene as an external standard.

3.6 Synthetic Applications of the Methodology

The utility of this methodology was evaluated in the synthesis of known intermediates toward two bioactive compounds (Figure 3.6). In the first example (Figure 3.6a), amide **3.38** underwent reductive arylation with boronate **3.39**, despite the notable electron deficiency of this nucleophile. This delivered alcohol **3.40**, a precursor to a known γ-secretase modulator (**3.41**).[43] We also targeted the interception of a known route to fluoxetine (**3.44**),[44] the active ingredient in the blockbuster drug Prozac®. Toward this end, amide **3.42**, derived from the corresponding

commercially available carboxylic acid, was coupled with boronate **3.6** (Figure 3.6b). This transformation furnished alcohol **3.43** in 69% yield, providing facile access to a known intermediate in the synthesis of **3.44** from commercially available materials.[44] These results not only further demonstrate the viability of leveraging a cross-coupling approach to add two disparate nucleophiles into an amide carbonyl carbon, but also showcase the practical utility of this reductive arylation protocol in the synthesis of complex chiral molecules.

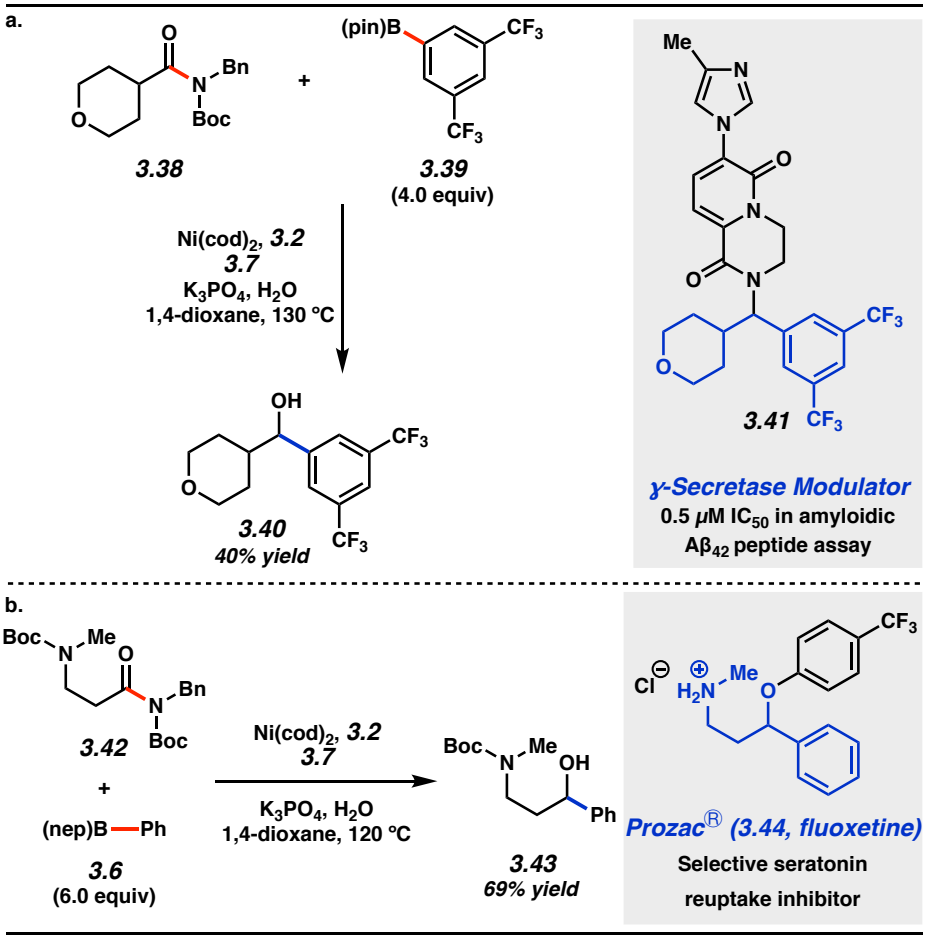

Figure 3.6. (a) Synthesis of alcohol **3.40**, an intermediate in the synthesis of γ-secretase modulator **3.41**. (b) Synthesis of alcohol **3.43**, intercepting a known synthetic route toward Prozac® (**3.44**, fluoxetine). See section 3.8.2.6 for details.

3.7 Conclusion

In summary, we have developed the first catalytic method for the direct intermolecular addition of two distinct nucleophiles to the amide carbonyl carbon. This transformation takes advantage of non-precious metal catalysis and allows for the facile conversion of amides to chiral alcohols via a cascade reaction involving Suzuki–Miyaura cross-coupling and subsequent transfer hydrogenation. The methodology has a broad scope with respect to both the amide and boronate cross-coupling partners. Additionally, it shows tolerance toward epimerizable stereocenters, select functional groups (i.e., alcohols, amines, esters, ethers, and secondary amides,) and a range of heterocycles. Moreover, the methodology can be used to access scaffolds of value to medicinal chemistry, as shown by the syntheses of **3.40** and **3.43**. This study validates the use of a cross-coupling approach to construct sp^3 carbon centers from the amide carbonyl carbon in a single operational step. We hope this study will prompt the development of additional processes that allow for the direct conversion of carboxylic acid derivatives to functional groups bearing stereogenic centers[45] via catalytic cascade processes.

3.8 Experimental Section

3.8.1 Materials and Methods.

Unless stated otherwise, reactions were conducted in flame-dried glassware under an atmosphere of nitrogen or argon and commercially obtained reagents were used as received. Amide substrates were synthesized following protocols specified in Section A in the Experimental Procedures. Alcohol **3.7** was prepared according to literature procedure.[46] Boronate esters **3.5**, **3.59**–**3.61**, **3.63**–**3.65**, **3.67** and **3.68** were obtained from Combi-Blocks. Boronate ester **3.6** was obtained from TCI Chemicals. Boronate ester **3.39** was obtained from AK Scientific. Boronate esters **3.62** and **3.66** were prepared according to literature procedure.[47] $Ni(cod)_2$ and Benz-ICy•HCl (**3.2**) were obtained from Strem Chemicals. [(TMEDA)Ni(*o*-tolyl)Cl] was prepared according to literature procedure.[48] Ligand A (**3.71**) was prepared according to literature procedure.[49] Potassium phosphate (K_3PO_4) was obtained from Acros. 1,4-dioxane was obtained from Fisher Scientific and purified by distillation over sodium metal degassed by sparging with N_2 for 1 h. Paraffin wax (mp 53–57 °C ASTM D 87) was obtained from Sigma-Aldrich and used as received). 1,3,5-trimethoxybenzene was obtained from Alfa Aesar and used as received. Reaction temperatures were controlled using an IKAmag temperature modulator, and unless stated otherwise, reactions were performed at room temperature (approximately 23 °C). Thin-layer chromatography (TLC) was conducted with EMD gel 60 F254 pre-coated plates (0.25 mm for analytical chromatography and 0.50 mm for preparative chromatography) and visualized using a combination of UV, anisaldehyde, iodine, and potassium permanganate staining techniques. Silicycle Siliaflash P60 (particle size 0.040–0.063 mm) was used for flash column chromatography. ^{1}H NMR spectra were recorded on Bruker spectrometers (400, 500, and 600 MHz were allowed for our provided spectra) and are reported relative to residual solvent signals.

Data for ^{1}H NMR spectra are reported as follows: chemical shift (δ ppm), multiplicity, coupling constant (Hz), integration. Data for ^{13}C NMR are reported in terms of chemical shift (at 125 MHz). IR spectra were recorded on a Perkin-Elmer UATR Two FT-IR spectrometer and are reported in terms of frequency absorption (cm^{-1}). DART-MS spectra were collected on a Thermo Exactive Plus MSD (Thermo Scientific) equipped with an ID-CUBE ion source and a Vapur Interface (IonSense Inc.). Both the source and MSD were controlled by Excalibur software v. 3.0. The analyte was spotted onto OpenSpot sampling cards (IonSense Inc.) using $CHCl_3$ or CH_2Cl_2 as the solvent. Ionization was accomplished using UHP He plasma with no additional ionization agents. The mass calibration was carried out using Pierce LTQ Velos ESI (+) and (–) Ion calibration solutions (Thermo Fisher Scientific). Determination of enantiopurity was carried out on a Mettler Toledo SFC (supercritical fluid chromatography) using Daicel ChiralPak AD–H columnn. Data for SFC are reported in enantiomeric excess (ee). For SFC chromatograms see section 3.8.2.11 of Experimental Procedures.

3.8.2 Experimental Procedures

3.8.2.1 Syntheses of Amide Substrates

Supporting information for the syntheses of amides **3.1**,[50] **3.45**–**3.48**,[50] **3.21**,[51] **3.38**,[51] **3.49**–**3.52**,[51] and **3.53**[52] have been published and spectral data match those previously reported.

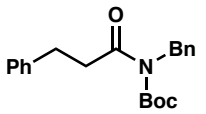

3.1

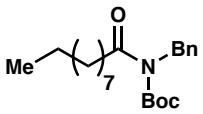

3.45

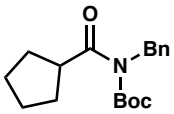

3.46

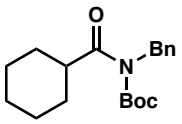

3.47

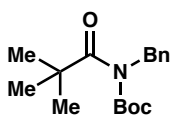

3.48

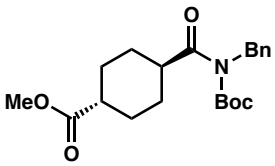

3.49

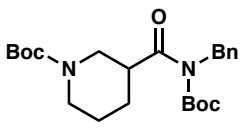

3.50

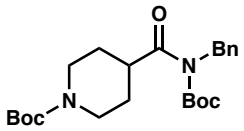

3.21

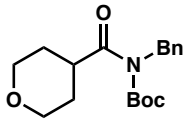

3.38

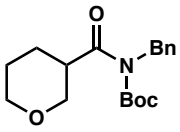

3.51

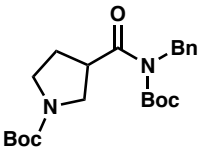

3.52

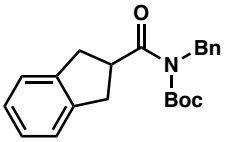

3.53

Syntheses for the remaining substrates shown in Figures 3.4 and 3.6 are as follows:

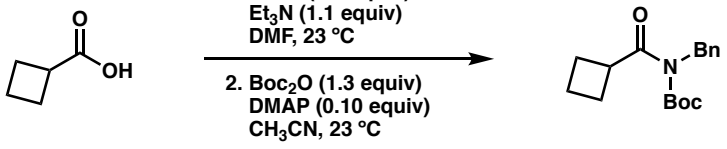

3.54 (32% yield, 2 steps) *3.55*

Amide 3.55. To a mixture of carboxylic acid **3.54** (65.0 mg, 0.650 mmol, 1.00 equiv), EDC•HCl (137 mg, 0.0720 mmol, 1.10 equiv), HOBt (109 g, 0.710 mmol, 1.10 equiv), triethylamine (0.100 mL, 0.710 mmol, 1.10 equiv), and DMF (5.00 mL, 0.130 M) was added benzylamine (78.0 µL, 0.710 mmol, 1.10 equiv). The resulting mixture was stirred at 23 ºC for 17 h, and then diluted with deionized water (5 mL) and transferred to a separatory funnel with brine (5 mL). The aqueous layer was extracted with EtOAc (3 x 10 mL), then the organic layers were combined and washed with deionized water (3 x 10 mL), dried over Na_2SO_4, and evaporated under reduced pressure. The resulting crude material was used in the subsequent step without further purification.

To a flask containing the crude material from the previous step was added DMAP (8.00 mg, 0.0650 mmol, 0.100 equiv) followed by acetonitrile (4.00 mL, 0.160 M). Boc_2O (184 g, 0.850

mmol, 1.30 equiv) was added in one portion and the reaction vessel was flushed with N_2, then the reaction mixture was allowed to stir at 23 ºC for 20 h. The reaction was quenched by addition of saturated aqueous $NaHCO_3$ (5 mL), transferred to a separatory funnel with EtOAc (10 mL) and H_2O (10 mL), and extracted with EtOAc (3 x 10 mL). The organic layers were combined, dried over Na_2SO_4, and evaporated under reduced pressure. The resulting crude residue was purified by flash column chromatography (29:1 Hexanes:EtOAc) to yield amide **3.55** (60.5 mg, 32% yield, over two steps) as a clear oil. Amide **3.55**: R_f 0.65 (5:1 Hexanes:EtOAc); ^{1}H NMR (600 MHz, C_6D_6): δ 7.30 (d, *J* = 7.5, 2H), 7.11 (t, *J* = 7.5, 2H), 7.03 (t, *J* = 7.5, 1H), 4.88 (s, 2H), 4.05 (quint, *J* = 8.3, 1H), 2.54–2.43 (m, 2H), 2.30–2.18 (m, 2H), 1.82–1.67 (m, 2H), 1.17 (s, 9H); ^{13}C NMR (125 MHz, $CDCl_3$): δ 178.0, 152.8, 138.6, 128.4, 127.6, 127.1, 83.0, 47.6, 41.4, 28.0, 25.8, 17.9; IR (film): 2980, 2869, 1732, 1687, 1144, 980 cm^{-1}; HRMS-APCI (*m/z*) $[M + H]^+$ calcd for $C_{17}H_{24}NO_3^+$, 290.17507; found 290.17377.

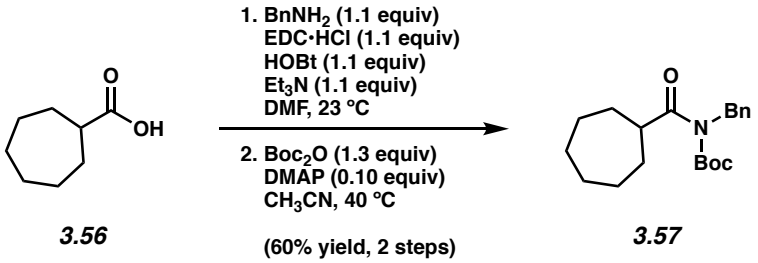

Amide 3.57. To a mixture of carboxylic acid **3.56** (1.00 g, 7.03 mmol, 1.00 equiv), EDC•HCl (1.48 g, 7.74 mmol, 1.10 equiv), HOBt (1.18 g, 7.74 mmol, 1.10 equiv), triethylamine (1.10 mL, 7.74 mmol, 1.10 equiv), and DMF (70 mL, 0.10 M) was added benzylamine (0.850 mL, 7.740 mmol, 1.10 equiv). The resulting mixture was stirred at 23 ºC for 20 h, and then diluted with deionized water (100 mL) and transferred to a separatory funnel with EtOAc (30 mL) and brine (15 mL). The aqueous layer was extracted with EtOAc (3 x 100 mL), then the organic layers were combined

and washed with deionized water (4 x 100 mL), dried over Na_2SO_4, and evaporated under reduced pressure. The resulting crude solid material was used in the subsequent step without further purification.

To a flask containing the crude material from the previous step was added DMAP (85.9 mg, 0.703 mmol, 0.100 equiv) followed by acetonitrile (35.0 mL, 0.200 M). Boc_2O (1.99 g, 9.14 mmol, 1.30 equiv) was added in one portion and the reaction vessel was flushed with N_2, then the reaction mixture was allowed to stir at 40 ºC for 16 h. The reaction was quenched by addition of saturated aqueous $NaHCO_3$ (100 mL), transferred to a separatory funnel with EtOAc (20 mL) and extracted with EtOAc (3 x 40 mL). The organic layers were combined, dried over Na_2SO_4, and evaporated under reduced pressure. The resulting crude residue was purified by flash chromatography (99:1 Hexanes:EtOAc $\rightarrow$ 9:1 Hexanes:EtOAc) to yield amide **3.57** as a white crystalline powder. Hot recrystallization of the purified product from *n*-heptane gave the recrystallized material (1.41 g, 60% yield over two steps) as white crystals. Amide **3.57**: mp: 57.7–62.8 ºC; R_f 0.57 (5:1 Hexanes:EtOAc); ^{1}H NMR (500 MHz, $CDCl_3$): δ 7.32–7.27 (m, 2H), 7.25–7.20 (m, 3H), 4.85 (s, 2H), 3.59 (tt, J = 9.7, 3.9, 1H), 1.97–1.87 (m, 2H), 1.81–1.70 (m, 2H), 1.70–1.44 (m, 8H), 1.40 (s, 9H); ^{13}C NMR (125 MHz, $CDCl_3$): δ 180.8, 153.3, 138.7, 128.4, 127.6, 127.1, 83.0, 47.8, 45.8, 31.9, 28.4, 28.0, 26.7; IR (film): 2977, 2928, 2858, 1734, 1694, 1369, 1148 cm^{-1}; HRMS-APCI (*m/z*) $[M + H]^+$ calcd for $C_{20}H_{30}NO_3^+$, 332.22202; found 332.22098.

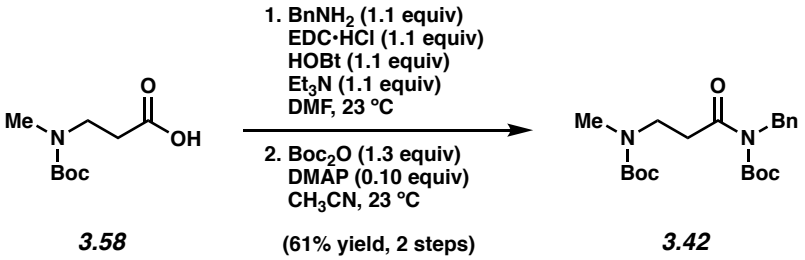

Amide 3.42. To a mixture of carboxylic acid **3.58** (500 mg, 2.46 mmol, 1.00 equiv), EDC•HCl (519 mg, 2.71 mmol, 1.10 equiv), HOBt (414 mg, 2.71 mmol, 1.10 equiv), triethylamine (0.380 mL, 2.71 mmol, 1.10 equiv), and DMF (25.0 mL, 0.100 M) was added benzylamine (0.300 mL, 2.71 mmol, 1.10 equiv). The resulting mixture was stirred at 23 ºC for 23 h, and then diluted with deionized water (100 mL) and transferred to a separatory funnel with EtOAc (30 mL) and brine (15 mL). The aqueous layer was extracted with EtOAc (3 x 80 mL), then the organic layers were combined and washed with deionized water (4 x 80 mL), dried over Na_2SO_4, and evaporated under reduced pressure. The resulting crude solid material was used in the subsequent step without further purification.

To a flask containing the crude material from the previous step was added DMAP (28.9 mg, 0.236 mmol, 0.100 equiv) followed by acetonitrile (12.0 mL, 0.200 M). Boc_2O (671 mg, 3.07 mmol, 1.30 equiv) was added in one portion and the reaction vessel was flushed with N_2, then the reaction mixture was allowed to stir at 23 ºC for 17 h. The reaction was quenched by addition of saturated aqueous $NaHCO_3$ (10 mL), transferred to a separatory funnel with EtOAc (20 mL) and extracted with EtOAc (3 x 40 mL). The organic layers were combined, dried over Na_2SO_4, and evaporated under reduced pressure. The resulting crude residue was purified by flash chromatography (19:1 Hexanes:EtOAc → 9:1 Hexanes:EtOAc) to yield amide **3.42** (0.57 g, 61% yield over two steps) as a clear oil. Amide **3.42**: R_f 0.38 (5:1 Hexanes:EtOAc); ^{1}H NMR (500 MHz, $CDCl_3$): δ 7.33–7.17 (m, 5H), 4.87 (br s, 2H), 3.55 (s, 2H), 3.15 (br s, 2H), 2.86 (br s, 3H),

1.45 (s, 9H), 1.40 (s, 9H); ^{13}C NMR (125 MHz, $CDCl_3$): δ 174.4, 155.7, 153.1, 138.3, 128.4, 127.6, 127.3, 83.5, 79.6, 79.5, 47.4, 45.6, 45.3, 37.2, 36.6, 35.0, 34.8, 28.6, 28.0; IR (film): 2977, 1734, 1691, 1368, 1145 cm^{-1}; HRMS-APCI (*m/z*) $[M + H]^+$ calcd for $C_{21}H_{33}N_2O_5^+$, 393.23840; found 393.23730.

*Note: **3.42** was obtained as a mixture of rotamers. These data represent empirically observed chemical shifts from the ^{1}H NMR and ^{13}C NMR spectra.*

3.8.2.2 Relevant Control Experiments

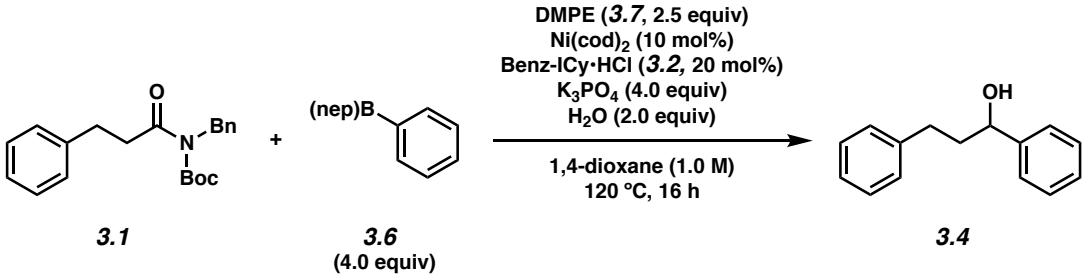

Representative Procedure for Conversion of Aliphatic Amides to Secondary Alcohols from Figure 3.3 (amide 3.1 and boronate ester 3.6 used as an example). A 1-dram vial was charged with anhydrous powder K_3PO_4 (170 mg, 0.800 mmol, 4.00 equiv) and a magnetic stir bar. The vial and its contents were flame-dried under reduced pressure and allowed to cool under N_2. Amide substrate **3.1** (67.9 mg, 0.200 mmol, 1.00 equiv), boronate ester nucleophile **3.6** (152 mg, 0.800 mmol, 4.00 equiv), and DMPE (**3.7**, 82.6 mg, 0.500 mmol, 2.50 equiv) were added. The vial was flushed with N_2 for 5 min, then water (7.21 μL, 0.400 mmol, 2.00 equiv), which had been sparged with N_2 for 10 min, was added. The vial was taken into a glovebox and charged with $Ni(cod)_2$ (5.50 mg, 0.0200 mmol, 10 mol%) and Benz-ICy•HCl (**3.2**, 12.8 mg, 0.0400 mmol, 20 mol%). Subsequently, 1,4-dioxane (200 μL, 1.00 M) was added. The vial was sealed with a Teflon-lined screw cap, removed from the glovebox, and stirred vigorously (800 RPM) at 120 ºC for 16 h. After

cooling to 23 ºC, the mixture was quenched by the addition of saturated aqueous NH_4Cl (1 mL) and extracted with EtOAc (3 x 2 mL). The combined organic layers were then filtered over a plug of silica gel (3 cm) and Na_2SO_4 (3 cm) using EtOAc (10 mL) as eluent. The volatiles were removed under pressure and the yield of alcohol **3.4** was determined by ^{1}H NMR analysis with 1,3,5-trimethoxybenzene as an external standard.

Any modifications of the conditions shown in the representative procedure above are specific below in Table 3.1.

Table 3.1. Relevant control experiments

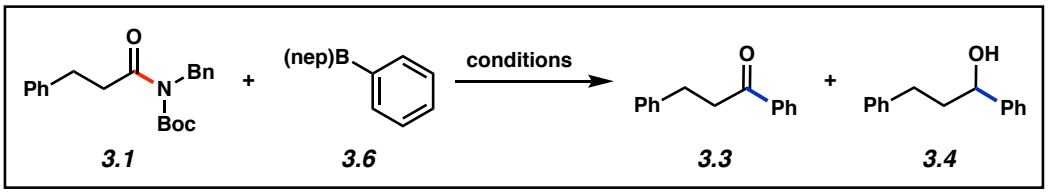

Reaction Conditions	Experimental Results[a] 3.1	3.3	3.4
3.6 (4.0 equiv), DMPE (***3.7***, 4.0 equiv), K_3PO_4 (4.0 equiv), H_2O (2.0 equiv) 1,4-dioxane (1.0 M), 120 °C, 16 h	5%[b]	0%	0%
3.6 (4.0 equiv), DMPE (***3.7***, 4.0 equiv), K_3PO_4 (4.0 equiv), H_2O (2.0 equiv) Benz-ICy·HCl (***3.2***, 20 mol%), 1,4-dioxane (1.0 M), 120 °C, 16 h	0%[b]	0%	0%
3.6 (4.0 equiv), DMPE (***3.7***, 4.0 equiv), K_3PO_4 (4.0 equiv), H_2O (2.0 equiv) $Ni(cod)_2$ (10 mol%), 1,4-dioxane (1.0 M), 120 °C, 16 h	12%[b]	0%	0%

[a] Yields determined by ^{1}H NMR analysis using 1,3,5-trimethoxybenzene as an external standard.

[b] Substantial amounts of the corresponding Boc-cleavage product (de-Boc amide starting material) were observed due to the elevated reaction temperature.

3.8.2.3 General Procedures for Methodology

3.8.2.3.1 General Procedure A. A 1-dram vial was charged with anhydrous powder K_3PO_4 (170 mg, 8.00 mmol, 4.00 equiv) and a magnetic stir bar. The vial and its contents were flame-dried under reduced pressure and allowed to cool under N_2. Amide substrate (0.200 mmol, 1.00 equiv), boronate ester nucleophile (152 mg, 0.800 mmol, 4.00 equiv), and DMPE (**3.7**, 82.6 mg, 0.500 mmol, 2.50 equiv) were added. The vial was flushed with N_2 for 5 min, then water (7.21 μL, 0.400 mmol, 2.00 equiv), which had been sparged with N_2 for 10 min, was added. The vial was taken into a glovebox and charged with $Ni(cod)_2$ (5.50 mg, 0.0200 mmol, 10 mol%) and Benz-ICy•HCl (**3.2**, 12.8 mg, 0.0400 mmol, 20 mol%). Subsequently, 1,4-dioxane (200 μL, 1.00 M) was added. The vial was sealed with a Teflon-lined screw cap, removed from the glovebox, and stirred vigorously (800 RPM) at 120 ºC for 16 h. After cooling to 23 ºC, the mixture was quenched by the addition of saturated aqueous NH_4Cl (1 mL) and extracted with EtOAc (3 x 2 mL). The combined organic layers were then filtered over a plug of silica gel (3 cm) and Na_2SO_4 (3 cm) using EtOAc (10 mL) as eluent and the volatiles were removed under pressure. The crude mixture was adsorbed onto silica gel (450 mg) under reduced pressure and purified by flash column chromatography on silica.

3.8.2.3.2 General Procedure B. A 1-dram vial was charged with anhydrous powder K_3PO_4 (170 mg, 8.00 mmol, 4.00 equiv) and a magnetic stir bar. The vial and its contents were flame-dried under reduced pressure and allowed to cool under N_2. Amide substrate (0.200 mmol, 1.00 equiv), boronate ester nucleophile (152 mg, 0.800 mmol, 4.00 equiv), and DMPE (**3.7**, 82.6 mg, 0.500 mmol, 2.50 equiv) were added. The vial was flushed with N_2 for 5 min, then water (7.21 μL, 0.400 mmol, 2.00 equiv), which had been sparged with N_2 for 10 min, was added. The vial was taken

into a glovebox and charged with $Ni(cod)_2$ (5.50 mg, 0.0200 mmol, 10 mol%) and Benz-ICy•HCl (**3.2**, 12.8 mg, 0.0400 mmol, 20 mol%). Subsequently, 1,4-dioxane (200 μL, 1.00 M) was added. The vial was sealed with a Teflon-lined screw cap, removed from the glovebox, and stirred vigorously (800 RPM) at 120 ºC for 16 h. After cooling to 23 ºC, the mixture was diluted with CH_2Cl_2 (1 mL) and washed with 2 M HCl (3 x 1 mL). The organic layer was then filtered over a plug of silica gel (3 cm) and Na_2SO_4 (3 cm) using EtOAc (10 mL) as eluent and the volatiles were removed under pressure. The crude mixture was adsorbed onto silica gel (450 mg) under reduced pressure and purified by flash column chromatography on silica.

3.8.2.3.3 General Procedure C. A 1-dram vial was charged with anhydrous powder K_3PO_4 (170 mg, 8.00 mmol, 4.00 equiv) and a magnetic stir bar. The vial and its contents were flame-dried under reduced pressure and allowed to cool under N_2. Amide substrate (0.200 mmol, 1.00 equiv), boronate ester nucleophile (228 mg, 1.20 mmol, 6.00 equiv), and DMPE (**3.7**, 82.6 mg, 0.500 mmol, 2.50 equiv) were added. The vial was flushed with N_2 for 5 min, then water (7.21 μL, 0.400 mmol, 2.00 equiv), which had been sparged with N_2 for 10 min, was added. The vial was taken into a glovebox and charged with $Ni(cod)_2$ (11.0 mg, 0.0400 mmol, 20 mol%) and Benz-ICy•HCl (**3.2**, 25.6 mg, 0.0800 mmol, 40 mol%). Subsequently, 1,4-dioxane (200 μL, 1.00 M) was added. The vial was sealed with a Teflon-lined screw cap, removed from the glovebox, and stirred vigorously (800 RPM) at 120 ºC for 16 h. After cooling to 23 ºC, the mixture was diluted with CH_2Cl_2 (1 mL) and washed with deionized H_2O (3 x 1 mL). The organic layer was then filtered over a plug of silica gel (3 cm) and Na_2SO_4 (3 cm) using EtOAc (10 mL) as eluent and the volatiles were removed under pressure. The crude mixture was adsorbed onto silica gel (450 mg) under reduced pressure and purified by flash column chromatography on silica.

Any modifications of the conditions shown in the representative procedures above are specified in the following schemes, which depict all of the results shown in Figures 3.4, 3.5, and 3.6.

3.8.2.4 Scope of Amide Substrates

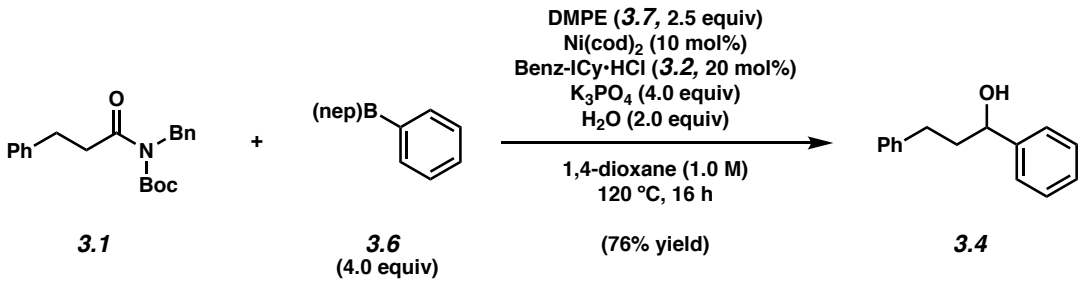

Alcohol 3.4. Crude alcohol **3.4** was synthesized following General Procedure A. Purification by flash column chromatography (99:1 Hexanes:EtOAc → 19:1 Hexanes:EtOAc) afforded alcohol **3.4** (76% yield, average of two experiments) as a white solid. Alcohol **3.4**: R_f 0.34 (5:1 Hexanes:EtOAc). ^{1}H NMR (500 MHz, $CDCl_3$): δ 7.40–7.34 (m, 4H), 7.32–7.27 (m, 3H), 7.23–7.16 (m, 3H), 4.70 (app t, J = 6.5, 1H), 2.76 (ddd, J = 13.9, 10.0, 5.8, 1H), 2.68 (ddd, J = 13.9, 9.6, 6.4, 1H), 2.21–1.98 (m, 2H), 1.92 (br s, 1H). Spectral data match those previously reported.[53]

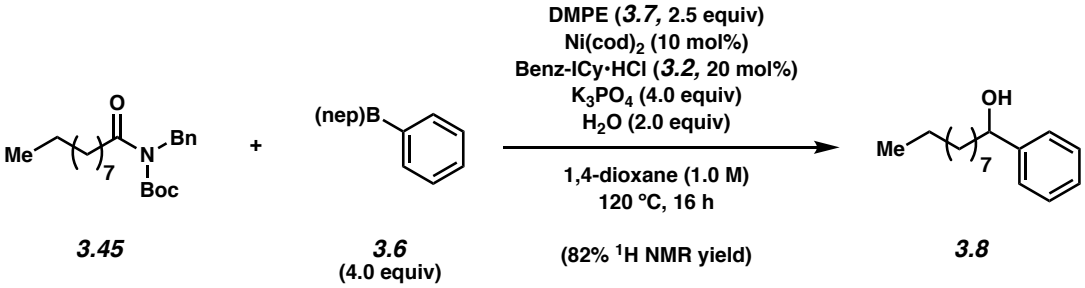

Alcohol 3.8. Crude alcohol **3.8** was synthesized following General Procedure A. ^{1}H NMR analysis of the crude reaction mixture indicated an 82% yield of alcohol **3.8** relative to 1,3,5-trimethoxybenzene external standard. Sequential purification by preparative thin-layer chromatography (3:1 Hexanes:Et_2O, then 4:1 Hexanes:Acetone) provided an analytical sample of

alcohol **3.8** as a clear oil. Alcohol **3.8**: R_f 0.52 (5:1 Hexanes:EtOAc). ^{1}H NMR (500 MHz, $CDCl_3$): δ 7.41–7.31 (m, 4H), 7.31–7.27 (m, 1H), 4.67 (dd, *J* = 7.5, 5.9, 1H), 1.87–1.75 (m, 2H), 1.75–1.65 (m, 1H), 1.49–1.36 (m, 1H), 1.36–1.16 (m, 13H), 0.87 (t, *J* = 6.8, 3H). Spectral data match those previously reported.[54]

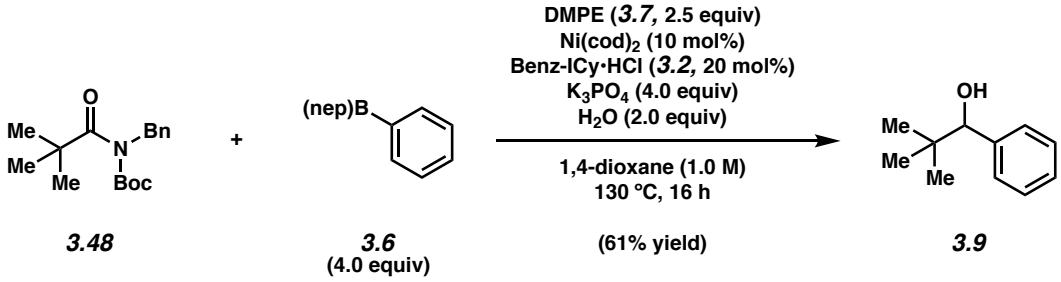

Alcohol 3.9. Crude alcohol **3.9** was synthesized following General Procedure A. Purification by flash column chromatography (39:1 Hexanes:Et_2O → 6.5:1 Hexanes:Et_2O) afforded alcohol **3.9** (61% yield, average of two experiments) as a clear oil. Alcohol **3.9**: R_f 0.48 (5:1 Hexanes:EtOAc). ^{1}H NMR (500 MHz, $CDCl_3$): δ 7.34–7.28 (m, 4H), 7.29–7.26 (m, 1H), 4.40 (s, 1H), 1.83 (s, 1H), 0.93 (s, 9H). Spectral data match those previously reported.[55]

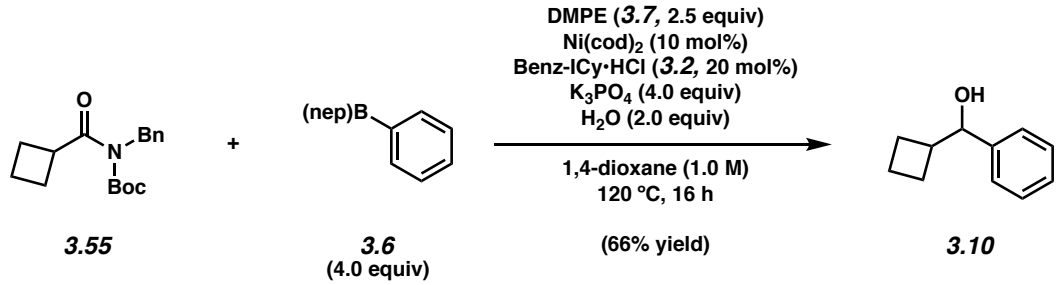

Alcohol 3.10. Crude alcohol **3.10** was synthesized following General Procedure A. Sequential purification by flash column chromatography (98:1:1 Hexanes:CH_2Cl_2:Et_2O → 3:1:1 Hexanes:CH_2Cl_2:Et_2O) followed by preparative thin-layer chromatography (1:1:1 CH_2Cl_2:Et_2O:Hexanes) afforded alcohol **3.10** (66% yield, average of two experiments) as a clear

oil. Alcohol **3.10**: R_f 0.38 (5:1 Hexanes:EtOAc). ^{1}H NMR (500 MHz, $CDCl_3$): δ 7.37–7.30 (m, 4H), 7.30–7.24 (m, 1H), 4.58 (d, *J* = 8.0, 1H), 2.69–2.56 (m, 1H), 2.15–1.96 (m, 2H), 1.92–1.75 (m, 5H). Spectral data match those previously reported.[55]

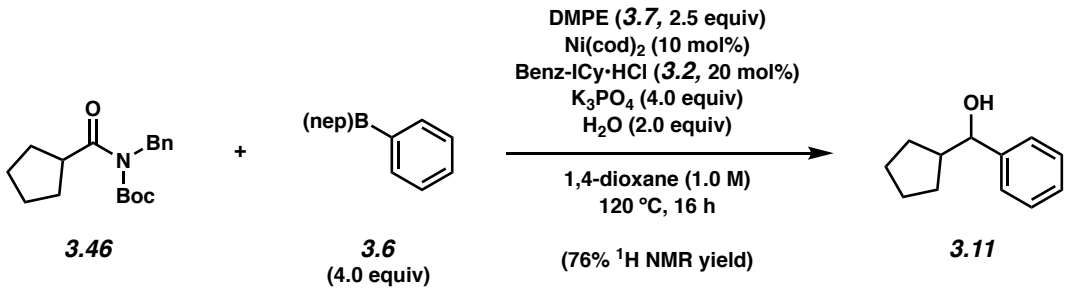

Alcohol 3.11. Crude alcohol **3.11** was synthesized following General Procedure A. ^{1}H NMR analysis of the crude reaction mixture indicated a 76% yield of alcohol **3.11** relative to 1,3,5-trimethoxybenzene external standard. Sequential purification by preparative thin-layer chromatography (5:1 Hexanes:EtOAc, then 5:1:1 Hexanes:CH_2Cl_2:Et_2O) afforded an analytical sample of alcohol **3.11** as a clear oil. Alcohol **3.11**: R_f 0.46 (5:1 Hexanes:EtOAc). ^{1}H NMR (500 MHz, $CDCl_3$): δ 7.36–7.26 (m, 5H), 7.30–7.27 (m, 1H), 4.41 (d, *J* = 8.5, 1H), 2.22 (app sext, *J* = 8.2, 1H), 1.95–1.78 (m, 2H), 1.70–1.63 (m, 1H), 1.54–1.44 (m, 3H), 1.42–1.33 (m, 1H), 1.19–1.10 (m, 1H). Spectral data match those previously reported.[56]

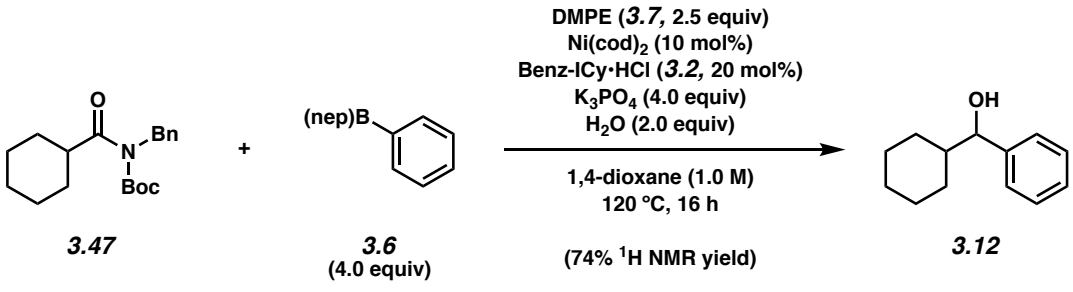

Alcohol 3.12. Crude alcohol **3.12** was synthesized following General Procedure A. ^{1}H NMR analysis of the crude reaction mixture indicated a 74% yield of alcohol **3.12** relative to 1,3,5-

trimethoxybenzene external standard. Alcohol **3.12**: R_f 0.44 (5:1 Hexanes:EtOAc). Spectral data match those previously reported.[57]

Note: The ^{1}H NMR spectrum of the crude material obtained using the reaction conditions above is provided and matches previously reported ^{1}H NMR data.

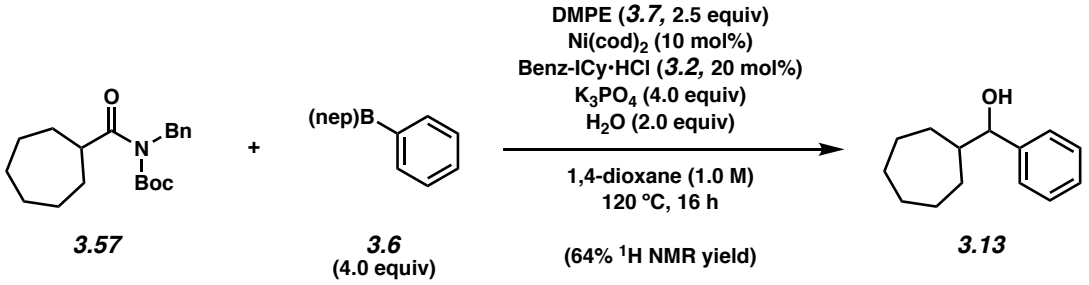

Alcohol 3.13. Crude alcohol **3.13** was synthesized following General Procedure A. ^{1}H NMR analysis of the crude reaction mixture indicated an 64% yield of alcohol **3.13** relative to 1,3,5-trimethoxybenzene external standard). Preparation of an authentic sample of alcohol **3.13** from cycloheptyl(phenyl)methanone (see section 3.8.2.7 for experimental details) allowed for direct comparison with the ^{1}H NMR spectrum of the crude reaction mixture and full characterization. Alcohol **3.13**: R_f 0.57 (5:1 Hexanes:EtOAc); ^{1}H NMR (600 MHz, $CDCl_3$): δ 7.35–7.23 (m, 5H), 4.47 (d, J = 6.7, 1H), 1.93–1.82 (m, 2H), 1.79 (br s, 1H), 1.72–1.65 (m, 1H), 1.65–1.30 (m, 9H), 1.23–1.09 (m, 1H); ^{13}C NMR (125 MHz, $CDCl_3$): δ 144.0, 128.3, 127.5, 126.8, 79.4, 46.4, 31.2, 29.4, 28.6, 28.5, 26.9, 26.7; IR (film): 3378, 2917, 2852, 1492, 699 cm^{-1}; HRMS-APCI (*m/z*) [M + H]$^+$ calcd for $C_{14}H_{21}O^+$, 205.15869; found 205.15788.

Note: ^{1}H NMR and ^{13}C NMR spectra of the authentic material, as prepared in section 3.8.2.7, are provided. A ^{1}H NMR spectrum of the crude material obtained using the reaction conditions above is also provided and matches the ^{1}H NMR spectrum of the authentic material.

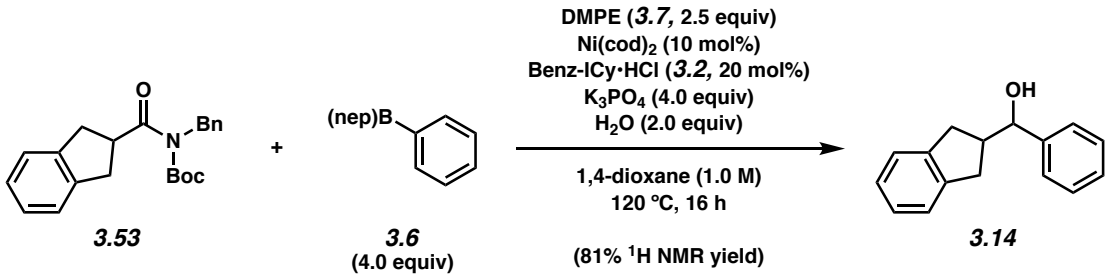

Alcohol 3.14. Crude alcohol **3.14** was synthesized following General Procedure A. ^{1}H NMR analysis of the crude reaction mixture indicated an 81% yield of alcohol **3.14** relative to 1,3,5-trimethoxybenzene external standard (average of two experiments). To the crude reaction mixture was added a Teflon-coated magnetic stir bar and CH_2Cl_2 (1 mL). The solution was stirred, cooled to 0 °C, TFA (200 μL) was slowly added, and the contents were stirred at 0 °C for 1 h. The volatiles were then removed under reduced pressure to give the crude material, which was purified by flash column chromatography (99:1 Hexanes:EtOAc → 19:1 Hexanes:EtOAc). Treatment of the purified product with a solution (4 mL total volume, 1:1 v/v) of MeOH:2M KOH and stirring the resulting solution at 23 °C for 2 h afforded an analytical sample of alcohol **3.14** as a white solid. Alcohol **3.14**: R_f 0.38 (5:1 Hexanes:EtOAc); ^{1}H NMR (500 MHz, $CDCl_3$): δ 7.43–7.29 (m, 5H), 7.23–7.22 (m, 1H), 7.14–7.11 (m, 3H), 4.63 (d, J = 8.5, 1H), 3.16 (dd, J = 16.0, 8.0, 1H), 3.06 (dd, J = 16.0, 8.0, 1H), 2.87 (app sext, J = 8.3, 1H), 2.69 (dd, J = 16.0, 8.0, 1H), 2.64 (dd, J = 16.0, 8.5, 1H); ^{13}C NMR (125 MHz, $CDCl_3$): δ 144.0, 143.2, 142.8, 128.7, 128.0, 126.7, 126.4, 126.3, 124.7, 124.5, 78.5, 47.3, 36.3, 36.1; IR (film): 3556, 3385, 3067, 3028, 2936 cm^{-1}; HRMS-APCI (*m/z*) $[M + NH_4]^+$ calcd for $C_{16}H_{20}NO^+$, 242.15394; found 242.15312.

*Note: **3.14** was obtained as a mixture of rotamers. These data represent empirically observed chemical shifts from the ^{1}H NMR and ^{13}C NMR spectra.*

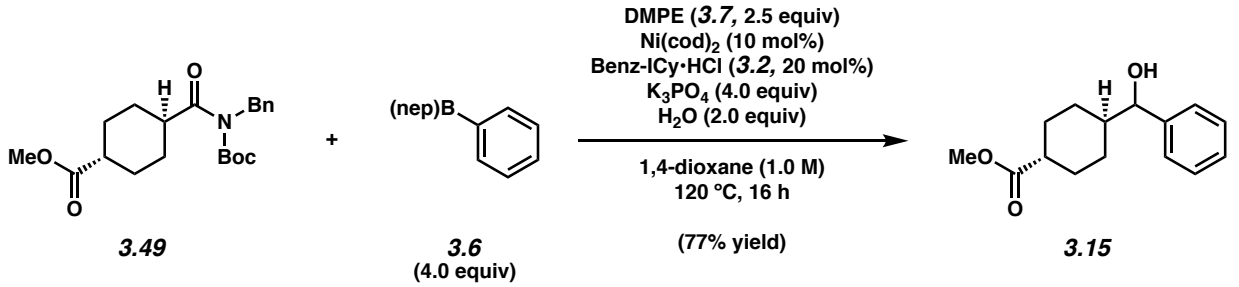

Alcohol 3.15. Crude alcohol **3.15** was synthesized following General Procedure A. Purification by flash column chromatography (99:1 Hexanes:Acetone → 9:1 Hexanes:Acetone) afforded a mixture of the trans and cis diastereomers of alcohol **3.15** (77% yield, 31:1 trans:cis diastereomers, average of two experiments) as a clear oil. Trans diastereomer alcohol **3.15**: R_f 0.22 (5:1 Hexanes:EtOAc); ^{1}H NMR (500 MHz, $CDCl_3$): δ 7.37–7.24 (m, 5H), 4.35 (d, J = 7.2, 1H), 3.63 (s, 3H), 2.20 (tt, J = 12.4, 3.6, 1H), 2.13–1.87 (m, 4H), 1.66–1.56 (m, 1H), 1.51–1.28 (m, 3H), 1.13–0.96 (m, 2H); ^{13}C NMR (125 MHz, $CDCl_3$): δ 176.6, 143.5, 128.4, 127.7, 126.7, 79.1, 51.6, 44.2, 43.3, 28.70, 28.68, 28.4, 27.9; IR (film): 3454, 2938, 1731, 1716, 1170 cm^{-1}; HRMS-APCI (*m/z*) $[M + H]^+$ calcd for $C_{15}H_{21}O_3^+$, 249.14852; found 249.14806.

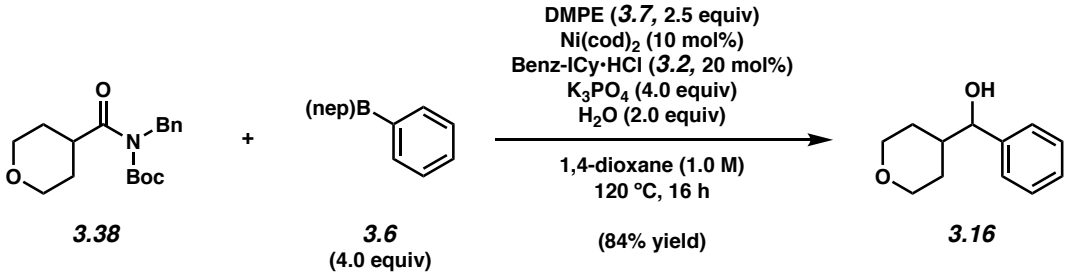

Alcohol 3.16. Crude alcohol **3.16** was synthesized following General Procedure B. Purification by flash column chromatography (19:1 Hexanes:EtOAc → 3:1 Hexanes:EtOAc) afforded alcohol **3.16** (84% yield, average of two experiments) as a white solid. Alcohol **3.16**: R_f 0.23 (3:1 Hexanes:EtOAc). ^{1}H NMR (500 MHz, $CDCl_3$): δ 7.38–7.26 (m, 5H), 4.32 (d, J = 7.7, 1H), 3.98

(app dd, J = 11.6, 4.6, 1H), 3.86 (app dd, J = 11.6, 4.6, 1H), 3.34 (td, J = 11.8, 2.2, 1H), 3.25 (td, J = 11.9, 2.3, 1H), 2.21 (br s, 1H), 1.94–1.86 (m, 1H), 1.86–1.72 (m, 1H), 1.50–1.36 (m, 1H), 1.36–1.20 (m, 1H), 1.20–1.07 (m, 1H). Spectral data match those previously reported.[58]

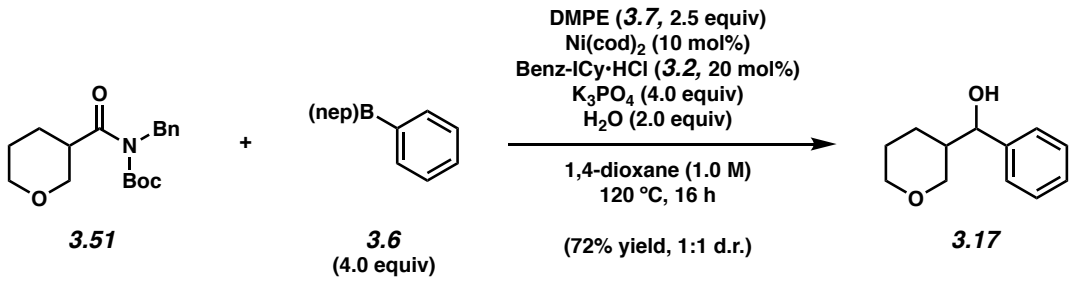

Alcohol 3.17. Crude alcohol **3.17** was synthesized following General Procedure B. Purification by flash chromatography (19:1 Hexanes:EtOAc → 1:1 Hexanes:EtOAc) afforded a mixture of diastereomers of alcohol **3.17** (72% yield, 1:1 d.r., average of two experiments) as a clear oil. Alcohol **3.17**: R_f 0.27 (3:1 Hexanes:EtOAc); ^{1}H NMR (500 MHz, $CDCl_3$): δ 7.37–7.26 (m, 10H), 4.50 (dd, J = 2.8, 7.0, 1H), 4.40 (dd, J = 2.9, 8.5, 1H), 4.16 (ddd, J = 1.8, 4.0, 11.3, 1H), 3.89–3.71 (m, 2H), 3.58 (ddd, J = 1.7, 4.0, 11.3, 1H), 3.49–3.30 (m, 3H), 3.20 (dd, J = 11.3, 9.4, 1H), 2.13, (d, J = 2.9, 1H), 2.10 (d, J = 3.0, 1H), 2.00–1.86 (m, 3H), 1.73–1.65 (m, 1H), 1.63–1.43 (m, 4H), 1.43–1.35 (m, 1H), 1.20–1.10 (m, 1H); ^{13}C NMR (125 MHz, $CDCl_3$, 19 of 20 observed): δ 143.1, 143.0, 128.60, 128.56, 128.0, 127.9, 126.7, 126.4, 76.6, 75.9, 70.8, 70.6, 68.6, 68.4, 43.0, 42.9, 26.4, 25.4, 25.3; IR (film): 3401, 2938, 2846, 1453, 1081 cm^{-1}; HRMS-APCI (*m/z*) $[M + H]^+$ calcd for $C_{12}H_{17}O_2^+$, 193.12231; found 193.12228.

*Note: **3.17** was obtained as a mixture of diastereomers. These data represent empirically observed chemical shifts from the ^{1}H NMR and ^{13}C NMR spectra.*

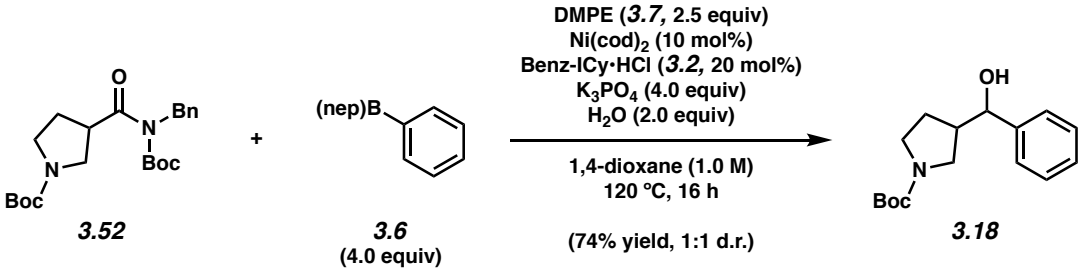

Alcohol 3.18. Crude alcohol **3.18** was synthesized following General Procedure B. Purification by flash chromatography (19:1 Hexanes:EtOAc → 1:1 Hexanes:EtOAc) afforded a mixture of diastereomers of alcohol **3.18** (74% yield, 1:1 d.r., average of two experiments) as a clear oil. Alcohol **3.18**: R_f 0.27 (9:1 PhH:Acetone). ^{1}H NMR (500 MHz, DMSO-d_6): 7.44–7.08 (m, 5H), 5.45–5.33 (m, 1H), 4.52–4.21 (m, 1H), 3.45–2.83 (m, 4H), 2.47–2.27 (m, 1H), 1.97–1.71 (m, 1H), 1.63–1.30 (m, 10H). Spectral data match those previously reported.[59]

*Note: **3.18** was obtained as a mixture of rotamers and diastereomers. These data represent empirically observed chemical shifts from the ^{1}H NMR spectra.*

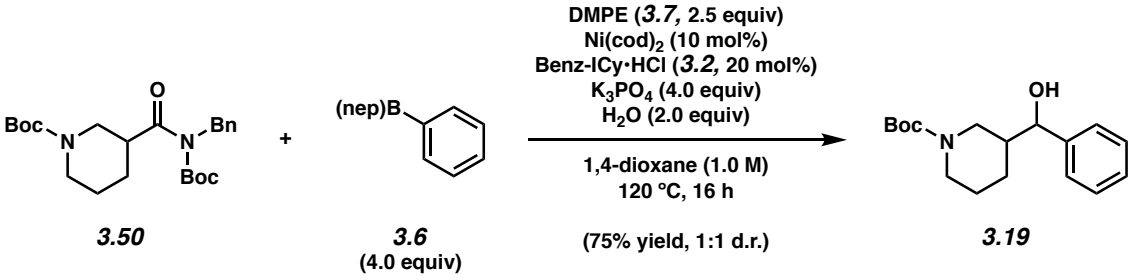

Alcohol 3.19. Crude alcohol **3.19** was synthesized following General Procedure B. Purification by flash column chromatography (PhH → 9:1 PhH:Acetone) afforded a mixture of diastereomers of alcohol **3.19** (75% yield, 1:1 d.r. average of two experiments) as a clear oil. Alcohol **3.19**: R_f 0.44 (9:1 PhH:Acetone); ^{1}H NMR (500 MHz, $CDCl_3$, 49 of 50 observed): δ 7.81–7.26 (m, 10H), 4.50 (br s, 1H), 4.43 (d, J = 8.5, 1H), 4.16–2.46 (m, 7H), 2.24–1.51 (m, 10H), 1.49–1.31 (m, 18H), 1.22–1.09 (m, 1H); ^{13}C NMR (125 MHz, $CDCl_3$, 23 of 26 observed): δ 155.4, 155.0, 142.9, 128.57,

128.56, 127.93, 127.91, 126.7, 126.5, 79.7, 79.4, 76.5, 75.9, 46.7, 44.5, 43.1, 43.0, 28.6, 28.5, 27.0, 26.3, 24.8, 24.0; IR (film): 3422, 2975, 2930, 1665, 1424 cm^{-1}; HRMS-APCI (*m/z*) $[M + H]^+$ calcd for $C_{17}H_{26}NO_3^+$, 292.19072; found 292.18998.

*Note: **3.19** was obtained as a mixture of rotamers and diastereomers. These data represent empirically observed chemical shifts from the ^1H NMR and ^{13}C NMR spectra.*

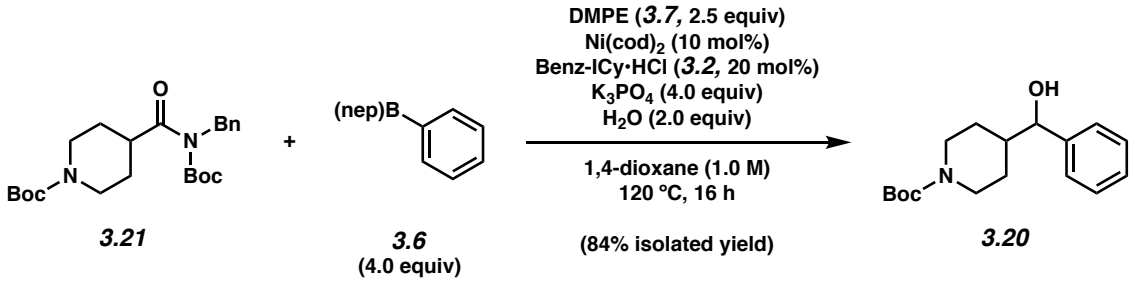

Alcohol 3.20. Crude alcohol **3.20** was synthesized following General Procedure B. Purification by flash column chromatography (PhH → 9:1 PhH:Acetone) afforded alcohol **3.20** (84% yield, average of two experiments) as a clear oil. Alcohol **3.20**: R_f 0.33 (9:1 PhH:Acetone). ^1H NMR (500 MHz, $CDCl_3$): 7.38–7.23 (m, 5H), 4.34 (d, J = 7.5, 1H), 4.29–3.81 (m, 2H), 2.77–2.38 (m, 2H), 2.26 (br s, 1H), 1.98–1.89 (m, 1H), 1.81–1.65 (m, 1H), 1.42 (s, 9H), 1.33–1.17 (m, 2H), 1.11 (app qd, J = 12.5, 4.4, 1H). Spectral data match those previously reported.[58]

3.8.2.5 Scope of Boronate Ester Nucleophiles

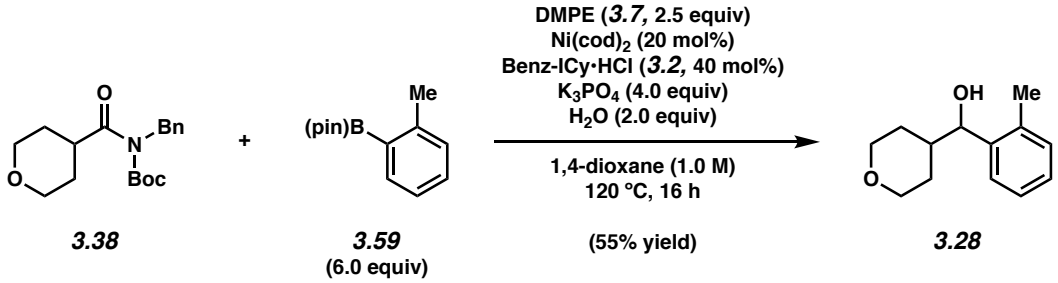

Alcohol 3.28. Crude alcohol **3.28** was synthesized following General Procedure B. Purification by flash column chromatography (19:1 Hexanes:EtOAc → 3:1 Hexanes:EtOAc) afforded alcohol **3.28** (55% yield, average of two experiments) as a crystalline solid. Alcohol **3.28**: mp: 62–64 ºC; R_f 0.32 (2:1 Hexanes:EtOAc); ^{1}H NMR (500 MHz, $CDCl_3$): δ 7.42 (dd, *J* = 7.7, 1.3, 1H), 7.23 (td, *J* = 7.5, 1.5, 1H), 7.21–7.12 (m, 2H), 4.69 (d, *J* = 7.3, 1H), 4.03 (dd, *J* = 11.2, 4.5, 1H), 3.90 (dd, *J* = 11.5, 4.5, 1H), 3.37 (td, *J* = 9.5, 2.3, 1H), 3.29 (td, *J* = 9.5, 2.3, 1H), 2.35 (s, 3H), 1.96–1.83 (m, 2H), 1.71 (br s, 1H), 1.60–1.48 (m, 1H), 1.42 (qd, *J* = 12.5, 4.6, 1H), 1.22–11.5 (m, 1H); ^{13}C NMR (125 MHz, $CDCl_3$): δ 141.3, 135.3, 130.6, 127.5, 126.39, 126.36, 74.6, 68.1, 67.9, 42.2, 29.4, 29.2, 19.6; IR (film): 3420, 2951, 2847, 1090, 1016 cm^{-1}; HRMS-APCI (*m/z*) $[M + H]^+$ calcd for $C_{13}H_{19}O_2^+$, 207.13796; found 207.13823.

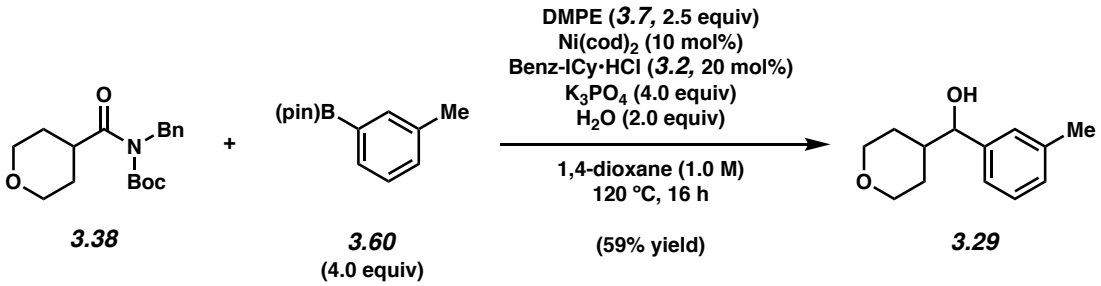

Alcohol 3.29. Crude alcohol **3.29** was synthesized following General Procedure B. Purification by flash chromatography (19:1 Hexanes:EtOAc → 3:1 Hexanes:EtOAc) afforded alcohol **3.29** (59%

yield, average of two experiments) as a white solid. Alcohol **3.29**: mp: 97–99 ºC; R_f 0.36 (2:1 Hexanes:EtOAc); ^{1}H NMR (500 MHz, $CDCl_3$): δ 7.23 (t, *J* = 7.5, 1H), 7.12–7.09 (m, 3H), 4.33 (d, *J* = 7.9, 1H), 4.02 (dd, *J* = 11.4, 4.4, 1H), 3.90 (dd, *J* = 11.4, 4.4, 1H), 3.37 (td, *J* = 11.9, 2.3, 1H), 3.29 (td, *J* = 11.9, 2.3, 1H), 2.36 (s, 3H), 1.93–1.90 (m, 1H), 1.89–1.79 (m, 2H), 1.47 (qd, *J* = 12.2, 4.5, 1H), 1.32 (qd, *J* = 12.2, 4.6, 1H), 1.18–1.15 (m, 1H); ^{13}C NMR (125 MHz, $CDCl_3$): δ 143.0, 138.2, 128.7, 128.4, 127.4, 123.8, 79.1, 68.0, 67.8, 42.5, 29.5, 29.4, 21.6; IR (film): 3409, 2950, 2848, 1135, 1089, 1035 cm^{-1}; HRMS-APCI (*m/z*) $[M + H]^+$ calcd for $C_{13}H_{19}O_2^+$, 207.13796; found 207.13826.

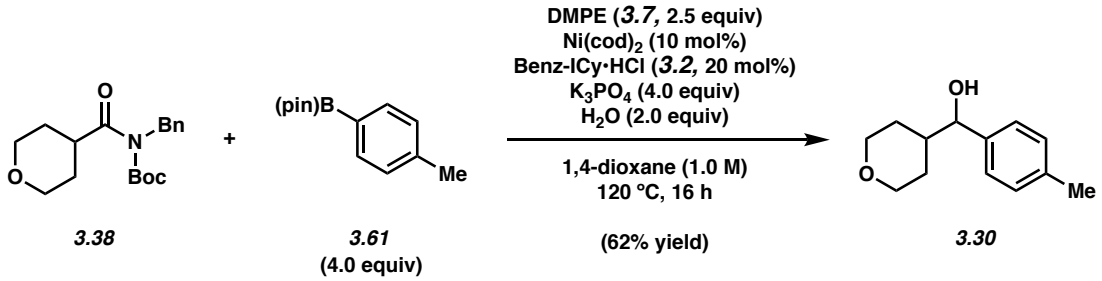

Alcohol 3.30. Crude alcohol **3.30** was synthesized following General Procedure B. Purification by flash chromatography (19:1 Hexanes:EtOAc → 3:1 Hexanes:EtOAc) afforded alcohol **3.30** (62% yield, average of two experiments) as a white solid. Alcohol **3.30**: mp: 71–74 ºC; R_f 0.25 (2:1 Hexanes:EtOAc); ^{1}H NMR (500 MHz, $CDCl_3$): δ 7.24–7.13 (m, 4H), 4.33 (d, *J* = 7.9, 1H), 4.02 (dd, *J* = 11.8, 4.4, 1H), 3.89 (dd, *J* = 11.2, 4.8, 1H), 3.37 (td, *J* = 11.9, 2.3, 1H), 3.28 (td, *J* = 11.9, 2.3, 1H), 2.34 (s, 3H), 1.94–1.91 (m, 1H), 1.86–1.79 (m, 1H), 1.46 (qd, *J* = 12.3, 4.7, 1H), 1.30 (qd, *J* = 12.3, 4.7, 1H), 1.17–1.13 (m, 1H); ^{13}C NMR (125 MHz, $CDCl_3$): δ 143.0, 137.6, 129.2, 126.7, 78.8, 68.0, 67.8, 42.5, 29.6, 29.3, 21.3; IR (film): 3410, 2950, 2847, 1089, 1033, 1017 cm^{-1}; HRMS-APCI (*m/z*) $[M + H]^+$ calcd for $C_{13}H_{19}O_2^+$, 207.13796; found 207.13823.

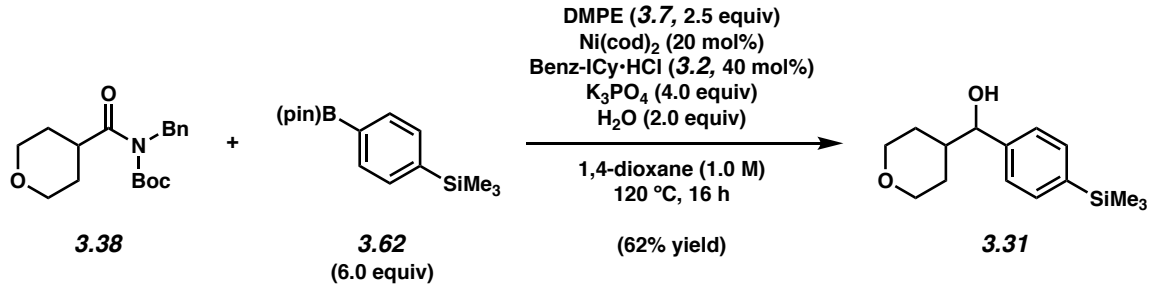

Alcohol 3.31. Crude alcohol **3.31** was synthesized following General Procedure B. Purification by flash chromatography (PhH → 9:1 PhH:Acetone) afforded alcohol **3.31** (62% yield, average of two experiments) as a clear oil. Alcohol **3.31**: R_f 0.26 (9:1 PhH:Acetone); ^{1}H NMR (500 MHz, $CDCl_3$): δ 7.51 (d, *J* = 8.1, 2H), 7.30 (d, *J* = 8.1, 2H), 4.37 (d, *J* = 7.5, 1H), 4.02 (dd, *J* = 11.4, 4.6, 1H), 3.90 (dd, *J* = 11.4, 4.6, 1H), 3.37 (td, *J* = 12.0, 2.3, 1H), 2.29 (td, *J* = 12.0, 2.3, 1H), 1.95–1.89 (m, 1H), 1.89–1.74 (m, 2H), 1.47 (app qd, *J* = 12.6, 4.7, 1H), 1.39–1.29 (m, 1H), 1.22–1.16 (m, 1H), 0.26 (s, 9H); ^{13}C NMR (125 MHz, $CDCl_3$): δ 143.5, 140.2, 133.6, 126.1, 79.0, 68.0, 67.8, 42.4, 29.4, 29.3, –0.98; IR (film): 3409, 2953, 2846, 1247, 831 cm^{-1}; HRMS-APCI (*m/z*) $[M + K]^+$ calcd for $C_{15}H_{24}O_2SiK^+$, 303.11771; found 303.11798.

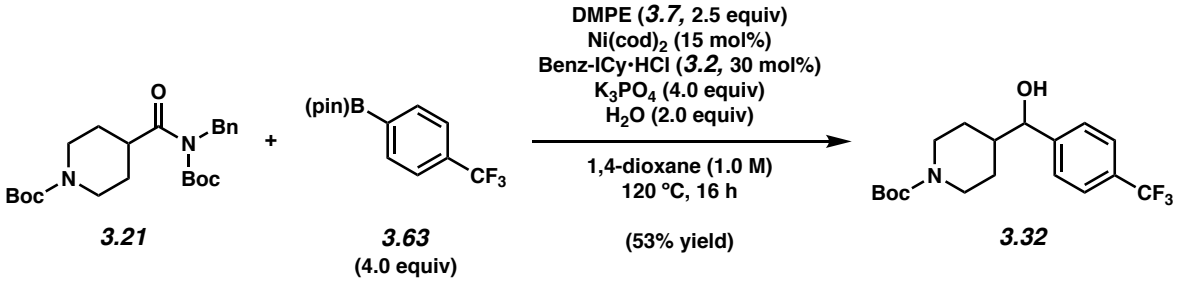

Alcohol 3.32. Crude alcohol **3.32** was synthesized following General Procedure B. Purification by flash chromatography (PhH → 9:1 PhH:Acetone) afforded alcohol **3.32** (53% yield, average of two experiments) as a clear oil. Alcohol **3.32**: mp: 140–143 ºC; R_f 0.29 (9:1 PhH:Acetone). ^{1}H NMR (500 MHz, $CDCl_3$): δ 7.61 (d, *J* = 8.3, 2H), 7.43 (d, *J* = 8.3, 2H), 4.48 (d, *J* = 7.1, 1H), 4.29–

3.93 (m, 2H), 2.77–2.45 (m, 2H), 2.01 (br s, 1H), 1.93–1.84 (m, 1H), 1.80–1.69 (m, 1H), 1.44 (s, 9H), 1.34–1.12 (m, 4H); ^{13}C NMR (125 MHz, $CDCl_3$): δ 154.9, 147.1, 130 (q, J = 32), 127.0, 125.4 (q, J = 3.6), 125.4, 125.3, 123.1, 79.6, 77.9, 43.7, 28.6, 28.4, 27.9; IR (film): 3418, 2932, 2859, 1666, 1325, 1162, 1125 cm^{-1}; HRMS-APCI (*m/z*) $[M]^+$ calcd for $C_{18}H_{24}F_3NO_3^+$, 359.17028; found 359.17126.

*Note: **3.32** was obtained as a mixture of rotamers. These data represent empirically observed chemical shifts from the ^{1}H NMR and ^{13}C NMR spectra.*

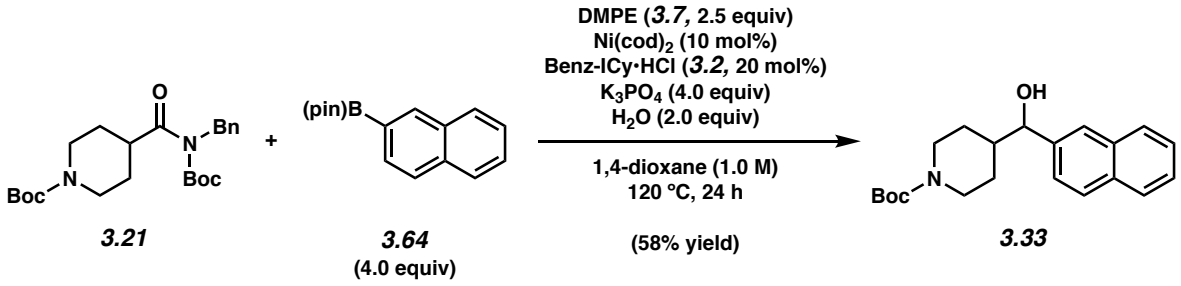

Alcohol 3.33. Crude alcohol **3.33** was synthesized following General Procedure B. Purification by flash chromatography (PhH → 9:1 PhH:Acetone) afforded alcohol **3.33** (58% yield, average of two experiments) as a clear oil. Alcohol **3.33**: R_f 0.39 (9:1 PhH:Acetone); ^{1}H NMR (500 MHz, $CDCl_3$): δ 7.89–7.80 (m, 3H), 7.73, (s, 1H), 7.53–7.43 (m, 3H), 4.56 (d, J = 7.5, 1H), 4.17 (app d, J = 13.4, 1H), 4.04 (app d, J = 13.4, 1H), 2.68 (td, J = 12.9, 2.7, 1H), 2.58 (td, J = 12.9, 2.7, 1H), 2.04–1.98 (m, 1H), 1.89–1.82 (m, 1H), 1.43 (s, 9H), 1.36–1.15 (m, 4H); ^{13}C NMR (125 MHz, $CDCl_3$, 16 of 17 observed): δ 154.9, 140.5, 133.3, 133.2, 128.4, 128.0, 127.8, 126.4, 126.1, 125.7, 124.5, 79.4, 78.8, 43.5, 28.6, 28.4; IR (film): 3418, 2974, 2929, 2856, 1666, 1425, 1162 cm^{-1}; HRMS-APCI (*m/z*) $[M + H]^+$ calcd for $C_{21}H_{28}NO_3^+$, 342.20637; found 342.20615.

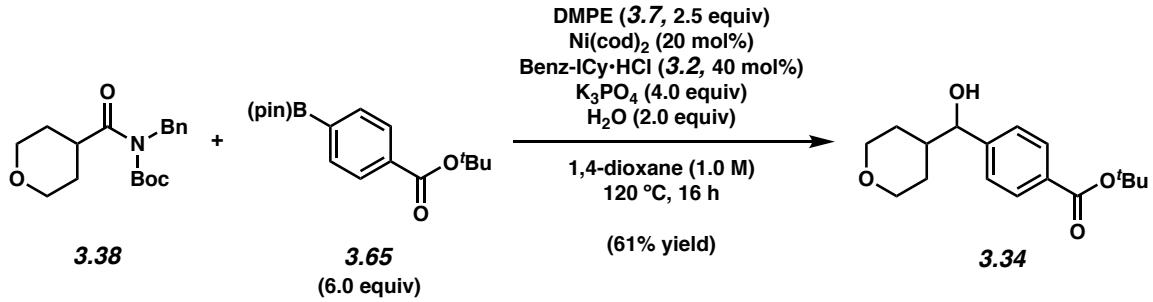

Alcohol 3.34. Crude alcohol **3.34** was synthesized following General Procedure B. Purification by flash chromatography (19:1 Hexanes:EtOAc → 3:1 Hexanes:EtOAc) generated alcohol **3.34** (61% yield, average of two experiments) as a clear oil. Alcohol **3.34**: R_f 0.18 (2:1 Hexanes:EtOAc); ^{1}H NMR (500 MHz, $CDCl_3$): δ 8.00–7.95 (m, 2H), 7.39–7.34 (m, 2H), 4.45 (d, J = 7.2, 1H), 4.01 (app dd, J = 11.4, 4.2, 1H), 3.90 (app dd, J = 11.4, 4.2, 1H), 3.35 (td, J = 12.0, 2.0, 1H), 3.27 (td, J = 12.0, 2.0, 1H), 1.91 (br s, 1H), 1.88–1.78 (m, 2H), 1.59 (s, 9H), 1.52–1.42 (m, 1H), 1.40–1.31 (m, 1H), 1.18–1.14 (m, 1H); ^{13}C NMR (125 MHz, $CDCl_3$): δ 165.7, 147.5, 131.6, 129.7, 128.5, 126.5, 81.2, 78.4, 68.0, 67.7, 42.6, 29.3, 29.1, 28.3; IR (film): 3417, 2953, 2848, 1710, 1292, 1117 cm^{-1}; HRMS-APCI (*m/z*) $[M + H]^+$ calcd for $C_{17}H_{25}O_4^+$, 293.17474; found 293.17416.

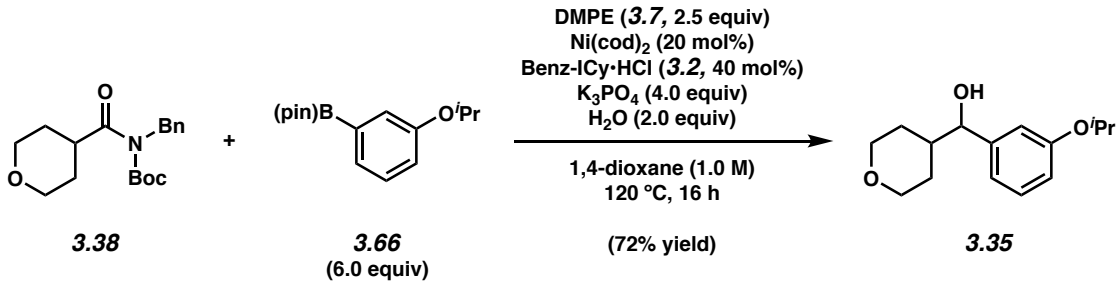

Alcohol 3.35. Crude alcohol **3.35** was synthesized following General Procedure B. Purification by flash chromatography (PhH → 9:1 PhH:Acetone) generated alcohol **3.35** (72% yield, average of two experiments) as a clear oil. Alcohol **3.35**: R_f 0.31 (9:1 PhH:Acetone); ^{1}H NMR (500 MHz, $CDCl_3$): δ 7.24 (t, J = 8.1, 1H), 6.87–6.84, (m, 2H), 6.81 (ddd, J = 8.1, 2.5, 0.85, 1H), 4.56 (sept,

J = 6.0, 1H), 4.32 (d, *J* = 7.6, 1H), 4.02 (app dd, *J* = 11.4, 4.2, 1H), 3.90 (app dd, *J* = 11.4, 4.2, 1H), 3.36 (td, *J* = 12.0, 2.2, 1H), 3.28 (td, *J* = 11.8, 2.2, 1H), 1.94–1.87 (m, 1H), 1.87–1.78 (m, 1H), 1.58 (br s, 1H) 1.46 (qd, *J* = 12.3, 4.6, 1H), 1.34 (d, *J* = 6.1), 1.33 (qd, *J* = 12.3, 4.4) (7H total), 1.23–1.15 (m, 1H); ^{13}C NMR (125 MHz, $CDCl_3$): δ 158.1, 144.7, 129.5, 118.9, 115.0, 114.3, 78.9, 69.9, 68.0, 67.8, 42.5, 29.4, 29.3, 22.2; IR (film): 3406, 2974, 2847, 1599, 1583, 1253, 1116 cm^{-1}; HRMS-APCI (*m/z*) $[M]^+$ calcd for $C_{15}H_{22}O_3^+$, 250.15635; found 250.15623.

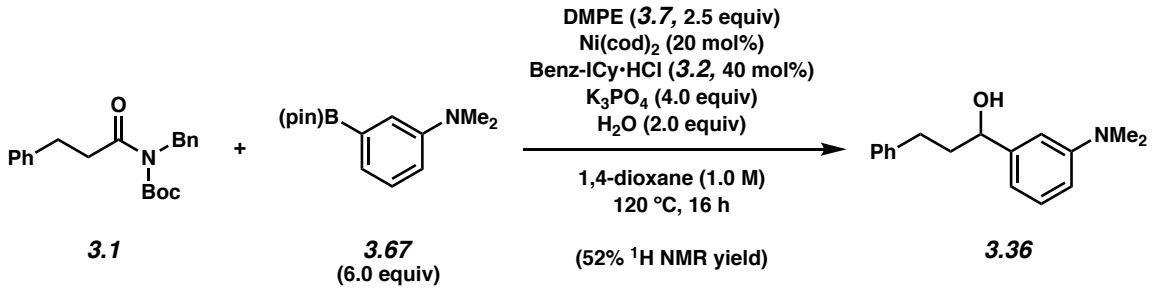

Alcohol 3.36. Crude alcohol **3.36** was synthesized following General Procedure C. ^{1}H NMR analysis of the crude reaction mixture indicated an 52% yield of alcohol **3.36** relative to 1,3,5-trimethoxybenzene external standard (average of two experiments). Purification by preparative thin-layer chromatography (9:1 PhH:Acetone) provided an analytical sample of alcohol **3.36** as a clear oil. Alcohol **3.36**: R_f 0.54 (2:1 Hex:EtOAc); ^{1}H NMR (500 MHz, $CDCl_3$): δ 7.30–7.26 (m, 2H), 7.25–7.14 (m, 3H), 6.75–6.72 (m, 1H), 6.70 (app d, *J* = 7.5, 1H), 6.66 (ddd, *J* = 8.5, 2.6, 0.8, 1H), 4.62 (ddd, *J* = 8.3, 5.4, 3.3, 1H), 2.96 (s, 6H), 2.77 (ddd, *J* = 14.5, 9.8, 5.8, 1H), 2.69 (ddd, *J* = 14.5, 9.8, 6.4, 1H), 2.20–2.10 (m, 1H), 2.10–1.99 (m, 1H), 1.81 (d, *J* = 3.3, 1H); ^{13}C NMR (125 MHz, $CDCl_3$): δ 151.0, 145.7, 142.1, 129.4, 128.6, 128.5, 125.9, 114.3, 112.1, 110.1, 74.6, 40.8, 40.4, 32.3; IR (film): 3366, 3025, 2918, 2858, 2801, 1602, 1495, 697 cm^{-1}; HRMS-APCI (*m/z*) $[M + H]^+$ calcd for $C_{17}H_{22}NO^+$, 256.16959; found 256.16915.

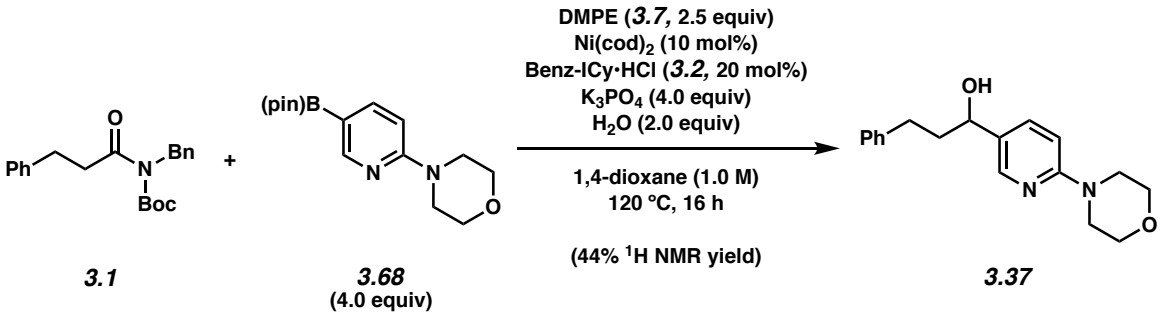

Alcohol 3.37. Crude alcohol **3.37** was synthesized following General Procedure C. ^{1}H NMR analysis of the crude reaction mixture indicated a 44% yield of alcohol **3.37** and 56% yield of the corresponding ketone intermediate relative to 1,3,5-trimethoxybenzene external standard (average of two experiments). Preparation of an authentic sample of alcohol **3.37** (see section 3.8.2.7 for experimental details) allowed for direct comparison with the ^{1}H NMR spectrum of the crude reaction mixture and full characterization. Alcohol **3.37**: R_f 0.45 (3:1 PhH:Acetone); ^{1}H NMR (500 MHz, $CDCl_3$): δ 8.15 (d, *J* = 2.4, 1H), 7.55 (dd, *J* = 8.8, 2.4, 1H), 7.31–7.26 (m, 2H), 7.22–7.15 (m, 3H), 6.65 (d, *J* = 8.8, 1H), 4.65–4.59 (m, 1H), 3.83 (app t, *J* = 4.8, 4H), 3.50 (app t, *J* = 4.8, 4H), 2.76–2.58 (m, 2H), 2.20–2.10 (m, 1H), 2.06–1.95 (m, 1H), 1.78–1.68 (m, 1H); ^{13}C NMR (125 MHz, $CDCl_3$): δ 159.6, 146.3, 141.7, 135.8, 129.5, 128.56, 128.55, 126.1, 107.1, 71.6, 66.9, 45.8, 40.0, 32.2; IR (film): 3391, 3025, 2918, 2855, 1605, 1494, 1245 cm^{-1}; HRMS-APCI (*m/z*) [M + H]$^+$ calcd for $C_{18}H_{23}N_2O_2^+$, 299.17540; found 299.17471.

Note: ^{1}H NMR and ^{13}C NMR spectra of the authentic material, as prepared in section 3.8.2.7, are provided. A ^{1}H NMR spectrum of the crude material obtained using the reaction conditions above is also provided and matches the ^{1}H NMR spectrum of the authentic material.

3.8.2.6 Syntheses of Alcohols 3.40 and 3.43

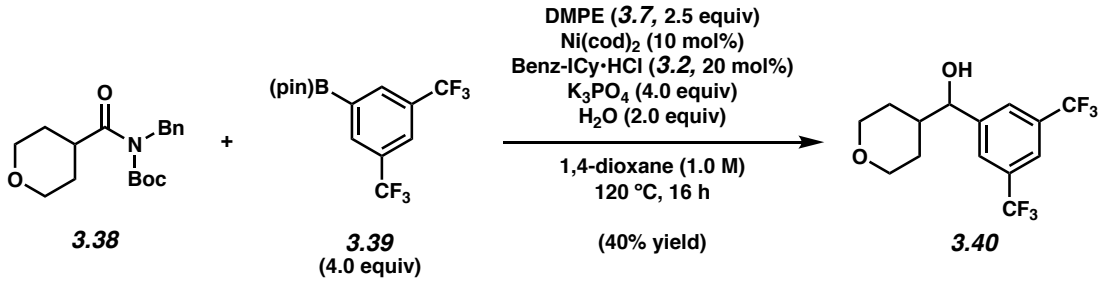

Alcohol 3.40. Crude alcohol **3.40** was synthesized following General Procedure B. Purification by flash column chromatography (19:1 Hexanes:EtOac → 3:1 Hexanes:EtOAc) afforded alcohol **3.40** (40% yield, average of two experiments) as a clear oil. Alcohol **3.40**: R_f 0.45 (2:1 Hexanes:EtOAc); ^{1}H NMR (500 MHz, $CDCl_3$): δ 7.81 (s, 1H), 7.78 (s, 2H), 4.58 (dd, *J* = 6.9, 3.5, 1H), 4.03 (app dd, *J* = 11.6, 4.3, 1H), 3.95 (app dd, *J* = 11.6, 4.2, 1H), 3.36 (td, *J* = 12.1, 2.0), 3.32 (td, *J* = 12.1, 2.0) (2H total), 2.08 (d, *J* = 3.5, 1H), 1.90–1.80 (m, 1H), 1.79–1.72 (m, 1H), 1.49 (qd, 12.3, 4.6), 1.43 (qd, *J* = 12.3, 4.7) (2H total), 1.29–1.19 (m, 1H); ^{13}C NMR (125 MHz, $CDCl_3$): δ 145.6, 131.8 (q, *J* = 33), 126.8, 126.7, 124.5, 122.3, 121.8 (sept, *J* = 3.7), 77.5, 67.8, 67.6, 42.6, 29.1, 28.4; IR (film): 3401, 2956, 2855, 1277, 1128 cm^{-1}; HRMS-APCI (*m/z*) $[M + H]^+$ calcd for $C_{14}H_{15}F_6O_2^+$, 329.09708; found 329.09637.

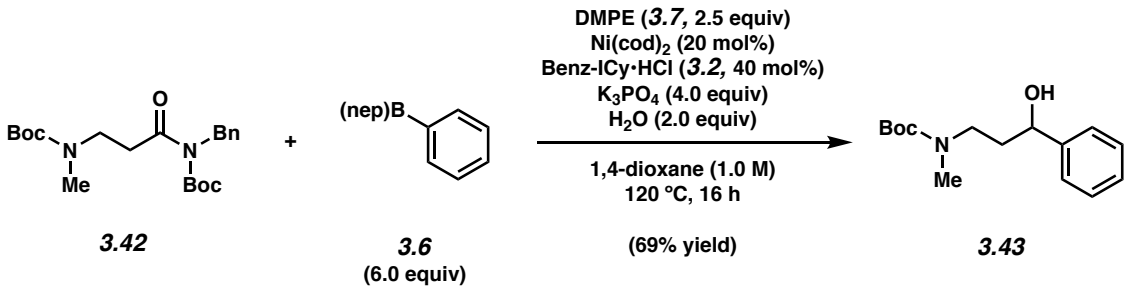

Alcohol 3.43. Crude alcohol **3.43** was synthesized following General Procedure B. Purification by flash column chromatography (PhH → 9:1 PhH:Acetone) yield alcohol **3.43** (69% yield, average of two experiments) as a clear oil. Alcohol **3.43**: R_f 0.48 (2:1 Hexanes:EtOAc); ^{1}H NMR (400

MHz, $CDCl_3$): δ 7.42–7.18 (m, 5H), 4.60 (br s, 1H), 4.33 (br s), 3.90 (br s), 3.47 (br s), 3.30–2.92 (m), 2.50 (br s), (total 3H), 2.87 (s, 3H), 2.00–1.88 (m, 1H), 1.88–1.67 (m, 1H), 1.47 (s, 9H). Spectral data match those previously reported.[60]

*Note: **3.43** was obtained as a mixture of rotamers. These data represent empirically observed chemical shifts from the ^1H NMR spectrum.*

3.8.2.7 Syntheses of Authentic Samples of Alcohols 3.13 and 3.37

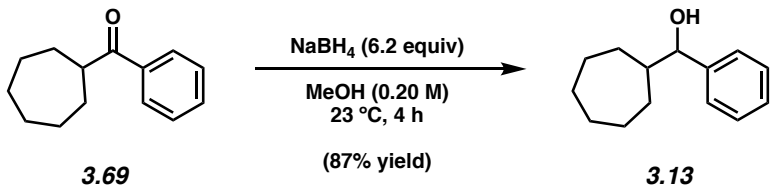

To a flame-dried 1-dram vial equipped with a magnetic stir bar was added the ketone **3.69** (11.4 mg, 0.0560 mmol, 1.00 equiv) in MeOH. The solvent was then evaporated under reduced pressure. The vial was then capped with a septum cap, and the atmosphere was purged with N_2. To the vial was added MeOH (0.300 mL, 0.190 M) and the reaction was stirred to give a homogeneous solution. $NaBH_4$ (6.80 mg, 0.180 mmol, 3.20 equiv) was added in a single portion and the vial was stirred at 23 °C. After 1 h, $NaBH_4$ (6.40 mg, 0.170 mmol, 3.00 equiv) was added in a single portion and the vial was stirred at 23 °C. After 3 h, the reaction was quenched with H_2O (2 mL). The aqueous layer was extracted with EtOAc (4 x 3 mL), the combined organic layers were dried over anhydrous $MgSO_4$, and the volatiles were removed under reduced pressure. The resulting crude residue was purified by preparative thin-layer chromatography (5:1 Hexanes:EtOAc) to yield alcohol **3.13** as a clear oil (10.0 mg, 87% yield).

Note: See section 3.8.2.4 for chemical shifts from the ^1H NMR and ^{13}C NMR spectra.

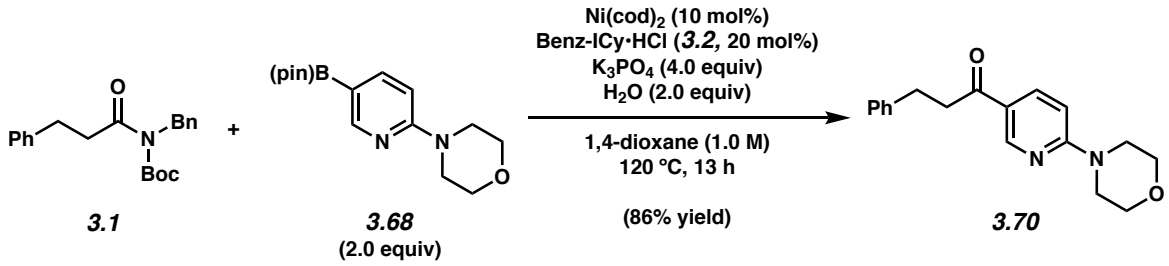

A 1-dram vial was charged with anhydrous powder K_3PO_4 (170 mg, 0.800 mmol, 4.00 equiv) and a magnetic stir bar. The vial and its contents were flame-dried under reduced pressure and allowed to cool under N_2. Amide substrate **3.1** (67.9 mg, 0.200 mmol, 1.00 equiv) and boronate ester nucleophile **3.68** (116 mg, 0.400 mmol, 2.00 equiv) were added. The vial was flushed with N_2 for 5 min, then water (7.21 μL, 0.400 mmol, 2.00 equiv), which had been sparged with N_2 for 10 min, was added. The vial was taken into a glovebox and charged with $Ni(cod)_2$ (5.50 mg, 10 mol%) and Benz-ICy•HCl (**3.2**, 12.8 mg, 20 mol%). Subsequently, 1,4-dioxane (200 μL, 1.00 M) was added. The vial was sealed with a Teflon-lined screw cap, removed from the glovebox, and stirred vigorously (800 RPM) at 120 ºC for 13 h. After cooling to 23 ºC, the mixture was quenched by the addition of saturated aqueous NH_4Cl (1 mL) and extracted with EtOAc (3 x 2 mL). The combined organic layers were then filtered over a plug of silica gel (3 cm) and Na_2SO_4 (3 cm) using EtOAc (10 mL) as eluent. The volatiles were removed under reduced pressure and the resulting crude residue was purified by flash column chromatography (9:1 Hexanes:EtOAc → EtOAc) to yield ketone **3.70** as a clear oil (10.0 mg, 87% yield). Alcohol **3.70**: ^{1}H NMR (500 MHz, $CDCl_3$): δ 8.78 (d, J = 2.3, 1H), 8.05 (dd, J = 9.1, 2.3, 1H), 7.32–7.28 (m, 2H), 7.26–7.18 (m, 3H), 6.60 (d, J = 9.1, 1H), 3.81 (t, J = 5.0, 4H), 3.67 (t, J = 5.0, 4H), 3.19 (t, J = 7.5, 4H), 3.05 (t, J = 7.5, 4H). Spectral data match those previously reported.[61]

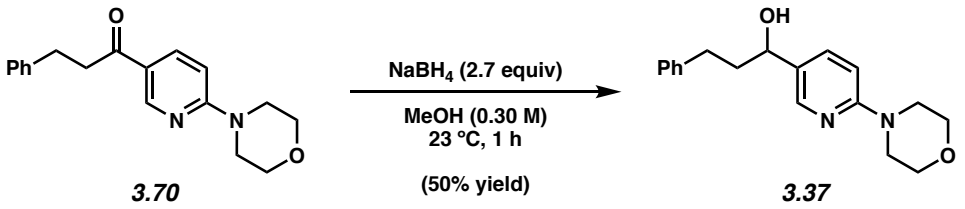

To a flame-dried 1-dram vial equipped with a magnetic stir bar was added $NaBH_4$ (17.0 mg, 0.450 mmol, 2.70 equiv). The ketone **3.70** (50.0 mg, 0.0170 mmol, 1.00 equiv) was dissolved in MeOH (0.60 mL, 0.30 M) and added to the vial. After 1 h, the reaction was quenched with H_2O (2 mL). The aqueous layer was extracted with EtOAc (4 x 3 mL), the combined organic layers were dried over anhydrous $NaSO_4$, and the volatiles were removed under reduced pressure. The resulting crude residue was purified by preparative TLC (1:1 Hexanes:EtOAc) to yield alcohol **3.37** as a clear oil (25.0 mg, 50% yield).

Note: See section 3.8.2.5 for chemical shifts from the ^{1}H NMR and ^{13}C NMR spectra.

3.8.2.8 Robustness Screen

Table 3.2. Evaluation of functional group compatibility in the Suzuki–Miyaura coupling and transfer hydrogenation cascade

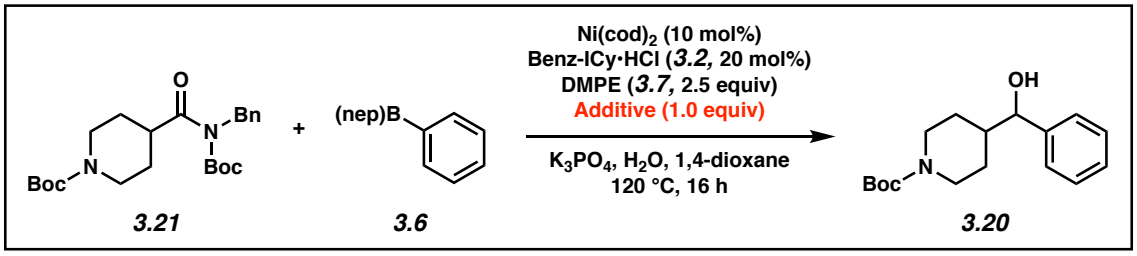

Entry	Additive	Yield of *3.20* (%)	Additive Remaining (%)	SM Remaining (%)
1	–	81	N.D.	0
2	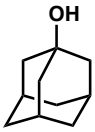	89	>99	0
3	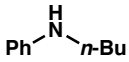	83	>99	0
4	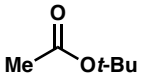	42	N.D.[b]	0
5	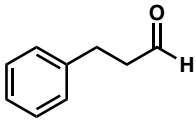	43	0	0
6	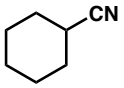	0	0	0
7	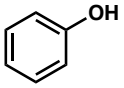	0	0	0
8	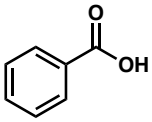	31	0	0
9	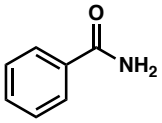	13	0	0
10	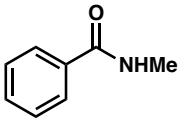	58	88	0
11		68	0	0
12		22	18	0
13	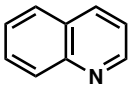	88	98	0
14	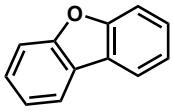	68	94	0
15	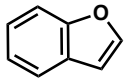	25	0	0
16	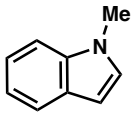	78	80	0

Conditions: amide **3.21** (0.20 mmol, 1.00 equiv), PhB(nep) (**3.6**, 0.80 mmol, 4.00 equiv), DMPE (**3.7**, 0.50 mmol, 2.50 equiv), additive (0.20 mmol, 1.00 equiv), $Ni(cod)_2$ (0.020 mmol, 10 mol%), Benz-ICy•HCl (**3.2**, 0.040 mmol, 20 mol%), K_3PO_4 (0.80 mmol, 4.00 equiv), H_2O (0.40 mmol, 2.00 equiv), and 1,4-dioxane (1.0 M) in a sealed vial at 120 °C for 16 h. Yields of coupled product, remaining additive, and remaining starting material were determined by ^1H NMR analysis using 1,3,5-trimethoxybenzene or hexamethylbenzene as an external standard.

3.8.2.9 Benchtop Variants of Methodology

3.8.2.9.1 Procedure A: Employing a paraffin wax encapsulation approach. Note: The supporting information for the preparation of Ni(cod)$_2$/Benz-ICy–paraffin capsules has been previously reported.[62]

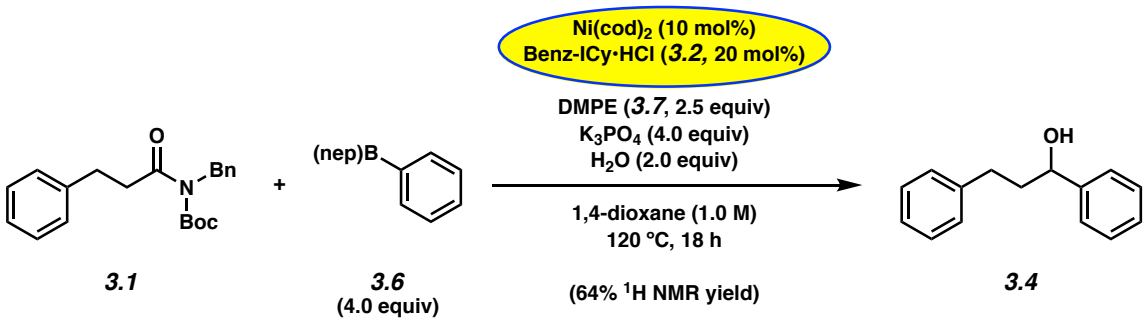

A 2-dram vial was charged with anhydrous powder K_3PO_4 (340 mg, 1.60 mmol, 4.00 equiv) and a magnetic stir bar (egg-shaped 3/8 x 3/16 in). The vial and its contents were flame-dried under reduced pressure and allowed to cool under N_2. The vial was then charged with amide substrate **3.1** (136 mg, 0.40 mmol, 1.00 equiv), boronate ester nucleophile **3.6** (304 mg, 1.60 mmol, 4.00 equiv), DMPE (**3.7**, 165 mg, 1.00 mmol, 2.50 equiv), and a paraffin wax capsule containing Ni(cod)$_2$ (11.0 mg, 0.0400 mmol, 10 mol%) and Benz-ICy•HCl (**3.2**, 25.5 mg, 0.0800 mmol, 20 mol%) were added. The vial was purged with N_2 and subsequently deionized water (14.0 μL, 0.80 mmol, 2.00 equiv) and 1,4-dioxane (0.400 mL, 1.00 M), which had been sparged with N_2 for 10 min, were added. The vial was capped with a Teflon-lined screw cap under a flow of N_2 and the reaction mixture was stirred vigorously (800 RPM) at 120 ºC for 18 h. After removing the vial from heat, the reaction mixture was transferred to a 100 mL pear-shaped flask containing 2.0 g of silica gel with hexanes (6 mL) and CH_2Cl_2 (6 mL). The mixture was adsorbed onto the silica gel under reduced pressure and filtered over a plug of silica gel (4.0 cm OD x 3.0 cm, 300 mL of hexanes eluent to remove paraffin, then 250 mL of EtOAc eluent). The volatiles were removed

under reduced pressure. ^{1}H NMR analysis of the crude reaction mixture indicated a 64% yield of alcohol **3.4** relative to 1,3,5-trimethoxybenzene external standard (average of two experiments).

3.8.2.9.2 Procedure B: Employing an air-stable Ni(II) pre-catalyst

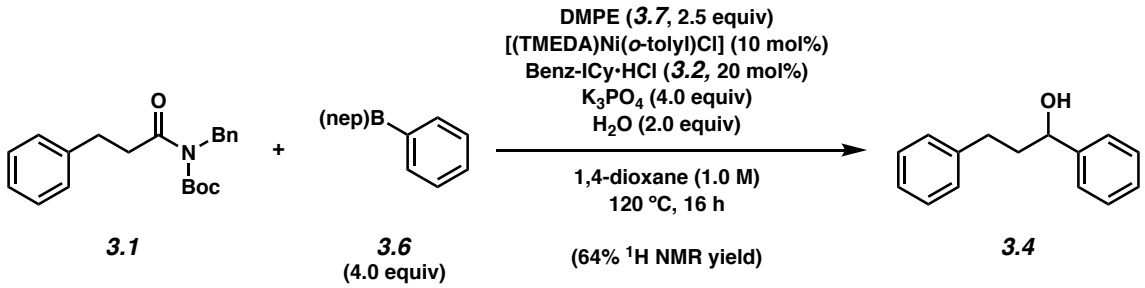

A 1-dram vial was charged with anhydrous powder K_3PO_4 (170 mg, 0.800 mmol, 4.00 equiv) and a magnetic stir bar. The vial and its contents were flame-dried under reduced pressure and allowed to cool under N_2. Amide substrate **3.1** (67.9 mg, 0.200 mmol, 1.00 equiv), boronate ester nucleophile **3.6** (152 mg, 0.800 mmol, 4.00 equiv), DMPE (**3.7**, 82.6 mg, 0.500 mmol, 2.50 equiv), [(TMEDA)Ni(*o*-tolyl)Cl][48] (6.03 mg, 0.0200 mmol, 10 mol%), and Benz-ICy•HCl (**3.2**, 12.8 mg, 0.0400 mmol, 20 mol%) were added. The vial was flushed with N_2 for 5 min, then water (7.21 μL, 0.400 mmol, 2.00 equiv) and 1,4-dioxane (200 μL, 1.00 M), which had been sparged with N_2 for 10 min, were added. The vial was capped with a Teflon-lined screw cap under a flow of N_2 and the reaction mixture was stirred vigorously (800 RPM) at 120 ºC for 16 h. After cooling to 23 ºC, the mixture was quenched by the addition of saturated aqueous NH_4Cl (1 mL) and extracted with EtOAc (3 x 2 mL). The combined organic layers were then filtered over a plug of silica gel (3 cm) and Na_2SO_4 (3 cm) using EtOAc (10 mL) as eluent. The volatiles were removed under reduced pressure. ^{1}H NMR analysis of the crude reaction mixture indicated a 64% yield of alcohol **3.4** relative to 1,3,5-trimethoxybenzene external standard.

3.8.2.10 Enantioselectivity Experiments

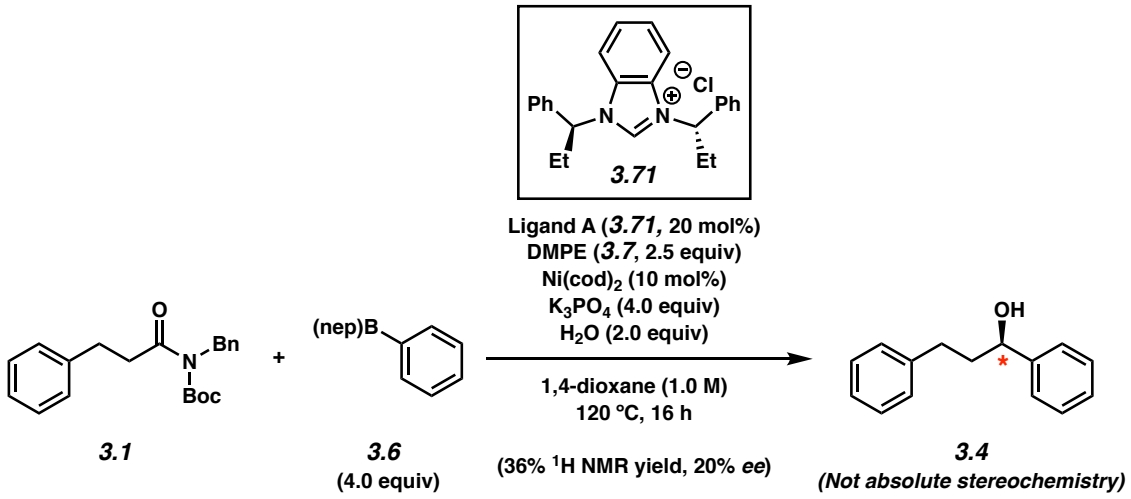

Alcohol 3.4. A 1-dram vial was charged with anhydrous powder K_3PO_4 (170 mg, 0.800 mmol, 4.00 equiv) and a magnetic stir bar. The vial and its contents were flame-dried under reduced pressure and allowed to cool under N_2. Amide substrate **3.1** (67.9 mg, 0.200 mmol, 1.00 equiv), boronate ester nucleophile **3.6** (152 mg, 0.800 mmol, 4.00 equiv), and DMPE (**3.7**, 82.6 mg, 0.500 mmol, 2.50 equiv) were added. The vial was flushed with N_2 for 5 min, then water (7.21 μL, 0.400 mmol, 2.00 equiv), which had been sparged with N_2 for 10 min, was added. The vial was taken into a glovebox and charged with $Ni(cod)_2$ (5.50 mg, 0.0200 mmol, 10 mol%) and Ligand A (**3.71**, 15.6 mg, 0.0400 mmol, 20 mol%). Subsequently, 1,4-dioxane (200 μL, 1.00 M) was added. The vial was sealed with a Teflon-lined screw cap, removed from the glovebox, and stirred vigorously (800 RPM) at 120 ºC for 16 h. After cooling to 23 ºC, the mixture was quenched by the addition of saturated aqueous NH_4Cl (1 mL) and extracted with EtOAc (3 x 2 mL). The combined organic layers were then filtered over a plug of silica gel (3 cm) and Na_2SO_4 (3 cm) using EtOAc (10 mL) as eluent. ^1H NMR analysis of the crude reaction mixture indicated a 36% yield of alcohol **3.4** relative to 1,3,5-trimethoxybenzene external standard. Purification by preparative thin-layer chromatography (4:1 Hexanes:EtOAc) provided an analytical sample of enantioenriched alcohol

3.4 as a clear oil. The spectral data match those previously reported in section 3.8.2.4 of Experimental Procedures for ***rac*-3.4**.

3.8.2.11 Verification of Enantioenrichment

Table 3.3. Conditions and results of chiral SFC analysis of alcohol products

Compound	Method Column/Temp.	Solvent	Method Flow Rate	Retention Times (min)	Enantiomeric Ratio (er)
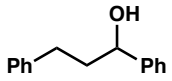 ***rac-3.4***	Daicel ChiralPak AD-H/35 °C	1% isopropanol in CO_2	3.5 mL/min	7.35/8.12	50:50
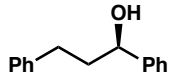 ***enantioenriched-3.4***	Daicel ChiralPak AD-H/35 °C	1% isopropanol in CO_2	3.5 mL/min	7.43/8.12	40:60

Figure 3.7. SFC trace of *rac*-**3.4** (Table 3.3, Entry 1).

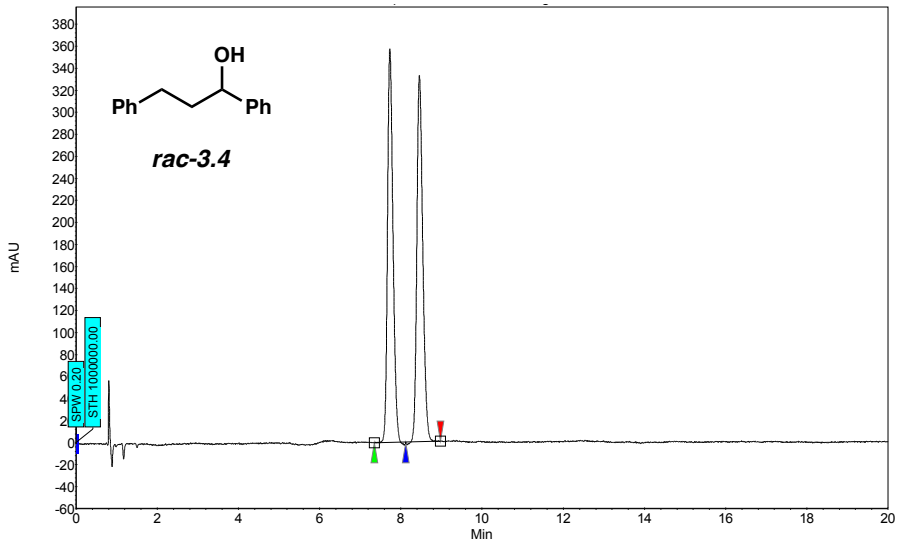

Index	Name	Start	Time	End	RT Offset	Quantity	Height	Area	Area
		[Min]	[Min]	[Min]	[Min]	[% Area]	[µV]	[µV.Min]	[%]
1	UNKNOWN	7.35	7.73	8.12	0.00	49.91	357.5	55.6	49.913
2	UNKNOWN	8.12	8.46	8.98	0.00	50.09	332.4	55.8	50.087
Total						100.00	689.9	111.4	100.000

Figure 3.8. SFC trace of *enantionenriched*-**3.4** (Table 3.3, Entry 2).

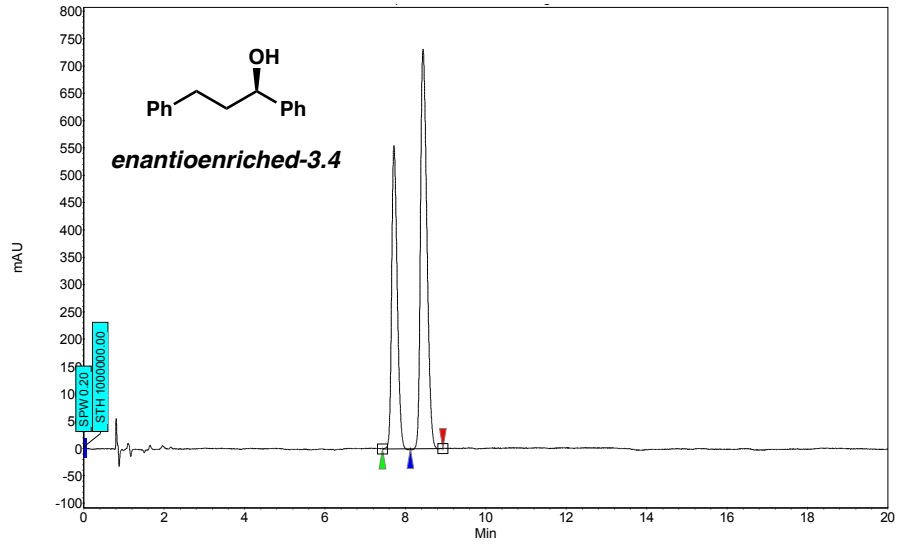

Index	Name	Start	Time	End	RT Offset	Quantity	Height	Area	Area
		[Min]	[Min]	[Min]	[Min]	[% Area]	[µV]	[µV.Min]	[%]
1	UNKNOWN	7.43	7.72	8.12	0.00	39.72	554.9	88.6	39.725
2	UNKNOWN	8.12	8.44	8.94	0.00	60.28	731.0	134.5	60.275
Total						100.00	1285.9	223.1	100.000

3.8.2.12 Deuterium Incorporation Experiments

3.8.2.12.1 Preparation of deuterated reducing agent *d*-DMPE (*d*-3.7)

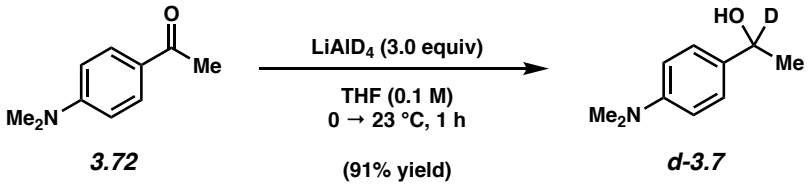

3.72 *d-3.7*

To a flame-dried flask equipped with a magnetic stir bar was added ketone **3.72** (50.0 mg, 0.307 mmol, 1.00 equiv) and THF (3.0 mL, 0.10 M). The flask was cooled to 0 °C and lithium aluminum deuteride (39 mg, 0.921 mmol. 3.00 equiv) was added in a single portion. The reaction was then warmed to 23 °C and stirred for 1 h. The reaction was cooled to 0 °C and quenched by the sequential addition of MeOH (5 mL), and deionized water (3 mL) and the resulting mixture was transferred to a separatory funnel with CH_2Cl_2 (10 mL) and water (10 mL). The aqueous layer was extracted with CH_2Cl_2 (3 x 10 mL), then the organic layers were combined, dried over Na_2SO_4, and evaporated under reduced pressure. Purification of the crude residue by flash chromatography (4:1 Hexanes:EtOAc) afforded deuterated alcohol ***d*-3.7** (46 mg, 91% yield) as a white solid. Alcohol ***d*-3.7**: R_f 0.33 (3:1 Hexanes:EtOAc). ^{1}H NMR (500 MHz, $CDCl_3$): δ 7.26 (d, J = 9.0, 2H), 6.73 (d, J = 9.0, 2H), 2.94 (s, 3 H), 1.62 (s, 1H), 1.48 (s, 3H).

3.8.2.12.2 Deuterium incorporation experiments using *d*-DMPE (*d*-3.7)

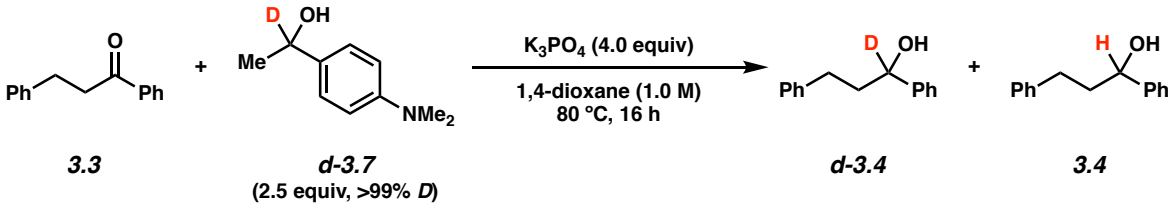

3.3 | *d-3.7* (2.5 equiv, >99% *D*) | *d-3.4* | *3.4*

Conversion	Yield of *d*-3.4	Yield of 3.4
75%	75%	0%

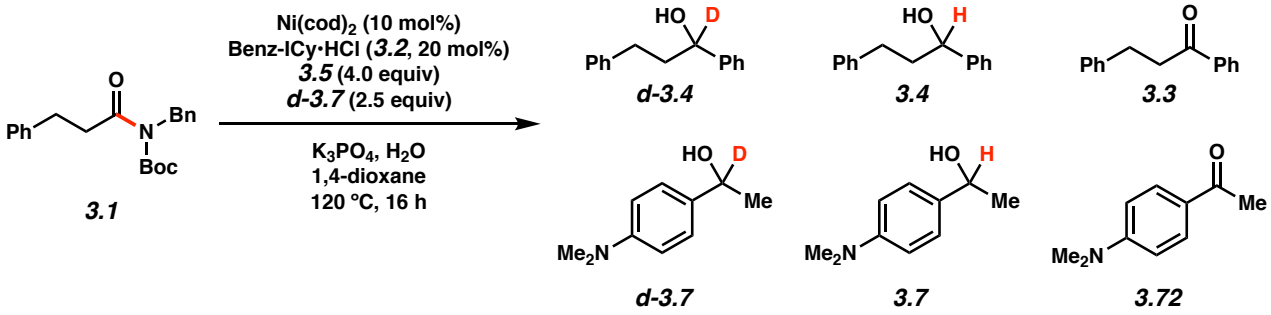

3.1 → *d-3.4*, *3.4*, *3.3*, *d-3.7*, *3.7*, *3.72*

Conversion	Yield *d*-3.4	Yield *3.4*	Yield *3.3*	Yield *d-3.7*	Yield *3.7*	Yield *3.72*
100%	0%	72%	15%	58%	1%	30%

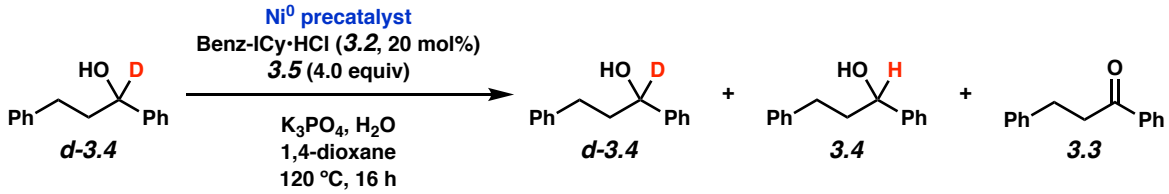

d-3.4 → *d-3.4*, *3.4*, *3.3*

Ni^0 pre-catalyst	Yield *d*-3.4	Yield *3.4*	Yield *3.3*
None	95%	0%	0%
Ni(cod)$_2$ (10 mol%)	12%	22%	20%

3.9 Spectra Relevant to Chapter Three:

Reductive Arylation of Amides via a Nickel-Catalyzed Suzuki–Miyaura Coupling and Transfer Hydrogenation Cascade

Milauni M. Mehta,† Timothy B. Boit,† Junyong Kim, Emma L. Baker and Neil K. Garg.

Angew. Chem., Int. Ed. **2021**, *60*, 2472–2477.

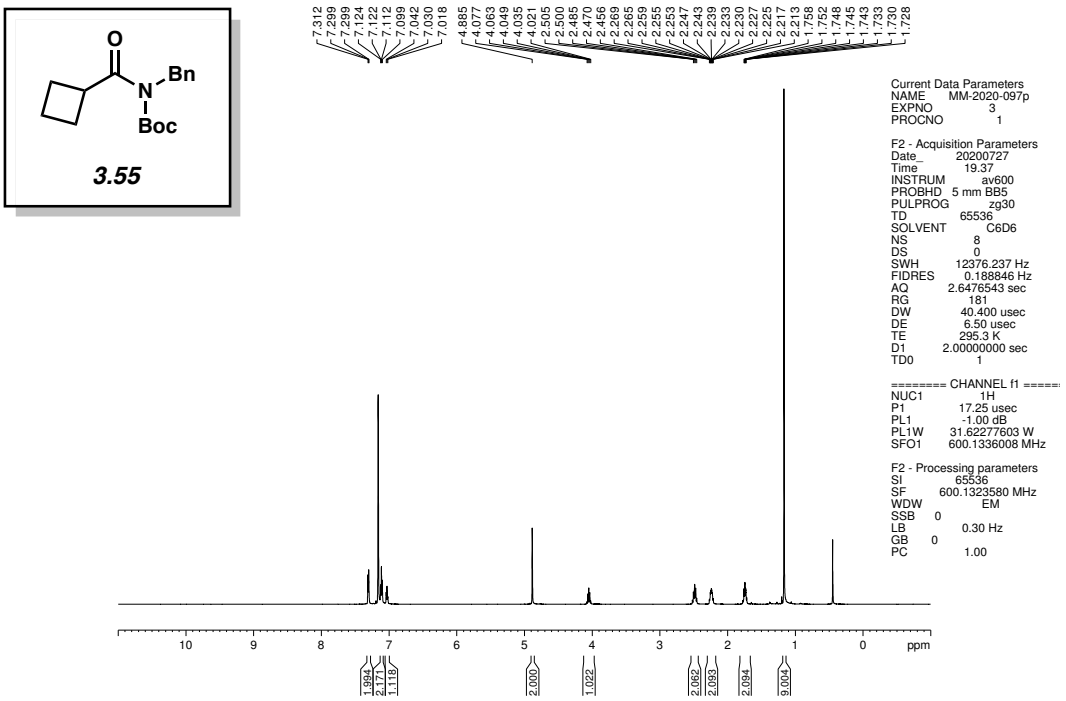

Figure 3.9 ^{1}H NMR (600 MHz, $CDCl_3$) of compound **3.55**.

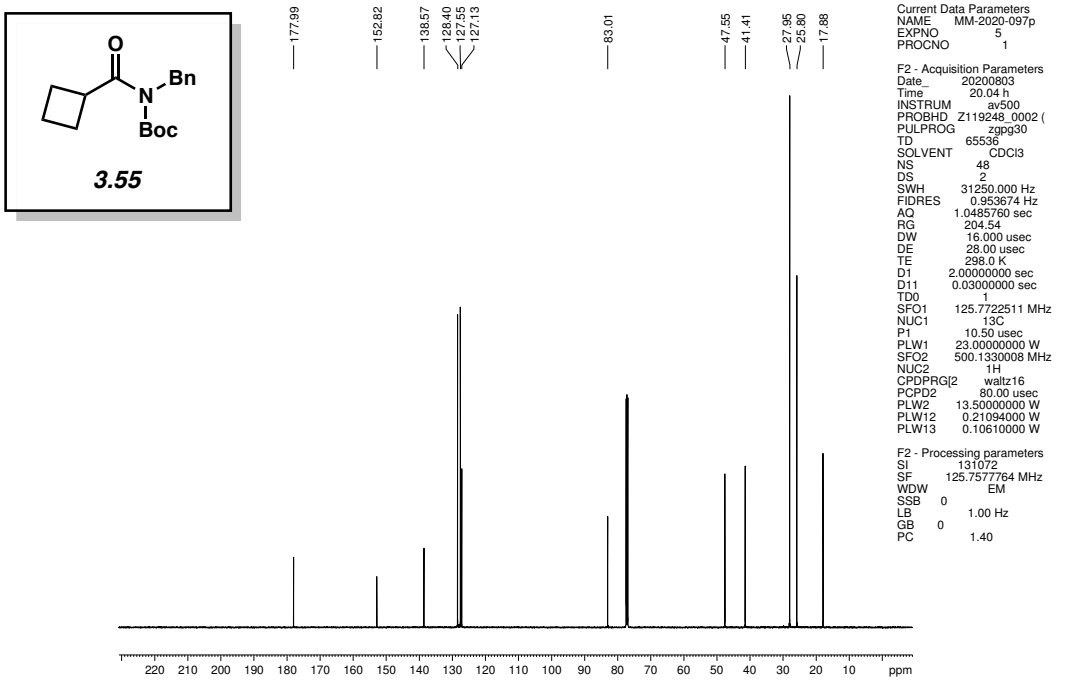

Figure 3.10 ^{13}C NMR (125 MHz, $CDCl_3$) of compound **3.55**.

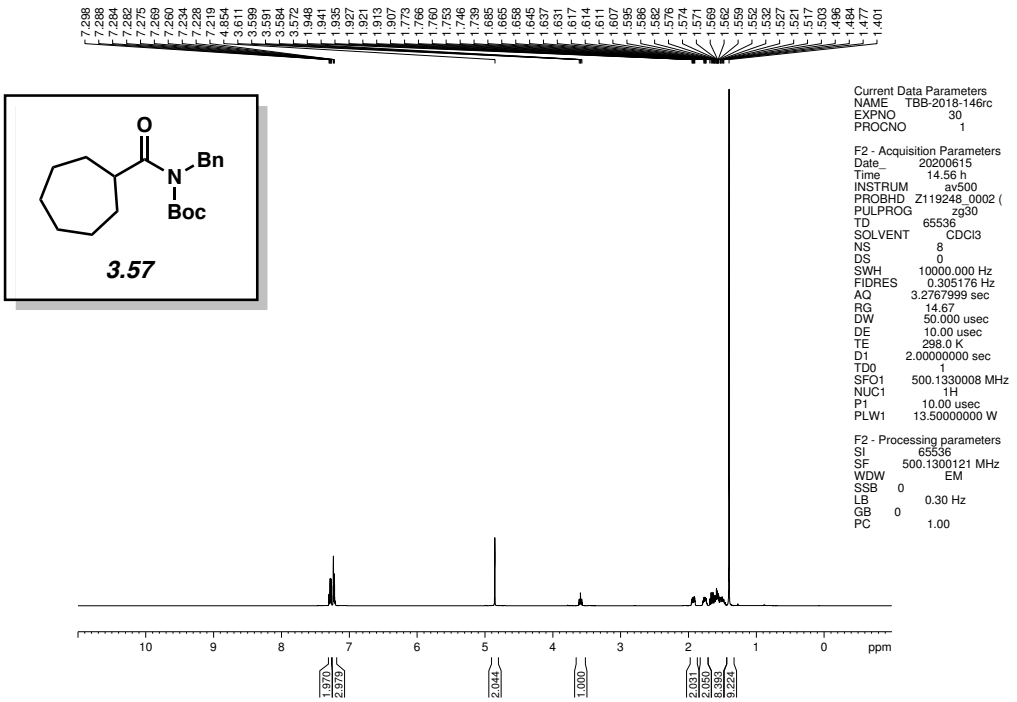

Figure 3.11 ^{1}H NMR (500 MHz, $CDCl_3$) of compound **3.57**.

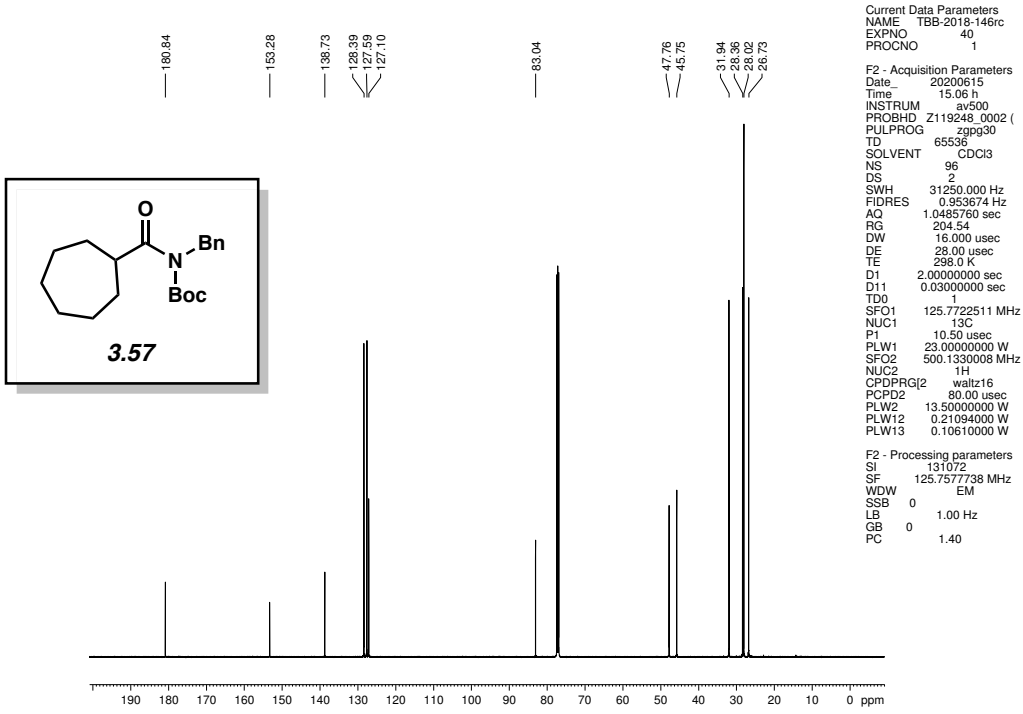

Figure 3.12 ^{13}C NMR (125 MHz, $CDCl_3$) of compound **3.57**.

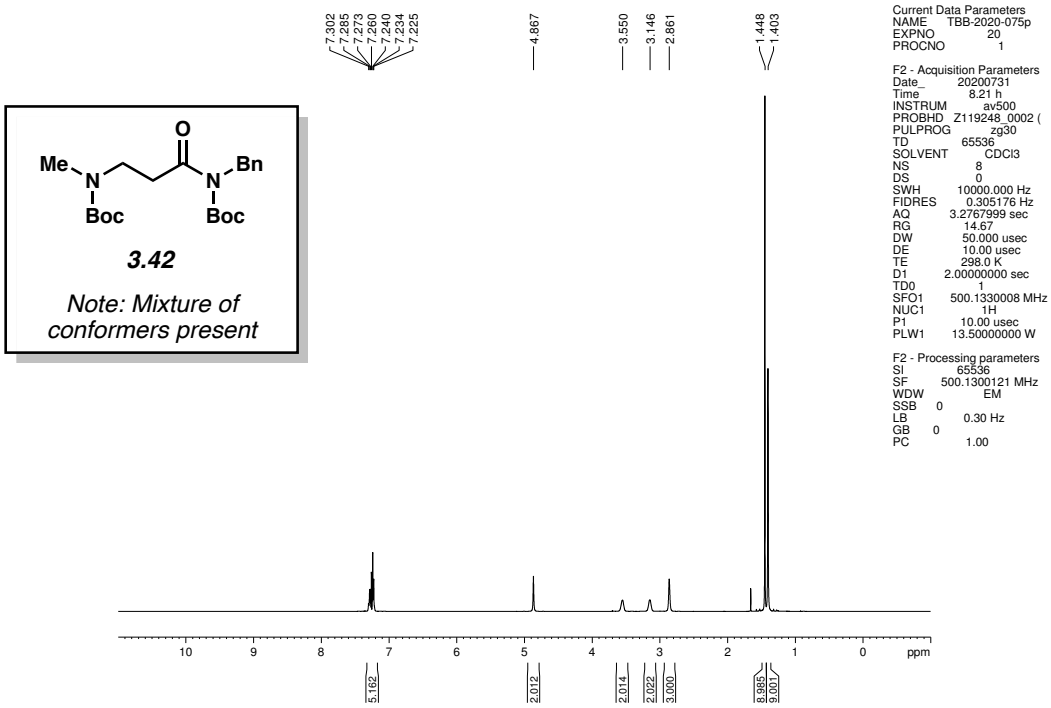

Figure 3.13 ^{1}H NMR (500 MHz, $CDCl_3$) of compound **3.42**.

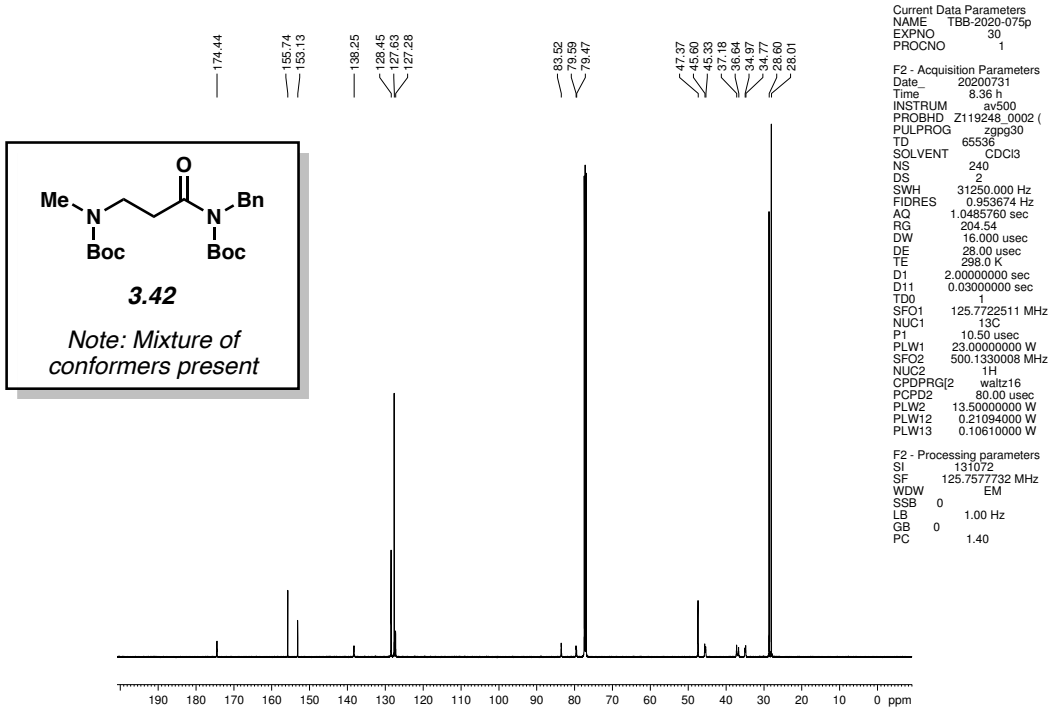

Figure 3.14 ^{13}C NMR (125 MHz, $CDCl_3$) of compound **3.42**.

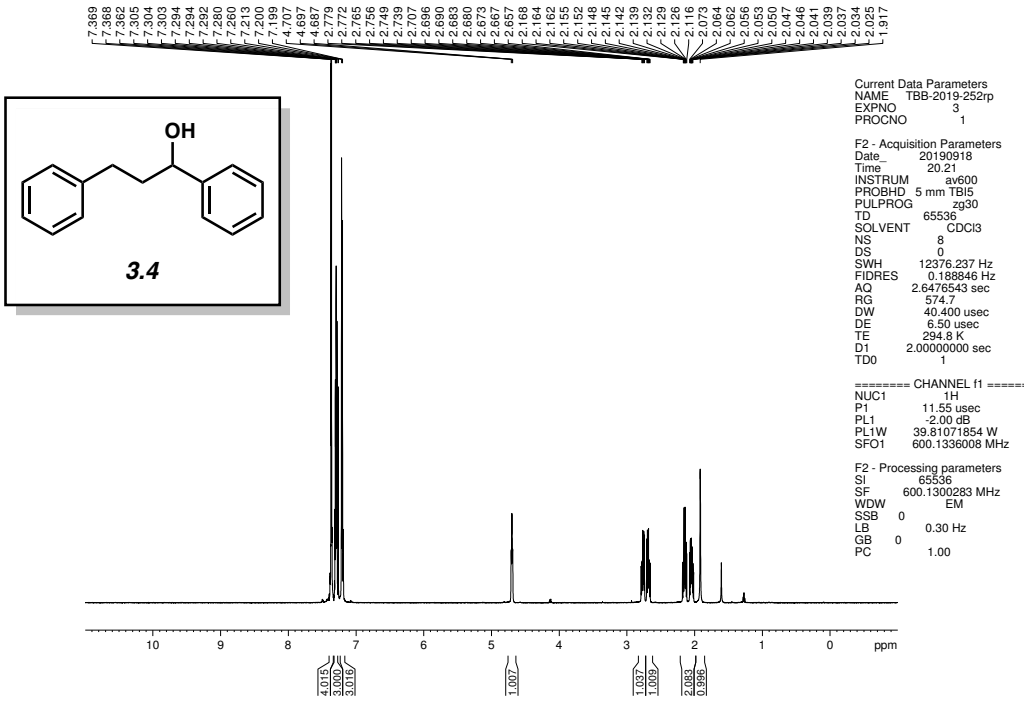

Figure 3.15 ^{1}H NMR (600 MHz, $CDCl_3$) of compound **3.4**.

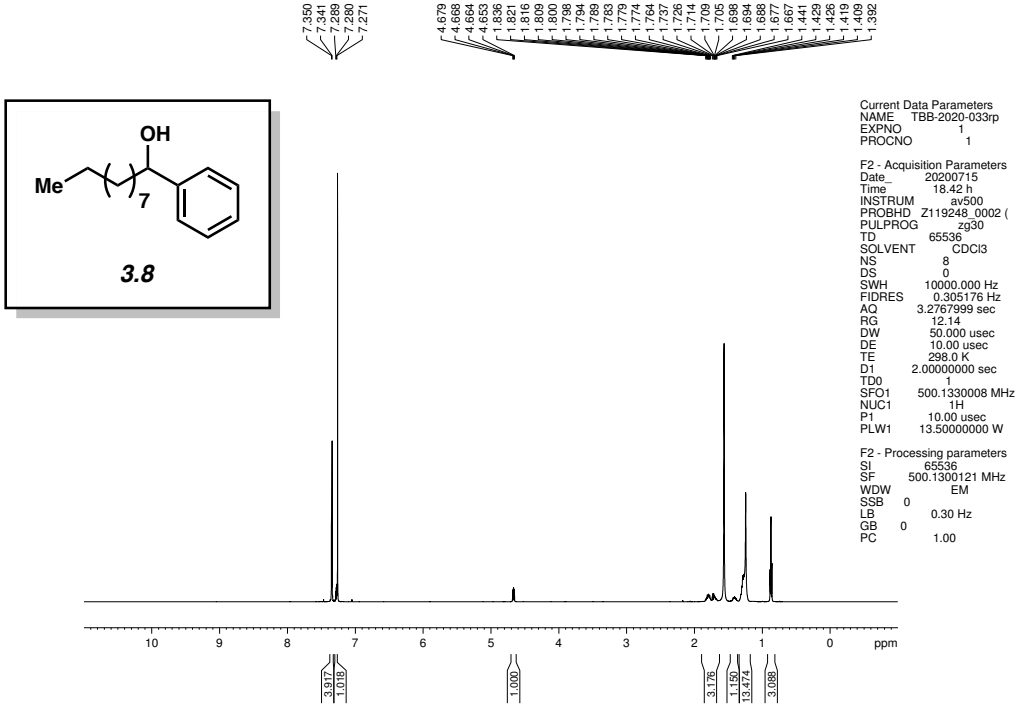

Figure 3.16 ^{1}H NMR (500 MHz, $CDCl_3$) of compound **3.8**.

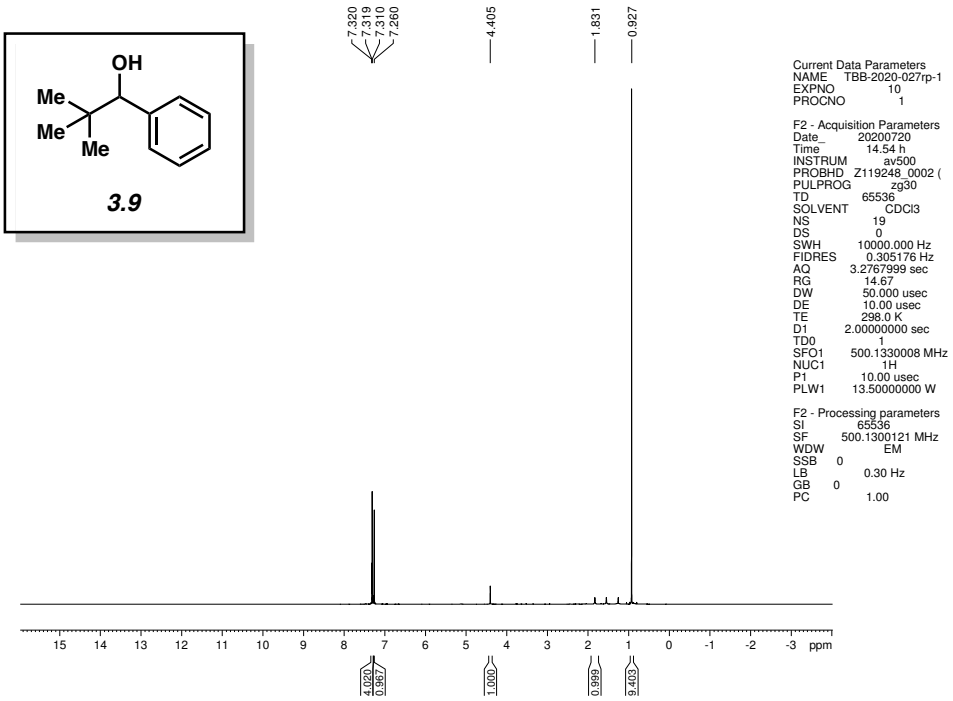

Figure 3.17 ^{1}H NMR (500 MHz, $CDCl_3$) of compound **3.9**.

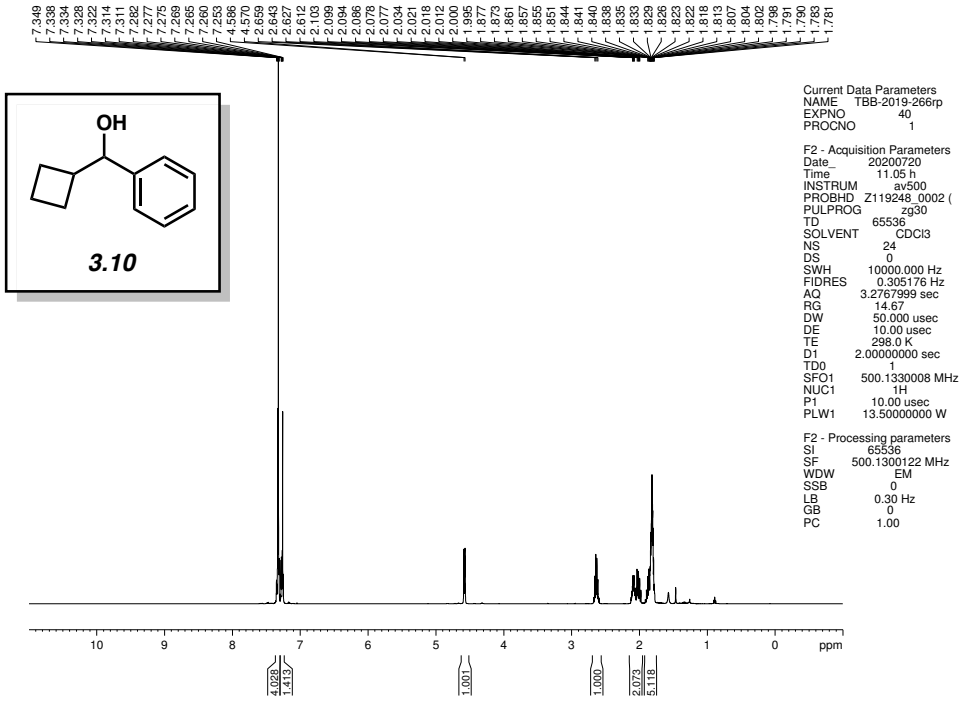

Figure 3.18 ^{1}H NMR (500 MHz, $CDCl_3$) of compound **3.10**.

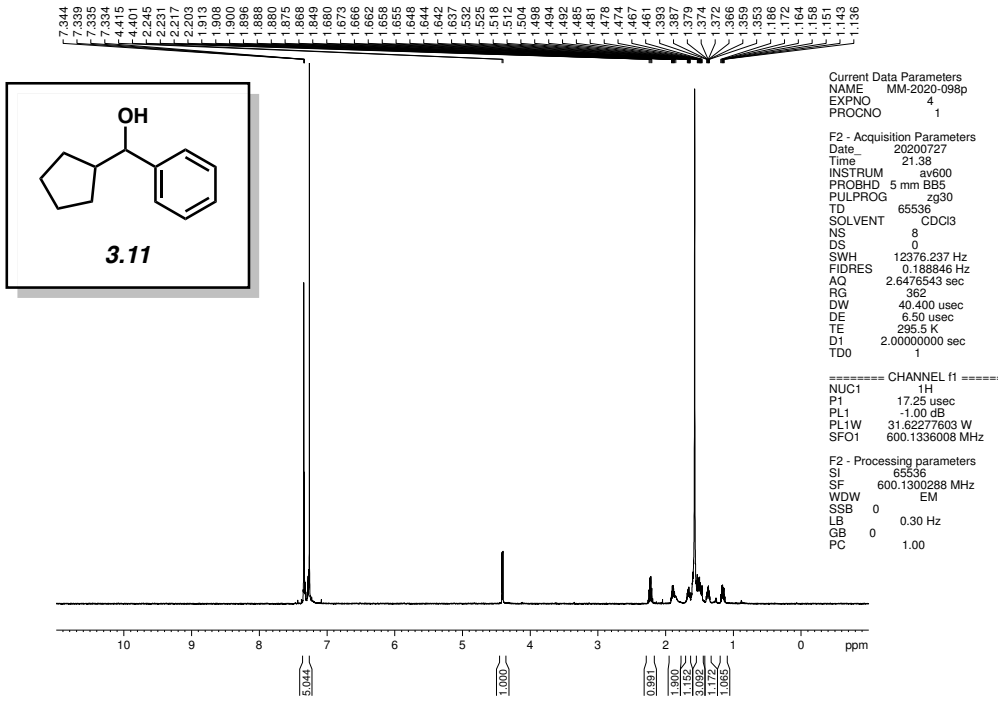

Figure 3.19 ^{1}H NMR (600 MHz, $CDCl_3$) of compound **3.11**.

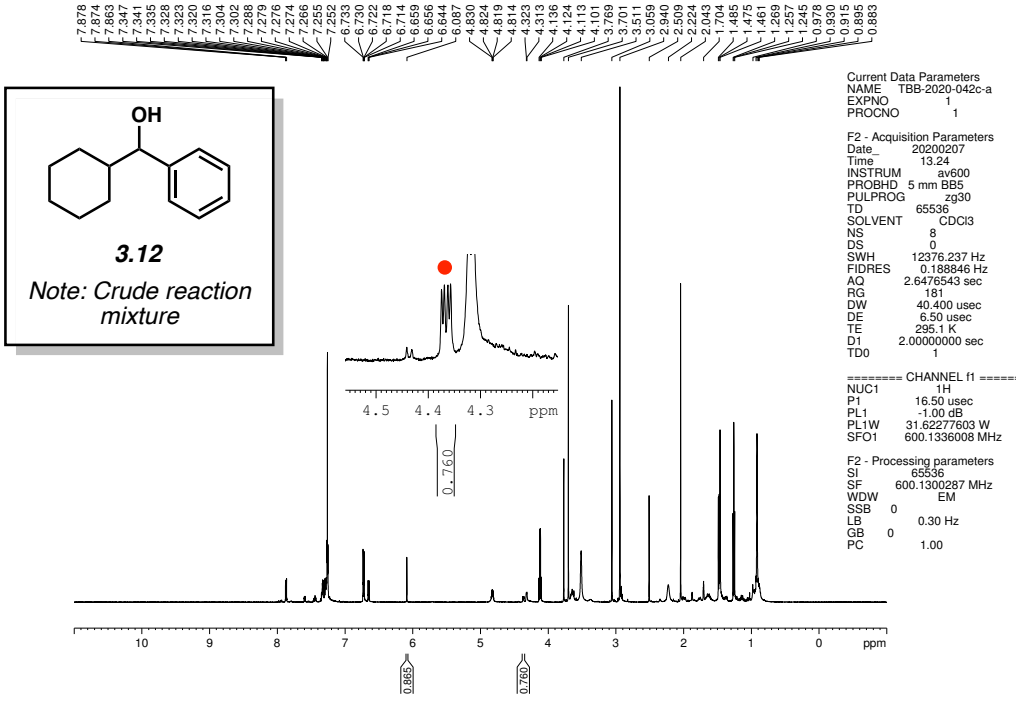

Figure 3.20 ^{1}H NMR (600 MHz, $CDCl_3$) of compound **3.12**.

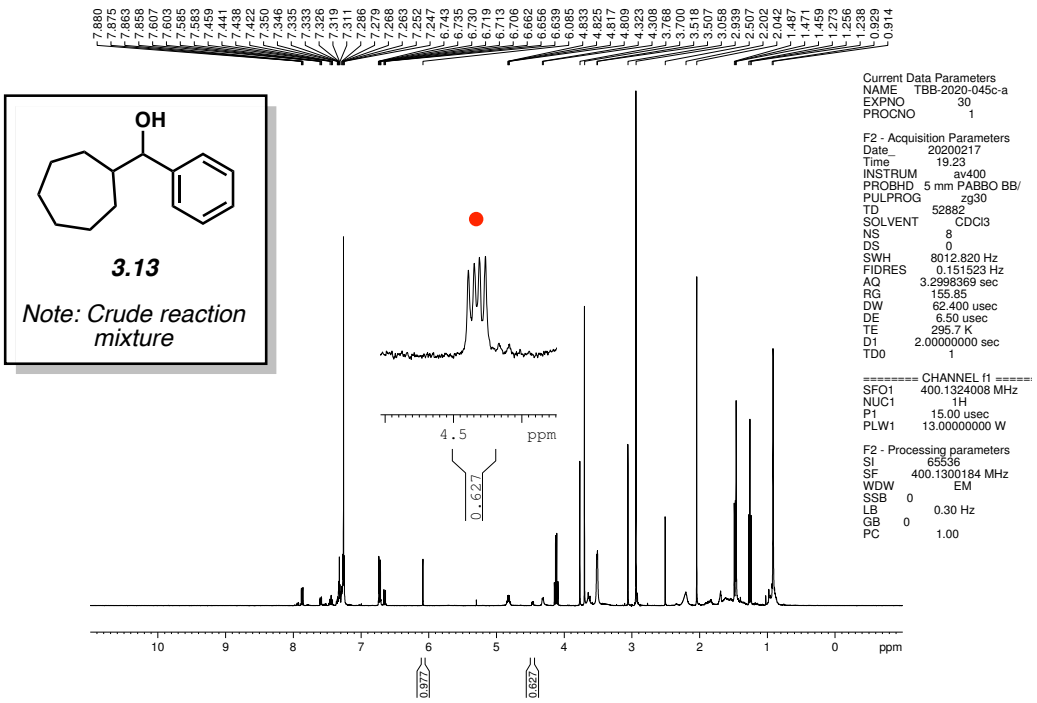

Figure 3.21 ^{1}H NMR (400 MHz, $CDCl_3$) of compound **3.13**.

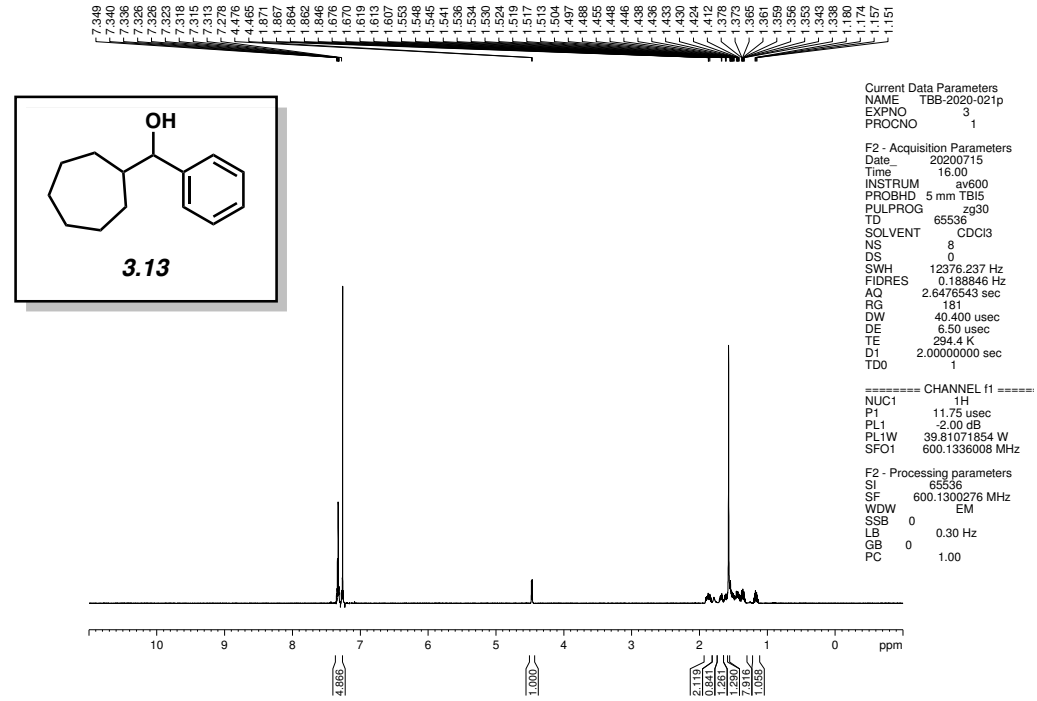

Figure 3.22 ^{1}H NMR (600 MHz, $CDCl_3$) of compound **3.13**.

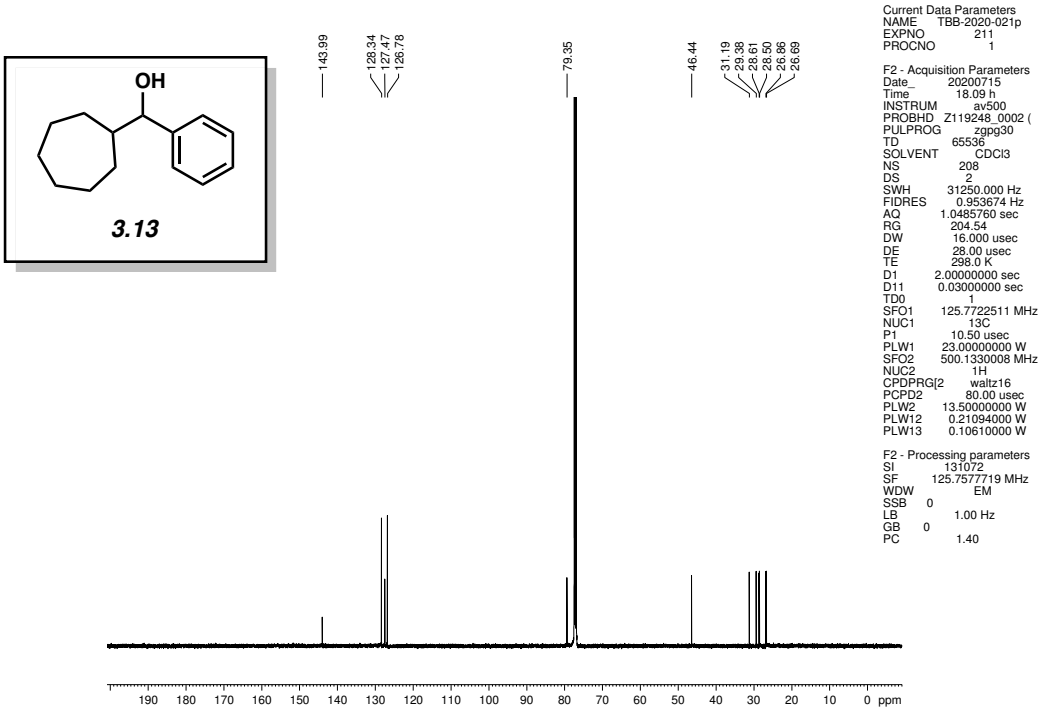

Figure 3.23 ^{13}C NMR (125 MHz, $CDCl_3$) of compound **3.13**.

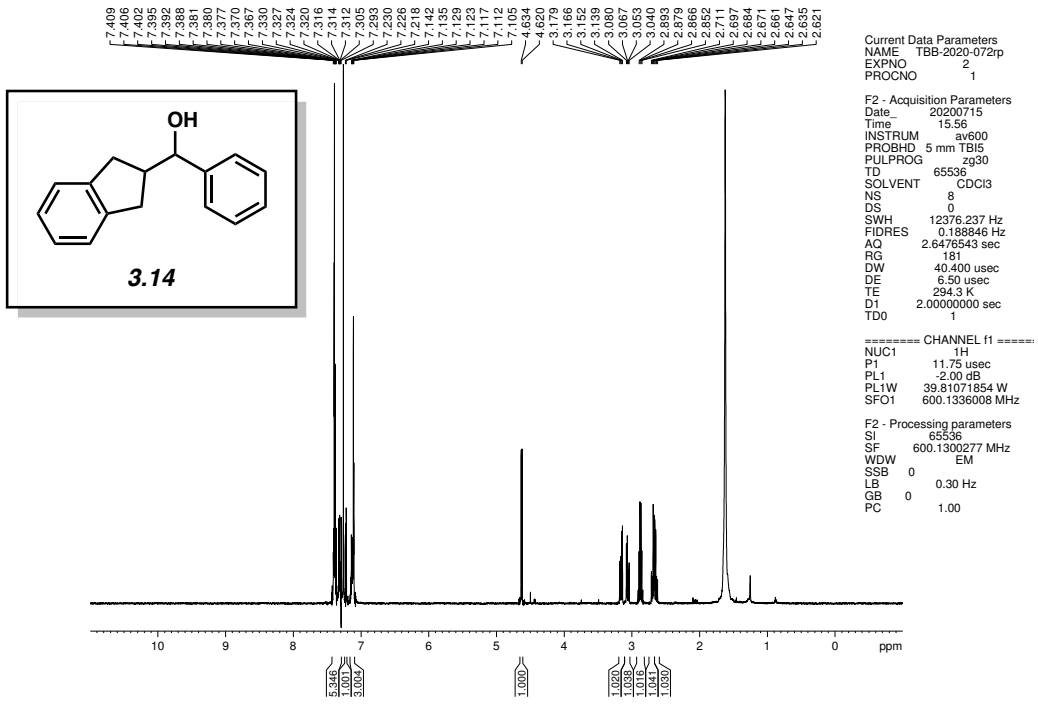

Figure 3.24 ^{1}H NMR (600 MHz, $CDCl_3$) of compound **3.14**.

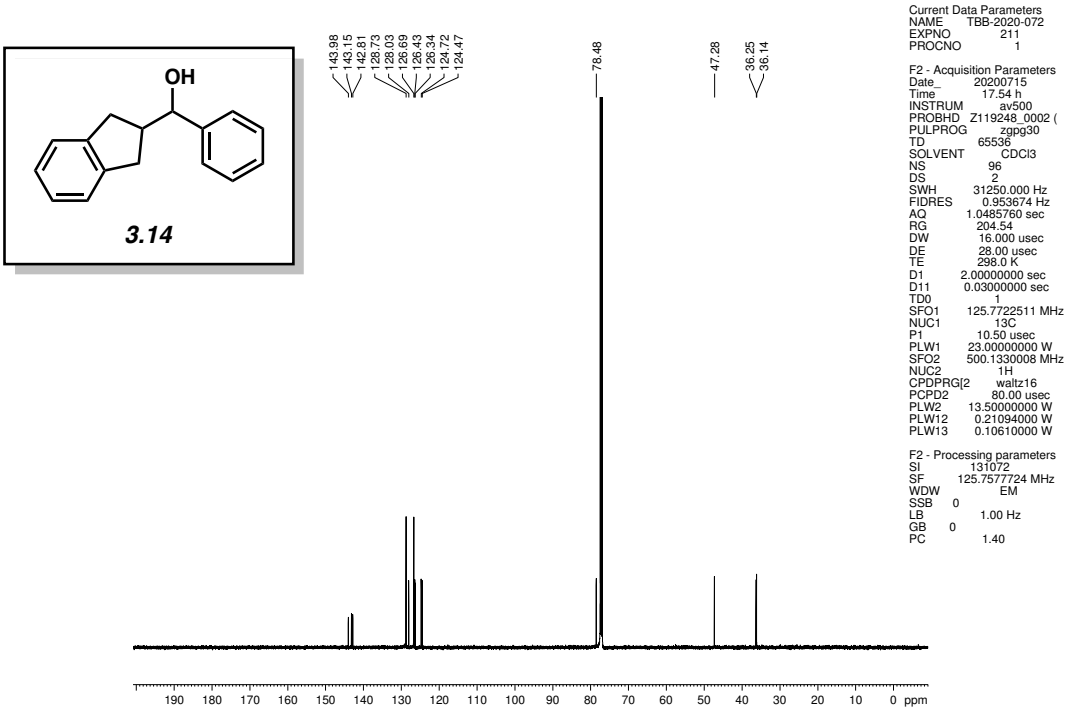

Figure 3.25 ^{13}C NMR (125 MHz, $CDCl_3$) of compound **3.14**.

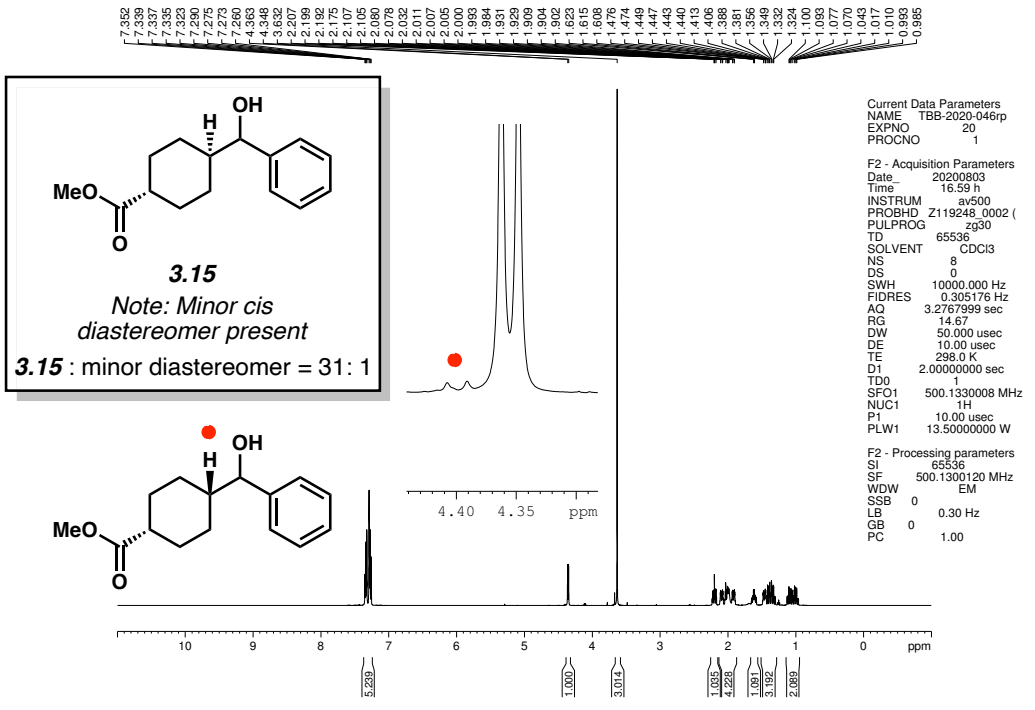

Figure 3.26 ^{1}H NMR (500 MHz, $CDCl_3$) of compound **3.15**.

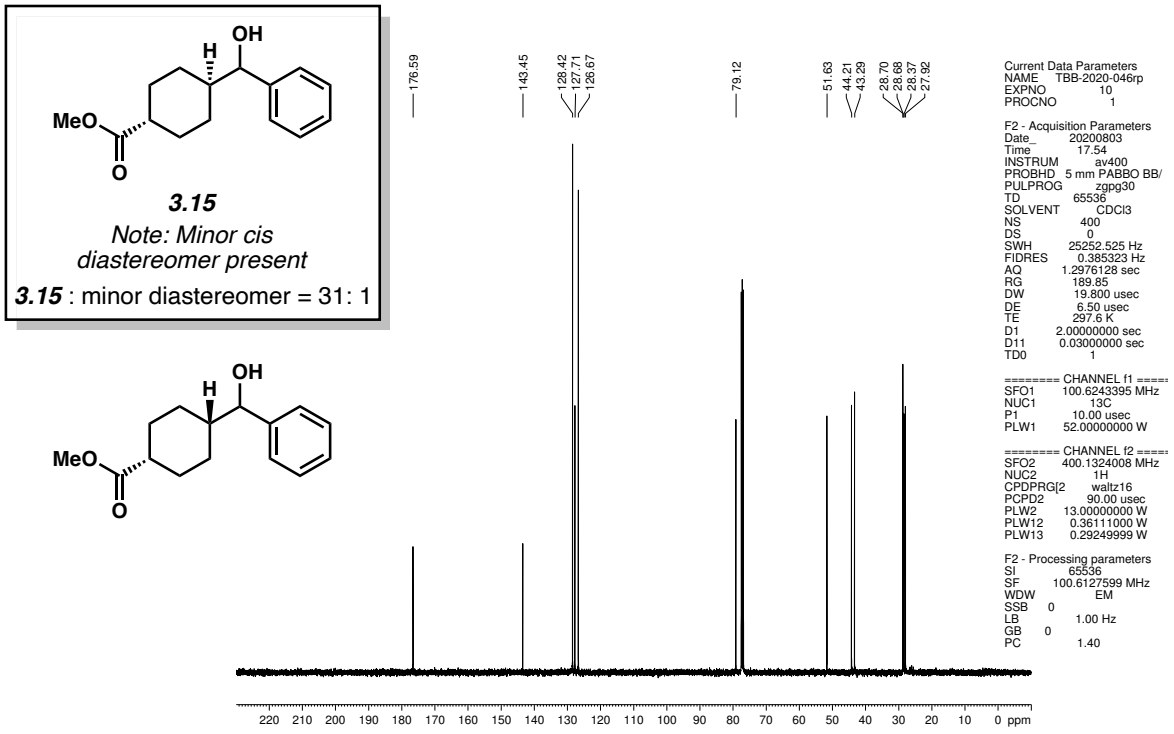

Figure 3.27 ^{13}C NMR (125 MHz, $CDCl_3$) of compound **3.15**.

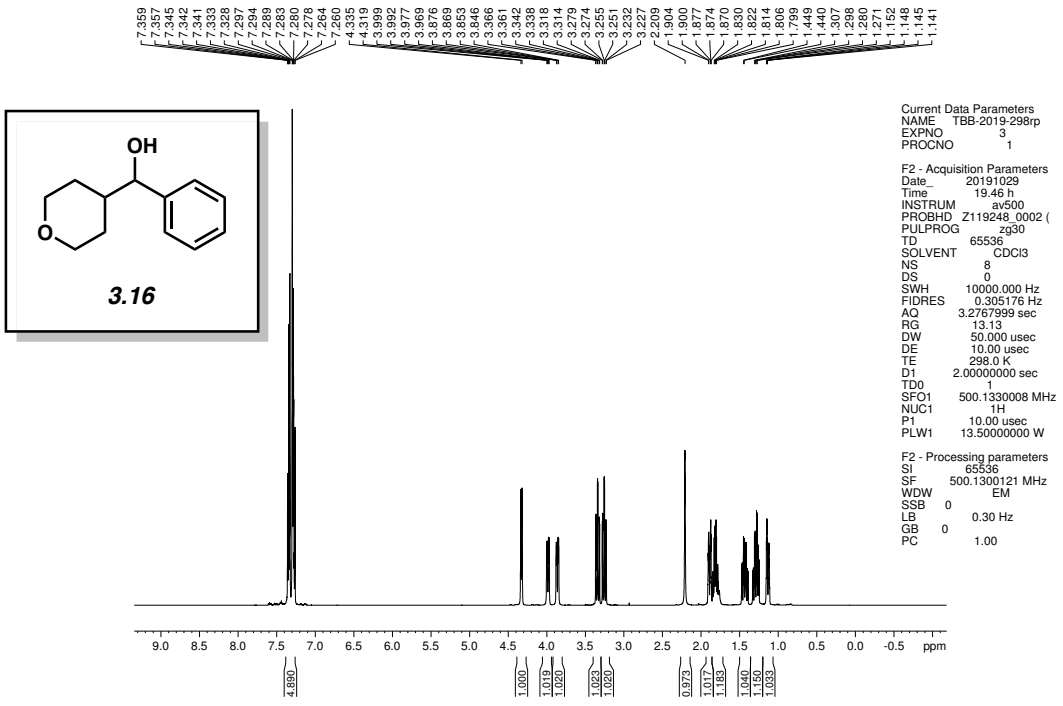

Figure 3.28 ^{1}H NMR (500 MHz, $CDCl_3$) of compound **3.16**.

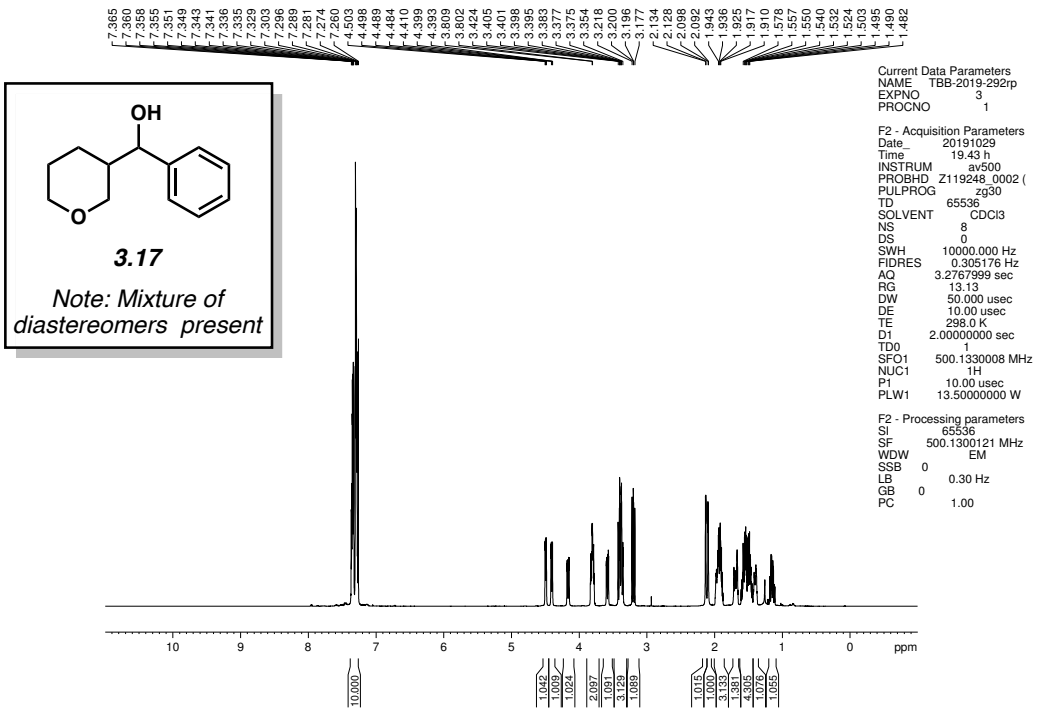

Figure 3.29 ^{1}H NMR (500 MHz, $CDCl_3$) of compound **3.17**.

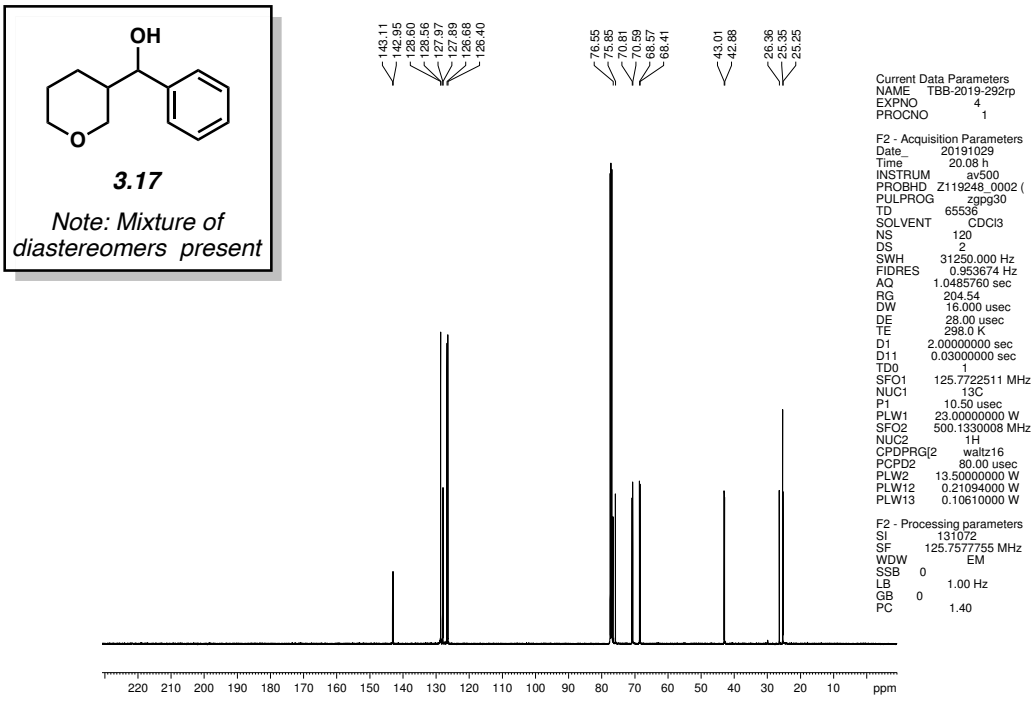

Figure 3.30 ^{13}C NMR (125 MHz, $CDCl_3$) of compound **3.17**.

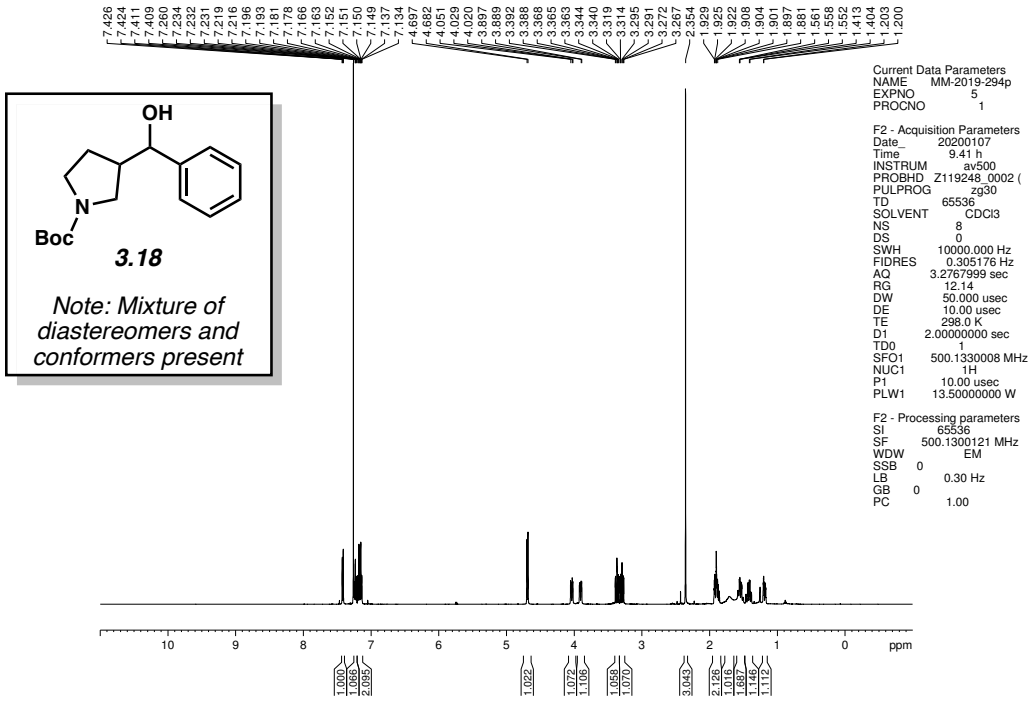

Figure 3.31 ^{1}H NMR (500 MHz, $CDCl_3$) of compound **3.18**.

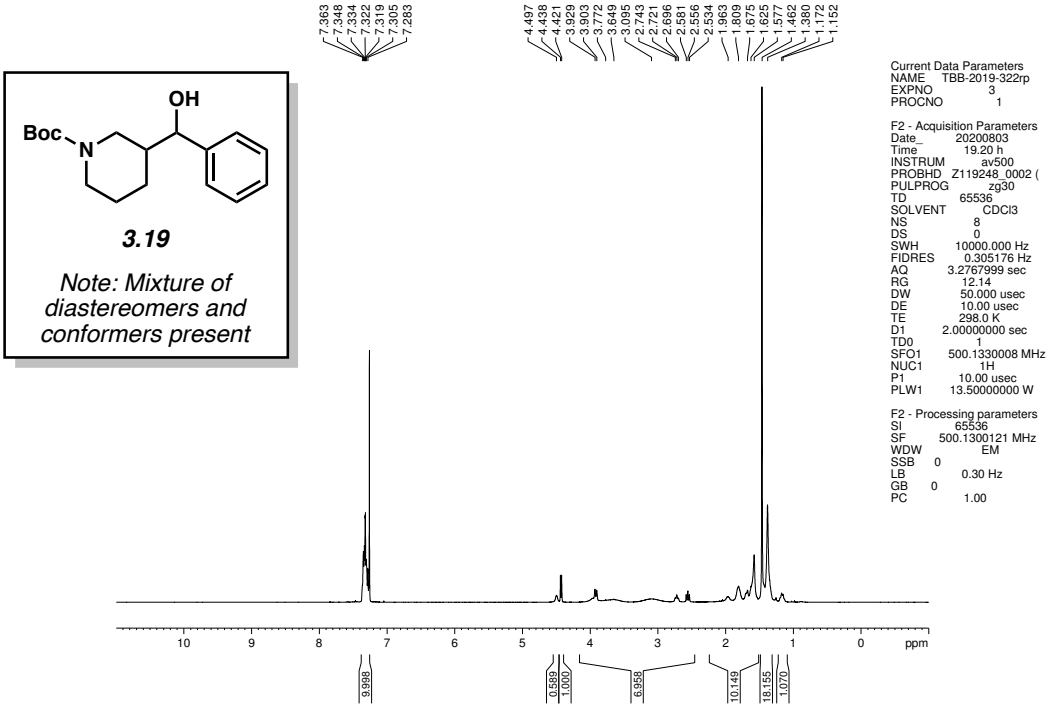

Figure 3.32 ^{1}H NMR (500 MHz, $CDCl_3$) of compound **3.19**.

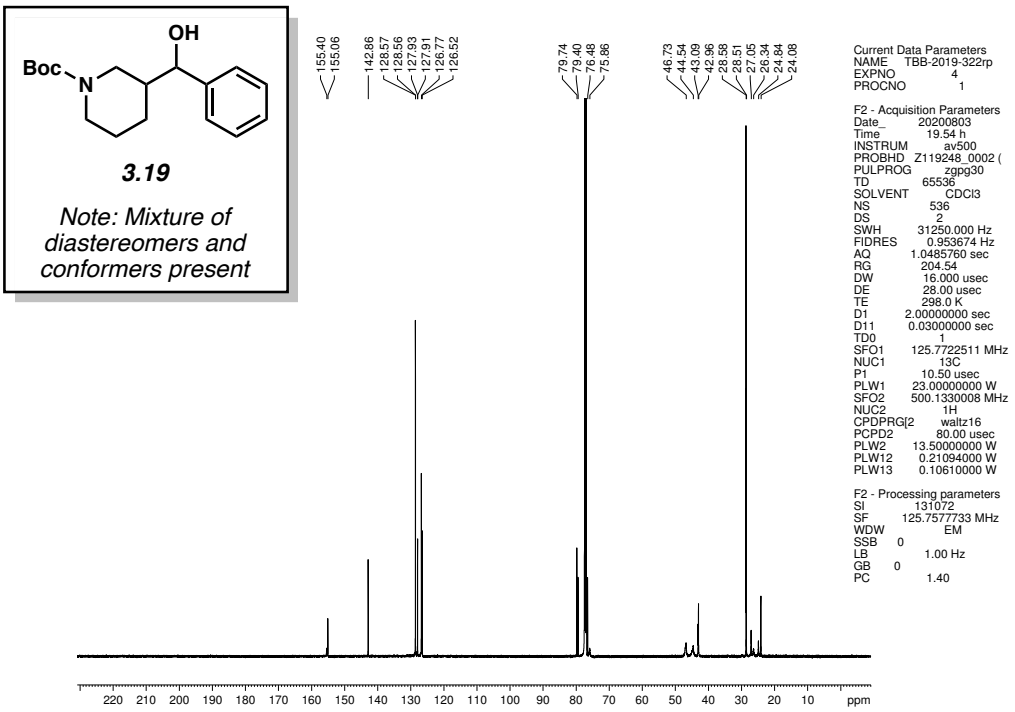

Figure 3.33 ^{13}C NMR (125 MHz, $CDCl_3$) of compound **3.19**.

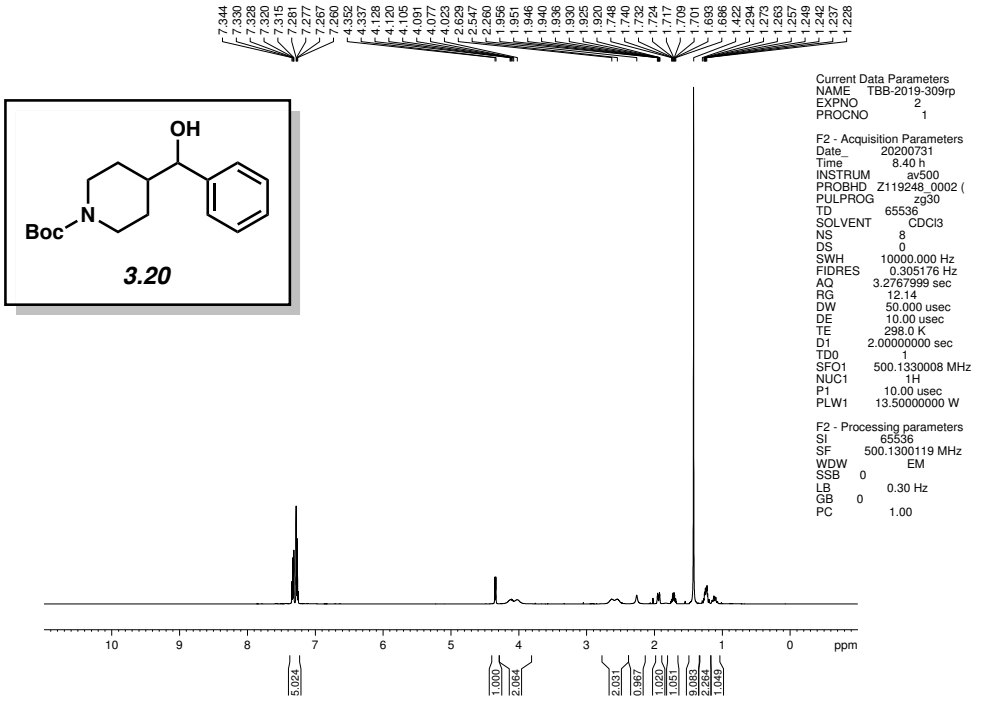

Figure 3.34 ^{1}H NMR (500 MHz, $CDCl_3$) of compound **3.20**.

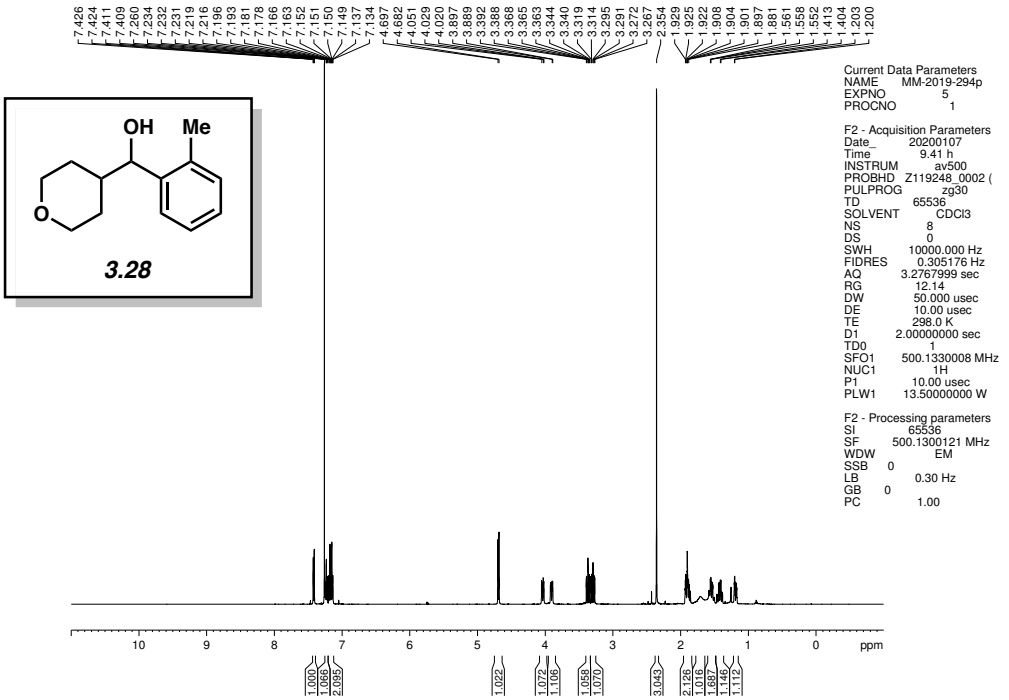

Figure 3.35 ^{1}H NMR (500 MHz, $CDCl_3$) of compound **3.28**.

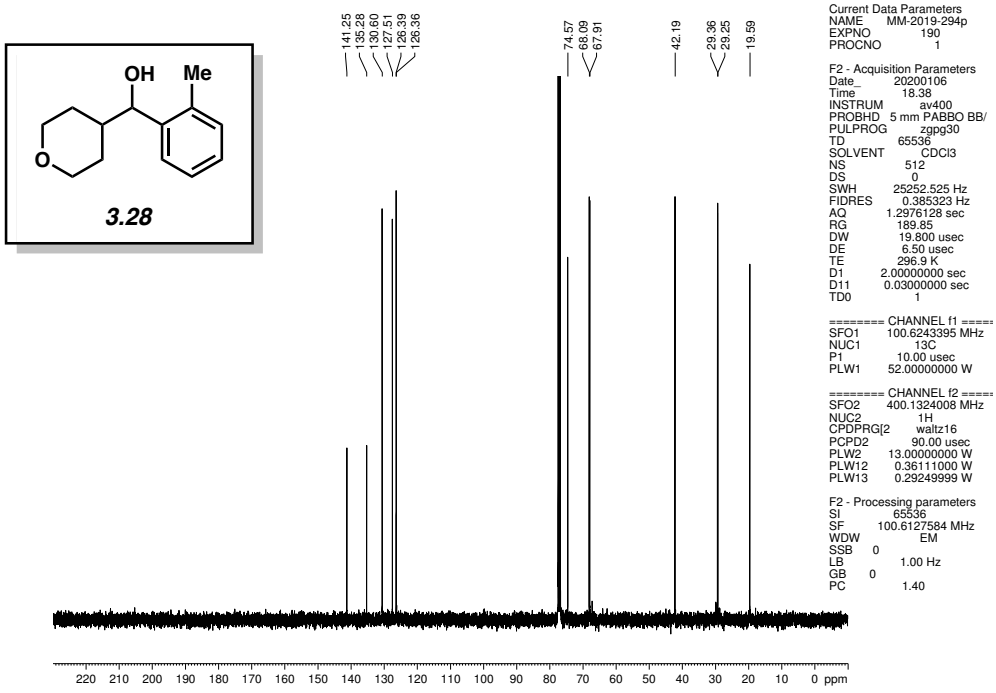

Figure 3.36 ^{13}C NMR (125 MHz, $CDCl_3$) of compound **3.28**.

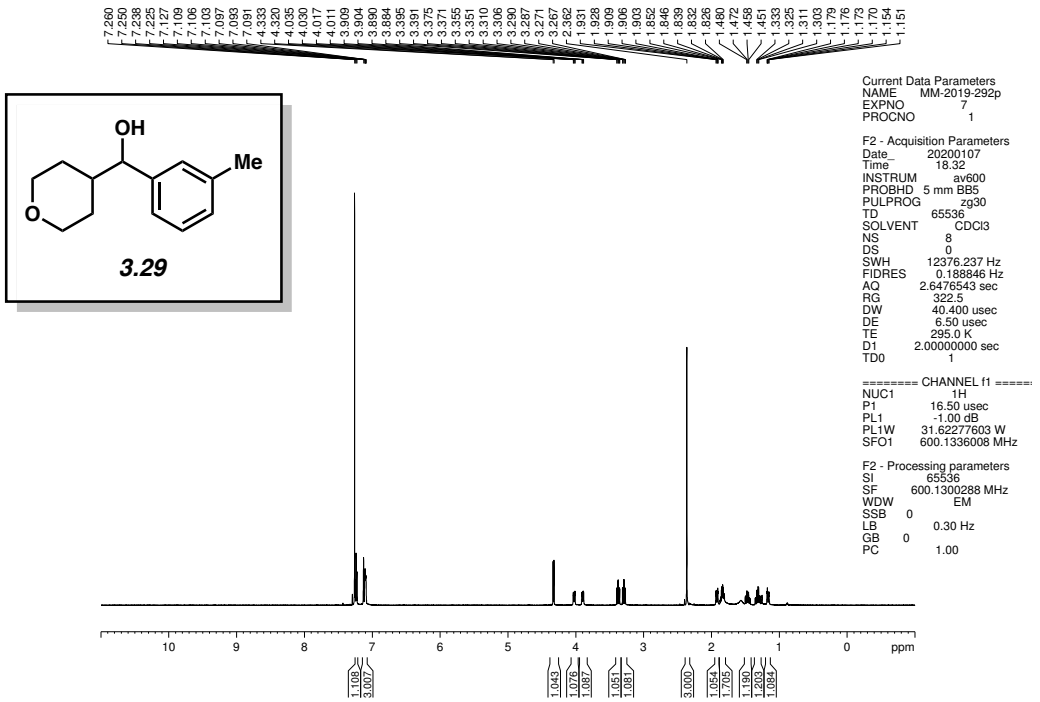

Figure 3.37 ^{1}H NMR (600 MHz, $CDCl_3$) of compound **3.29**.

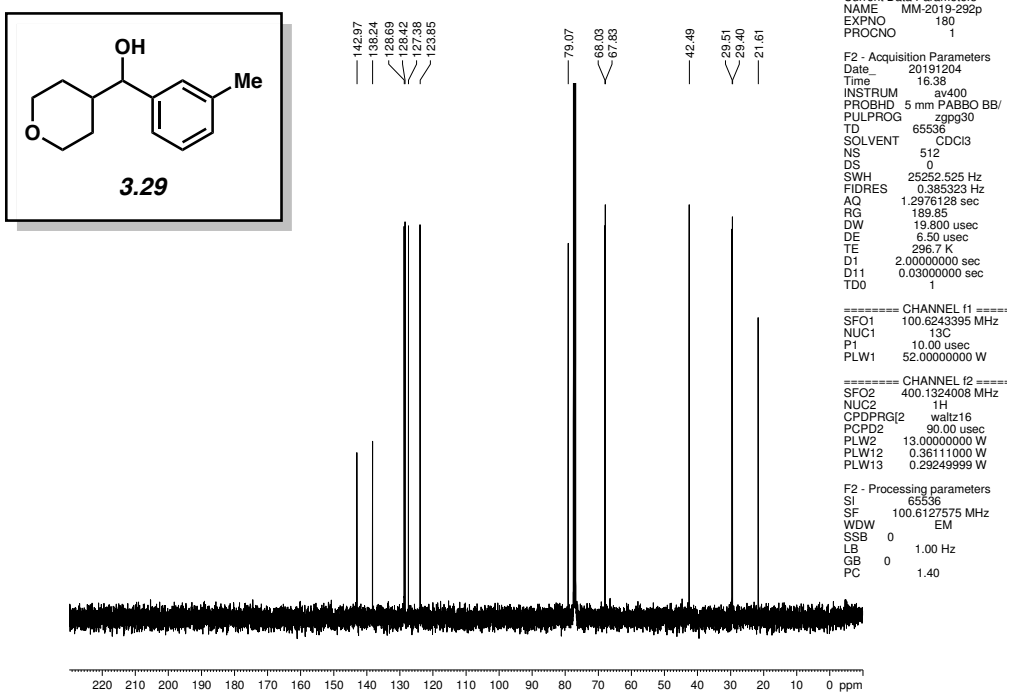

Figure 3.38 ^{13}C NMR (125 MHz, $CDCl_3$) of compound **3.29**.

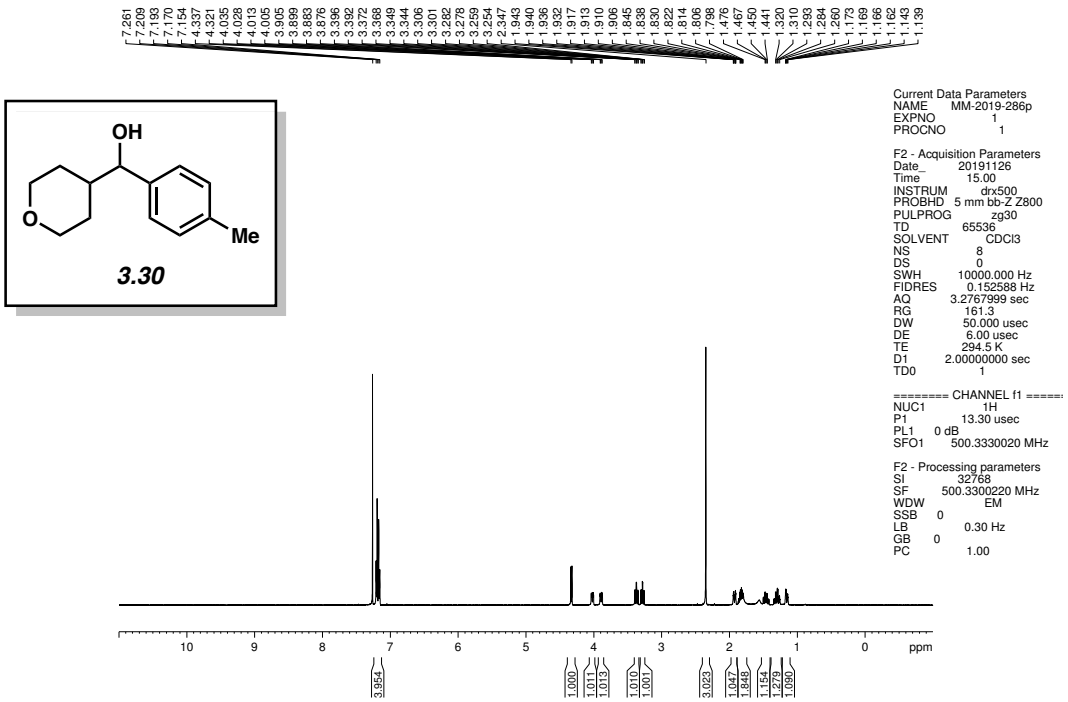

Figure 3.39 ^{1}H NMR (500 MHz, $CDCl_3$) of compound **3.30**.

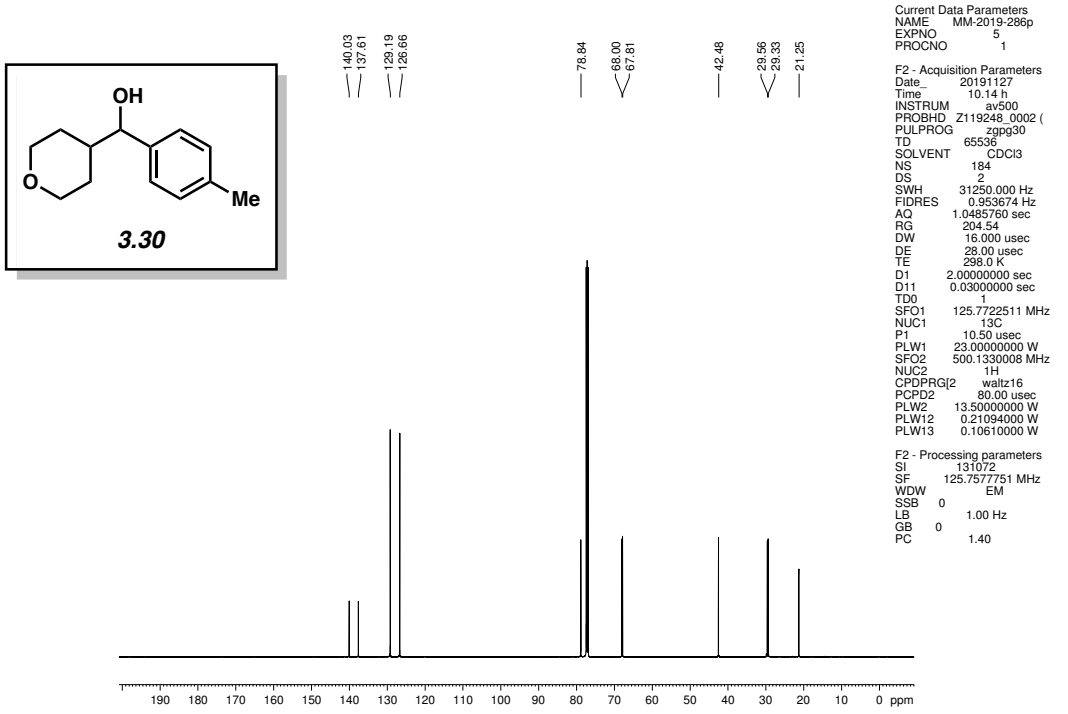

Figure 3.40 ^{13}C NMR (125 MHz, $CDCl_3$) of compound **3.30**.

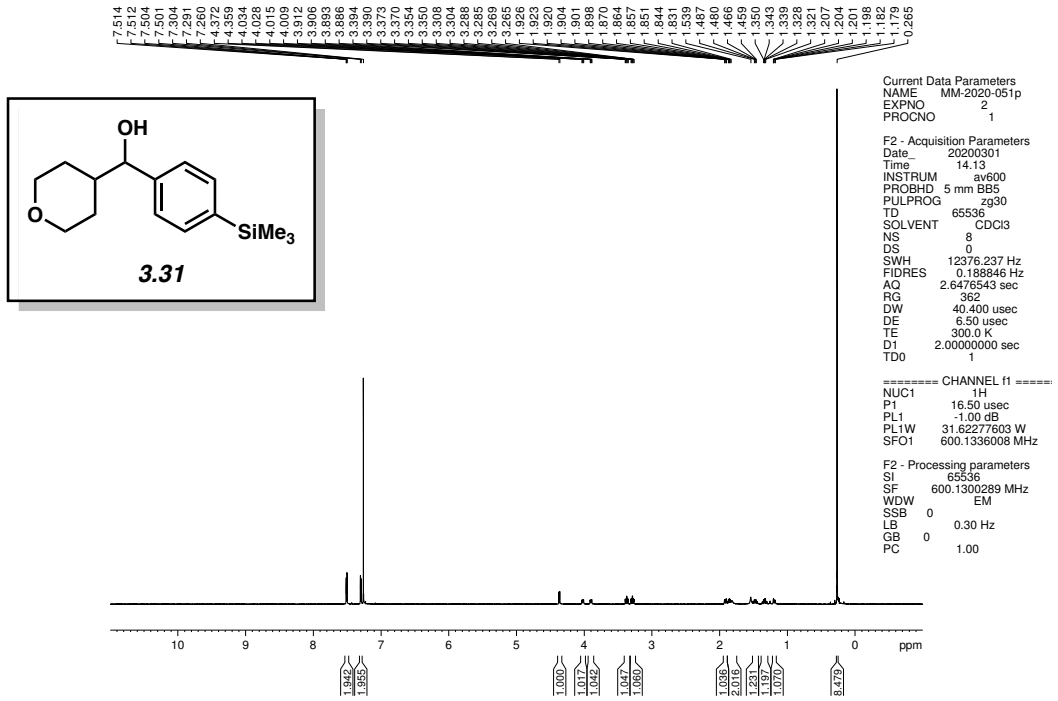

Figure 3.41 ^{1}H NMR (600 MHz, $CDCl_3$) of compound **3.31**.

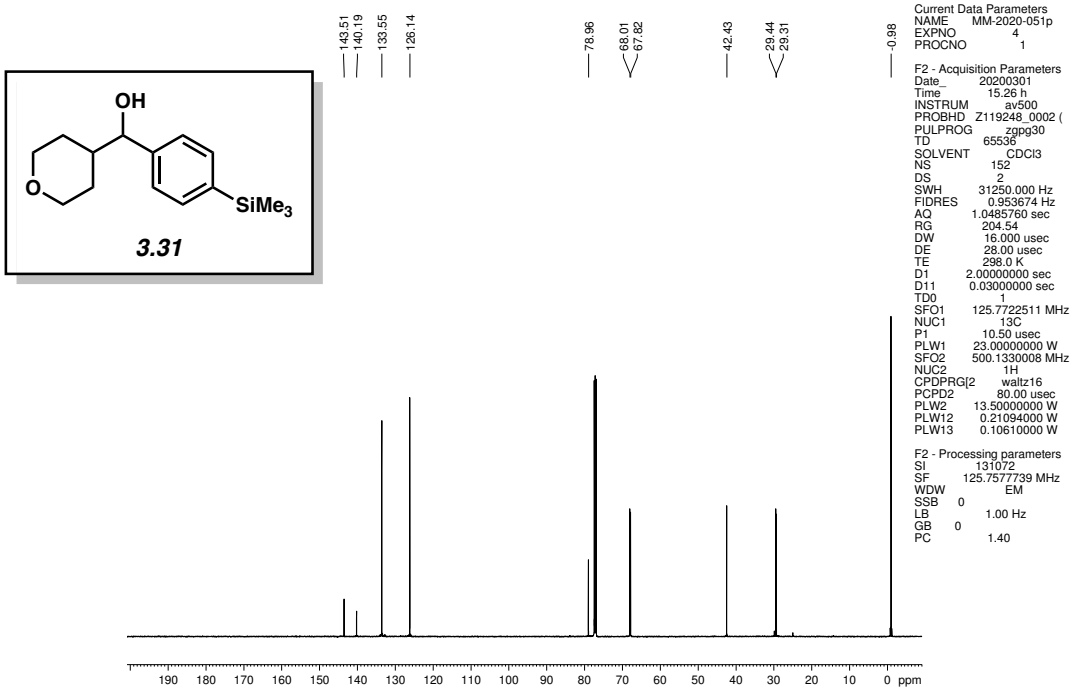

Figure 3.42 ^{13}C NMR (125 MHz, $CDCl_3$) of compound **3.31**.

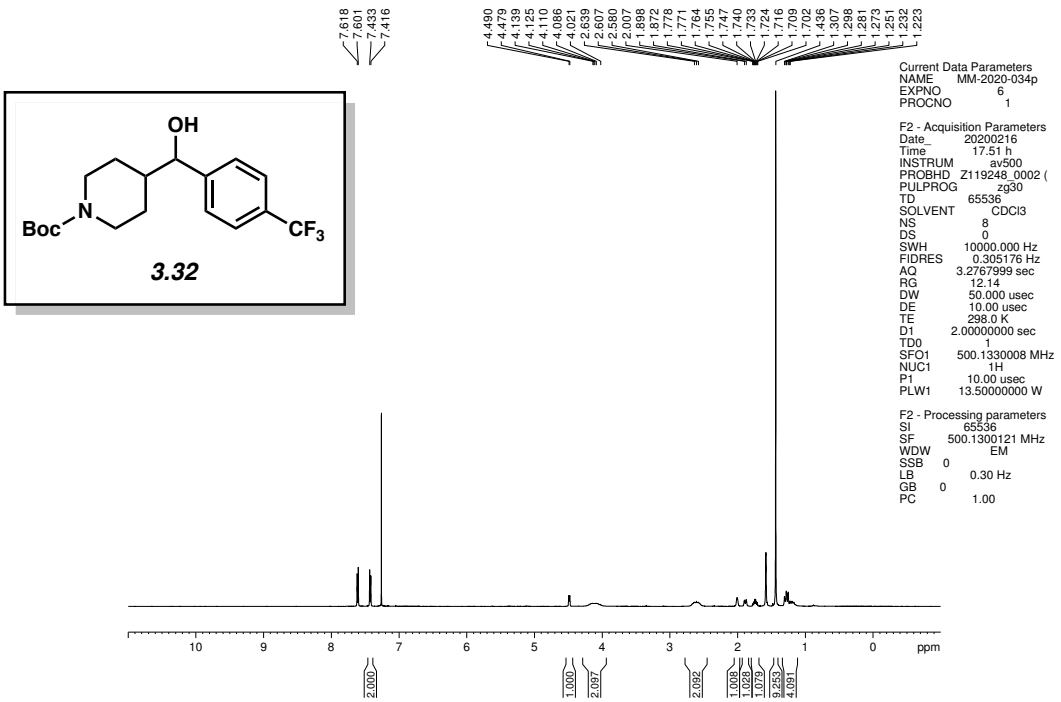

Figure 3.43 ^{1}H NMR (500 MHz, $CDCl_3$) of compound **3.32**.

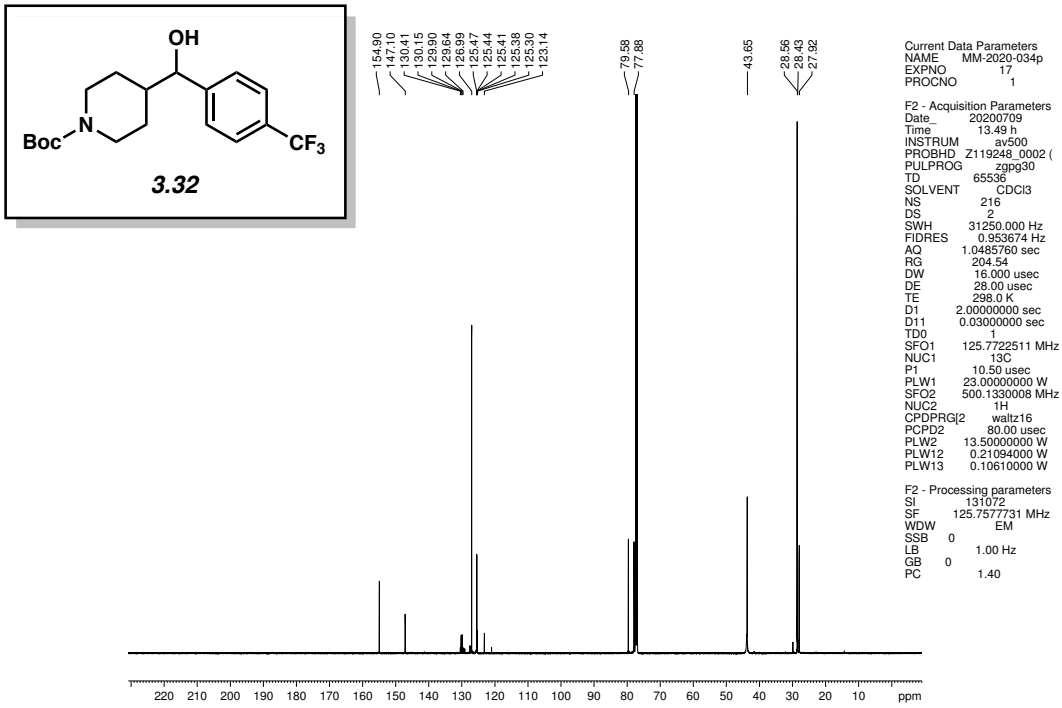

Figure 3.44 ^{13}C NMR (125 MHz, $CDCl_3$) of compound **3.32**.

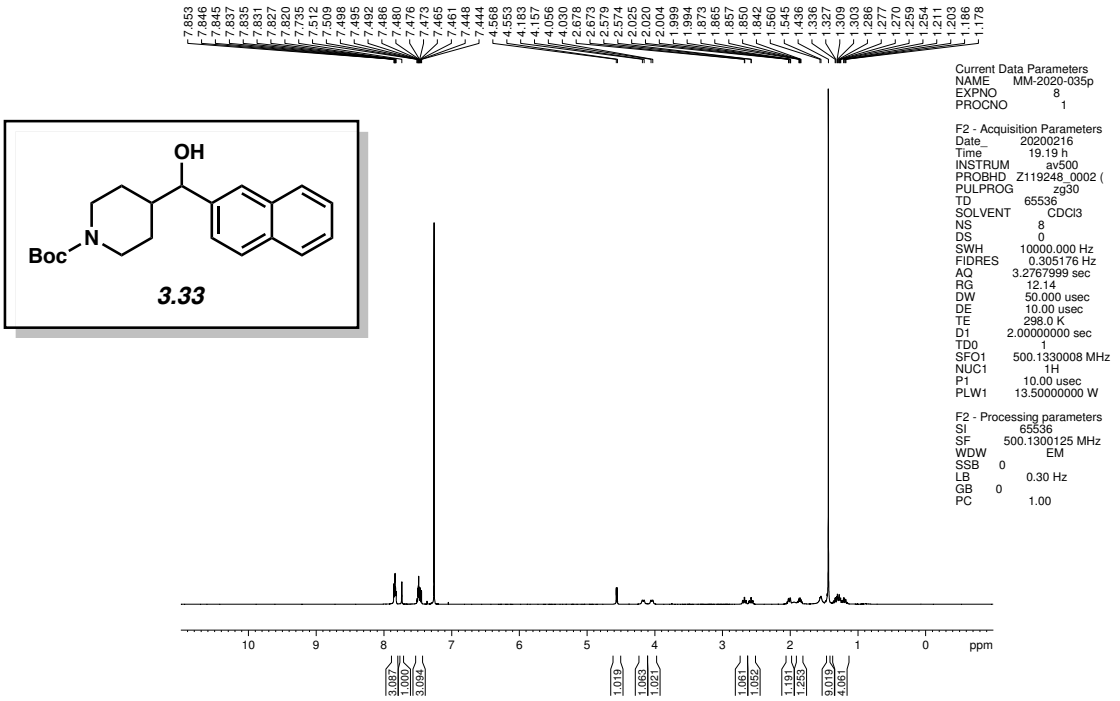

Figure 3.45 ^{1}H NMR (500 MHz, $CDCl_3$) of compound **3.33**.

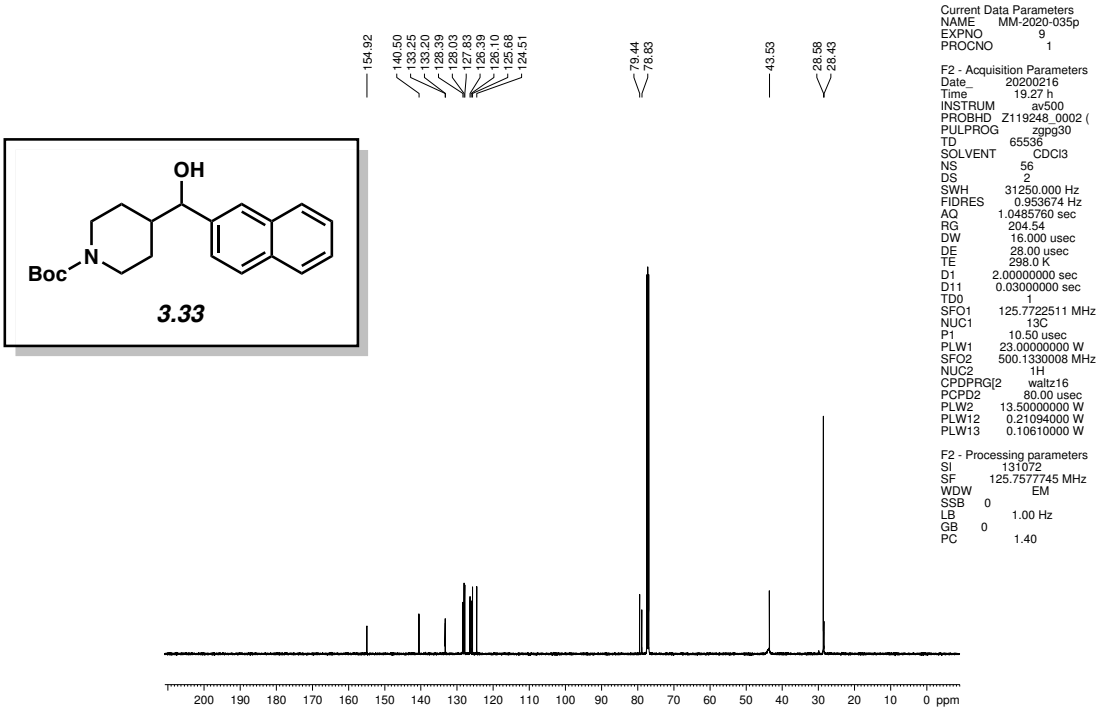

Figure 3.46 ^{13}C NMR (125 MHz, $CDCl_3$) of compound **3.33**.

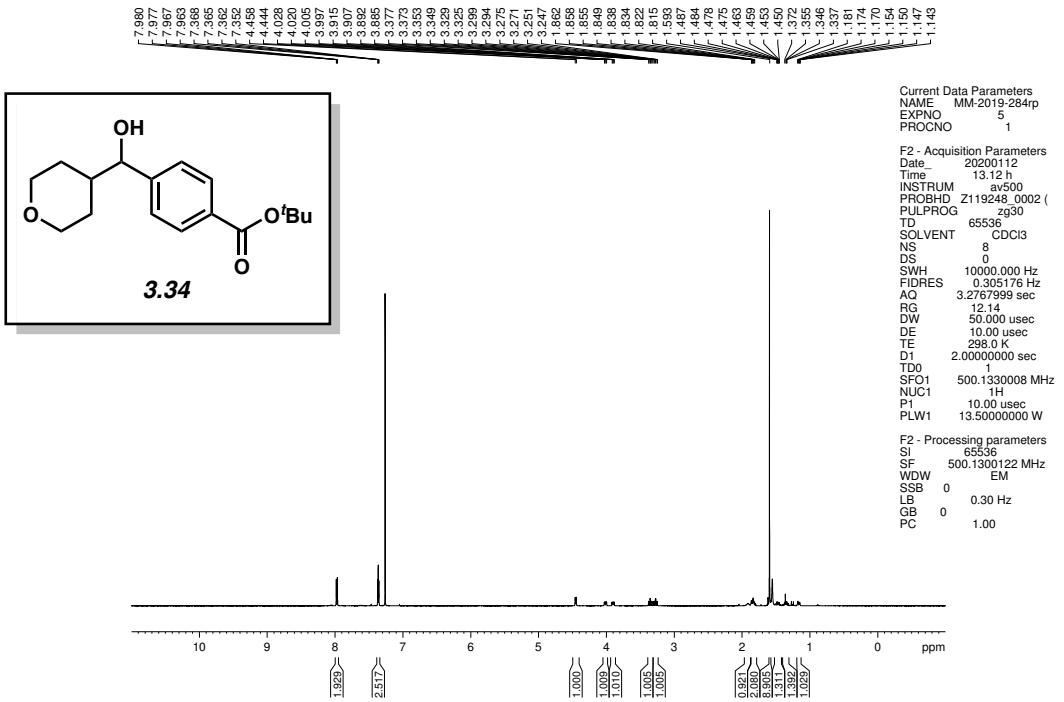

Figure 3.47 ^{1}H NMR (500 MHz, $CDCl_3$) of compound **3.34**.

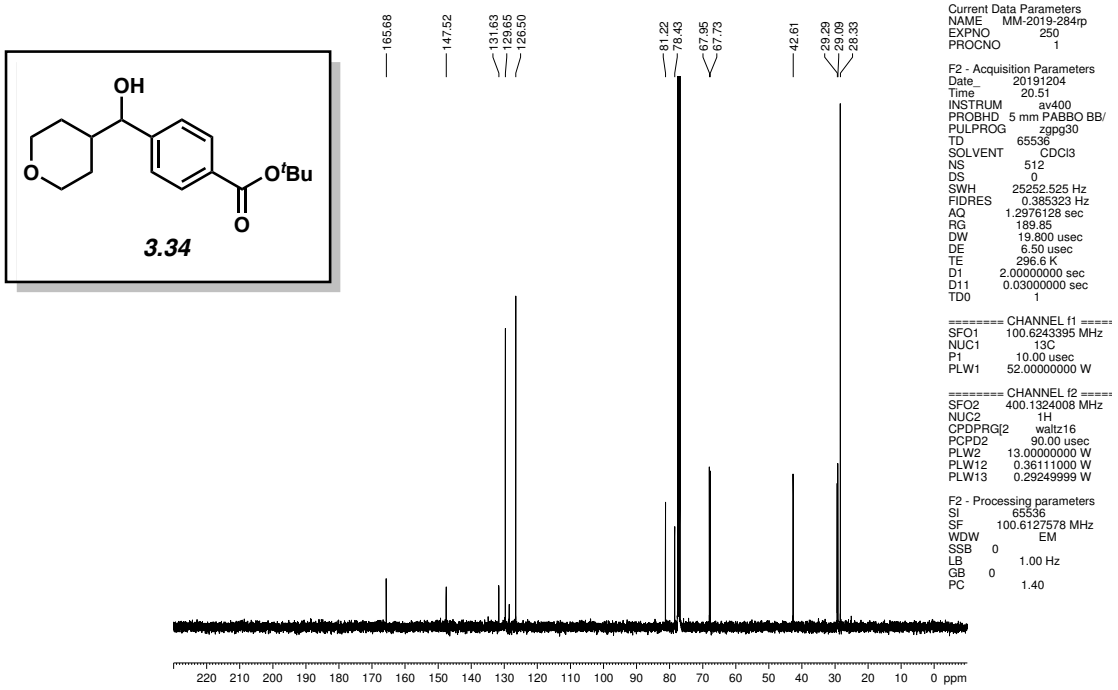

Figure 3.48 ^{13}C NMR (100 MHz, $CDCl_3$) of compound **3.34**.

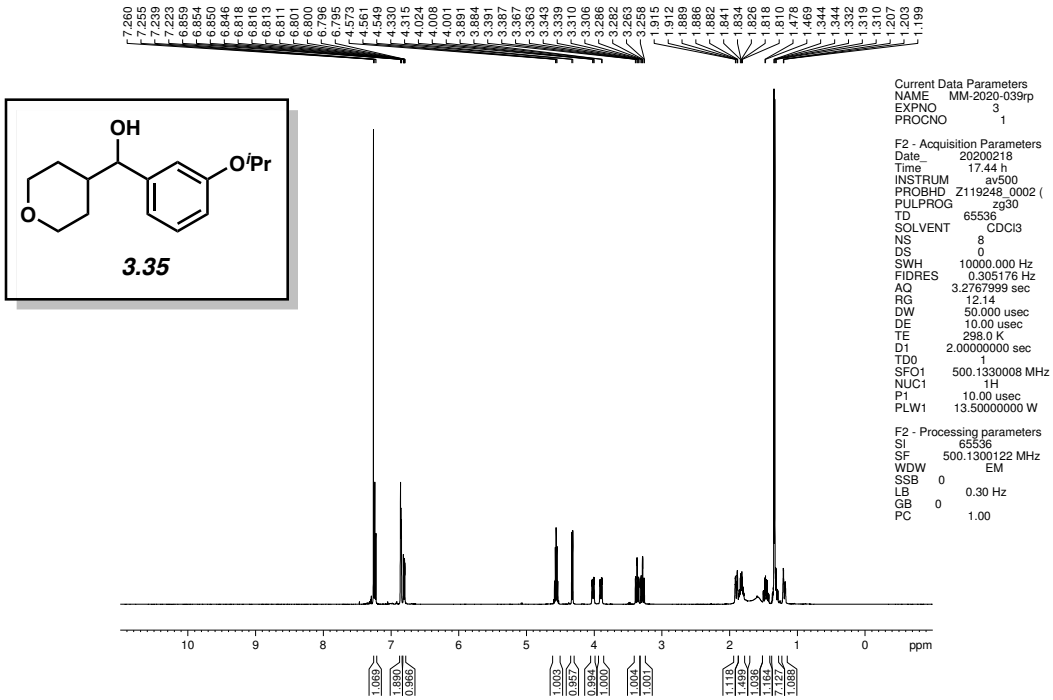

Figure 3.49 ^{1}H NMR (500 MHz, $CDCl_3$) of compound **3.35**.

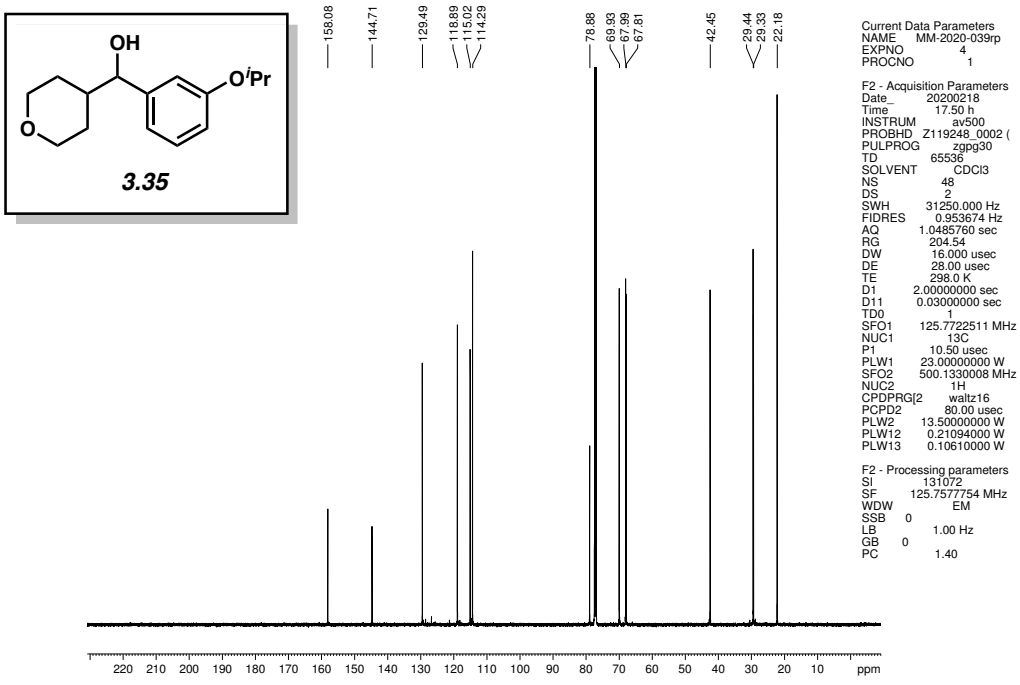

Figure 3.50 ^{13}C NMR (125 MHz, $CDCl_3$) of compound **3.35**.

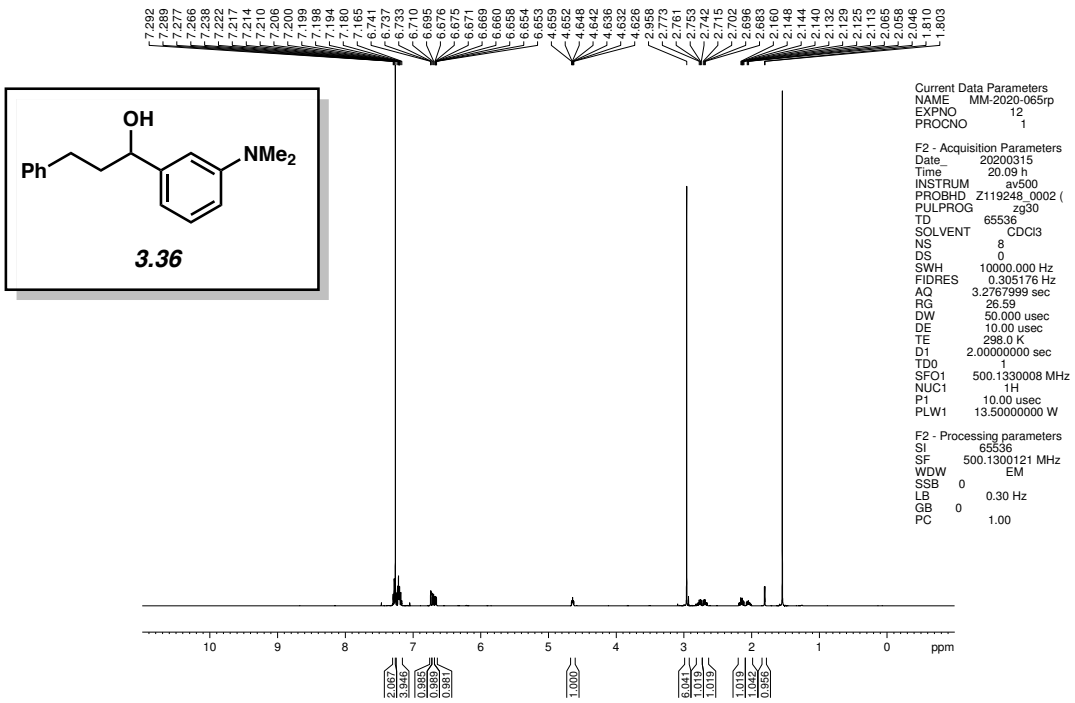

Figure 3.51 ^{1}H NMR (500 MHz, $CDCl_3$) of compound **3.36**.

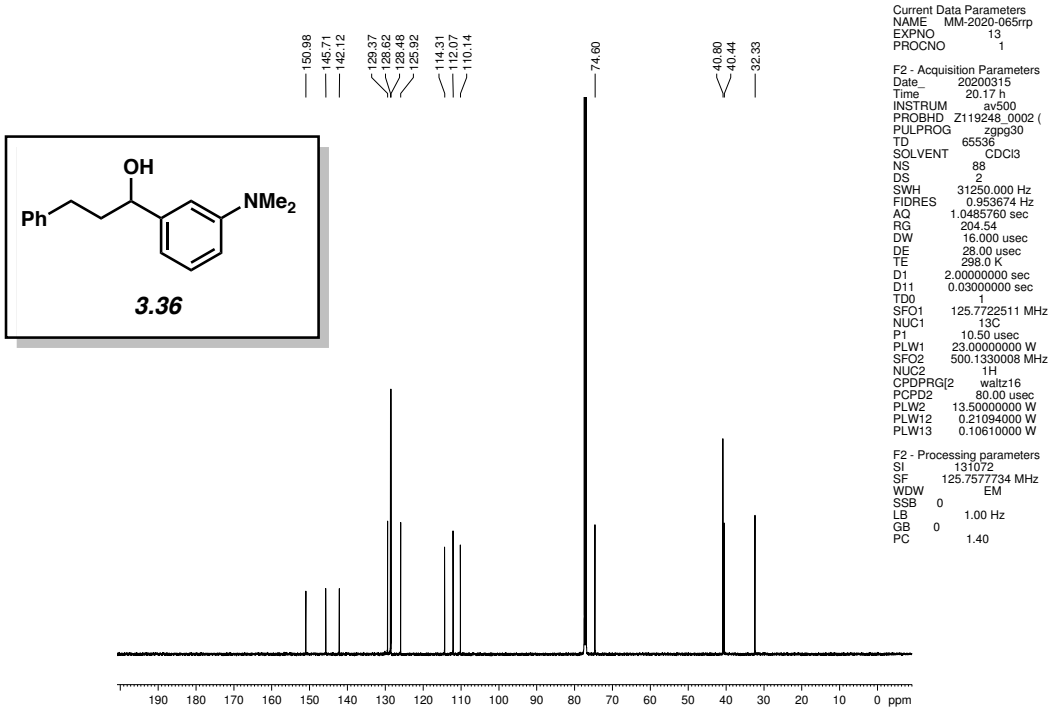

Figure 3.52 ^{13}C NMR (125 MHz, $CDCl_3$) of compound **3.36**.

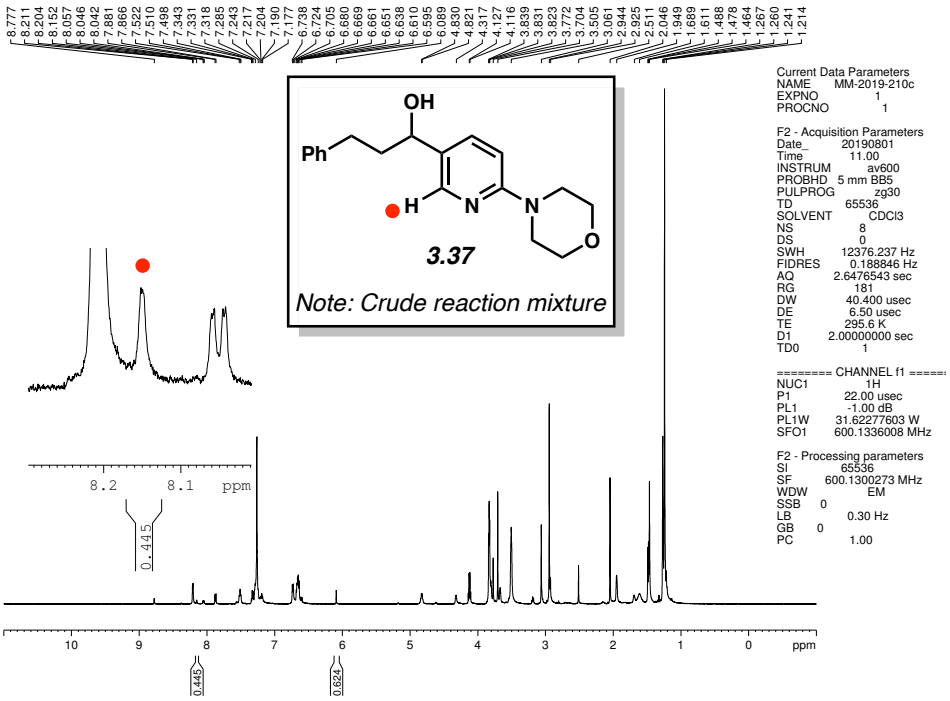

Figure 3.53 ^{1}H NMR (600 MHz, $CDCl_3$) of compound **3.37**.

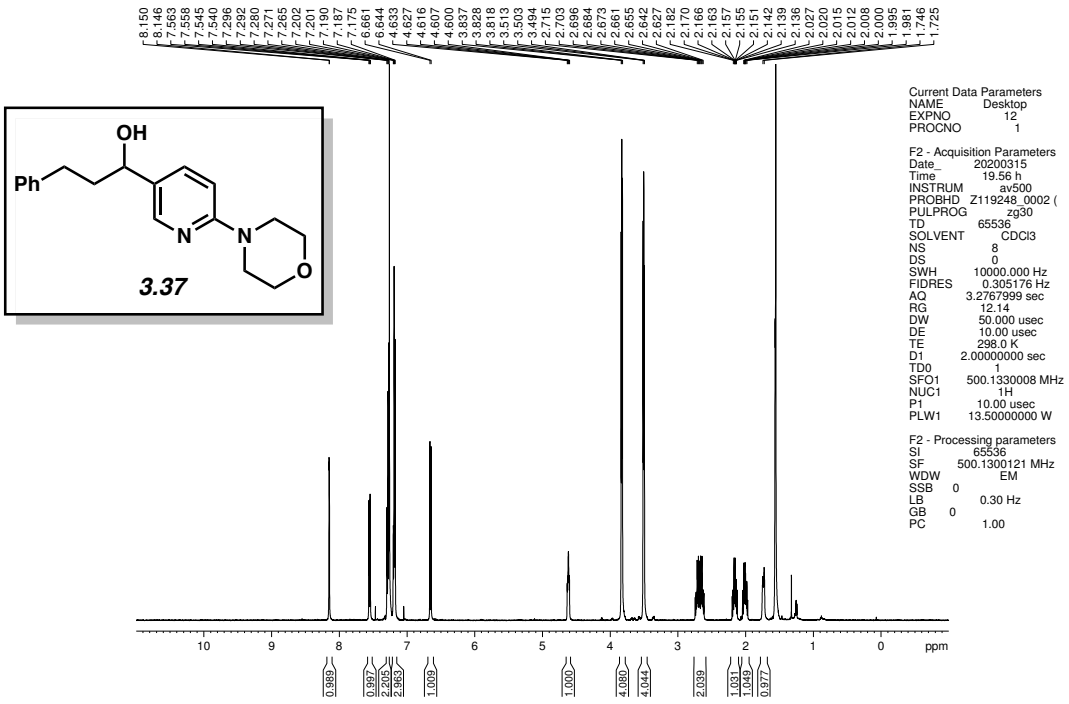

Figure 3.54 ^{1}H NMR (500 MHz, $CDCl_3$) of compound **3.37**.

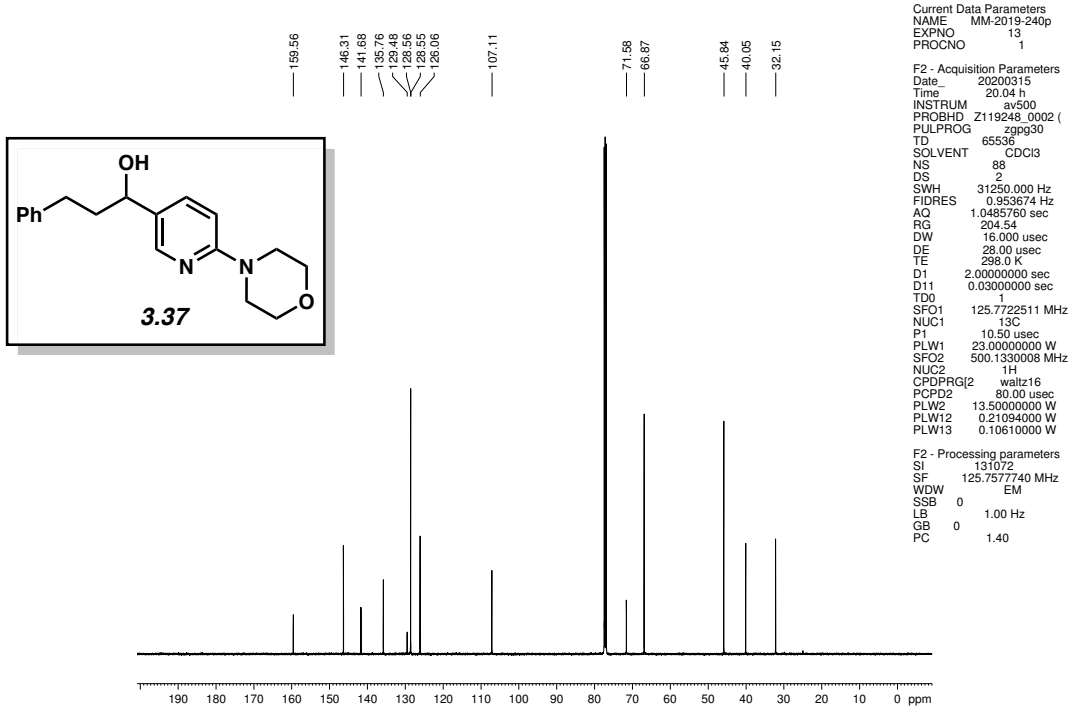

Figure 3.55 ^{13}C NMR (125 MHz, $CDCl_3$) of compound **3.37**.

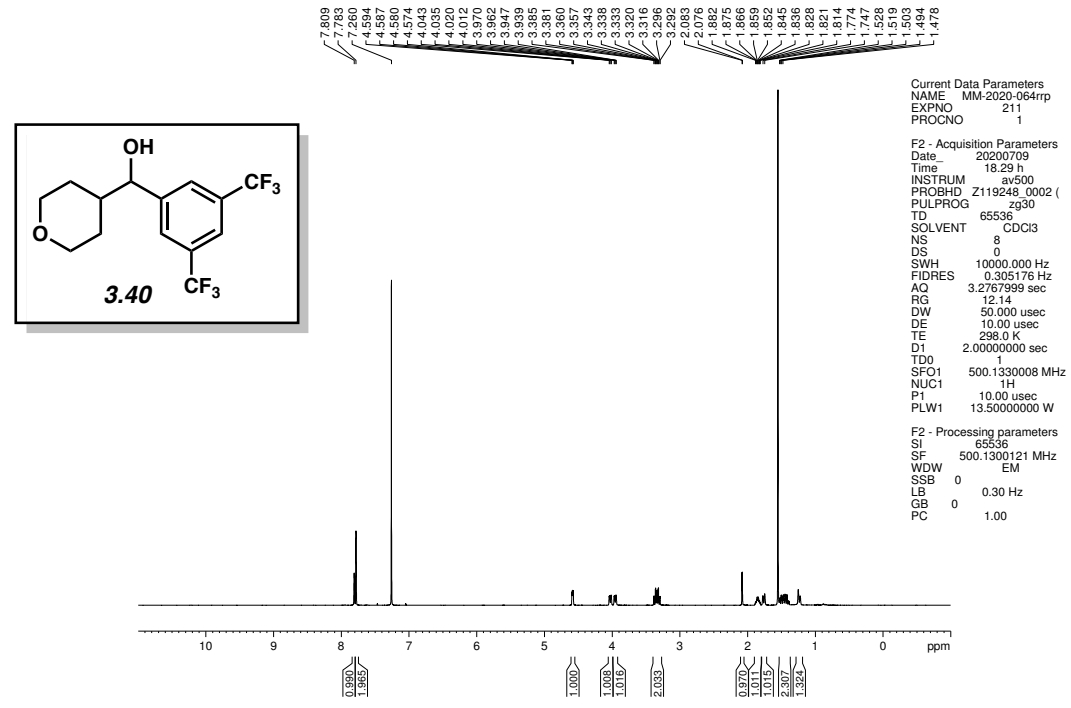

Figure 3.56 ^{1}H NMR (500 MHz, $CDCl_3$) of compound **3.40**.

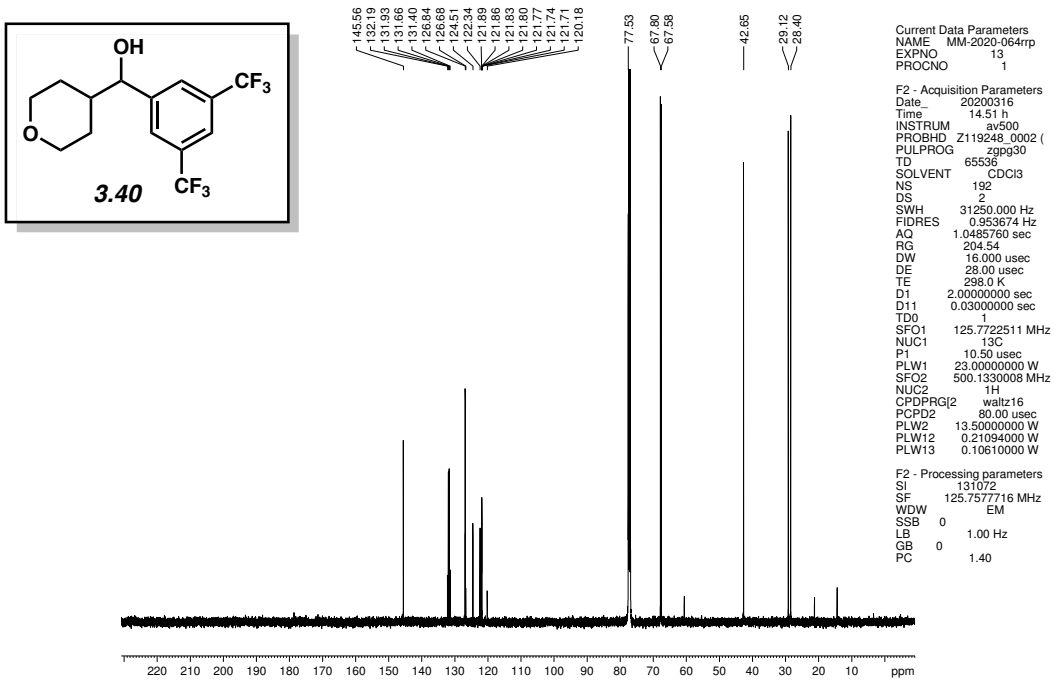

Figure 3.57 ^{13}C NMR (125 MHz, $CDCl_3$) of compound **3.40**.

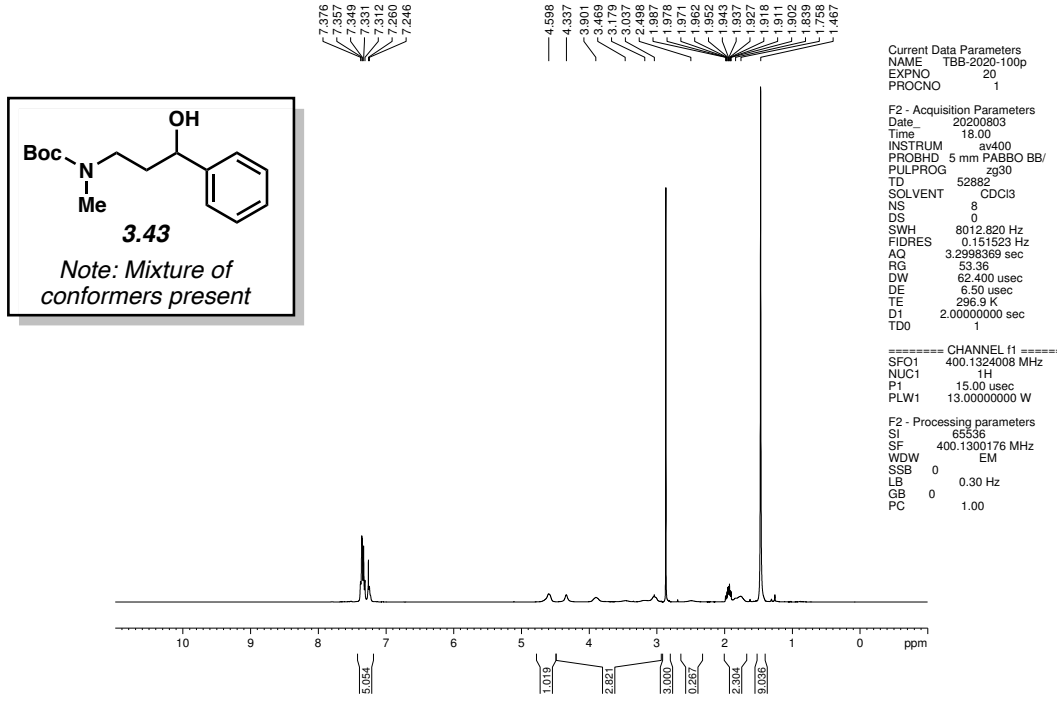

Figure 3.58 ^{1}H NMR (400 MHz, $CDCl_3$) of compound **3.43**.

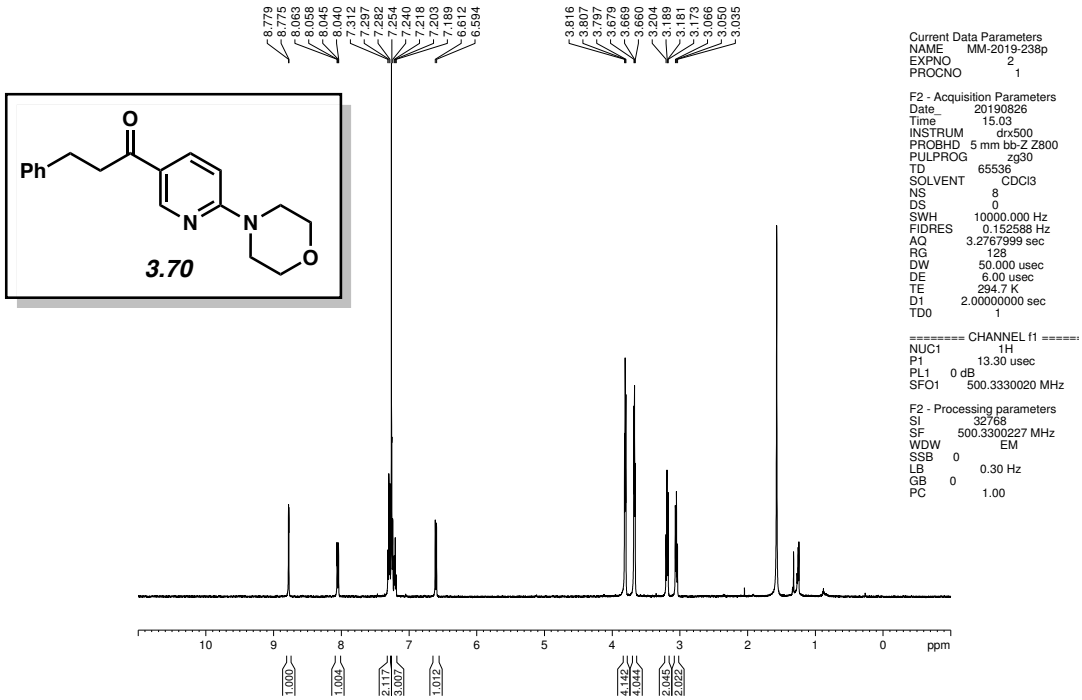

Figure 3.59 ^{1}H NMR (500 MHz, $CDCl_3$) of compound **3.70**.

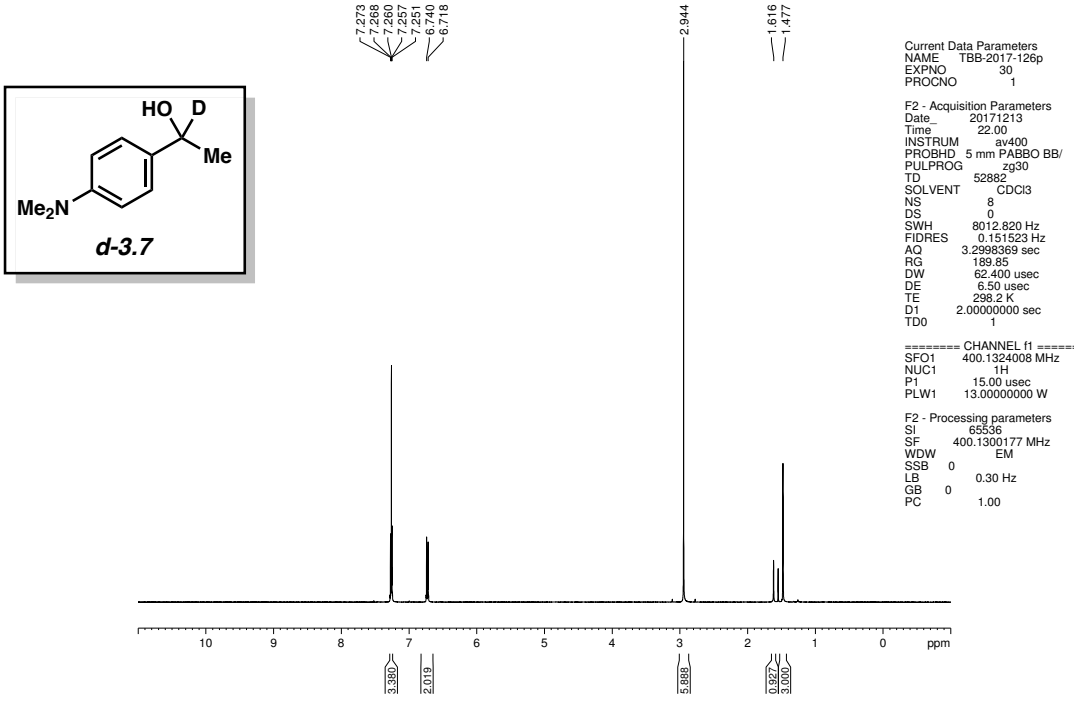

Figure 3.60 ^{1}H NMR (400 MHz, $CDCl_3$) of compound ***d*-3.7**.

3.10 Notes and References

(1) Larock, R. C. *Comprehensive Organic Transformations: A Guide to Functional Group Preparation*; 2nd Ed. John Wiley & Sons: New York, 1997.

(2) For the classic Weinreb amide synthesis of ketones from amides via a tetrahedral intermediate, see: Nahm, S.; Weinreb, S. M. *N*-Methoxy-*N*-methylamides as Effective Acylating Agents *Tetrahedron Lett.* **1981**, *22*, 3815–3818.

(3) For a related synthetic method that allows for the addition of two nucleophiles to substituted ureas, thus affording ketone products, see: Heller, S. T.; Newton, J. N.; Fu, T.; Sarpong, R. One-pot Unsymmetrical Ketone Synthesis Employing a Pyrrole-Bearing Formal Carbonyl Dication Linchpin Reagent. *Angew. Chem., Int. Ed.* **2015**, *54*, 9839–9843.

(4) For representative reviews and publications on the non-decarbonylative transition metal-catalyzed cross-coupling of carboxylic acid derivatives, see: (a) Liebeskind, L. S.; Srogl, J. Thiol Ester−Boronic Acid Coupling. A Mechanistically Unprecedented and General Ketone Synthesis. *J. Am. Chem. Soc.* **2000**, *122*, 45, 11260–11261. (b) Cheng, H.-G.; Chen, H.; Liu, Y.; Qianghui, Z. The Liebeskind–Srogl Cross-Coupling Reaction and its Synthetic Applications. *Asian J. Org. Chem.* **2008**, *7*, 490–508. (c) Johnson, J. B.; Rovis, T. Enantioselective Cross-Coupling of Anhydrides with Organozinc Reagents: The Controlled Formation of Carbon−Carbon Bonds through the Nucleophilic Interception of Metalacycles. *Acc. Chem. Res.* **2008**, *41*, 327–338. (d) Gooßen, L. J.; Rodriguez, N.; Gooßen, K. Carboxylic Acids as Substrates in Homogeneous Catalysis. *Angew. Chem., Int. Ed.* **2008**, *47*, 3100–3120. (e) Albano, G.; Aronica, L. A. Acyl Sonogashira Cross-Coupling: State of the Art and Application to the Synthesis of Heterocyclic Compounds. *Catalysts* **2020**, *10,* 25–61. (f)

Blangetti, M.; Rosso, H.; Prandi, C.; Deagostino, A.; Venturello, P. Suzuki–Miyaura Cross-Coupling in Acylation Reactions, Scope and Recent Developments. *Molecules* **2013**, *18*, 1188–1213. (g) Hirschbeck, V.; Gehrtz, P. H.; Fleischer, I. Metal-Catalyzed Synthesis and Use of Thioesters: Recent Developments. *Chem. Eur. J*. **2018**, *24*, 7092–7107. (h) Ogiwara, Y.; Sakai, N. Acyl Fluorides in Late-Transition-Metal Catalysis. *Angew. Chem., Int. Ed.* **2020**, *59*, 574–594. (i) Gooßen, L. J.; Gooßen, K.; Rodriguez, N.; Blanchot, M.; Linder, C.; Zimmermann, B. New Catalytic Transformations of Carboxylic Acids. *Pure Appl. Chem.* **2008**, *80*, 1725–1733. (j) Meng, G.; Shi, S.; Szostak, M. Cross-Coupling of Amides by N–C Bond Activation. *Synlett* **2016**, *27*, 2530–2540. (k) Liu, C.; Szostak, M. Twisted Amides: From Obscurity to Broadly Useful Transition-Metal-Catalyzed Reactions by N−C Amide Bond Activation. *Chem. Eur. J.* **2017**, *23*, 7157–7173. (l) Dander, J. E.; Garg, N. K. Breaking Amides using Nickel Catalysis. *ACS Catal.* **2017**, *7*, 1413–1423. (m) Takise, R.; Muto, K.; Yamaguchi, J. Cross-Coupling of Aromatic Esters and Amides. *Chem. Soc. Rev.* **2017**, *46*, 5864–5888. (n) Meng, G.; Szostak, M. N-Acyl-Glutarimides: Privileged Scaffolds in Amide N–C Bond Cross-Coupling. *Eur. J. Org. Chem.* **2018**, 2352–2365. (o) Buchspies, J.; Szostak, M. Recent Advances in Acyl Suzuki Cross-Coupling. *Catalysts* **2019**, *9,* 53–75.

(5) Hu, J.; Zhao, Y.; Liu, J.; Zhang, Y.; Shi, Z. Nickel-Catalyzed Decarbonylative Borylation of Amides: Evidence for Acyl C−N Bond Activation. *Angew. Chem., Int. Ed.* **2016**, *55*, 8718–8722.

(6) These cascade reactions could involve either one or two catalytic steps. For discussion on the definitions of cascade and tandem processes, see: (a) Fogg, D. E.; dos Santos, E. N. Tandem

Catalysis: A Taxonomy and Illustrative Review. *Coord. Chem. Rev.* **2004**, *248*, 2365–2379. (b) Hayashi, Y. Pot Economy and One-Pot Synthesis. *Chem. Sci.* **2016**, *7*, 866–880.

(7) For representative examples of one-pot, sequential protocols for the reductive functionalization of amides, see: (a) Meyers, A.; Comins, D. *N*-Methylamino Pyridyl Amides (mapa) II. An Efficient Acylating Agent for Various Nucleophiles and Sequential Addition to Unsymmetrical *tert*-Alcohols. *Tetrahedron Lett.* **1978**, *19*, 5179–5182. (b) Oda, Y.; Sato, T.; Chida, N. Direct Chemoselective Allylation of Inert Amide Carbonyls. *Org. Lett.* **2012**, *14*, 950–953. (c) Zheng, X.; Liu, J.; Ye, C.-X.; Wang, A.; Wang, A.-E.; Huang, P.-Q. SmI_2-Mediated Radical Coupling Strategy to Securinega Alkaloids: Total Synthesis of (−)-14, 15-Dihydrosecurinine and Formal Total Synthesis of (−)-Securinine. *J. Org. Chem.* **2015**, *80*, 1034–1041. (d) Dander, J. E.; Giroud, M.; Racine, S.; Darzi, E. R.; Alvizo, O.; Entwistle, D.; Garg, N. K. Chemoenzymatic Conversion of Amides to Enantioenriched Alcohols in Aqueous Medium. *Commun. Chem.* **2019**, *2*, 82. (e) Ong, D. Y.; Fan, D.; Dixon, D. J.; Chiba, S. Transition-Metal-Free Reductive Functionalization of Tertiary Carboxamides and Lactams for α-Branched Amine Synthesis. *Angew. Chem., Int. Ed.* **2020**, *59*, 11903–11907.

(8) Kaiser, D.; Bauer, A.; Lemmerer, M.; Maulide, N. Amide Activation: An Emerging Tool for Chemoselective Synthesis. *Chem. Soc. Rev.* **2018**, *47*, 7899–7925.

(9) Hie, L.; Fine Nathel, N. F.; Shah, T.; Baker, E. L.; Hong, X.; Yang, Y.-F.; Liu, P.; Houk, K. N.; Garg, N. K. Conversion of Amides to Esters by the Nickel-Catalysed Activation of Amide C–N Bonds. *Nature* **2015**, *524*, 79–83

(10) Pauling, L.; Corey, R. B. Configurations of Polypeptide Chains with Favored Orientations Around Single Bonds: Two New Pleated Sheets. *Proc. Natl. Acad. Sci. USA* **1951**, *37*, 729–740.

(11) Gabriel, P.; Gregory, A. W.; Dixon, D. J. Iridium-Catalyzed Aza-Spirocyclization of Indole-Tethered Amides: An Interrupted Pictet–Spengler Reaction. *Org. Lett.* **2019**, *21*, 6658–6662.

(12) For examples of one-pot, *sequential* reductive functionalizations of tertiary amides, see: (a) Gregory, A. W.; Chambers, A.; Hawkins, A.; Jakubec, P.; Dixon, D. J. Iridium-Catalyzed Reductive Nitro-Mannich Cyclization. *Chem. Eur. J.* **2015**, *21*, 111–114. (b) Tan, P. W.; Seayad, J.; Dixon, D. J. Expeditious and Divergent Total Syntheses of Aspidosperma Alkaloids Exploiting Iridium (I)-Catalyzed Generation of Reactive Enamine Intermediates. *Angew. Chem., Int. Ed.* **2016**, *55*, 13436–13440. (c) Xie, L-G.; Dixon, D. J. Tertiary Amine Synthesis via Reductive Coupling of Amides with Grignard Reagents. *Chem. Sci.* **2017**, *8*, 7492–7497. (d) Fuentes de Arriba, Á. L.; Lenci, E.; Sonawane, M.; Formery, O.; Dixon, D. J. Iridium-Catalyzed Reductive Strecker Reaction for Late-Stage Amide and Lactam Cyanation. *Angew. Chem., Int. Ed.* **2017**, *56*, 3655–3659. (e) Xie, L.-G.; Dixon, D. J. Iridium-Catalyzed Reductive Ugi-Type Reactions of Tertiary Amides. *Nat. Commun.* **2018**, *9*, 2841. (f) Gabriel, P.; Xie, L.-G.; Dixon, D. J. Iridium-Catalyzed Reductive Coupling of Grignard Reagents and Tertiary Amides. *Org. Synth.* **2019**, *96*, 511–527. (g) T. Rogova, P. Gabriel, S. Zavitsanou, J. A. Leitch, F. Duarte, D. J. Dixon. Reverse Polarity Reductive Functionalization of Tertiary Amides via a Dual Iridium-Catalyzed Hydrosilylation and Single Electron Transfer Strategy. *ACS Catal.* **2020**, *10*, 11438–11447. (h) For a review, see: Matheau-Raven, D.; Gabriel, P.; Leitch, J. A.; Almehmadi, Y. A.; Yamazaki, K.; Dixon, D. J. Catalytic

Reductive Functionalization of Tertiary Amides using Vaska's Complex: Synthesis of Complex Tertiary Amine Building Blocks and Natural Products. *ACS Catal.* **2020**, *10*, 8880–8897.

(13) Although definitions for step count vary widely in the literature, here we employ the term "operational step" to indicate the number of reagent additions. Cascade reactions involving a single operational step enjoy certain practical advantages, such as operational simplicity, over complementary cascade reactions requiring multiple reagent additions. Moreover, cascade reactions involving one operational step present additional challenges to the organic chemist including the design of reaction conditions suitable for both transformations.

(14) Wu, X.; Li, X.; Huang, W.; Wang, Y.; Xu, H.; Cai, L.; Qu, J.; Chen, Y. Direct Transformation of Aryl 2-Pyridyl Esters to Secondary Benzylic Alcohols by Nickel Relay Catalysis. *Org. Lett.* **2019**, *21*, 2453–2458.

(15) Bandar, J. S.; Ascic, E.; Buchwald, S. L. Enantioselective CuH-Catalyzed Reductive Coupling of Aryl Alkenes and Activated Carboxylic Acids. *J. Am. Chem. Soc.* **2016**, *138*, 5821–5824.

(16) Zhang, S.; del Pozo, J.; Romiti, F.; Mu, Y.; Torker, S.; Hoveyda, A. Delayed Catalyst Function Enables Direct Enantioselective Conversion of Nitriles to NH_2-Amines. *Science* **2019**, *364*, 45–51.

(17) Further advantages of cascade reactions in regard to efficiency include the avoidance of intermediate purification, improved atom economy, and reduced waste generation. For general reviews on cascade reactions, see: (a) Ref. 6. (b) Tietze, L. F.; Brasche, G.; Gericke, K. *Domino Reactions in Organic Synthesis*, Wiley-VCH, Weinheim, **2006.** (c) Tietze, L. F.;

Beifuss, U. Sequential Transformations in Organic Chemistry: A Synthetic Strategy with a Future. *Angew. Chem., Int. Ed.* **1993**, *32*, 131–163. (d) Tietze, L. F. Domino Reactions in Organic Synthesis. *Chem. Rev.* **1996**, *96*, 115–136. (e) Ho, T.-L. *Tandem Organic Reactions*, Wiley, New York, **1992**. (f) Bunce, R. A. Recent Advances in the Use of Tandem Reactions for Organic Synthesis. *Tetrahedron* **1995**, *51*, 13103–13159. (g) Trost, B. M. The Atom Economy–A Search for Synthetic Efficiency. *Science* **1991**, *254*, 1471–1477. (h) Trost, B. M. Atom Economy—A Challenge for Organic Synthesis: Homogeneous Catalysis Leads the Way. *Angew. Chem., Int. Ed.* **1995**, *34*, 259–281. (i) Nicolaou, K. C.; Edmonds, D. J.; Bulger, P. G. Cascade Reactions in Total Synthesis. *Angew. Chem., Int. Ed.* **2006**, *45*, 7134–7186. (j) Romiti, F.; del Pozo, J.; Paioti, P. H. S.; Gonsales, S. A.; Li, X.; Hartrampf, F. W. W.; Hoveyda, A. Different Strategies for Designing Dual-Catalytic Enantioselective Processes: From Fully Cooperative to Non-Cooperative Systems. *J. Am. Chem. Soc.* **2019**, *141*, 17952–17961. (k) Jones, A.; Stoltz, B. M.; May, J. A.; Sarpong, R. S. Toward a Symphony of Reactivity: Cascades Involving Catalysis and Sigmatropic Rearrangements. *Angew. Chem., Int. Ed.* **2014**, *535*, 2556–2591.

(18) For reviews on nickel catalysis see: (a) Tasker, S. Z.; Standley, E. A.; Jamison, T. F. Recent Advances in Homogeneous Nickel Catalysis. *Nature* **2014**, *509*, 299–309. (b) Rosen, B. M.; Quasdorf, K. W.; Wilson, D. A.; Zhang, N.; Resmerita, A.-M.; Garg, N. K.; Percec, V. Nickel-Catalyzed Cross-Couplings Involving Carbon–Oxygen Bonds. *Chem. Rev.* **2011**, *111*, 1346–1416.

(19) For our laboratory's nickel-catalyzed Suzuki–Miyaura couplings of amides, see: (a) Weires, N. A.; Baker, E. L.; Garg, N. K. Nickel-Catalysed Suzuki–Miyaura Coupling of Amides. *Nat.*

Chem. **2016**, *8*, 75–79. (b) Boit, T. B.; Weires, N. A.; Kim, J.; Garg, N. K. Nickel-Catalyzed Suzuki–Miyaura Coupling of Aliphatic Amides. *ACS Catal.* **2018**, *8*, 1003–1008.

(20) Johnstone, R. A. W.; Wilby, A. H.; Entwistle, I. D. Heterogeneous Catalytic Transfer Hydrogenation and its Relation to Other Methods for Reduction of Organic Compounds. *Chem. Rev*. **1985**, *85*, 129−170.

(21) This catalytic reductive *arylation* protocol complements the known catalytic reductive *alkylation* and reductive *allylation* methods shown in Figure 3.1b.

(22) Despite its air-sensitivity, $Ni(cod)_2$ has been used in more than 800 synthetic methodology studies (see ref 23a). Moreover, it has been used in several process research studies, suggesting its value in manufacturing. For select studies, see: (a) Dawson, D. D.; Jarvo, E. R. Stereospecific Nickel-Catalyzed Cross-Coupling Reactions of Benzylic Ethers with Isotopically-Labeled Grignard Reagents. *Org. Process Res. Dev.* **2015**, *19*, 1356–1359. (b) Liu, J.; Gao, S.; Chen, M. Preparation of Bifunctional Allylboron Reagent and Application to Aldehyde Allylboration. *Org. Process Res. Dev.* **2019**, *23*, 1659–1662.

(23) For the use of $Ni(cod)_2$ on the benchtop, paraffin wax encapsulation has proven to be an effective strategy, including for the Suzuki–Miyaura coupling of aliphatic amides; see: a) Dander, J. E.; Weires, N. A.; Garg, N. K. *Org. Lett*. **2016**, *18*, 3934–3936. (b) Mehta, M. M.; Boit, T. B.; Dander, J. E.; Garg, N. K. Ni-Catalyzed Suzuki–Miyaura Cross-Coupling of Aliphatic Amides on the Benchtop. *Org. Lett.* **2020**, *22*, 1–5.

(24) In our prior studies, we have shown that the Suzuki–Miyaura coupling of aliphatic amides requires high temperatures, presumably to facilitate the transmetalation step.

(25) For seminal publications, see: (a) Meerwein, H.; Schmidt, R. Ein neues Verfahren zur Reduktion von Aldehyden und Ketonen. *Liebigs Ann*. **1925**, *444*, 221−238. (b) Verley, A. The Exchange of Functional Groups Between Two Molecules. The Passage of Ketones to Alcohols and the Reverse. *Bull. Soc. Chim. Fr*. **1925**, *37*, 871−874. (c) Ponndorf, W. Z. Der reversible Austausch der Oxydationsstufen zwischen Aldehyden oder Ketonen einerseits und primären oder sekundären Alkoholen anderseits. *Angew. Chem*. **1926**, *39*, 138−143.

(26) For reviews, see: (a) Cha, J. S. Recent Developments in Meerwein−Ponndorf−Verley and Related Reactions for the Reduction of Organic Functional Groups Using Aluminum, Boron, and Other Metal Reagents: A Review. *Org. Process Res. Dev*. **2006**, *10*, 1032−1053. (b) de Graauw, C. F.; Peters, J. A.; van Bekkum, H.; Huskens, J. Meerwein–Ponndorf–Verley Reductions and Oppenauer Oxidations: An Integrated Approach. *Synthesis* **1994**, 1007−1017. (c) Inch, T. D. Asymmetric Synthesis. *Synthesis* **1970**, 466−473. (d) Nishide, K.; Node, M. Recent Development of Asymmetric Syntheses Based on the Meerwein–Ponndorf–Verley Reduction. *Chirality* **2002**, *14*, 759−767. (e) Ooi, T.; Miura, T.; Itagaki, Y.; Ichikawa, H.; Maruoka, K. Catalytic Meerwein–Ponndorf–Verley (MPV) and Oppenauer (OPP) Reactions: Remarkable Acceleration of the Hydride Transfer by Powerful Bidentate Aluminum Alkoxides. *Synthesis* **2002**, 279−291. (f) Wilds, A. L. *Org. React*. **2011**, *2*, 178−223. (g) Djerassi, C. The Oppenauer Oxidation. *Org. React*. **2011**, *6*, 207−272.

(27) When using *i*-PrOH as the solvent, up to 39% yield of the corresponding ester product was observed by ^{1}H NMR.

(28) Boit, T. B.; Mehta, M. M.; Garg, N. K. Base-Mediated Meerwein–Ponndorf–Verley Reduction of Aromatic and Heterocyclic Ketones. *Org. Lett.* **2019**, *21*, 6447–6451.

(29) We anticipated that the stability of the doubly vinylogous amide byproduct resulting from oxidation of DMPE (**3.7**) would drive the transfer hydrogenation reaction forward.

(30) (a) Verheyen, T.; van Turnhout, L.; Vandavasi, J. K.; Isbrandt, E. S.; De Borggraeve, W. M.; Newman, S. G. Ketone Synthesis by a Nickel-Catalyzed Dehydrogenative Cross-Coupling of Primary Alcohols. *J. Am. Chem. Soc.* **2019**, *141*, 6869–6874. (b) Bera, S.; Bera, A.; Banerjee, D. Nickel-Catalyzed Hydrogen-Borrowing Strategy: Chemo-Selective Alkylation of Nitriles with Alcohols. *Chem. Commun.* **2020**, *56*, 6850–6853. (c) Berini, C.; Brayton, D. F.; Mocka, C.; Navarro, O. Homogeneous, Anaerobic (N-Heterocyclic Carbene)-Pd or -Ni Catalyzed Oxidation of Secondary Alcohols at Mild Temperatures. *Org. Lett.* **2009**, *11*, 4244–4247.

(31) It should be noted that for subsequent evaluation of the scope of the methodology, boronates derived from both pinacol and neopentyl glycol were used. We generally recommend the use of boronates derived from neopentyl glycol. However, the superior commercial availability of boronates derived from pinacol can sometimes be advantageous.

(32) Notably, the reductive arylation of amide **3.1** could be performed on the benchtop by employing either (a) a paraffin wax capsule charged with the precatalyst/ligand combination, $Ni(cod)_2$/Benz-ICy•HCl, or (b) the air-stable Ni(II) precatalyst [(TMEDA)Ni(*o*-tolyl)Cl]. See section 3.8.2.9 for details.

(33) When amides derived from benzoic acids were employed, using a $Ni(cod)_2$ / SIPr catalyst/ligand system and 3-pentanol as the alcohol reductant in toluene at 50 °C for 16 h, the corresponding ester was observed in 85% yield as determined by ^{1}H NMR analysis using hexamethylbenzene as an external standard.

(34) Notably, under our standard Suzuki–Miyaura coupling conditions of the parent amide, epimerization of the stereocenter α to the amide carbonyl is observed affording a mixture of *cis* and *trans* diastereomers (see ref. 19b.)

(35) For transition metal-catalyzed cleavage of the acyl C–O bond of esters, see: (a) Muto, K.; Yamaguchi, J.; Musaev, D. G.; Itami, K. Decarbonylative Organoboron Cross-Coupling of Esters by Nickel Catalysis. *Nat. Commun.* **2015**, *6*, 7508. (b) LaBerge, N. A.; Love, J. A. Nickel-Catalyzed Decarbonylative Coupling of Aryl Esters and Arylboronic Acids. *Eur. J. Org. Chem.* **2015**, 5546–5553. (c) Halima, T. B.; Vandavasi, J. K.; Shkoor, M.; Newman, S. G. A Cross-Coupling Approach to Amide Bond Formation from Esters. *ACS Catal.* **2017**, *7*, 2176–2180. (d) Kruckenberg, A.; Wadepohl, H.; Gade, L. H. Bis(diisopropylphosphinomethyl)amine Nickel(II) and Nickel(0) Complexes: Coordination Chemistry, Reactivity, and Catalytic Decarbonylative C–H Arylation of Benzoxazole. *Organometallics* **2013**, *32*, 5153–5170. (e) Yue, H.; Guo, L.; Liao, H.-H.; Cai, Y.; Zhu, C.; Rueping, M. Catalytic Ester and Amide to Amine Interconversion: Nickel-Catalyzed Decarbonylative Amination of Esters and Amides by C–O and C–C Bond Activation. *Angew. Chem., Int. Ed.* **2017**, *56*, 4282–4285. (f) Yu, H.; Guo, L.; Lee, S.-C.; Liu, X.; Rueping, M. Selective Reductive Removal of Ester and Amide Groups from Arenes and Heteroarenes through Nickel-Catalyzed C–O and C–N Bond Activation. *Angew. Chem., Int. Ed.* **2017,** *56*, 3972–3976. (g) Halima, T. B.; Zhang, W.; Yalaoui, I.; Hong, X.; Yang, Y.; Houk, K. N.; Newman, S. G. Palladium-Catalyzed Suzuki–Miyaura Coupling of Aryl Esters. *J. Am. Chem. Soc.* **2017**, *139*, 1311–1318. (h) Halima, T. B.; Masson-Makdissi, J.; Newman, S. G. Nickel-Catalyzed Amide Bond Formation from Methyl Esters. *Angew. Chem., Int. Ed.* **2018**, *57*,

12925–12929. (i) Zheng, Y.-L.; Newman, S. G. Methyl Esters as Cross-Coupling Electrophiles: Direct Synthesis of Amide Bonds. *ACS Catal.* **2019**, *9*, 4426–4433. (j) Zheng, Y.-L.; Newman, S. G. Nickel-Catalyzed Domino Heck-Type Reactions Using Methyl Esters as Cross-Coupling Electrophiles. *Angew. Chem., Int. Ed.* **2019**, *58*, 18159–18164.

(36) Vitaku, E.; Smith, D. T.; Njardarson, J. T. Analysis of the Structural Diversity, Substitution Patterns, and Frequency of Nitrogen Heterocycles Among US FDA Approved Pharmaceuticals: Miniperspective. *J. Med. Chem.* **2014**, *57*, 10257–10274.

(37) Collins, K. D.; Glorius, F. A Robustness Screen for the Rapid Assessment of Chemical Reactions. *Nat. Chem.* **2013**, *5*, 597–601.

(38) The robustness screen was carried out using amide **3.21** and boronate **3.6**, with one equivalent of additive. Additives **3.22**–**3.27** were recovered in near quantitative yields and did not significantly hinder the reductive arylation reaction. See section 3.8.2.8 for details.

(39) The amide coupling partner was varied in order to simplify isolation of purified products.

(40) For nickel-catalyzed cleavage of the aryl C–O bond of aryl ethers, see: (a) Wenkert, E.; Michelotti, E. L.; Swindell, C. S. Nickel-Induced Conversion of Carbon–Oxygen into Carbon–Carbon Bonds. One-Step Transformations of Enol Ethers into Olefins and Aryl Ethers into Biaryls. *J. Am. Chem. Soc*. **1979**, *101*, 2246–2247. (b) Wenkert, E.; Michelotti, E. L.; Swindell, C. S.; Tingoli, M. Transformation of Carbon-Oxygen into Carbon-Carbon Bonds Mediated by Low-Valent Nickel Species. *J. Org. Chem.* **1984**, *49*, 4894–4899. (c) Dankwardt, J. W. Nickel-Catalyzed Cross-Coupling of Aryl Grignard Reagents with Aromatic Alkyl Ethers: An Efficient Synthesis of Unsymmetrical Biaryls. *Angew. Chem., Int. Ed.* **2004**, *43*, 2428–2432. (d) Guan, B.-T.; Xiang, S.-K.; Wu, T.; Sun, Z.-P.; Wang, B.-Q.;

Zhao, K.-Q.; Shi, Z.-J. Methylation of Arenes via Ni-Catalyzed Aryl C–O/F Activation. *Chem. Commun.* **2008**, 1437–1439. (e) Tobisu, M.; Shimasaki, T.; Chatani, N. Nickel-Catalyzed Cross-Coupling of Aryl Methyl Ethers with Aryl Boronic Esters. *Angew. Chem., Int. Ed.* **2008**, *47*, 4866–4869. (f) Sergeev, A. G.; Hartwig, J. F. Selective, Nickel-Catalyzed Hydrogenolysis of Aryl Ethers. *Science* **2011**, *322*, 439–443.

(41) For the nickel-catalyzed cleavage of the aryl C–N bond of dimethylanilines, see: Cao, Z.-C.; Xie, S.-J.; Fang, H.; Shi, Z.-J. Ni-Catalyzed Cross-Coupling of Dimethyl Aryl Amines with Arylboronic Esters Under Reductive Conditions. *J. Am. Chem. Soc*. **2018**, *140*, 13575−13579.

(42) When boronates bearing para electron-donating groups were employed, a significant amount of the ketone intermediate was observed. For example, the coupling of amide **3.1** with p-NMe_2Ph–B(pin) under our standard reaction conditions gave the corresponding ketone and alcohol in 17% and 42% yields, respectively.

(43) Rombouts, F. J. R.; Trabanco-Suárez, A. A.; Gijsen, H. J. M.; Macdonald, G. J.; Bischoff, F. P.; Alonso-de Diego, S.-A.; Velter, A. I.; Van Roosbroeck, Y. E. M. Substituted 3,4-Dihydro-2H-pyrido[1,2-a]pyrazine-1,6-dione Derivatives Useful for the Treatment of (Inter Alia) Alzheimer's Disease. (Janssen Pharmaceuticals, Inc.), WO2013171712A1, **2013**.

(44) Zhao, S.; Guo, Y.; Han, E.-J.; Luo, J.; Liu, H.-M.; Liu, C.; Xie, W.; Zhang, W.; Wang, M. Copper (II)-Catalyzed Trifluoromethylation of Iodoarenes Using Chen's Reagent. *Org. Chem. Front.* **2018**, *5,* 1143–1147.

(45) An exciting opportunity lies in catalytic asymmetric variants of our strategy. In an encouraging preliminary result, we have found that the use of a chiral NHC ligand allows for the synthesis of **3.4** in 36% yield and 20% ee. See sections 3.8.2.10 and 3.8.2.11 for details.

(46) Boit, T. B.; Mehta, M. M.; Garg, N. K. Base-Mediated Meerwein–Ponndorf–Verley Reduction of Aromatic and Heteroaromatic Ketones. *Org. Lett.* **2019**, *21*, 6447–6451.

(47) Fier, P. S.; Luo, J.; Hartwig, J. F. Copper-mediated fluorination of arylboronate esters. Identification of a copper(III) fluoride complex. *J. Am. Chem. Soc.* **2013***, 135,* 2552–2559

(48) Shields, J. D.; Gray, E. E.; Doyle, A. G. A modular air-stable nickel precatalyst. *Org. Lett.* **2020**, *17*, 2166–2169.

(49) He, W.; Zhao, W.; Zhou, B.; Liu, H.; Li, X.; Li, L.; Li, J.; Shi, J. Synthesis of C_2-symmetric benzimidazolium salts and their application in palladium-catalyzed enantioselective intramolecular α-arylation of amides. *Molecules* **2016**, *21*, 742–748.

(50) Hie, L.; Baker, E. L.; Anthony, S. M.; Desrosiers, J. -N.; Senanayake, C.; Garg, N. K. Nickel-catalyzed esterification of aliphatic amides. *Angew. Chem., Int. Ed.* **2016**, *65*, 15129–15132.

(51) Boit, T. B.; Weires, N. A.; Kim, J.; Garg, N. K. Nickel-catalyzed Suzuki–Miyaura coupling of aliphatic amides. *ACS Catal.* **2018**, *8*, 1003–1008.

(52) Dander, J. E.; Baker, E. L.; Garg, N. K. Nickel-catalyzed transamidation of aliphatic amide derivatives. *Chem. Sci.* **2017**, *8*, 6433–6438.

(53) Lamani, M.; Ravikumara, G. S.; Prabhu, K. R. Iron(III) chloride-catalysed aerobic reduction of olefins using aqueous hydrazine at ambient temperature. *Adv. Synth. Catal*. **2012**, *354*, 1437–1442.

(54) Genc, S.; Arslan, B.; Gulcemal, S.; Gunnaz, S.; Cetinkaya, B.; Gulcemal, D. Iridium(I)-catalyzed C–C and C–N bond forming reactions via the borrowing hydrogen strategy. *J. Org. Chem.* **2019**, *84*, 6286–6297.

(55) Rahaim, R. J.; Maleczka, R. E. C–O hydrogenolysis catalyzed by Pd-PMHS nanoparticles in the company of chloroarenes. *Org. Lett*. **2011**, *13*, 584–587.

(56) Kabalka, G. W.; Wu, Z.; Ju, W. Alkylation of aromatic aldehydes with alkylboron chloride derivatives. *Tetrahedron* **2001**, *57*, 1663–1670.

(57) Gaykar, R. N.; Bhunia, A.; Biju, A. T. Employing arynes for the generation of aryl anion equivalents and subsequent reaction with aldehydes. *J. Org. Chem*. **2018**, *83*, 11333–11340.

(58) Orjales, A.; Mosquera, R.; Toledo, A.; Pumar, M. C.; Garcia, N.; Cortizo, L.; Labeaga, L.; Innerarity, A. Syntheses and binding studies of new [(aryl)(aryloxy)methyl]piperidine derivatives and related compounds as potential antidepressant drugs with high affinity for serotonin (5-HT) and norepinephrine (NE) transporters. *J. Med. Chem*. **2003**, *46*, 5512–5532.

(59) Van Orden, L. J.; Van Dyke, P. M.; Saito, D. R.; Church, T. J.; Chang, R.; Smith, J. A. M.; Martin, W. J.; Jaw–Tsai, S.; Strangeland, E. L. A novel class of 3-(phenoxy-phenyl-methyl)-pyrrolidines as potent and balanced norepinephrine and serotonin reuptake inhibitors: synthesis and structure-activity relationships. *Bioorg & Med Chem. Lett.* **2013**, *23*, 1456–1461.

(60) Jakobsson, J. E.; Gronnevik, G.; Riss, P. J. Organocatalyst-assisted Ar–^{18}F bond formation: a universal procedure for direct aromatic radiofluorination. *Chem. Commun.* **2017**, *53*, 12906–12909.

(61) Perner, R. J.; Gu, Y.-G.; Lee, C.-H.; Bayburt, E. K.; McKie, J.; Alexander, K. M.; Kohlhaas, K. L.; Wismer, C. T.; Mikusa, J.; Jarvis, M. F.; Kowaluk, E. A.; Bhagwat, S. S. 5,6,7-Trisubstituted 4-Aminopyrido[2,3-*d*]pyrimidines as novel inhibitors of adenosine kinase. *J. Med. Chem*. **2003**, *46*, 5249–5257.

(62) Mehta, M. M.; Boit, T. B.; Dander, J. E.; Garg, N. K. Ni-catalyzed Suzuki–Miyaura cross-coupling of aliphatic amides on the benchtop. *Org. Lett.* **2020**, *22*, 1–5.

CHAPTER FOUR

Cyclic Allene Approach to the Manzamine Alkaloid Keramaphidin B

Milauni M. Mehta, Jordan A. M. Gonzalez, James L. Bachman, and Neil K. Garg.

Manuscript submitted.

4.1 Abstract

Strained cyclic allenes are valuable synthetic building blocks for the assembly of complex scaffolds. In contrast to their close relatives, arynes and cyclic alkynes, cyclic allenes have seen sparse use in the context of total synthesis. We report an approach to access the core of the manzamine alkaloid keramaphidin B that relies on the strain-promoted Diels–Alder cycloaddition of an azacyclic allene with a pyrone trapping partner. We show that the cycloaddition is tolerant of nitrile and primary amide functional groups and can be dovetailed with a subsequent retro-Diels–Alder step to access advanced intermediates. These studies demonstrate that strained cyclic allenes can be used to build significant structural complexity and should encourage further exploration of these fleeting intermediates in complex molecule synthesis.

4.2 Introduction

Manzamine alkaloids serve as attractive synthetic targets due to their impressive structural complexity. Some members of this class of natural products display important biological activities, including but not limited to anti-cancer, anti-bacterial, and anti-inflammatory properties.[1,2,3] The present study pertains to the manzamine alkaloid keramaphidin B (**4.1**, Figure 4.1), which was first isolated in 1994 as a racemate and features a pentacyclic framework with an azadecalin core.[4,5] The eastern portion of the azadecalin core bears a [2.2.2]-bridged bicycle containing four

stereogenic centers, one of which is quaternary (C8a). Additionally, the natural product possesses 11- and 13-membered macrocyclic rings. Two prior syntheses of keramaphidin B (**4.1**) have been achieved: Baldwin's biomimetic synthesis of (±)-**4.1** in 1998[6,7,8] and Fürstner's synthesis of (+)-**4.1** via an intermolecular Michael/Michael addition cascade to generate the central core in 2021.[9]

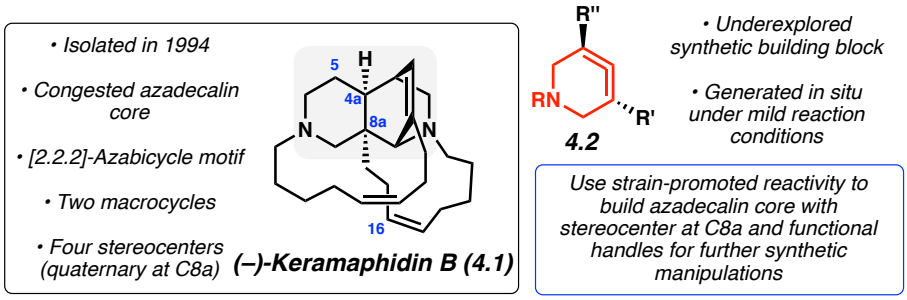

Figure 4.1. (–)-Keramaphidin B (**4.1**), a complex manzamine alkaloid, and azacyclic allenes **4.2**, an underutilized synthetic building block.

We viewed keramaphidin B (**4.1**) as a suitable target to probe the scope and limitations of strained cyclic allene methodology in a complex setting. Specifically, we questioned if azacyclic allenes (**4.2**) could be used to assemble the azadecalin core and generate the C8a quaternary stereocenter of keramaphidin B (**4.1**, Figure 4.1). The use of strained cyclic allenes in the context of total synthesis has remained underexplored, especially in comparison to related aryne chemistry, which has been used in >100 total syntheses to date.[10,11,12] Encouraged by our group's recent success in using an azacyclic allene (**4.2**) in the total synthesis of (–)-lissodendoric acid A,[13] we sought to further expand cyclic allene chemistry by utilizing these fleeting intermediates to build the highly complex bridged azadecalin core of keramaphidin B (**4.1**).

Strained cyclic allenes provide new tools for the rapid generation of highly complex, sp^3-rich scaffolds under mild reaction conditions. Although they were experimentally discovered over 50 years ago,[14,15,16,17] they have recently emerged as valuable synthetic building blocks.[13,18,19,20,21,22,23,24,25,26,27,28,29,30,31,32,33,34,35,36,37,38,39,40,41] Most relevant to the studies described herein, it has been demonstrated that azacyclic allenes (**4.2**) serve as competent dienophiles in

strain-promoted Diels–Alder cycloadditions due to their appreciable strain energy of ~27 kcal/mol.[37] Generally, studies have focused on the use of electron-rich dienes, but in the context of our total synthesis studies,[13] we found that regioselectivity of the cycloaddition with respect to the olefins of the cyclic allene can be modulated by using relatively electron-deficient pyrones. This approach has also proven useful in assembling the azadecalin core of keramaphidin B (**4.1**) in the presence of potentially reactive functional groups, as we describe in this report.

4.3 Retrosynthetic Analysis

Figure 4.2 shows our retrosynthetic analysis of keramaphidin B (**4.1**). The natural product **4.1** was expected to arise from [2.2.2]-azabicycle **4.3** through late-stage functional group manipulations and installation of the 13-membered macrocycle. Next, we envisioned the assembly of [2.2.2]-azabicycle **4.3** via a series of cycloaddition processes. [2.2.2]-Azabicycle **4.3** would be accessed from intermediate **4.4**, which would be generated in situ from precursor **4.5**, via an intramolecular iminium or *N*-acyl iminium Diels–Alder (ImDA) cycloaddition.[42,43,44] In turn, intermediate **4.5** would arise from cycloadduct **4.6** via a retro-Diels–Alder reaction that proceeds with loss of carbon dioxide. Lastly, cycloadduct **4.6** would be accessed from strained cyclic allene **4.7** and pyrone **4.8** via the key strain-promoted Diels–Alder cycloaddition. This step would simultaneously introduce a quaternary center and construct the azadecalin core of the natural product. As will be discussed herein, several variations of this overall strategy were considered,[45] including the tether length (n) for the ImDA step, the oxidation state for the ImDA precursor (i.e., iminium vs *N*-acyl iminium),[46] and whether cycloadduct **4.6** was isolated in the Diels–Alder/retro-Diels–Alder sequence.

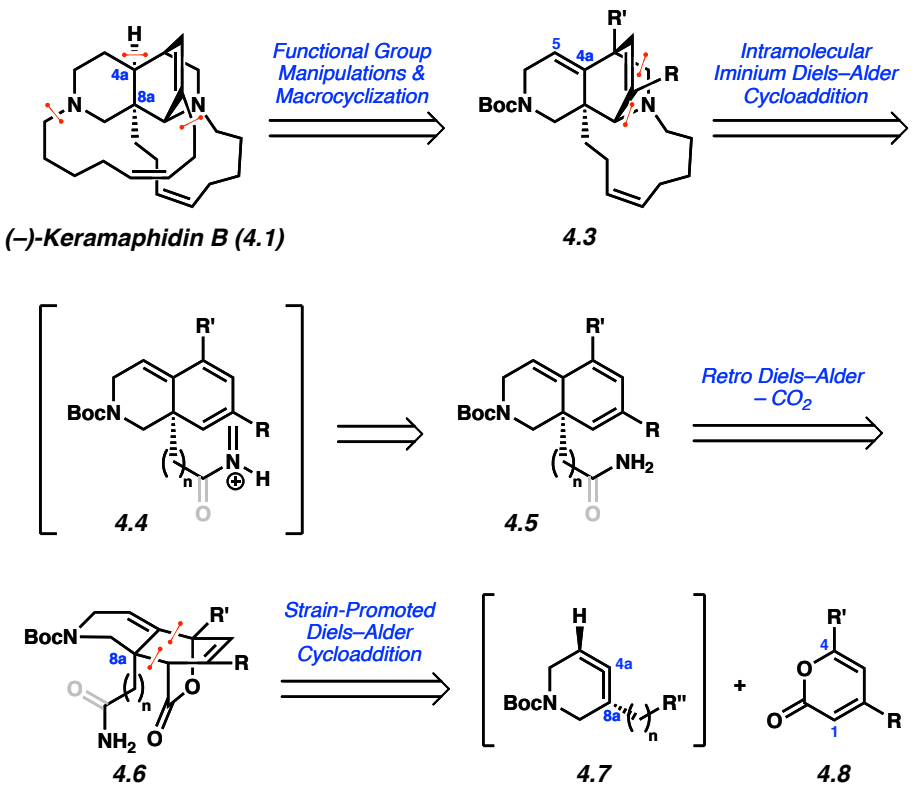

Figure 4.2. Retrosynthetic analysis of (–)-keramaphidin B (**4.1**).

4.4 Model System Studies

We first attempted to prepare a cycloadduct of type **4.6** with a pendant primary amine (see Figure 4.2; n = 7), as this could plausibly allow for direct assembly of the core of keramaphidin B (**4.1**) and install all the carbons necessary for the 11-membered macrocycle (Figure 4.3). The model system[47] shown is proposed to provide valuable insight into the fundamental reactivity of the strained cyclic allene for constructing the bicyclic core of the natural product. The necessary silyl triflate **4.11** was derived from known silyl ketone **4.9**[13] using a scalable three-step cross-metathesis, hydrogenation, and triflation sequence. This route, which mimics a general strategy developed by our laboratory for prior studies, gave access to **4.11** in 26% yield over 3 steps. To evaluate the key step, **4.11** was subjected to pyrone **4.12** in the presence of CsF at 23 °C. Notably, pyrone **4.12** was chosen as the trapping partner for this cycloaddition as it has been demonstrated to be a competent diene for the strain-promoted Diels–Alder cycloaddition with azacyclic

allenes.[13] We were delighted to obtain cycloadduct **4.14** in 56% yield. Of note, this key steps forms two new C–C bonds and sets three new stereocenters, including a quaternary carbon at C8a, which highlights the utility of cyclic allene methodology to generate structural complexity in a single synthetic step.

The strain-promoted Diels–Alder cycloaddition of the cyclic allene proceeds with high regio- and diastereoselectivity, presumably via an approach shown in transition structure **4.13** (Figure 4.3). With regard to regioselectivity,[48] cycloaddition could occur at either olefin of the cyclic allene; however, the more substituted, relatively electron-rich olefin preferentially undergoes the reaction with the relatively electron-deficient pyrone, presumably via an inverse electron demand Diels–Alder cycloaddition.[13] Considering the diastereoselectivity, the pyrone is thought to approach the allene in an *endo* fashion, with favorable orbital overlap between the diene and the non-reactive olefin of the cyclic allene.[34] In this case, these stereoelectronic factors led to the formation of **4.14** with excellent regio- and diastereoselectivity.

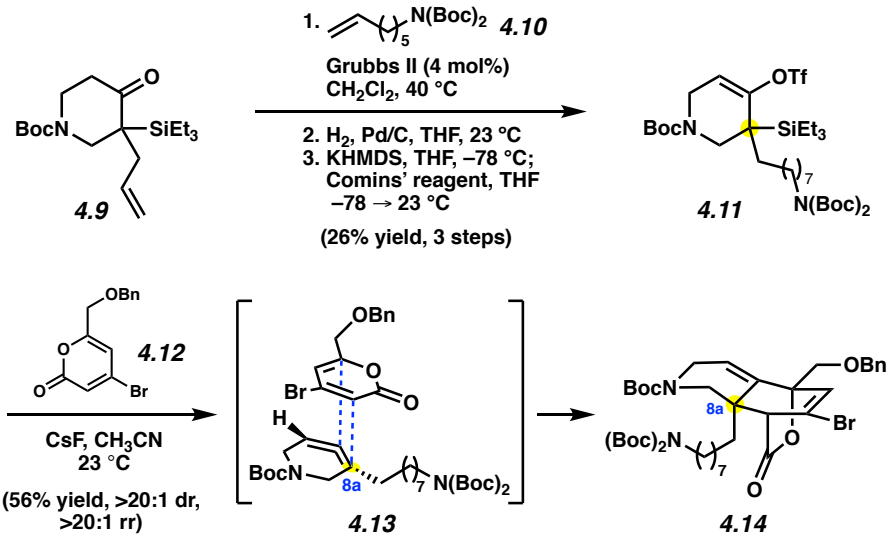

Figure 4.3. Model system for assembly of azadecalin scaffold (**4.14**).

With cycloadduct **4.14** in hand, we aimed to construct the desired [2.2.2]-azabicycle via an ImDA reaction (Figure 4.4). We first sought to reduce the C4a–C5 alkene in the piperidinyl ring

to install the requisite stereochemistry at C4a.[49] This was achieved by subjecting cycloadduct **4.14** to allylic oxidation conditions, followed by a diastereoselective 1,4-reduction using modified Stryker's reagent.[13] Product **4.15** was obtained in 48% yield over two steps with >20:1 dr. Next, heating **4.15** to 80 °C in acetonitrile facilitated a retro-Diels–Alder reaction. Treatment of the product with TFA led to removal of the Boc protecting groups, thus affording the desired substrate **4.16**. Considerable effort was put forth to enable the desired intramolecular ImDA[50] and generate the [2.2.2]-azabicyclic core. Although the formation of the iminium intermediate was validated,[51] exhaustive attempts to access the desired product **4.17** were not successful. We hypothesize that there is a significant entropic penalty to achieve the necessary reactive conformation for the ImDA reaction, resulting from the lengthy tether.[52] Consequently, we opted to pursue a modified substrate, bearing a shorter and more geometrically constrained tether.

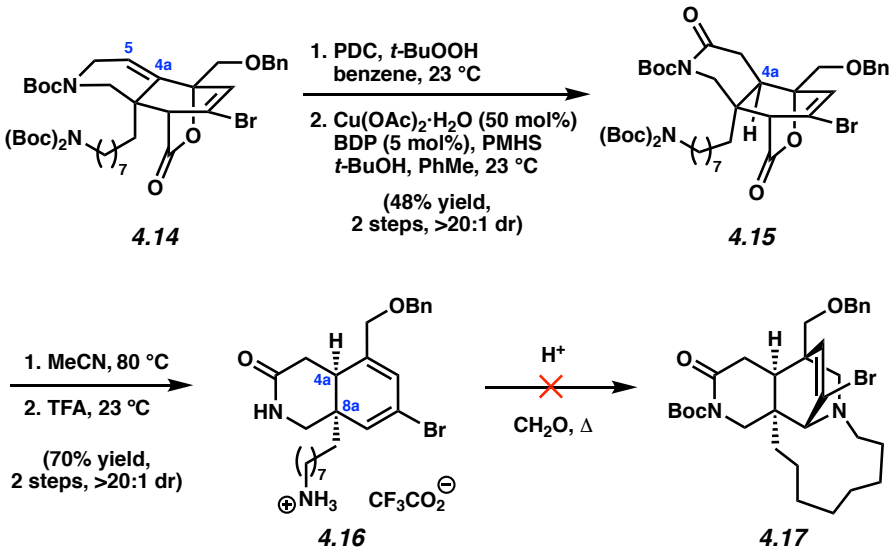

Figure 4.4. Synthesis of ImDA precursor **4.16** and evaluation of intramolecular ImDA reaction.

4.5 Revised Strategy and Experimental Results

Our revised approach to synthesize the [2.2.2]-azabicycle is shown in Figure 4.5. We envisioned accessing cyclic allenes **4.18**, which bear a shorter tether with either pendant nitrile or primary amide functional groups for the introduction of *N*-substituents. Trapping with pyrone **4.8**

and a subsequent retro-Diels–Alder reaction would furnish cycloadducts **4.19**. If the primary amide and nitrile functional groups are tolerated in this transformation, this step would expand upon known azacyclic allene cycloaddition chemistry. Subsequently, the s-cis diene present in **4.19** could engage in the intramolecular *N*-acyl ImDA or ImDA cycloaddition,[46] depending on the oxidation state at C16, to furnish **4.20**. Cleavage of the C16–N bond[53] could enable introduction of the 11-membered macrocycle.

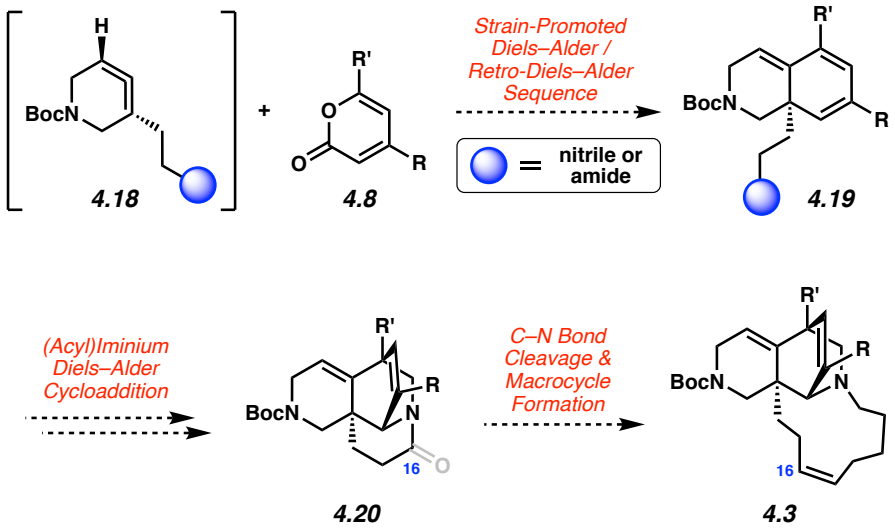

Figure 4.5. Revised strategy to construct the [2.2.2]-azabicycle.

The requisite cyclic allene precursors were synthesized as shown in Figure 4.6. Silyl triflate **4.21**, accessible in one step from ketone **4.9** (see Section 4.7 for details), was elaborated to nitrile-containing silyl triflate **4.22a** through a hydroboration/oxidation, oxidation, and nitrile formation sequence.[54] To access the other desired silyl triflate, nitrile **4.22a** was treated with the Ghaffar–Parkins catalyst to furnish primary amide **4.22b** in 84% yield.[55] It is notable that the silyl triflate motif withstands the various reaction conditions shown in Figure 4.6, thus demonstrating its utility in multistep synthesis.

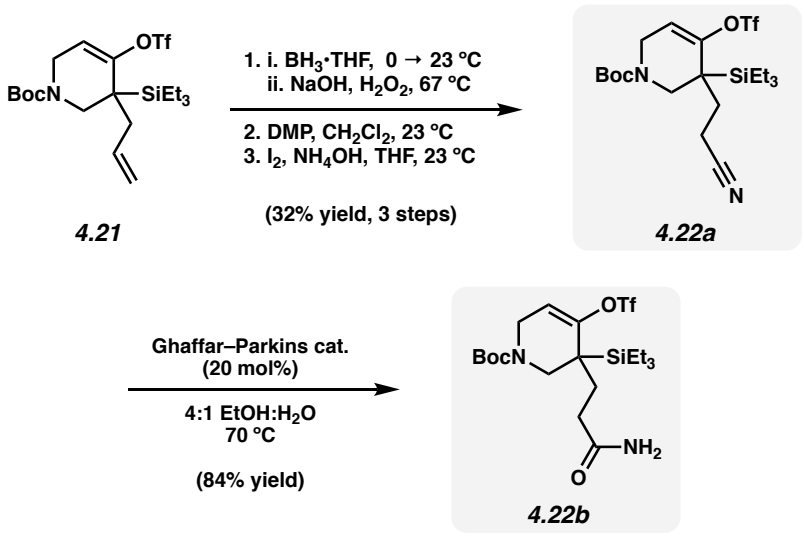

Figure 4.6. Synthesis of cyclic allene precursors **4.22a** and **4.22b**.

With silyl triflates **4.22a** and **4.22b** in hand, we evaluated each compound in a strain-promoted Diels–Alder cycloaddition/retro-Diels–Alder cascade (Figure 4.7). Each substrate was independently subjected to pyrone **4.12** and CsF in acetonitrile. At ambient temperatures, as described previously, cyclic allene generation and Diels–Alder trapping occurred leading to the formation of two new C–C bonds and installation of the C8a quaternary carbon. By directly heating the reactions to 80 °C, the subsequent CO_2 extrusion was achieved in one pot to generate trienes **4.23a** and **4.23b** in 51% and 27% yield,[56] respectively. The presumed mechanism is depicted for the reaction of amide **4.22b** (**4.22b→4.25→4.26→4.23b**), with regio- and diastereoselectivity in the key cyclic allene trapping step paralleling observations described earlier (see Figure 4.3). Despite the low yield of **4.23b**, it is notable that the primary amide functional group is tolerated in this complexity-generating step given the known electrophilicity of strained cyclic allenes.[57] Although extensive efforts to access **4.24** using ImDA and *N*-acyl ImDA approaches were ultimately curtailed due to the exploration of an alternative approach, our current results underscore the synthetic utility of strained cyclic allene intermediates for the generation of complex scaffolds in the context of a total synthesis study.

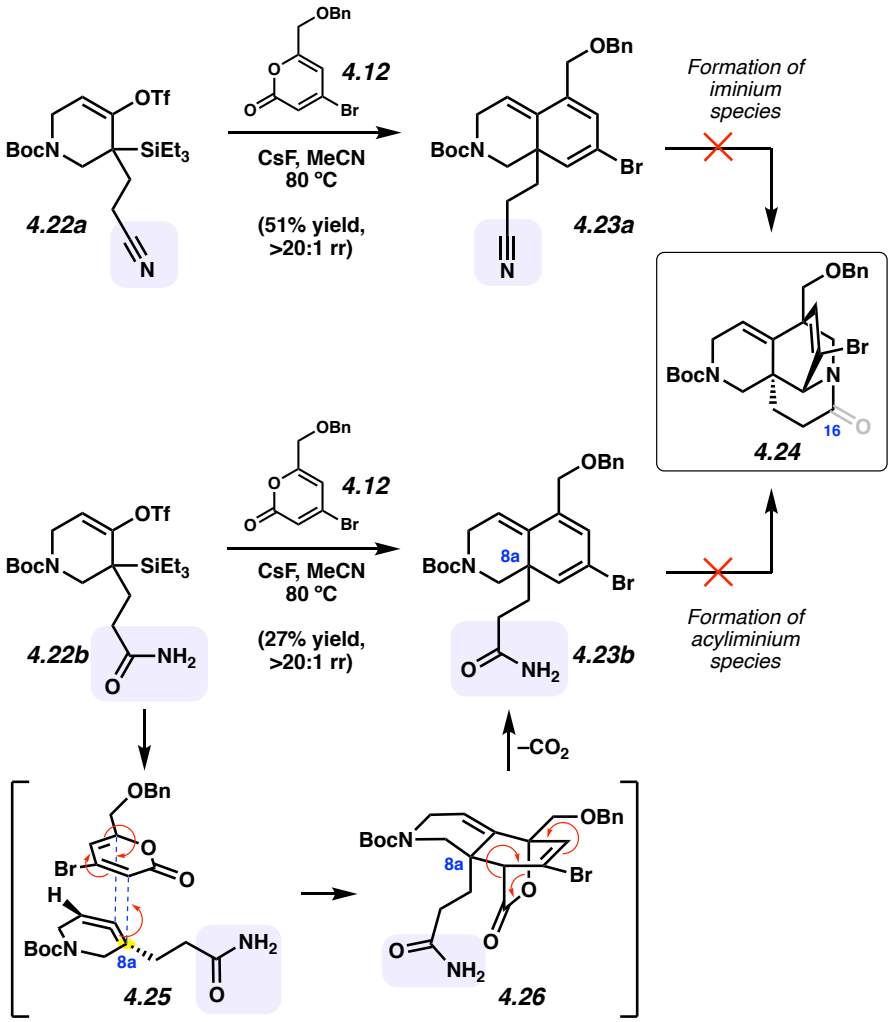

Figure 4.7. One-pot cycloaddition and CO_2 extrusion to generate trienes **4.23a** and **4.23b**.

4.6 Conclusion

Strained cyclic allenes have seen sparse use in total synthesis, especially in comparison to their close relatives, arynes and cyclic alkynes. In this study, we have validated that these relatively understudied fleeting intermediates can be used to generate significant structural complexity in the context of a synthetic approach to the manzamine alkaloid keramaphidin B (**4.1**). Our key step involves the regio- and diastereoselective trapping of a strained azacyclic allene with a pyrone, leading to the formation of two new C–C bonds and three stereocenters, including a quaternary carbon center. Moreover, we showed that the nitrile and primary amide moieties are tolerated in the context of a cascade variant of this key step, wherein a subsequent retro-Diels–Alder reaction

with loss of CO_2 takes place directly. These efforts should inform future synthetic design plans, including our ongoing efforts to assemble the bridged azadecalin core of keramaphidin B (**4.1**). Furthermore, we expect these studies will help fuel the exploration of strained azacyclic allenes for the assembly of complex structural architectures.

4.7 Experimental Section

4.7.1 Materials and Methods.

Unless stated otherwise, reactions were conducted in flame-dried glassware under an atmosphere of nitrogen using anhydrous solvents (either freshly distilled or passed through activated alumina columns). All commercially obtained reagents were used as received unless otherwise specified. Non-commercially available substrates were synthesized according to known preparations or following protocols specified in the Experimental Procedures. Dimethylformamide (DMF), tetrahydrofuran (THF), dichloromethane, benzene, methanol (MeOH), toluene (PhMe), and acetonitrile (MeCN) were passed through an activated alumina column prior to use. Cesium carbonate, Grubbs' 2nd generation catalyst, Brockman Grade activated basic alumina (60 mesh powder), potassium bis(trimethylsilyl)amide (KHMDS), pyridinium dichromate (PDC), *tert*-butyl hydroperoxide (*t*-BuOOH) 70 wt% in H_2O, 1,2-bis(diphenylphosphino)benzene (BDP), trifluoroacetic acid (TFA), borane-tetrahydrofuran complex 1M in THF, sodium hydroxide (NaOH), and ammonium hydroxide (NH_4OH) were obtained from Sigma-Aldrich. *tert*-Butanol (*t*-BuOH), H_2O_2 30 wt% in H_2O, and Dess–Martin periodinane (DMP) were purchased from Fischer Scientific. Ghaffar–Parkins catalyst, cesium fluoride (CsF), and Pd/C were purchased from Strem Chemicals. Iodine and poly(methylhydrosiloxane) (PMHS) were purchased from Alfa Aesar. Copper(II) acetate monohydrate ($Cu(OAc)_2•H_2O$) was purchased from TCI chemicals. *N*-(5-chloro-2-pyridyl)bis(trifluoromethanesulfonimide) (Comins' Reagent) was purchased from Combi-Blocks. Di-*tert*-butyl iminodicarbonate ($NH(Boc)_2$) was purchased from Ambeed. PMHS and *t*-BuOH were sparged with N_2 prior to use. Reaction temperatures at or above 23 °C were controlled using an IKAmag temperature modulator. Thin-layer chromatography (TLC) was conducted with EMD gel 60 F_{254} pre-coated plates (0.25 mm for analytical chromatography and

0.50 mm for preparative chromatography) and visualized using a combination of UV light, anisaldehyde and potassium permanganate staining. Silicycle Siliaflash P60 (particle size 0.040–0.063 mm) was used for flash column chromatography. ^{1}H NMR spectra were recorded on Bruker spectrometers (at 400, 500, and 600 MHz) and are reported relative to the residual solvent signal. Data for ^{1}H NMR spectra are reported as follows: chemical shift (δ ppm), multiplicity, coupling constant (Hz) and integration. ^{13}C NMR spectra were recorded on Bruker spectrometers (at 100, 125, and 150 MHz) and are reported relative to the residual solvent signal. Data for ^{13}C-NMR spectra are reported in terms of chemical shift (δ ppm) and, when necessary, multiplicity and coupling constant (Hz). ^{19}F NMR spectra were recorded on Bruker spectrometers (at 376 MHz) and reported in terms of chemical shift (δ ppm). IR spectra were obtained on a Perkin-Elmer UATR Two FT-IR spectrometer and are reported in terms of frequency of absorption (cm^{-1}). DART-MS spectra were collected on a Thermo Exactive Plus MSD (Thermo Scientific) equipped with an ID-CUBE ion source, a Vapur Interface (IonSense Inc.), and an Orbitrap mass analyzer. Both the source and MSD were controlled by Excalibur software v. 3.0. The analyte was spotted onto OpenSpot sampling cards (IonSense Inc.) using $CDCl_3$ or CH_2Cl_2 as the solvent. Ionization was accomplished using UHP He (Airgas Inc.) plasma with no additional ionization agents. The mass calibration was carried out using Pierce LTQ Velos ESI (+) and (–) Ion calibration solutions (Thermo Fisher Scientific).

Note: Supporting information for the syntheses of silyl ketone **4.9** and pyrone **4.12** have been published and spectral data match those previously reported.[13]

4.7.2 Experimental Procedures

4.7.2.1 Synthesis of Compound 4.16

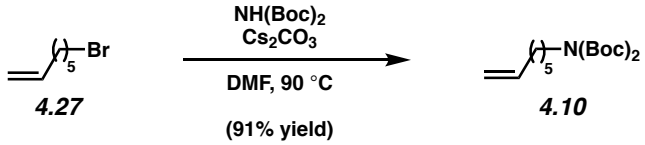

Alkene 4.10: To a solution of bromide **4.27** (4.00 g, 22.6 mmol, 1.00 equiv) in DMF (75.3 mL, 0.30 M) was added di-*tert*-butyl iminodicarbonate (5.40 g, 24.8 mmol, 1.10 equiv) and cesium carbonate (8.10 g, 24.8 mmol, 1.10 equiv). The reaction mixture was heated to 90 °C for 15 h. After this time, the mixture was allowed to cool to 23 ºC, transferred to a separatory funnel, and diluted with water (100 mL) and CH_2Cl_2 (50 mL). The layers were separated and the aqueous layer was extracted with CH_2Cl_2 (3 x 100 mL). The combined organic layers were washed with water (3 x 100 mL), washed with brine (2 x 100 mL), dried over Na_2SO_4, filtered, and concentrated under reduced pressure. The crude residue was purified via flash chromatography (100% hexanes → 9:1 hexanes:EtOAc) to afford alkene **4.10** (6.47 g, 91% yield) as a colorless oil. Alkene **4.10**: R_f 0.45 (9:1 hexanes:EtOAc); ^{1}H NMR (500 MHz, $CDCl_3$): δ 5.79 (ddt, J = 17.3, 9.8, 6.6, 1H), 4.98 (d, J = 16.9, 1H), 4.93 (d, J = 10.2, 1H), 3.54 (t, J = 7.6, 2H), 2.04 (q, J = 7.0, 2H), 1.56 (t, J = 7.5, 2H), 1.50 (s, 18H), 1.44–1.35 (m, 2H), 1.34–1.23 (m, 2H); ^{13}C NMR (100 MHz, $CDCl_3$): δ 152.8, 138.9, 114.5, 82.0, 46.5, 33.8, 29.0, 28.6, 28.2, 26.4; IR (film): 2979, 2932, 1746, 1717, 1695 cm^{-1}; HRMS-APCI (m/z) $[M + H]^+$ calcd for $C_{17}H_{32}NO_4^+$, 314.2326; found 314.2325.

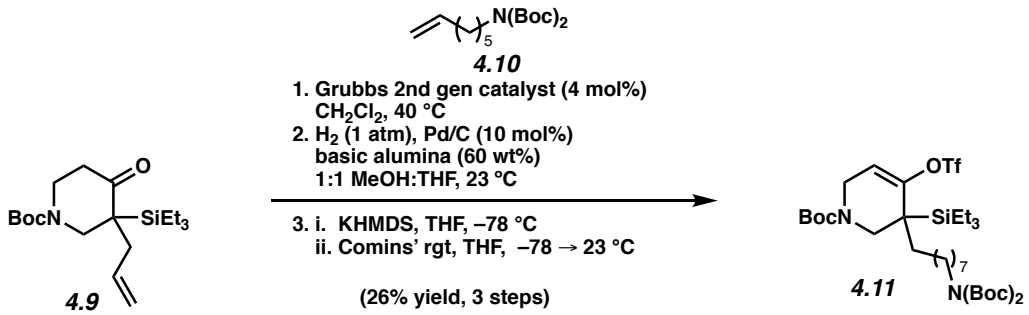

Silyl triflate 4.11: To a flask in the glovebox was added Grubbs' 2nd generation catalyst (96.0 mg, 113 μmol, 4.00 mol%). The flask was then removed from the glovebox and silyl ketone **4.9** (1.00 g, 2.83 mmol, 1.00 equiv) and alkene **4.10** (4.43 g, 14.1 mmol, 5.00 equiv) were added to the flask. The mixture was then dissolved in CH_2Cl_2 (18.9 mL, 0.15 M) and stirred to create a homogenous mixture. The flask was fitted with a reflux condenser and heated to 40 °C for 20 h under nitrogen. After this time, the reaction was removed from heat and cooled to 23 ºC. The solvent was evaporated under reduced pressure and the crude residue was purified via flash chromatography (95:5 → 85:15 hexanes:EtOAc) to afford the cross-metathesis product (1.14 g, 1.78 mmol), which was used directly in the subsequent step.

To a solution of the cross-metathesis product (1.00 g, 1.57 mmol, 1.00 equiv) in THF (24 mL, 0.033 M) and MeOH (24 mL) was added basic alumina (600 mg) and Pd/C (167 mg, 10.0 wt%, 157 μmol, 10.0 mol%). The headspace of the flask was then flushed with H_2 from a balloon and the reaction was left to stir under an atmosphere of H_2 (1 atm) for 16 h. The reaction was then filtered over celite (5 cm, Monstr pipette) with CH_2Cl_2 as the eluent (25 mL) and the solvent was removed under reduced pressure. The crude residue was purified via flash chromatography (4:1 hexanes:EtOAc) to afford the silyl ketone product (883 mg, 1.38 mmol), which was used directly in the subsequent step.

To a flask in the glovebox was added KHMDS (164 mg, 824 μmol, 1.20 equiv). The flask was then removed from the glovebox, charged with THF (2.00 mL), and cooled to –78 °C. To

another flask was added the silyl ketone product (440 mg, 686 μmol, 1.00 equiv) and THF (3.00 mL). The ketone solution was then added dropwise over 10 min to the KHMDS solution at –78 °C. After stirring for 3 h at –78 °C, a solution of Comins' Reagent (350 mg, 892 μmol, 1.30 equiv) in THF (2.00 mL) was added dropwise over 5 min at –78 °C. The reaction was allowed to stir at –78 ºC for 30 min and then allowed to warm to 23 ºC and stirred for 16 h. After this time, the reaction was quenched with saturated aq. $NaHCO_3$ (15 mL) and diluted with Et_2O (20 mL). The layers were separated and the aqueous layer was extracted with Et_2O (2 x 50 mL). The combined organic layers were dried over Na_2SO_4, filtered, and concentrated under reduced pressure to provide the crude residue. The crude residue was purified via flash chromatography (95:5 → 85:15 hexanes:EtOAc) to afford silyl triflate **4.11** (260 mg, 26% yield over three steps) as a clear colorless oil. Silyl triflate **4.11**: R_f 0.56 (5:1 Hexanes:EtOAc); ^{1}H NMR (500 MHz, $CDCl_3$): δ 5.65 (s, 1H), 4.17 (dd, *J* = 18.3, 4.0, 1H), 3.80–3.60 (m, 2H), 3.57–3.48 (m, 2H), 3.48–3.27 (m, 1H), 1.55–1.52 (m, 2H), 1.50 (s, 18H), 1.46 (s, 9H), 1.25 (br s, 12H), 0.99 (t, *J* = 8.0, 9H), 0.73–0.66 (m, 6H); ^{13}C NMR (125 MHz, $CDCl_3$): δ 154.3, 153.5, 152.9, 118.5 (q, *J* = 319), 110.3, 82.1, 80.5, 47.5, 46.8, 46.7, 42.4, 41.9, 35.4, 33.0, 32.6, 30.58, 30.51, 29.7, 29.5, 29.22, 29.15, 28.5, 28.2, 27.04, 26.96, 25.0, 24.6, 8.1, 6.9, 6.7, 5.9, 5.8, 2.9; ^{19}F NMR (376 MHz, $CDCl_3$): δ –74.8; IR (film): 2933, 2879, 1697, 1415, 1171 cm^{-1}; HRMS–APCI (*m/z*) $[M + H]^+$ calcd for $C_{35}H_{64}F_3N_2O_9SSi^+$, 773.4048; found 773.4034.

*Note: **4.11** was obtained as a mixture of rotamers. These data represent empirically observed chemical shifts from the ^{1}H NMR and ^{13}C NMR spectrum.*

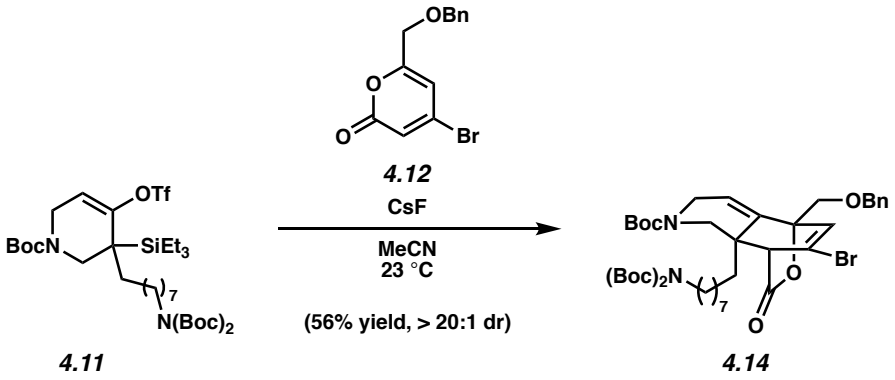

Cycloadduct 4.14: To a solution of silyl triflate **4.11** (53.0 mg, 68.6 µmol, 1.00 equiv) and pyrone **4.12** (101 mg, 343 µmol, 5.00 equiv) in MeCN (687 µL, 0.10 M) was added CsF (52.1 mg, 343 µmol, 5.00 equiv). The reaction mixture was allowed to stir at 1000 RPM at 23 °C for 20 h. After this time, the reaction mixture was filtered through a short plug of silica gel (3 cm silica) eluting with EtOAc (~10 mL) and then concentrated under reduced pressure. The crude residue was purified via flash chromatography (9:1 → 4:1 hexanes:EtOAc) to afford the cycloadduct **4.14** (27.0 mg, 56% yield) as an amorphous yellow foam. Cycloadduct **4.14**: R_f 0.22 (5:1 Hexanes:EtOAc); ^{1}H NMR (500 MHz, $CDCl_3$): δ 7.40–7.32 (m, 5H), 6.54 (dd, *J* = 19.3, 2.2, 1H), 5.67 (ddd, *J* = 22.8, 2.7, 2.1, 1H), 4.67 (s, 2H), 4.38–4.09 (m, 2H), 4.03 (dd, *J* = 10.9, 5.4, 1H), 3.92 (d, *J* = 10.9, 1H), 3.68 (dd, *J* = 13.2, 2.0, 1H), 3.62 (td, *J* = 19.8, 5.0, 1H), 3.55–3.48 (m, 2H), 2.31 (dd, *J* = 33.8, 12.2, 1H), 1.50 (s, 18H), 1.48 (d, *J* = 8.0, 9H), 1.25 (br s, 14H); ^{13}C NMR (125 MHz, $CDCl_3$): δ 169.2, 169.1, 155.2, 155.0, 152.9, 138.8, 138.3, 137.3, 137.2, 133.5, 133.0, 128.8, 128.30, 128.27, 128.14, 128.11, 119.2, 118.8, 117.5, 117.1, 85.2, 85.1, 82.13, 82.09, 80.6, 80.4, 74.2, 67.9, 67.8, 57.4, 57.3, 46.6, 45.6, 44.8, 43.0, 42.5, 40.8, 40.7, 34.4, 30.0, 29.9, 29.8, 29.6, 29.5, 29.3, 29.2, 28.6, 28.5, 28.2, 27.0, 26.9, 23.5, 23.3; IR (film): 2981, 2926, 2857, 1771, 1697 cm^{-1}; HRMS–APCI (*m/z*) $[M + H – Boc]^+$ calcd for $C_{36}H_{52}BrN_2O_7^+$, 703.2952; found 703.2948.

*Note: **4.14** was obtained as a mixture of rotamers. These data represent empirically observed chemical shifts from the ^{1}H NMR and ^{13}C NMR spectrum.*

The structure of **4.14** was retroactively verified based on 2D-NOESY analysis of **4.15**.

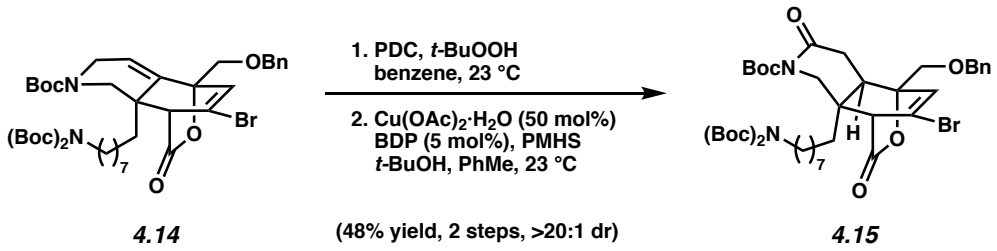

4.14 *4.15*

Amide 4.15: To a solution of cycloadduct **4.14** (126 mg, 157 μmol, 1.00 equiv) in benzene (15.7 mL, 0.01 M) was added PDC (177 mg, 470 μmol, 3.00 equiv) and *t*-BuOOH (65.0 μL, 70 wt% in H_2O, 470 μmol, 3.00 equiv). The solution was stirred at 23 °C for 24 h. At this point, celite (90 mg) was added and the solution was allowed to stir for 30 min. Next, the mixture was filtered over a pad of celite (5 cm, Monstr pipette) and rinsed with EtOAc (10 mL). The filtrate was diluted with saturated aq. sodium thiosulfate solution (10 mL) and water (10 mL). The solution was transferred to a separatory funnel, shaken, and the layers were separated. The aqueous layer was extracted with EtOAc (3 x 15 mL). The combined organic layers were washed with water (3 x 15 mL) and brine (15 mL), dried over Na_2SO_4, filtered, and concentrated to a crude brown oil. The crude oil was purified via flash column chromatography (9:1 → 3:2 hexanes:EtOAc) to obtain the enamide intermediate (76 mg, 93 μmol), which was used in the next step.

A flask was charged with copper(II) acetate monohydrate (9.2 mg, 46 μmol, 50 mol%) and BDP (4.1 mg, 9.2 μmol, 10 mol%). The solids were dissolved in sparged *t*-BuOH (87 μL, 917 μmol, 10.0 equiv) and toluene (352 μL, 0.26 M). The contents of the flask were sonicated for 2 min and then stirred for 20 min, during which the solution turned blue. At this point, PMHS (520 μL, 275 μmol, 3.00 equiv) was added dropwise over 3 min, then the solution was allowed to stir for 40 min during which it turned yellow/green. A solution of enamide (75 mg, 92 μmol) in toluene (352 μL, 0.26 M) was then added to the Stryker reagent dropwise over 3 min. The reaction was stirred at 23 °C for 20 h, after which it was diluted with EtOAc (2 mL). The solution was

transferred to a separatory funnel and sequentially washed with 1N NaOH (2 mL), 1N HCl (2 mL), saturated aq. $NaHCO_3$ solution (2 mL), and brine (2 mL). The combined aqueous layers were extracted with EtOAc (3 x 5 mL). The organic layers were combined, dried over Na_2SO_4, and concentrated under reduced pressure. The crude material was purified via flash chromatography (100% hexanes → 2:1 hexanes:EtOAc) to obtain amide **4.15** (38 mg, 30% yield over two steps) as a white foam. Amide **4.15**: R_f 0.56 (2:1 hexanes:EtOAc); ^{1}H NMR (500 MHz, $CDCl_3$): δ 7.40–7.30 (m, 5H), 6.46 (s, 1H), 4.66 (d, *J* = 12.1, 1H), 4.57 (d, *J* = 12.1, 1H), 4.24 (d, *J* = 13.9, 1H), 3.83 (d, *J* = 11.2, 1H), 3.65 (d, *J* = 11.2, 1H), 3.59 (s, 1H), 3.53 (t, *J* = 7.5, 2H), 3.20 (d, *J* = 13.9, 1H), 2.59 (dd, *J* = 14.5, 5.7, 1H), 2.29 (dd, *J* = 11.9, 5.7, 1H), 2.04 (dd, *J* = 14.6, 12.0, 1H), 1.68–1.60 (m, 1H), 1.53 (s, 9H), 1.50 (s, 18H), 1.35–1.18 (m, 13H); ^{13}C NMR (125 MHz, $CDCl_3$): δ 169.2, 169.0, 152.9, 151.2, 137.0, 131.0, 128.8, 128.4, 128.1, 122.4, 86.6, 84.1, 82.1, 74.2, 69.1, 56.8, 46.6, 45.9, 44.7, 43.5, 38.4, 37.5, 29.9, 29.51, 29.47, 29.2, 28.2, 28.1, 27.0, 23.2; IR (film): 2983, 1771, 1730, 1367, 1132 cm^{-1}; HRMS–APCI (*m/z*) $[M + H - CO_2]^+$ calcd for $C_{40}H_{60}BrN_2O_8^+$, 775.3528; found 775.3573.

The structure of **4.15** was verified by 2D-NOESY, as the following interaction was observed:

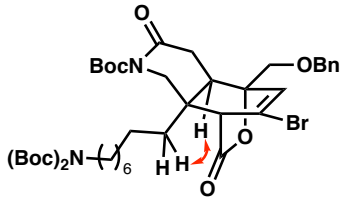

4.15

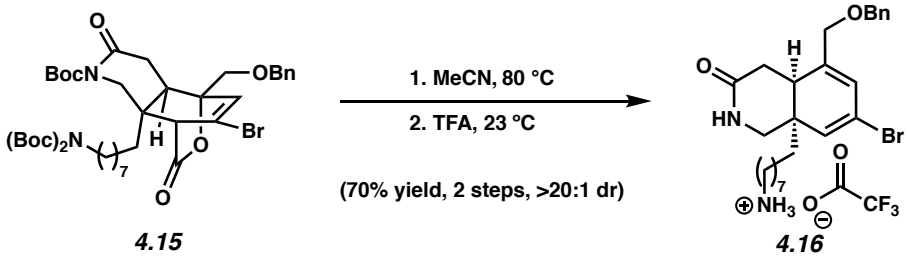

4.15 ***4.16***

Amine 4.16: A vial was charged with amide **4.15** (17.0 mg, 21.0 μmol, 1.00 equiv) and MeCN (410 μL, 0.05 M). The vial was heated to 80 °C for 16 h, after which it was allowed to cool to 23 °C. The reaction mixture was concentrated under reduced pressure and purified via preparative TLC (2:1 hexanes:EtOAc) to afford the desired diene intermediate (11.5 mg, 14.8 μmol) with the Boc protecting groups intact, which was used in the subsequent step.

A vial was charged with the diene intermediate (11.5 mg, 14.8 μmol, 1.00 equiv) and CH_2Cl_2 (0.20 mL, 0.074 M). Trifluoroacetic acid (0.10 mL, 9.00 equiv) was added dropwise to the diene solution over 2 min. The reaction mixture was allowed to stir at 23 ºC for 1 h. At this point, the septum was pierced with a nitrogen inlet and vent needle and the reaction mixture was allowed to concentrate at 23 ºC. CH_2Cl_2 (0.5 mL, 0.05 M) was added to resuspend the crude material and then subsequently evaporated off with a nitrogen inlet and vent needle. This was repeated twice more to afford amine **4.16** as the TFA salt (10 mg, 70% yield, two steps). Amine **4.16**: R_f 0.67 (2:1 CH_2Cl_2:MeOH); ^{1}H NMR (500 MHz, MeOD-d_4): δ 7.37–7.26 (m, 5H), 5.96 (s, 1H), 5.89 (s, 1H), 4.56 (d, J = 11.8, 1H), 4.52 (d, J = 11.8, 1H), 4.12 (d, J = 13.5, 1H), 4.02 (d, J = 13.5, 1H), 3.20 (d, J = 12.9, 1H), 2.89 (t, J = 7.6, 2H), 2.57–2.48 (m, 2H), 2.14 (td, J = 11.7, 8.8, 1H), 1.76–1.69 (m, 1H), 1.66–1.58 (m, 2H), 1.40–1.22 (m, 15H); ^{13}C NMR (125 MHz, MeOD-d_4): δ 175.8, 162.8, 143.6, 139.5, 133.9, 129.5, 128.8, 124.3, 118.3, 73.6, 72.0, 50.3, 42.3, 40.7, 38.0, 37.9, 33.9, 31.3, 30.8, 30.2, 30.1, 28.6, 27.4, 25.0; IR (film): 3064, 1678, 1204, 1136, 801 cm^{-1}; HRMS–APCI (*m/z*) $[M + H - C_2O_2F_3]^+$ calcd for $C_{25}H_{36}BrN_2O_2^+$, 475.19547; found 475.19370.

4.7.2.2 Syntheses of Silyl Triflates 4.22a and 4.22b

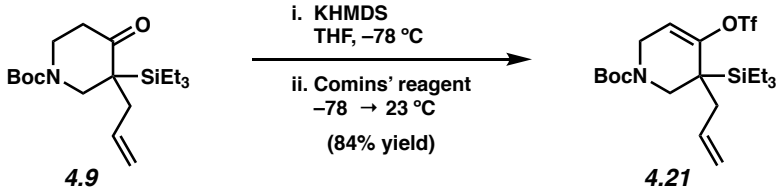

4.9 *4.21*

Silyl Triflate 4.21. A flask in the glovebox was charged with KHMDS (3.07 g, 15.4 mmol, 1.62 equiv). The flask was brought out of the glovebox and the contents were dissolved in THF (32 mL). This solution was then cooled to –78 ºC and ketone **4.9** (3.36 g, 9.50 mmol, 1.00 equiv) in THF (32 mL) was added dropwise over 15 min at –78 ºC. The solution was stirred at –78 ºC for 2.5 h. Then, a solution of Comins' reagent (4.66 g, 11.9 mmol, 1.25 equiv) in THF (32 mL) was added to the reaction mixture dropwise over 10 min at –78 ºC. The reaction was stirred for 1 h at –78 ºC, then warmed to 23 ºC and stirred for 2.5 h. After this time, the reaction was quenched with saturated aq. $NaHCO_3$ (75 mL). The reaction was then transferred to a separatory funnel, the layers were separated, and the aqueous layer was extracted with ethyl acetate (3 x 75 mL). The organic layers were combined and washed with brine (75 mL), then dried over Na_2SO_4, filtered, and concentrated under reduced pressure. The crude material was purified via flash column chromatography (100% hexanes → 95:5 hexanes:EtOAc) to yield silyl triflate **4.21** (3.87 g, 84% yield) as a yellow oil. Silyl triflate **4.21**: R_f 0.71 (9:1 pentane:EtOAc); ^{1}H NMR (500 MHz, $CDCl_3$): δ 5.83–5.73 (m, 1H), 5.73–5.63 (m, 1H), 5.15–4.98 (m, 2H), 4.09 (dd, *J* = 18.2, 3.6, 1H), 3.95–3.80 (m, 1H), 3.78–3.43 (m, 2H), 2.56–2.43 (m, 1H), 2.25 (dd, *J* = 14.4, 8.4, 1H), 1.46 (s, 9H), 1.00 (t, *J* = 7.9, 9H), 0.78–0.68 (m, 6H); ^{13}C NMR (125 MHz, $CDCl_3$): δ 154.3, 153.0, 133.5, 133.3, 128.5, 118.5, 118.3 (q, *J* = 319), 118.2, 110.2, 82.6, 80.6, 80.4, 47.4, 46.6, 42.4, 42.0, 36.8, 35.4, 31.4, 28.5, 28.3, 8.0, 7.0, 6.7, 6.6, 5.9, 2.8; ^{19}F NMR (376 MHz, $CDCl_3$): δ –74.7; IR (film): 2961, 1701, 1415, 1209, 882 cm^{-1}; HRMS-APCI (*m/z*) $[M + H]^+$ calcd for $C_{20}H_{35}F_3NO_5SSi^+$, 486.1952; found 486.1985.

*Note: **4.21** was obtained as a mixture of rotamers. These data represent empirically observed chemical shifts from the ^{1}H NMR and ^{13}C NMR spectrum.*

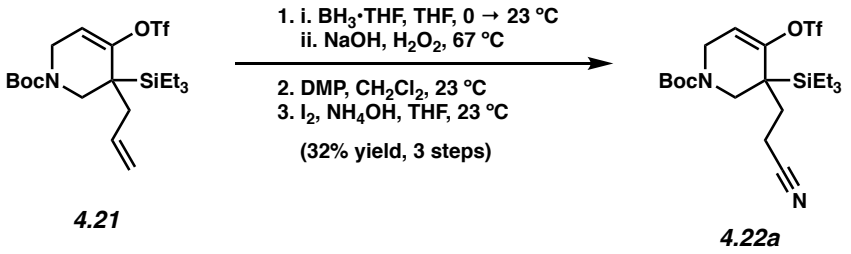

4.21 ***4.22a***

Silyl Triflate 4.22a: A vial was charged with silyl triflate **4.21** (1.18 g, 2.43 mmol, 1.00 equiv) and THF (12.1 mL, 0.20 M) and then cooled to 0 ºC. BH_3•THF (7.29 mL, 7.29 mmol, 2.00 equiv, 1.0 M in THF) was added dropwise at 0 ºC over 5 min. The reaction mixture was allowed to warm to 23 ºC over 30 min, and then allowed to stir for 3 h at 23 ºC. After this time, the reaction was cooled to 0 ºC and NaOH (24.3 mL, 24.3 mmol, 10.0 equiv, 1.0 M) and H_2O_2 (2.48 mL, 24.3 mmol, 10.0 equiv, 30 wt% in H_2O) were added sequentially to the reaction mixture. The reaction mixture was allowed to warm to 23 ºC over 10 min, then maintained at 67 ºC for 1 h. After this time, the solution was cooled to 23 ºC and diluted with H_2O (10 mL) and EtOAc (10 mL). The solution was transferred to a separatory funnel and the aqueous layer was extracted with EtOAc (3 x 50 mL). The combined organic layers were dried over Na_2SO_4, filtered and concentrated under reduced pressure. The crude material was purified by flash chromatography (9:1 → 1:1 hexanes:EtOAc) to afford the primary alcohol (954 mg, 1.89 mmol), which was used in the subsequent step.

To a solution of the primary alcohol (950 mg, 1.89 mmol, 1.00 equiv) in CH_2Cl_2 (18.9 mL, 0.10 M) was added Dess–Martin periodinane (960 mg, 2.26 mmol, 1.20 equiv). The reaction mixture was allowed to stir at 23 ºC for 1 h. After this time, the reaction mixture was quenched with saturated aq. sodium thiosulfate (10 mL) and diluted with CH_2Cl_2 (10 mL). The mixture was transferred to a separatory funnel, the layers were separated, and the aqueous layer was extracted with CH_2Cl_2 (3 x 30 mL). The combined organic layers were washed with brine (40 mL), dried over $MgSO_4$, filtered, and concentrated under reduced pressure. The crude material was dissolved

in hexanes, filtered over a short celite plug (3 x 5 cm) eluting with hexanes (40 mL), concentrated under reduced pressure, and purified by flash chromatography (9:1 → 5:1 hexanes:EtOAc) to afford the aldehyde product (512 mg, 1.02 mmol), which was used in the subsequent step.

To a vial was added the aldehyde product (256 mg, 510 μmol, 1.00 equiv), ammonium hydroxide (6.78 mL, 51.0 mmol, 10.0 equiv, 30 wt% in H_2O), and THF (3.40 mL, 0.15 M). The vial was then wrapped in aluminum foil to exclude light. Iodine (142 mg, 561 μmol, 1.10 equiv) was added and the reaction mixture was allowed to stir at 23 ºC for 1 h. After this time, the reaction mixture was quenched with saturated aq. sodium thiosulfate (10 mL). The mixture was transferred to a separatory funnel and shaken. The layers were separated and the aqueous layer was extracted with EtOAc (3 x 10 mL). The organic layers were combined, washed with brine (20 mL), dried over Na_2SO_4, filtered, concentrated under reduced pressure, and purified by flash chromatography (100% hexanes → 9:1 hexanes:EtOAc) to afford silyl triflate **4.22a** (95 mg, 32% yield over three steps) as a clear oil. Silyl triflate **4.22a**: R_f 0.51 (5:1 hexanes:EtOAc); ^{1}H NMR (500 MHz, $CDCl_3$): δ 5.83 (s, 1H), 4.31 (dd, *J* = 18.5, 4.7, 1H), 4.12–3.78 (m, 1H), 3.69 (dd, *J* = 18.3, 1.5, 1H), 3.48–3.98 (m, 1H), 2.42 (t, *J* = 8.3, 2H), 2.20–2.04 (m, 1H), 2.04–1.90 (m, 1H), 1.48 (s, 9H), 1.01 (t, *J* = 8.0, 9H), 0.72 (qd, *J* = 7.7, 3.3, 6H); ^{13}C NMR (125 MHz, $CDCl_3$): δ 154.2, 150.6, 119.7, 118.4 (q, *J* = 320), 113.6, 81.5, 46.8, 42.3, 34.9, 29.3, 28.5, 13.0, 8.0, 2.4; ^{19}F NMR (376 MHz, $CDCl_3$): δ –74.2; IR (film): 2962, 2881, 2246, 1698, 1414 cm^{-1}; HRMS–APCI (*m/z*) $[M + H]^+$ calcd for $C_{20}H_{34}F_3N_2O_5SSi^+$, 499.1904; found 499.1902.

*Note: **4.22a** was obtained as a mixture of rotamers. These data represent empirically observed chemical shifts from the ^{1}H NMR and ^{13}C NMR spectrum.*

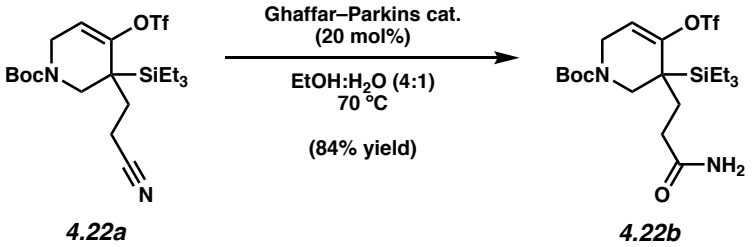

4.22a ***4.22b***

Silyl Triflate 4.22b: To a vial in the glovebox was added Ghaffar–Parkins catalyst (64.6 mg, 150 μmol, 0.20 equiv). The vial was removed from the glovebox and then a separate solution of silyl triflate **4.22a** (375 mg, 752 μmol, 1.00 equiv) in sparged EtOH:H_2O (4:1, 2.50 mL, 0.30 M) was added to the vial containing the catalyst. The reaction mixture was allowed to stir at 70 ºC for 1 h. After this time, the solution was cooled to 23 ºC, diluted with CH_2Cl_2 (5 mL), and filtered over a short silica plug with Na_2SO_4 layered on top of the silica (5 cm, Monstr pipette) eluting with 95:5 CH_2Cl_2:MeOH (10 mL). The crude reaction solution was concentrated under reduced pressure and purified by flash chromatography (100% CH_2Cl_2 → 95:5 CH_2Cl_2:MeOH) to afford silyl triflate **4.22b** (328 mg, 84% yield) with minor silyl impurities. An aliquot of this material was repurified via preparative TLC (3:1 benzene:acetone) to give the desired product as an amorphous white foam for analytical purposes. Silyl triflate **4.22b**: R_f 0.58 (3:1 benzene:acetone); ^{1}H NMR (500 MHz, MeOD-d_4): δ 5.84 (s, 1H), 4.35–3.99 (m, 1H), 3.89 (dd, J = 18.4, 2.8, 1H), 3.83–3.38 (m, 2H), 2.37–2.20 (m, 2H), 2.05–1.87 (m, 2H), 1.48 (s, 9H), 1.05 (t, J = 8.13, 9H), 0.84–0.73 (m, 6H); ^{13}C NMR (125 MHz, MeOD-d_4): δ 178.0, 155.9, 153.5, 119.7 (q, J = 319), 113.3, 82.1, 47.6, 43.4, 42.9, 36.0, 32.8, 31.5, 28.6, 26.2, 23.7, 21.0, 19.1, 14.4, 11.8, 8.2, 3.6; ^{19}F NMR (376 MHz, MeOD-d_4): δ –76.5, –80.1; IR (film): 3344, 3196, 2960, 2881, 1674 cm^{-1}; HRMS–APCI (*m/z*) [M + H]$^+$ calcd for $C_{20}H_{36}F_3N_2O_6SSi^+$, 517.2010; found 517.2011.

*Note: **4.22b** was obtained as a mixture of rotamers. These data represent empirically observed chemical shifts from the ^{1}H NMR and ^{13}C NMR spectrum.*

4.7.2.3 Syntheses of Trienes 4.23a and 4.23b

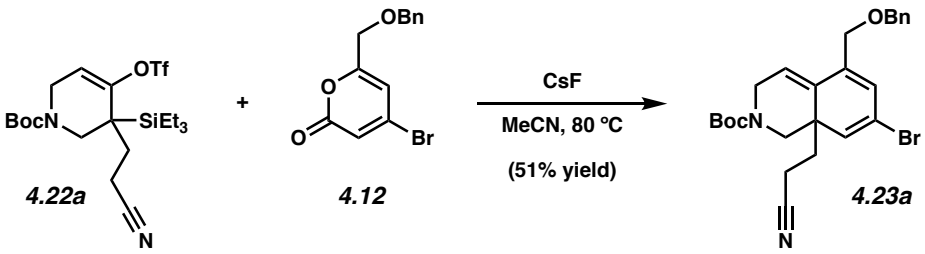

Triene 4.23a: To a solution of silyl triflate **4.22a** (50.0 mg, 100 μmol, 1.00 equiv) and pyrone **4.12** (136 mg, 461 μmol, 4.60 equiv) in MeCN (1.00 mL, 0.10 M) was added CsF (76.2 mg, 501 μmol, 5.00 equiv). The reaction mixture was allowed to stir at 1000 RPM at 80 °C for 1 h. After this time, the reaction mixture was filtered through a short plug of silica gel (3 cm, Monstr pipette) eluting with EtOAc (~10 mL) and then concentrated under reduced pressure. The crude residue was purified via flash chromatography (100% hexanes → 4:1 hexanes:EtOAc) to afford triene **4.23a** (25 mg, 51% yield) as a yellow oil. Triene **4.23a**: R_f 0.33 (5:1 hexanes:EtOAc); ^{1}H NMR (600 MHz, $CDCl_3$): δ 7.40–7.29 (m, 5H), 6.00 (s, 1H), 5.91 (d, *J* = 26.8, 1H), 5.76 (s, 1H), 4.54 (s, 2H), 4.39 (dd, *J* = 66.4, 20.5, 1H), 4.17 (s, 1H), 4.00 (dd, *J* = 103.6, 13.0, 1H), 3.79 (dd, *J* = 46.0, 26.8, 1H), 2.95 (dd, *J* = 66.9, 13.1, 1H), 2.54–2.35 (m, 1H), 2.34–2.25 (m, 1H), 2.02–1.93 (m, 1H), 1.74–1.66 (m, 1H), 1.49 (s, 9H); ^{13}C NMR (150 MHz, $CDCl_3$): δ 155.1, 137.8, 129.6, 129.1, 128.7, 128.1, 128.0, 125.8, 125.5, 124.8, 124.1, 80.9, 80.8, 73.0, 72.9, 69.2, 69.0, 48.4, 47.0, 44.6, 44.1, 43.9, 35.2, 29.9, 28.5, 12.7; IR (film): 2979, 2920, 2851, 2241, 1694 cm^{-1}; HRMS–APCI (*m/z*) $[M + H]^+$ calcd for $C_{25}H_{30}BrN_2O_3^+$, 485.1434; found 485.1425.

*Note: **4.23a** was obtained as a mixture of rotamers. These data represent empirically observed chemical shifts from the ^{1}H NMR and ^{13}C NMR spectrum.*

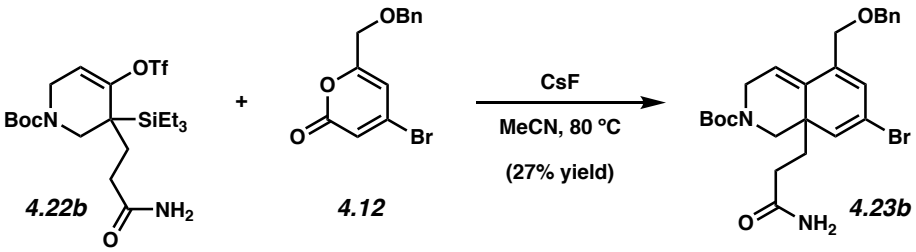

Triene 4.23b: To a solution of silyl triflate **4.22b** (15.0 mg, 29.0 μmol, 1.00 equiv) and pyrone **4.12** (42.8 mg, 145 μmol, 5.00 equiv) in MeCN (290 μL, 0.10 M) was added CsF (22.1 mg, 145 μmol, 5.00 equiv). The reaction mixture was allowed to stir at 1000 RPM at 80 °C for 3.5 h. After this time, the reaction mixture was filtered through a short plug of silica gel (3 cm silica, Monstr pipette) eluting with EtOAc (~10 mL) and then concentrated under reduced pressure. The crude residue was purified via preparative TLC (95:5 CH_2Cl_2:MeOH) to afford triene **4.23b** (4.0 mg, 27% yield) as a yellow oil. Triene **4.23b**: R_f 0.26 (95:5 CH_2Cl_2:MeOH); ^{1}H NMR (500 MHz, $CDCl_3$): δ 7.39–7.28 (m, 5H), 5.97 (s, 1H), 5.93–5.72 (m, 2H), 5.28–5.01 (m, 1H), 4.53 (d, J = 10.2, 2H), 4.36 (dd, J = 40.6, 20.8, 1H), 4.23–4.10 (m, 3H), 3.97–3.70 (m, 1H), 2.93 (dd, J = 54.2, 13.0, 1H), 2.44–2.10 (m, 2H), 1.81 (dtd, J = 91.8, 12.6, 4.1, 1H), 1.47 (s, 9H), 1.25 (br s, 2H); ^{13}C NMR (150 MHz, $CDCl_3$): 175.4, 155.4, 137.9, 136.8, 134.4, 130.8, 128.7, 128.1, 128.01, 127.97, 125.8, 125.6, 123.5, 122.8, 117.7, 80.6, 72.8, 72.5, 69.4, 69.1, 60.6, 48.9, 46.1, 44.7, 44.5, 44.4, 43.8, 35.1, 34.5, 31.1, 30.5, 29.9, 28.6; IR (film): 3415, 3343, 3195, 2922, 2862, 1673 cm^{-1}; HRMS–APCI (*m/z*) $[M + H]^+$ calcd for $C_{25}H_{32}BrN_2O_4^+$, 503.1540; found 503.1540.

*Note: **4.23b** was obtained as a mixture of rotamers. These data represent empirically observed chemical shifts from the ^{1}H NMR and ^{13}C NMR spectrum.*

4.8 Spectra Relevant to Chapter Four:

Cyclic Allene Approach to the Manzamine Alkaloid Keramaphidin B

Milauni M. Mehta, Jordan A. M. Gonzalez, James L. Bachman, and Neil K. Garg.

Manuscript submitted.

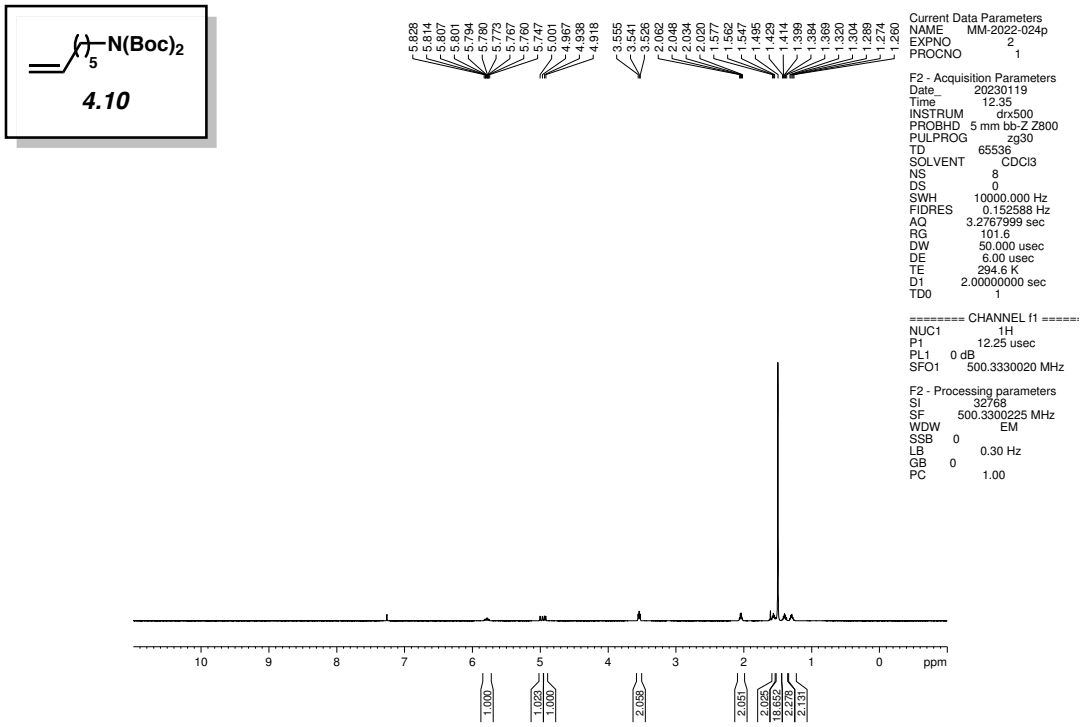

Figure 4.8 ^{1}H NMR (500 MHz, $CDCl_3$) of compound **4.10**.

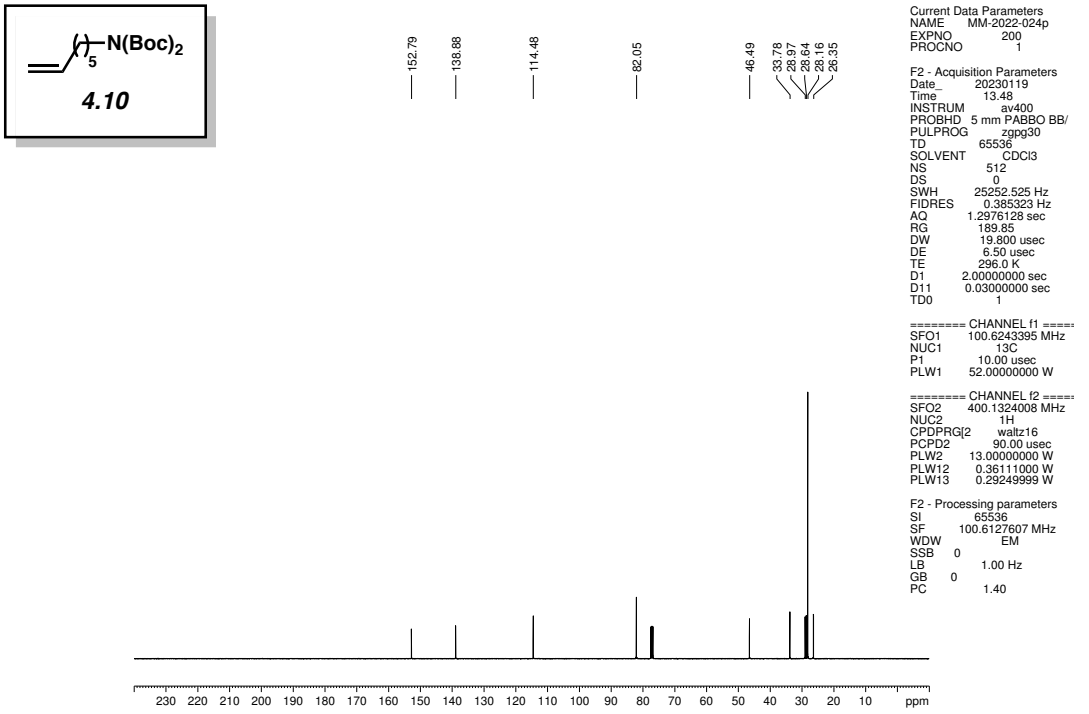

Figure 4.9 ^{13}C NMR (100 MHz, $CDCl_3$) of compound **4.10**.

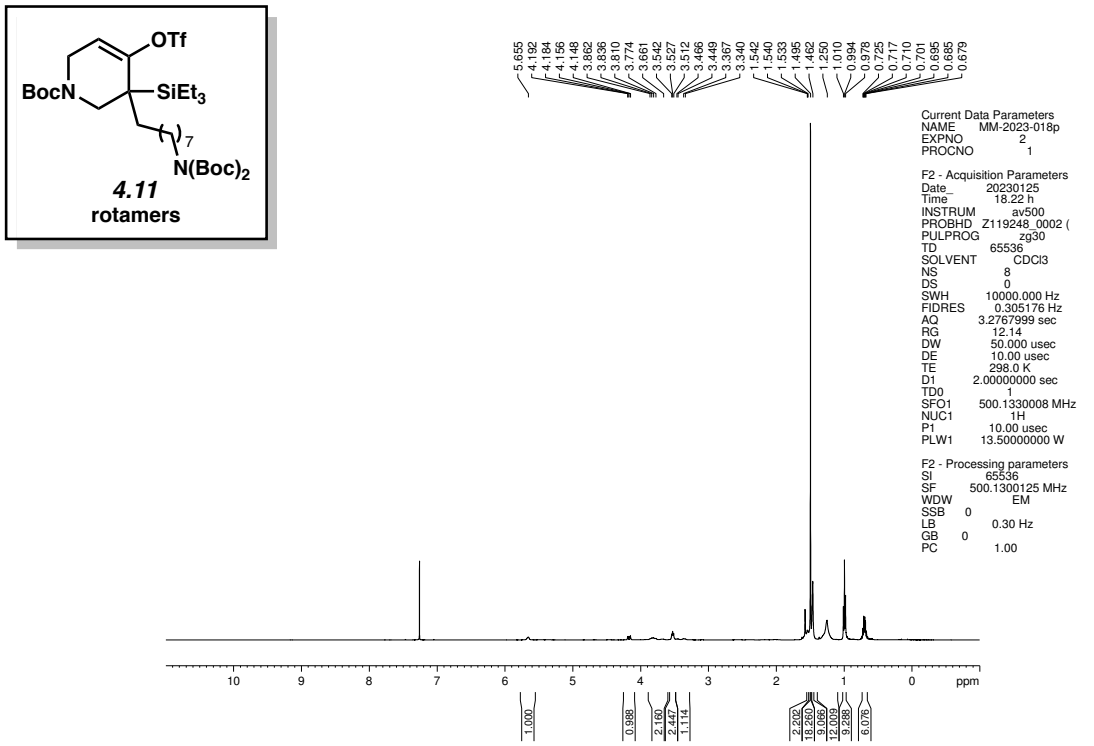

Figure 4.10 ^{1}H NMR (500 MHz, $CDCl_3$) of compound **4.11**.

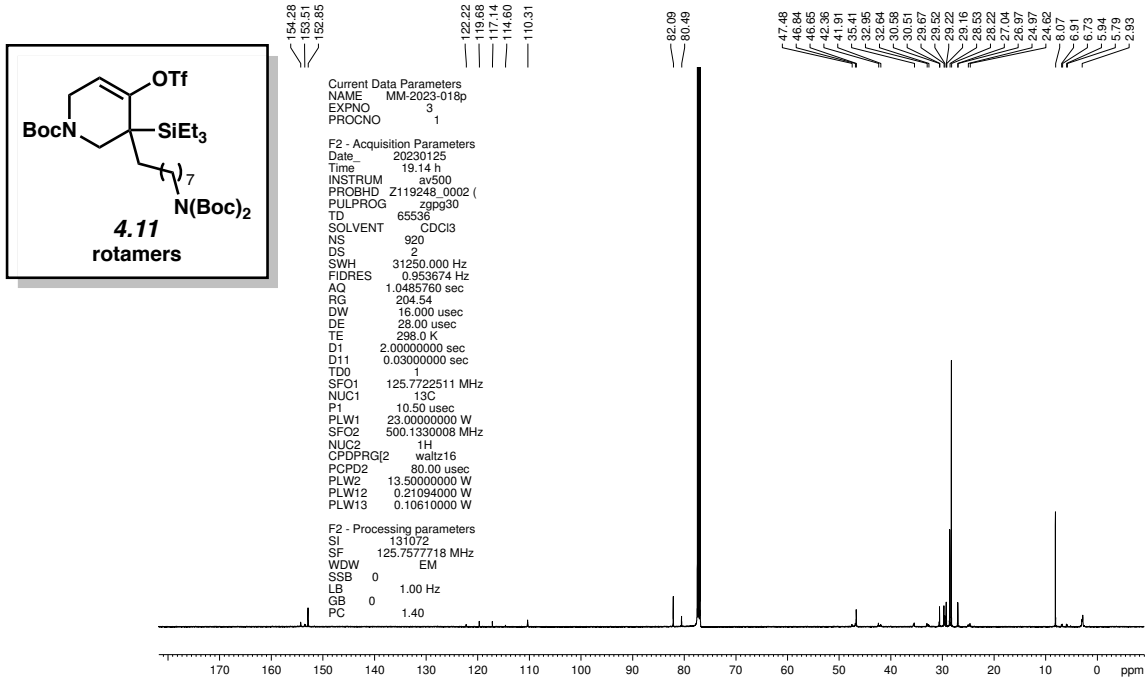

Figure 4.11 ^{13}C NMR (125 MHz, $CDCl_3$) of compound **4.11**.

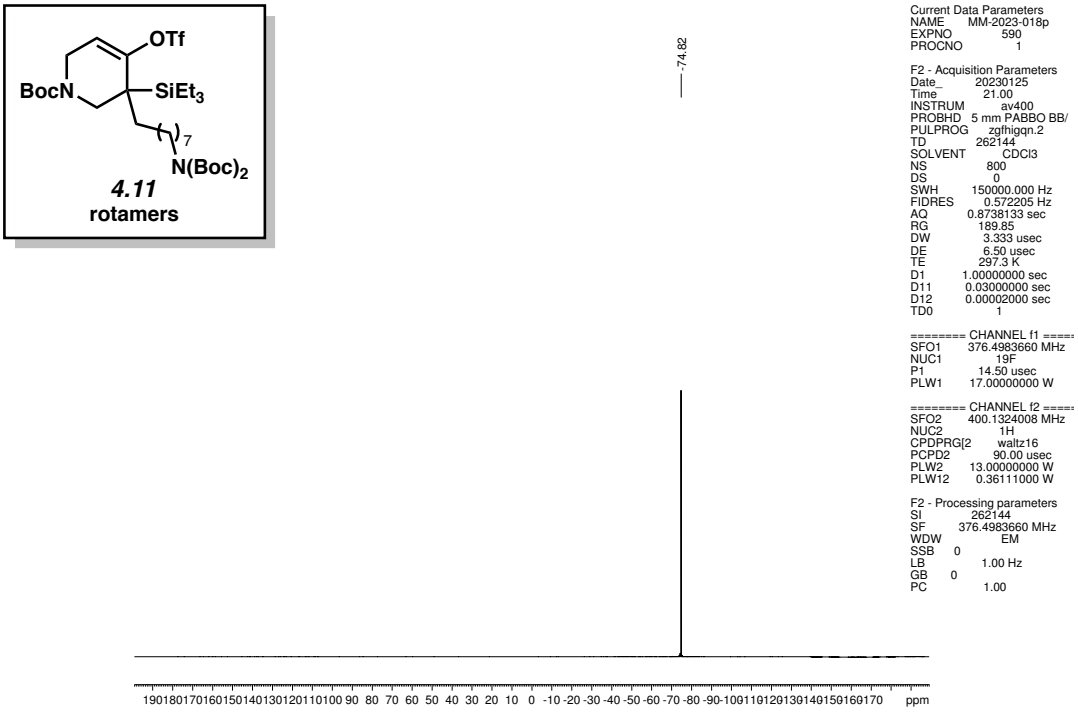

Figure 4.12 ^{19}F NMR (376 MHz, $CDCl_3$) of compound **4.11**.

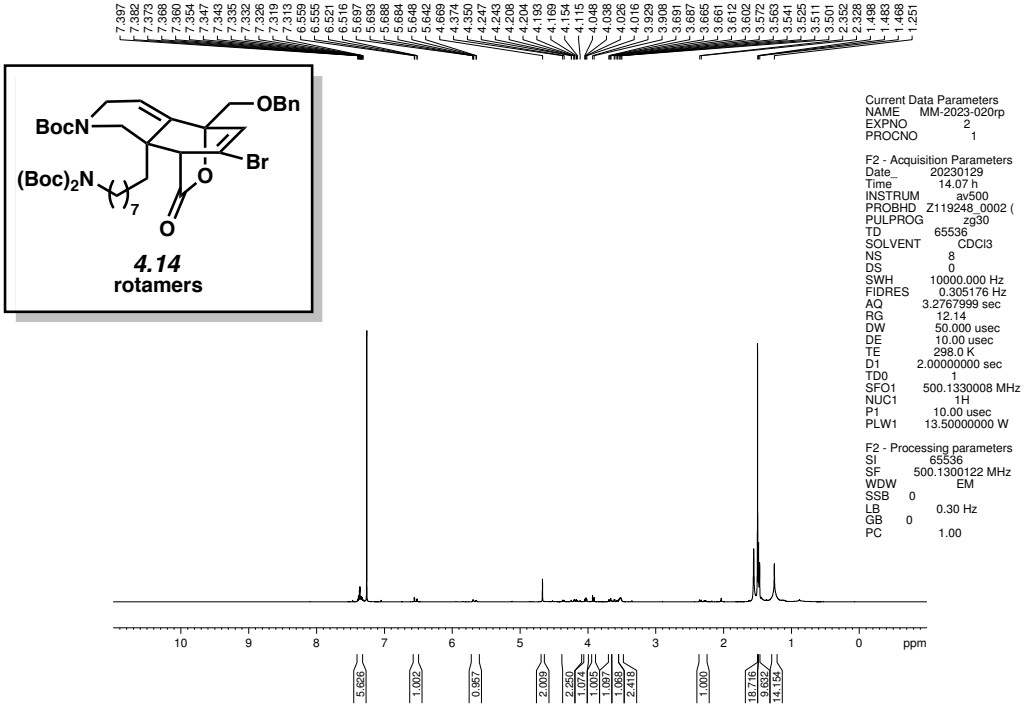

Figure 4.13 ^{1}H NMR (500 MHz, $CDCl_3$) of compound **4.14**.

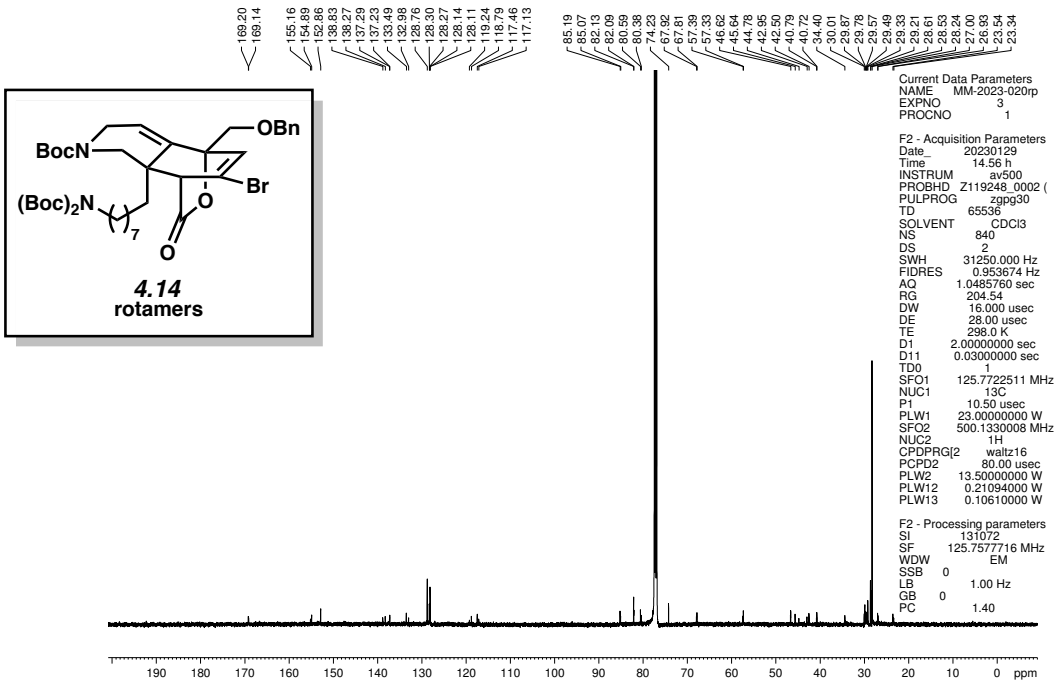

Figure 4.14 ^{13}C NMR (125 MHz, $CDCl_3$) of compound **4.14**.

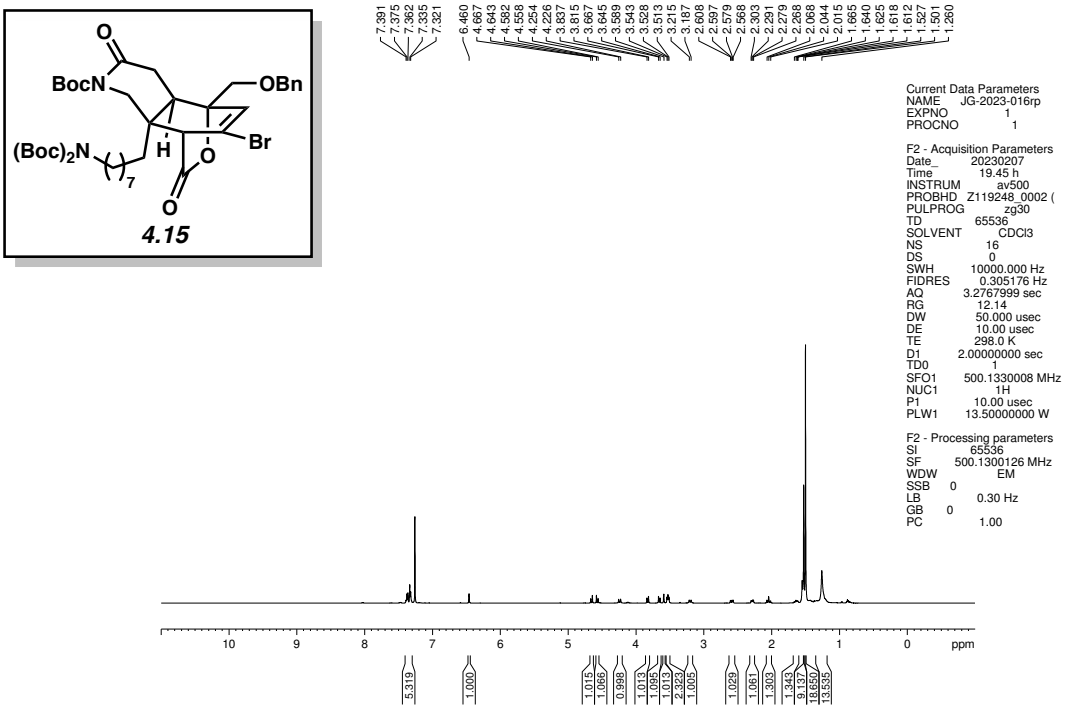

Figure 4.15 ^{1}H NMR (500 MHz, $CDCl_3$) of compound **4.15**.

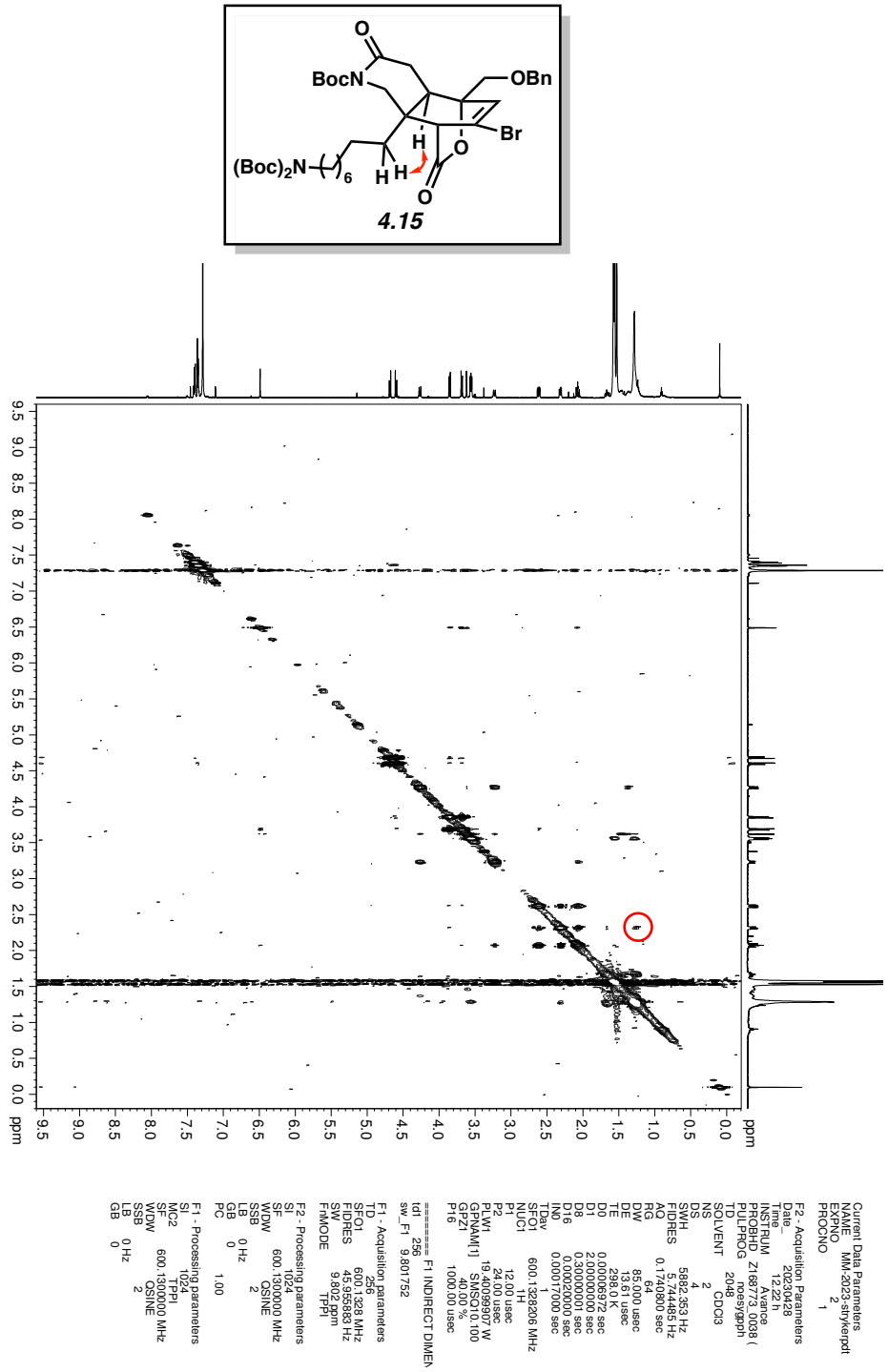

Figure 4.16 NOESY (600 MHz, $CDCl_3$) of compound **4.15**.

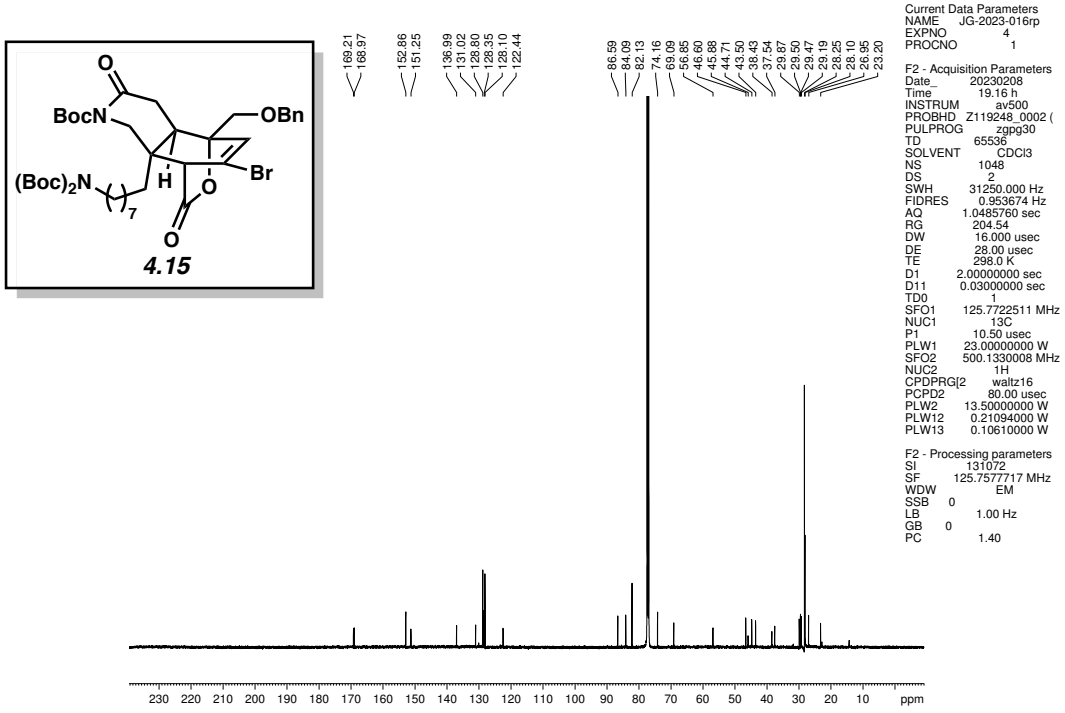

Figure 4.17 ^{13}C NMR (125 MHz, $CDCl_3$) of compound **4.15**.

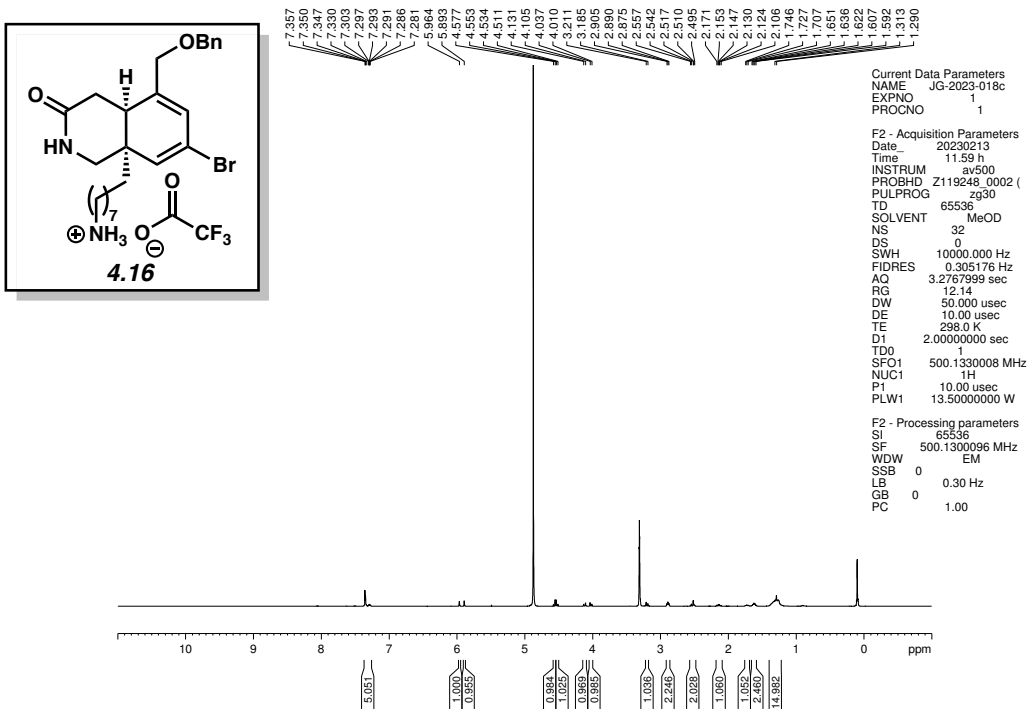

Figure 4.18 ^{1}H NMR (500 MHz, MeOD) of compound **4.16**.

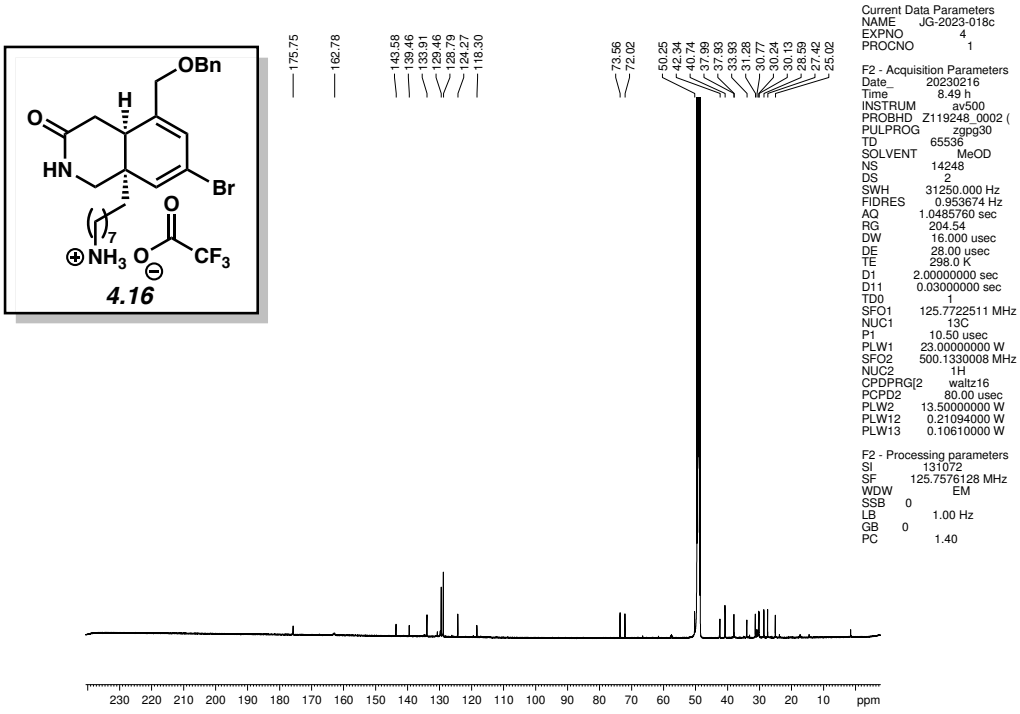

Figure 4.19 ^{13}C NMR (125 MHz, MeOD) of compound **4.16**.

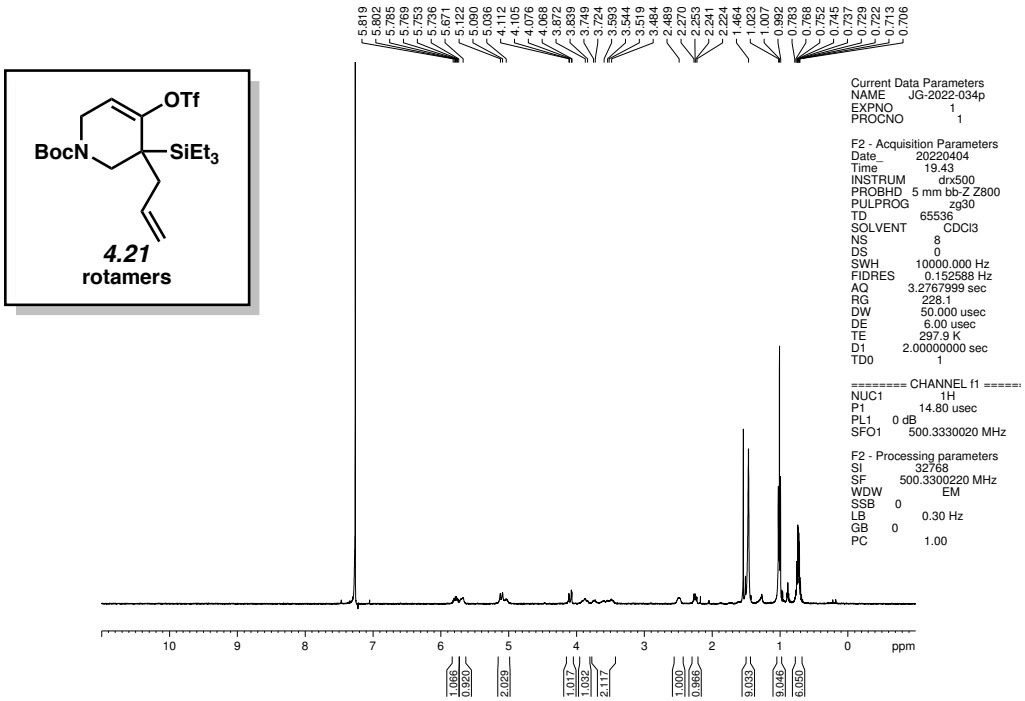

Figure 4.20 ^{1}H NMR (500 MHz, $CDCl_3$) of compound **4.21**.

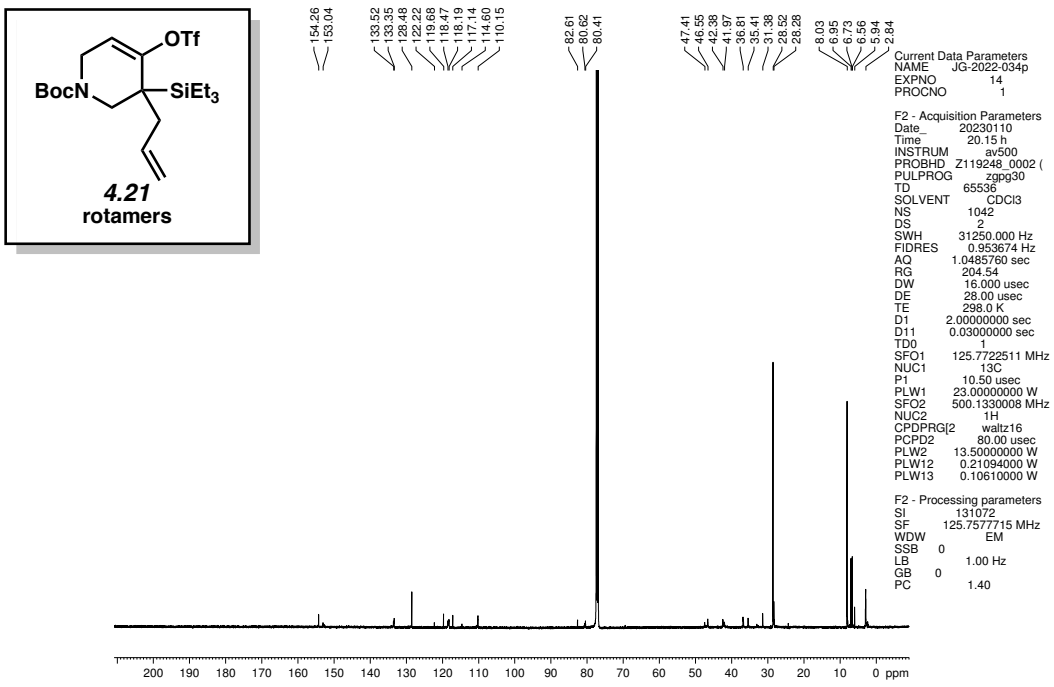

Figure 4.21 ^{13}C NMR (125 MHz, $CDCl_3$) of compound **4.21**.

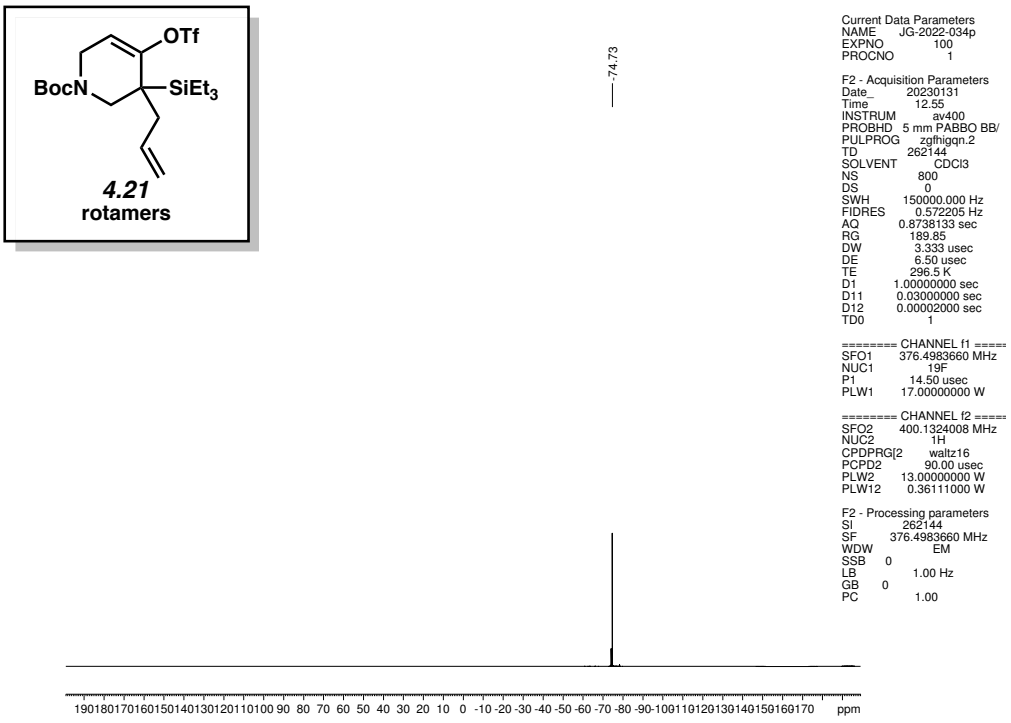

Figure 4.22 ^{19}F NMR (376 MHz, $CDCl_3$) of compound **4.21**.

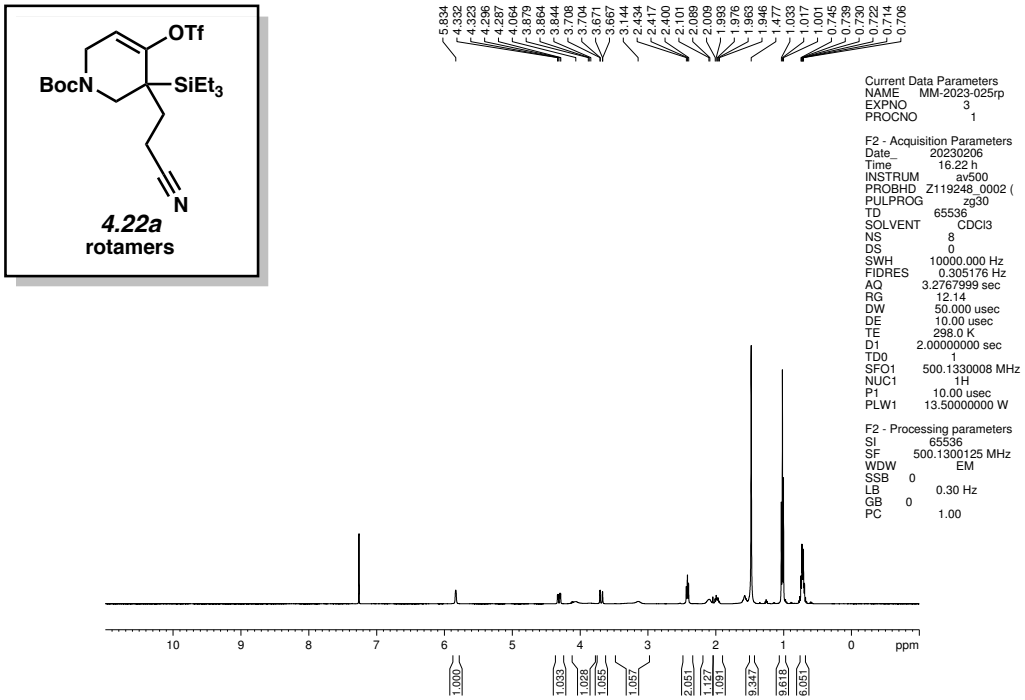

Figure 4.23 ^{1}H NMR (500 MHz, $CDCl_3$) of compound **4.22a**.

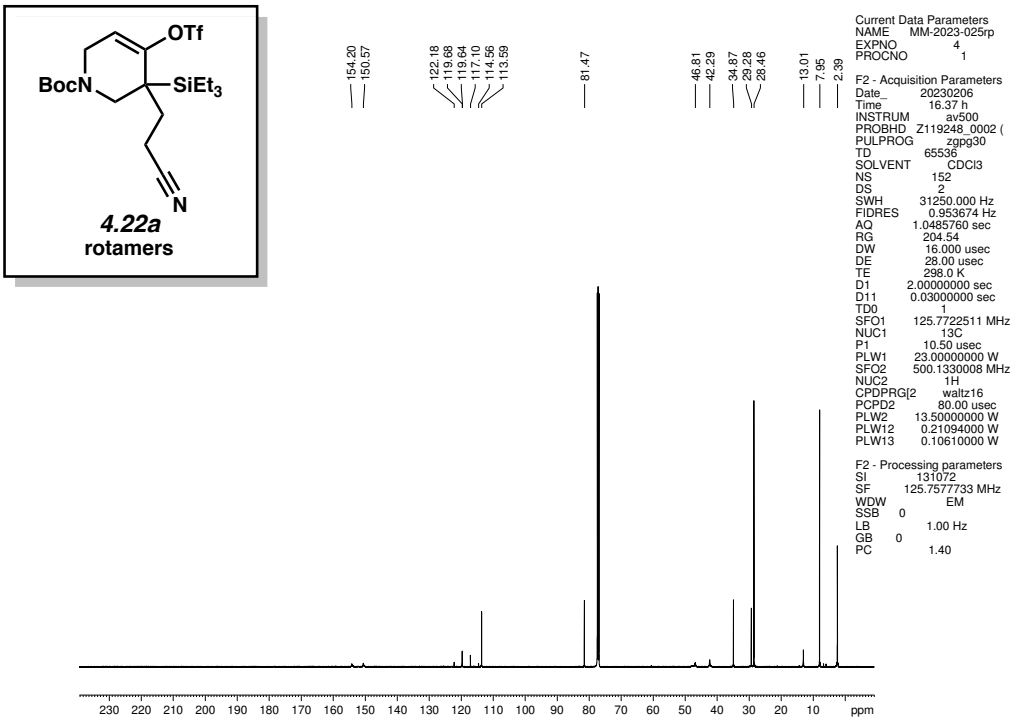

Figure 4.24 ^{13}C NMR (125 MHz, $CDCl_3$) of compound **4.22a**.

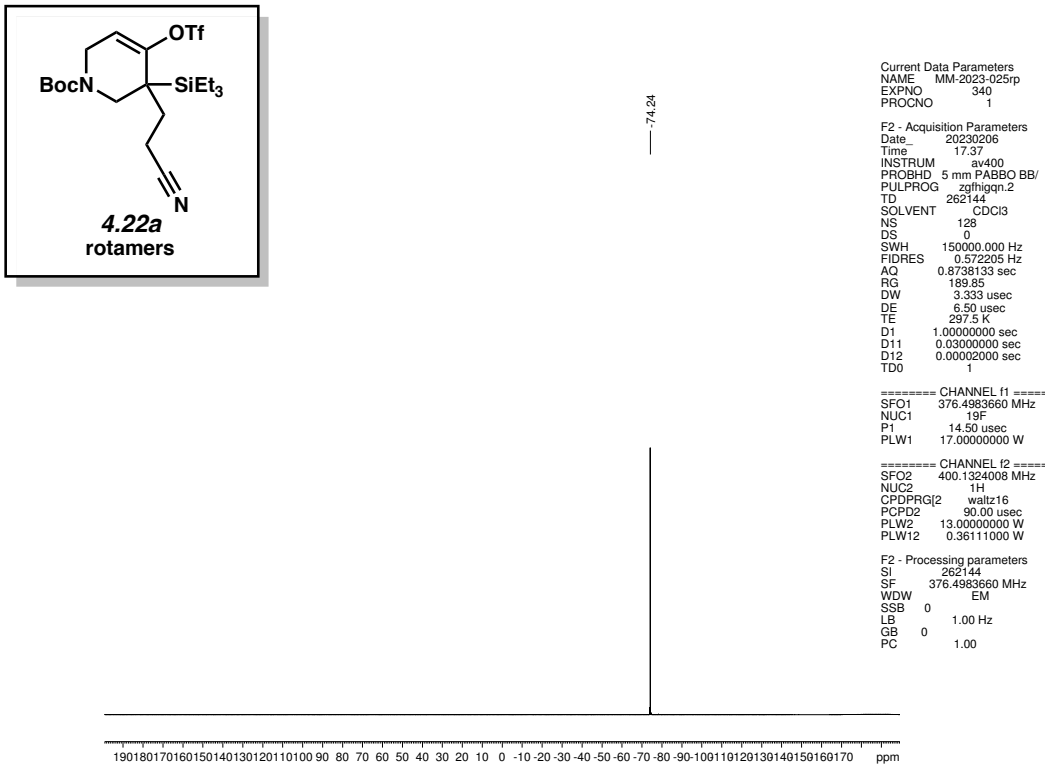

Figure 4.25 ^{19}F NMR (376 MHz, $CDCl_3$) of compound **4.22a**.

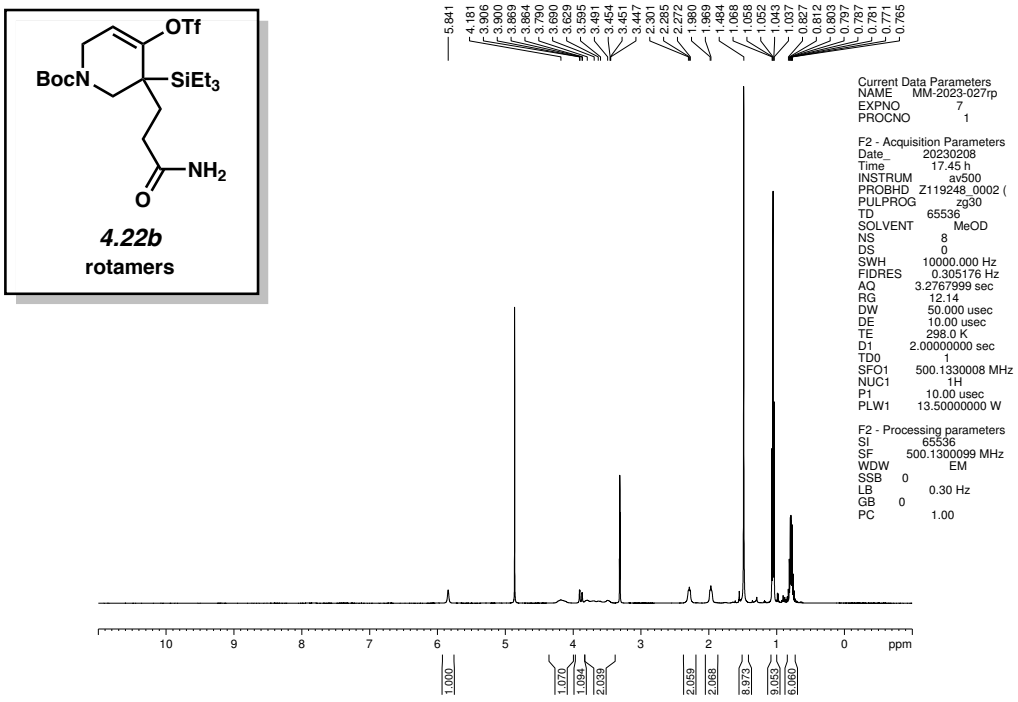

Figure 4.26 ^{1}H NMR (500 MHz, MeOD) of compound **4.22b**.

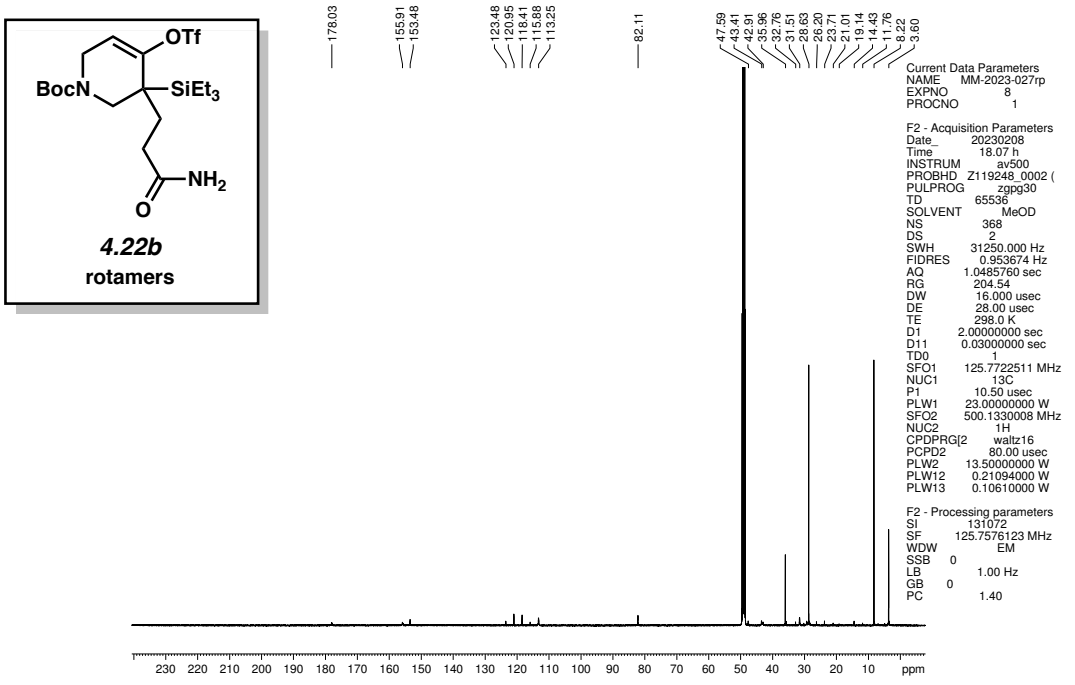

Figure 4.27 ^{13}C NMR (125 MHz, MeOD) of compound **4.22b**.

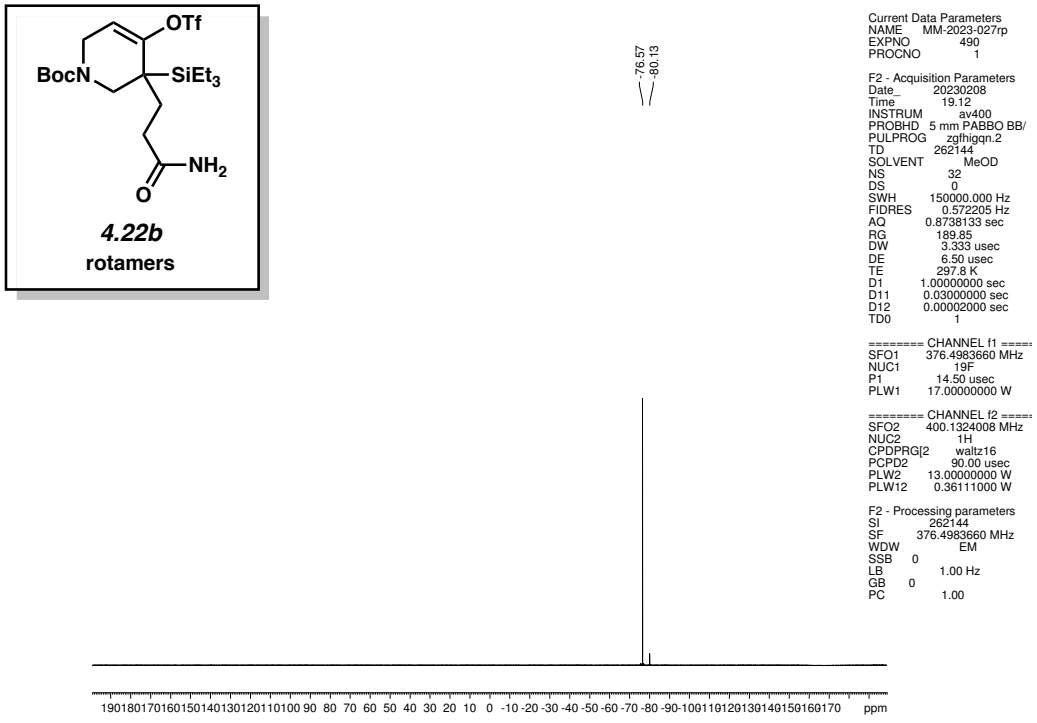

Figure 4.28 ^{19}F NMR (376 MHz, MeOD) of compound **4.22b**.

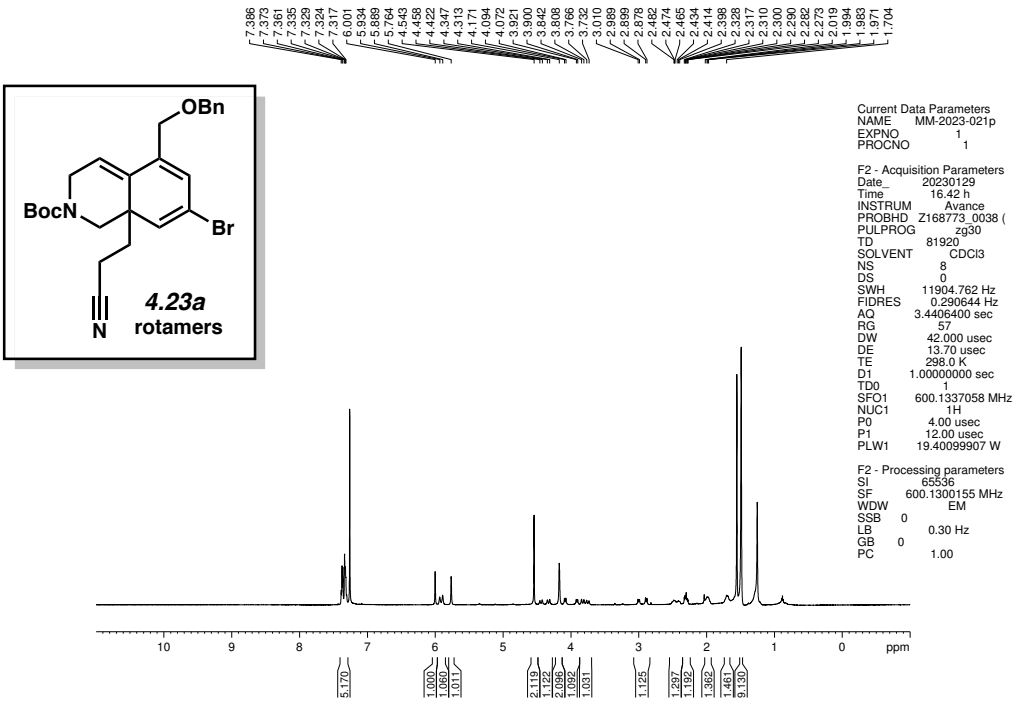

Figure 4.29 ^{1}H NMR (600 MHz, $CDCl_3$) of compound **4.23a**.

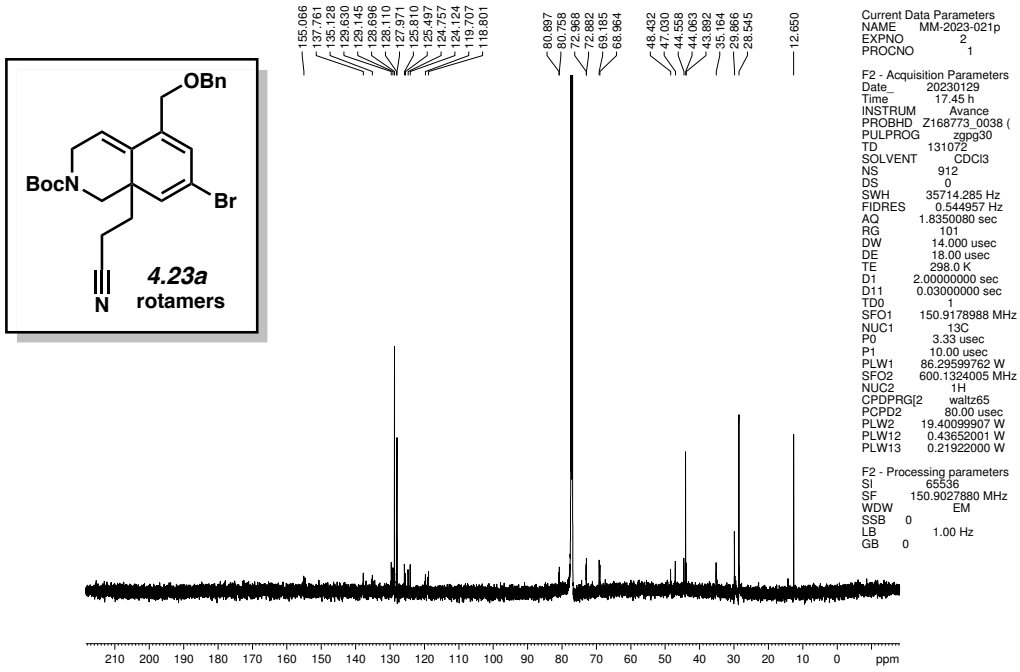

Figure 4.30 ^{13}C NMR (150 MHz, $CDCl_3$) of compound **4.23a**.

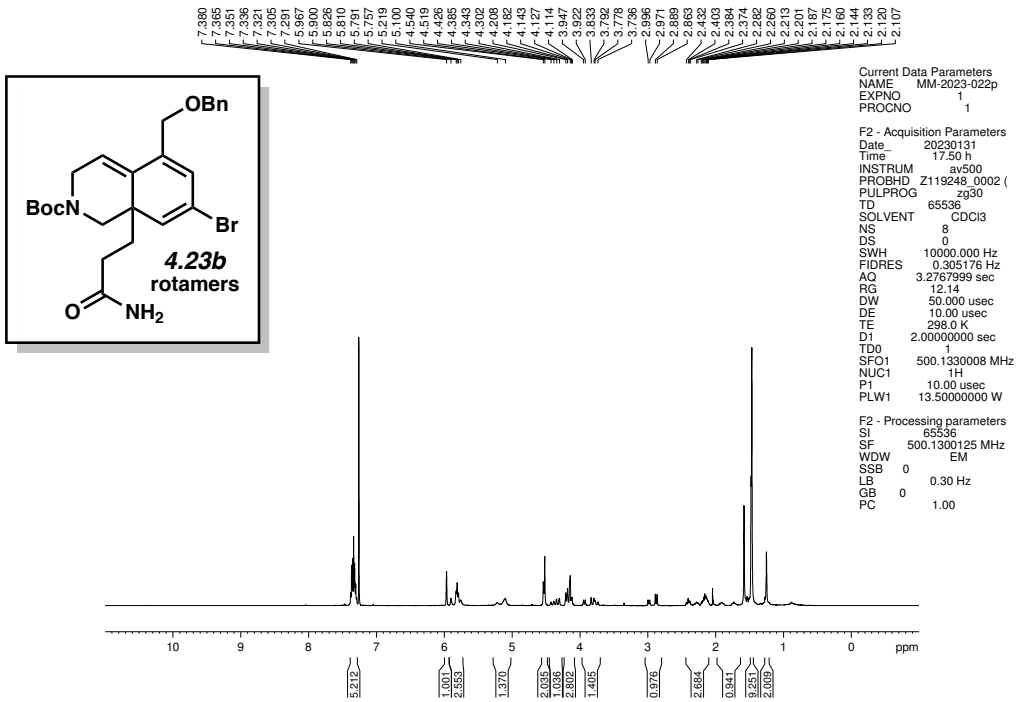

Figure 4.31 ^{1}H NMR (500 MHz, $CDCl_3$) of compound **4.23b**.

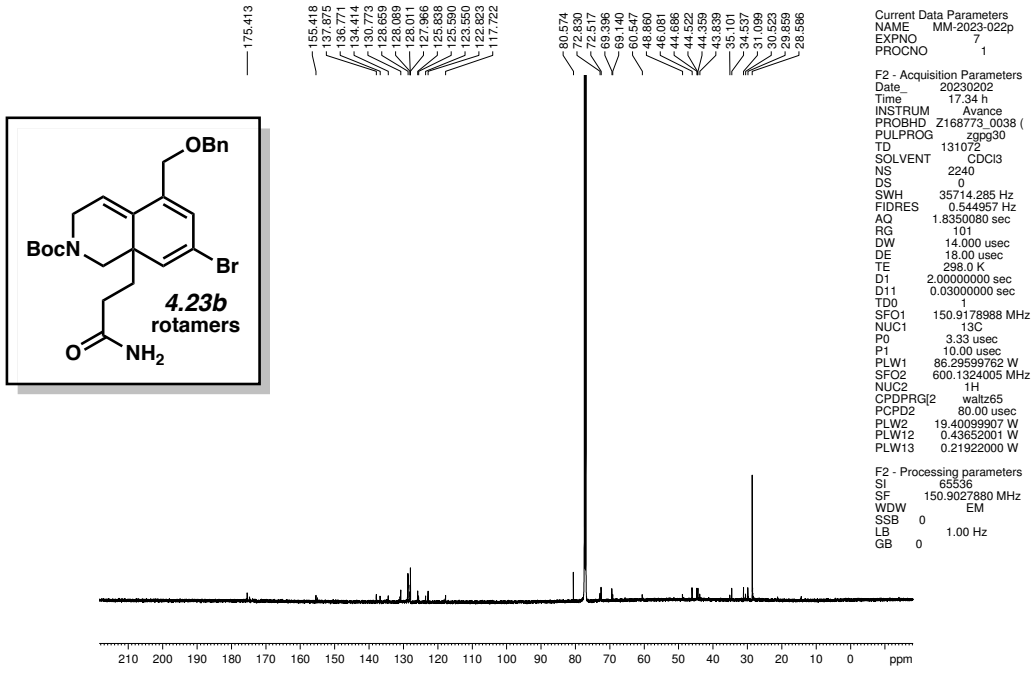

Figure 4.32 ^{13}C NMR (150 MHz, $CDCl_3$) of compound **4.23b**.

4.9 Notes and References

(1) Magnier, E.; Langlois, Y. Manzamine Alkaloids, Syntheses and Synthetic Approaches. *Tetrahedron* **1998**, *54*, 6201–6258.

(2) Radwan, M.; Hanora, A.; Khalifa, S.; Abou-El-Ela, S. H. Manzamines. *Cell Cycle* **2012**, *11*, 1765–1772.

(3) Ashok, P.; Ganguly, S.; Murugesan, S. Manzamine Alkaloids: Isolation, Cytotoxicity, Antimalarial Activity and SAR Studies. *Drug Discov. Today* **2014**, *19*, 1781–1791.

(4) Kobayashi, J. i.; Tsuda, M.; Kawasaki, N.; Matsumoto, K.; Adachi, T. Keramaphidin B, A Novel Pentacyclic Alkaloid from a Marine Sponge Amphimedon sp.: A Plausible Biogenetic Precursor of Manzamine Alkaloids. *Tetrahedron Lett.* **1994**, *35*, 4383–43864

(5) Tsuda, M.; Inaba, K.; Kawasaki, N.; Honma, K.; Kobayashi, J. Chiral Resolution of (±)–Keramaphidin B and Isolation of Manzamine L, a New β-Carboline Alkaloid from a Sponge Amphimedon sp. *Tetrahedron* **1996**, *52*, 2319−2324.

(6) Baldwin, J. E.; Claridge, T. D. W.; Culshaw, A. J.; Heupel, F. A.; Lee, V.; Spring, D. R.; Whitehead, R. C. Studies on the Biomimetic Synthesis of the Manzamine Alkaloids. *Chem. Eur. J.* **1999**, *5*, 3154−3161.

(7) Baldwin, J. E.; Claridge, T. D. W.; Culshaw, A. J.; Heupel, F. A.; Lee, V.; Spring, D. R.; Whitehead, R. C.; Boughtflower, R. J.; Mutton, I. M.; Upton, R. J. Investigations into the Manzamine Alkaloid Biosynthetic Hypothesis. *Angew. Chem., Int. Ed.* **1998**, *37*, 2661−2663.

(8) Baldwin, J. E.; Whitehead, R. C. On the Biosynthesis of Manzamines. *Tetrahedron Lett.* **1992**, *33*, 2059–2062.

(9) Meng, Z.; Spohr, S. M.; Tobegen, S.; Farès, C.; Fürstner, A. A Unified Approach to Polycyclic Alkaloids of the Ingenamine Estate: Total Syntheses of Keramaphidin B, Ingenamine, and Nominal Njaoamine I. *J. Am. Chem. Soc.* **2021**, *143*, 14402–14414.

(10) Tadross, P. M.; Stoltz, B. M. A Comprehensive History of Arynes in Natural Product Total Synthesis. *Chem*. *Rev*. **2012**, *112*, 3550–3577.

(11**)** Gampe, C. M.; Carreira, E. M. Arynes and Cyclohexyne in Natural Product Synthesis. *Angew*. *Chem*., *Int*. *Ed*. **2012,** *51*, 3766–3778.

(12) Takikawa, H.; Nishii, A.; Sakai, T.; Suzuki, K. Aryne-Based Strategy in the Total Synthesis of Naturally Occurring Polycyclic Compounds. *Chem*. *Soc*. *Rev*. **2018**, *47*, 8030–8056.

(13) Ippoliti, F. M.; Adamson, N. J.; Wonilowicz, L. G.; Nasrallah, D. J.; Darzi, E. R.; Donaldson, J. S.; Garg, N. K. Total Synthesis of Lissodendoric Acid A via Stereospecific Trapping of a Strained Cyclic Allene. *Science* **2023**, *379*, 261–265.

(14) Moser, W. R. The Reactions of *gem*-Dihalocyclopropanes with Organometallic Reagents. Ph.D. Dissertation, Massachusetts Institute of Technology Cambridge, MA, **1964**.

(15) Wittig, G.; Fritze, P. On the Intermediate Occurrence of 1,2-Cyclohexadiene. *Angew. Chem., Int. Ed.* **1966**, *5*, 846.

(16) Uyegaki, M.; Ito, S., Sugihara, Y.; Murata, I. 1-Benzoxepin and Its Valence Isomers, 4,5-benz-3-oxatricyclo[4.1.0.0^{2,7}]heptane and 3,4-benz-2-oxabicyclo-[3.2.1]-hepta-3,6-diene. *Tetrahedron Lett.* **1976**, *49*, 4473–4476.

(17) Christl, M., Braun, M., Wolz, E. & Wagner, W. 1-Phenyl-1-aza-3,4- Cyclohexadien, Das Erste Isodihydropyridin: Ertzeugung und Abfangreaktionen. *Chem. Ber.* **1994**, *127*, 1137–1142.

(18) Quintana, I.; Peña, D.; Pérez, D.; Guitián, E. Generation and Reactivity of 1,2-Cyclohexadiene Under Mild Reaction Conditions. *Eur. J. Org. Chem.* **2009**, *2009*, 5519−5524.

(19) Peña, D.; Iglesias, B.; Quintana, I.; Pérez, D.; Guitián, E.; Castedo, L. Synthesis and Reactivity of New Strained Cyclic Allene and Alkyne Precursors. *Pure Appl. Chem.* **2006**, *78*, 451−455.

(20) Jankovic, C. L.; West, F. G. 2+2 Trapping of Acyloxy-1,3-cyclohexadienes with Styrenes and Electron-Deficient Olefins. *Org. Lett.* **2022**, *24*, 9497–9501.

(21) Lofstrand, V. A.; West, F. G. Efficient Trapping of 1,2-Cyclohexadienes with 1,3-Dipoles. *Chem. Eur. J.* **2016**, *22*, 10763−10767.

(22) Lofstrand, V. A.; McIntosh, K. C.; Almehmadi, Y. A.; West, F. G. Strain-activated Diels−Alder Trapping of 1,2-Cyclohexadienes: Intramolecular Capture by Pendent Furans. *Org. Lett.* **2019**, *21*, 6231−6234.

(23) Almehmadi, Y. A.; West, F. G. A Mild Method for the Generation and Interception of 1,2-Cycloheptadienes with 1,3-dipoles. *Org. Lett.* **2020**, *22*, 6091−6095.

(24) Wang, B.; Constantin, M. G.; Singh, S.; Zhou, Y.; Davis, R. L.; West, F. G. Generation and Trapping of Electron-Deficient 1,2-Cyclohexadienes. Unexpected Hetero-Diels–Alder Reactivity. *Org. Biomol. Chem.* **2021**, *19*, 399–405.

(25) Hioki, Y.; Mori, A.; Okano, K. Steric Effects on Deprotonative Generation of Cyclohexynes and 1,2-Cyclohexadienes from Cyclohexenyl Triflates by Magnesium Amides. *Tetrahedron* **2020**, *76*, 131103.

(26) Inoue, K.; Nakura, R.; Okano, K.; Mori, A. One-pot Synthesis of Silylated Enol Triflates from Silyl Enol Ethers for Cyclohexynes and 1,2-Cyclohexadienes. *Eur. J. Org. Chem.* **2018**, 3343−3347.

(27) Westphal, M. V.; Hudson, L.; Mason, J. W.; Pradeilles, J. A.; Zecri, F. J.; Briner, K.; Schreiber, S. L. Water-Compatible Cycloadditions of Oligonucleotide-Conjugated Strained Allenes for DNA-Encoded Library Synthesis. *J. Am. Chem. Soc.* **2020**, *142*, 7776−7782.

(28) Anthony, S. M.; Wonilowicz, L. G.; McVeigh, M. S.; Garg, N. K. Leveraging Fleeting Strained Intermediates to Access Complex Scaffolds. *JACS Au* **2021**, *1*, 897–912.

(29) Kelleghan, A. V.; Witkowski, D. C.; McVeigh, M. S.; Garg, N. K. Palladium-Catalyzed Annulations of Strained Cyclic Allenes. *J. Am. Chem. Soc.* **2021**, *143*, 9338–9342.

(30) Yamano, M. M.; Kelleghan, A. V.; Shao, Q.; Giroud, M.; Simmons, B. J.; Li, B.; Chen, S.; Houk, K. N.; Garg, N. K. Intercepting Fleeting Cyclic Allenes with Asymmetric Nickel Catalysis. *Nature* **2020**, *586*, 242–247.

(31) McVeigh, M. S.; Kelleghan, A. V.; Yamano, M. M.; Knapp, R. R.; Garg, N. K. Silyl Tosylate Precursors to Cyclohexyne, 1,2-Cyclohexadiene, and 1,2-Cycloheptadiene. *Org. Lett.* **2020**, *22*, 4500−4504.

(32) Yamano, M. M.; Knapp, R. R.; Ngamnithiporn, A.; Ramirez, M.; Houk, K. N.; Stoltz, B. M.; Garg, N. K. Cycloadditions of Oxacyclic Allenes and a Catalytic Asymmetric Entryway to Enantioenriched Cyclic Allenes. *Angew. Chem., Int. Ed.* **2019**, *58*, 5653−5657.

(33) Barber, J. S.; Styduhar, E. D.; Pham, H. V.; McMahon, T. C.; Houk, K. N.; Garg, N. K. Nitrone Cycloadditions of 1,2-Cyclohexadiene. *J. Am. Chem. Soc.* **2016**, *138*, 2512−2515.

(34) Ramirez, M.; Svatunek, D.; Liu, F.; Garg, N. K.; Houk, K. N. Origins of *Endo* Selectivity in Diels–Alder Reactions of Cyclic Allene Dienophiles. *Angew. Chem., Int. Ed.* **2021**, *60*, 14989–14997.

(35) McVeigh, M. S.; Garg, N. K. Interception of 1,2-Cyclohexadiene with TEMPO Radical. *Tetrahedron Lett.* **2021**, *87*, 153539–153543.

(36) Spence, K. A.; Tena Meza, A.; Garg, N. K. Merging Metals and Strained Intermediates. *Chem Catalysis* **2022**, *2*, 1870–1879.

(37) Barber, J. S.; Yamano, M. M.; Ramirez, M.; Darzi, E. R.; Knapp, R. R.; Liu, F.; Houk, K. N.; Garg, N. K. Diels–Alder Cycloadditions of Strained Azacyclic Allenes. *Nat. Chem*. **2018**, *10*, 953–960.

(38) Nendel, M.; Tolbert, L. M.; Herring, L. E.; Islam, M. N.; Houk, K. N. Strained Allenes as Dienophiles in the Diels–Alder Reaction: An Experimental and Computational Study. *J. Org. Chem.* **1999**, *64*, 976–983.

(39) For a comprehensive review of strained cyclic allene chemistry through 2003, see: Christl, M. Cyclic Allenes Up to Seven-Membered Rings. *Modern Allene Chemistry*; Krause, N., Kashmi, S. A. K., Eds.; Wiley-VCH: Weinheim, 2005; pp 243–357.

(40) Xu, Q.; Hoye, T. R. A Distinct Mode of Strain-Driven Cyclic Allene Reactivity: Group Migration to the Central Allene Carbon Atom. *J. Am. Chem. Soc.* **2023**, *145*, 9867–9875.

(41) Witkowski, D. C.; McVeigh, M. S.; Scherer, G. M.; Anthony, S. M.; Garg, N. K. Catalyst-Controlled Annulations of Strained Cyclic Allenes with π-Allylpalladium Complexes. *J. Am. Chem. Soc.* **2023**, Accepted Article, https://doi.org/10.1021/jacs.3c03102.

(42) Wu, P.; Nielson, T. E. Scaffold Diversity from *N*-Acyliminium Ions. *Chem. Rev.* **2017**, *117*, 7811–7856.

(43) Memeo, M. G.; Quadrelli, P. Iminium Ions as Dienophiles in Aza-Diels–Alder Reactions: A Closer Look. *Chem. Eur. J.* **2012**, *18*, 12554–12582.

(44) Erkkilä, A.; Majander, I.; Pihko, P. M. Iminium Catalysis. *Chem. Rev.* **2007**, *107*, 5416–5470.

(45) Although our exploratory studies were performed without attempts to control absolute stereochemistry, our prior studies have demonstrated the feasibility of asymmetric synthesis of an allene precursor to provide enantioenriched cycloadducts; see Reference 13.

(46) We opted to pursue both variants of the ImDA reaction simultaneously to maximize likelihood of success and provide options for late-stage manipulations. In general, *N*-acyl ImDA reactions tend to utilize harsher reaction conditions. For pertinent reviews, see references 42, 43, and 44.

(47) This approach would omit the macrocyclic alkene, but was pursued as a model system due to relative ease of substrate synthesis.

(48) The regioisomeric ratios reported in this study are reflective of the selectivity with respect to the two olefins of the cyclic allene. A single regioisomer is consistently observed where bonds are formed between C8a of the allene with C1 of the pyrone and C4a of the allene with C4 of the pyrone (see Figure 4.2 for atom numbering).

(49) We opted to introduce the required stereochemistry at C4a early in the synthesis for the model system route to investigate the intramolecular ImDA with a diene trapping partner (**4.16**). However, if this olefin is not reduced, retro-Diels–Alder with loss of CO_2 leads to a triene motif, which we also explored as a trapping partner for the iminium and *N*-acyl-iminium Diels–Alder reaction (see Figure 4.7).

(50) Grieco, P. A.; Parker, D. T. Quinolizidine Synthesis via Intramolecular Immonium Ion Based Diels–Alder Reactions. Total Synthesis of (+)-Lupine, (+)-Epilupine, (+)-Cryptopleurine, and (+)-Julandine. *J. Org. Chem.* **1988**, *53*, 3325–3330.

(51) Formation of the iminium intermediate was validated via reductive amination control experiments following Fukuyama's approach; see the following reference for conditions employed: Ueda, H.; Satoh, H.; Matsumoto, K.; Sugimoto, K.; Fukuyama, T. Total Synthesis of (+)-Haplophytine. *Angew. Chem., Int. Ed.* **2009**, *48*, 7600–7603.

(52) Such challenges are inherent to macrocyclization processes. For a pertinent review, see: Marti-Centelles, V.; Mrituanjay, D. P.; Burguete, M. I.; Luis, S. V. Macrocyclization Reactions: The Importance of Conformational, Configurational, and Template-Induced Preorganization. *Chem. Rev.* **2015**, *115*, 8736–8834.

(53) One attractive approach involves cleavage of a twisted amide; for a pertinent review, see: Liu, C.; Szostak, M. Twisted Amides: From Obscurity to Broadly Useful Transition-Metal-Catalyzed Reactions by N–C Amide Bond Activation. *Chem*. *Eur*. *J*. **2017**, *23*, 7157–7173.

(54) Haydl, A. M.; Xu, K.; Breit, B. Regio- and Enantioselective Synthesis of *N*-Substituted Pyrazoles by Rhodium-Catalyzed Asymmetric Addition to Allenes. *Angew Chem., Int. Ed.* **2015**, *54*, 7149–7153.

(55) Cadierno, V. Synthetic Applications of the Parkins Nitrile Hydration Catalyst [PtH{(PMe2O)2H}(PMe2OH)]: A Review. *Appl. Sci.* **2015**, *5*, 380-401.

(56) The poor mass balance for the cycloaddition with silyl triflate **4.22b** is attributed to the general decomposition observed in the NMR of the crude reaction mixture.

(57) Dillon, P. W.; Underwood, G. R. Cyclic Allenes. I. The Electronic Structure and Probably Deformation of the Allene Linkage When Included in a Ring. An INDO-MO Study. *J. Am. Chem. Soc.* **1974**, *96*, 779–787.

CHAPTER FIVE

Strain-Promoted Diels–Alder Cycloadditions of Heterocyclic Allenes and α-Pyrones

Milauni M. Mehta,[†] Laura Wonilowicz,[†] and Neil K. Garg*

Manuscript in Preparation

5.1 Abstract

Strained cyclic intermediates that contain a functional group with a preferred linear geometry constrained in a six-membered ring are valuable synthetic building blocks. Diels–Alder cycloadditions of such intermediates are particularly useful as they generate two new bonds and multiple stereocenters. Whereas Diels–Alder cycloadditions of strained cyclic alkynes, such as arynes and cyclic alkynes, are most well-studied, the corresponding reactions of heterocyclic allenes are less developed. Specifically, most examples of Diels–Alder reactions with strained cyclic allenes involve the use of electron-rich diene trapping partners. This study focuses on the use of α-pyrones, which are ambiphilic reaction partners, in Diels–Alder trappings of heterocyclic allenes. We investigate regioselectivity trends with respect to both coupling partners and perform competition experiments to assess the influence of structural features on reaction rates. Additionally, the first ester-substituted oxacyclic allene is accessed and evaluated in a Diels–Alder reaction with α-pyrone. Lastly, we demonstrate the scalability of this methodology. This study provides insight into strained cyclic allene reactivity, as well as new synthetic tools for the rapid construction of complex, heterocyclic scaffolds.

5.2 Introduction

Intermediates containing a functional group with preferred linear geometry constrained within a six-membered ring can be leveraged to build structural complexity. Cycloadditions of

strained intermediates are particularly useful as they typically generate two new bonds and multiple stereocenters. In the 1950s–1960s, furans (**5.2**, where X = O, Figure 5.1), which are commonly employed as electron-rich dienes in Diels–Alder (DA) cycloadditions, were used to validate the existence of the strained cyclic intermediates benzyne[1,2,3,4] and cyclohexyne[5,6] (**5.3**, Figure 5.1). In contrast to furans, pyrones (**5.4**)[7] are relatively understudied dienes in DA reactions with strained cyclic alkynes (**5.3**). The first examples of benzyne[8,9] and cyclohexyne[10] undergoing the DA cycloaddition with α-pyrone were published in 1997 and 1998, respectively, three decades after furans had been demonstrated as competent reaction partners in the DA cycloadditions with strained cyclic alkynes.[11,12,13,14] To note, cycloadducts **5.5** are often unstable due to facile extrusion of CO_2 and subsequent aromatization; thus, although this method is useful for generating sp^2-rich molecules, the structural and stereochemical complexity built in the Diels–Alder reaction is typically ablated.[15,16,17,18,19]

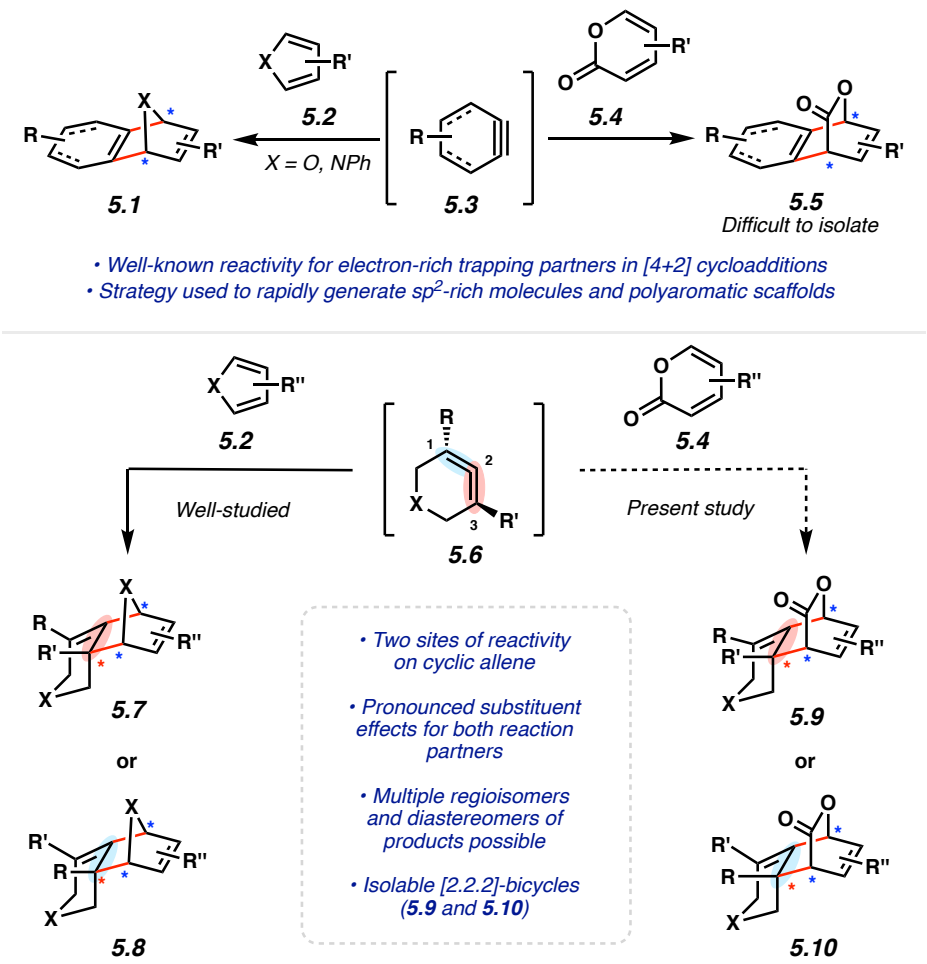

Figure 5.1. Overview of scaffolds accessible from strain-promoted Diels–Alder cycloadditions of intermediates **5.3** or **5.6** with furans **5.2** or pyrones **5.4**.

We were interested in evaluating a related class of strained intermediates, cyclic allenes (**5.6**, Figure 5.1),[20] in Diels–Alder cycloadditions with α-pyrones (**5.4**). Several factors motivated these studies: a) Similar to cyclic alkynes **5.3**, cyclic allenes **5.6** can be generated under mild reaction conditions and exhibit strain-promoted reactivity;[21,22,23,24,25,26,27,28,29,30,31,32,33,34,35,36,37,38,39,40,41,42,43,44,45] b) cyclic allenes **5.6** have two sites of reactivity that can be differentiated based on substituent effects, potentially allowing for the controlled formation of isomeric products; c) like linear allenes, cyclic allenes are chiral, providing long-term opportunities to control stereochemistry; d) although Diels–Alder trappings of cyclic allenes **5.6** have been known for

decades, nearly all studies focus on the use of electron-rich dienes **5.2** to provide cycloadducts **5.7** or **5.8**. The use of ambiphilic pyrones, which relies on the electronics of the substituents of both reaction partners to guide selectivity parameters of the cycloaddition,[46] are not well explored, but can deliver structurally complex and isolable[47] cycloadducts **5.9** or **5.10**. There is only one report describing DA cycloadditions between strained cyclic allenes and pyrones, which recently enabled the first total synthesis of the manzamine alkaloid lissodendoric acid A.[48]

In this manuscript, we study Diels–Alder reactions of strained heterocyclic allenes and α-pyrones. We describe the scope of the heterocyclic allene and pyrone components with a focus on electronic perturbations and principles that guide regioselectivity. In addition, we demonstrate the scalability and functional group tolerance of the cycloaddition. We also perform competition experiments to gauge relative reaction rates when employing different cyclic allene / pyrone combinations. Overall, this study provides insight into strained cyclic allene reactivity and selectivity trends, as well as new synthetic tools for the assembly of highly functionalized, sp^3-rich cycloadducts.

5.3 Scope of Cycloadditions with Methyl-Substituted Heterocyclic Allenes

We initiated our studies by investigating cycloadditions with allenes bearing either electron-donating or electron-withdrawing groups, beginning with methyl-substituted heterocyclic allene precursors **5.11** (Figure 5.2).[49] The use of Kobayashi-type silyl triflate precursors[12] **5.11** allows for cyclic allene generation under mild fluoride-based conditions. Both the oxygen- and nitrogen-containing variants of cyclic allenes were evaluated in this transformation, to compare their efficiency in the transformations, while also providing access to a variety of poly-heterocyclic cycloadducts. For the scope of the pyrone trapping partners, we evaluated unsubstituted pyrone

5.15, 4-chloro pyrone **5.16**, pyrone **5.17** with electron-donating groups, and pyrone **5.18** with an electron-withdrawing substituent. We observed that the combination of the ambiphilic nature of pyrones **5.15** and **5.16** with allenes **5.12** leads to a mixture of isomers **5.19a**/**b**, **5.20a/b**, **5.21a/b**, and **5.22a/b** (Entries 1 and 2, Figure 5.2).[50] It is inferred that the C1–C2 and C2–C3 olefins lack the electronic distinction required for a highly selective cycloaddition of one olefin over the other. Pyrone **5.17** did not undergo the DA cycloaddition with either oxa- or azacyclic allene **5.12**; instead, only dimers **5.23** and **5.24** were observed in moderate yields (Entry 3, Figure 5.2). Excitingly, ester-substituted pyrone **5.18** underwent the DA cycloaddition with allenes **5.12** to give cycloadducts with high regioselectivity. More specifically, cycloadducts **5.25** and **5.26** were isolated in 39% and 36% yield, respectively, as single observed isomers with >20:1 dr (Entry 4, Figure 5.2). These studies suggest that methyl-substituted cyclic allenes generally behave as relatively electron-rich dienophiles due to the electron-donating effect of the methyl group; as such, strongly electron-withdrawing substituents are required on the pyrone for the cycloadditions to proceed with high regioselectivity. It is also worth noting that all major Diels–Alder cycloadducts obtained reflect endo-selectivity, which is consistent with prior studies. [48,51]

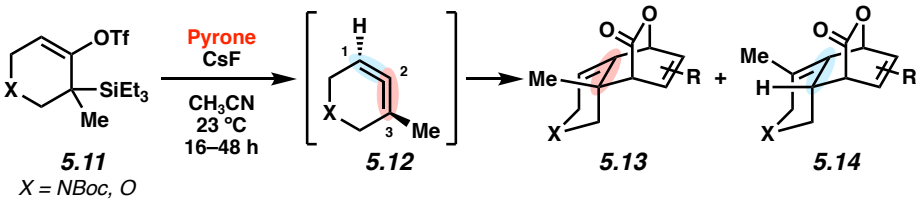

Entry	Pyrone	Products and yields[a] (dr)	
1	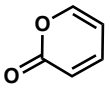 5.15	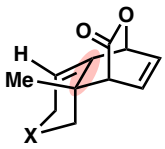 **5.19a** X = NBoc, 41% yield (>20:1 dr) **5.20a** X = O, 27% yield (>20:1 dr)	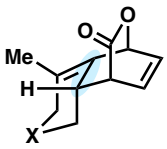 **5.19b** X = NBoc, 41% yield (>20:1 dr) **5.20b** X = O, 43% yield (>20:1 dr)
2	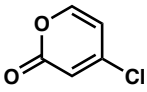 5.16	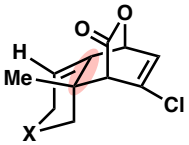 **5.21a** X = NBoc, 46% yield (>20:1 dr) **5.22a** X = O, 29% yield (>20:1 dr)	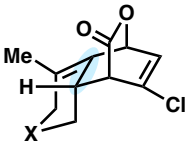 **5.21b** X = NBoc, 24% yield (>20:1 dr) **5.22b** X = O, 25% yield (>20:1 dr)
3	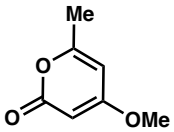 5.17	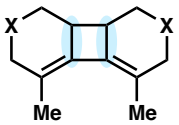	**5.23** X = NBoc, 49% yield (>20:1 dr) **5.24** X = O, 36% yield (>20:1 dr)
4	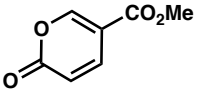 5.18	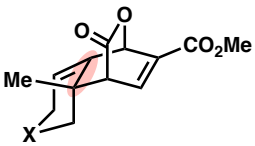	**5.25** X[b] = NBoc, 36% yield (>20:1 dr) **5.26** X[c] = O, 39% yield (>20:1 dr)

Figure 5.2. Scope of the DA cycloaddition with methyl-substituted oxa and azacyclic allenes (**5.12**) and pyrones **5.15**–**5.18**. Conditions unless otherwise stated: silyl triflate substrate (1.0 equiv), pyrone (5.0 equiv), CsF (5.0 equiv), acetonitrile (0.1 M) at 23 °C. Yields reflect the average of two experiments. [a]Yield determined by ^{1}H NMR analysis using 1,3,5-trimethoxybenzene as an external standard. [b]Reaction performed with 10.0 equiv CsF for 48 h. [c]Reaction performed with 2.5 equiv TBAF in THF for 16 h.

5.4 Cycloadditions with Ester-Substituted Oxacyclic Allenes

We also investigated cycloadditions of ester-substituted cyclic allenes **5.27** and **5.31** with both α-pyrone (**5.15**) and 2,5-dimethylfuran (**5.29**) as trapping partners (Figure 5.3). Cyclic allenes **5.27** and **5.31** were accessed from their corresponding silyl triflate precursors, whose syntheses are described in Section 5.8.2.1. We first evaluated ester-substituted allene **5.27** with pyrone **5.15** and observed a 33% yield of cycloadduct **5.28** with 4:1 dr. To further perturb the electronics of the system, we evaluated the corresponding cyclic allene bearing an additional methyl group (**5.31**) with **5.15**. The Diels–Alder trapping proceeded with similar regioselectivity, with cycloadduct **5.32** observed as the major product in 55% yield and 9:1 dr. Recognizing the strong influence of the ester substituents in determining the electronic nature of cyclic allenes **5.27** and **5.31**, we explored the use of 2,5-dimethylfuran (**5.29**) as an electron-rich trapping partner. In both cases, the cycloaddition proceeded with excellent yield and dr to provide cycloadducts **5.30** and **5.33**, which arose from cycloaddition on the C2–C3 olefins of **5.27** and **5.31**, respectively. Notably, these are the first strain-promoted Diels–Alder cycloadditions with ester-substituted oxacyclic allenes. These results suggest that the greater electronic matching between ester-substituted allenes and electron-rich trapping partners leads to more efficient and selective reactions in comparison to those with ambiphilic trapping partners.

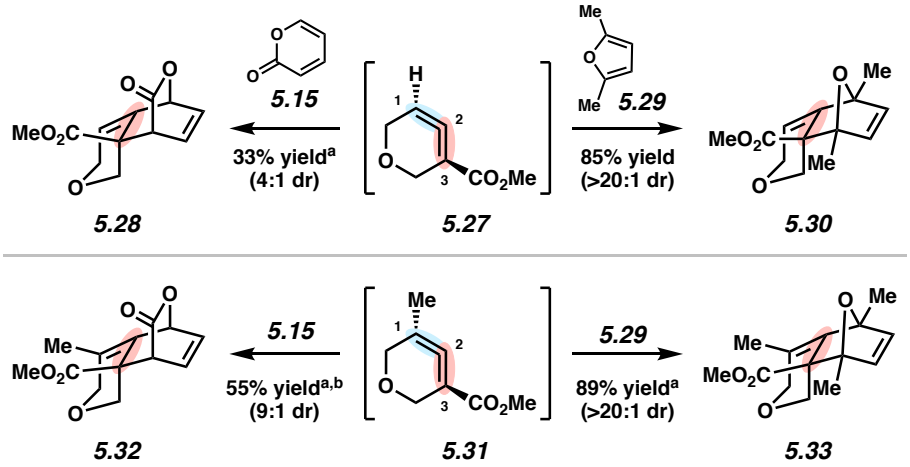

Figure 5.3. Cycloaddition reactions with α-pyrone (**5.15**) and 2,5-dimethylfuran (**5.29**) with ester-substituted oxacyclic allene **5.27** and disubstituted oxacyclic allene **5.31**. Conditions: silyl triflate substrate (1.0 equiv), pyrone (5.0 equiv), CsF (5.0 equiv), acetonitrile (0.1 M) at 23 ºC. [a]Yield determined by ^{1}H NMR analysis using 1,3,5-trimethoxybenzene as an external standard. [b]A constitutional isomer of **5.32** was also observed in ~20% yield, see Section 5.8.2.3 for further details.

Several aspects of the DA cycloadditions of strained cyclic allenes and pyrones should be noted. In particular, the reactions occur at ambient temperature and are enabled by the high ring strain of the cyclic allene as compared to the typically elevated temperature required for DA cycloadditions with pyrones as dienes.[21,46] Two new C–C bonds and three new stereocenters are formed in addition to other elements of structural complexity, such as a bicyclic ring system. Additionally, the use of reaction partners with either highly electron-donating or electron-withdrawing substituents resulted in the cycloaddition proceeding with high regioselectivity. To note, the cycloadducts arising from methyl-substituted allenes (**5.12**) displayed excellent diastereoselectivity, whereas the cycloadducts arising from the allenes with ester substituents (**5.27** and **5.31**) displayed a slightly lower diastereomeric ratio. While this is an empirical observation, we hypothesize that the difference in diastereomeric ratios of the cycloadducts is attributed to the different proposed mechanisms for the cycloadditions for methyl- vs ester-substituted allenes.[41,51]

5.5 Competition Experiments

Competition experiments were performed to compare the relative reaction efficiency of α-pyrone (**5.15**) and 2,5-dimethylfuran (**5.29**) with cyclic allenes generated from cyclic allene precursors **5.34** and **5.35** (Figure 5.4). In the first experiment, **5.34**, bearing an electron-donating methyl group, was treated with cesium fluoride in acetonitrile at 23 ºC for 16 hours in the presence of equimolar amounts of **5.15** and **5.29**. We observed that cycloaddition with pyrone **5.15** occurred preferentially to give the mixture of isomers **5.20a** and **5.20b** in 56% overall yield and >20:1 dr for each regioisomer. In the second experiment, allene precursor **5.35**, bearing the electron-withdrawing ester substituent, was subjected to the same reaction conditions with equimolar amounts of **5.15** and **5.29**. In this experiment, we observed almost exclusive cycloaddition between the ester-substituted allene and 2,5-dimethylfuran (**5.29**), which gave rise to cycloadduct **5.30** in 89% yield (>20:1 dr), with cycloadduct **5.28** observed in <5% yield. Whereas the methyl-substituted oxacyclic allene arising from **5.34** can be generally considered electron-rich thus leading to selective reactivity with electron-deficient pyrone over electron-rich furan, there is insufficient electronic bias between the two cyclic allene olefins to yield one constitutional isomer of the cycloadduct **5.20**. In the case of **5.35**, the electron-deficient cyclic allene generated in situ preferentially reacts with the electron rich diene **5.29**. The observation of the single constitutional isomer of **5.30** also suggests better electronic matching between the Diels–Alder partners. Overall, these findings underscore that electronic matching of the cycloaddition partners is largely influenced by the substituents on both the cyclic allene (i.e., methyl vs ester) and the pyrone.

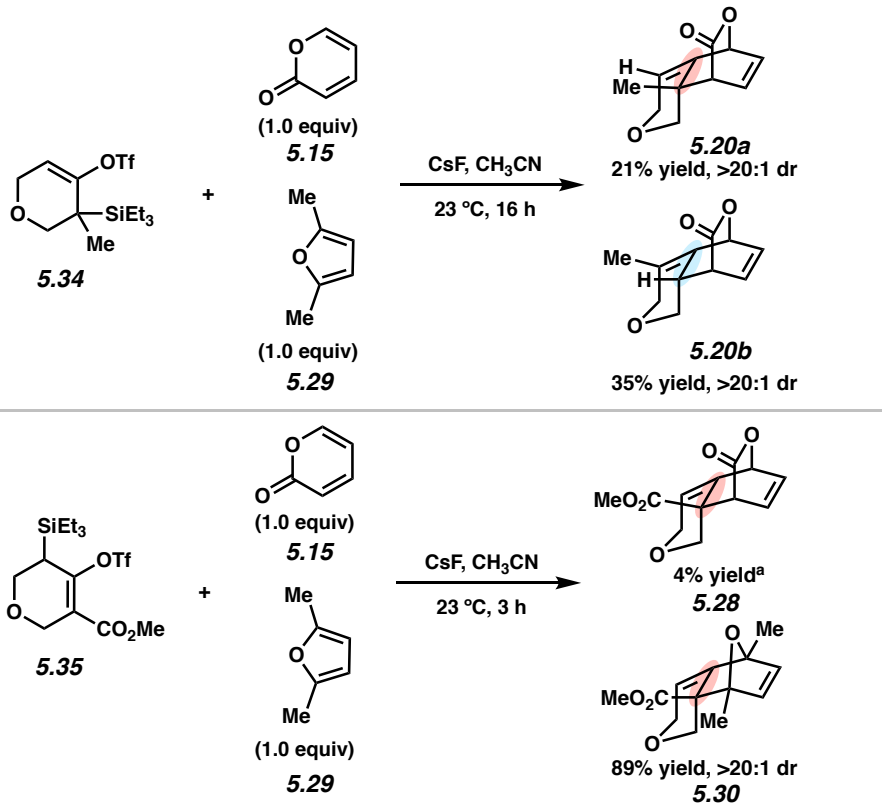

Figure 5.4. Competition experiments with allene precursors **5.34** and **5.35** with 2,5-dimethylfuran (**5.29**) and α-pyrone (**5.15**). Conditions unless otherwise stated: silyl triflate substrate (1.0 equiv), pyrone (5.0 equiv), CsF (5.0 equiv), acetonitrile (0.1 M) at 23 ºC. [a]Yield determined by ^{1}H NMR analysis using 1,3,5-trimethoxybenzene as an external standard.

5.6 1 mmol Scale Reaction

Strained heterocyclic allene/pyrone cycloadditions show promise for the scalable synthesis of structurally complex products bearing multiple functional groups. To demonstrate the scalability of this transformation, allyl-substituted silyl triflate **5.36** and ester-substituted pyrone **5.18** were treated with TBAF in THF at 23 °C for 16 h on a one mmol scale. In alignment with our previous results (Entry 4, Figure 5.2), the reaction proceeded with high regioselectivity giving rise to cycloadduct **5.37** in 60% yield with >20:1 dr. This example highlights the scalability and chemoselectivity of strain-promoted reactivity where, at ambient temperature, the cycloaddition occurs with the olefin of the cyclic allene over the olefin of the allyl group. Furthermore, **5.37**

contains several functional groups that are well poised for chemoselective elaboration to more complex products, including the allyl and ester groups, the lactone bridge, and the three distinct olefins. This demonstrates the utility of selective strain-promoted DA cycloadditions of cyclic allenes and pyrones in generating highly functionalized, sp^3-rich heterocycles.

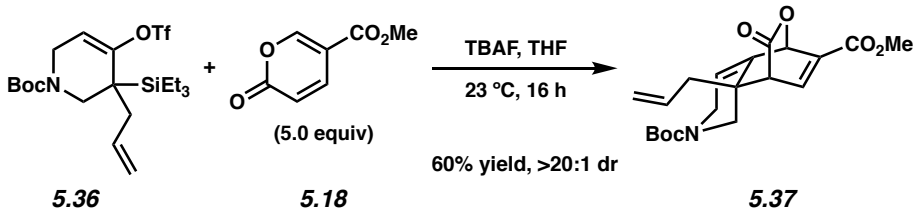

Figure 5.5. Strain-promoted DA cycloaddition with allene precursor **5.36** and pyrone **5.18** on one mmol scale. Conditions: silyl triflate substrate (1.0 equiv), pyrone (5.0 equiv), TBAF (2.5 equiv), THF (0.1 M) at 23 ºC.

5.7 Conclusion

We have conducted a systematic investigation of reactions between strained heterocyclic allenes and α-pyrones. Substituents on both reactants can be modulated to impart electronic bias, and, in turn, regioselectivity in the Diels–Alder cycloaddition reactions. Based on the competition experiments reported, it is hypothesized that predictable selectivity of the cycloaddition can be observed provided there is significant electronic bias between the two reaction partners. These studies provide fundamental insight into strained cyclic allene reactivity, new tools for the assembly of complex, sp^3-rich scaffolds, and the impetus for further studies geared toward the understanding of selectivity-guiding principles in strained cyclic allene trapping reactions.

5.8 Experimental Procedures

5.8.1 Materials and Methods.

Unless stated otherwise, reactions were conducted in flame-dried glassware under an atmosphere of nitrogen using anhydrous solvents (either freshly distilled or passed through activated alumina columns). All commercially obtained reagents were used as received unless otherwise specified. Non-commercially available substrates were synthesized according to known preparations or following protocols specified in the Experimental Procedures. Tetrahydrofuran (THF), diethyl ether (Et_2O), and acetonitrile (MeCN) were passed through an activated alumina column prior to use. Iodomethane (MeI), n-butyllithium (n-BuLi), potassium bis(trimethylsilyl)amide (KHMDS), diisopropylamine, hexamethylphosphoramide (HMPA), methyl cyanoformate (Mander's reagent), sodium hydride (NaH, 60 wt%), and tetrabutylammonium fluoride (TBAF, 1.0 M in THF) were obtained from Sigma-Aldrich. Sodium hydride was washed with pentane prior to use and stored in a Nitrogen-filled glovebox. Cesium fluoride (CsF) was purchased from Strem Chemicals. Triethylsilylchloride (TESCl) was obtained from Oakwood Prodcts, Inc. *N*-(5-chloro-2-pyridyl)bis(trifluoromethanesulfonimide) (Comins' Reagent), trifluoromethanesulfonic acid (Tf_2O), and methyl coumalate (**5.18**) were purchased from Combi-Blocks. Furan was purchased from Alfa Aesar. α-Pyrone (**5.15**) was purchased from Fischer Scientific. 4-chloro-2H-pyran-one (**5.16**) was purchased from Enamine. 4-methoxy-6-methyl-2H-pyran-2H-one (**5.17**) was purchased from Ambeed. Tf_2O, HMPA, and diisopropylamine were distilled over CaH_2 prior to use. Reaction temperatures at or above 23 °C were controlled using an IKAmag temperature modulator. Thin-layer chromatography (TLC) was conducted with EMD gel 60 F_{254} pre-coated plates (0.25 mm for analytical chromatography and 0.50 mm for preparative chromatography) and visualized using a combination of UV light,

anisaldehyde and potassium permanganate staining. Silicycle Siliaflash P60 (particle size 0.040–0.063 mm) was used for flash column chromatography. ^{1}H NMR, 2D-NOESY, 2D-HSQC, and 2D-HMBC spectra were recorded on Bruker spectrometers (at 400, 500, and 600 MHz) and are reported relative to the residual solvent signal. Data for ^{1}H NMR spectra are reported as follows: chemical shift (δ ppm), multiplicity, coupling constant (Hz) and integration. ^{13}C NMR spectra were recorded on Bruker spectrometers (at 100, 125, and 150 MHz) and are reported relative to the residual solvent signal. Data for ^{13}C-NMR spectra are reported in terms of chemical shift (δ ppm). ^{19}F NMR spectra were recorded on Bruker spectrometers (at 376 MHz) and reported in terms of chemical shift (δ ppm). IR spectra were obtained on a Perkin-Elmer UATR Two FT-IR spectrometer and are reported in terms of frequency of absorption (cm^{-1}). DART-MS spectra were collected on a Thermo Exactive Plus MSD (Thermo Scientific) equipped with an ID-CUBE ion source, a Vapur Interface (IonSense Inc.), and an Orbitrap mass analyzer. Both the source and MSD were controlled by Excalibur software v. 3.0. The analyte was spotted onto OpenSpot sampling cards (IonSense Inc.) using $CDCl_3$ or CH_2Cl_2 as the solvent. Ionization was accomplished using UHP He (Airgas Inc.) plasma with no additional ionization agents. The mass calibration was carried out using Pierce LTQ Velos ESI (+) and (–) Ion calibration solutions (Thermo Fisher Scientific).

Silyl enol ether **5.38**,[45] silyl ketone **5.41**,[45] and silyl triflate **5.44**[41] are known compounds. ^{1}H NMR spectral data match those reported in literature.

5.8.2 Experimental Procedure

5.8.2.1 Synthesis of Silyl Triflates

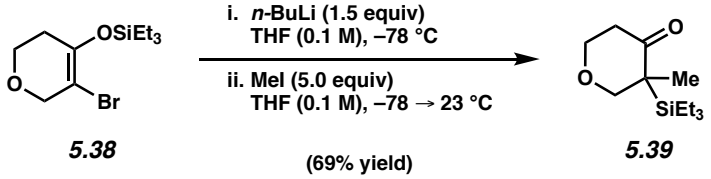

Silyl ketone 5.39: To a solution of silyl enol ether **5.38** (1.00 g, 3.41 mmol, 1.00 equiv) in THF (40 mL) at –78 °C was added *n*-BuLi (2.09 mL, 2.4 M in hexanes, 5.11 mmol, 1.50 equiv) over 3 min. The reaction was stirred at –78 °C for 1 h. Neat MeI (2.42 g, 1.07 mL, 17.0 mmol, 5.00 equiv) was then added over 4 min at –78 °C and the reaction was allowed to stir at this temperature for 2 h. The reaction was then warmed to 23 °C and stirred for an additional 5 h, after which it was quenched by the addition of deionized water (100 mL). The layers were shaken, then separated and the aqueous layer was extracted with EtOAc (4 x 50 mL). The combined organic layers were dried over $MgSO_4$, filtered, and concentrated under reduced pressure. The crude residue was purified by flash column chromatography (19:1 hexanes:EtOAc → 4:1 hexanes:EtOAc) to afford silyl ketone **5.39** as a colorless oil (540 mg, 69% yield). Silyl ketone **5.39**: R_f 0.29 (9:1 hexanes:EtOAc); ^{1}H NMR (500 MHz, $CDCl_3$): δ 4.26–4.18 (m, 2H), 3.70 (td, J = 3.6, 11.9, 1H), 3.38 (d, J = 11.4, 1H), 2.60 (ddd, J = 7.8, 12.1, 15.8, 1H), 2.36–2.30 (m, 1H), 1.08 (s, 3H), 0.99 (t, J = 7.9, 9H), 0.79–0.65 (m, 6H); ^{13}C NMR (150 MHz, $CDCl_3$): δ 209.9, 75.1, 67.9, 46.9, 41.5, 15.9, 7.8, 2.8; IR (film): 2956, 2878, 1687, 1460 cm^{-1}; HRMS–APCI (*m/z*) $[M + H]^+$ calcd for $C_{12}H_{25}O_2Si^+$, 229.1618; found 229.1621.

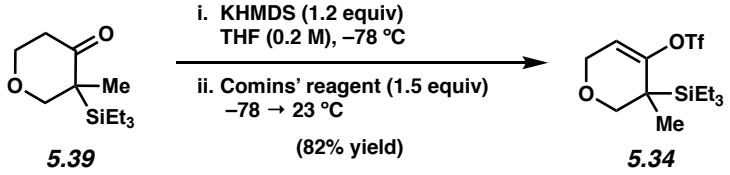

5.39 *5.34*

Silyl triflate 5.34: To a flask in the glovebox was added KHMDS (331 mg, 1.66 mmol, 1.20 equiv). The flask was then removed from the glovebox, charged with THF (2.30 mL), and cooled to –78 °C. To another flask was added the silyl ketone **5.39** (316 mg, 1.38 mmol, 1.00 equiv) and THF (2.30 mL). The ketone solution was then added dropwise over 5 min to the KHMDS solution at –78 °C. After stirring for 1 h at –78 °C, a solution of Comins' Reagent (812 mg, 2.07 mmol, 1.50 equiv) in THF (2.30 mL) was added dropwise over 3 min at –78 °C. The reaction was allowed to gradually warm to 23 ºC and stirred for 16 h. After this time, the reaction was quenched with saturated aq. NH_4Cl (15 mL) and diluted with deionized water (10 mL). The layers were shaken, then separated and the aqueous layer was extracted with Et_2O (3 x 15 mL). The combined organic layers were dried over $MgSO_4$, filtered, and concentrated under reduced pressure to provide the crude residue. The crude residue was purified via flash chromatography (7:1 → 1:1 hexanes:benzene) to afford silyl triflate **5.34** (408 mg, 82% yield) as a clear colorless oil. Silyl triflate **5.34**: R_f 0.52 (3:2 hexanes:benzene); ^{1}H NMR (600 MHz, $CDCl_3$): δ 5.67 (t, J = 2.89, 1H), 4.29 (dd, J = 3.2, 16.1, 1H), 4.19 (dd, J = 2.6, 16.1, 1H), 3.84 (d, J = 11.3, 1H), 3.58 (d, J = 11.4, 1H), 1.20 (s, 3H), 1.00 (t, J = 7.85, 9H), 0.72–0.66 (m, 6H); ^{13}C NMR (125 MHz, $CDCl_3$): δ 153.8, 118.5 (q, J = 319.3), 111.5, 73.7, 64.8, 31.3, 17.7, 7.8, 2.5; ^{19}F NMR (376 MHz, $CDCl_3$): δ –74.5; IR (film): 2958, 2880, 2835, 1670, 1416 cm^{-1}.

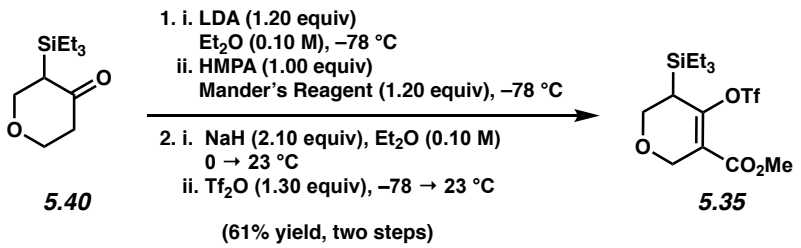

Silyl Triflate 5.35: To a solution of diisopropylamine (0.45 mL, 3.22 mmol, 1.20 equiv) in Et_2O (13 mL) at –78 ºC was added *n*-BuLi (1.34 mL, 2.4 M in hexanes, 3.22 mmol, 1.20 equiv) over 10 min. The reaction was stirred at –78 ºC for 20 min, then allowed to stir at 23 ºC for 10 min. Then the reaction mixture was cooled to –78 ºC and a solution of ketone **5.40** (575 mg, 2.68 mmol, 1.00 equiv) in Et_2O (13 mL) was added dropwise over 15 min and stirred at –78 ºC for 1 h. Then HMPA (467 μL, 2.68 mmol, 1.00 equiv) and Mander's reagent (256 μL, 3.22 mmol, 1.20 equiv) were added dropwise sequentially over 3 min at –78 ºC. The reaction was stirred at –78 ºC for 1 h, then quenched by the addition of cold deionized water (0 ºC, 15 mL) and allowed to warm to 23 ºC. The layers were separated and the aqueous layer was extracted with Et_2O (3 x 20 mL). The combined organic layers were dried over Na_2SO_4, filtered, and concentrated under reduced pressure to provide the crude product, which was purified by flash column chromatography (hexanes → 9:1 hexanes:EtOAc) to afford the β-keto ester as a colorless oil (605 mg, 2.22 mmol). This material was used directly in the next step.

To a flask in the glovebox was added NaH (68.5 mg, 2.85 mmol, 2.10 equiv). The flask was removed from the glovebox, CH_2Cl_2 (7 mL) was added, and the suspension was cooled to 0 ºC. A solution of the β-keto ester (370 mg, 1.36 mmol, 1.00 equiv) in CH_2Cl_2 (7 mL) was added dropwise over 10 min and allowed to warm to 23 ºC. After stirring for 1 h, the reaction was cooled to – 78 ºC and Tf_2O (298 μL, 1.77 mmol, 1.30 equiv) was added dropwise over 5 min. After stirring for 15 min, the reaction was allowed to warm to 23 ºC and stirred for 2 h. The reaction was cooled to 0 ºC and was quenched by the addition of deionized water (15 mL). The layers were separated

and the aqueous layer was extracted with CH_2Cl_2 (3 x 20 mL). The combined organic layers were dried over Na_2SO_4, filtered, and concentrated under reduced pressure to provide the crude product, which was purified by flash chromatography (9:1 hexanes:EtOAc) to afford silyl triflate **5.35** (364 mg, 60% yield, two steps) as a clear oil. Silyl triflate **5.35**: R_f 0.55 (5:1 hexanes:EtOAc); ^{1}H NMR (500 MHz, $CDCl_3$): δ 4.55 (dd, *J* = 16.2, 3.0, 1H), 4.36 (dd, *J* = 16.1, 1.8, 1H), 3.93 (d, *J* = 3.8, 2H), 3.78 (s, 3H), 2.12–2.07 (m, 1H), 1.00 (t, *J* = 7.9, 9H), 0.71 (q, *J* = 7.7, 6H); ^{13}C NMR (125 MHz, $CDCl_3$): δ 163.1, 154.6, 118.4 (q, *J* = 320.2), 117.5, 66.5, 65.6, 52.1, 30.2, 7.2, 2.9; ^{19}F NMR (376 MHz, $CDCl_3$): δ –74.3; (IR (film): 2957, 2880, 1716, 1655, 1424 cm^{-1}; HRMS–APCI (*m/z*) $[M + H]^+$ calcd for $C_{14}H_{24}F_3O_6SSi^+$, 405.1010; found 405.1005.

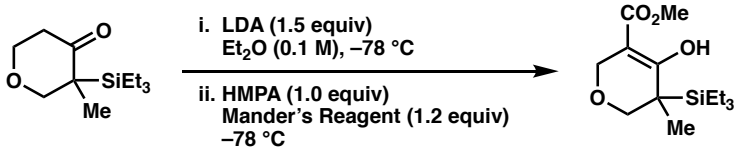

5.39 **(62% yield)** ***5.41***

β-Keto Ester 5.41: To a solution of diisopropylamine (0.29 mL, 2.07 mmol, 1.50 equiv) in Et_2O (5.5 mL) at –78 ºC was added *n*-BuLi (863 μL, 2.4 M in hexanes, 2.07 mmol, 1.50 equiv) over 10 min. The reaction was stirred at –78 ºC for 20 min, then allowed to stir at 23 ºC for 10 min. Then the reaction mixture was cooled to –78 ºC and a solution of ketone **5.39** (315 mg, 1.38 mmol, 1.00 equiv) in Et_2O (8.3 mL) was added dropwise over 7 min and stirred at –78 ºC for 1 h. Then HMPA (240 μL, 1.38 mmol, 1.00 equiv) and Mander's reagent (132 μL, 1.656 mmol, 1.20 equiv) were added dropwise sequentially over 5 min at –78 ºC. The reaction was stirred at –78 ºC for 3 h, then quenched by the addition of saturated aq. $NaHCO_3$ (10 mL) and allowed to warm to 23 ºC. The reaction further diluted with deionized water (25 mL) and Et_2O (25 mL). The layers were separated and the aqueous layer was extracted with Et_2O (3 x 20 mL). The combined organic layers were

dried over $MgSO_4$, filtered, and concentrated under reduced pressure to provide the crude product, which was purified by flash column chromatography (40:1 hexanes:EtOAc → 5:1 hexanes:EtOAc) to afford β-keto ester **5.41** (243 mg, 62% yield) as a light pink oil. β-keto ester **5.41**: R_f 0.60 (9:1 hexanes:EtOAc); ^{1}H NMR (500 MHz, $CDCl_3$): δ 4.32 (d, J = 13.7, 1H), 4.25 (d, J = 13.6, 1H), 3.84 (d, J = 11.3, 1H), 3.74 (s, 3H), 3.46 (d, J = 11.4, 1H), 1.20 (s, 3H), 0.98 (t, J = 8.1, 9H), 0.75–0.67 (m, 6H); ^{13}C NMR (125 MHz, $CDCl_3$): δ 177.5, 171.1, 94.5, 73.2, 64.2, 51.4, 32.3, 17.4, 7.9, 2.8; IR (film): 2954, 2877, 1746, 1653, 1607 cm^{-1}; HRMS–APCI (*m/z*) $[M + H]^+$ calcd for $C_{14}H_{27}O_4Si^+$, 287.1673; found 287.1682.

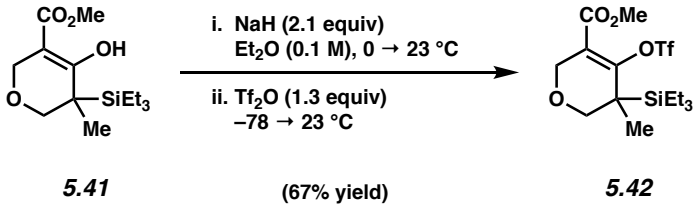

5.41 **(67% yield)** ***5.42***

Silyl Triflate 5.42: To a flask in the glovebox was added NaH (17.6 mg, 733 μmol, 2.10 equiv). The flask was removed from the glovebox and Et_2O (1.75 mL) was added at 0 ºC. Next, a solution of β-keto ester **5.41** (100 mg, 349 μmol, 1.00 equiv) in Et_2O (1.75 mL) was added dropwise over 3 min and the suspension was allowed to warm to 23 ºC. After stirring for 1 h, the reaction was cooled to –78 ºC and Tf_2O (76.7 μL, 454 μmol, 1.30 equiv) was added dropwise over 1 min. After stirring for 2 h at –78 °C, the reaction was allowed to warm to 23 ºC and stirred for 15 h. The reaction was quenched by the addition of deionized water (5 mL). The layers were separated and the aqueous layer was extracted with Et_2O (3 x 5 mL). The combined organic layers were dried over $MgSO_4$, filtered, and concentrated under reduced pressure to provide the crude product, which was purified by flash chromatography (19:1 hexanes:EtOAc → 5:1 hexanes:EtOAc) to afford silyl triflate **5.42** (98.5 mg, 67% yield) as a clear oil. Silyl triflate **5.42**: R_f 0.47 (9:1 hexanes:EtOAc);

^{1}H NMR (500 MHz, $CDCl_3$): δ 4.67 (d, *J* = 16.0, 1H), 4.17 (d, *J* = 16.0, 1H), 3.76 (s, 3H), 3.71 (m, 2H), 1.31 (s, 3H), 1.0 (t, *J* = 8.0, 9H), 0.71 (q, *J* = 7.6, 6H); ^{13}C NMR (125 MHz, $CDCl_3$): δ 163.8, 156.0, 118.8, 118.5 (q, *J* = 320.4), 74.2, 66.6, 52.3, 33.5, 17.7, 7.7, 2.4; ^{19}F NMR (376 MHz, $CDCl_3$): δ –72.5; IR (film): 2958, 2882, 1724, 1651, 1423 cm^{-1}; HRMS–APCI (*m/z*) $[M + H]^+$ calcd for $C_{15}H_{26}F_3O_6SSi^+$, 419.1166; found 419.1183.

5.8.2.2 Scope of Cycloadditions with Methyl-Substituted Heterocyclic Allenes

General Procedure: To a solution of silyl triflate **5.11** (0.10 mmol, 1.00 equiv) and pyrone (5.00 equiv) in MeCN (1.00 mL, 0.10 M) was added CsF (5.00 equiv). The reaction mixture was allowed to stir at 1000 RPM at 23 °C. After this time, the reaction mixture was filtered through a short plug of silica gel (3 cm silica) eluting with EtOAc (~10 mL) and then concentrated under reduced pressure. Yields were determined as an average of two experiments via NMR analysis using 1,3,5-trimethoxybenzene as an external standard.

Any deviations from the General Procedure are detailed below. For all compounds in which the diastereomeric ratio was >20:1, the minor diastereomer was not observed in the ^{1}H NMR of the crude reaction mixture.

*Note: Cycloadducts **5.19a/b**, **5.21a/b**, **5.23**, and **5.25** are isolated as a mixture of N-epimers. Protons in the ^{1}H NMR spectra are integrated together for each N-epimer. J-coupling values are provided for a single epimer. With regard to the ^{13}C NMR spectra, some peaks overlap, leading to less peaks than expected for the two N-epimers.*

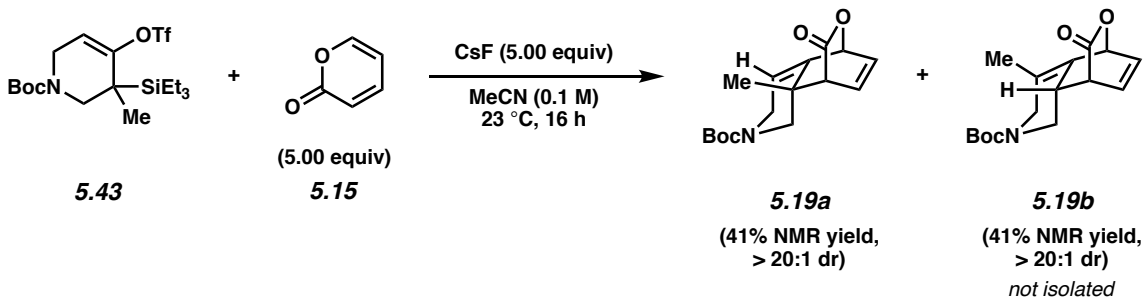

5.43 (5.00 equiv) ***5.15*** ***5.19a*** (41% NMR yield, > 20:1 dr) ***5.19b*** (41% NMR yield, > 20:1 dr) *not isolated*

Cycloadduct **5.19a**: An analytical sample of **5.19a** was obtained via preparative TLC (9:1 benzene:acetone). Cycloadduct **5.19a**: R_f 0.42 (9:1 benzene:acetone); ^{1}H NMR (500 MHz, $CDCl_3$): δ 6.49–6.41 (m, 1H), 6.39–6.30 (m, 1H), 5.68 (d, J = 3.3, 1H), 5.43 (d, J = 4.9, 1H), 4.25 (d, J =19.6, 1H), 3.93 (d, J = 11.4, 1H), 3.69–3.55 (m, 1H), 3.37 (t, J = 6.5, 1H), 2.21 (d, J = 11.6, 1H), 1.48 (s, 9H), 1.15 (s, 3H); ^{13}C NMR (125 MHz, $CDCl_3$): δ 171.7, 155.6, 155.3, 137.7, 137.3, 132.8, 132.5, 128.4, 128.1, 117.7, 117.2, 80.44, 80.39, 51.5, 51.3, 50.1, 43.2, 42.7, 35.6, 35.5, 28.6, 22.3, 22.2; IR (film): 2979, 2928, 1761, 1696, 1399 cm^{-1}; HRMS–APCI (*m/z*) $[M + H]^+$ calcd for $C_{16}H_{22}NO_4^+$, 292.1543; found 292.1526.

*Note: Regioisomeric cycloadduct **5.19b** was observed in the ^{1}H NMR spectrum of the crude material, but an analytical sample could not be obtained due to decomposition. The yield of cycloadduct **5.19b** reported in Figure 5.2 is based on integration of peaks analogous to those observed for cycloadduct **5.20b**.*

The structure of **5.19a** was verified by 2D-NOESY, as the following interactions were observed.

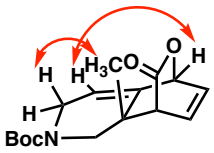

5.19a

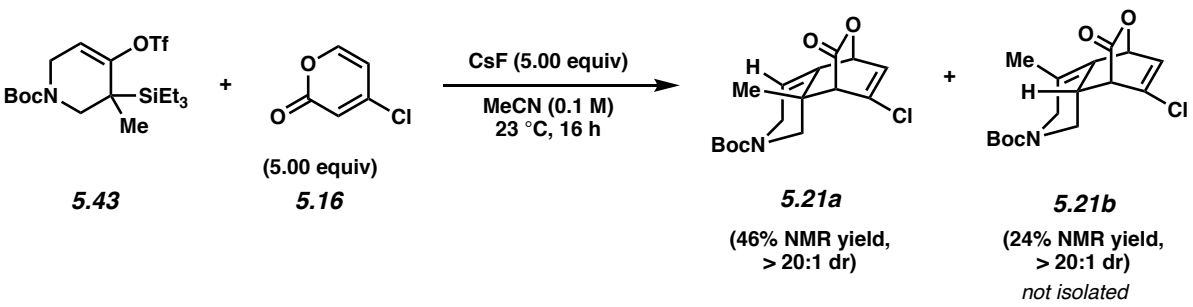

5.43 ***5.16*** ***5.21a*** ***5.21b***

(46% NMR yield, > 20:1 dr) **(24% NMR yield, > 20:1 dr)** *not isolated*

Cycloadduct **5.21a**: An analytical sample of **5.21a** was obtained via preparative TLC (1:1:1 hexanes:CH_2Cl_2:Et_2O). Cycloadduct **5.21a**: R_f 0.46 (1:1:1 hexanes:CH_2Cl_2:Et_2O); ^{1}H NMR (500 MHz, $CDCl_3$): δ 6.39 (ddd, J = 13.9, 5.6, 2.3, 1H), 5.76–5.64 (m, 1H), 5.42, (d, J = 5.7, 1H), 4.38–4.17 (m, 1H), 4.03 (dd, J = 89.2, 11.6, 1H), 3.65 (td, J = 20.0, 4.5, 1H), 3.49–3.41 (m, 1H), 2.41 (dd, J = 31.3, 11.7, 1H), 1.49 (s, 9H), 1.16 (s, 3H); ^{13}C NMR (125 MHz, $CDCl_3$): δ 169.4, 155.6, 155.3, 137.3, 136.7, 133.0, 132.6, 127.6, 127.2, 118.3, 117.9, 80.7, 80.6, 59.2, 59.1, 50.2, 49.1, 43.1, 42.6, 36.0, 35.9, 28.6, 22.0, 21.9; IR (film): 2975, 2936, 2876, 1768, 1697 cm^{-1}; HRMS–APCI (*m/z*) $[M + H]^+$ calcd for $C_{16}H_{21}ClNO_4^+$, 326.1154; found 326.1137.

*Note: Regioisomeric cycloadduct **5.21b** was observed in the ^{1}H NMR spectrum of the crude material, but an analytical sample could not be obtained due to decomposition. The yield of cycloadduct **5.21b** reported in Figure 5.2 is based on integration of peaks analogous to those observed for cycloadduct **5.20b**.*

The structure of **5.21a** was verified by 2D-NOESY, as the following interactions were observed.

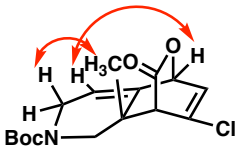

5.21a

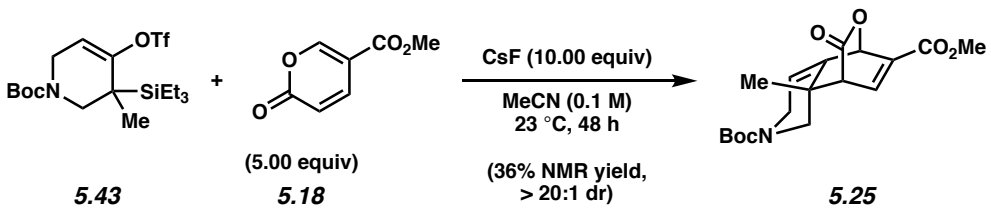

5.43 ***5.18*** ***5.25***

Cycloadduct **5.25**: 10.0 equivalents of CsF were added to this reaction mixture and the reaction was allowed to stir for 48 h. An analytical sample of **5.25** was obtained via preparative TLC (1:1:1 hexanes:CH_2Cl_2:Et_2O). Cycloadduct **5.25**: R_f 0.36 (1:1:1 hexanes:CH_2Cl_2:Et_2O); ^{1}H NMR (500 MHz, $CDCl_3$): δ 7.19–7.14 (m, 1H), 5.91 (s, 1H), 5.81 (d, J = 29.4, 1H), 4.26 (dd, J = 53.7, 19.7, 1H), 3.98 (dd, J = 90.5, 11.5, 1H), 3.81 (s, 3H), 3.67–3.57 (m, 1H), 3.53 (t, J = 5.6, 1H), 2.15 (dd, J = 46.1, 11.4, 1H), 1.47 (s, 9H), 1.19 (s, 3H); ^{13}C NMR (125 MHz, $CDCl_3$): δ 170.1, 162.1, 162.0, 155.5, 155.1, 137.1, 136.9, 136.7, 136.6, 136.5, 136.0, 119.1, 118.7, 80.64, 80.59, 52.61, 52.58, 51.9, 51.4, 50.1, 43.2, 42.7, 36.3, 36.2, 28.6, 22.3, 22.2; IR (film): 2974, 2860, 1769, 1723, 1697 cm^{-1}; HRMS–APCI (*m/z*) $[M + H]^+$ calcd for $C_{18}H_{24}NO_6^+$, 350.1598; found 350.1577.

The structure of **5.25** was verified by 2D-NOESY, as the following interactions were observed.

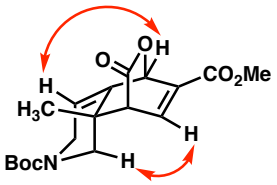

5.25

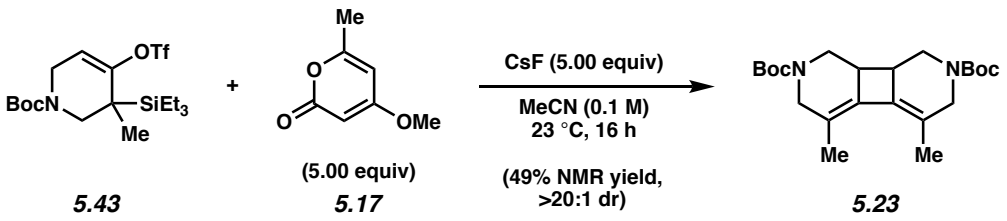

5.43 *5.17* *5.23*

Dimer **5.23**: An analytical sample of **5.23** was obtained via preparative TLC (2:1 hexanes:EtOAc). Dimer **5.23**: R_f 0.41 (5:1 hexanes:EtOAc); ^{1}H NMR (500 MHz, $CDCl_3$): δ 4.49–4.11 (m, 4H), 3.38 (t, J = 18.5, 2H), 2.62–2.34 (m, 4H), 1.76 (s, 6H), 1.46 (s, 18H); ^{13}C NMR (125 MHz, $CDCl_3$): δ 155.1, 134.4, 133.8, 118.2, 117.6, 79.9, 47.7, 47.1, 45.6, 44.4, 42.9, 28.6, 16.9; IR (film): 2975, 2926, 2857, 1695, 1404 cm^{-1}; HRMS–APCI (*m/z*) $[M + H]^+$ calcd for $C_{22}H_{35}N_2O_4^+$, 391.2591; found 391.2567.

*Note: **5.23** was isolated as a single isomer, but as an unassigned diastereomer due to the dimeric nature of the product.*

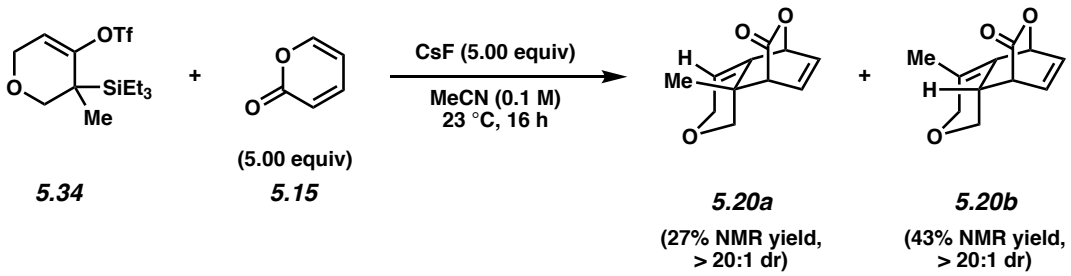

5.34 *5.15* ***5.20a*** ***5.20b***

(27% NMR yield, > 20:1 dr) **(43% NMR yield, > 20:1 dr)**

Cycloadducts **5.20a** and **5.20b**: An analytical sample of 1.4:1 mixture of **5.20a** and **5.20b** was obtained via preparative TLC (9:1 benzene:MeCN followed by 19:1 CH_2Cl_2:Et_2O). The cycloadducts were characterized as a mixture. Cycloadducts **5.20a** and **5.20b**: R_f 0.17 (2:1 hexanes:EtOAc) ^{1}H NMR (500 MHz, $CDCl_3$): **5.20a** (major isomer, proximal cycloadduct): δ 6.48–6.43 (m, 1H), 6.31–6.26 (m, 1H), 5.64 (br s, 1H), 5.45 (d, J = 5.2, 1H), 4.44 (d, J = 17.5, 1H), 4.08 (dd, J = 3.3, 17.7, 1H), 3.64 (d, J = 9.4, 1H), 3.30 (d, J = 5.9, 1H), 2.77 (d, J = 9.2, 1H), 1.29 (s, 3H); **5.20b** (minor isomer, distal cycloadduct): δ 6.55–6.51 (m, 1H), 6.20–6.15 (m, 1H),

5.74 (d, J = 5.0, 1H), 4.19 (d, J = 16.7, 1H), 4.03 (dd, J = 4.3, 9.3, 1H), 3.94–3.88 (m, 1H), 3.57–3.53 (m, 1H), 2.70–2.64 (m, 1H), 2.62–2.57 (m, 1H), 1.69 (s, 3H); ^{13}C NMR (125 MHz, $CDCl_3$): δ 172.5, 171.6, 136.5, 133.1, 132.5, 127.7, 126.5, 126.2, 126.0, 118.7, 77.3, 74.5, 71.7, 68.7, 67.4, 64.6, 50.6, 43.9, 34.3, 32.0, 22.5, 13.8; IR (film): 2981, 2922, 2886, 1759, 1382 cm^{-1}.

*Note: Compounds **5.20a** and **5.20b** were characterized as a mixture of regioisomers. Due to the selective decomposition of regioisomer **5.20b**, the ratio of cycloadducts **5.20a**:**b** changes upon purification of the crude reaction mixture.*

The structure of **5.20a** and **5.20b** was verified by 2D-NOESY, as the following interactions were observed.

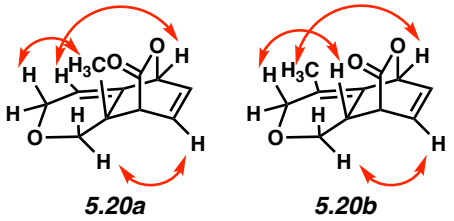

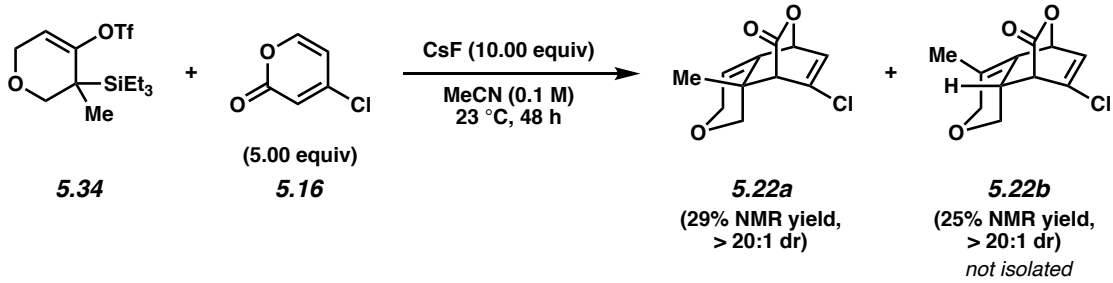

Cycloadduct **5.22a**: 10.0 equivalents of CsF were added to this reaction mixture and the reaction was allowed to stir for 48 h. An analytical sample of **5.22a** was obtained via preparative TLC (9:1 benzene:MeCN followed by 19:1 CH_2Cl_2:Et_2O). Cycloadduct **5.22a**: R_f 0.40 (2:1 hexanes:EtOAc); ^{1}H NMR (500 MHz, $CDCl_3$): δ 6.39 (dd, J = 2.1, 5.57, 1H), 5.67 (br s, 1H), 5.44 (d, J = 5.7, 1H), 4.44 (d, J = 17.8, 1H), 4.12 (dd, J = 3.2, 17.7, 1H), 3.74 (d, J = 9.6, 1H), 3.38 (d, J = 1.48, 1H), 2.97 (d, J = 9.5, 1H), 1.31 (s, 3H); ^{13}C NMR (125 MHz, $CDCl_3$): δ 169.3, 136.1, 132.4, 127.8,

119.4, 77.1, 70.6, 64.6, 58.2, 34.7, 22.2; IR (film): 2981, 2932, 2862, 1765, 1611 cm^{-1}; HRMS–APCI (*m/z*) $[M + H]^+$ calcd for $C_{11}H_{12}ClO_3^+$, 227.0470; found 227.0465.

*Note: Regioisomeric cycloadduct **5.22b** was observed in the ^1H NMR spectrum of the crude material, but an analytical sample could not be obtained due to decomposition. The yield of cycloadduct **5.22b** reported in Figure 5.2 is based on integration of peaks analogous to those observed for cycloadduct **5.20b**.*

The structure of **5.22a** was verified by 2D-NOESY, as the following interactions were observed.

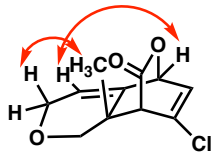

5.22a

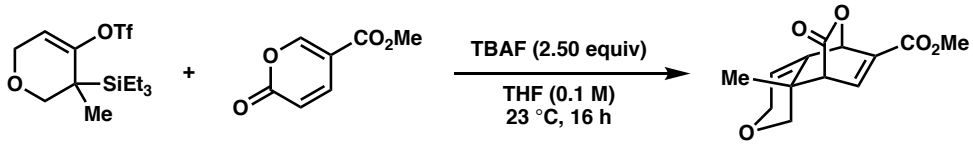

5.34 (5.00 equiv) ***5.18*** ***5.26***

Cycloadduct **5.26**: To a solution of silyl triflate **5.34** (36.0 mg, 0.10 mmol, 1.00 equiv) and pyrone **5.18** (77.1 mg, 0.50 mmol, 5.00 equiv) in THF (10.0 mL, 0.10 M) was added TBAF (0.25 mL, 0.25 mmol, 2.50 equiv). The reaction mixture was allowed to stir at 1000 RPM at 23 °C for 16 h. After this time, the reaction mixture was filtered through a short plug of silica gel (3 cm silica) eluting with EtOAc (~10 mL) and then concentrated under reduced pressure. The yield was determined as an average of two experiments via NMR analysis using 1,3,5-trimethoxybenzene as an external standard. An analytical sample of **5.26** was obtained via preparative TLC (3:1 hexanes:EtOAc, followed by 19:1 CH_2Cl_2:Et_2O, followed by 4:1:1 hexanes:CH_2Cl_2:Et_2O, followed by 5:1 benzene:acetone). Cycloadduct **5.26**: R_f 0.17 (2:1 hexanes:EtOAc); ^1H NMR (500 MHz, $CDCl_3$): δ 7.11 (dd, *J* = 1.7, 6.3, 1H), 5.94 (s, 1H), 5.77 (br s, 1H), 4.44 (d, *J* = 17.8, 1H),

4.07 (dd, J = 3.2, 18.1, 1H), 3.81 (s, 3H), 3.67 (d, J = 9.5 1H), 3.46 (d, J = 6.3, 1H), 2.70 (d, J = 9.5, 1H), 1.33 (s, 3H); ^{13}C NMR (125 MHz, $CDCl_3$): δ 169.9, 162.1, 137.4, 136.4, 135.3, 120.1, 76.7, 71.6, 64.7, 52.6, 51.0, 34.8, 22.5; IR (film): 2981, 2882, 1771, 1721, 1354 cm^{-1}; HRMS–APCI (*m/z*) $[M + H]^+$ calcd for $C_{13}H_{15}O_5^+$, 251.0914; found 251.0909.

The structure of **5.26** was verified by 2D-NOESY, as the following interactions were observed.

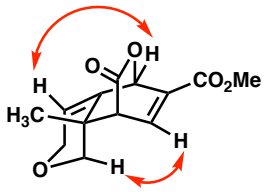

5.26

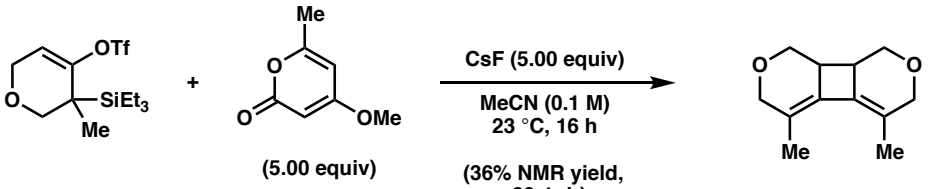

5.34 (5.00 equiv) ***5.17*** (36% NMR yield, >20:1 dr) ***5.24***

Dimer **5.24**: An analytical sample of **5.24** was obtained via preparative TLC (3:1 hexanes:EtOAc, followed by 4:1:1 hexanes:CH_2Cl_2:Et_2O, followed by a short plug of silica gel (3 cm silica) washing with hexanes (10 mL) and eluting with EtOAc (10 mL)). Dimer **5.24**: R_f 0.20 (5:1 hexanes:EtOAc); ^{1}H NMR (500 MHz, $CDCl_3$): δ 4.18 (d, J = 16.1, 2H), 4.05 (dd, J = 5.6, 10.0, 2H), 3.96 (d, J = 16.1, 2H), 3.15 (t, J = 9.7, 2H), 2.67 (br s, 2H), 1.69 (s, 6H); ^{13}C NMR (125 MHz, $CDCl_3$): δ 133.3, 118.1, 68.6, 67.4, 42.6, 15.1; IR (film): 2981, 2915, 2850, 1374, 1252 cm^{-1}; HRMS–APCI (*m/z*) $[M + H]^+$ calcd for $C_{12}H_{16}O_2^+$, 193.1223; found 193.1232.

*Note: **5.24** was isolated as a single isomer, but as an unassigned due to the dimeric nature of the product.*

5.8.2.3 Cycloadditions with Ester-Substituted Oxacyclic Allenes

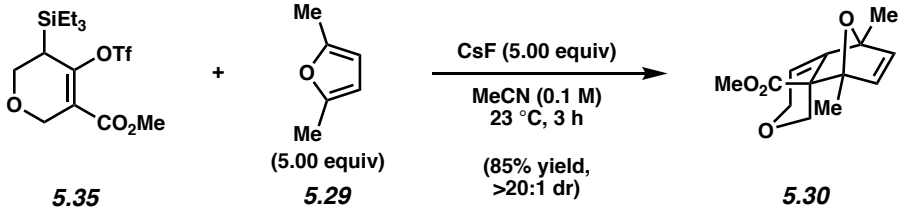

5.35 *5.29* *5.30*

Cycloadduct **5.30**: Silyl triflate **5.35** (20 mg, 0.05 mmol, 1.00 equiv) and furan **5.29** (27 µL, 0.25 mmol, 5.0 equiv) were added to the reaction flask and dissolved in MeCN (0.50 mL, 0.10 M). The solution was purged with nitrogen for 5 min and then CsF (38 mg, 0.25 mmol, 5.00 equiv) was added to the vial. The reaction mixture was then allowed to stir at 1000 RPM at 23 °C for 3 h. After this time, the reaction mixture was filtered through a short plug of silica gel (3 cm silica) eluting with EtOAc (~10 mL) and then concentrated under reduced pressure. Purification by flash chromatography (9:1 → 1:1 hexanes:EtOAc) afforded cycloadduct **5.30** as a clear oil (85% yield). Cycloadduct **5.30**: R_f 0.48 (1:1 hexanes:EtOAc); ^{1}H NMR (500 MHz, $CDCl_3$): δ 6.22 (d, J = 5.3, 1H), 5.89 (d, J = 5.3, 1H), 5.57–5.52 (m, 1H), 4.54 (d, J = 9.4, 1H), 4.31 (d, J = 17.0, 1H), 4.00–3.92 (m, 1H), 3.76–3.70 (m, 3H), 2.41 (d, J = 9.4, 1H), 1.73 (s, 3H), 1.58 (s, 3H); ^{13}C NMR (125 MHz, $CDCl_3$): δ 172.6, 142.7, 142.1, 133.8, 115.4, 88.6, 87.1, 70.7, 64.8, 57.4, 52.5, 16.8, 14.8; IR (film): 3090, 2933, 1722, 1452, 1217 cm^{-1}; HRMS–APCI (*m/z*) $[M + H]^+$ calcd for $C_{13}H_{17}O_4^+$, 237.1121; found 237.1121.

The structure of **5.30** was verified by 2D-NOESY, as the following interactions were observed.

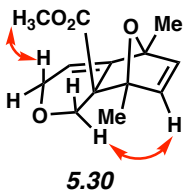

5.30

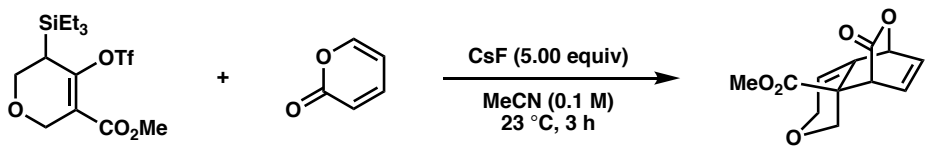

5.35 *5.15* *5.28*

Cycloadduct **5.28**: Silyl triflate **5.35** (21 mg, 0.05 mmol, 1.00 equiv) and pyrone **5.15** (21 µL, 0.26 mmol, 1.0 equiv) were added to the reaction flask and dissolved in MeCN (0.52 mL, 0.10 M). The solution was purged with nitrogen for 5 min and then CsF (39 mg, 0.26 mmol, 5.00 equiv) was added to the vial. The reaction mixture was then allowed to stir at 1000 RPM at 23 °C for 3 h. After this time, the reaction mixture was filtered through a short plug of silica gel (3 cm silica) eluting with EtOAc (~10 mL) and then concentrated under reduced pressure. Yields were determined via NMR analysis using 1,3,5-trimethoxybenzene as an external standard. An analytical sample of **5.28** was obtained via preparative TLC (1:1 hexanes:EtOAc). Cycloadduct **5.28**: R_f 0.21 (1:1 hexanes:EtOAc); ^{1}H NMR (500 MHz, $CDCl_3$): δ 6.57 (t, J = 6.0, 1H), 6.34–6.25 (m, 1H), 5.85 (s, 1H), 5.58 (d, J = 4.5, 1H), 4.52–4.33 (m, 2H), 4.11 (d, J = 18.3, 1H), 3.79 (d, J = 6.1, 1H), 3.75 (s, 3H), 2.75 (d, J = 9.5, 1H); ^{13}C NMR (125 MHz, $CDCl_3$): δ 171.3, 169.7, 135.4, 134.6, 131.8, 127.7, 126.4, 121.4, 76.4, 69.9, 69.1, 65.5, 65.4, 53.4, 49.0, 47.4, 47.2; IR (film): 3089, 2862, 1758, 1733, 1478 cm^{-1}; HRMS–APCI (*m/z*) $[M + H]^+$ calcd for $C_{12}H_{13}O_5^+$, 237.0758; found 237.0761.

The structure of **5.28** was verified by 2D-NOESY, as the following interaction was observed.

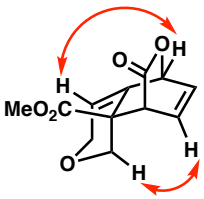

5.28

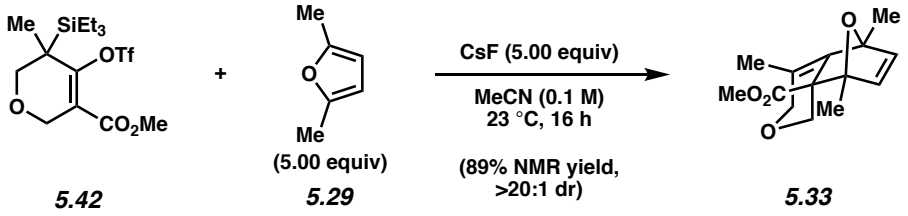

5.42 *5.29* *5.33*

Cycloadduct **5.33**: Silyl triflate **5.42** (42 mg, 0.1 mmol, 1.00 equiv) and furan **5.29** (53 µL, 0.50 mmol, 1.0 equiv) were added to the reaction flask and dissolved in MeCN (1.0 mL, 0.10 M). CsF (76 mg, 0.50 mmol, 5.00 equiv) was added to the vial. The reaction mixture was then allowed to stir at 1000 RPM at 23 °C for 16 h. After this time, the reaction mixture was filtered through a short plug of silica gel (3 cm silica) eluting with EtOAc (~10 mL) and then concentrated under reduced pressure. The yield was determined via NMR analysis using 1,3,5-trimethoxybenzene as an external standard. An analytical sample of **5.33** was obtained via preparative TLC (2:1 hexanes:EtOAc). Cycloadduct **5.33**: R_f 0.23 (1:1 hexanes:EtOAc); ^{1}H NMR (500 MHz, $CDCl_3$): δ 6.36 (d, J = 5.3, 1H), 5.87 (d, J = 5.3, 1H), 4.49 (d, J = 9.4, 1H), 4.07 (d, J = 16.4, 1H), 3.72 (s, 3H), 3.69 (d, 16.4, 1H), 2.38 (d, J = 9.4, 1H), 1.88 (s, 3H), 1.68 (s, 3H), 1.55 (s, 3H); ^{13}C NMR (125 MHz, $CDCl_3$): δ 173.0, 141.6, 135.3, 134.4, 123.1, 87.8, 87.6, 70.7, 68.6, 57.0, 52.4, 17.7, 16.8, 13.8; IR (film): 2981, 2867, 1721, 1453, 1384 cm^{-1}.

The structure of **5.33** was verified by 2D-NOESY (red) and 2D-HMBC (blue), as the following interactions were observed.

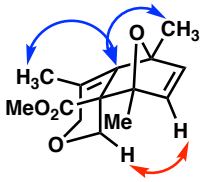

5.33

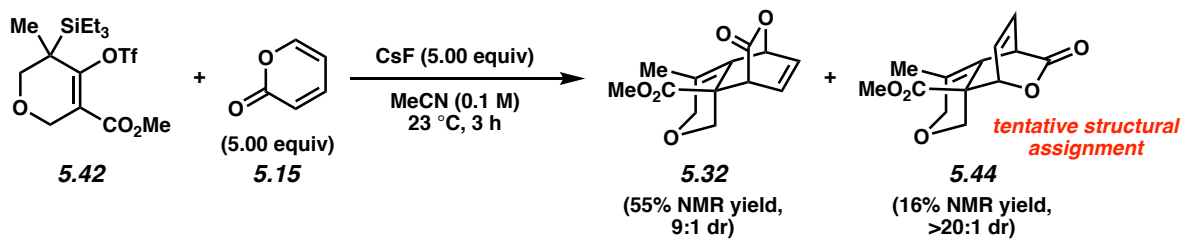

Cycloadducts **5.32** and **5.44**: Silyl triflate **5.42** (42 mg, 0.1 mmol, 1.00 equiv) and pyrone **5.15** (48 mg, 0.50 mmol, 1.0 equiv) were added to the reaction flask and dissolved in MeCN (1.0 mL, 0.10 M). CsF (76 mg, 0.50 mmol, 5.00 equiv) was added to the vial. The reaction mixture was then allowed to stir at 1000 RPM at 23 °C for 16 h. After this time, the reaction mixture was filtered through a short plug of silica gel (3 cm silica) eluting with EtOAc (~10 mL) and then concentrated under reduced pressure. Yields were determined via NMR analysis using 1,3,5-trimethoxybenzene as an external standard. Analytical samples of regioisomers **5.32** and **5.44** were obtained via preparative TLC (2:1 hexanes:EtOAc followed by 2:1:1 benzene:CH_2Cl_2:Et_2O). Cycloadduct **5.32** (major product): R_f 0.28 (1:1 hexanes:EtOAc); ^{1}H NMR (600 MHz, $CDCl_3$): 6.60–6.56 (m, 1H), 6.29–6.25 (m, 1H), 5.86 (dd, J = 1.5, 5.2, 1H), 4.36 (d, J = 9.4, 1H), 4.25 (d, J = 17.1, 1H), 3.92 (d, J = 17.0, 1H), 3.77 (dd, J = 1.6, 6.2, 1H), 3.74 (s, 3H), 2.76 (d, J = 9.4, 1H), 1.74 (s, 3H); ^{13}C NMR (125 MHz, $CDCl_3$): 171.8, 170.2, 133.9, 128.4, 126.7, 124.9, 74.0, 70.4, 68.8, 53.3, 47.2, 46.9, 14.1; IR (film): 2981, 2922, 1757, 1737, 1453 cm^{-1}. Cycloadduct **5.44** (minor product): R_f 0.23 (1:1 hexanes:EtOAc); ^{1}H NMR (600 MHz, $CDCl_3$): 6.56–6.52 (m, 1H), 6.50–6.46 (m, 1H), 5.26 (dd, J = 1.7, 4.6, 1H), 4.47 (d, J = 6.0, 1H), 4.34 (d, J = 10.0, 1H), 4.23 (d, J = 16.9, 1H), 4.00 (d, J = 16.9, 1H), 3.67 (s, 3H), 3.38 (d, J = 10.0, 1H), 1.81 (s, 3H); ^{13}C NMR (125 MHz, $CDCl_3$): 171.1, 169.2, 133.4, 131.5, 130.4, 117.7, 74.6, 69.5, 69.3, 52.8, 52.7, 45.3, 14.4; IR (film): 2981, 2886, 1749, 1728, 1382 cm^{-1}.

The structure of **5.32** and **5.44** was verified by 2D-NOESY and 2D-HMBC (blue), as the following interactions were observed.

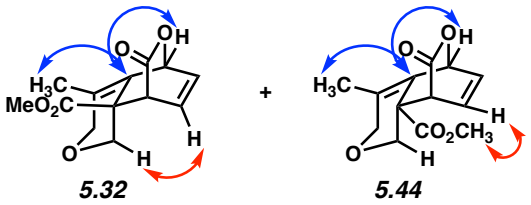

5.8.2.4 Competition Experiments

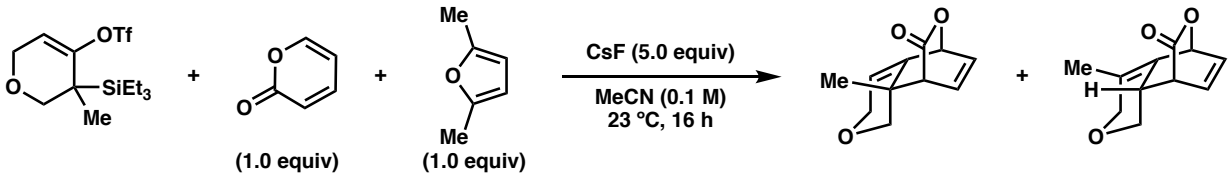

Silyl triflate **5.34** (18.0 mg, 50 µmol, 1.00 equiv), furan **5.29** (5.3 µL, 50 µmol, 1.0 equiv), and pyrone **5.15** (4.8 mg, 50 µmol, 1.0 equiv) were added to the reaction flask and dissolved in MeCN (500 µL, 0.10 M). CsF (38.0 mg, 250 µmol, 5.00 equiv) was added to the vial. The reaction mixture was then allowed to stir at 1000 RPM for 16 h at 23 °C. After this time, the reaction mixture was filtered through a short plug of silica gel (3 cm silica) eluting with EtOAc (~10 mL) and then concentrated under reduced pressure. Yields were determined via NMR analysis using 1,3,5-trimethoxybenzene as an external standard. Characterization data for **5.20a** and **5.20b** are detailed in Section 5.8.2.3.

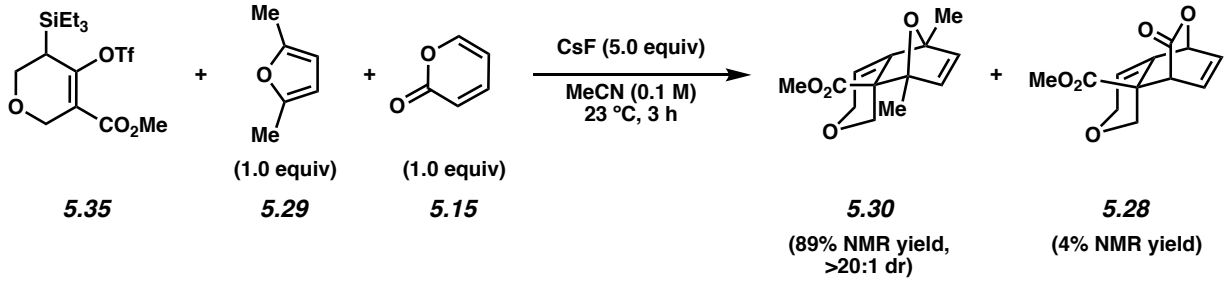

Silyl triflate **5.35** (20.0 mg, 49.4 µmol, 1.00 equiv), furan **5.29** (5.3 µL, 49 µmol, 1.0 equiv), and pyrone **5.15** (3.4 µL, 49 µmol, 1.0 equiv) were added to the reaction flask and dissolved in MeCN

(494 μL, 0.10 M). The solution was purged with nitrogen for 5 min and then CsF (37.6 mg, 247 μmol, 5.00 equiv) was added swiftly to the vial. The reaction mixture was then allowed to stir at 1000 RPM at 23 °C for 3 h. After this time, the reaction mixture was filtered through a short plug of silica gel (3 cm silica) eluting with EtOAc (~10 mL) and then concentrated under reduced pressure. Yields were determined via NMR analysis using 1,3,5-trimethoxybenzene as an external standard. Characterization data for **5.30** and **5.28** are detailed in Section 5.8.2.3.

5.8.2.5 1 mmol Scale Reaction

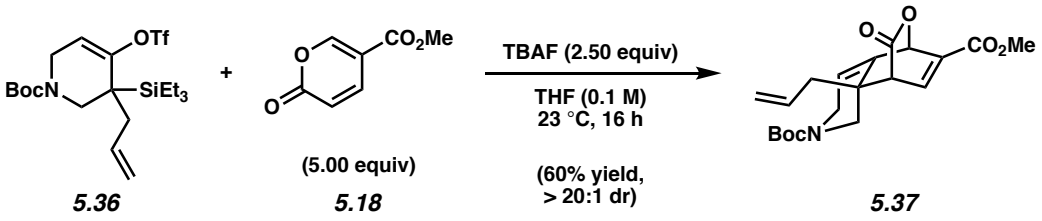

Cycloadduct 5.37: To a solution of silyl triflate **5.36** (486 mg, 1.00 mmol, 1.00 equiv) and pyrone **5.18** (771 mg, 5.00 mmol, 5.00 equiv) in THF (10.0 mL, 0.10 M) was added TBAF (2.50 mL, 2.50 mmol, 2.50 equiv). The reaction mixture was allowed to stir at 1000 RPM at 23 °C for 16 h. After this time, the reaction mixture was filtered through a short plug of silica gel (3 cm silica) eluting with EtOAc (75 mL) and then concentrated under reduced pressure. The crude material was purified by column chromatography (9:1 → 1:1 hexanes:EtOAc) to afford **5.37** (227 mg, 60% yield) as an amorphous white foam. Cycloadduct **5.37**: R_f 0.54 (1:1 hexanes:EtOAc); ^{1}H NMR (500 MHz, DMSO-d_6): δ 7.28 (td, J = 6.4, 2.0, 1H), 6.00 (s, 1H), 5.95 (dd, J = 19.3, 3.3, 1H), 5.88–5.71 (m, 1H), 5.22 (dd, J = 27.2, 10.2, 1H), 5.08 (t, J = 18.0, 1H), 4.19–3.99 (m, 2H), 3.79 (dd, J = 9.9, 6.4, 1H), 3.74 (s, 3H), 3.57 (qd, J = 19.4, 4.8, 1H), 2.31–2.16 (m, 1H), 1.93 (dd, J = 63.0, 12.1, 1H), 1.82–1.71 (m, 1H), 1.41 (d, J = 4.6, 9H); ^{13}C NMR (125 MHz, DMSO-d_6): δ 170.3, 162.0, 154.7, 154.3, 138.23, 138.16, 136.7, 136.5, 135.9, 135.8, 131.9, 131.8, 120.8, 120.7,

120.2, 120.1, 79.8, 76.5, 76.4, 55.4, 52.8, 48.3, 48.3, 47.1, 46.1, 43.2, 42.9, 38.5, 28.5; IR (film): 3082, 2872, 1767, 170, 1698 cm^{-1}; HRMS–APCI (*m/z*) $[M + H]^+$ calcd for $C_{20}H_{26}NO_6^+$, 376.1755; found 376.1753.

The structure of **5.37** was verified by 2D-NOESY (red) and 2D-HMBC (blue), as the following interactions were observed.

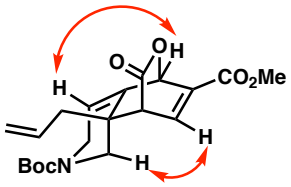

5.37

5.9 Spectra Relevant to Chapter Five:

Strain-Promoted (4+2) Cycloadditions of Heterocyclic Allenes and α-Pyrones

Milauni M. Mehta,[†] Laura Wonilowicz,[†] and Neil K. Garg*

Manuscript in Preparation

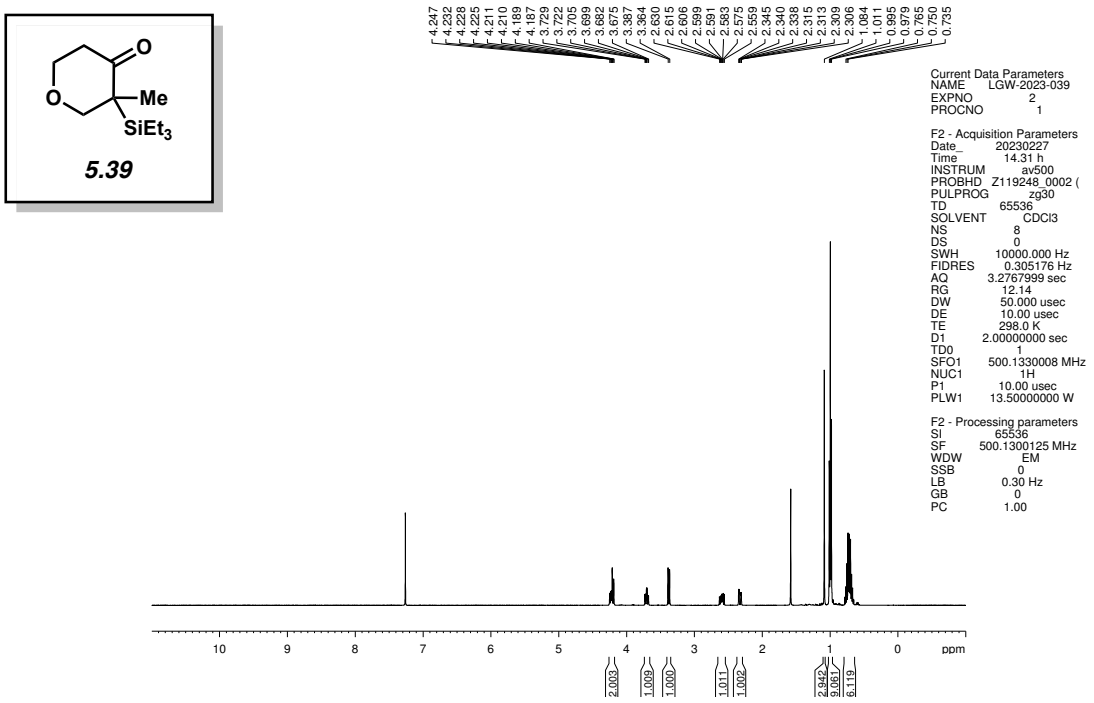

Figure 5.6. ^{1}H NMR (500 MHz, $CDCl_3$) of compound **5.39**.

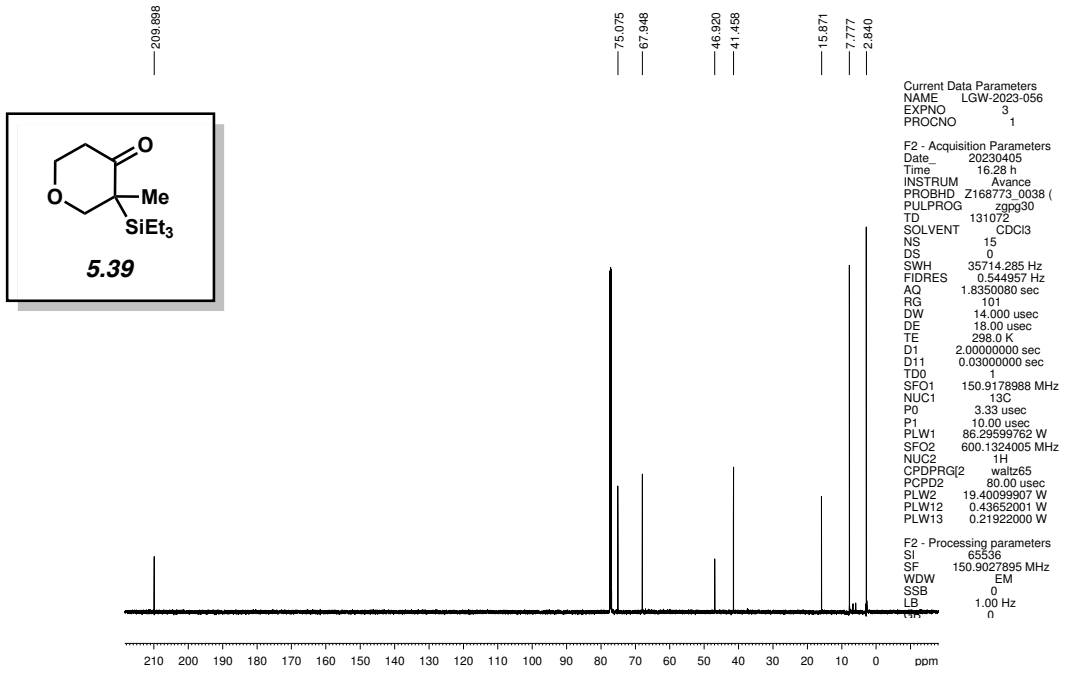

Figure 5.7. ^{13}C NMR (150 MHz, $CDCl_3$) of compound **5.39**.

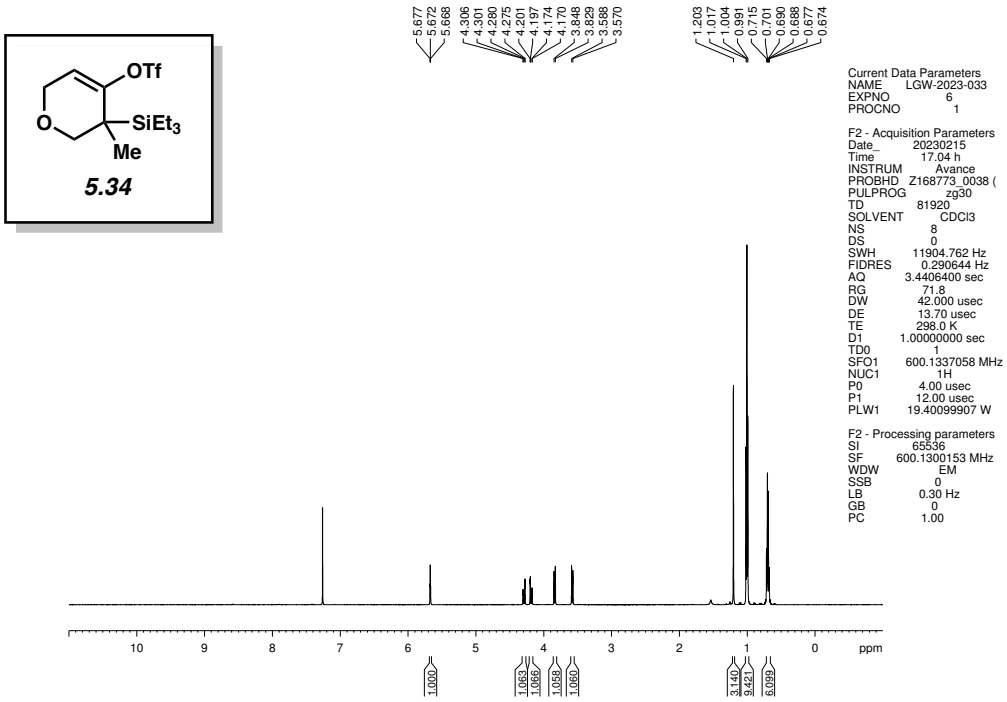

Figure 5.8. ^{1}H NMR (600 MHz, $CDCl_3$) of compound **5.34**.

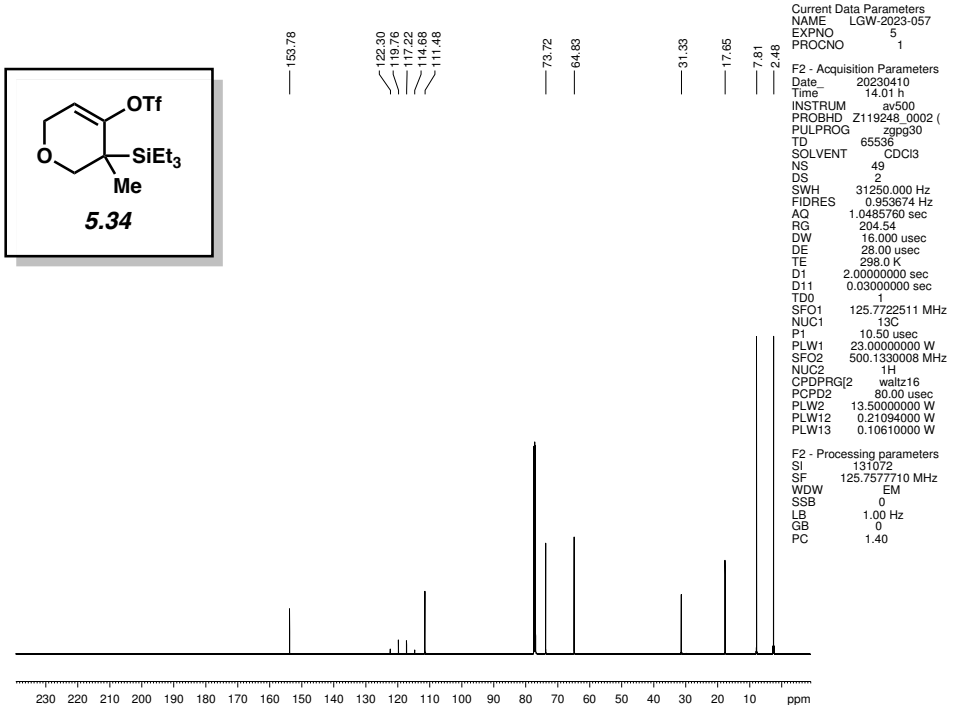

Figure 5.9. ^{13}C NMR (125 MHz, $CDCl_3$) of compound **5.34**.

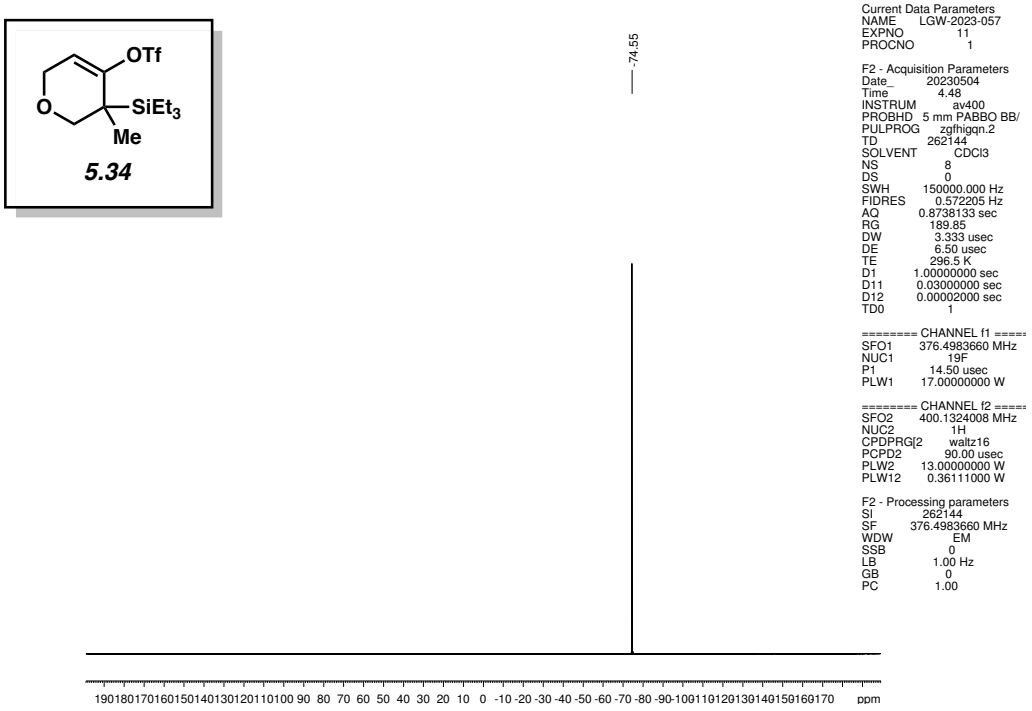

Figure 5.10. ^{19}F NMR (376 MHz, $CDCl_3$) of compound **5.34**.

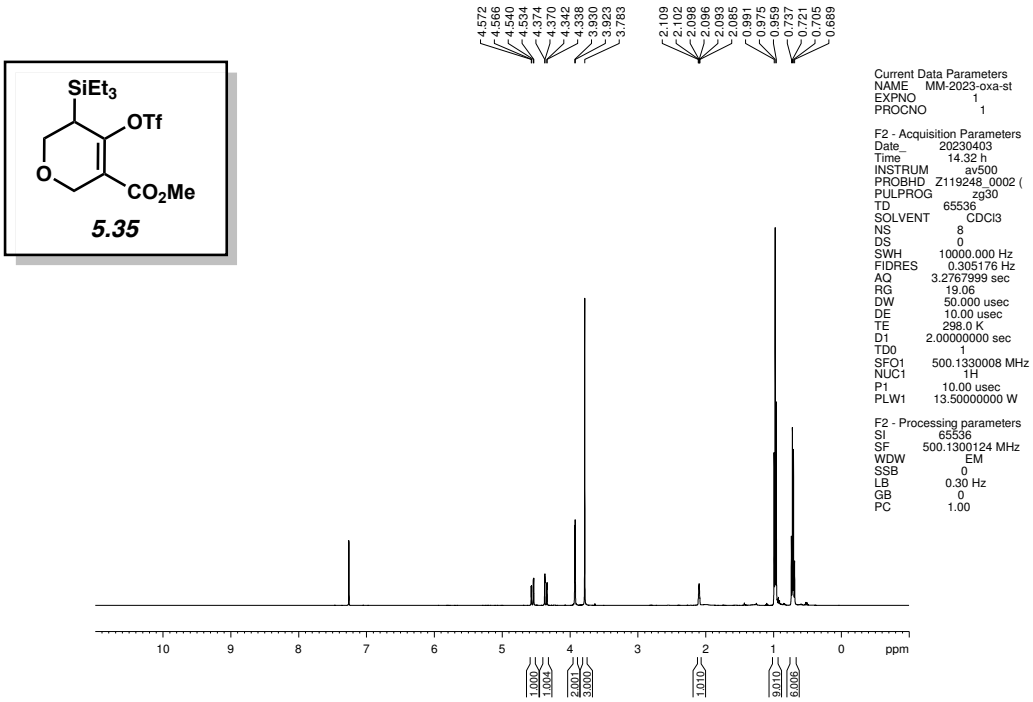

Figure 5.11. ^{1}H NMR (500 MHz, $CDCl_3$) of compound **5.35**.

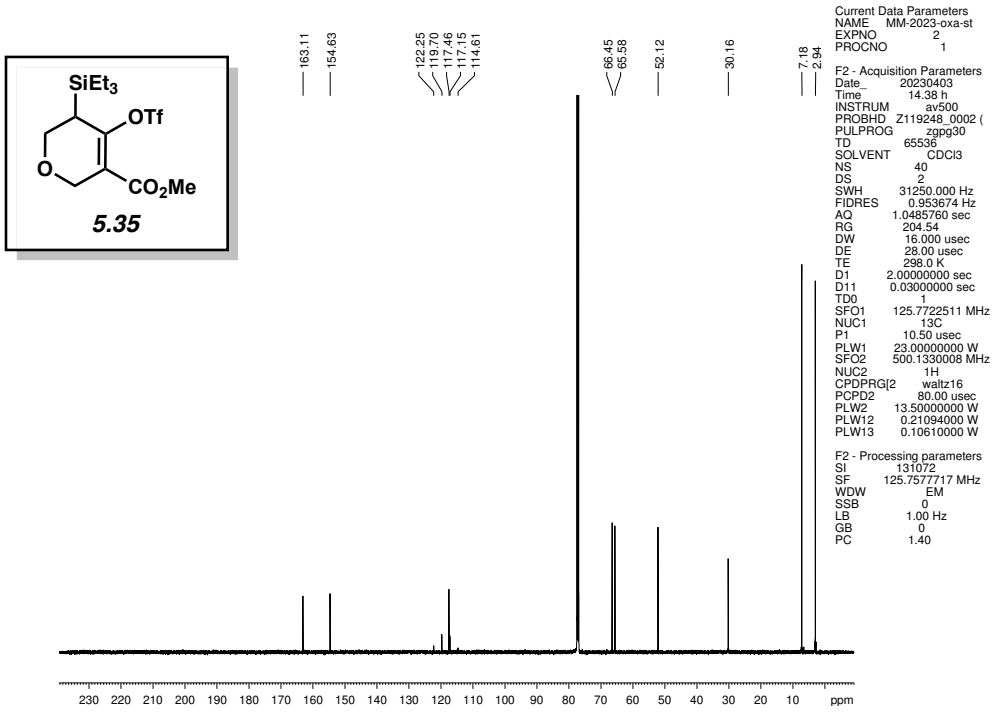

Figure 5.12. ^{13}C NMR (125 MHz, $CDCl_3$) of compound **5.35**.

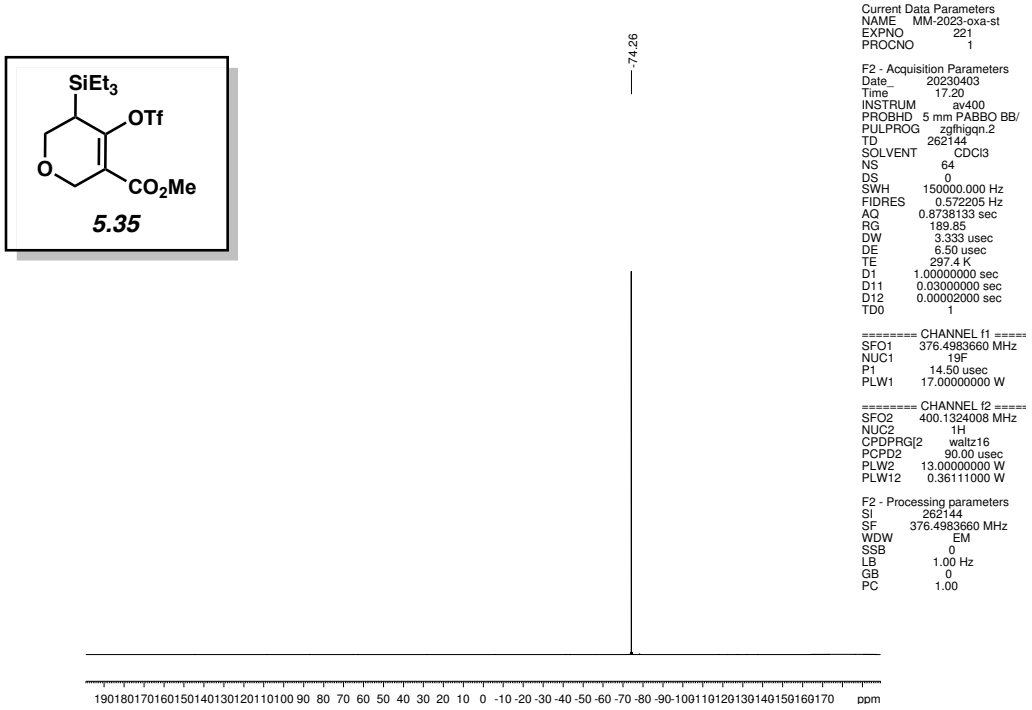

Figure 5.13. ^{19}F NMR (376 MHz, $CDCl_3$) of compound **5.35**.

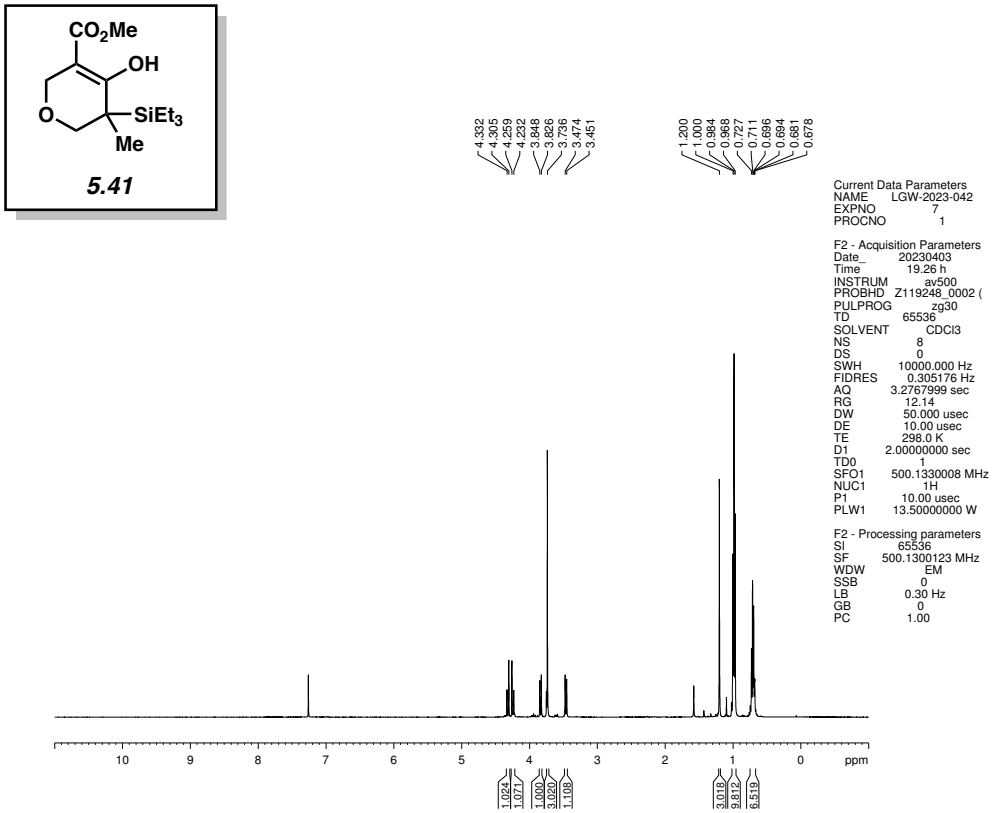

Figure 5.14. ^{1}H NMR (500 MHz, $CDCl_3$) of compound **5.41**.

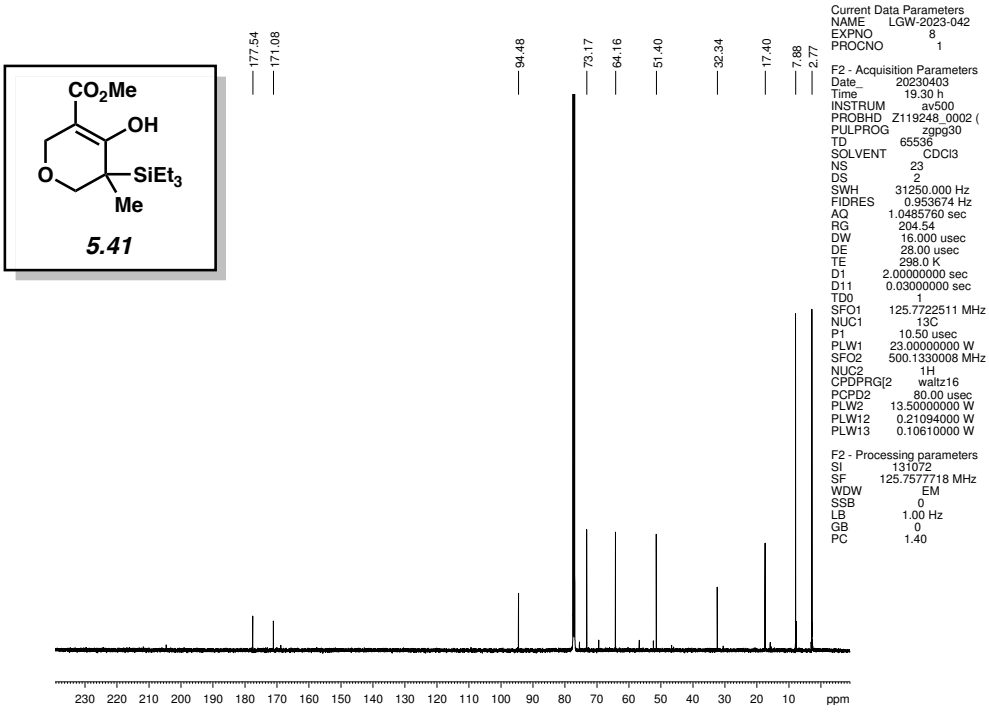

Figure 5.15. ^{13}C NMR (125 MHz, $CDCl_3$) of compound **5.41**.

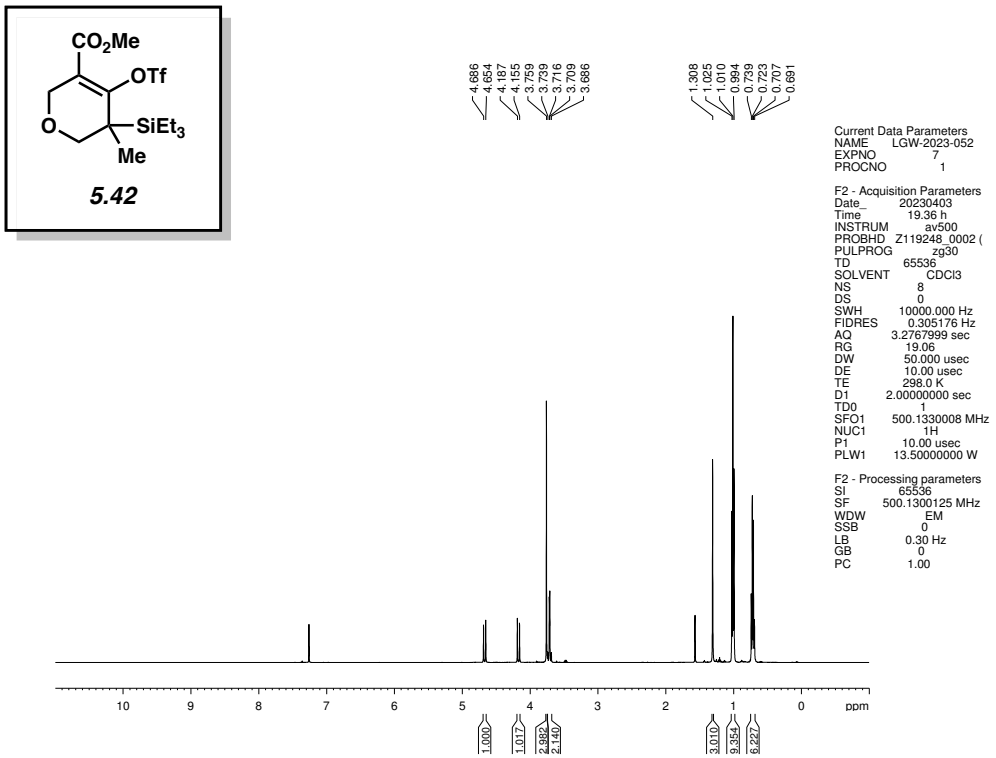

Figure 5.16. ^{1}H NMR (500 MHz, $CDCl_3$) of compound **5.42**.

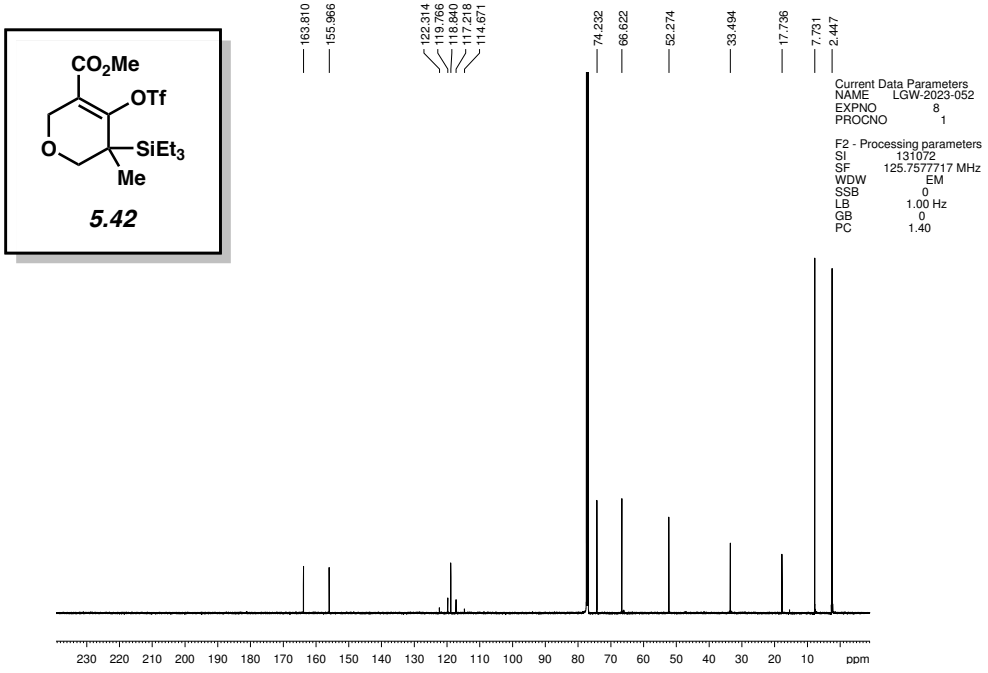

Figure 5.17. ^{13}C NMR (125 MHz, $CDCl_3$) of compound **5.42**.

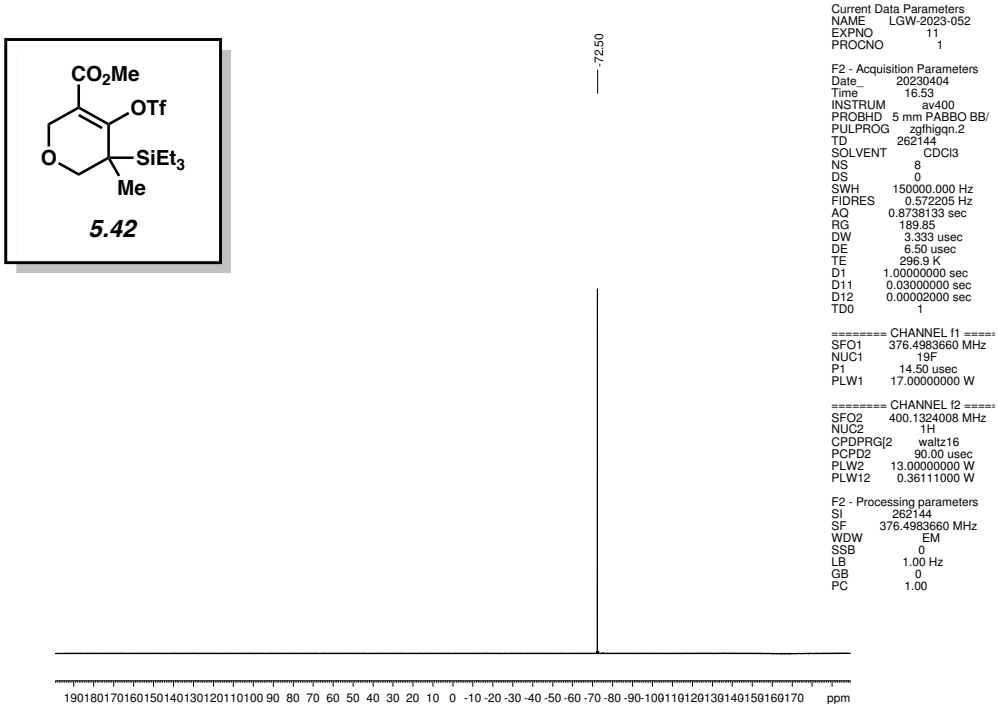

Figure 5.18. ^{19}F NMR (376 MHz, $CDCl_3$) of compound **5.42**.

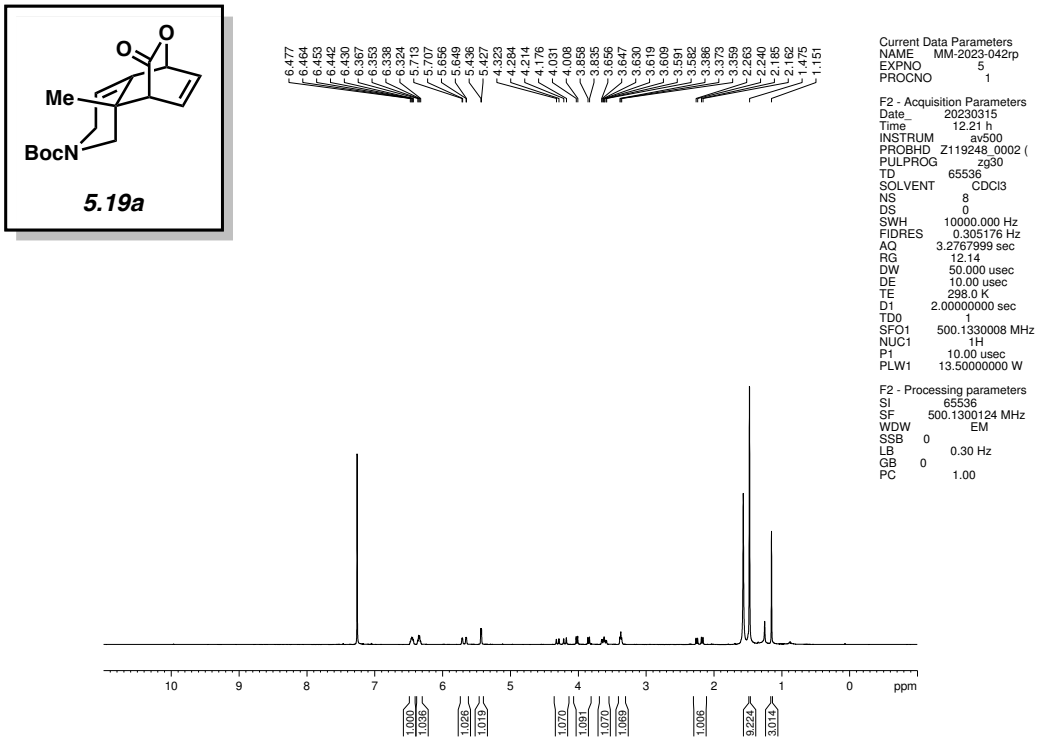

Figure 5.19. ^{1}H NMR (500 MHz, $CDCl_3$) of compound **5.19a**.

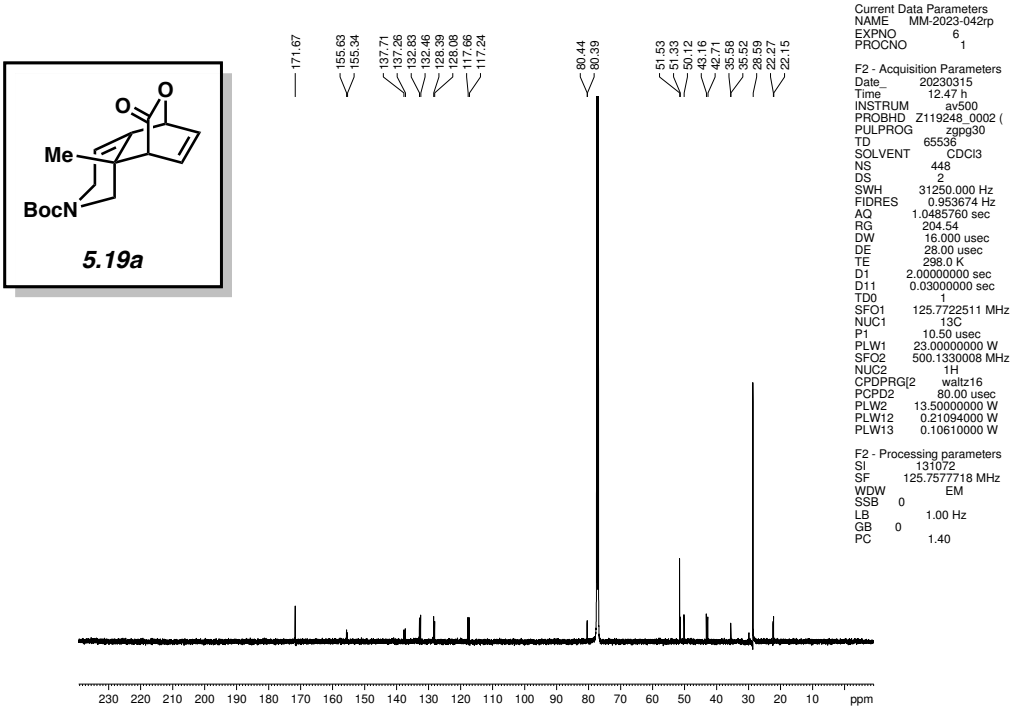

Figure 5.20. ^{13}C NMR (125 MHz, $CDCl_3$) of compound **5.19a**.

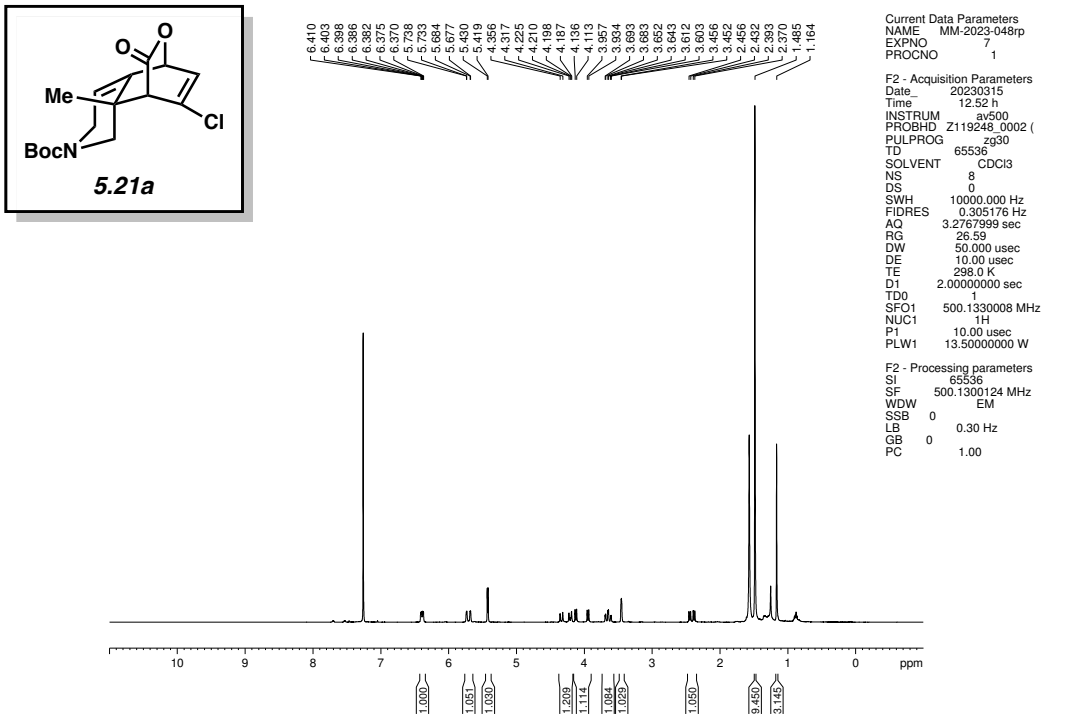

Figure 5.21. ^{1}H NMR (500 MHz, $CDCl_3$) of compound **5.21a**.

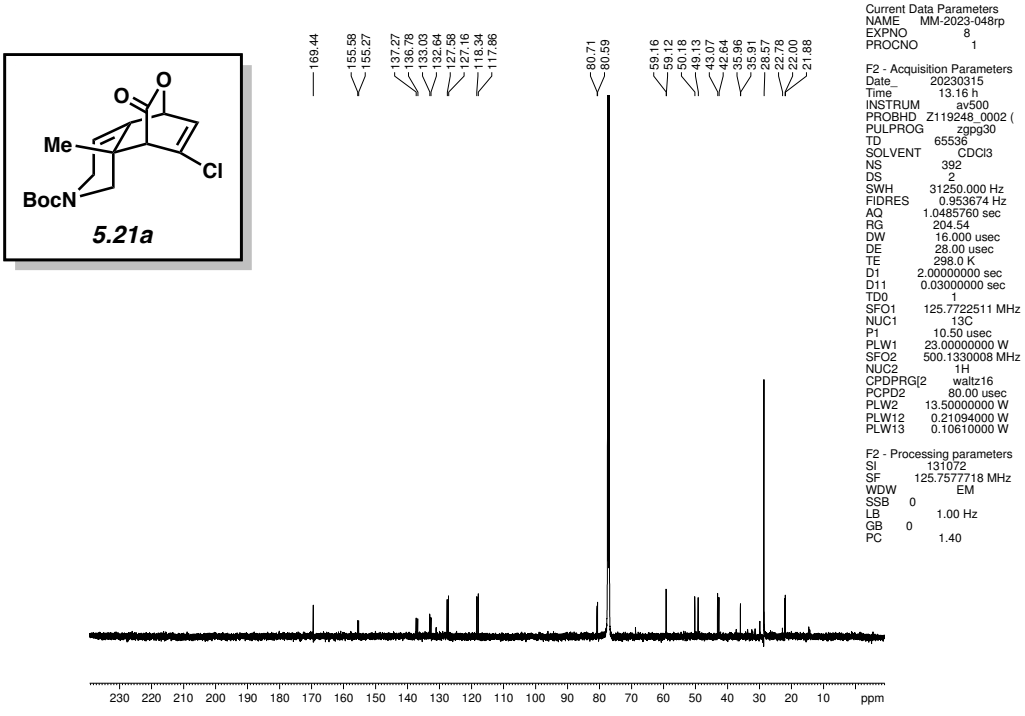

Figure 5.22. ^{13}C NMR (125 MHz, $CDCl_3$) of compound **5.21a**.

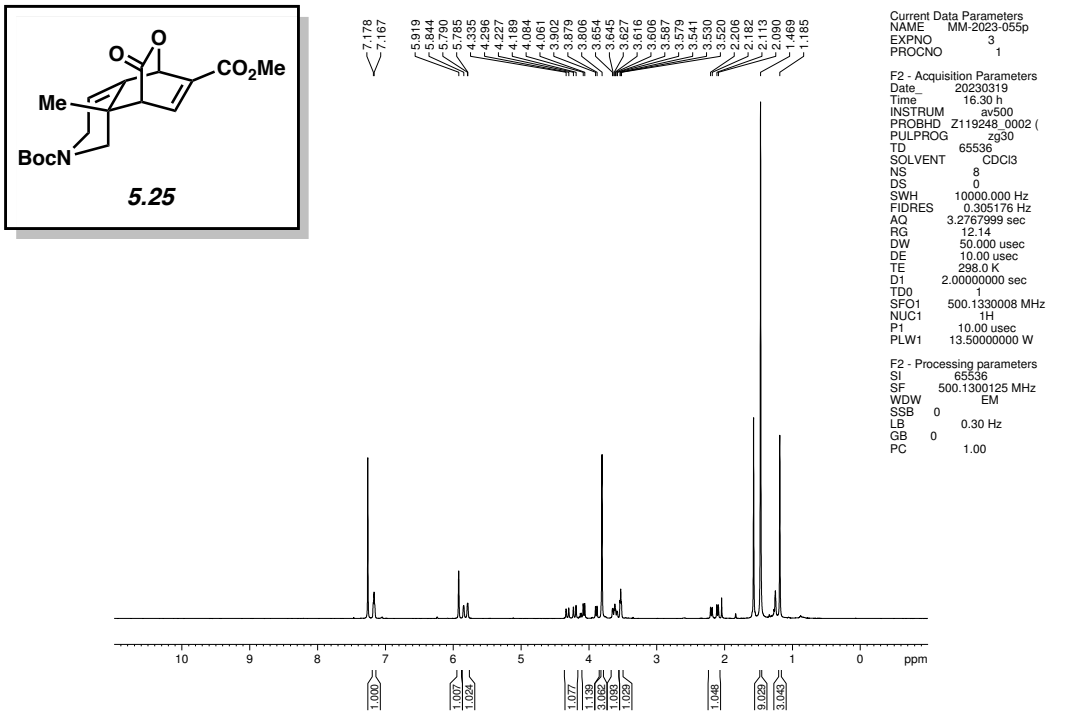

Figure 5.23. ^{1}H NMR (500 MHz, $CDCl_3$) of compound **5.25**.

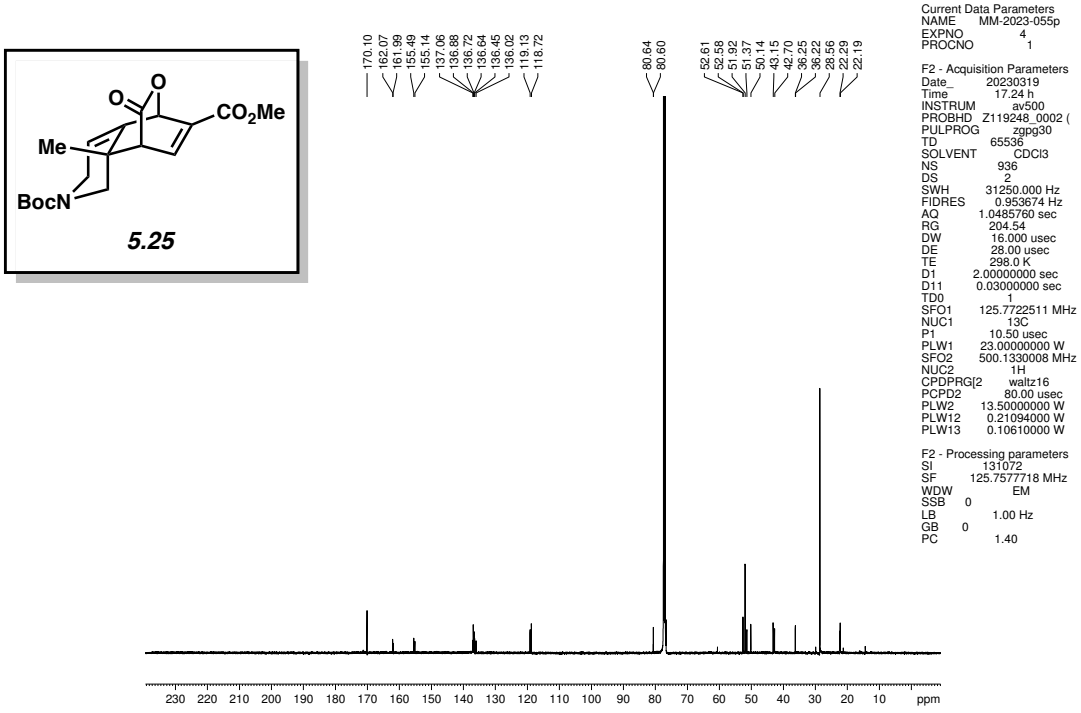

Figure 5.24. ^{13}C NMR (125 MHz, $CDCl_3$) of compound **5.25**.

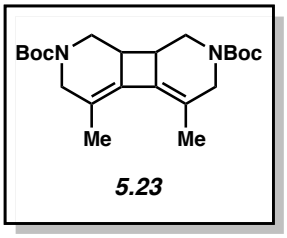

Figure 5.25. ^{1}H NMR (400 MHz, $CDCl_3$) of compound **5.23**.

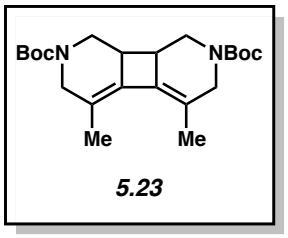

Figure 5.26. ^{13}C NMR (100 MHz, $CDCl_3$) of compound **5.23**.

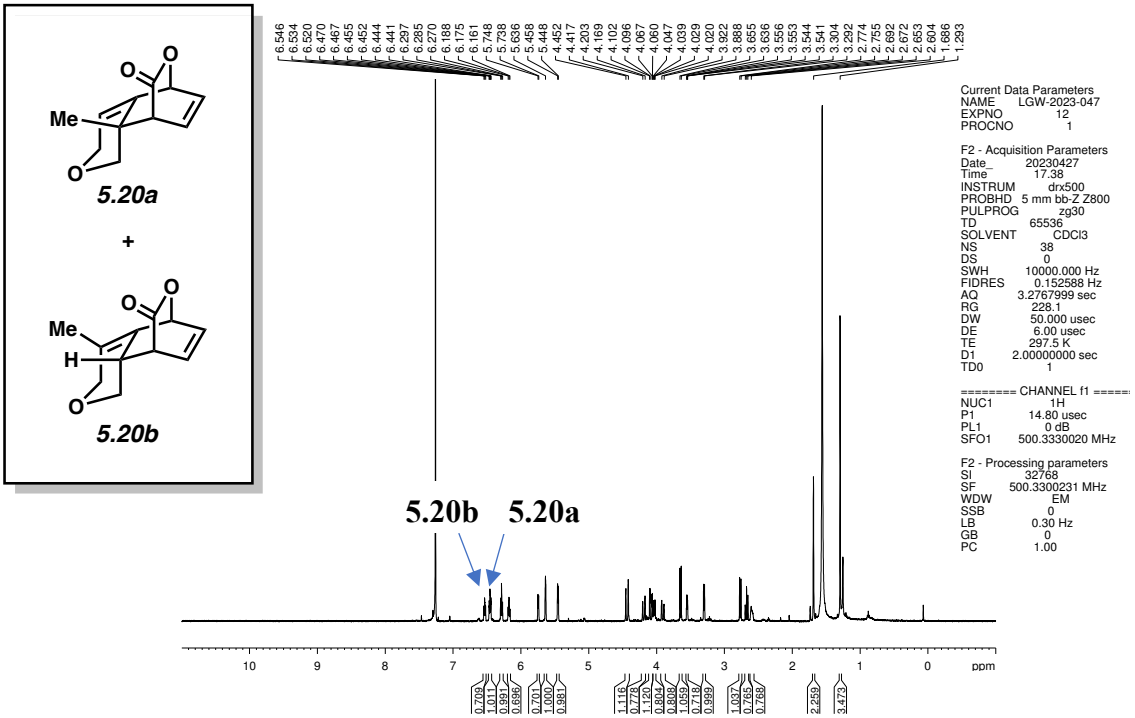

Figure 5.27. ^{1}H NMR (500 MHz, $CDCl_3$) of compounds **5.20a** and **5.20b**.

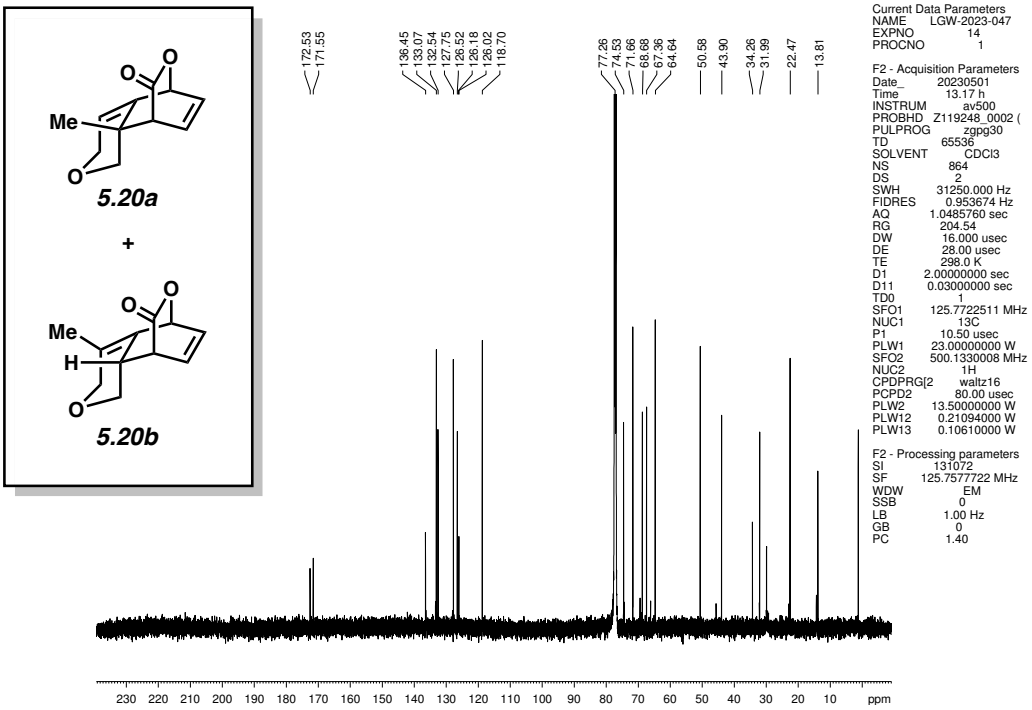

Figure 5.28. ^{13}C NMR (125 MHz, $CDCl_3$) of compounds **5.20a** and **5.20b**.

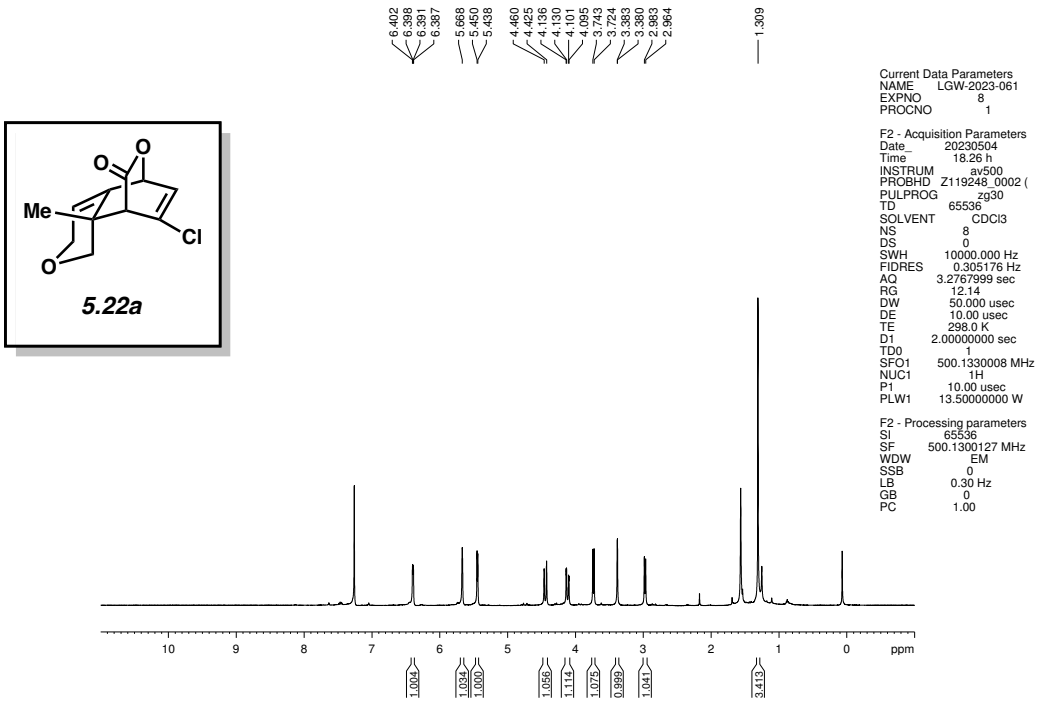

Figure 5.29. ^{1}H NMR (500 MHz, $CDCl_3$) of compound **5.22a**.

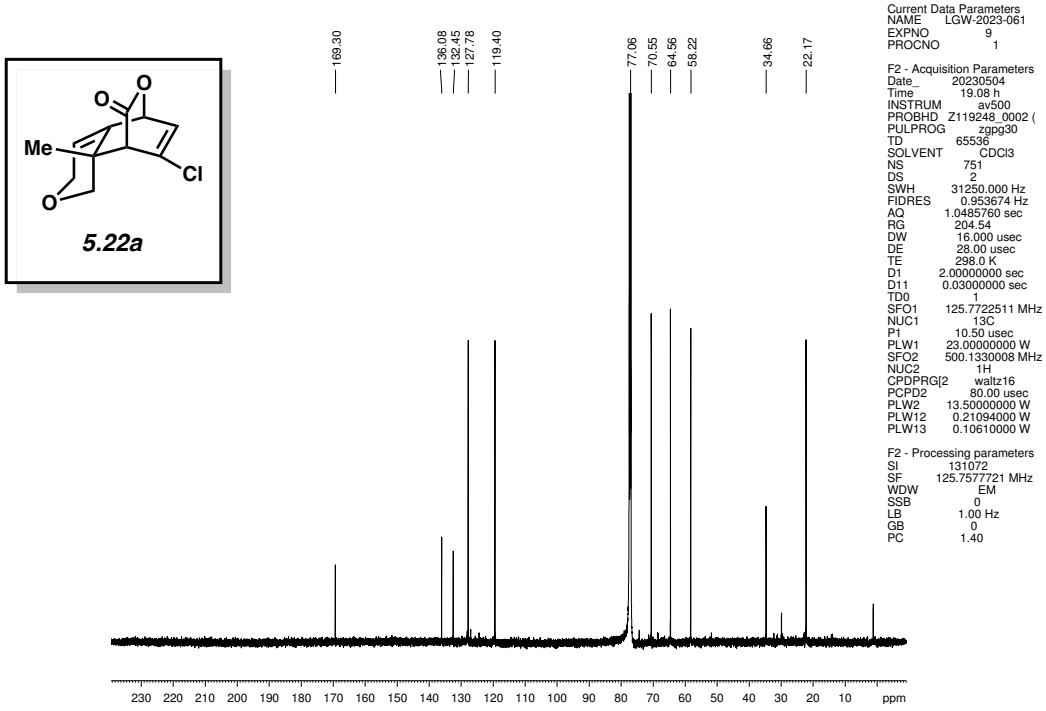

Figure 5.30. ^{13}C NMR (125 MHz, $CDCl_3$) of compound **5.22a**.

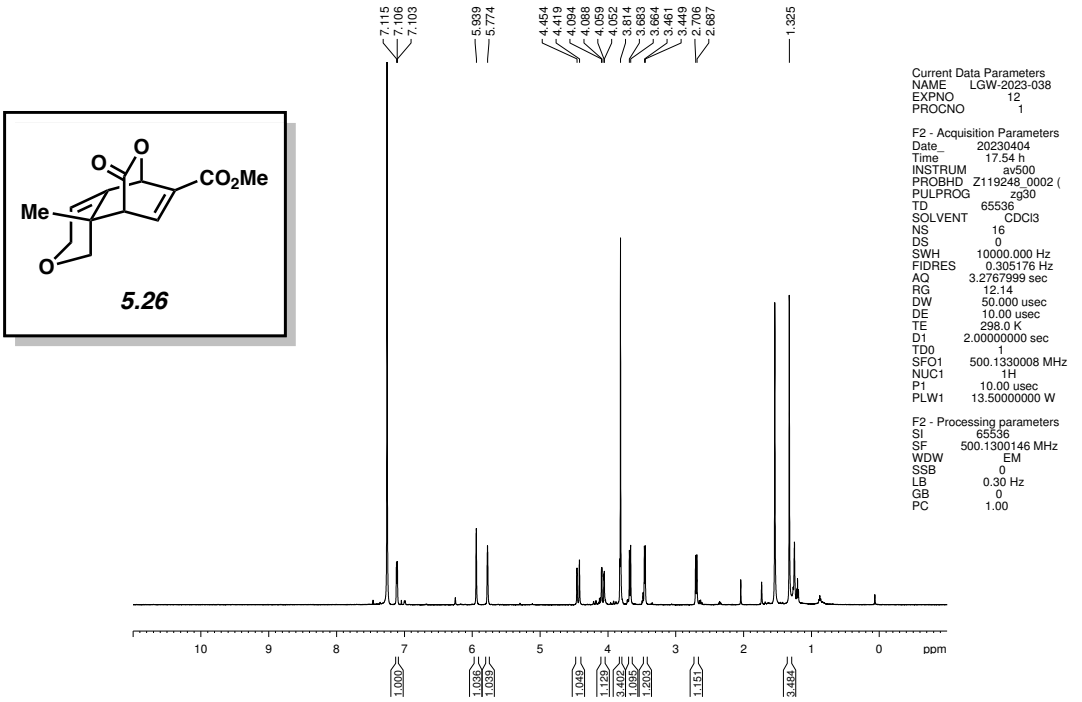

Figure 5.31. ^{1}H NMR (500 MHz, $CDCl_3$) of compound **5.26**.

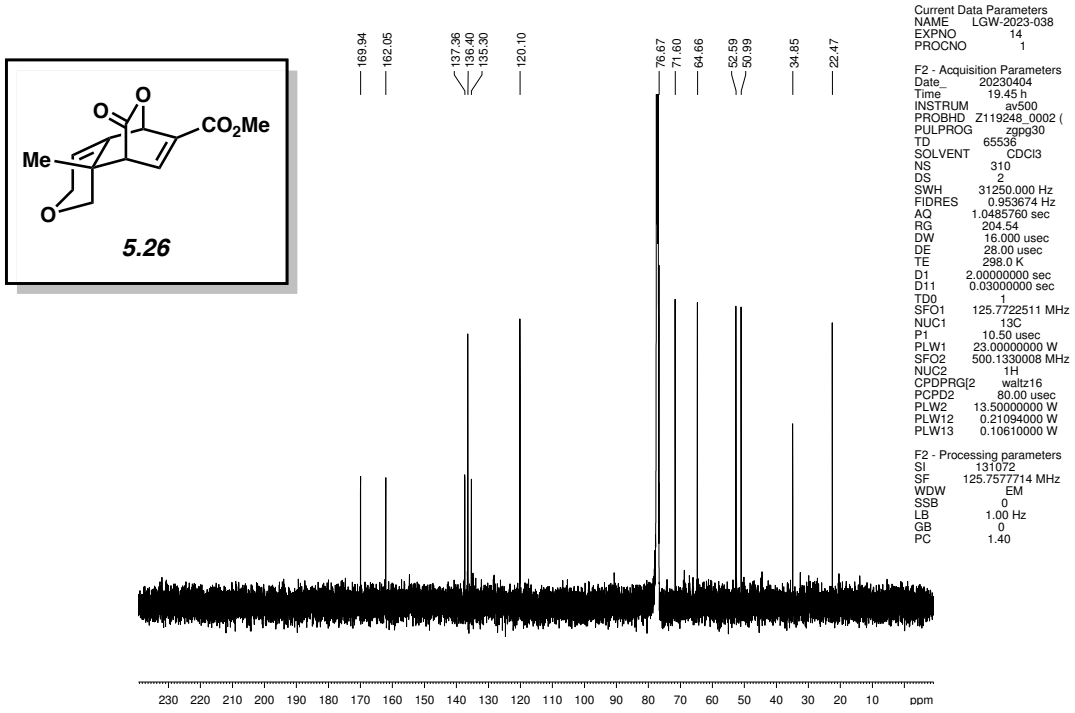

Figure 5.32. ^{13}C NMR (125 MHz, $CDCl_3$) of compound **5.26**.

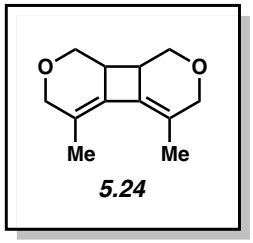

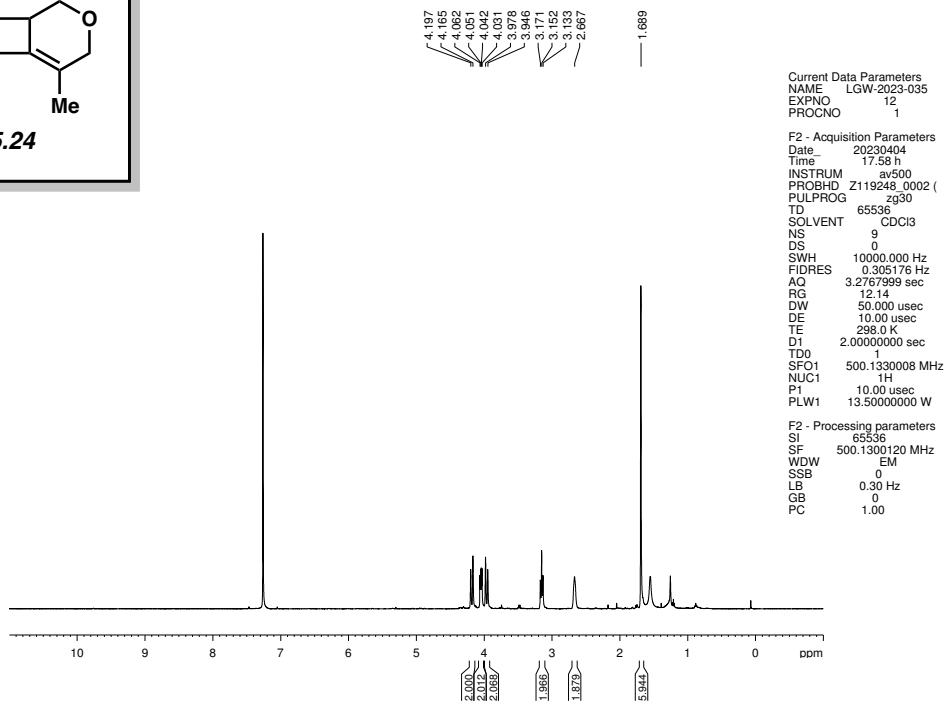

Figure 5.33. ^{1}H NMR (500 MHz, $CDCl_3$) of compound **5.24**.

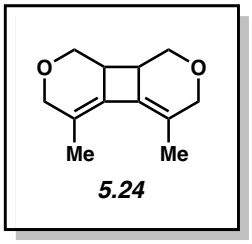

Figure 5.34. ^{13}C NMR (125 MHz, $CDCl_3$) of compound **5.24**.

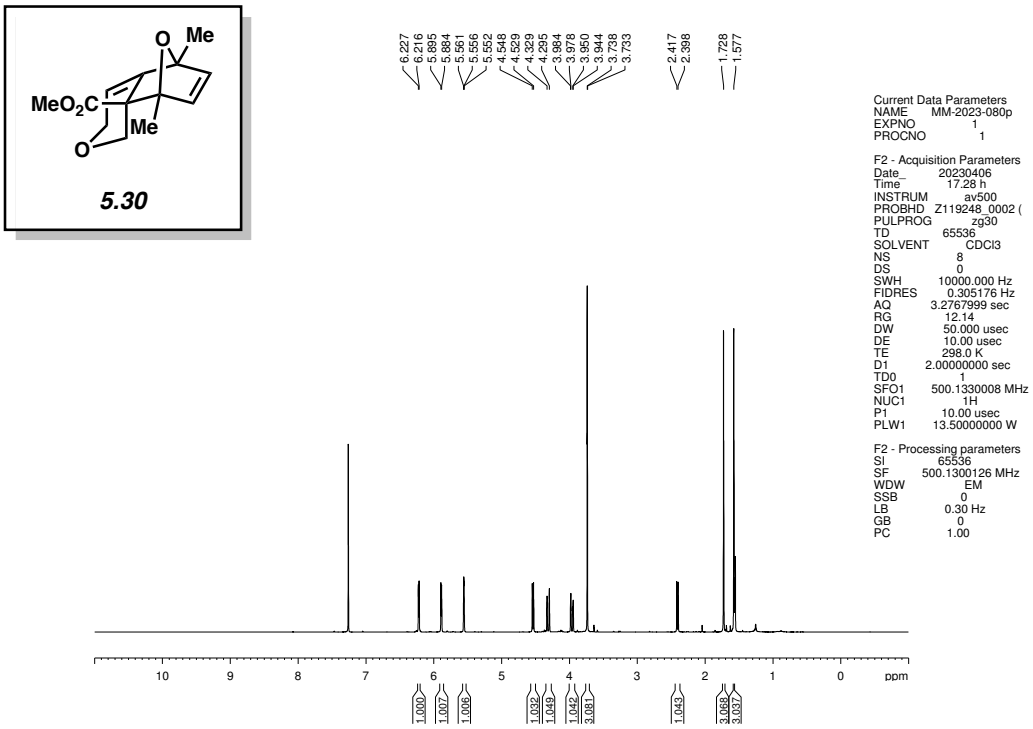

Figure 5.35. ^{1}H NMR (500 MHz, $CDCl_3$) of compound **5.30**.

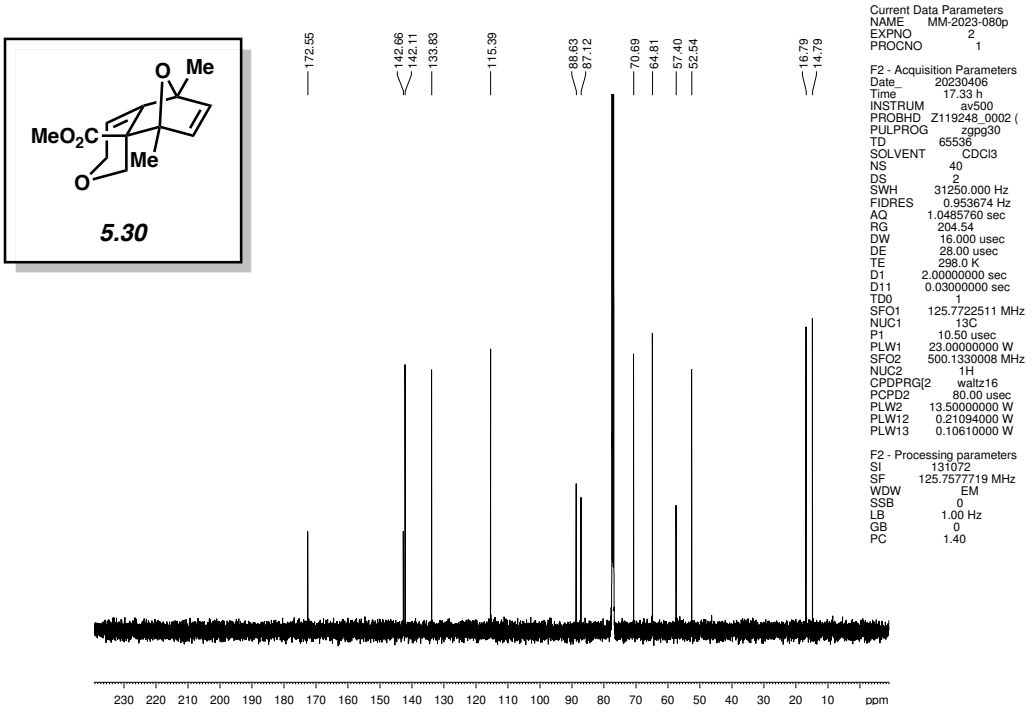

Figure 5.36. ^{13}C NMR (125 MHz, $CDCl_3$) of compound **5.30**.

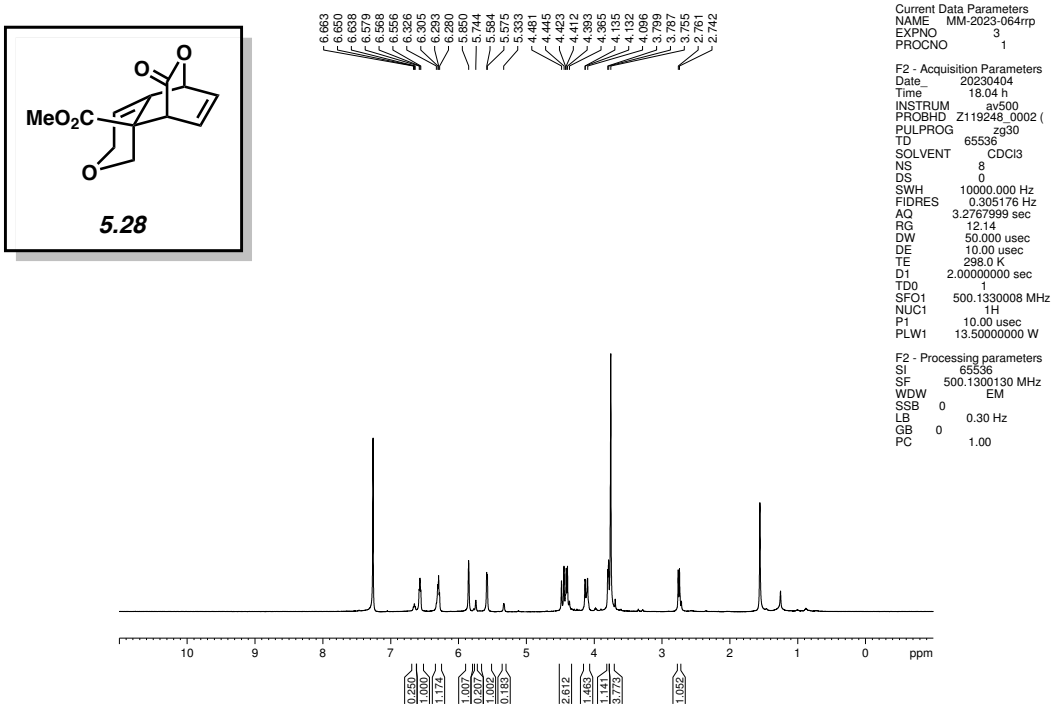

Figure 5.37. ^{1}H NMR (500 MHz, $CDCl_3$) of compound **5.28**.

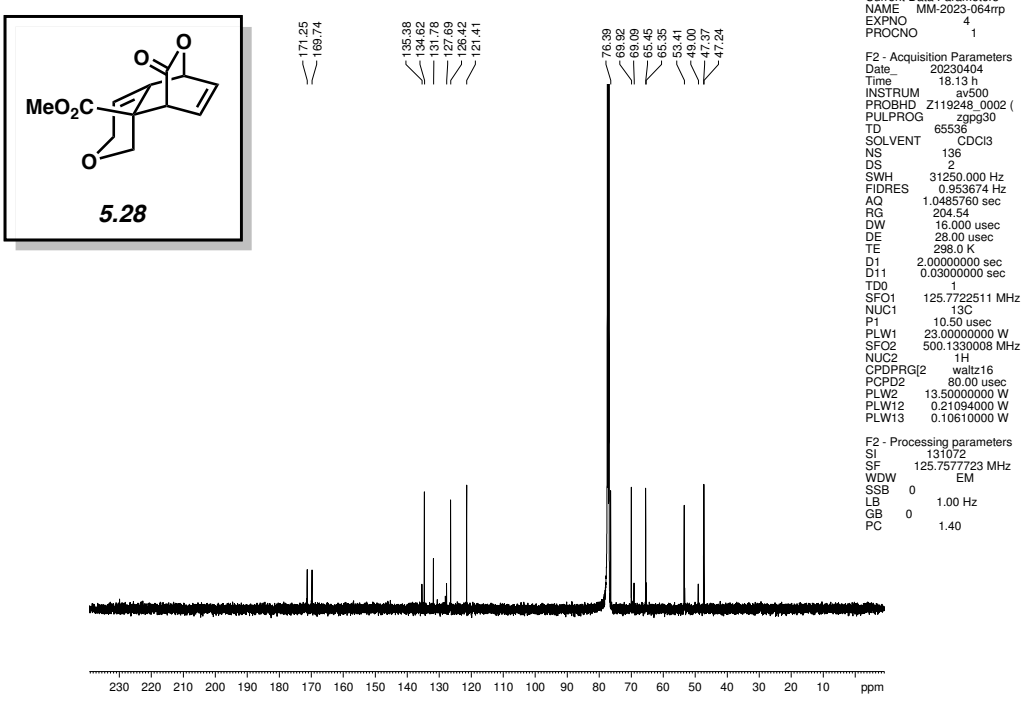

Figure 5.38. ^{13}C NMR (125 MHz, $CDCl_3$) of compound **5.28**.

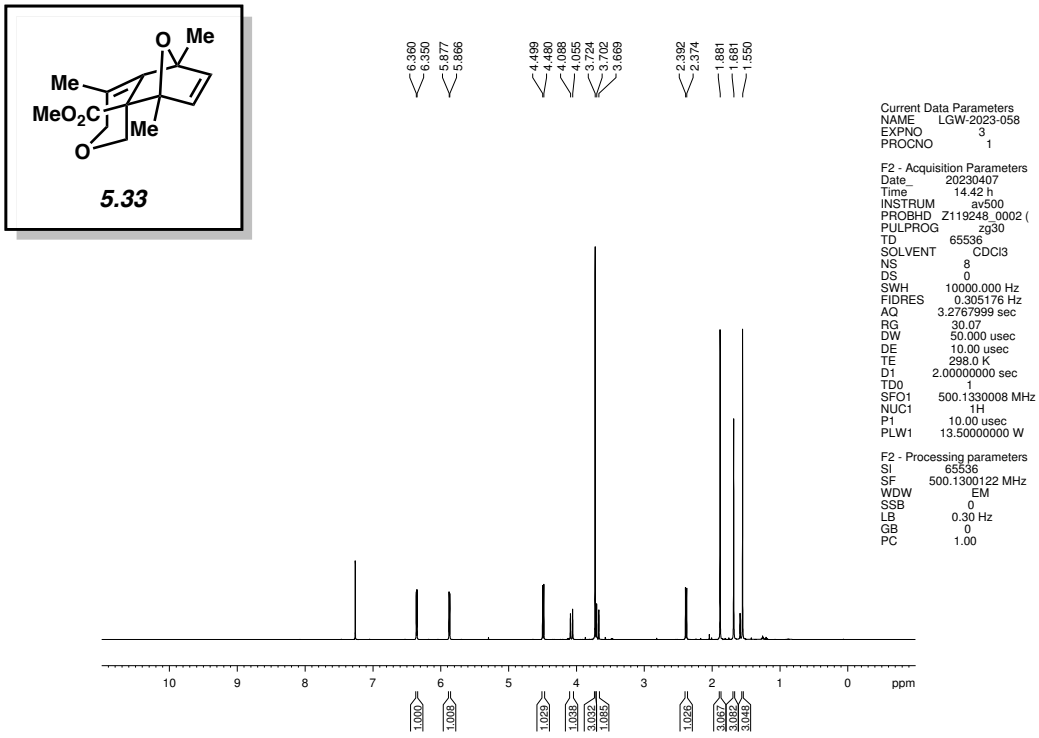

Figure 5.39. ^{1}H NMR (500 MHz, $CDCl_3$) of compound **5.33**.

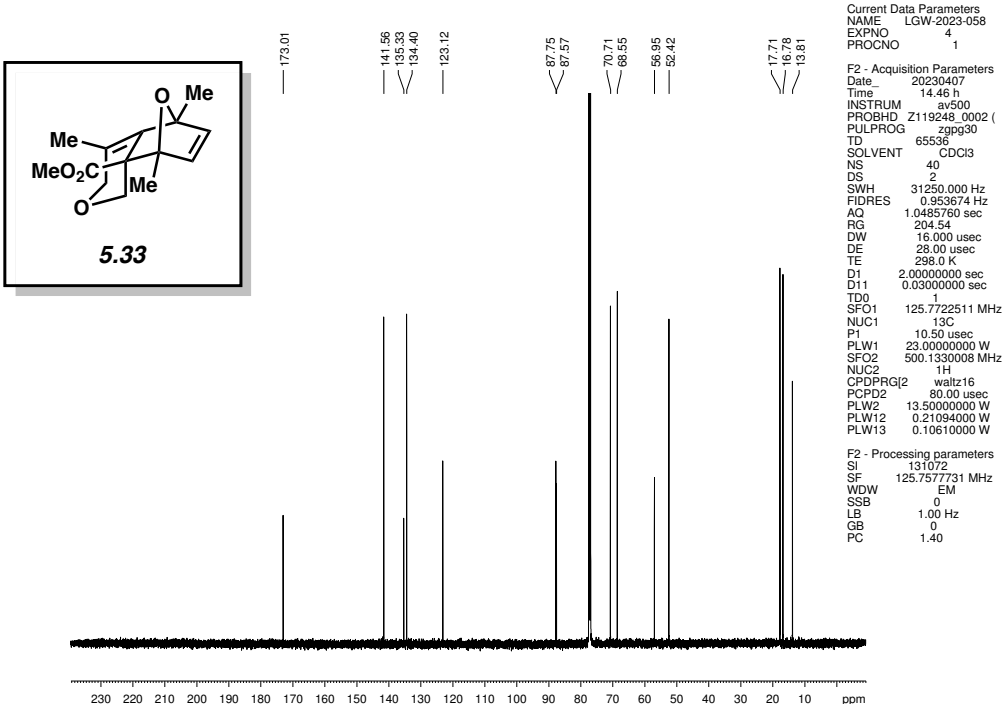

Figure 5.40. ^{13}C NMR (125 MHz, $CDCl_3$) of compound **5.33**.

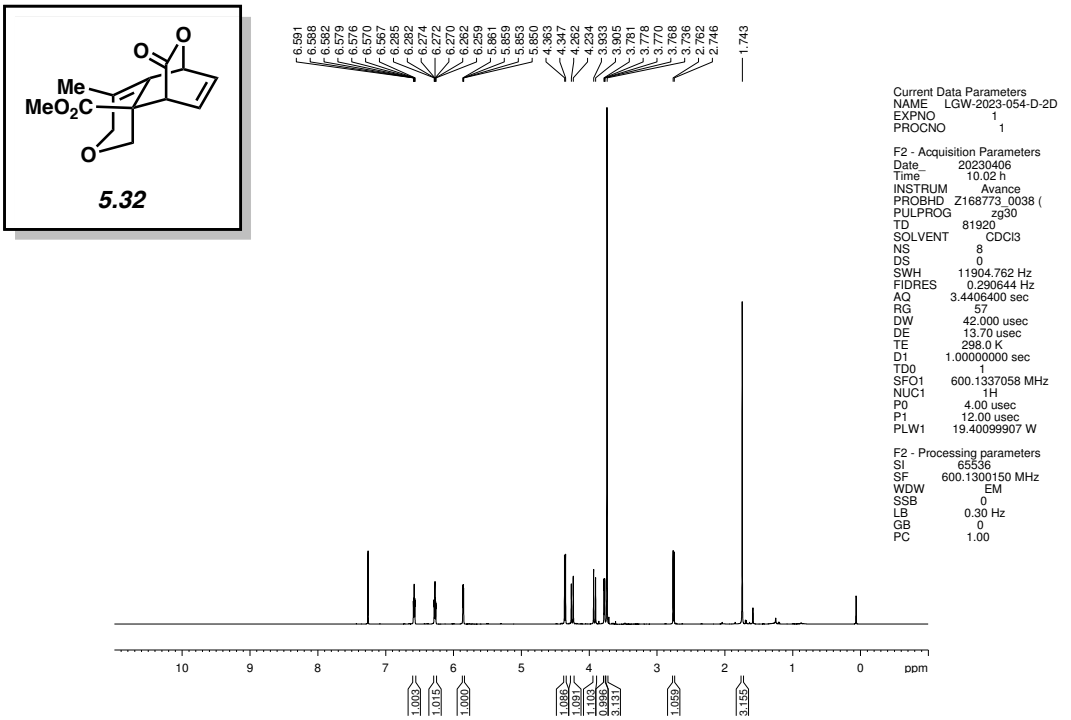

Figure 5.41. ^{1}H NMR (600 MHz, $CDCl_3$) of compound **5.32**.

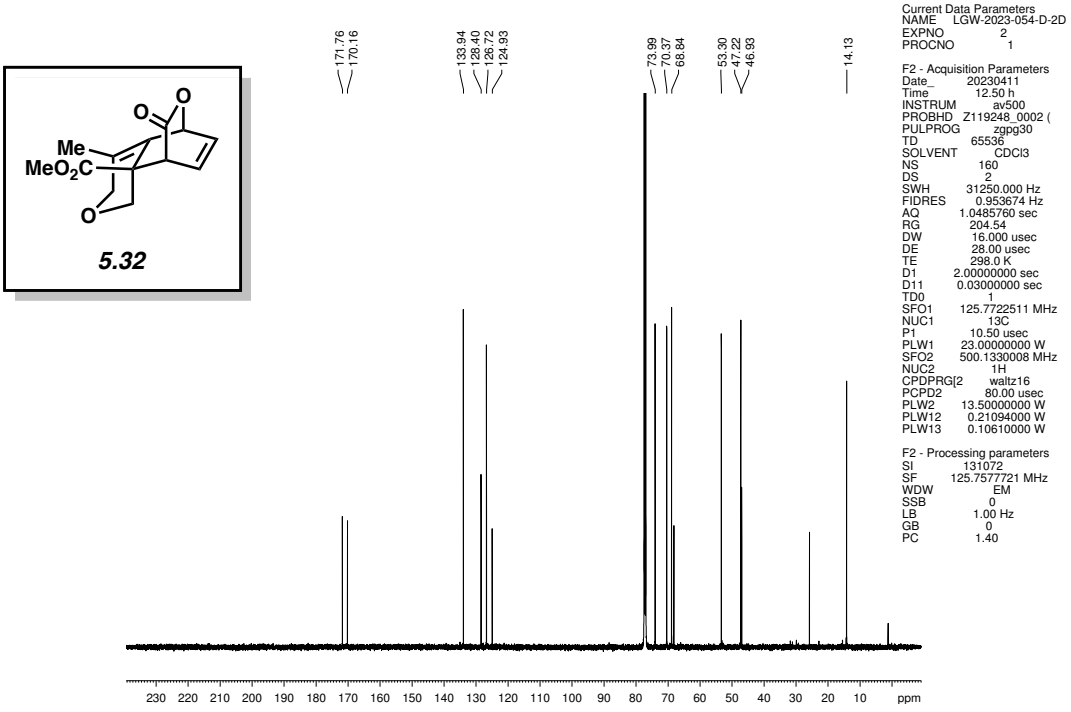

Figure 5.42. ^{13}C NMR (125 MHz, $CDCl_3$) of compound **5.32**.

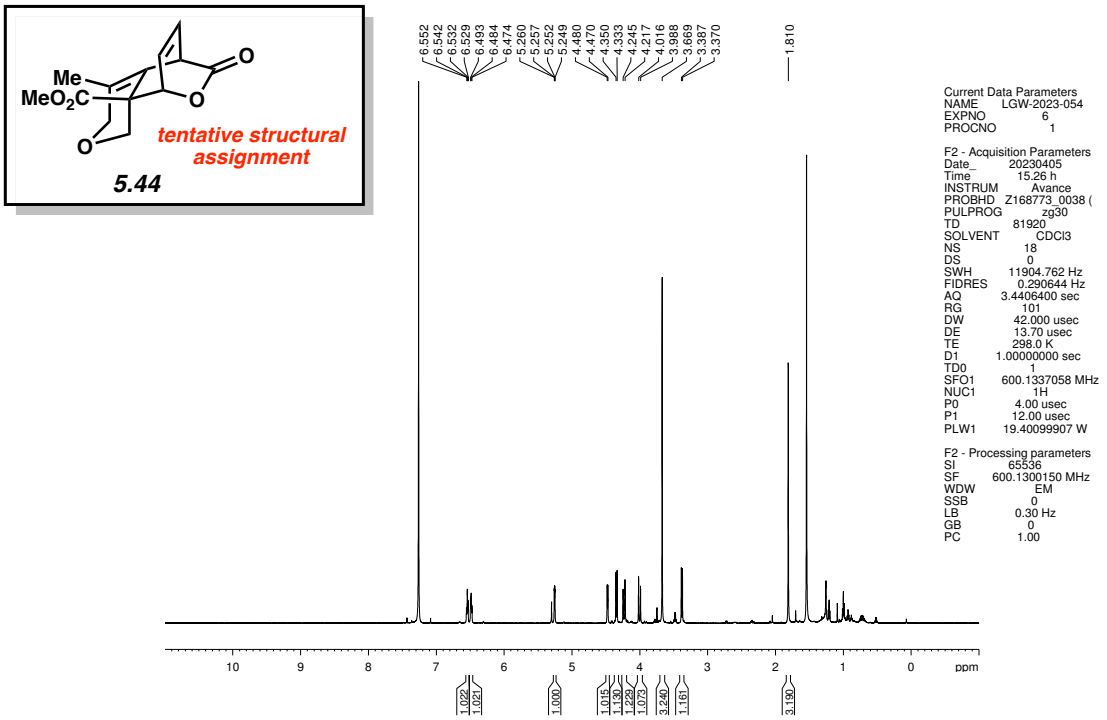

Figure 5.43. ^{1}H NMR (600 MHz, $CDCl_3$) of compound **5.44**.

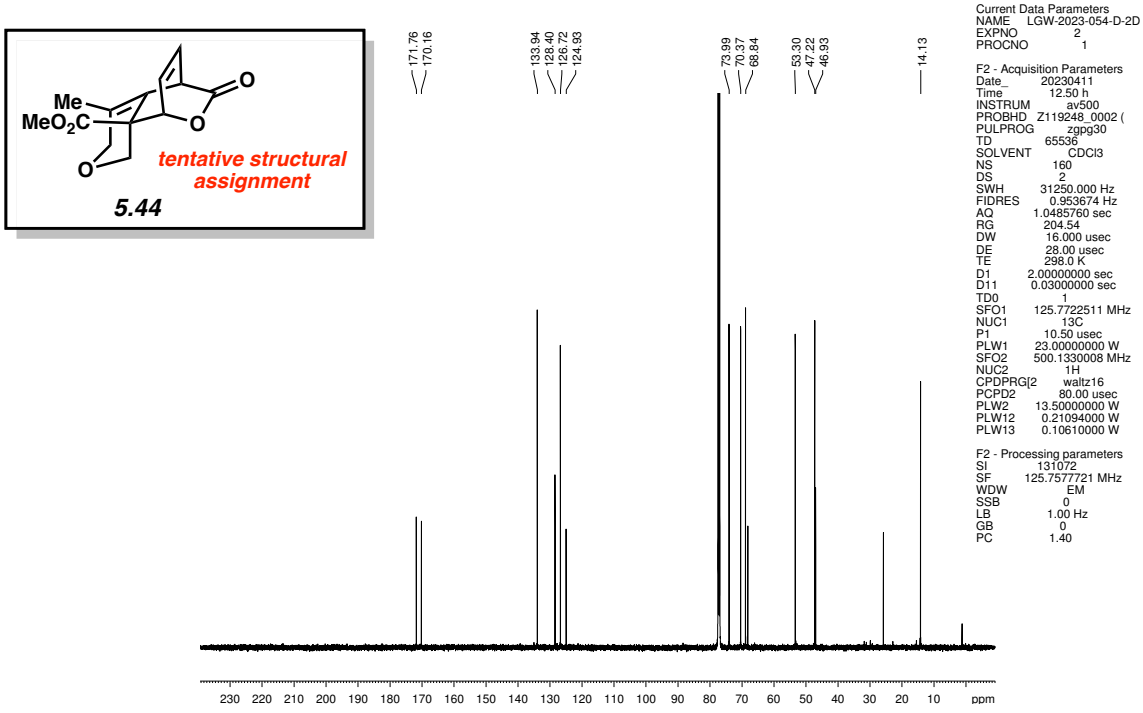

Figure 5.44. ^{13}C NMR (125 MHz, $CDCl_3$) of compound **5.44**.

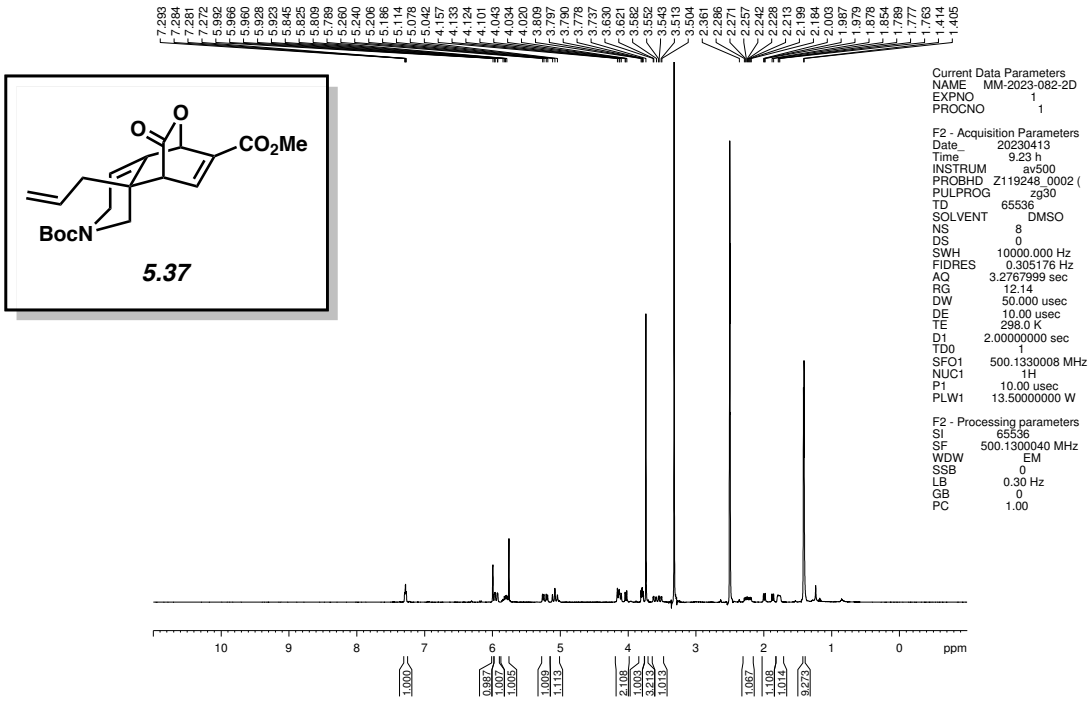

Figure 5.45. ^{1}H NMR (500 MHz, DMSO-d_6) of compound **5.37**.

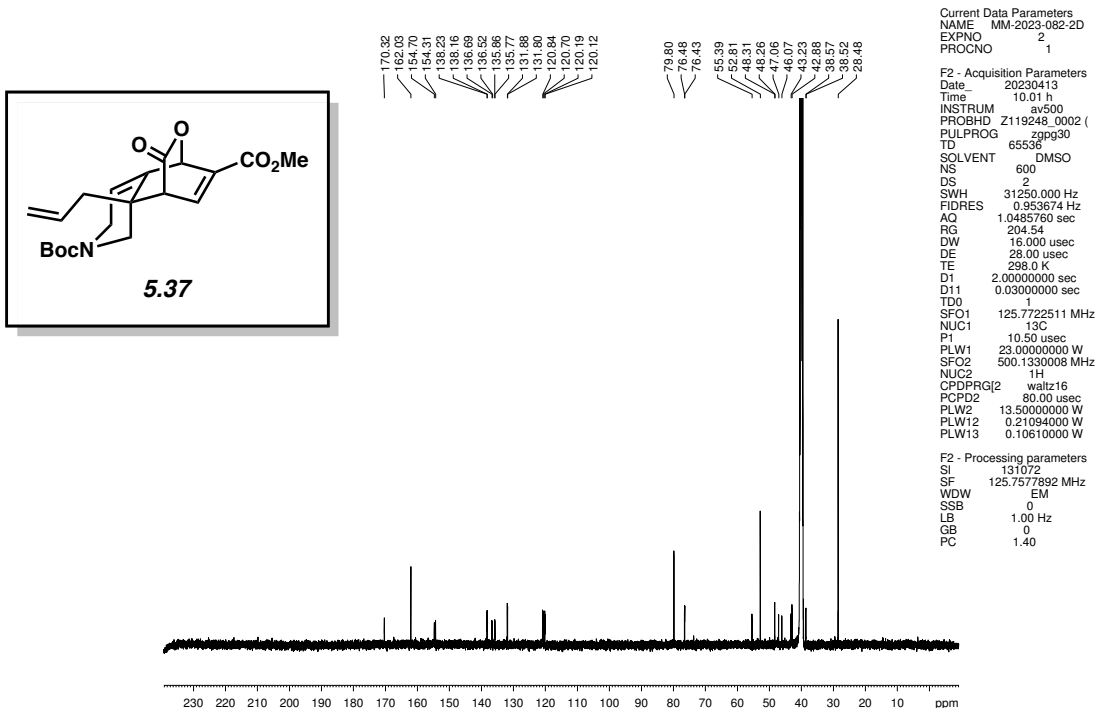

Figure 5.46. ^{13}C NMR (125 MHz, DMSO-d_6) of compound **5.37**.

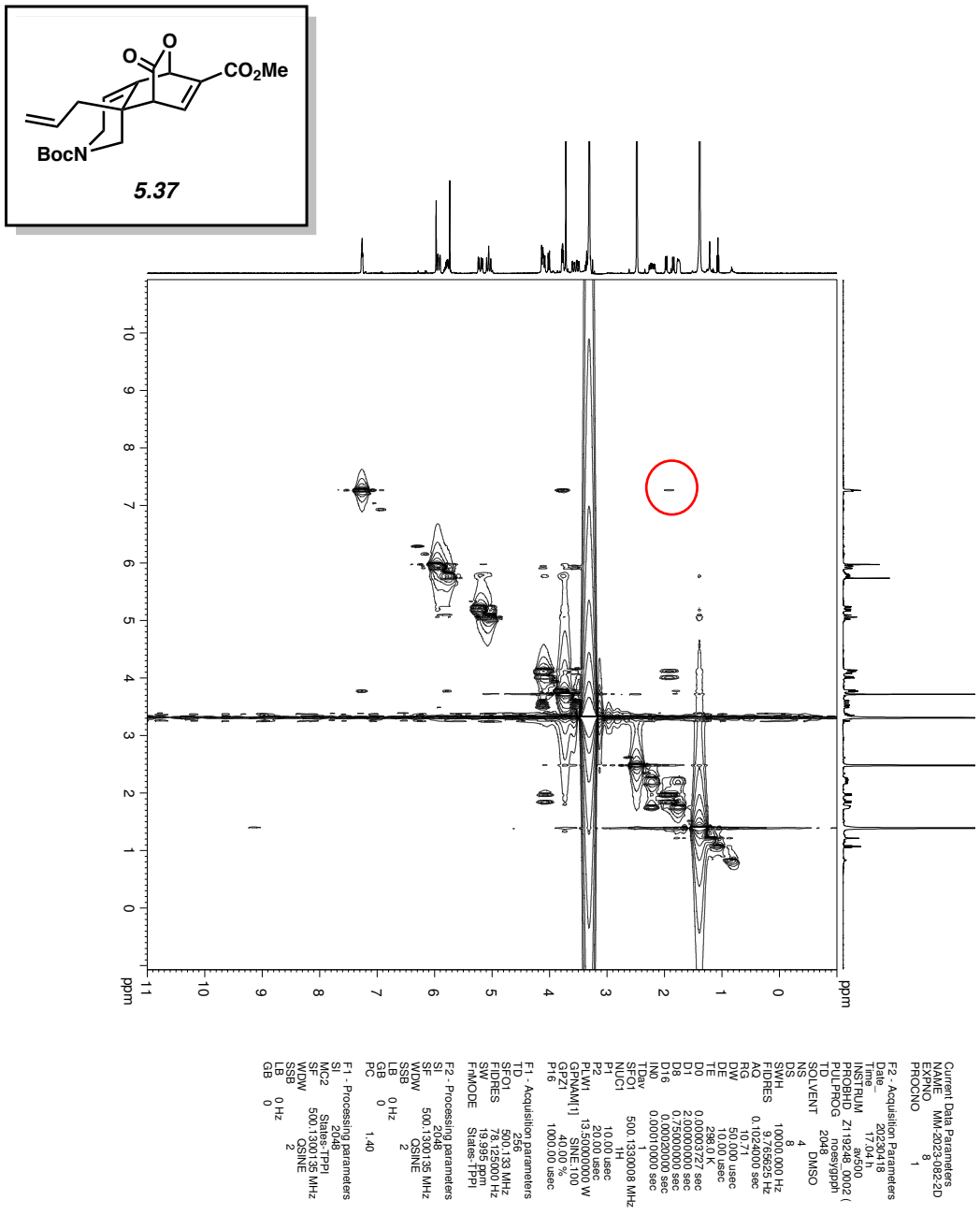

Figure 5.47. NOESY (500 MHz, DMSO-d_6) of compound **5.37**.

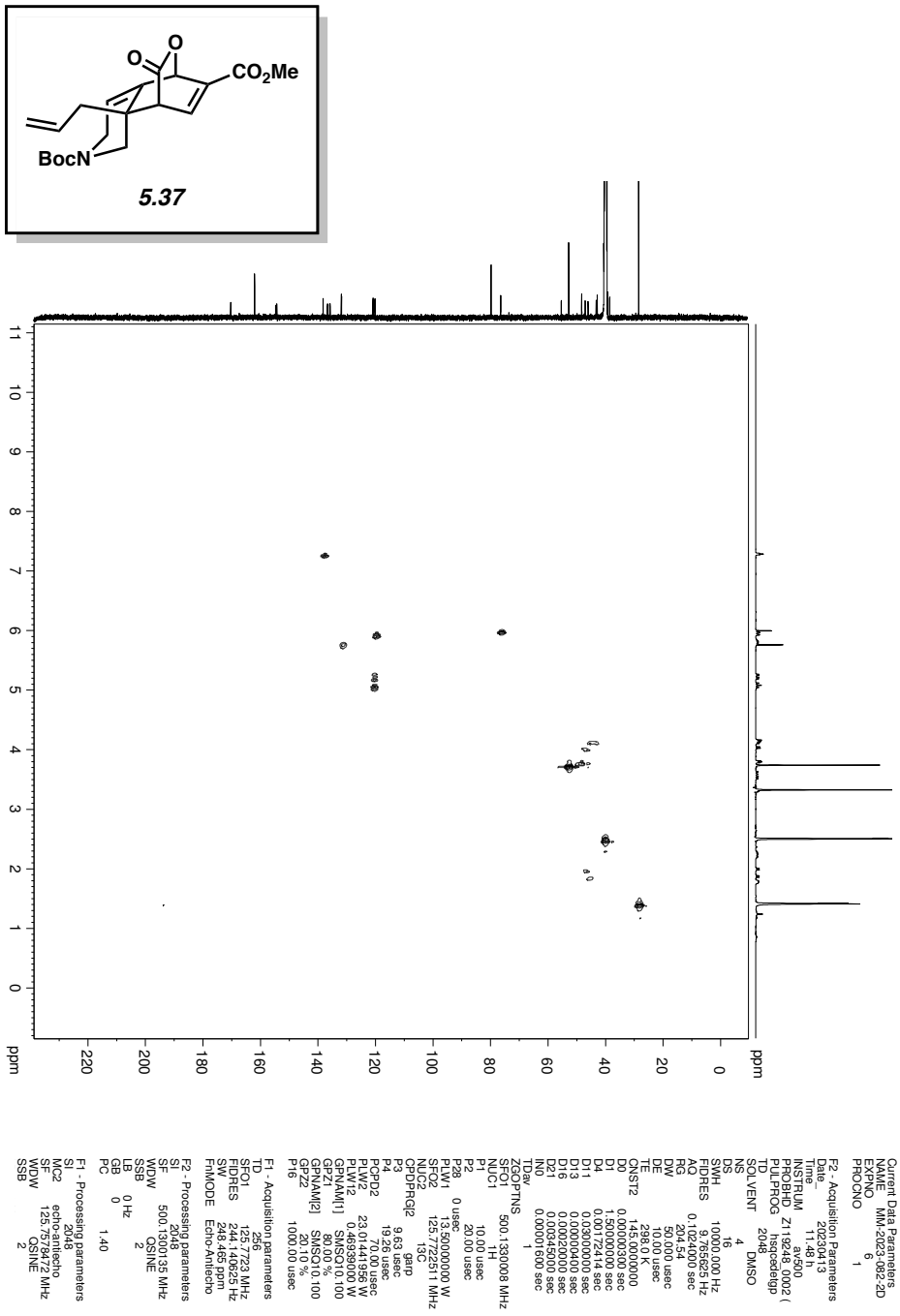

Figure 5.48. HSQC (600 MHz, DMSO-d_6) of compound **5.37**.

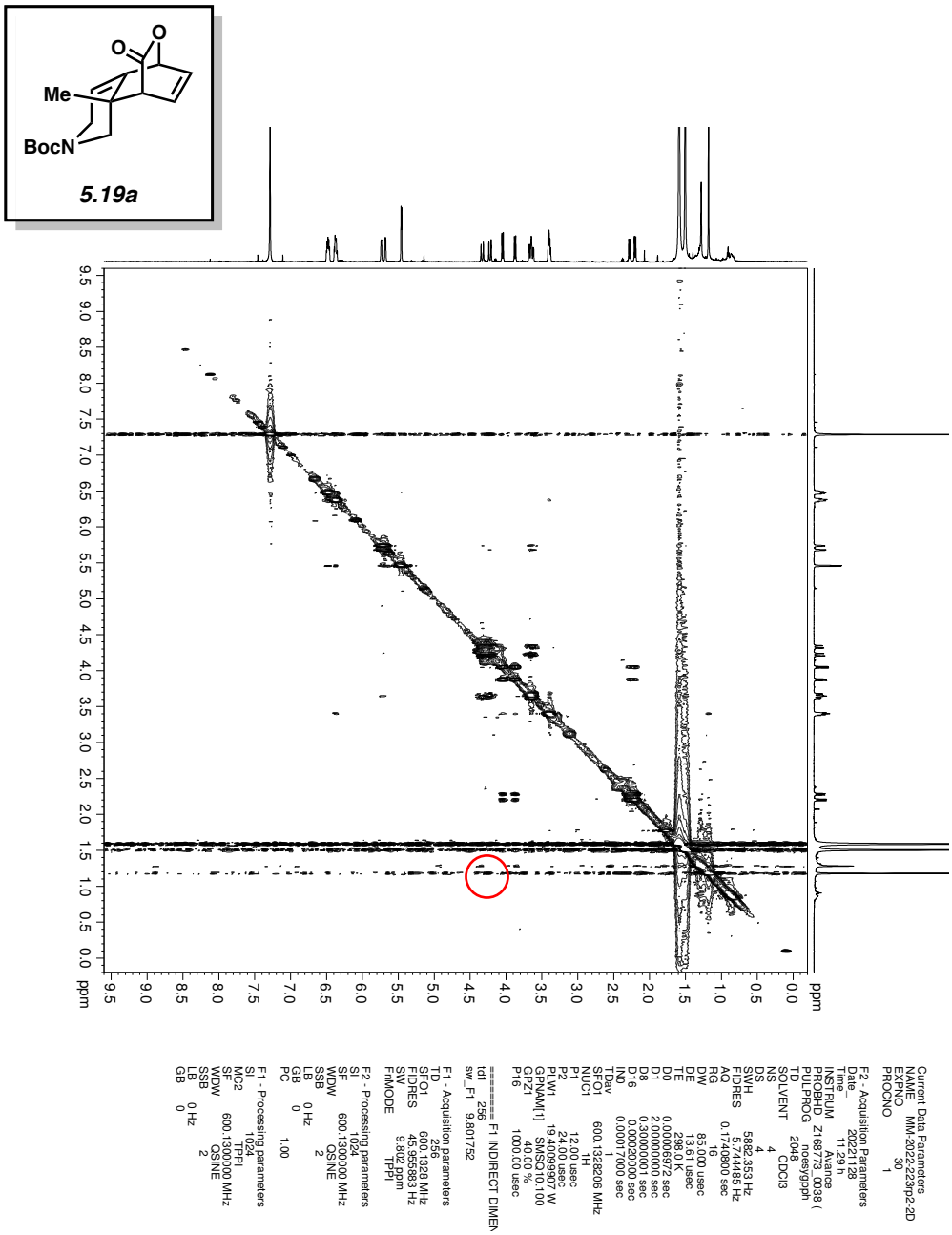

Figure 5.49. NOESY (600 MHz, $CDCl_3$) of compound **5.19a**.

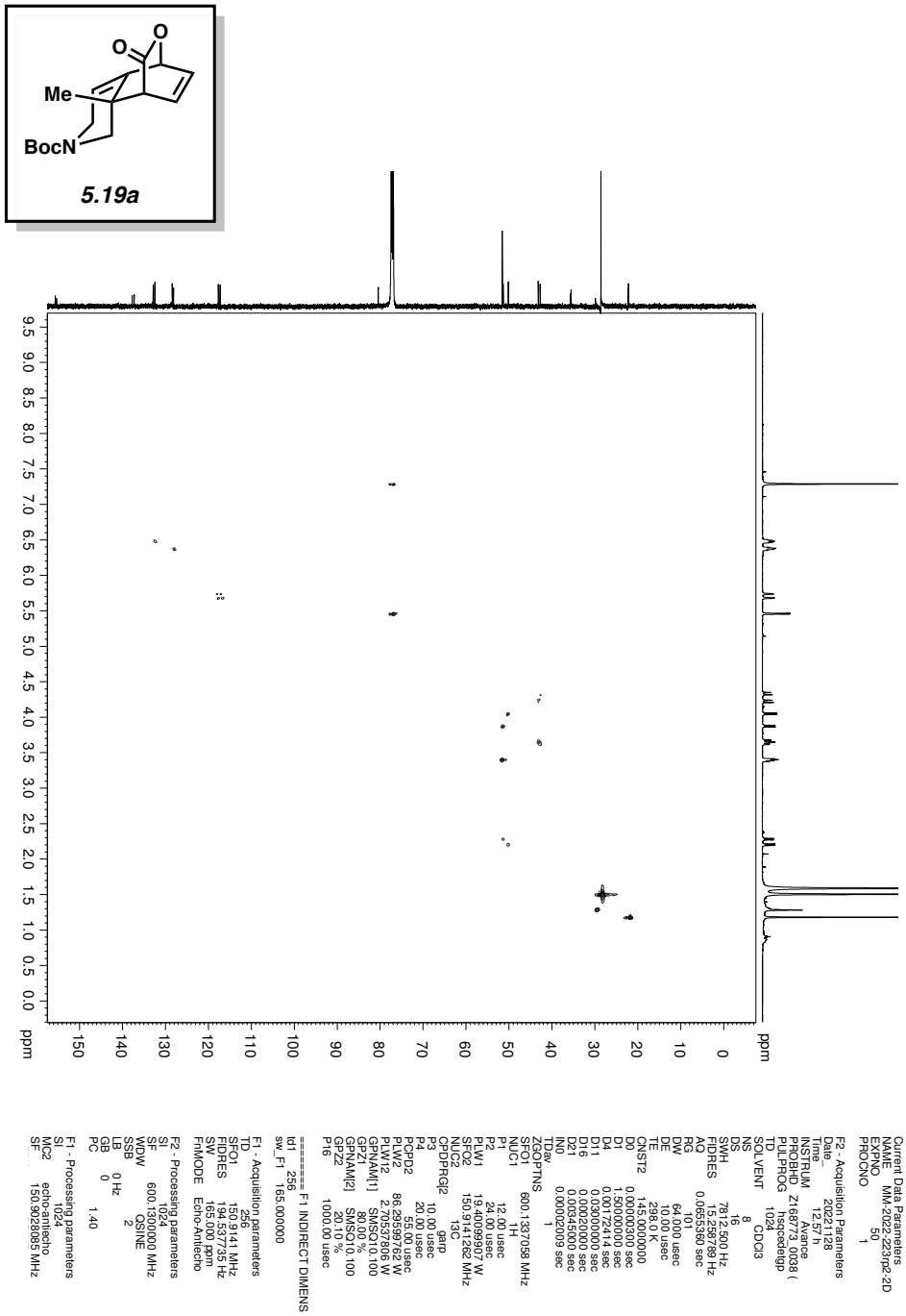

Figure 5.50. HSQC (600 MHz, $CDCl_3$) of compound **5.19a**.

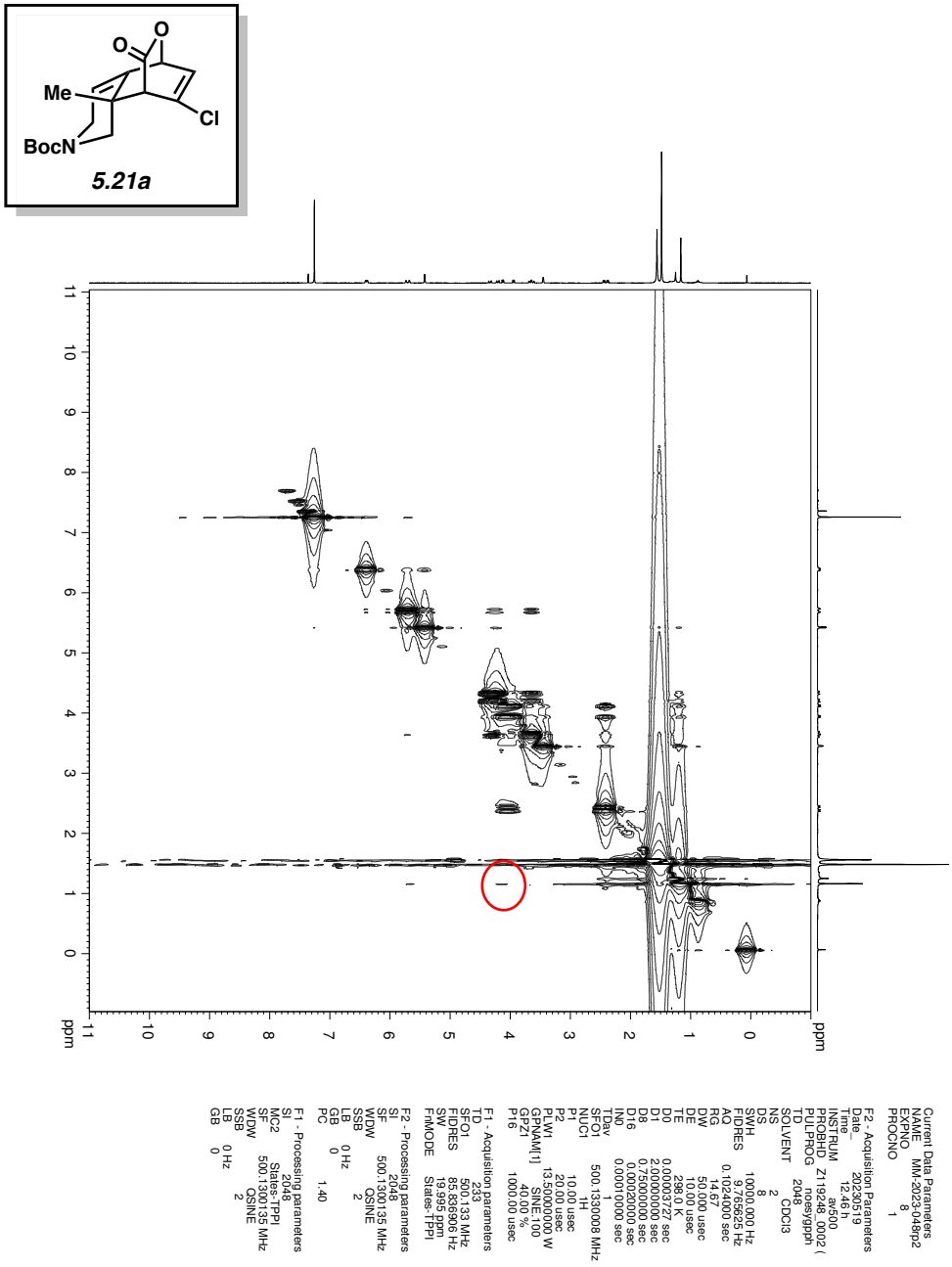

Figure 5.51. NOESY (500 MHz, $CDCl_3$) of compound **5.21a**.

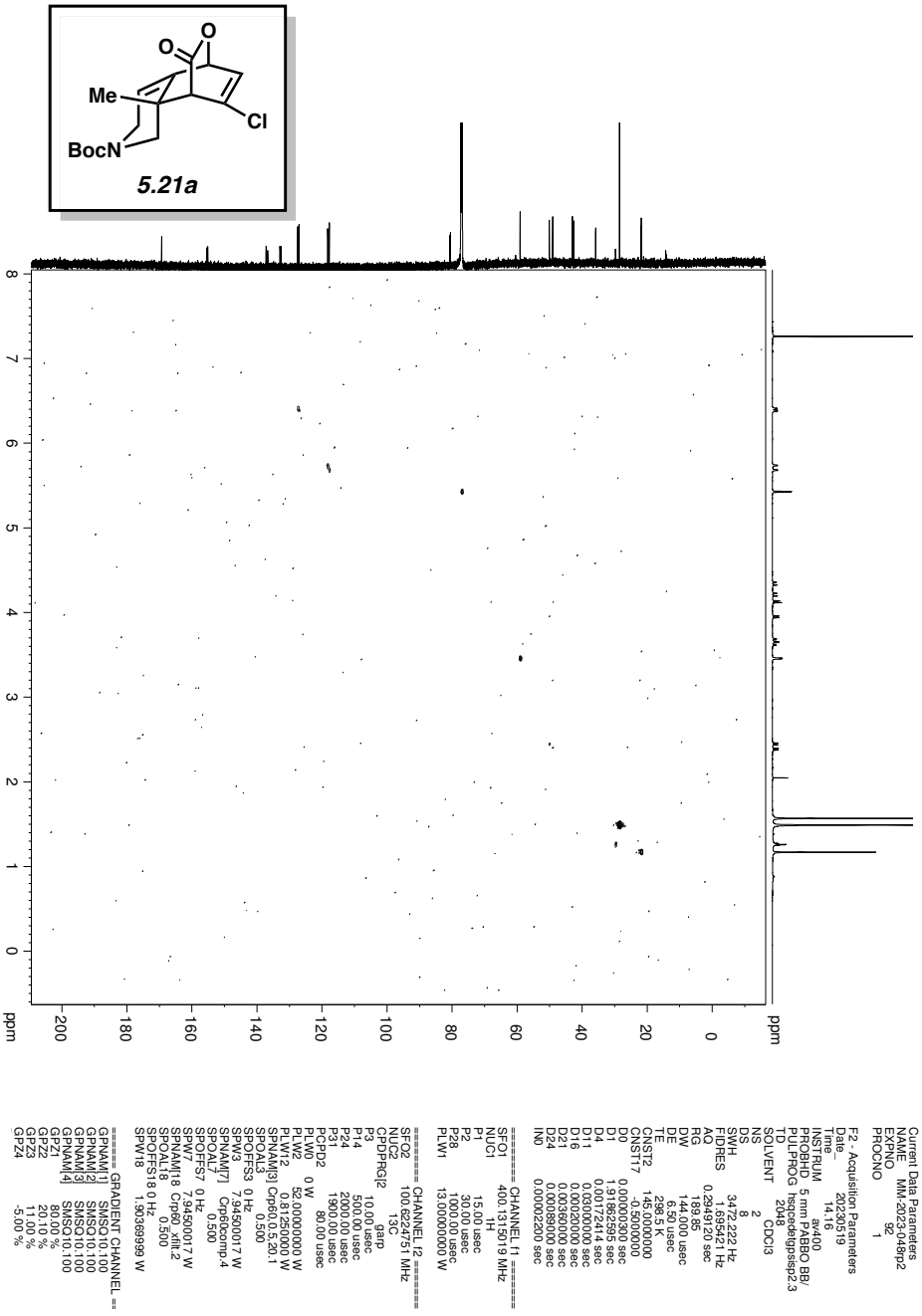

Figure 5.52. HSQC (400 MHz, $CDCl_3$) of compound **5.21a**.

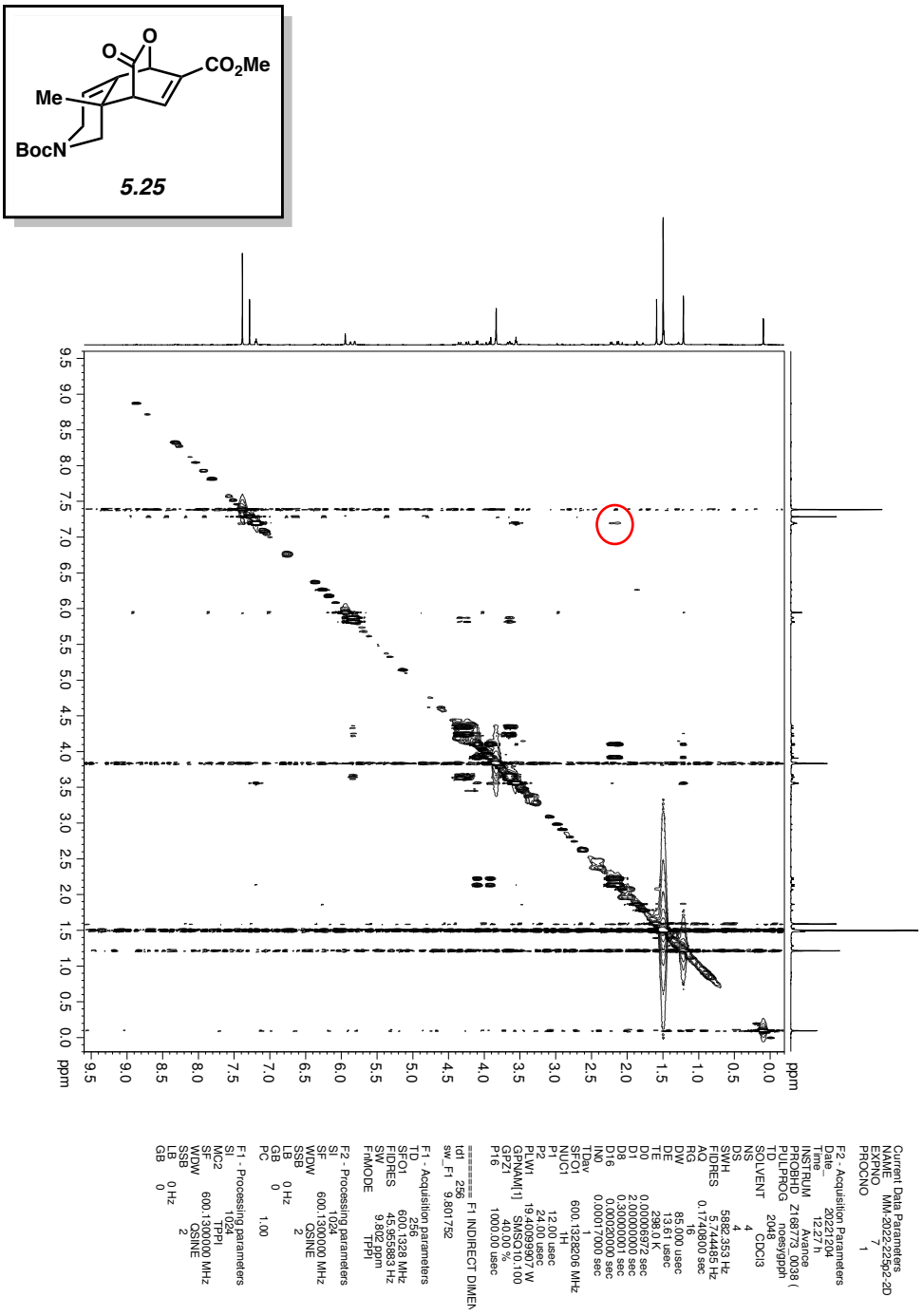

Figure 5.53. NOESY (600 MHz, $CDCl_3$) of compound **5.25**.

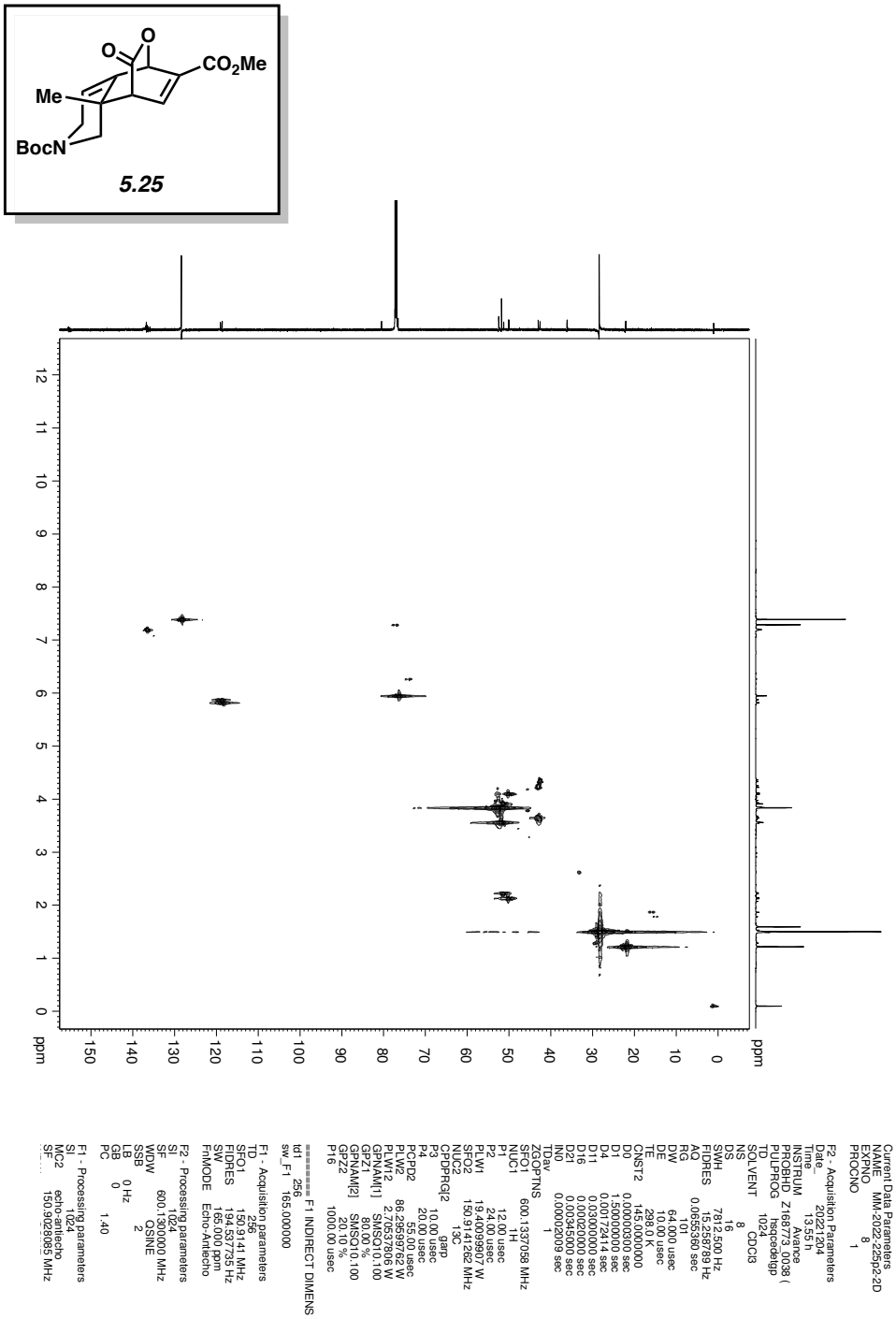

Figure 5.54. HSQC (600 MHz, $CDCl_3$) of compound **5.25**.

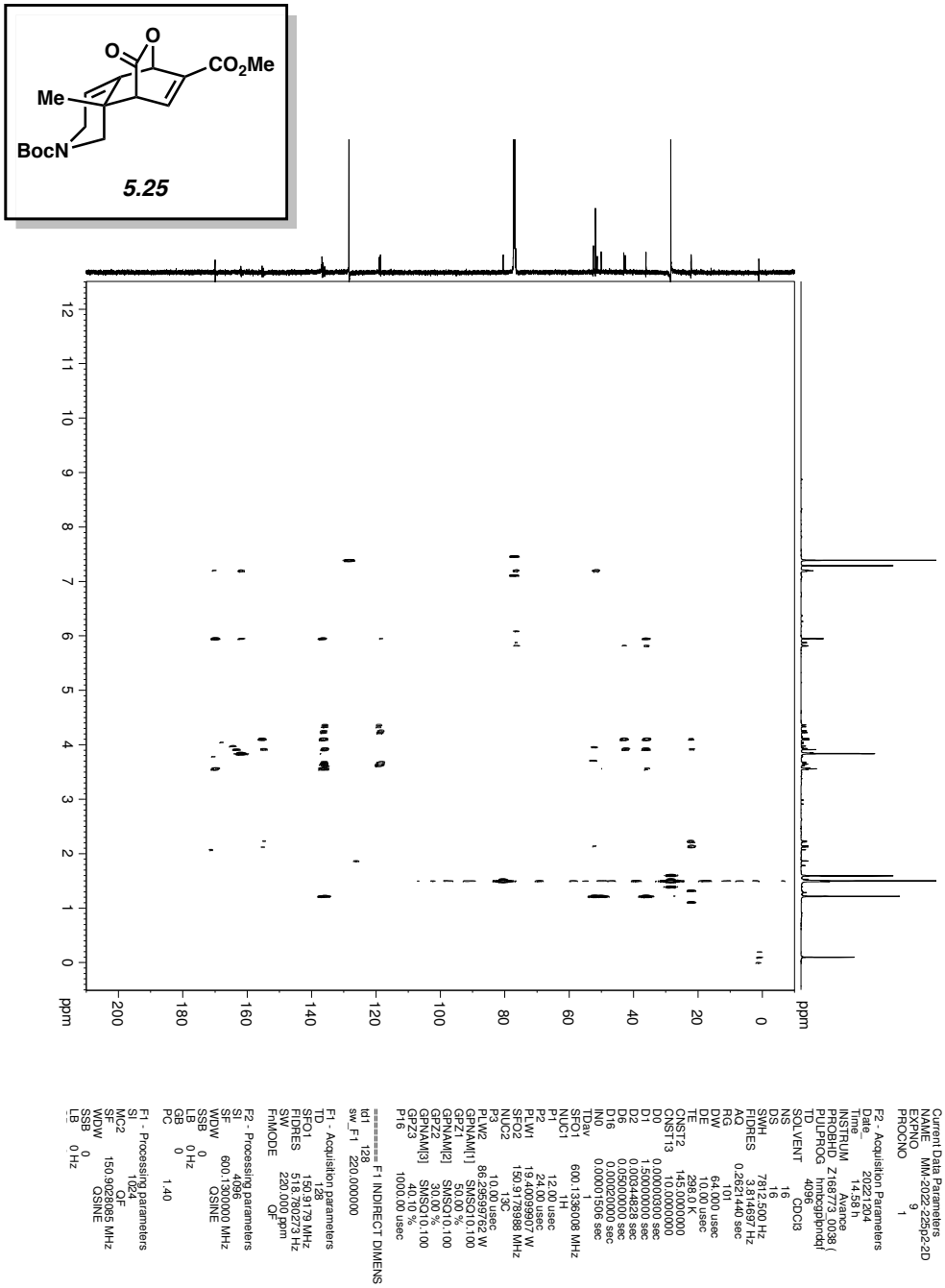

Figure 5.55. HMBC (600 MHz, $CDCl_3$) of compound **5.25**.

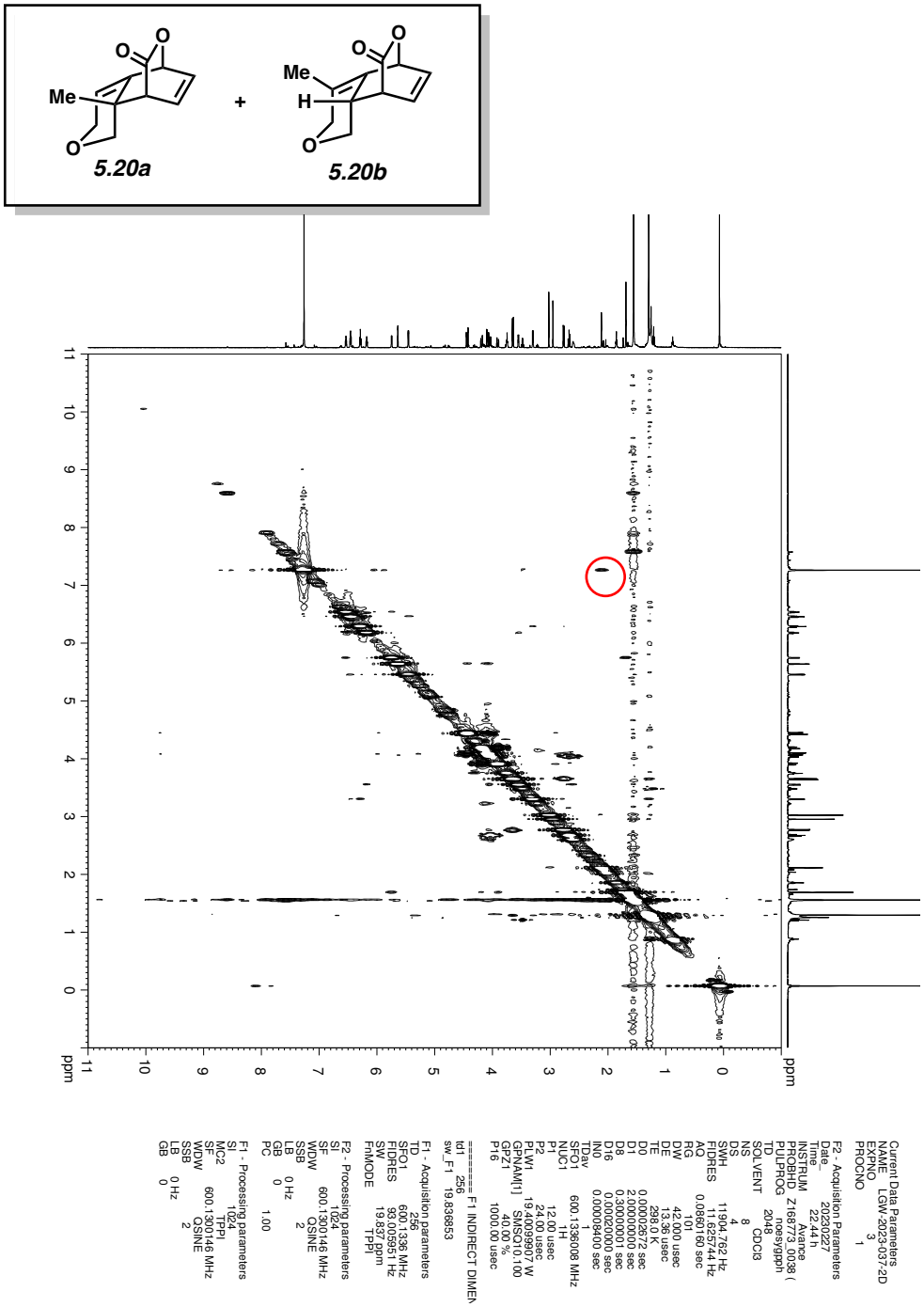

Figure 5.56. NOESY (600 MHz, $CDCl_3$) of compound **5.20a** and **5.20b**.

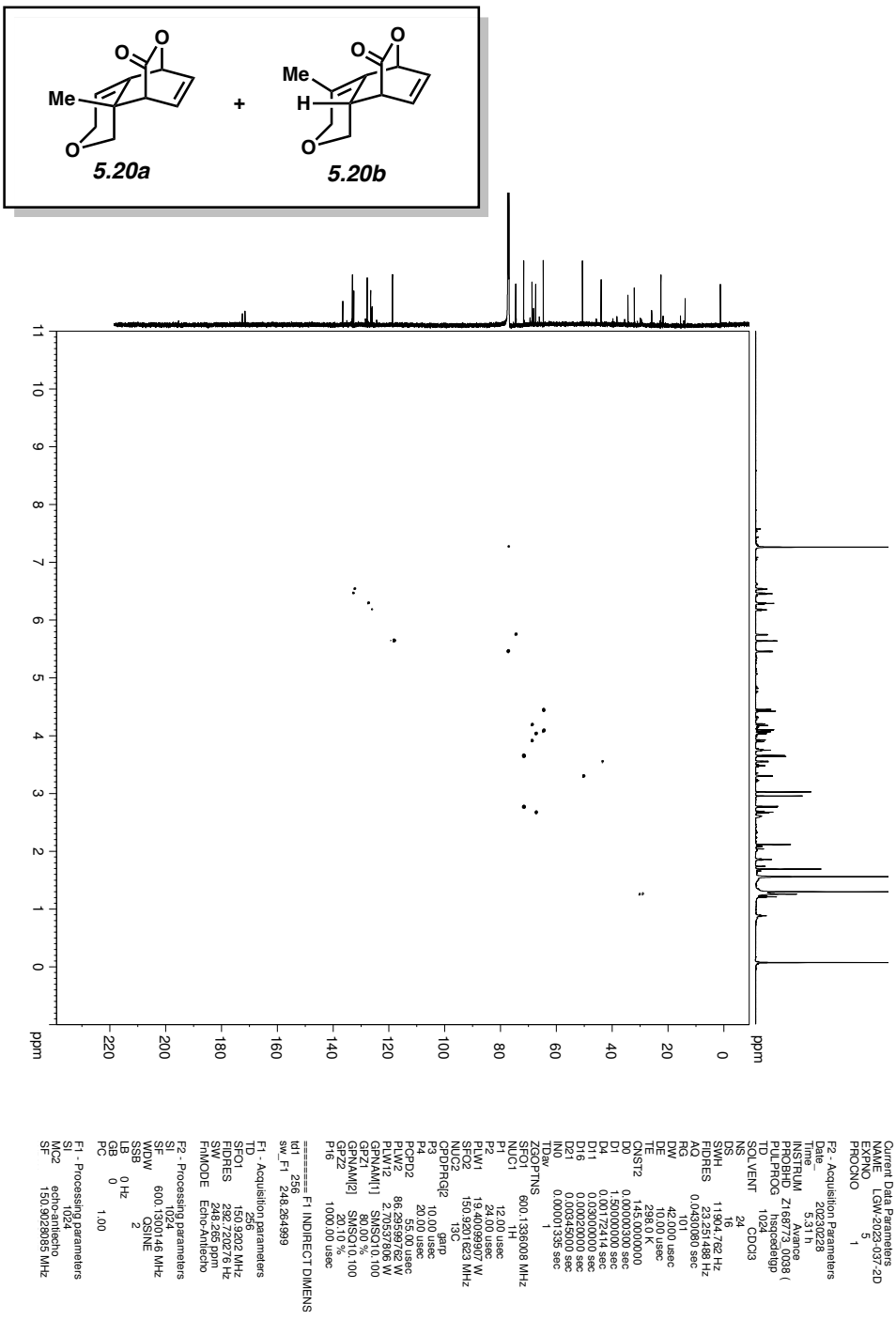

Figure 5.57. HSQC (600 MHz, $CDCl_3$) of compound **5.20a** and **5.20b**.

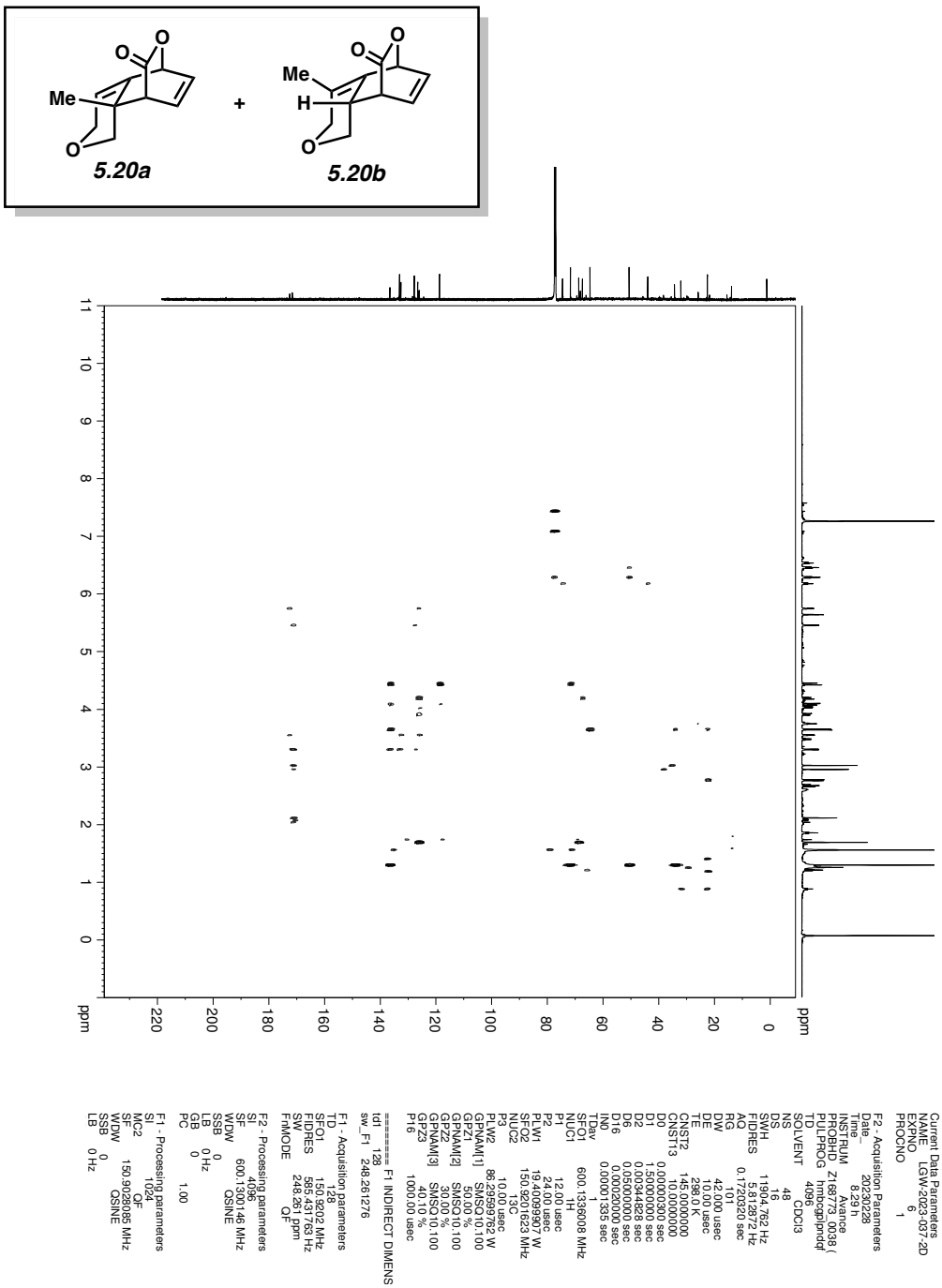

Figure 5.58. HMBC (600 MHz, $CDCl_3$) of compound **5.20a** and **5.20b**.

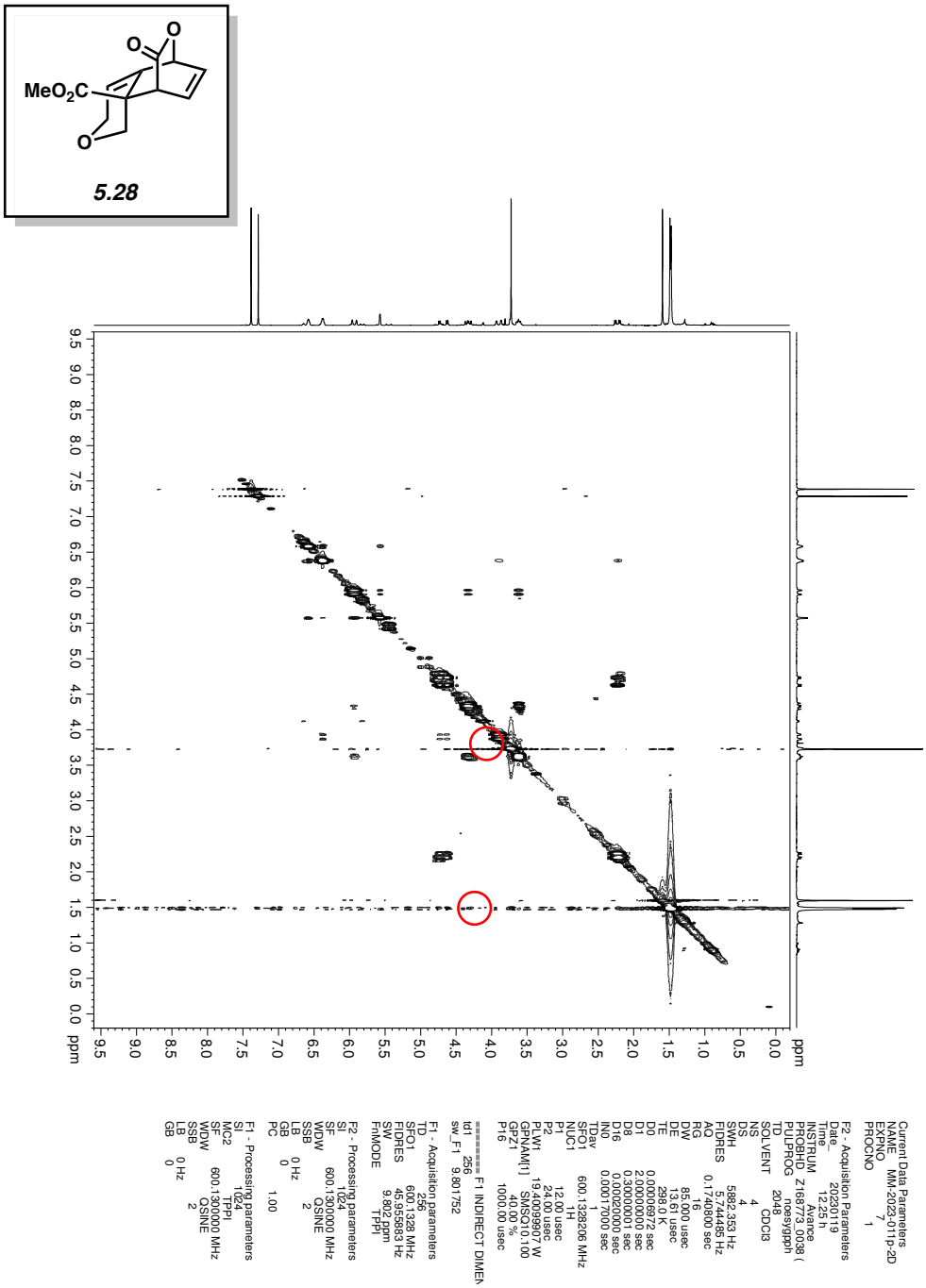

Figure 5.59. NOESY (600 MHz, $CDCl_3$) of compound **5.28**.

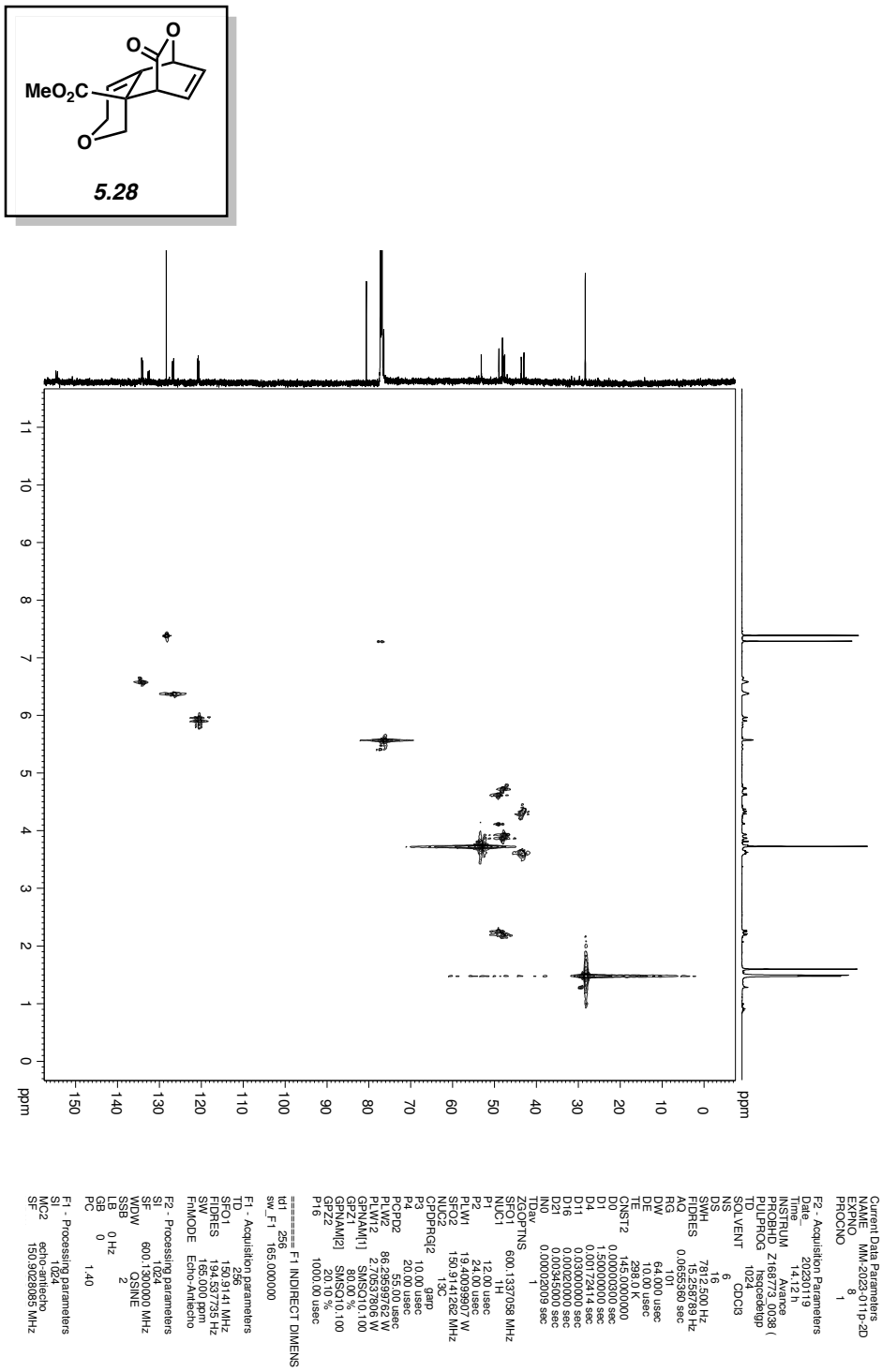

Figure 5.60. HSQC (600 MHz, $CDCl_3$) of compound **5.28**.

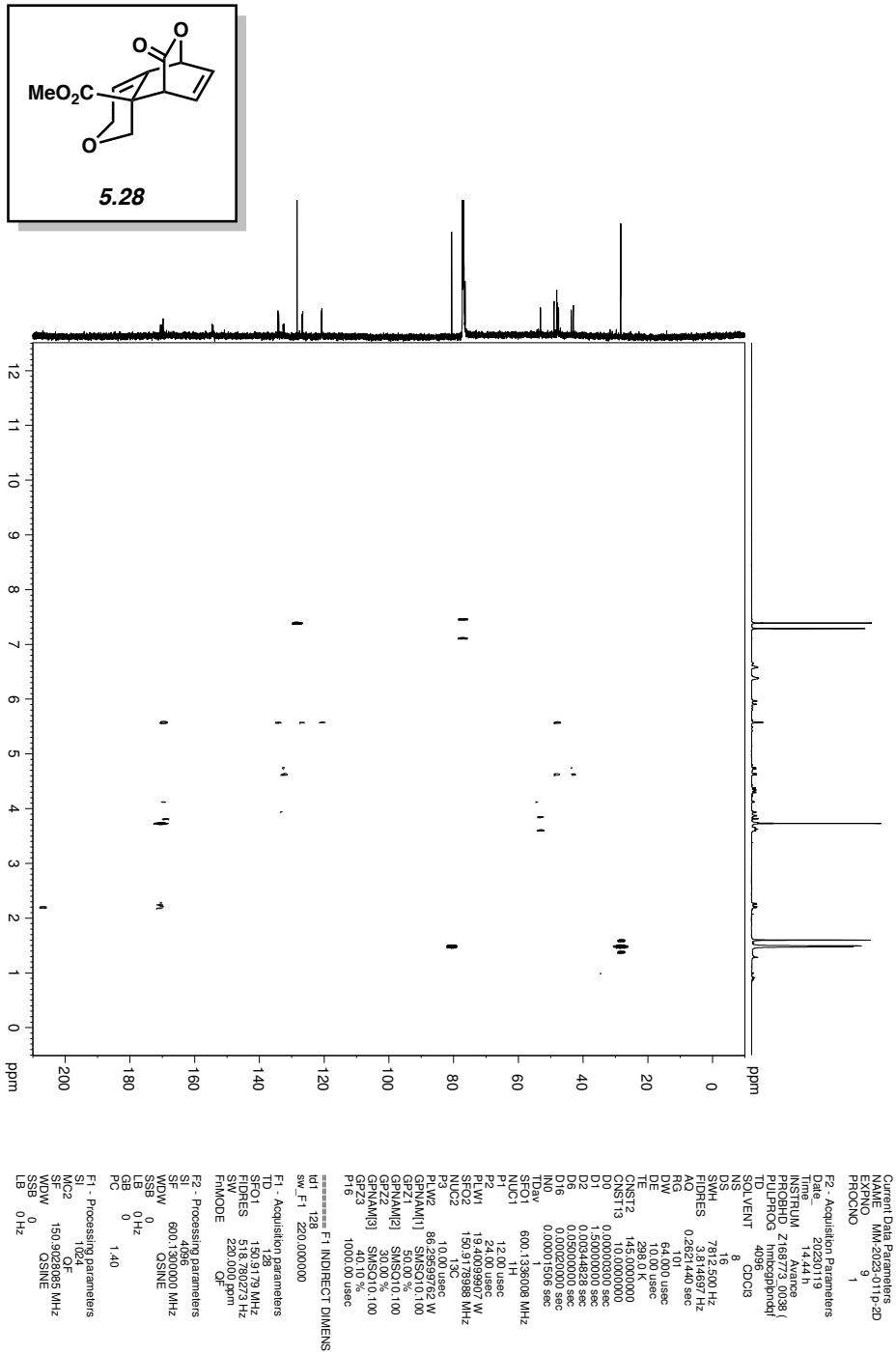

Figure 5.61. HMBC (600 MHz, $CDCl_3$) of compound **5.28**.

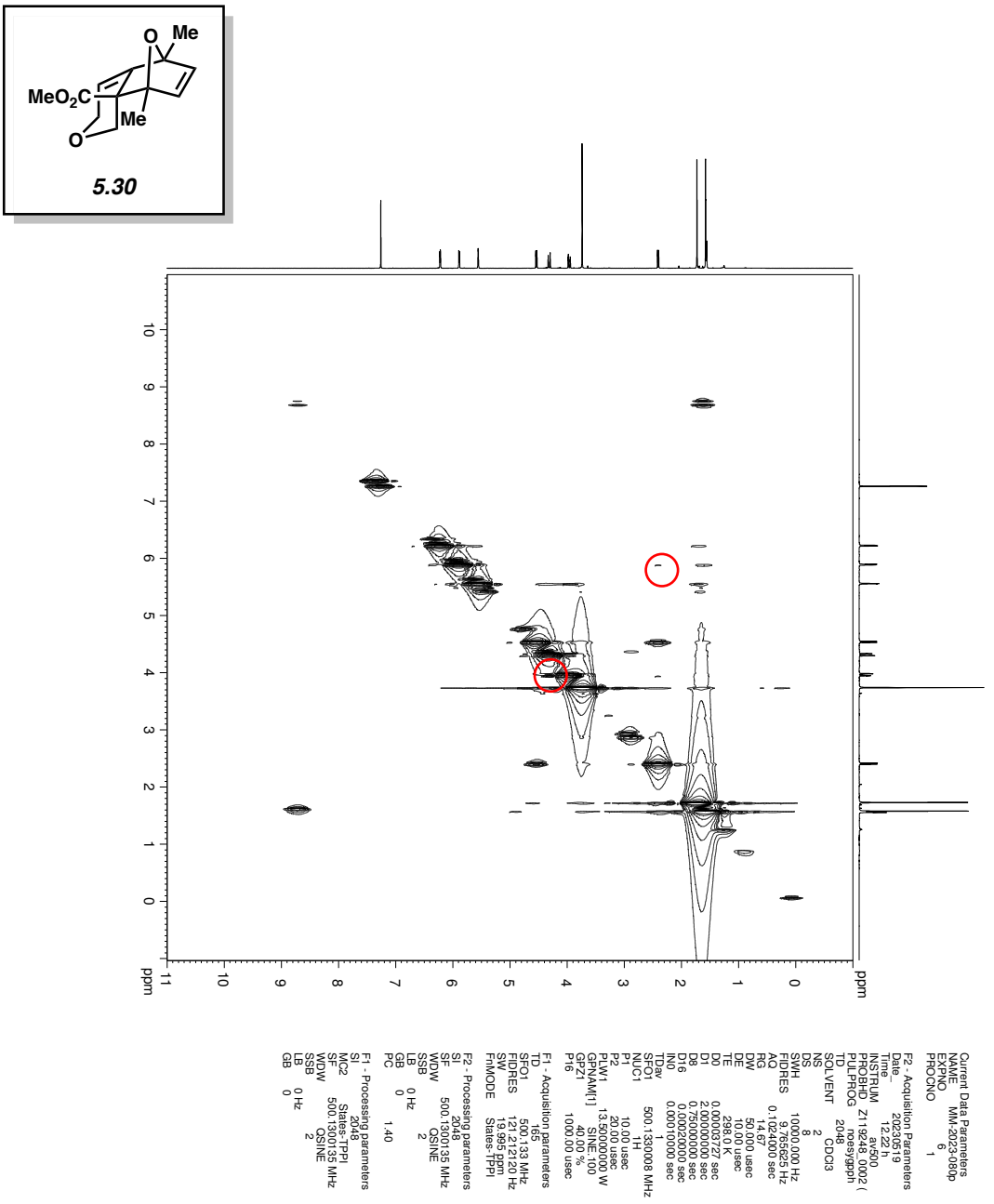

Figure 5.62. NOESY (600 MHz, $CDCl_3$) of compound **5.30**.

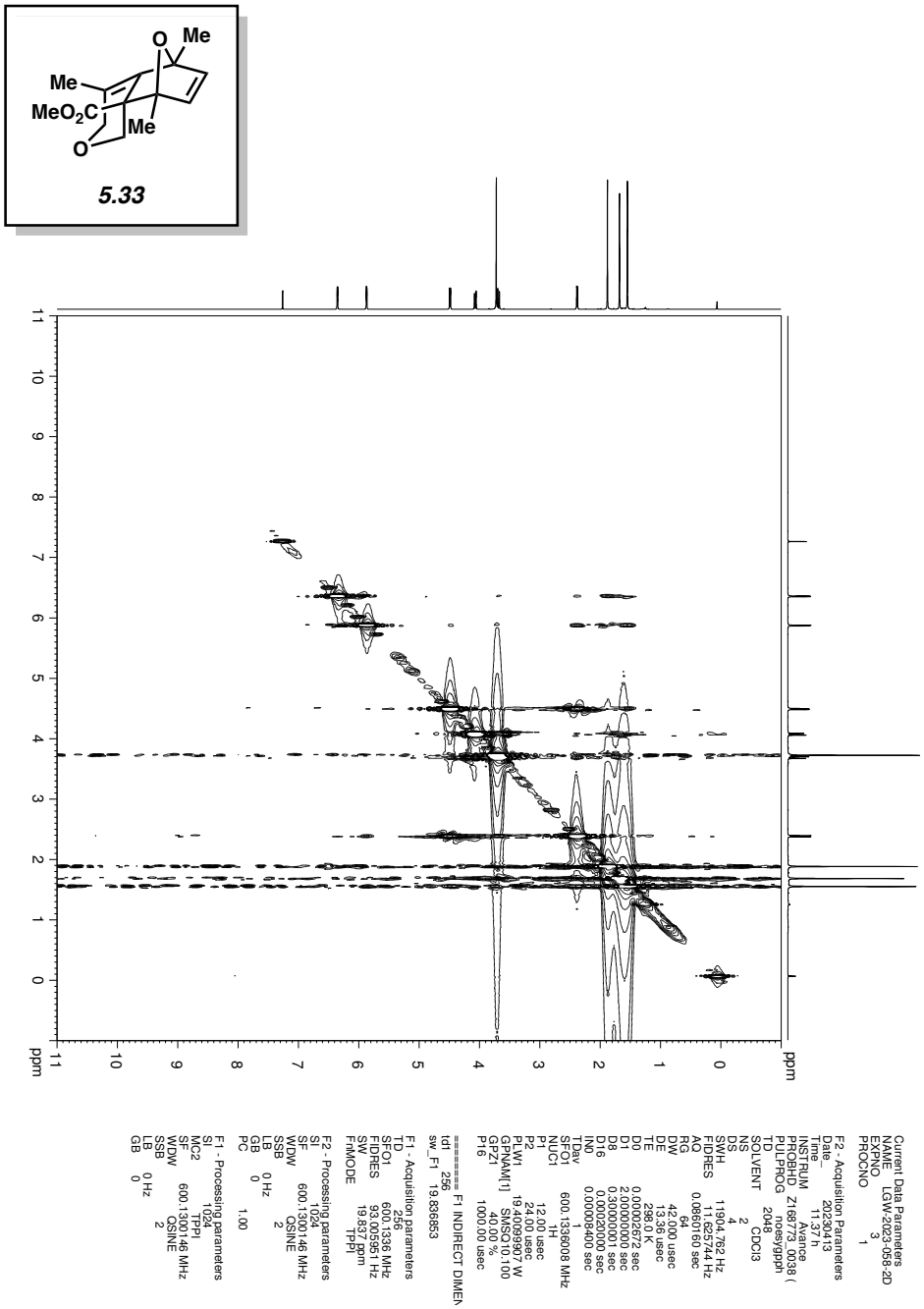

Figure 5.63. NOESY (600 MHz, $CDCl_3$) of compound **5.33**.

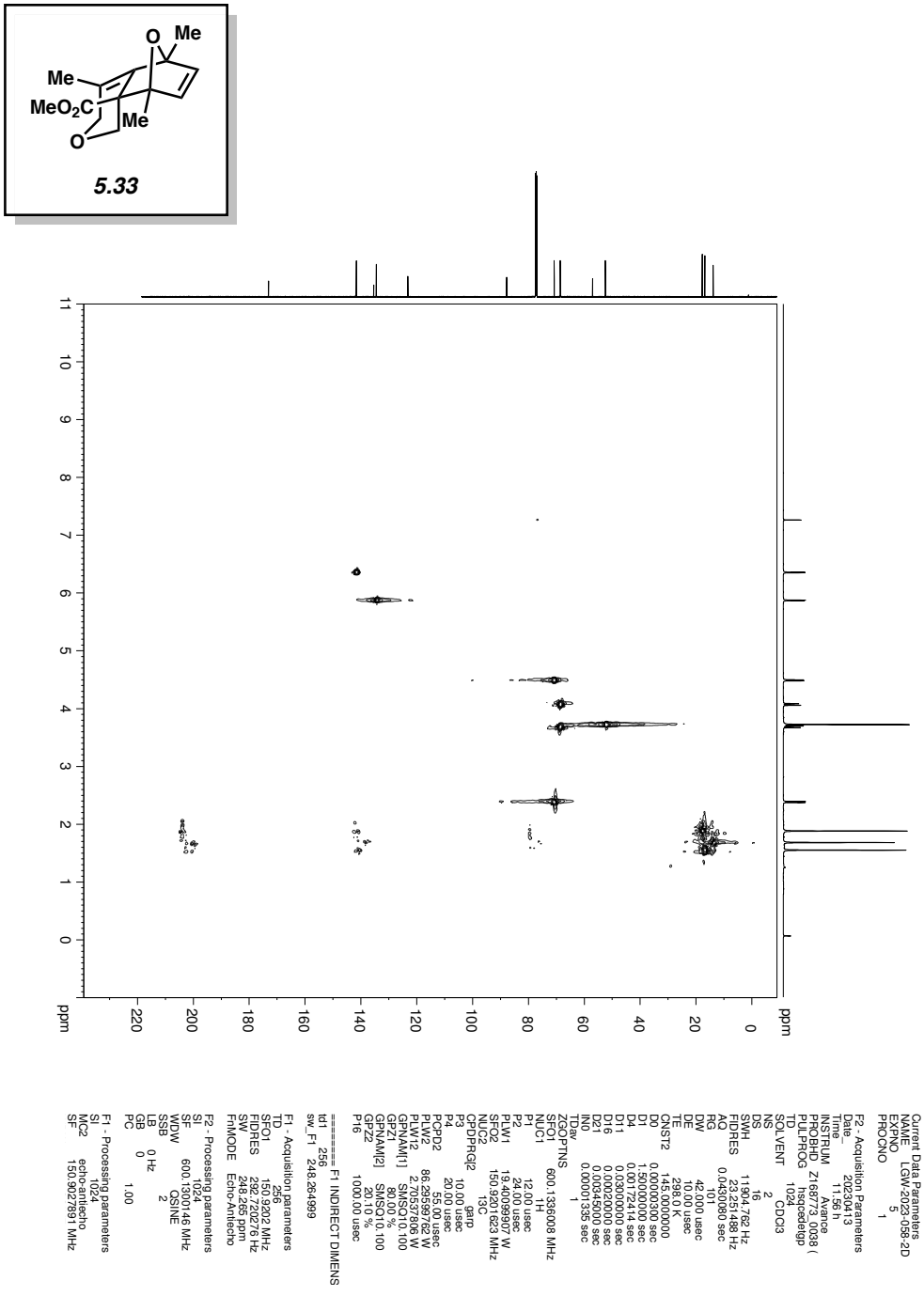

Figure 5.64. HSQC (600 MHz, $CDCl_3$) of compound **5.33**.

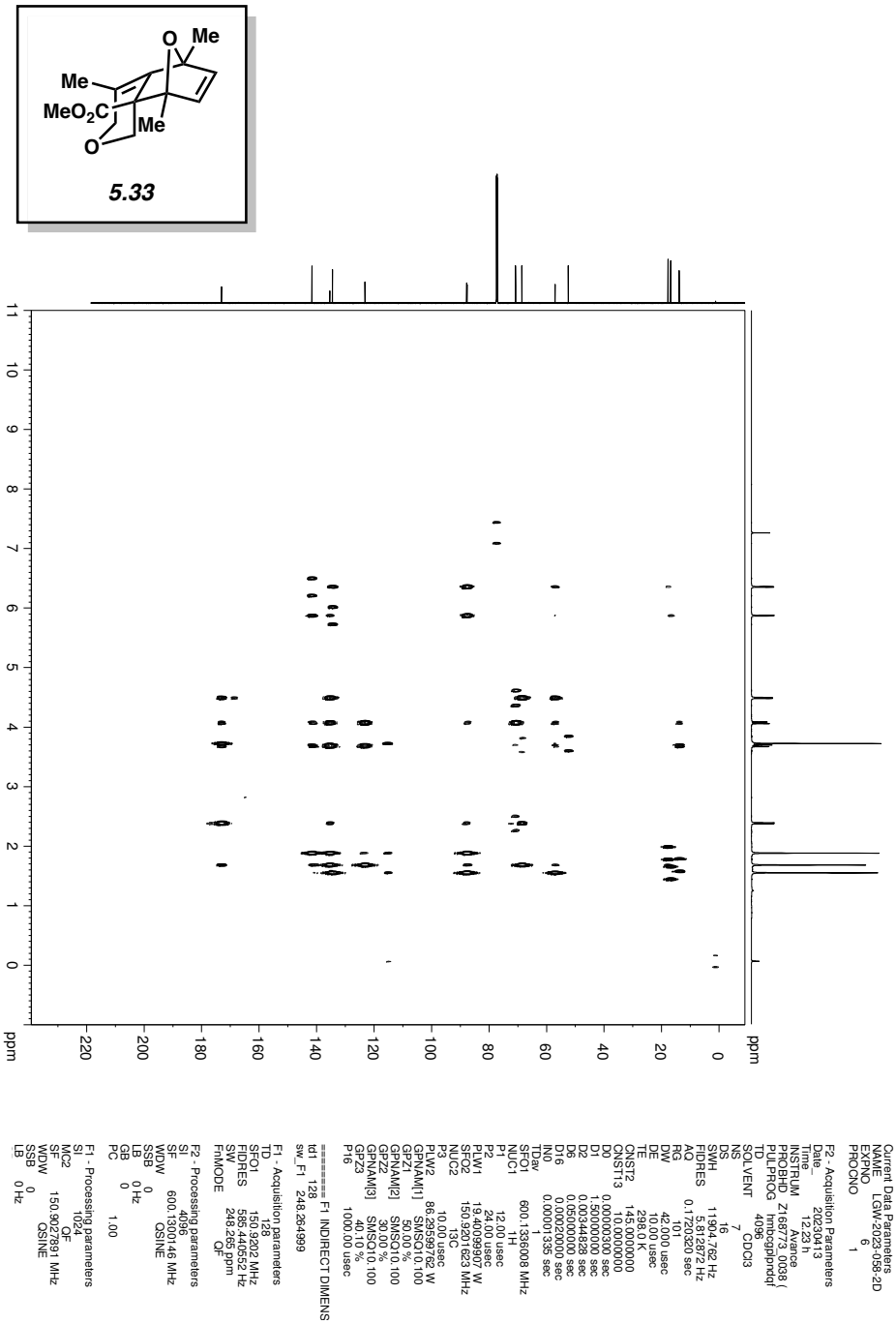

Figure 5.65. HMBC (600 MHz, $CDCl_3$) of compound **5.33**.

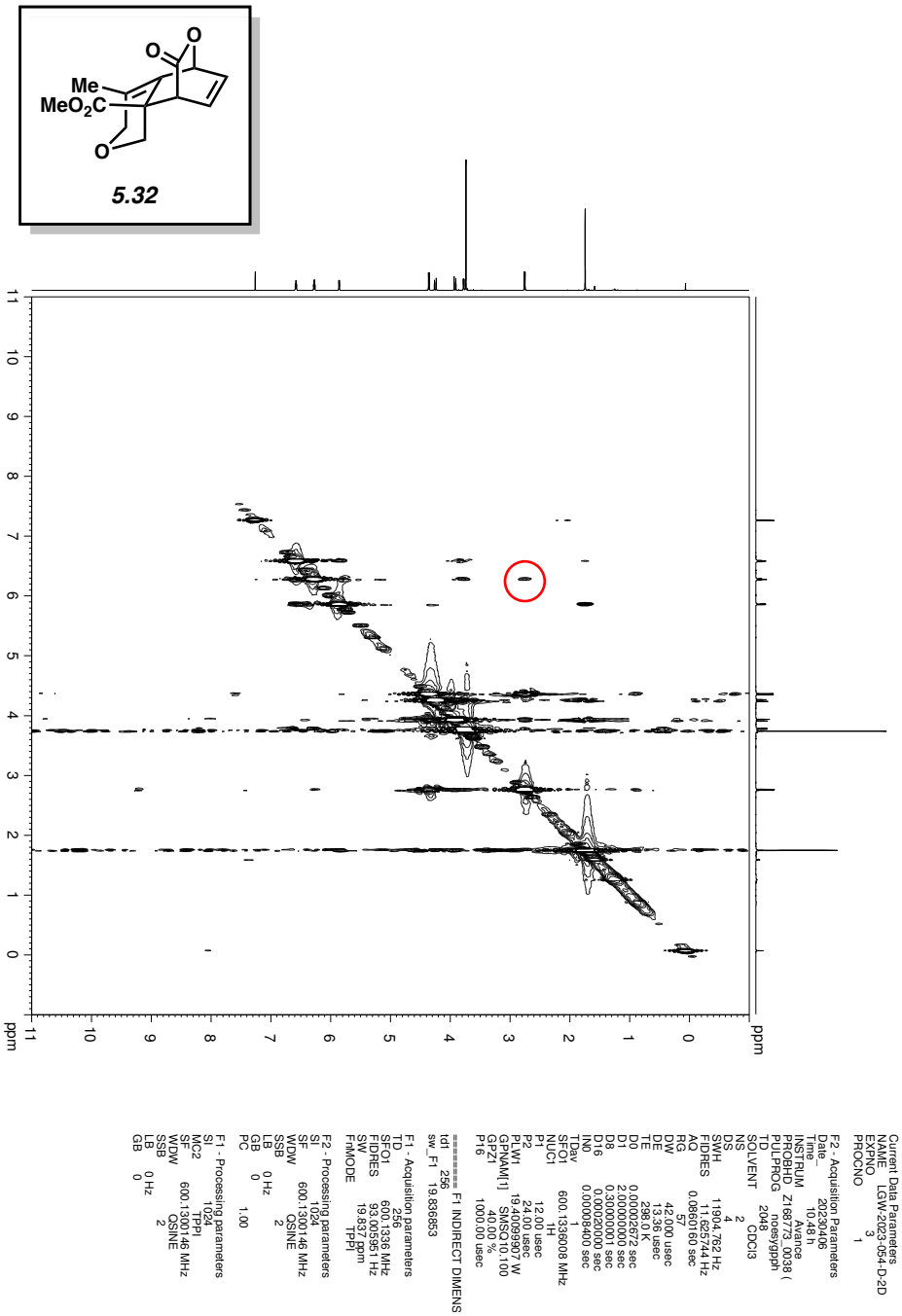

Figure 5.66. NOESY (600 MHz, $CDCl_3$) of compound **5.32**.

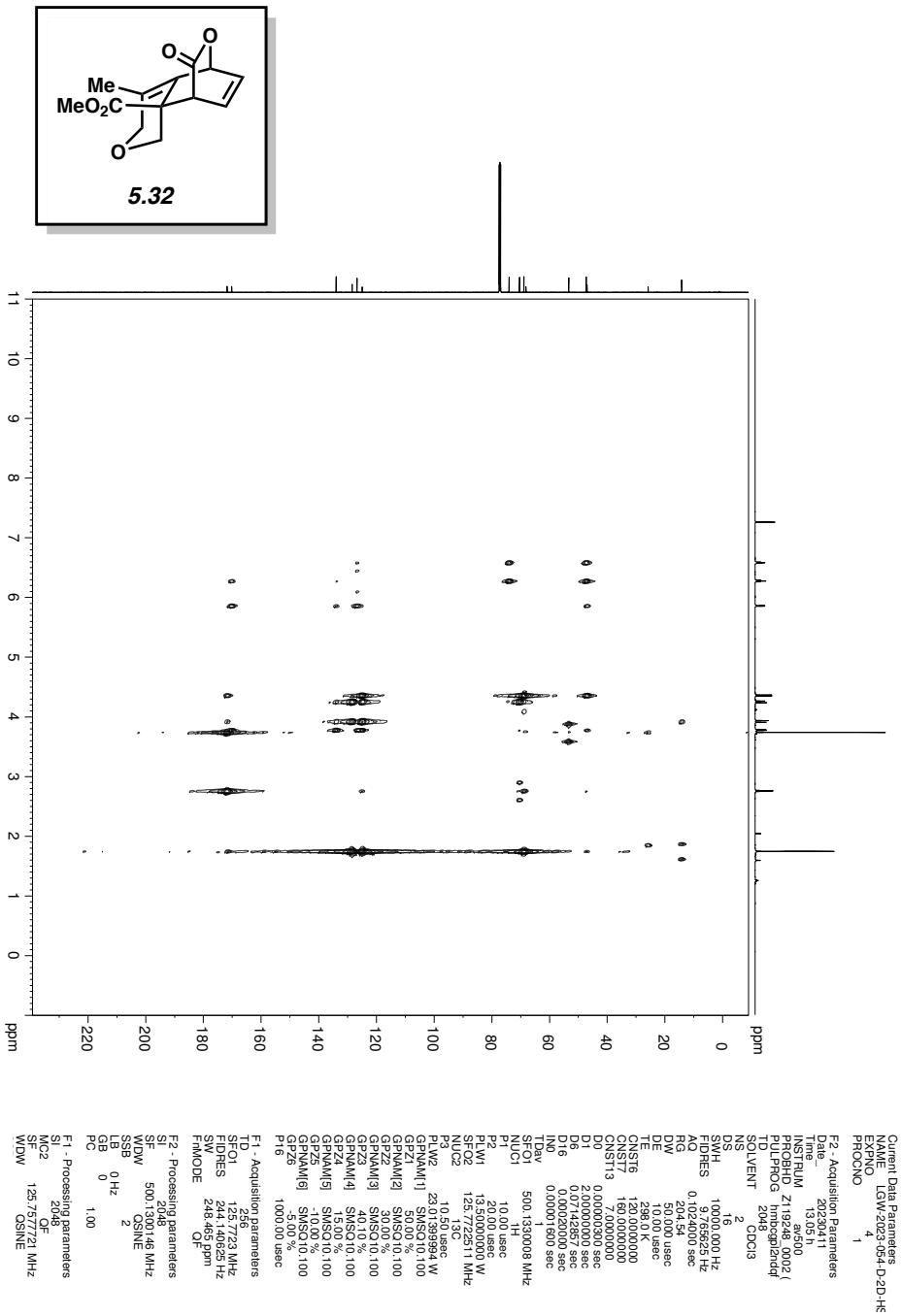

Figure 5.67. HMBC (600 MHz, $CDCl_3$) of compound **5.32**.

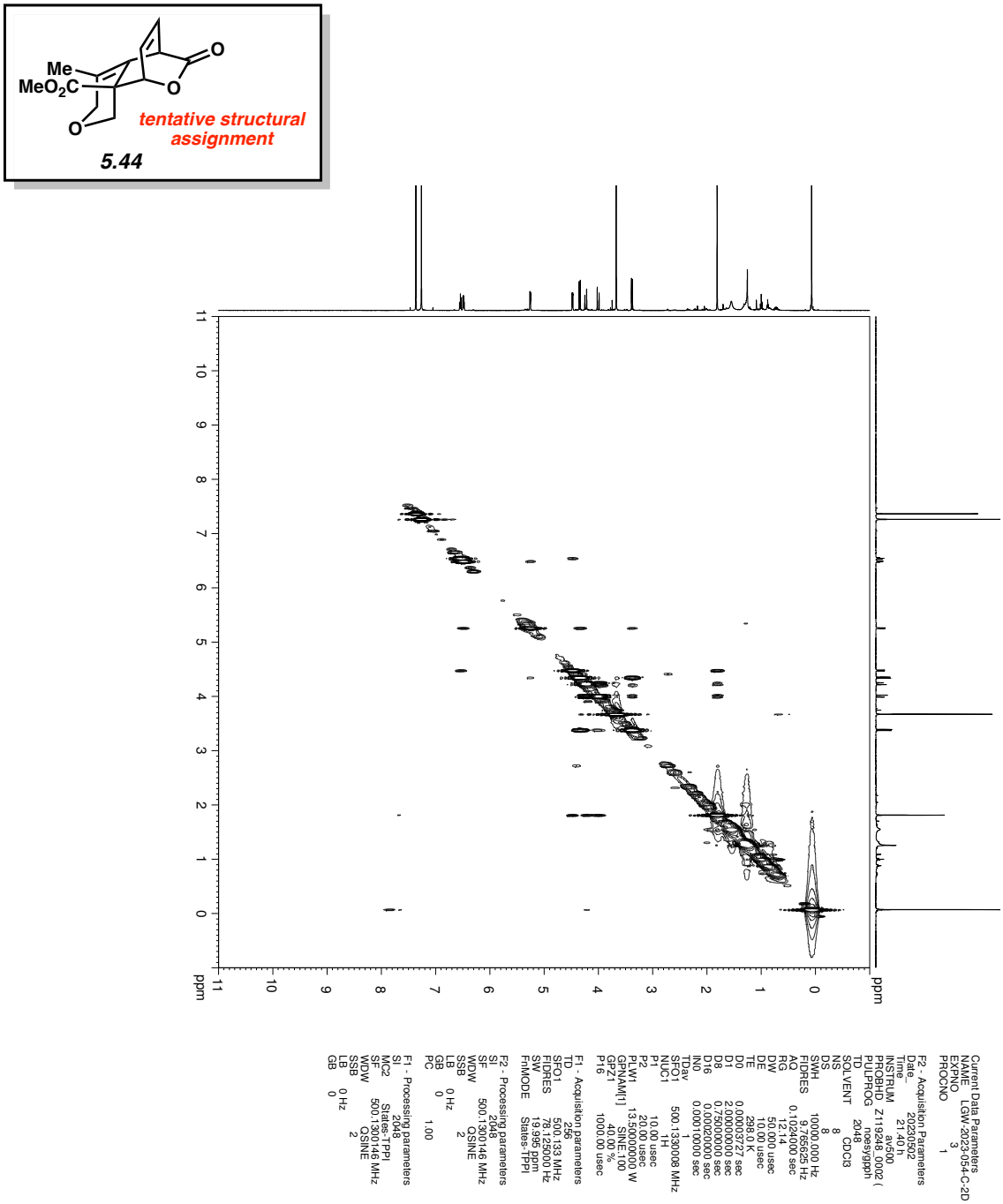

Figure 5.68. NOESY (600 MHz, $CDCl_3$) of compound **5.44**.

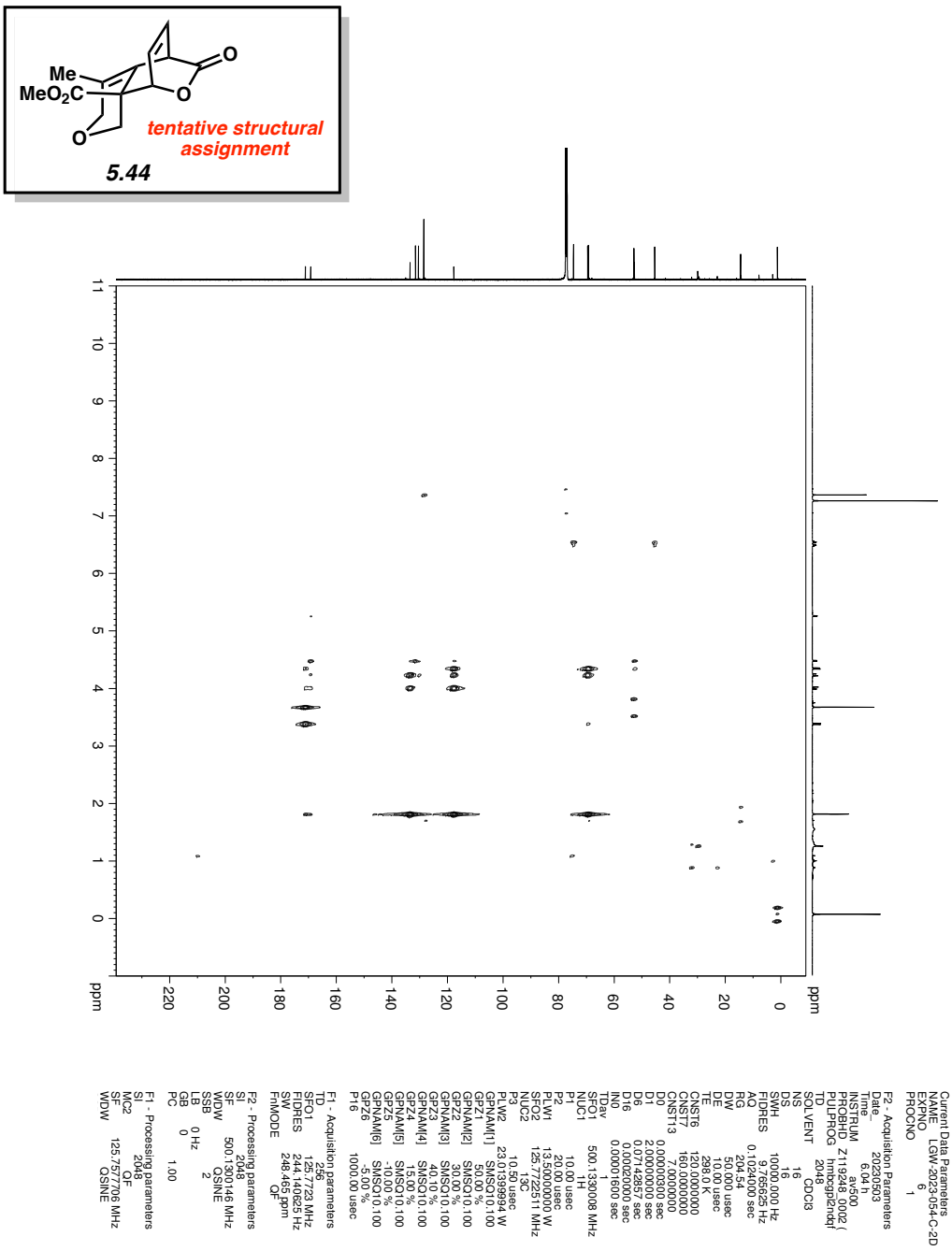

Figure 5.69. HMBC (600 MHz, $CDCl_3$) of compound **5.44**.

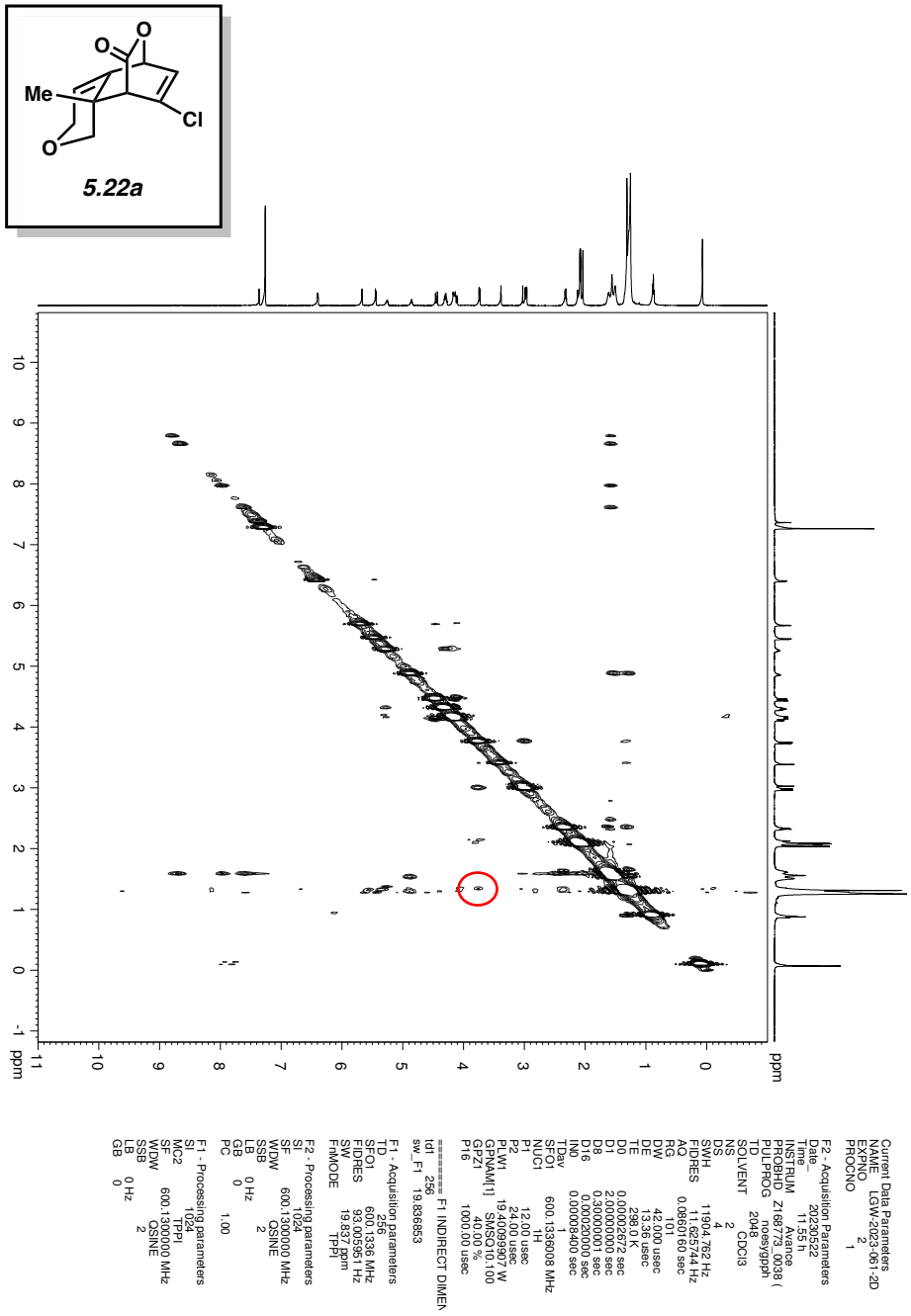

Figure 5.70. NOESY (600 MHz, $CDCl_3$) of compound **5.22a**.

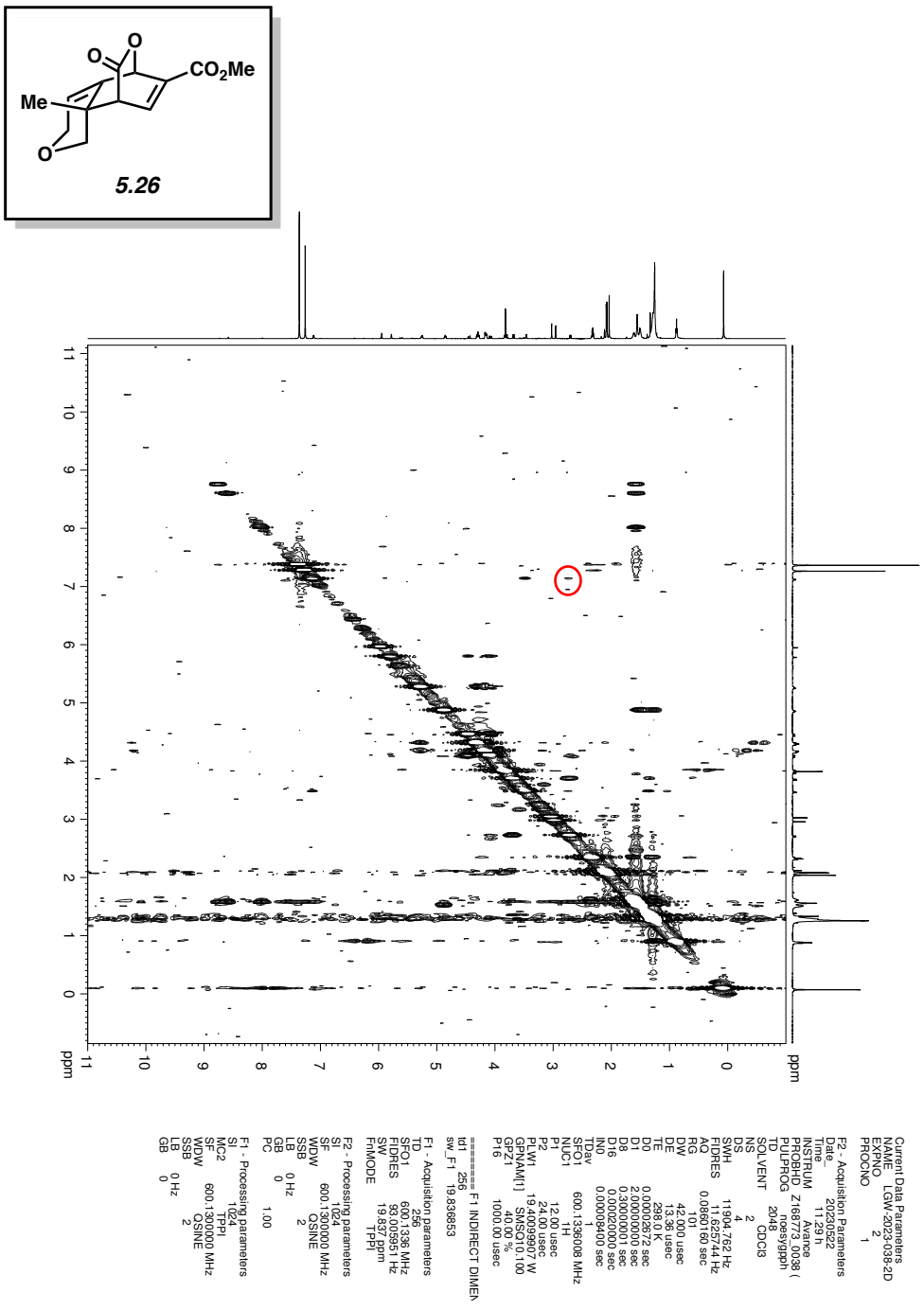

Figure 5.71. NOESY (600 MHz, $CDCl_3$) of compound **5.26**.

5.10 Notes and References

(1) Huisgen, R.; Rist, H. Über Umlagerungen bei nucleophilen Substitutionen in der aromatischen Reihe und ihre Deutung. *Naturwissenschaften* **1954**, *41*, 358–359.

(2) Roberts, J. D.; Simmons, H. E.; Carlsmith, L. A.; Vaughan, C. W. Rearrangement in the reaction of chlorobenzene-1-C14 with potassium amide. *J. Am. Chem. Soc.* **1953**, *75*, 3290−3291.

(3) Wittig, G.; Pohmer, L., Intermediäre Bildung von Dehydrobenzol (Cyclohexa-dienin). *Angew. Chem.* **1955**, *67*, 348–348.

(4) Wittig, G.; Pohmer, L., Über das intermediäre Auftreten von Dehydrobenzol. *Chem. Ber.* **1956**, *89*, 1334–1351.

(5) Scardiglia, F.; Roberts, J. D. Evidence for cyclohexyne as an intermediate in the coupling of phenyllithium with 1-chlorocyclohexene. *Tetrahedron* **1957**, *1*, 343−344.

(6) Wittig, G.; Mayer, U. Bildung und Verhalten von Cyclohexin. *Chem. Ber.* **1963**, *96*, 329–341.

(7) Dobler, D.; Leitner, M.; Moor, N.; Reiser, O. 2-Pyrone – A Privileged Heterocycle and Widespread Motif in Nature. *Eur. J. Org. Chem.* **2021**, *2021*, 6180–6205.

(8) Escudero, S.; Perez, D.; Castedo, L.; Guitian, E. [4+2] Cycloadditions between 2-Pyrones and Benzyne. Application to the Synthesis of Binaphthyls. *Tetrahedron Lett.* **1997**, *38*, 5375–5378.

(9) Takikawa, H.; Nishii, A.; Sakai, T.; Suzuki, K. Aryne-based strategy in the total synthesis of naturally occurring polycyclic compounds. *Chem. Soc. Rev.* **2018**, *47*, 8030–8056.

(10) Atanes, N.; Escudero, S.; Pérez.; Guitián, E.; Castedo, L. Generation of Cyclohexyne and its Diels–Alder Reaction with α-Pyrones. *Tetrahedron Lett.* **1998**, *39*, 3039–3040.

(11) Wenk, H. H.; Winkler, M.; Sander, W. One century of aryne chemistry. *Angew. Chem., Int. Ed*. **2003**, *42*, 502−528.

(12) Shi, J.; Li, L.; Li, Y. o-Silylaryl triflates: A journey of Kobayashi aryne precursors. *Chem. Rev.* **2021**, *121*, 3892−4044.

(13) Tadross, P. M.; Stoltz, B. M. A Comprehensive History of Arynes in Natural Product Total Synthesis. *Chem. Rev.* **2012**, *112*, 3550−3577.

(14) Gampe, C. M.; Carreira, E. M. Arynes and Cyclohexyne in Natural Product Synthesis. *Angew. Chem., Int. Ed.* **2012**, *51*, 3766−3778.

(15) Kim, J.-Y.; Kim, D.-H.; Jeon, T.-H.; Kim, W.-H.; Cho, C.-G. Total syntheses of Ningalins D and G. *Org. Lett.* **2017**, *19*, 4688–4691.

(16) Darzi, E. R.; Barber, J. S.; Garg, N. K. Cyclic alkyne approach to heteroatom-containing polycyclic aromatic hydrocarbon scaffolds. *Angew. Chem., Int. Ed.* **2019**, *58*, 94119–9424.

(17) Ramirez, M.; Darzi, E. R.; Donaldson, J. S.; Houk, K. N.; Garg, N. K. Cycloaddition cascades of strained alkynes and oxadiazinones. *Angew. Chem., Int. Ed.* **2021**, *60*, 18201–18208.

(18) Chinta, B. S.; Lee, D.; Hoye, T. R. Coumarin (5,6-Benzo-2-pyrone) Trapping of an HDDA-Benzyne. *Org. Lett.* **2021**, *23*, 2189–2193.

(19) Meguro, T.; Chen, S.; Kanemoto, K.; Yoshida, S.; Hosoya, T. Modular Synthesis of Unsymmetrical Doubly-Ring-Fused Benzene Derivatives Based on a Sequential Ring Construction Strategy Using Oxadiazinones as a Platform Molecule. *Chem. Lett.* **2019**, *48*, 582–585.

(20) For a comprehensive review of strained cyclic allene chemistry through 2003, see: Christl, M. Cyclic Allenes Up to Seven-Membered Rings. *Modern Allene Chemistry*; Krause, N., Kashmi, S. A. K., Eds.; Wiley-VCH: Weinheim, 2005; pp 243–357.

(21) Strain energies for benzyne: ~50 kcal/mol; cyclohexyne: ~40 kcal/mol; and cyclic allenes: ~30 kcal/mol. See Reference 32 for details.

(22) Moser, W. R. The Reactions of *gem*-Dihalocyclopropanes with Organometallic Reagents. Ph.D. Dissertation, Massachusetts Institute of Technology Cambridge, MA, **1964**.

(23) Wittig, G.; Fritze, P. On the Intermediate Occurrence of 1,2-Cyclohexadiene. *Angew. Chem., Int. Ed.* **1966**, *5*, 846.

(24) Uyegaki, M.; Ito, S., Sugihara, Y.; Murata, I. 1-Benzoxepin and Its Valence Isomers, 4,5-benz-3-oxatricyclo[4.1.0.0^{2,7}]heptane and 3,4-benz-2-oxabicyclo-[3.2.1]-hepta-3,6-diene. *Tetrahedron Lett.* **1976**, *49*, 4473–4476.

(25) Christl, M., Braun, M., Wolz, E. & Wagner, W. 1-Phenyl-1-aza-3,4- Cyclohexadien, Das Erste Isodihydropyridin: Ertzeugung und Abfangreaktionen. *Chem. Ber.* **1994**, *127*, 1137–1142.

(26) Quintana, I.; Peña, D.; Pérez, D.; Guitián, E. Generation and Reactivity of 1,2-Cyclohexadiene Under Mild Reaction Conditions. *Eur. J. Org. Chem.* **2009**, *2009*, 5519−5524.

(27) Peña, D.; Iglesias, B.; Quintana, I.; Pérez, D.; Guitián, E.; Castedo, L. Synthesis and Reactivity of New Strained Cyclic Allene and Alkyne Precursors. *Pure Appl. Chem.* **2006**, *78*, 451−455.

(28) Almehmadi, Y. A.; West, F. G. A Mild Method for the Generation and Interception of 1,2-Cycloheptadienes with 1,3-dipoles. *Org. Lett.* **2020**, *22*, 6091−6095.

(29) Wang, B.; Constantin, M. G.; Singh, S.; Zhou, Y.; Davis, R. L.; West, F. G. Generation and Trapping of Electron-Deficient 1,2-Cyclohexadienes. Unexpected Hetero-Diels–Alder Reactivity. *Org. Biomol. Chem.* **2021**, *19*, 399–405.

(30) Hioki, Y.; Mori, A.; Okano, K. Steric Effects on Deprotonative Generation of Cyclohexynes and 1,2-Cyclohexadienes from Cyclohexenyl Triflates by Magnesium Amides. *Tetrahedron* **2020**, *76*, 131103.

(31) Inoue, K.; Nakura, R.; Okano, K.; Mori, A. One-pot Synthesis of Silylated Enol Triflates from Silyl Enol Ethers for Cyclohexynes and 1,2-Cyclohexadienes. *Eur. J. Org. Chem.* **2018**, *2018*, 3343−3347.

(32) Westphal, M. V.; Hudson, L.; Mason, J. W.; Pradeilles, J. A.; Zecri, F. J.; Briner, K.; Schreiber, S. L. Water-compatible Cycloadditions of Oligonucleotide-conjugated Strained Allenes for DNA-encoded Library Synthesis. *J. Am. Chem. Soc.* **2020**, *142*, 7776−7782.

(33) Anthony, S. M.; Wonilowicz, L. G.; McVeigh, M. S.; Garg, N. K. Leveraging Fleeting Strained Intermediates to Access Complex Scaffolds. *JACS Au* **2021**, *1*, 897–912.

(34) Kelleghan, A. V.; Witkowski, D. C.; McVeigh, M. S.; Garg, N. K. Palladium-Catalyzed Annulations of Strained Cyclic Allenes. *J. Am. Chem. Soc.* **2021**, *143*, 25, 9338–9342.

(35) Yamano, M. M.; Kelleghan, A. V.; Shao, Q.; Giroud, M.; Simmons, B. J.; Li, B.; Chen, S.; Houk, K. N.; Garg, N. K. Intercepting Fleeting Cyclic Allenes with Asymmetric Nickel Catalysis. *Nature* **2020**, *586*, 242–247.

(36) McVeigh, M. S.; Kelleghan, A. V.; Yamano, M. M.; Knapp, R. R.; Garg, N. K. Silyl Tosylate Precursors to Cyclohexyne, 1,2-Cyclohexadiene, and 1,2-Cycloheptadiene. *Org. Lett.* **2020**, *22*, 4500−4504.

(37) Barber, J. S.; Styduhar, E. D.; Pham, H. V.; McMahon, T. C.; Houk, K. N.; Garg, N. K. Nitrone Cycloadditions of 1,2-Cyclohexadiene. *J. Am. Chem. Soc.* **2016**, *138*, 2512−2515.

(38) McVeigh, M. S.; Garg, N. K. Interception of 1,2-Cyclohexadiene with TEMPO Radical. *Tetrahedron Lett.* **2021**, *87*, 153539–153543.

(39) Spence, K. A.; Tena Meza, A.; Garg, N. K. Merging Metals and Strained Intermediates. *Chem Catalysis* **2022**, *2*, 1870–1879.

(40) Nendel, M.; Tolbert, L. M.; Herring, L. E.; Islam, M. N.; Houk, K. N. Strained Allenes as Dienophiles in the Diels–Alder Reaction: An Experimental and Computational Study. *J. Org. Chem.* **1999**, *64*, 976–983.

(41) Barber, J. S.; Yamano, M. M.; Ramirez, M.; Darzi, E. R.; Knapp, R. R.; Liu, F.; Houk, K. N.; Garg, N. K. Diels–Alder Cycloadditions of Strained Azacyclic Allenes. *Nat. Chem*. **2018**, *10*, 953–960.

(42) Jankovic, C. L.; West, F. G. 2+2 Trapping of Acyloxy-1,2-cyclohexadienes with Styrenes and Electron-Deficient Olefins. *Org. Lett.* **2022**, *24*, 9457–9501.

(43) Lofstrand, V. A.; West, F. G. Efficient Trapping of 1,2-Cyclohexadienes with 1,3-Dipoles. *Chem*. *Eur*. *J*. **2016**, *22*, 10763−10767.

(44) Lofstrand, V. A.; McIntosh, K. C.; Almehmadi, Y. A.; West, F. G. Strain-activated Diels−Alder Trapping of 1,2-Cyclohexadienes: Intramolecular Capture by Pendent Furans. *Org*. *Lett*. **2019**, *21*, 6231−6234.

(45) Yamano, M. M.; Knapp, R. R.; Ngamnithiporn, A.; Ramirez, M.; Houk, K. N.; Stoltz, B. M.; Garg, N. K. Cycloadditions of Oxacyclic Allenes and a Catalytic Asymmetric Entryway to Enantioenriched Cyclic Allenes. *Angew*. *Chem*., *Int*. *Ed*. **2019**, *58*, 5653−5657.

(46) Afarinkia, K.; Vinader, V.; Nelson, T. D.; Posner, G. H. Diels–Alder Cycloadditions of 2-pyrones and 2-pyridones. *Tetrahedron* **1992**, *48*, 9111–9171.

(47) The [2.2.2]-bicyclic products arising from DA cycloadditions between pyrones and cyclic allenes can be isolated. To enable CO_2 expulsion, more forcing thermal conditions are typically required.

(48) Ippoliti, F. M.; Adamson, N. J.; Wonilowicz, L. G.; Nasrallah, D. J.; Darzi, E. R.; Donaldson, J. S.; Garg, N. K. Total Synthesis of Lissodendoric Acid A via Stereospecific Trapping of a Strained Cyclic Allene. *Science* **2023**, *379*, 261–265.

(49) The structures of the cycloadducts throughout this study were assigned using 2D NMR analysis. The isomer of the cycloaddition with respect to the olefins of the cyclic allene were determined using the number of vinyl protons observed in the HSQC of the product.

(50) The regioisomeric ratios reported in this study are reflective of the selectivity with respect to the two olefins of the cyclic allene. A single regioisomer is consistently observed for the methyl-substituted allene examples where bonds are formed between C2 of the allene with the carbon alpha to the oxygen of the pyrone and C3 of the allene with the carbon alpha to the carbonyl of the pyrone (see Figure 5.2 for atom numbering).

(51) Ramirez, M.; Svatunek, D.; Liu, F.; Garg, N. K.; Houk, K. N. Origins of *Endo* Selectivity in Diels–Alder Reactions of Cyclic Allene Dienophiles. *Angew. Chem., Int. Ed.* **2021**, *60*, 14989–14997.